NASW-4066

Abstracts for the

52nd Annual Meeting of the METEORITICAL SOCIETY

Vienna, Austria
July 31 – August 4, 1989

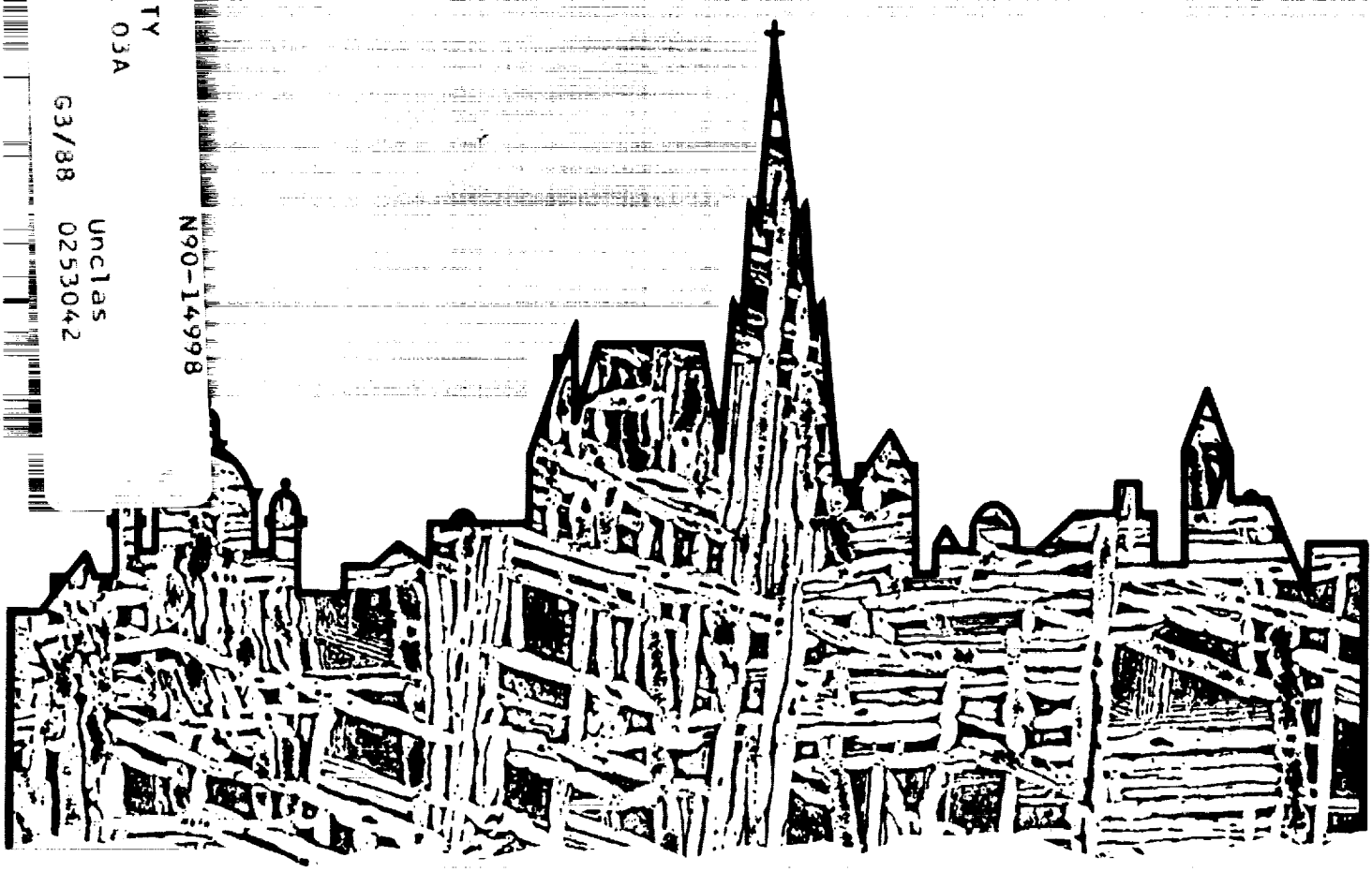

ABSTRACTS AND PROGRAM FOR THE

52ND ANNUAL MEETING OF THE METEORITICAL SOCIETY

Vienna, Austria
July 31 - August 4, 1989

Hosted by
Institute of Geochemistry, University of Vienna
Naturhistorisches Museum, Vienna

Sponsored by
University of Vienna
Naturhistorisches Museum, Vienna
Lunar and Planetary Institute, Houston
Ministry of Science and Research, Vienna

Co-sponsored by
The Barringer Crater Company
Vienna Tourist Board
City of Vienna
Austrian Space Agency
ÖMV, Vienna
Zentralsparkasse, Vienna
Nuclear Data, Inc.
Emtek Corporation
Springer Verlag
Fa. P. Haack, Vienna
Fa. K. Neumayer
Olympus Microscopes

LPI CONTRIBUTION 712

Compiled in 1989 by the

Lunar and Planetary Institute
3303 NASA Road 1
Houston, TX 77058-4399

The Lunar and Planetary Institute is operated by the Universities Space Research Association under Contract No. NASW-4066 with the National Aeronautics and Space Administration.

INTRODUCTION

This volume contains abstracts that have been accepted by the Program Committee for the 52nd Annual Meeting of the Meteoritical Society.

ORGANIZING COMMITTEE

Members of the Organizing Committee are Christian Koeberl (Chair; University of Vienna), Franz Brandstätter (Naturhistorisches Museum), Wolfgang Kiesl (University of Vienna), Gero Kurat (Naturhistorisches Museum), Thomas Meisel (University Vienna), and Helmut H. Weinke (University of Vienna). For the organization of the field trips the committee was assisted by G. Hoinkes (University of Graz), A. Preisinger (TU Vienna), P. Jakes, and St. Vrána (Geological Survey, Prague).

Logistics and administrative support were provided by the Projects Office of the Lunar and Planetary Institute and colleagues and students at the University of Vienna and the Naturhistorisches Museum. This abstract volume was prepared by the Publications Services staff of the Lunar and Planetary Institute.

PROGRAM COMMITTEE

Members of the Program Committee are Christian Koeberl (Chair; University of Vienna), Franz Brandstätter (Naturhistorisches Museum), Pamela Jones (Lunar and Planetary Institute, Houston), Wolfgang Kiesl (University of Vienna), Gero Kurat (Naturhistorisches Museum), and Ludolf Schultz (Max-Planck-Institut, Mainz).

STUDENT GRANTS

We gratefully acknowledge the contributions of The Barringer Crater Company, the Ministry of Science and Research, and other sponsors that made possible the student grants for the following students and recent graduates to help them attend this meeting:

S. Bajt (MPI Heidelberg, FRG)
J. D. Batchelor (University of Arkansas, Fayetteville, USA)
D. T. Britt (Brown University, Providence, USA)
W. Calvin (U.S. Geological Survey, Denver, USA)
H. C. Connolly (Rutgers University, New Brunswick, USA)
T. Dickinson (NASA Johnson Space Center, Houston, USA)
S. Engel (University of Arizona, Tucson, USA)
D. Fink (University of Pennsylvania, Philadelphia, USA)
M. Fomenkova (Space Research Institute, Moscow, USSR)
X. Gao (University of California, La Jolla, USA)
J. D. Gilmour (University of Manchester, UK)
R. E. Grimm (Southern Methodist University, Dallas, USA)
H. Haack (Geophysical Institute, Copenhagen, Denmark)
R. P. Harvey (University of Pittsburgh, Pittsburgh, USA)
C. F. Heavilon (Washington University, St. Louis, USA)
A. R. Hildebrandt (University of Arizona, Tucson, USA)
D. Iseri (University of New Mexico, Albuquerque, USA)
L. P. Keller (Arizona State University, Tempe, USA)
Kong Ping (IHEP, Academia Sinica, Beijing, China)
F. Langenhorst (University of Münster, FRG)
Y. T. Lin (MPI Heidelberg, FRG)
K. J. Mathew (PRL, Ahmedabad, India)
E. McFarlane (University of Arizona, Tucson, USA)
T. Michel (University of Bern, Switzerland)
R. H. Nichols (Washington University, St. Louis, USA)
M. C. Nolan (University of Arizona, Tucson, USA)

F. J. Stadermann (Washington University, St. Louis, USA)
M. K. Weisberg (American Museum of Natural History, New York, USA)
P. D. Yates (Open University, Milton Keynes, UK)
J. Zhang (Lehigh University, Bethlehem, USA)

GENERAL INFORMATION

Meeting Location

All the scientific sessions are held in the main building of the University of Vienna on the Ringstrasse. Two sessions will be held simultaneously in lecture rooms 1 (Kleiner Festsaal) and 2 (Hörsaal 33) on the first floor of the University (see maps in the program booklet). The registration and coffee area are located on street level at the Institute of Geochemistry (see map). [Please note that European and U.S. floor counts differ and that there is an intermediate floor between the basement (street level) floor and the first floor.] The opening ceremony (Monday, July 31, 1989, 9:00 a.m.) takes place in the Grosser Festsaal (next to Room 1, see map).

Plenary Addresses

We would like to draw your attention to the following addresses, which will be delivered during the meeting:

- **Barringer Address**, Monday, July 31, 15:30–16:00, Room 2
  Origin of Tektites by Virgil E. Barnes
  (Introduction: E. A. King)

- **Leonard Address**, Monday, July 31, 16:00–16:30, Room 1
  Problems of Origin of Asteroids and Comets by Victor S. Safronov
  (Introduction: G. W. Wetherill)

- **Invited paper**, Tuesday, August 1, 14:00–14:30, Room 1
  Twenty Years Since Apollo 11: What Have we Learned about The Moon? by S. Ross Taylor

- **Invited paper**, Tuesday, August 1, 14:30–15:00, Room 1
  Remembrances of the Lunar Receiving Laboratory by Elbert A. King

- **Invited paper**, Tuesday, August 1, 15:00–15:30, Room 1
  Thermal State of the Early Earth by Michael J. Drake

- **Invited paper**, Tuesday, August 1, 15:30–16:00, Room 1
  Allende: Landmark in Meteoritics by John A. Wood

MEETING LOGISTICS

Oral Presentations

Contributed oral presentations are limited to 10 minutes plus 5 minutes for discussion and transition to the next speaker. Plenary session papers have been allotted 20 minutes plus 10 minutes for discussion. We ask each speaker and session chairman to strictly observe these time limits.

Visual Aids

Please arrange your slides in the correct order and orientation as described in the instructions on the visual aids information sheet (additional forms available from the projectionists) and give them to the projectionists before the start of the session in which you are talking. Do not forget to number your slides. Two standard 35-mm slide projectors are available in each room. In addition, one overhead projector, which must be operated by the speaker, is available in each room.

Poster Presentations
Posters will be on display in the poster viewing area in front of Room I. To accommodate the large number of poster papers and to allow authors an opportunity to present their results, we have scheduled two special poster sessions. Posters associated with Monday and Tuesday sessions will be on display during these two days, with a dedicated poster session on Monday, July 31, 1989, 17:45–19:00. Posters associated with Wednesday through Friday sessions will be on display during these three days, with a dedicated poster session on Thursday, August 3, 1989, 12:00–13:00. We request that poster authors be present at their posters during the respective poster sessions in order to present their poster and to be available for questions.

Publication of Abstracts
Note that your one-page abstract as printed in this abstract volume may not be suitable for publication in *Meteoritics*. For publication in *Meteoritics*, abstracts must be no longer than 550 words. If you want to include figures or tables you must reduce the length of the text accordingly. More information on *Meteoritics* submission has been given in the third circular. Please fill out the abstract information form (included in the registration materials) and turn it in at the registration desk during the meeting. Note that revised abstracts must reach the *Meteoritics* office (Institute of Geophysics, University of California, Los Angeles, CA 90024, USA) not later than August 18, 1989. The abstract fee of $35 for publication of abstracts in *Meteoritics* is payable to the Treasurer of the Society.

Administrative Meetings
The Council Meeting will be held at 14:00 in the Seminar Room of the Institute of Petrology (close to the registration area; please ask for assistance at the registration desk) on Sunday, July 30, 1989.

The Nomenclature Committee meeting will be held at 12:30 in the Conference Room of the Hotel Rathauspark (just behind the University) on Monday, July 31, 1989.

The Business Meeting of the Meteoritical Society will be held from 12:00-12:30 in Room I on Tuesday, August 1, 1989. All are asked to attend.

SOCIAL EVENTS

Please note that badges and, if applicable, invitation cards are mandatory for attending the social events.

There will be a Welcome Party on Sunday, July 30, 1989, 18:30–22:30 at the Naturhistorisches Museum (Museum of Natural History) at the Ringstrasse. There will be an opportunity to visit the mineral and meteorite collections. Enter through the main entrance of the museum (see map).

An excursion and banquet will be held Wednesday, August 2, 1989, 13:30–24:00. We will leave the University by bus between 13:30 and 13:45 for a sightseeing trip to the Wachau province at the Danube in Lower Austria, ending up at the banquet place. The Leonard and Barringer medals will be presented at the banquet, and there will be musical entertainment with dancing after dinner. Buses will leave for Vienna between 23:00 and 24:00.

Upon invitation by the Mayor of Vienna, a reception will be held at the Rathaus (City Hall) on Thursday, August 3, 1989, starting at 17:00. The Rathaus is across the street from the University. The reception is followed at 20:00 by a symphonic concert (by invitation of the City of Vienna) in the Arcade Courtyard of the Rathaus. There will not be time to return to the hotels between the reception and the concert. In case of bad weather, the concert will be held in the Konzerthaus, about a 20-minute walk from the Rathaus.

A Farewell Party will be held Friday, August 4, 1989, 16:30–19:30, immediately following the afternoon sessions, at the Arcade Courtyard of the University.

LOCAL ARRANGEMENTS

Registration
The Registration Desk is located at the Institute of Geochemistry (see maps for entrance) and will be open Sunday, July 30, from 14:00 18:00, and Monday, July 31, from 8:00-17:00. No registration is possible on Sunday after 18:00. On other days the registration desk (and the Institute) will open at 8:30.

Transportation
Because the hotels are in easy walking distance from the meeting place, no transportation will be provided to and from hotels. Transportation to the airport can be arranged at the hotels.

Taxis can be found at a taxi stand on the Ringstrasse across the street from the University, or by calling one of the radio dispatch services (e.g., Tel. No. 3130, 4369, 9101).

We strongly recommend using the public transport system. Tickets are available at tourist information offices, certain tobacco shops, and Vienna Public Transit Authority offices (one is close to the University at the underground station "Schottentor"). Information material is included in the registration package.

Travel information (e.g., flight information) and assistance is available at a special desk of the Austropa/ Austrian National Travel Agency Congress Department, which is situated in the registration area. The desk will be staffed for several hours per day during the entire meeting. A schedule is posted.

Messages
A message center will be established in the registration desk area at the Institute of Geochemistry. People who need to contact attendees during the meeting should be instructed to call 43-222-4300-2020; from outside of Europe, call 43-1-4300-2020. This is the phone number of the registration desk. Alternatively, important communications may be relayed through 43-1-4300-2360 (through the Organizing Committee).

Fax transmissions can be sent to the University fax machine at 43-1-4300-2307 (marked for C. Koeberl).

Electronic mail messages can be sent to C. Koeberl at A8631DAB@AWIUNI11.BITnet.

Banks
Several banks are located across the street from the University (e.g., Creditanstalt-Bankverein, or Z - Zentralsparkasse). The usual business hours are from 8:00 15:00, except on Thursday until 17:30. Several banks are closed for lunch between 12:30 and 13:30.

Post Offices
Most post offices are open between 8:00 and 18:00, but some have extended business hours. Post offices in the vicinity of the University are at Wallnerstrasse 5-7 (Office A-1014 Vienna; extended business hours), Museumstrasse 12 (Office A-1016 Vienna), and Garnisongasse 7 (Office A-1096 Vienna). The main post office is at Fleischmarkt 19 and is open 24 hours a day. No stamps are available at the registration desk.

Restaurants
There are numerous restaurants of all price levels within a few minutes walking distance from the University. A special list of local restaurants with a location map and a general Vienna restaurant guide booklet are included with the registration materials. The famous Vienna wine taverns ("Heurige") can be found mainly in the outskirts of Vienna, e.g., near the terminal stations of streetcar lines 38, 41, 43, and D.

Guest Program
A sightseeing tour by bus (City tour "Historic Vienna") takes place on Monday, July 31, 1989, in the morning and is free for registered guests (badges and tickets are required). It starts at 9:30 a.m. (following the opening ceremony) at the University.

For a list of other guest programs available, please see the meeting calendar, the second circular, or contact the Austropa desk in the registration area. Tickets for all tours should be reserved, paid for, and picked up at least one day before the tour at the Austropa/Austrian National Travel Agency in the registration/coffee area.

Field Trips
Field trip participants have been notified by separate letters during early July. These letters included specific information and instructions. You may have received additional information with your registration material. If you did not pay the full fee for the field trip in advance, you need to pay the balance at the registration desk. Both trips start simultaneously on Sunday, August 6, 1989, at about 9:00. Pick-up places are given in the special field trip information.

Additional Information
Please consult the various brochures and maps that are included in the registration materials.

ACKNOWLEDGMENTS

The Chairman of the Organizing Committee wants to thank all sponsoring agencies for generous financial assistance, the members of the Organizing and Program Committees for their help in setting up the meeting and the program, and other colleagues and students, too many to be named individually, for technical assistance. Special thanks go to Pamela Jones (Projects Office, LPI, Houston) for patience, organizational help, personal advice, and numerous other invaluable contributions. Thanks also to Joan Shack (Publications Services Office, LPI, Houston) for skillfully handling all the abstracts and producing this abstract volume, and to Donna Jalufka Chady (Publications Services Office, LPI, Houston) for perfect artwork.

MEETING CALENDAR

Sunday, July 30

14:00-18:00: Registration at the Institute of Geochemistry, University of Vienna

18:30-22:30: Welcome Party at the Naturhistorisches Museum (Museum of Natural History), with an opportunity to visit the mineral and meteorite collections.

Monday, July 31

9:00-9:30: Opening Ceremony, Grosser Festsaal (Large Hall)

10:00-12:30: Room 1, Carbonaceous Chondrites

10:00-12:30: Room 2, Cosmogenic Nuclides and Effects

AM Guest Program: City tour "Historic Vienna." Free of charge for registered guests. Coach tour of the Ringstrasse buildings including the State Opera, the Hofburg, the Parliament, the City Hall, and the Museums. Includes visits to Belvedere Palace and Schönbrunn Palace. Starts at the University at 9:30.

14:00-17:45: Room 1, Early Solar System Processes and Planetary Bodies

14:00-18:00: Room 2, Impact Cratering and Tektites

PM Guest Program: Art Nouveau in Vienna. During this tour you will be shown some of the most beautiful buildings constructed in the Art Nouveau style. Highlight is a visit of the "Steinhof" Church, constructed by the famous architect Otto Wagner. Starts 14:30 at the University.

17:45-19:00: Poster Session I (Posters associated with Monday and Tuesday sessions). Located near Room 1

Evening Free

Tuesday, August 1

9:00-12:00: Room 1, Unique and Ordinary Chondrites

9:00-12:00: Room 2, Irons and Stony Irons

AM Guest Program: Walk through Old Vienna with visits to St. Stephen's Cathedral, Mozart's House, and St. Ruprecht's Church. Starts 9:30 at the University.

Children's Program: Visit to the Zoo of Schönbrunn (near Schönbrunn Palace) Starts 9:15 at the University

12:00-12:30: Room 1, Business Meeting, Meteoritical Society

14:00-16:00: Room 1, Plenary Session

16:30-18:15: Room 1, Meteorite Search and Antarctic Studies

16:30-18:15: Room 2, Allende and Olivines

PM Guest Program: Museum of Fine Arts (Kunsthistorisches Museum). Starts 14:30 at the Museum.

Evening Free

Wednesday, August 2

9:00-12:00: Room 1, Chondrules

9:00-12:00: Room 2, ECs, Ureilites, and Fellow Travelers

AM Guest Program: Imperial Showrooms and Treasury at the Hofburg. Starts 10:00 at the Hofburg.

13:30-24:00: Excursion and Banquet. Buses leave the University at 13:45.

23:00: First bus leaves banquet for Vienna
24:00: Last bus leaves banquet for Vienna

Thursday, August 3

9:00-12:00: Room 1, CAIs

9:00-12:00: Room 2, HEDs and Angrites

AM Guest Program: Tour of Belvedere Palace. Starts 9:30 at the University.

AM Children's Program: Tour to the Prater and ride on the Giant Ferris Wheel and the "Liliput-Bahn" (miniature train). Starts 9:15 at the University.

12:00-13:00: Poster Session II (Posters associated with Wednesday, Thursday and Friday sessions). Located near Room 1.

14:00-16:45: Room 1, Pre-Solar Grains and Processes

14:00-16:45: Room 2, Geological Boundaries and Early Earth

PM Guest Program: Kahlenberg - Klosterneuburg. Drive through "Heurigen" (Viennese wine taverns) villages to the Kahlenberg. Visit to the Abbey of the Augustinian Friars at Klosterneuburg. Starts 13:00 at the University.

16:45: Walk across the street to the Rathaus

17:00-22:00: Reception by the City of Vienna at the Rathaus, followed at 20:00 by a symphonic evening concert at the Arcade Courtyard of the Rathaus.

Friday, August 4

9:00-12:45: Room 1, Cosmic Dust and Spherules

9:00-12:45: Room 2, Noble Gases and Chronology

AM Guest Program: **(A)** Hofburg - Kapuzinergruft. Guided tour through the tombs of the emperors in the crypt of the "Kapuzinerkirche," and visit of the Augustine Church with the "Herzgruft" (tomb of the hearts). Visit the Baroque National Library / Stateroom at the Hofburg. Starts 10:00 in front of the State Opera. **(B)** Museum of Fine Arts (alternative tour)

14:00-16:30: Room 1, Isotopic Studies

14:00-16:30: Room 2, Lunar Studies

PM Guest Program: Vienna Woods - Heiligenkreuz. Drive via Lichtenstein Castle to the Vienna Woods south of the city, followed by a visit of the Cistercian Abbey at Heiligenkreuz and of the Carmelite Convent of Mayerling. Starts 13:00 at the University.

16:30-19:30: Farewell Party at the Arcade Courtyard of the University

UNIVERSITY, Street (basement) Level
(Registration, Coffee Area)

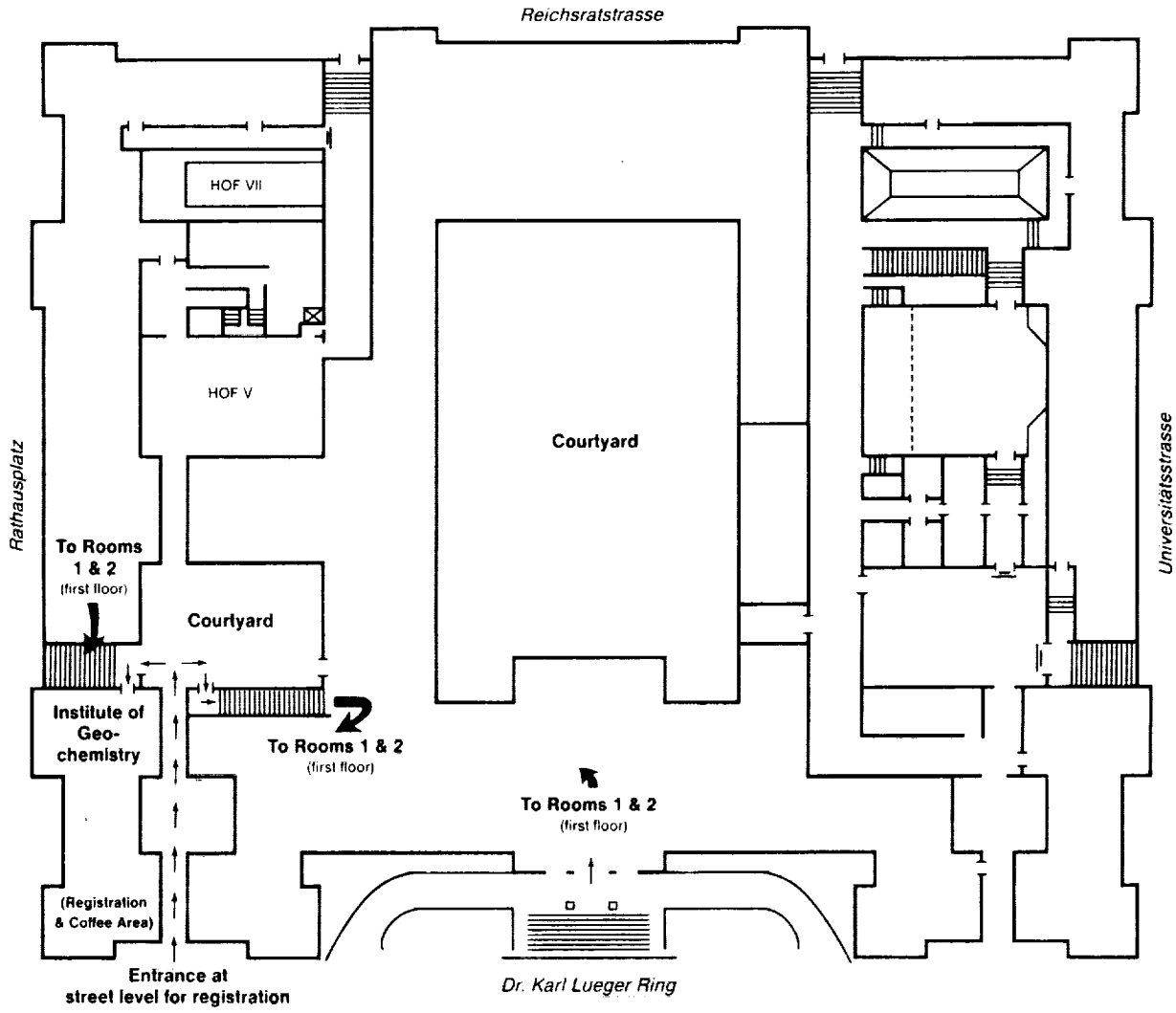

UNIVERSITY, 1st Floor
(Lecture Rooms, Poster Area)

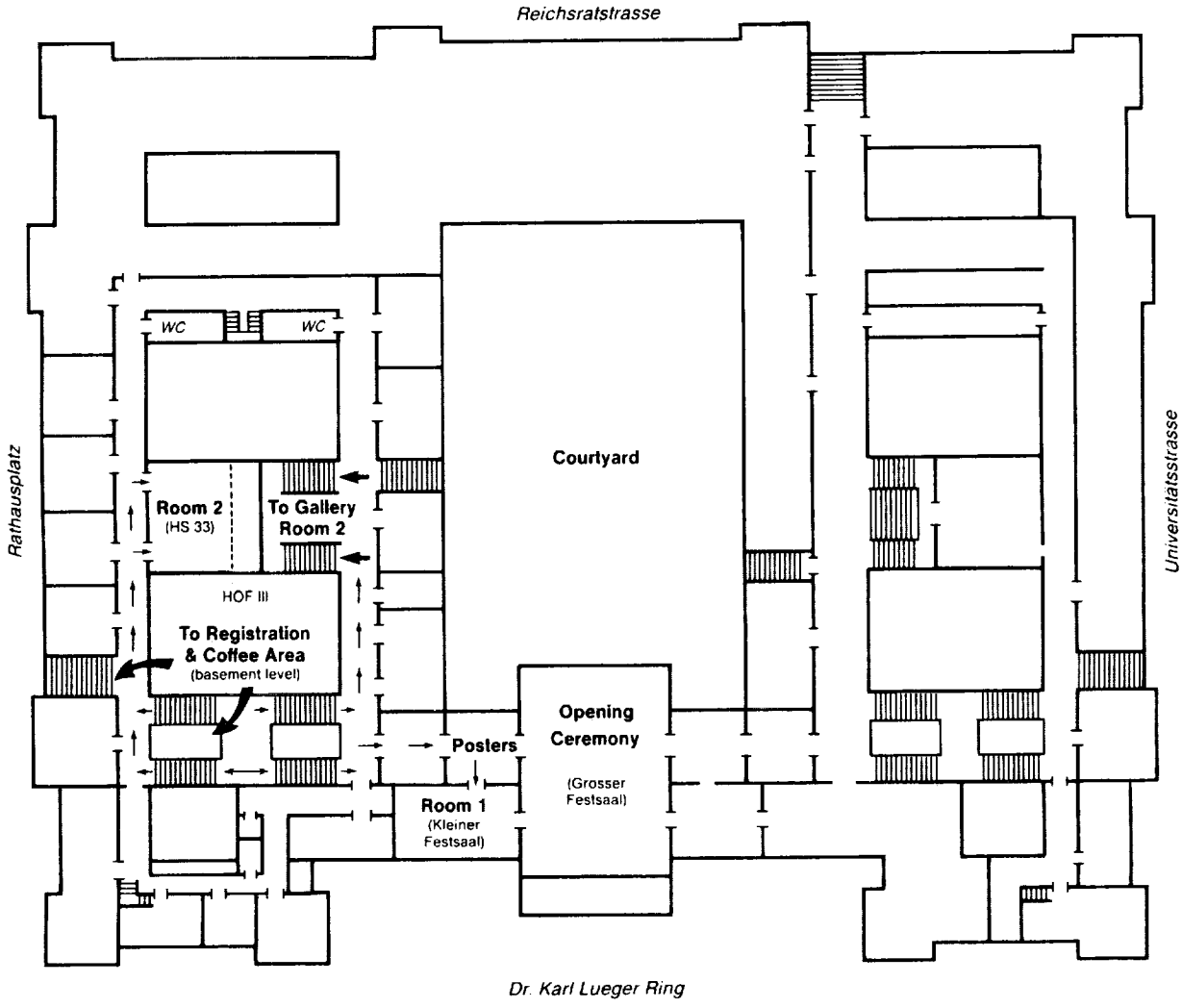

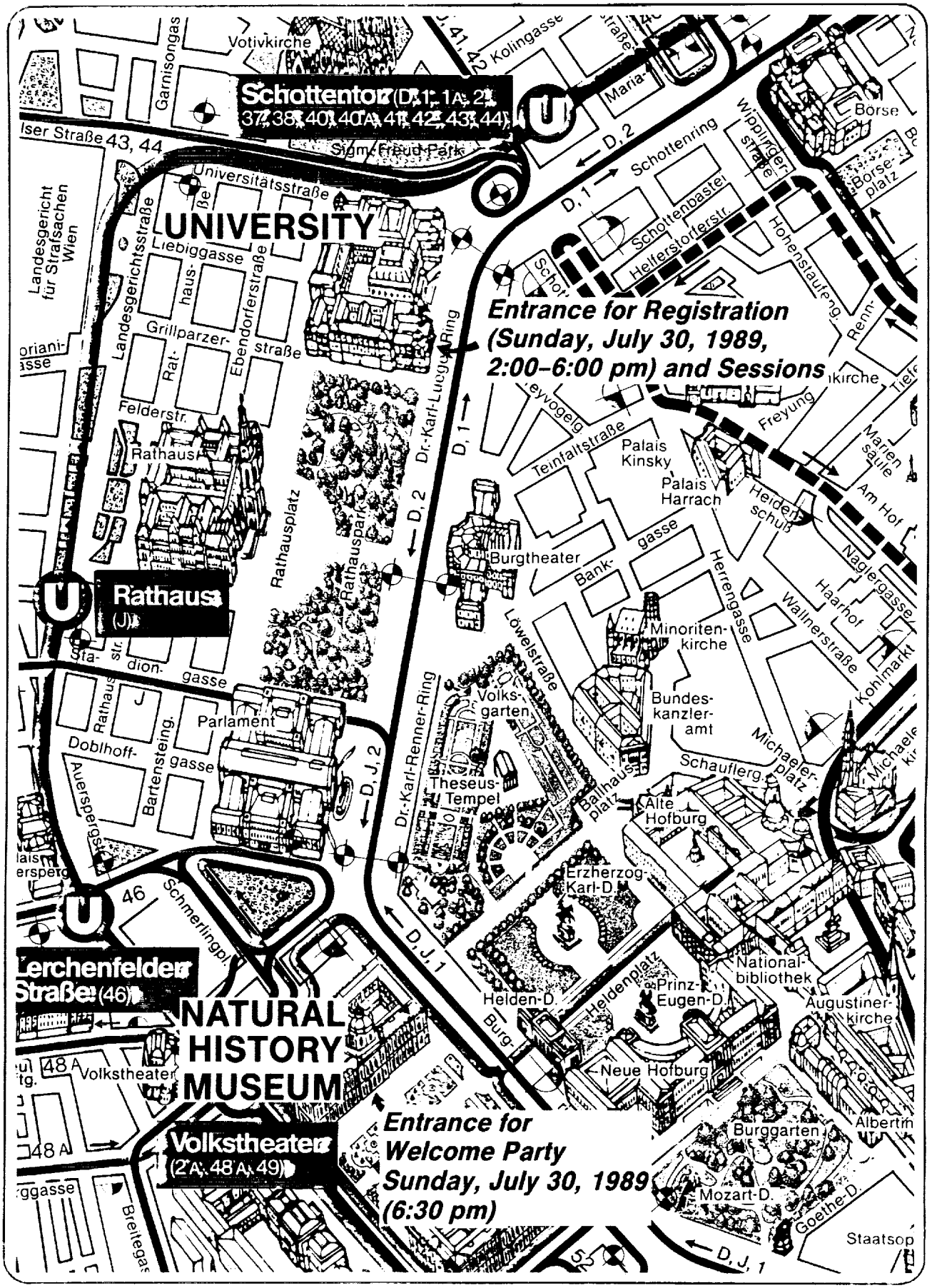

52ND ANNUAL METEORITICAL SOCIETY MEETING
July 31 - August 4, 1989
Vienna, Austria

* Indicates Speaker

Monday, July 31st

Chairman: C. Koeberl

9:00-9:30 Opening Ceremony, Grosser Festsaal (Large Hall)

9:30-10:00 COFFEE BREAK

SESSION A - CARBONACEOUS CHONDRITES

Monday a.m., Room 1 (Kleiner Festsaal)

Chairmen: H. Y. McSween
M. K. Weisberg

A-1 10:00-10:15 Paul R. L. Lipschutz M. E.*
A Modest Proposal for Carbonaceous Chondrite Classification in Light of the Antarctic Samples

A-2 10:15-10:30 Hartmetz C. P.* Gibson E. K. Jr.
In Situ Determination of Volatiles in CM2 Chondrites

A-3 10:30-10:45 Kallemeyn G. W.*
Compositional Studies of Types 4-6 Carbonaceous Chondrites

A-4 10:45-11:00 Grimm R. E.* McSween H. Y. Jr.
Water and the Thermal Evolution of Carbonaceous Chondrite Parent Bodies

A-5 11:00-11:15 Keller L. P.* Buseck P. R.
Aqueous Alteration of the Kaba CV3 Carbonaceous Chondrite

A-6 11:15-11:30 Weisberg M. K.* Prinz M. Clayton R. N. Mayeda T. K.
The Renazzo-Type CR Chondrites

A-7 11:30-11:45 Franchi I. A.* Exley R. A. Gilmour I. Pillinger C. T.
Stable Isotope and Abundance Measurements of Hydrocarbons in Murchison

A-8 11:45-12:00 Zenobi R.* Philippoz J. Buseck P. R. Zare R. N.
Organic Analysis of Individual Meteorite Inclusions by Two-Step Laser Desorption/Laser Multiphoton Ionization Mass Spectrometry

A-9 12:00-12:15 Kojima H.* Yanai K.
Origin of PCP

A-10 12:15-12:30 Scott E. R. D.* Jones R. H.
Chondrules in CO3 Chondrites Keys to Unlocking Their Nebular and Asteroidal Secrets

POSTERS - SESSION A
CARBONACEOUS CHONDRITES

A-11 Brearley A. J.
Matrix Mineralogy of the Bells CM2 Carbonaceous Chondrite and the In-Situ Observation of Titanium Oxides (Magneli Phases)

A-12 Fang H. Feng X. Chai C. Ouyang Z.
An Aluminium-Rich Pyroxene in the Ningqiang Chondrite (CV3) Refractory Inclusions

A-13 Fisenko A. V. Karpenko S. F. Semjonova L. F. Ljalikov A. V. Spiridonov V. G. Lavrukhina A.K.
143-Nd and 146-Nd in HNO_3- and $HClO_4$-Soluble Fractions of the Efremovka Carbonaceous Chondrite

A-14 Fisenko A. V. Semjonova L. F. Ljul A. Yu. Lavrukhina A. K.
HCl, HF - Insoluble Fraction of the Efremovka Carbonaceous Chondrite

A-15 Geiger T. Bischoff A.
Mineralogy of Metamorphosed Carbonaceous Chondrites

A-16 Lavrukhina A. K. Ustinov V. I. Fugzan M. M. Baryshnikova G. V. Shukolyukov Yu. A.
The Oxygen Isotopic Composition and the ^{40}Ar-^{39}Ar Age of the Kainsaz CO Chondrules

A-17 Ulyanov A. A. Kononkova N. N. Korovkin M. A.
Chemistry and Isotopic Composition of Xenoliths in Carbonaceous Chondrites

A-18 Weckwerth G.
Chemical Fractionation of Primitive Meteorites

A-19 Zolensky M. E. Mittlefehldt D. W.* Lipschutz M. E. Xiao X. Clayton R. N. Mayeda T. K. Barrett R. A.
The Composition of EET 83334: A Progress Report

Monday, July 31st

SESSION B - COSMOGENIC NUCLIDES AND EFFECTS

Monday a.m., Room 2 (Hörsaal 33)

Chairmen: P. Englert
R. C. Reedy

B-1 10:00-10:15 Nishiizumi K. Arnold J. R.* Fink D. Klein J. Middleton R. Brownlee D. E. Maurette M.
Cosmogenic Radionuclides in Individual Cosmic Particles

B-2 10:15-10:30 Fink D.* Klein J. Middleton R. Vogt S. Herzog G.
^{41}Ca in Iron Meteorites

B-3 10:30-10:45 Michel Th.* Eugster O.
Cosmic-Ray Exposure Ages of Howardites, Eucrites, and Diogenites

Burger M.* Eugster O. Krähenbühl U.
Refractory Trace Elements in Different Classes of Achondrites by RNAA and INAA and Some Noble Gas Data

B-4 10:45-11:00 Weber H. W.* Schultz L. Begemann F.
Exposure Ages of H4-Chondrite Falls

B-5 11:00-11:15 Nichols R. H. Jr.* Hohenberg C. M. Olinger C. T. Goswami J. N.
Extended Regolith Histories or an Active Early Sun: Another Piece of the Puzzle

B-6 11:15-11:30 Klein J.* Fink D. Herzog G. F. Pierazzo E. Middleton R. Vogt S.
SCR Produced ^{41}Ca in Lunar Basalt 74275

B-7 11:30-11:45 Pellas P.* Fiéni C. Perron C.
Spallation Recoil Tracks and Fission Tracks in Chondritic Merrillites

B-8 11:45-12:00 Bhandari N.* Bonino G. Castagnoli G. C.
Cosmic Ray Interactions in Meteorites and Solar Activity

B-9 12:00-12:15 Reedy R. C.* Marti K. Lavielle B.
Solar-Proton-Produced ^{81}Kr in Lunar Rocks

B-10 12:15-12:30 Mathew K. J.* Rao M. N. Michel R. Precsher K.
Xenon Isotope Production Cross-Sections from Ba-Targets by Protons in the 12 to 45 MeV Energy Range

POSTERS - SESSION B
COSMOGENIC NUCLIDES AND EFFECTS

B-11 Alexeev V. A.
Cosmogenic Radionuclides in Meteorites

B-12 Heusser G.
Doubts on Meteorites as Cosmic Ray Probes

B-13 Nishiizumi K. Kubik P. W. Sharma P. Arnold J. R.
^{129}I Depth Profiles in Cores from Jilin and the Moon

B-14 Perelygin V. P. Stetsenko S. G. Otgonsuren O. Petrova R. I. Bankova G. G.
The Results of Calibrating Meteoritic Olivine Crystals with ^{238}U Nuclei at the Bevalac Accelerator

B-15 Rajan R. S. Lugmair G. W.
Solar Flare Tracks and Neutron Capture Effects in the Carbonaceous Gas-Rich Meteorite Murchison

SESSION C - EARLY SOLAR SYSTEM PROCESSES AND PLANETARY BODIES

Monday p.m., Room 1 (Kleiner Festsaal)

Chairmen: W. Benz
W. K. Hartmann

C-1 14:00-14:15 Nolan M. C.* Greenberg R.
Stochastic Evolution of Asteroids to Produce the Ordinary Chondrites

C-2 14:15-14:30 Benz W.* Slattery W. L. Cameron A. G. W.
Tilting Uranus in a Giant Impact

C-3 14:30-14:45 Cruikshank D. P. Hartmann W. K.* Tholen D. J. Bell J. F. Brown R. H.
Basaltic Achondrites: Discovery of Source Asteroids

C-4 14:45-15:00 Calvin W. M.* Clark R. N.
Mineralogy of the Non-Ice Material on Callisto: Clues from Reflectance Modeling

C-5 15:00-15:15 Fegley B. Jr.*
Chemical Models of Outgassing and Oxidation Reactions on Chondrite Parent Bodies

C-6 15:15-15:30 Wetherill G. W.*
Cometary Cratering Rates on the Terrestrial Planets

15:30-16:00 COFFEE BREAK

C-7 16:00-16:30 Safronov V. S.*: Leonard Medal Address
Introduction: G. Wetherilll
Problems of Origin of Asteroids and Comets

C-8 16:30-16:45 Hashimoto A.* Holmberg B. B. Wood J. A.
Effects of Melting on Evaporation Kinetics

C-9 16:45-17:00 Nagahara H.* Kushiro I.
Dynamic Vaporization Experiments in the System Forsterite-Anorthite and Its Implication for the Origin of CAIs and Chondrules

C-10 17:00-17:15 Engel S.* Lewis J. S. Lunine J. I.
Is Comet Halley a Solar Nebula Condensate?

C-11 17:15-17:30 Ehlers K.* Fegley B. Jr.
Chemical Consequences of High Temperature Oxidizing Conditions in the Solar Nebula: Diagnostic Signatures and New Constraints

C-12 17:30-17:45 Makalkin A. B.* Gruzinskaya B. Dorofeyeva V.A.
Temperature Conditions in the Preplanetary Disk, Implication for Meteorites and Planets

POSTERS - SESSION C
EARLY SOLAR SYSTEM PROCESSES AND PLANETARY BODIES

C-13 Bell J. F. Lucey P. G. Gradie J. C. Granahan J. C. Tholen D. J. Piscitelli J. R. Lebofsky L. A.
Reflection Spectroscopy of Phobos and Deimos

C-14 Budka P. Z. Milillo F. F.
Gravitational Body Force as a Variable in Meteorite Formation

C-15 De Laeter J. R. Rosman K. J. R. Loss R. D.
Solar System Abundances Around the Magic Proton Tin Peak

C-16 Hartmann W. K. Tholen D. J. Meech K. J. Cruikshank D. P.
"Asteroid" 2060 Chiron: Blurring the Distinction Between Asteroids and Comets

C-17 Jones T. D. Lebofsky L. A. Lewis J. S.
Mid-IR Reflectance Spectra of Carbonaceous Chondrites: Applications to Low-Albedo Asteroids

C-18 Köhler A. V. Palme H. Geiger T. Müller K.
Condensation or Evaporation: The Origin of Moderately Volatile Elements in Chondritic Meteorites

C-19 Lang B. Grochowski T.
Graph-Theoretical Indices Probing Cosmochemical Efficacity: Cyanopolyynes as Tracers

C-20 Lebofsky L. A. Jones T. D.
The Nature of Low Albedo Asteroids from 3-Micrometer Multi-Color Photometry and Spectrophotometry

C-21 Mendybaev R. A. Kuyunko N. S. Lavrukhina A. K.
Interaction of Fe, Ni-Metal with Preplanetary Nebula Gases H_2O, H_2S, CO, CO_2): Physicochemical Aspect

C-22 Tsuchiyama A.
Condensation Experiments and Their Application to the Chemical Compositions of Chondrites

C-23 Uyeda C. Okano J. Tsuchiyama A.
Magnesium Isotope Abundances of Silicates Produced in Gas-Condensation Furnace

PRESENTED BY TITLE ONLY

C-24 Wood J. A. Hashimoto A.
Calculation of Mineral Equilibrium in the Nebula by Energy-Minimization Techniques

POSTER SESSION I

17:45-19:00 *Posters associated with Monday and Tuesday Sessions—Near Room 1*

SESSION D - IMPACT CRATERING AND TEKTITES

Monday p.m., Room 2 (Hörsaal 33)

Chairmen: B. P. Glass
D. Stöffler

D-1 14:00-14:15 Iseri D. A.* Geissman J. W. Newsom H. E. Graup G.
Paleomagnetic and Rock Magnetic Examination of the Natural Remanent Magnetization of Suevite Deposits at Ries Crater, West Germany

D-2 14:15-14:30 Grieve R.* Robertson P. Bouchard M. Orth C. Attrep M. Bottomley R.
Impact Melt Rocks from New Quebec Crater

D-3 14:30-14:45 Bishop J.* Koeberl C. Reimold W. U.
Geochemistry of the Roter Kamm Impact Crater, SWA/Namibia

D-4 14:45-15:00 Schärer U.* Deutsch A.
Rb-Sr and U-Pb Systematics in Highly Shocked Minerals: Haughton Impact Structure, Arctic Canada

Deutsch A.* Schärer U. Langenhorst F.
U-Pb Systematics in Zircons and Titanites, Shocked Experimentally up to 59.0 GPa

D-5 15:00-15:15 Masaitis V. L.*
Structural Features of Giant Astroblemes

D-6 15:15-15:30 Wasson J. T.*
Climate and Tektite Origin

D-7 15:30-16:00 Barnes V. E.*: Barringer Medal Address
Introduction: F. A. King
Origin of Tektites

16:00-16:30 COFFEE BREAK

16:30-16:45 Bouška V.*
Distribution of Moldavites and Their Stratigraphic Position

D-9 16:45-17:00 Fernandes A. Glass B. P.*
Upper Eocene Impact Ejecta from DSDP Site 612 off New Jersey

D-10 17:00-17:15 Koeberl C.* Bottomley R. J. Glass B. P. Storzer D. York D.
Geochemistry and Age of Ivory Coast Tektites

D-11 17:15-17:30 Storzer D.* Koeberl C.
Fission Track Evidence for Multiple Source Components of Zhamanshin Impactites, and New Fission Track Ages

D-12 17:30-17:45 Matthies D.* Sauerer A. Koeberl C.
Volatile Element Geochemistry of Target Rocks and Impact Glasses at the Zhamanshin Crater (USSR) and Other Impact Craters

D-13 17:45-18:00 Izokh E. P.*
Relationship Between Austral-Asian Tektite Strewn-Field and Zhamanshin Crater: Clue to the Origin of Tektites

POSTERS - SESSION D
IMPACT CRATERING AND TEKTITES

D-14 Badjukov D. D. Nazarov M. A.
Possible Constraints on Abundance of Shocked Quartz in Sedimentary Rocks

D-15 Barnes V. E. Barnes V. E. II
Comets and the Origin of Tektites

D-16 Burns C. A. Glass B. P.
Source Region for the Australasian Tektite Strewn Field

D-17 Ernstson K. Claudin F.
Pelarda Formation (Eastern Iberian Chains, NE Spain)-- Continuous Deposit of the Azuara Impact Structure

D-18 Fedosova S. P. Sazonova L. V. Feldman V. I.
Particularities of Diaplectic Transformation of Hornblende from Puchezh-Katunk Astrobleme (USSR)

D-19 Feldman V. I.
Crystallochemical Control of Diaplectical Transformation

D-20 Kapustkina I. G.
The Projectile Reconstruction by the Meteorite Matter in the Impactites

D-21 Langenhorst F.
Experimentally Shocked Plagioclase: Changes of Refractive Indices and Optic Axial Angle in the 10-30 GPa Range

D-22 Meisel T. Koeberl C. Jedlicka J.
Geochemical Studies of Muong Nong Type Indochinites and Possible Muong Nong Type Moldavites

D-23 Orlova A. O. Sazonova L. V. Feldman V. I.
Correlation Between Plagioclase Crystal Morphology and Cooling Kinetic of Boltysh Astrobleme Impact Melt (USSR)

D-24 Papagiannis M. D.
Photographs from Geostationary Satellites Indicate the Possible Existence of a Huge 300 km Impact Crater in the Bohemian Region of Czechoslovakia

D-25 Preuss E. Pohl J.
Microtektites in Muong Nong Tektites

D-26 Rondot J.
Pseudotachylite and Mylolisthenite

D-27 Sazonova L. V. Korotaeva N. N.
Chemical Diaplectic Changes of Plagioclases from Impactites (Popigai and Puchezh-Katunk Astroblemes, USSR)

D-28 Stöffler D. Avermann M. Bischoff L. Brockmeyer P. Deutsch A. Dressler B. O. Lakomy R. Müller-Mohr V.
Sudbury, Canada: Remnant of the Only Multi-Ring (?) Impact Basin on Earth

D-29 Surenian R.
Shock Metamorphism in the Koefels Structure

D-30 Vrána S.
Petrology and Chemistry of Probable Impact Melt Rocks at the Sevetin Crater

D-31 Wu S.
Impact-Produced Fluidization of Duolun Crater, China

POSTER SESSION I

18:00-19:00 *Posters associated with Monday and Tuesday Sessions – Near Room 1*

EVENING FREE

Tuesday, August 1, 1989

SESSION E - UNIQUE AND ORDINARY CHONDRITES

Tuesday a.m., Room 1 (Kleiner Festsaal)

Chairmen: K. Fredriksson
R. T. Dodd

This session is dedicated to Professor Hans Suess in recognition of his achievements in meteoritics on the occasion of his 80th birthday.

9:00-9:05 G. J. Wasserburg: Introduction of H. Suess

E-1 9:05-9:20 MacPherson G. J.* Davis A. M. Grossman J. N.
Refractory Inclusions in the Unique Chondrite ALH85085

E-2 9:20-9:35 Kimura M.* El Goresy A.
Discovery of E-Chondrite Assemblages and Silica-Bearing Objects in ALH85085: Link Between E- and C-Chondrites

E-3 9:35-9:50 Hutchison R.*
Are Chondrites Primitive? A Paper for Discussion

E-4 9:50-10:05 Wasilewski P. J.
Thermomagnetic Characterization of Meteorites

E-5 10:05-10:20 Skinner W. R.* McSween H. Y. Jr. Patchen A. D.
Bleached Chondrules and the Diagenetic Histories of Ordinary Chondrite Parent Bodies

10:20-10:45 COFFEE BREAK

E-6 10:45-11:00 McSween H. Y. Jr.* Patchen A. D.
On the Absence of Pressure Effects in Metamorphosed Ordinary Chondrites

E-7 11:00-11:15 Brearley A. J.*
Carbon-rich Aggregates in Type 3 Ordinary Chondrites: Origin and Implications for Thermal Histories

E-8 11:15-11:30 Britt D. T.* Pieters C. M.
Black Chondrite Meteorites: An Analysis of Fall Frequency and the Distribution of Petrologic Types

E-9 11:30-11:45 Graf T.* Marti K.
H-Chondrites: Exposure Ages and Thermal Events on Parent Bodies

E-10 11:45-12:00 Dodd R. T.*
H Chondrite Clusters and Streams

POSTERS - SESSION E
UNIQUE AND ORDINARY CHONDRITES

E-11 Bukovanska M. Janicke J. Brandstätter F.
Sazovice I5 and Wessely H5 Chondrites (Czechoslovakia)-Mineralogy and Classification

E-12 Chen Y. Pernicka E. Wang D. Wei H.
Composition of Three Recently Fallen Chinese Ordinary Chondrites

E-13 Danon J. Azevedo I. S. Scorzelli R. B.
Mössbauer Spectroscopy Study of the Nickel-Iron Alloys in Metal Particles of Cherokee Spring LL6 Chondrite

E-14 Grokhovsky V. I. Kirov S. M.
The Structure Peculiarities of Taenite Particles and Two Stages of Its Thermal History in Okhansk H4 Meteorite

E-15 Hartmetz C. P. Gibson E. K. Jr. Socki R. A.
Total Carbon and Sulfur Abundances in Antarctic Carbonaceous Chondrites, Ordinary Chondrites, and Eucrites

E-16 Kashkarov L. L. Kashkarova V. G.
Radiation and Thermal History for the Ordinary Chondrites Saratov L4 and Elenovka L5: Thermoluminescence Study for Chondrules

E-17 Kashkarov L. L. Korotkova N. N. Skripnik A. Ya. Lavrukhina A. Y.
Accretion of Ordinary Chondrites on Data of Track Studies

E-18 Levi-Donati G. R. Prinz M.
Petrology of Three Undescribed Hungarian Chondrites: Kisvarsany, Mike and Ofeherto

E-19 Lu J. DeHart J. M. Sears D. W. G.
Cathodoluminescence Properties of St. Mary's County, a Type 3.3 Ordinary Chondrite, Compared with Other Type 3 Ordinary Chondrites

E-20 Morse A. D. Wright I. P. Pillinger C. T.
Hydrogen in the Inman Ordinary Chondrite

E-21 Sugiura N. Hashizume K.
A Preliminary Report on Nitrogen Abundances and Isotopes in LL Chondrites

PRESENTED BY TITLE ONLY

E-22 Murty S. V. S. Goel P. S.
Unusual Distribution of N and Li in Ambapur Nagla

12:00-12:30 METEORITICAL SOCIETY BUSINESS MEETING, Room 1

12:30-14:00 LUNCH BREAK

SESSION F - IRONS AND STONY IRONS

Tuesday a.m., Room 2 (Hörsaal 33)

Chairmen: V. F. Buchwald
J. T. Wasson

This session is dedicated to the memory of Hans Voshage.

9:00-9:05 L. Schultz: In Memoriam Hans Voshage

F-1 9:05-9:20 Buchwald V. F.*
On the Corrosion of Meteorites

F-2 9:20-9:35 Plotkin H. Buchwald V. F. Clarke R. S. Jr.*
The Port Orford Meteorite Hoax

F-3 9:35-9:50 Haack H.*
Asteroid Core Crystallization by Inwards Growth

F-4 9:50-10:05 Zhang J.* Williams D. B. Goldstein J. I.
Where Is the Tetrataenite Phase in the Iron Meteorite Santa Catharina?

F-5 10:05-10:20 Niemeyer S.* Gerlach D. Russ G. P. III
Re-Os Dating of IIIAB and Silicate-Bearing Iron Meteorites

F-6 10:20-10:35 Johnson C. A.* Prinz M. Weisberg M. K.
Magnetite in Silicate Inclusions in the Bocaiuva Iron: Formation by Reaction of CO3 Chondritic Silicates and Metal

10:35-11:00 COFFEE BREAK

F-7 11:00-11:15 Köhler T.* Palme H. Brey G.
Cooling History of IAB-Silicate Inclusions and Related Chondritic Meteorites

F-8 11:15-11:30 Neal N. J.* Franchi I. A. Pillinger C. T.
Nitrogen Isotope Variation in Iron Meteorites

F-9 11:30-11:45 Collinson D. W.*
Magnetic Properties of the Estherville Mesosiderite

F-10 11:45-12:00 Monod Th.*
New Approaches to the Chinguetti Meteorite Problem

POSTERS SESSION F
IRONS AND STONY IRONS

F-11 Engström E. U.
Secondary Ion Mass Spectrometry of Cape York

F-12 Harper C. L.
Meteoritic Zircon Revisited: A New Separation from Toluca

F-13 Hassanzadeh J. Rubin A. E. Wasson J. T.
Large Metal Nodules in Mesosiderites

F-14 Ogilvie R. E. Chang J.
Orientation and Plane of Polish of Octahedrites— Method I

F-15 Ogilvie R. E.
Orientation and Plane of Polish of Octahedrites— Method II

F-16 Pedersen H. Lindgren H. Canut de Bon C.
Strewn-fields of Imilac and Vaca Muerta

F-17 Schultz L. Spettel B. Weber H. W. Höfle H. C. Buchwald V. Bremer K. Herpers U. Neubauer J. Heumann K. G.
Mt. Wegener, a New Antarctic Iron Meteorite

F-18 Vistisen L. Roy-Poulsen N. O. Clarke R. S. Jr.
Corrosion of the Santa Catharina Meteorite

12:00-12:30 METEORITICAL SOCIETY BUSINESS MEETING, Room 1

12:30-14:00 LUNCH BREAK

SESSION Fa: PLENARY

Tuesday p.m., Room 1 (Kleiner Festsaal)

Chair: U. B. Marvin

Fa-1 14:00-14:30 Taylor S. R.*
Twenty Years Since Apollo 11: What Have We Learned About the Moon?

Fa-2 14:30-15:00 King E. A.*
Remembrances of the Lunar Receiving Laboratory

Fa-3 15:00-15:30 Drake M. J.*
Thermal State of the Early Earth

Fa-4 15:30-16:00 Wood J. A.*
Allende: Landmark in Meteoritics

16:00-16:30 COFFEE BREAK

SESSION G - METEORITE SEARCH AND ANTARCTIC STUDIES

Tuesday p.m., Room 1 (Kleiner Festsaal)

Chairmen: M. M. Grady
J. O. Annexstad

G-1 16:30-16:45 Yanai K.*
Over 2,000 New Antarctic Meteorites, Recovered Near the Sør Rondane Mountains, East Antarctica

G-2 16:45-17:00 Delisle G.* Sievers J.
Meteorites, Concentration Mechanisms at the Allan Hills, Victoria Land, Antarctica

G-3 17:00-17:15 Annexstad J. O.* Schultz L.
The 1988/89 Remeasurement of the Triangulation Network at the Allan Hills Icefield, Victoria Land, Antarctica

G-4 17:15-17:30 Harvey R.
The Search for Extraterrestrial Material in Sediment from a Lake Along the Margin of the Lewis Cliff Ice Tongue, East Victoria Land, Antarctica

G-5 17:30-17:45 Velbel M. A.* Long D. T. Gooding J. L.
Meteoritic Source of Large-Ion Lithophile Elements in Terrestrial Nesquehonite from Antarctic Meteorite LEW 85320 (H5)

G-6 17:45-18:00 Mittlefehldt D. W.* Lindstrom M. M.
Weathering in Antarctic Meteorites: An INAA-SEM Study

G-7 18:00-18:15 Bevan A. W. R.* Binns R. A.
Further Meteorite Recoveries from the Nullarbor Region, Western Australia

POSTERS - SESSION G
METEORITE SEARCH AND ANTARCTIC STUDIES

G-8 Dod B. D. Urbanik R. T. Sipiera P. P.
A Study of Surface Conditions and Sediment Accumulation in Blowout Areas of Roosevelt County, New Mexico, as Evidence for Meteorite Concentration Mechanisms

G-9 Samuels S. M.
Applications of Statistics to Antarctic, Non-Antarctic Differences

G-10 Wacker J. F.
A Survey of 26-Aluminum in Antarctic Meteorites

G-11 Wlotzka F. Spettel B. Palme H. Schultz L.
Two New CM Chondrites from Antarctica: Different Mineralogy, But Same Chemistry

G-12 Yates A. M.
Weathering in Ordinary Chondrites as Evidenced by Chemical Analyses (Old and New)

SESSION H - ALLENDE AND OLIVINES

Tuesday p.m., Room 2 (Hörsaal 33)

Chairmen: H. Palme
C. E. Nehru

H-1 16:30-16:45 Kurat G.* Zinner E. Palme H.
Primitive Olivines with High Trace Element Contents in Allende-AF Aggregates

H-2 16:45-17:00 Weinbruch S.* Zinner E. K. Steele I. M. El Goresy A. Palme H.
Oxygen-Isotopic Compositions of Allende Olivines

H-3 17:00-17:15 Fredriksson K.*
Allende Chondrule vs. Whole Rock Analyses

H-4 17:15-17:30 Spettel B.* Palme H. Kurat G.
Have Different Parts of Allende Sampled Compositionally Different Chondrules?

H-5 17:30-17:45 Keck B. D.*
Boron Abundances in Bulk Fragments and Separated Phases of Allende

H-6 17:45-18:00 Klöck W.* Thomas K. L. McKay D. S. Zolensky M. E.
Comparison of Olivine Compositions in IDPs and Chondrite Matrices

H-7 18:00-18:15 Brandstätter F.* Kurat G. Franke H.
Olivines Rich in Minor Elements from Ordinary Chondrites

Wednesday, August 2, 1989

SESSION I - CHONDRULES

Wednesday a.m., Room 1 (Kleiner Festsaal)

Chairmen: R. Hutchison
D. W. G. Sears

I-1 9:00-9:15 Kring D. A. Boynton W. V.
Chemical Memory in Chondrules of Precursor Dust with Fractionated Compositions

I-2 9:15-9:30 Rubin A. E.* Wasson J. T.
An Olivine-Microchondrule-Bearing Clast in Krymka and the Origin of Microchondrules

I-3 9:30-9:45 Prinz M.* Weisberg M. K. Han R. Zolensky M. E.
Chondrules in the B7904 CI2 Chondrite

I-4 9:45-10:00 Sears D. W. G.* DeHart J. M.
Chondrule Mesostasis Cathodoluminescence and Composition: Implications for (1) Metamorphism and Aqueous Alteration in Low Type 3 Ordinary Chondrites and (2) Selection Effects in Chondrule Studies

I-5 10:00-10:15 Jones R. H.* Ullmann S.
Experimental Devitrification of Chondrule Mesostasis: Implications for the Thermal History of Chondrules

10:15-10:45 COFFEE BREAK

I-6 10:45-11:00 Pernicka E.* Bajt S. Traxel K. Kurat G. Brandstätter F.
Composition and Interrelationship of Chondrules, Lithic Fragments and Fine-grained Matrix from Chainpur (LL-3)

I-7 11:00-11:15 Connolly H. C. Jr.* Hewins R. H.
Influence of Bulk Composition on Olivine Chondrule Textures

I-8 11:15-11:30 Bajt S.* Pernicka E. Traxel K.
Trace-Element Zoning in Chondrules and Relict Forsterite Grains in Semarkona

I-9 11:30-11:45 Nehru C. E.* Prinz M. Weisberg M. K.
Chondrules in EH3 Chondrites

I-10 11:45-12:00 Lofgren G. E.*
Limits on Chondrule Formation Processes Imposed by Dynamic Crystallization Experiments

POSTERS - SESSION I
CHONDRULES

I-11 Marakushev A. A. Granovsky L. B. Zinovyeva N. G. Mitreikina O. B.
Genetic Relations Between Chondrules and Matrix in Chondrite Saratov

I-12 Wasilewski P. J.
Chondrule Magnetic Properties

12:00-13:30 LUNCH BREAK

EXCURSION AND BANQUET:

13:30-13:45 Meet outside of University to board the buses for afternoon excursion and banquet

13:45 Leave for excursion and banquet

15:00-16:00 Arrive at Melk Monastery; guided tour of the Monastery

16:15 Leave Melk, drive to Dürnstein

16:45-17:45 Unguided walk at Dürnstein

17:45 Leave Dürnstein, drive to Grafenegg

18:30 Arrive in Grafenegg, welcome drink in the courtyard of the palace

19:30 Walk over to the "Reitschule" ("Riding School Hall"), where the banquet will take place

19:45-24:00 Banquet

23:00-24:00 Buses leave for Vienna; <1 h drive

SESSION J - ECs, UREILITES, AND FELLOW TRAVELERS

Wednesday a.m., Room 2 (Hörsaal 33)

Chairmen: H. Takeda
A. El Goresy

J-1 9:00-9:15 Chen Y.* Pernicka E. Lin Y. Wang D.
REE and Some Other Trace Element Distributions of Oldhamite in Qingzhen (EH3) Chondrite

J-2 9:15-9:30 Lin Y. T.* El Goresy A. Ouyang Z. Wang D.
Evidence for Different and Complex Thermal Histories of Individual Aggregates in Some EH Chondrites

J-3 9:30-9:45 Warren P. H.* Kallemeyn G. W.
Geochemistry of Seven Ureilites: The Case of the Missing Aluminum

J-4 9:45-10:00 Jones J. H.* Goodrich C. A.
Siderophile Trace Element Partitioning in the Fe-Ni-C System: Preliminary Results with Application to Ureilite Petrogenesis

J-5 10:00-10:15 Spitz A. H.* Ruiz J. Boynton W. V.
Trace Element Analysis of Ureilite Meteorites: A Progress Report

J-6 10:15-10:30 Wheelock M. M.* Keil K. Taylor G. J.
Coarse-Grained Oldhamite in an Igneous Clast in the Norton County Aubrite

10:30-11:00 COFFEE BREAK

J-7 11:00-11:15 Ntaflos Th.* Keil K. Newsom H. E.
Petrology of Sulfides and Fe-Ni Metal from Khor Temiki Aubrite

J-8 11:15-11:30 Lodders K.* Palme H.
Europium Anomaly Produced by Sulfide Separation and Implications for the Formation of Enstatite Achondrites (Aubrites)

J-9 11:30-11:45 Heavilon C. F.* Wheelock M. Keil K. Strait M. M. Crozaz G.
New Chemical Constraints on the Origin of Aubrites

J-10 11:45-12:00 Swindle T. D.* Hohenberg C. M. Nichols R. H. Olinger C. T. Garrison D. H.
Excess Fission Xenon in Meteorites

POSTERS - SESSION J
ECs, UREILITES, AND FELLOW TRAVELERS

J-11 Nagel H.-J. Lin Y. T. El Goresy A.
Sphalerite Compositions in Meteorites: A Dilemma of an Originally Promising Cosmobarometer

12:00-13:30 LUNCH BREAK

13:30-24:00 EXCURSION AND BANQUET; SEE ROOM 1

Thursday, August 3, 1989

SESSION K - CAIs

Thursday a.m., Room 1 (Kleiner Festsaal)

Chairmen: G. J. MacPherson
E. Zinner

K-1 9:00-9:15 El Goresy A.* Zinner E. Caillet C.
Allende TE Revisited I: Petrographic Anatomy and Mineral Chemistry

K-2 9:15-9:30 Zinner E.* Virag A. Weinbruch S. El Goresy A.
Allende TE Revisited II: Magnesium and Oxygen Isotopic Stratigraphy

K-3 9:30-9:45 Sylvester P.* Ward B. Grossman L.
Chemical Compositions of Fremdlinge from an Allende Inclusion

K-4 9:45-10:00 Hashimoto A. Davis A. M.* Clayton R. N. Mayeda T. K.
Correlated Isotopic Mass Fractionation of Oxygen, Magnesium and Silicon in Forsterite Evaporation Residues

K-5 10:00-10:15 Prombo C. A.* Nyquist L. E. Wiesmann H.
Titanium Isotopes in Allende Inclusions

K-6 10:15-10:30 Völkening J. Papanastassiou D. A.*
Fe Isotope Anomalies

10:30-11:00 COFFEE BREAK

K-7 11:00-11:15 Loss R. D.* Lugmair G. W.
On the Distribution of Zinc Isotope Anomalies Within Allende CAIs

K-8 11:15-11:30 Hutcheon I. D.* Palme H. Kennedy A. Spettel B.
Trace Elements in the Fun Inclusion C-1: Absence of Ce and W Anomalies

K-9 11:30-11:45 Palme H.* Köhler A. V. Spettel B. Hutcheon I. D.
Loss of Tungsten from Refractory Metal Condensates by High-Temperature Oxidation

K-10 11:45-12:00 Ireland T. R.* Zinner E. K.
Oxygen Isotopic Compositions of Murchison Refractory Inclusions

POSTERS - SESSION K
CAIs

K-11 Kring D. A. Boynton W. V. Yarn A. Jest N.
Heat Source for the Melting of CAI in the Solar Nebula

POSTER SESSION II

12:00-13:00 *Posters associated with Wednesday, Thursday and Friday Sessions—Near Room 1*

13:00-14:00 LUNCH BREAK

SESSION L - HEDs AND ANGRITES

Thursday a.m., Room 2 (Hörsaal 33)

Chairmen: R. H. Hewins
M. Prinz

L-1 9:00-9:15 Boctor N. Z.* Carlson R. W. Tera F.
Petrology of Vitric and Basaltic Clasts from the Bouvante Eucrite

L-2 9:15-9:30 Batchelor J. D.* Sears D. W. G.
Thermoluminescence of the Eucrite Association Meteorites

L-3 9:30-9:45 Delaney J. S.* Sutton S. R.
In Situ Analyses of Trace Elements in Basaltic Achondrite Plagioclase

L-4 9:45-10:00 Newsom H. E.* Sims K. W. Gladney E. S.
W, Sb and As Depletions in the Pomozdino Eucrite and Angra Dos Reis

L-5 10:00-10:15 Reid A. M.* Buchanan P. C. Barrett R. A. Zolensky M. E.
Carbonaceous Fragments in the Bholghati Howardite

L-6 10:15-10:30 Takeda H.* Hidaka O.
Association of Diogenites and Cumulate Eucrites in Yamato 791439 and Their Genetic Link

L-7 10:30-10:45 Kozul J. M. Hewins R. H.*
Fayalite-Bearing Eucrites and the Origins of HED Magmas

10:45-11:15 COFFEE BREAK

L-8 11:15-11:30 McKay G.* Miyamoto M. Takeda H.
Cooling History of Angrite LEW 86010

L-9 11:30-11:45 Lugmair G. W.* Galer S. J. G.
Isotopic Evolution and Age of Angrite LEW 86010

L-10 11:45-12:00 Wright I. P.* Grady M. M. Pillinger C. T.
C and N in LEW 86010

POSTERS - SESSION L
HEDs AND ANGRITES

L-11 Bobe K. D. Bischoff A. Stöffler D.
Impact and Thermal Metamorphism as Fundamental Processes in the Evolution of the Stannern, Juvinas, Jonzac, Peramiho, and Millbillillie Eucrite Parent Body

L-12 Boctor N. Z. Tera F. Carlson R. W.
Petrologic and Pb Isotope Investigations of Binda Eucrite

L-13 Kashkarov L. L. Genaeva L. I.
Track Study of Pesyanoe Achondrite Radiation History

L-14 Monteiro J. F.
Preliminary Study of Chaves Howardite

L-15 Wang M.-S. Lipschutz M. E.
Volatile/Mobile Trace Elements in Angrites

PRESENTED BY TITLE ONLY

L-16 Clayton R. N. Mayeda T. K.
Oxygen Isotopic Composition of LEW 86010

POSTER SESSION II

12:00-13:00 *Posters associated with Wednesday, Thursday and Friday Sessions—Near Room 1*

13:00-14:00 LUNCH BREAK

SESSION M - PRE-SOLAR GRAINS AND PROCESSES

Thursday p.m., Room 1 (Kleiner Festsaal)

Chairmen: U. Ott
C. T. Pillinger

M-1 14:00-14:15 Amari S.* Lewis R. S.
Interstellar SiC and Its Noble Gas Components

M-2 14:15-14:30 Pillinger C. T.* Ash R. D. Arden J. W.
The Role of CVD in the Production of Interstellar Grains

M-3 14:30-14:45 Wopenka B.* Virag A. Zinner E. Amari S. Lewis R. S. Anders E.
Isotopic and Optical Properties of Large Individual SiC Crystals from the Murchison Chondrite

M-4 14:45-15:00 Huss G. R.* Lewis R. S.
Interstellar Diamonds and SiC from Type 3 Ordinary Chondrites

15:00-15:30 COFFEE BREAK

M-5 15:30-15:45 Alexander C. M. O'D.* Swan P. D. Arden J. W. Pier J. G. Walker R. M. Pillinger C. T.
Observation of SiC in Ordinary Chondrites

M-6 15:45-16:00 Lorin J. C.* Slodzian G. Dennebouy R.
Direct Measuremnt of Oxygen-Isotope Ratios in Individual Mineral Grains of Refractory Inclusions by Means of Secondary-Ion Mass Spectrometry

M-7 16:00-16:15 Amari S. Anders E.* Virag A. Zinner E.
Two Types of Interstellar Amorphous Carbon in the Murchison Meteorite

M-8 16:15-16:30 Ott U.* Kallas K. Schmitt-Strecker S. Begemann F.
Correlated Isotopic Anomalies of Xe and Ba in Murchison

M-9 16:30-16:45 Lewis R. S.* Amari S.
Multiple Stellar Sources of s-Process Krypton

POSTERS - SESSION M
PRE-SOLAR GRAINS AND PROCESSES

M-10 Ash R. D. Arden J. W. Pillinger C. T.
Light Nitrogen Associated with SiC in Cold Bokkeveld

SESSION N - GEOLOGICAL BOUNDARIES AND EARLY EARTH

Thursday p.m., Room 2 (Hörsaal 33)

Chairmen: C. R. Chapman
R. A. F. Grieve

N-1 14:00-14:15 Chapman C. R.* Morrison D. Bowell E.
Hazards from Earth-Approachers: Implications of 1989 FC's "Near Miss"

N-2 14:15-14:30 Kong P.* Chai C.
Studies on Chemical Speciation of Anomalous Iridium at Cretaceous-Tertiary Boundary

N-3 14:30-14:45 Robert F.* Rejou-Michel A. Javoy M.
A Nitrogen Isotope Anomaly at the K-T Boundary

N-4 14:45-15:00 Hildebrand A. R.* Boynton W. V.
Hg Anomalies at the K/T Boundary: Evidence for Acid Rain?

N-5 15:00-15:15 Bohor B. F.* Foord E. E. Betterton W. J.
Trace Minerals in K-T Boundary Clays

15:15-15:45 COFFEE BREAK

N-6 15:45-16:00 Nazarov M. A.* Badjukov D. D. Kolesnikov E. M. Barsukova L. D. Kolesov G. M.
Geology, Geochemistry and Geochronology of the Kara Impact Structure

N-7 16:00-16:15 Preisinger A.*
Consequences of a Giant Impact Exemplified at Cretaceous/Tertiary Boundaries in Austria

N-8 16:15-16:30 McFarlane E. A.* Drake M. J. Gąsparik T.
Mineral/Melt Partitioning and the Early Thermal History of the Earth

N-9 16:30-16:45 Jagoutz E.*
Pb-Sr-Nd Isotopic Evolution on Mars and Earth

POSTERS - SESSION N
GEOLOGICAL BOUNDARIES AND EARLY EARTH

N-10 Miura Y.
Various Formation Processes of the K-T Boundary Samples from Density Variation of Quartz Minerals

N-11 Mao X. Chai C. Ma J.
Ir/Au Ratio—Indicator of Origin of Geological Event

N-12 Musselwhite D. S. Drake M. J. Swindle T. D.
Early Outgassing of the Earth and Mars

PRESENTED BY TITLE ONLY

N-13 Zhou Y. Chai C. Mao X. Ma S. Ma J.
A Mixed Model on the Permian-Triassic Boundary Event

Friday, August 4, 1989

SESSION O - COSMIC DUST AND SPHERULES

Friday a.m., Room 1 (Kleiner Festsaal)

Chairmen: R. P. Harvey
F. Rietmeijer

O-1 9:00-9:15 Stadermann F. J.* Walker R. M. Zinner E.
Ion Microprobe Measurements of Nitrogen Isotopic Variations in Individual IDPs

O-2 9:15-9:30 Olinger C. T.* Walker R. M. Hohenberg C. M. Maurette M.
Noble Gas Measurements of Extraterrestrial Particles from Antarctic Sediment

O-3 9:30-9:45 Raisbeck G. M.* Yiou F.
Cosmic Ray Exposure Ages of Cosmic Spherules

O-4 9:45-10:00 Bradley J. P.*
Mineralogy of Nanometer-Sized Grains in Chondritic Interplanetary Dust

O-5 10:00-10:15 Thomas K. L.* Klöck W. Zolensky M. E. McKay D. S.
Bulk Chemistry and Mineral Composition of a Chondritic Interplanetary Dust Particle

O-6 10:15-10:30 Rietmeijer F. J. M.*
Reflections on Mineral Loci of Elements in Interplanetary Dust Particles: Extraterrestrial Sulfur in the Lower Stratosphere

10:30-11:00 COFFEE BREAK

O-7 11:00-11:15 Flynn G. J.* Sutton S. R.
Minor and Trace Element Abundances in Eight "Chondritic" Stratospheric Particles: Evidence for Ni Depletions

Sutton S. R.* Flynn G. J.
Density Estimates for Eleven Cosmic Dust Particles Based on Synchrotron X-ray Fluorescence Analyses

O-8 11:15-11:30 Jessberger E. K.*
Halley's Grains, Interplanetary and Interstellar Dust

O-9 11:30-11:45 Fomenkova M. N.* Evlanov E. N. Mukhin L. M. Prilutski O. F. Sagdeev R. Z. Zubkov B. V.
Chemical Composition and Properties of Comet Halley Dust Particles as Obtained During Vega Mission

O-10 11:45-12:00 Maurette M.* Bradley J. P. Jouret C. Veyssieres P.
High Resolution Electron Microscope Studies of "Cap-Prudhomme" Unmelted Micrometeorites. Preliminary Comparisons with Stratospheric IDPs and Primitive Meteorites

O-11 12:00-12:15 Yates P. D.* Wright I. P. Pillinger C. T. Hutchison R.
Isotopically Heavy Carbon in Deep-Sea Spherules

O-12 12:15-12:30 Kolesnikov E. M.*
Search for Dispersed Tunguska Meteorite Matter

O-13 12:30-12:45 Peng H.* Lui Z.
Measurement of the Annual Flux of Cosmic Dust in Deep-Sea Sediments

POSTERS - SESSION O
COSMIC DUST AND SPHERULES

O-14 Lorin J. C. Levy C.-M. Slodzian G. Dennebouy R. Bourot-Denise M.
Isotopic and Minor Elements Signature of Coarse-Grained Micrometeorites from Greenland Blue Ice Lakes

O-15 Yiou F. Raisbeck G. M.
Influx of Cosmic Spherules to the Earth During the Last 100,000 Years as Deduced From Concentrations in Antarctic Ice Cores

PRESENTED BY TITLE ONLY

O-16 Sykes M. V.
Asteroidal Sources of Dust at the Earth's Orbit

12:45-14:00 LUNCH BREAK

SESSION P - NOBLE GASES AND CHRONOLOGY

Friday a.m., Room 2 (Hörsaal 33)

Chairmen: J. H. Reynolds
T. D. Swindle

P-1 9:00-9:15 Gilmour J. D.* Hewett S. M. Lyon I. C. Stringer M. R. Turner G.
Resonance Ionization Mass Spectrometry of Meteoritic Xenon

P-2 9:15-9:30 Marti K.* Kim J. S. Lavielle B. Pellas P. Perron C.
Xenon in Chondritic Metal

P-3 9:30-9:45 Metzler K.* Bischoff A.
Formation of Accretionary Dust Mantles in the Solar Nebula as Confirmed by Noble Gas Data of CM-Chondrites

P-4 9:45-10:00 Wieler R.* Baur H. Signer P. Lewis R. S.
Planetary Noble Gases in Nitric Acid-Soluble Fractions of Carbonaceous Chondrites

P-5 10:00-10:15 Shukolyukov Yu. A.*
About the Nature of "Atmospherelike" Xenon in Meteorites

P-6 10:15-10:30 Trieloff M.* Jessberger E. K. Oehm J.
Ar-Ar Ages of LL Chondrites

P-7 10:30-10:45 Levsky K. L.* Ott U. Begemann F.
Noble Gas Components in Krymka (LL3.0)

10:45-11:15 COFFEE BREAK

P-8 11:15-11:30 Wacker J. F.*
On the Origin of Trapped Noble Gases in Meteorites

P-9 11:30-11:45 Turner G.* Burgess R. Chatzitheodoridis E.
Is There Martian Surface Water in Nakhla?

P-10 11:45-12:00 Macdougall J. D.* Lugmair G. W.
Chronology of Chemical Change in the Orgueil CI Chondrite Based on Sr Isotope Systematics

P-11 12:00-12:15 Göpel C.* Manhes G. Allègre C. J.
U-Pb Study of Phosphates in Chondrites

P-12 12:15-12:30 McConville P. Reynolds J. H.*
Cosmogenic Helium and Volatile-rich Mantle Fluid in Sierra Leone Diamonds

P-13 12:30-12:45 Nyquist L. E.* Wiesmann H. Bansal B. M. Shih C.-Y.
^{147}Sm-^{143}Nd Age and Initial $^{146}Sm/^{144}Sm$ Ratio of an Eucrite Clast in the Bholghati Howardite

POSTER SESSION P
NOBLE GASES AND CHRONOLOGY

P-14 Hagee B. Bernatowicz T. Podosek F.
Elemental Abundances of Trapped Noble Gases in Primitive Meteorites Determined by Isotope Dilution

P-15 Kaneoka I. Takaoka N. Yanai K.
^{40}Ar-^{39}Ar Age and Noble Gases of a H-Chondritic Clast in a Shocked L6-Chondrite from Antarctica

P-16 Stephan T. Jessberger E. K.
Shock-Induced Disturbance of the K-Ar System—A Comparison Between Experimental and Natural Shock

12:45-14:00 LUNCH BREAK

SESSION Q - ISOTOPIC STUDIES

Friday p.m., Room 1 (Kleiner Festsaal)

Chairmen: C. A. Prombo
J. C. Lorin

Q-1 14:00-14:15 Lundberg L. L.* Crozaz G. Zinner E. El Goresy A.
Rare Earth Elements and Calcium Isotopes in the Oldhamite of Unequilibrated Enstatite Chondrites

Q-2 14:15-14:30 Rotaru M.* Birck J. L. Allègre C. J.
Cr Isotopic Diversity in Carbonaceous Chondrites

Q-3 14:30-14:45 Gao X.* Thiemens M. H.
Multi-Isotopic Sulfur Isotope Ratios ($\delta^{33}S$, $\delta^{34}S$, $\delta^{36}S$) in Meteorites

Q-4 14:45-15:00 Hoppe P.* Geiss J. El Goresy A.
Nitrogen Isotopes in Sinoite Grains from the Yilmia Enstatite Chondrite

Q-5 15:00-15:15 Grady M. M.* Pillinger C. T.
Carbon and Nitrogen Stable Isotope Analyses of Two Lunar Meteorites

Q-6 15:15-15:30 Goel P. S.* Thakur A. N.
Variable $^{196}Hg/^{202}Hg$ Ratio in Meteorites

Q-7 15:30-15:45 Rowe M. W. Clayton R. N.* Mayeda T. K.
Oxygen Isotopes in Separated Components of CI and CM Chondrites

Mayeda T. K. Clayton R. N.* Sodonis A.
Internal Oxygen Isotope Variations in Two Unequilibrated Chondrites

Q-8 15:45-16:00 Virag A.* Zinner E. Lewis R. S. Amari S.
Oxygen Isotopic Compositions of Spinel and Corundum Grains from the Murchison Carbonaceous Chondrite

Q-9 16:00-16:15 Wen J-S. Thiemens M. H.*
A Non-Equilibrium Isotopic Fractionation: Thermal Decomposition of Ozone

Q-10 16:15-16:30 Park M. Hong S. M. Yang J.*
The Isotopic Fractionation Effects of Thermal Unimolecular Decomposition of Ozone

POSTERS - SESSION Q
ISOTOPIC STUDIES

Q-11 Gawinowski G. Birck J. L. Allègre C. J.
Zinc Isotopic Composition in Meteorites

Q-12 Lorin J. C. Slodzian G. Levy M. C-M. Kurat G. Palme H.
The Oxygen of Rusty Ornans

16:30-19:30 FAREWELL PARTY AT THE ARCADE COURTYARD OF THE UNIVERSITY

SESSION R - LUNAR STUDIES

Friday p.m., Room 2 (Hörsaal 33)

Chairmen: G. Ryder
P. W. Warren

R-1 14:00-14:15 Kerridge J. F.* Bochsler P. Geiss J.
Modelling the Evolution of N and $^{15}N/^{14}N$ in the Lunar Regolith

R-2 14:15-14:30 Stöffler D.* Jessberger E. K. Lingner S.
On Canonical Interpretations of Lunar Highland Rock Ages: Late Cataclysm or Intense Early Bombardment?

R-3 14:30-14:45 Ryder G.* Martinez R.
Zoned and Exsolved Complex Pyroxenes in Evolved Highlands Rocks from the Apennine Front

R-4 14:45-15:00 Dickinson T.* Jones J. H.
Ba and Th Partitioning Between Immiscible Silicate Melts: Further Evaluation of the Role of Silicate Liquid Immiscibility in the Petrogenesis of Lunar Granites

R-5 15:00-15:15 Marvin U. B.* Holmberg B. B. Lindstrom M. M.
Granoblastic Lunar "Dunites" Revisited

R-6 15:15-15:30 Taylor L. A.*
Lunar Regolith: Its Characterization as a Potential Resource for a Lunar Base

R-7 15:30-15:45 Shaw D. M.* Middleton T. A. Smith P. A.
Lunar Boron, Samarium, Gadolinium Correlations

R-8 15:45-16:00 Neal C. R.* Taylor L. A.
Characterization of a Pure urKREEP Signature by Identifying the "Dregs" of the Lunar Magma Ocean

R-9 16:00-16:15 Wentworth S. J.* McKay D. S. Takeda H.
Glasses in Lunar Meteorite Y82193: Comparisons to Apollo 16 Feldspathic Fragmental and Regolith Breccias

R-10 16:15-16:30 Simon S. B.*
Comparative Petrology of Lunar Regolith Breccias and Soils, and Implications for the Howardite Parent Body Regolith

POSTERS - SESSION R
LUNAR STUDIES

R-11 Ryder G.
Ages of Lunar Impact Melts and Lunar Bombardment

16:30-19:30 FAREWELL PARTY AT THE ARCADE COURTYARD OF THE UNIVERSITY

CONTENTS

Observation of SiC in ordinary chondrites.

Alexander C.M.O'D.[1], Swan P.D.[1], Arden J.W.[2], Pier J.G.[1], Walker R.M.[1] and Pillinger C.T.[3] 1) McDonnell Center for Space Sciences and Physics Department, Washington University, St Louis, MO 63130 USA. 2) Dept. of Earth Sciences, Oxford University, Oxford OX1 3PR, U.K. 3) Dept. of Earth Sciences, The Open University, Milton Keynes MK7 6AA, U.K.

SiC crystals of unusual isotopic composition have previously been found in acid residues of the CM meteorites Murray, Murchison (Bernatowicz *et al.*, 1987; Zinner *et al.*, 1987) and Cold Bokkeveld (Ash, pers. comm.). Bulk concentrations of SiC in these meteorites are approximately 4-6 ppm. SiC has yet to be identified the CV chondrite Allende and must be present at concentrations not greater than 0.02ppm. We report here the first observations of SiC in acid residues prepared from the type 3 ordinary chondrites Inman (L3.4), Tieschitz (H3.6) and Clovis (L3.9).

The residues of bulk Inman and a Tieschitz 'matrix' separate were prepared by attack with HF/HCl at room temperature followed by treatment with chromic and perchloric acid. In addition to SiC these residues contain spinel, Cδ (Ash *et al.*, 1989), hibonite, corundum, titanium oxide and zircon. Titanium oxide and zircon have been found in residues prepared by several laboratories, but further work is necessary to determine whether or not they are terrestrial contamination. The Clovis sample was treated with HF/HNO_3 at 180°C in a Teflon bomb which primarily left unidentified carbonaceous material and minor quantities of SiC.

The SiC grains in the residues of both ordinary and CM chondrites were identified by the recently described X-ray mapping technique (Swan *et al.*, 1989) at a magnification of 1600X. In the CM chondrites most of the SiC crystals have apparent sizes that lie in the range 0.2 to 2μm, although a few up to 20μm in size have been observed. In Tieschitz and Inman the size distributions are similar to the CM chondrites, except for the absence of the very large grains. However, the failure to find very large SiC grains in Inman and Tieschitz may simply be a result of the small quantities of the residues examined so far. The SiC in the Clovis residue is present in very low concentrations making statistically valid comparisons difficult at present. The concentration of SiC in the residues studied were obtained by pixel counting and recalculated to the bulk samples are estimated to be: Murchison, 4ppm; Inman, 1ppm; Tieschitz 'matrix', 0.5ppm; and Clovis, 0.06ppm.

Stepwise combustion experiments have shown that both Inman and Tieschitz contain refractory, heavy carbon bearing components (Alexander *et al.*, 1989a). In Inman the release profile and isotopic composition (+1242‰) of the heavy carbon component is essentially identical to that of the CM chondrites (Alexander *et al.*, 1989b). It seems likely, therefore, that in Inman, as in the CM chondrites, the SiC is the carrier of the heavy carbon. In Tieschitz the heavy carbon release profile is more complex, with 2 or possibly 3 components and a peak isotopic composition of only +511‰ (Alexander *et al.*, 1989b). Also, the release temperatures of the heavy carbon are significantly lower than in the CM chondrites. This appears to be true for all the ordinary chondrites in which heavy carbon has been found, with the exception of Inman (Alexander *et al.*, 1989a,b). It is possible that the carrier of heavy carbon in Tieschitz, and possibly the other ordinary chondrites, is also SiC. However, for this to be true there would have to be subtle differences, in grainsize or polytype for instance, compared to that in Inman and the CM chondrites.

Alexander *et al.*, (1989a) Lunar Planet. Sci. XX, 7-8 . Alexander *et al.*, (1989b) in prep. Ash *et al.*, (1989) Nature, submitted. Bernatowicz *et al.*, (1987) Nature 330, 728-730. Swan *et al.*, (1989) Lunar Planet. Sci. XX, 1093-1094. Zinner *et al.*, (1987) Nature 330, 730-732.

COSMOGENIC RADIONUCLIDES IN METEORITES; V.A.Alexeev. Vernadsky Institute of Geochemistry and Analytical Chemistry, USSR Academy of Sciences, Moscow, USSR.

We have analysed the distribution of the saturated contents of long-lived cosmogenic radionuclides Al-26, Be-10 and Mn-53 in Antarctic and non-Antarctic ordinary chondrites of two groups: meteorites with low ($T \leq 8$ Myr) and high ($T > 8$ Myr) radiation ages. The average saturated contents of these radionuclides in non-Antarctic H chondrites with low radiation ages were found higher of those with high radiation ages. Differences (Δ,%) between the average saturated contents (A) of radionuclides are shown in the Table, where $\Delta = 100[A(T \leq 8) - A(T > 8)]/A(T > 8)$.

Table
The values of Δ(%) in non-Antarctic chondrites.

Radio-nuclide	$T_{1/2}$ Myr	Meteorites H	L,LL
Al-26	0.72	6 ± 4	-2 ± 5
Be-10	1.5	12 ± 5	-8 ±10
Mn-53	3.7	29 ± 8	10 ±13

We can see the found effect in H chondrites depends on the half-life of radionuclide and has maximum value for Mn-53. The value of Δ can be approximated by $\Delta = 0.43 + 7.7 \times T_{1/2}$, where $T_{1/2}$ is half-life of radionuclide. This dependence is seen only for non-Antarctic H chondrites. Antarctic H chondrites showed the same trend, but small number of meteorites with known radiation ages does not allow to evaluate this effect quantitatively. Neither non-Antarctic nor Antarctic L and LL chondrites showed this regularity.

About 45% of H chondrites are placed within of the main peak of radiation ages of ~6.5 Myr. These meteorites possible belong to compact group of bodies and form the stable "meteorite swarm" in resonant orbit (Hughes, 1982). Small frequency of strong collisions of bodies in such group in the space allowed to preserve the sizes of these bodies and the accumulated quantities of radionuclides in them. On the other hand H chondrites of high radiation ages possible have been often collided and therefore decreased their sizes and contents of radionuclides. In this case we shall have the observed effect. Absence of this effect in L, LL chondrites may be stipulated by often collisions all these meteorites in the space. Alternative explanation of the data is the changes of cosmic ray intensity due to changes of orbital parameters of H chondrites.

Hughes D.W. (1982) Nature, 299, 14.

INTERSTELLAR SiC AND ITS NOBLE GAS COMPONENTS

Sachiko Amari and Roy S. Lewis

Enrico Fermi Institute, University of Chicago, Chicago, IL 60637-1433, USA.

Meteoritic SiC contains at least two exotic noble-gas components--Xe-S and Ne-E(H) (Tang and Anders, 1988a)--and since Xe-S is accompanied by more than one kind of Kr-S (Ott *et al.*, 1988), the actual number of SiC types must be greater than two. Following up indications that these SiC types differ in grain size, combustion temperature, and perhaps association with spinel, we have analyzed by stepped pyrolysis a set of narrowly sized, >90% pure, SiC fractions covering the following nominal size ranges (μm): LQB (0.05-0.15), LQC (0.15-0.3) and LQD (0.3-0.5). Three parent or sibling fractions were analyzed by stepped combustion. Kr data are reported by Lewis and Amari (1989).

Procedure. An 88-g sample of Murchison--mainly fusion-crust-rich flakes--was dissolved in HCl-HF by the usual Chicago procedure (Tang and Anders, 1988a). To permit recovery of Cα, the residue was not immediately heated with $HClO_4$ but was first treated with $K_2Cr_2O_7$ and other oxidants, and then fractionated by grain size and density (Amari *et al.*, 1989). Further fractionations were carried out on the residue after $HClO_4$ treatment, yielding separates of SiC (Lewis and Amari, 1989, Wopenka *et al.*, 1989), spinel, and corundum (Virag *et al.*, 1989).

Noble-gas trends. Combined with earlier Murchison data, these samples show several distinct trends in the size interval 0.03-10 μ: 1) Ne_E^{22} increases ~3× from LQB to LQD but then levels off, 2) Xe_S^{130} decreases ~60×, 3) Xe_S^{130}/Ne_E^{22} decreases ~100×, 4) bulk Ne^{20}/Ne^{22} decreases ~10×, 5) Kr_S^{82}/Xe^{130} rises from 0.27 to 0.67 (LQB to LQD only), 6) Murray separates have higher Xe-S/Ne-E ratios than do Murchison separates.

The first 3 trends confirm that the Xe-S carrier is finer-grained than the Ne-E carrier (Tang and Anders, 1988a), but since the coarser size separates stubbornly retained some fine particles, it seems likely that the size distributions of these two carriers overlap less than the noble-gas data indicate. We did not confirm earlier conjectures that the Ne-E carrier is occluded by, or otherwise associated with, spinel (Tang and Anders, 1988a); the observed coherence of these two phases seems to be due only to adhesiont.

The trend in Ne^{20}/Ne^{22} reflects mainly the rise in Ne_E^{22} with grain size. For example, in LQB-LQD Ne^{22} rises by 2.8× while Ne^{20} remains nearly constant. This trapped Ne^{20} (and accompanying Kr, Xe) cannot come from Cδ diamond, as it is released at higher T in stepped combustion and does not closely match the isotopic or elemental ratios of Cδ gases. Presumably these trapped gases reside in some or all of the SiC.

Presolar Exposure Age of SiC. On a 20/22 vs 21/22 plot, the data fall on a straight line with a positive x-intercept of 1.6×10^{-3}, less than the value of $(2.4\text{-}2.6) \times 10^{-3}$ for a set of coarser-grained SiC samples from Murchison and Murray (Tang and Anders, 1988b) but again indicating the presence of cosmogenic Ne_c^{21}. Only 2-7% of this Ne^{21} can come from the recent cosmic-ray irradiation of the meteorite; the rest presumably comes from a presolar cosmic-ray exposure. *The mean presolar exposure age for the 3 samples (corrected for Ne^{21} recoil losses as in Tang and Anders, 1988b) is 36 ± 10 Myr, compared to 41 ±8 Myr for the previous set (both based on the production rate of Reedy, 1989). These values are considerably shorter than the estimated 500 Myr lifetime of refractory interstellar grains, perhaps due to late outgassing of a major part of the SiC (Tang and Anders, 1988b).*

Acknowledgment. We thank Edward Anders for designing the separation procedure.

References. Amari S., Anders E., Virag A., and Zinner E. (1989) *Meteoritics*, this volume. Lewis R. S. and Amari S. (1989) *Meteoritics*, this volume. Ott U., Begemann F., Yang J., and Epstein S. (1988) *Nature* **332**, 700-702. Reedy R. C. (1989) *Lunar Planet. Sci.* **20**, 888-889. Tang M. and Anders E. (1988a) *Geochim. Cosmochim. Acta* **52**, 1235-1244. Tang M. and Anders E. (1988b) *Astrophys. J.* **335**, L31-L34. Virag A., Zinner E., Lewis R. S., and Amari S. (1989) *Meteoritics*, this volume. Wopenka B., Virag A., Zinner E., Amari S., Lewis R. S., and Anders E. (1989) *Meteoritics*, this volume.

TWO TYPES OF INTERSTELLAR AMORPHOUS CARBON IN THE MURCHISON METEORITE

Sachiko Amari*, Edward Anders*, Alois Virag† and Ernst Zinner†

*Enrico Fermi Institute, University of Chicago, Chicago, IL 60637-1433, USA;

†McDonnell Center for the Space Sciences, Washington University, St. Louis, MO 63130-4899, USA.

The carrier of Ne-E(L)--called Cα--has not been isolated thus far. But it appears to be carbonaceous, with $\rho \simeq 2.0$-2.5 g/cm^3, gas release and combustion T$\simeq$ 600° C, grain size 1-10 μm, bulk $\delta C^{13} = +340$ ‰, and abundance ~5 ppm (Anders, 1988). We have tried to isolate it from the Murchison C2 chondrite by a series of chemical treatments and density separations, and have examined the samples by noble gas and ion probe mass spectrometry and SEM (EDX). Two fractions are appreciably enriched in Ne^{22}-E(L):

LFC (1.75 - 2.2 g/cm^3; >95% C)	>1300 x 10^{-8} cc/g
LFD (2.2 - 2.5 g/cm^3; ~5% C)	500 x 10^{-8} cc/g

On the ion probe, LFC turned out to comprise at least two distinct kinds of carbon grains. The dominant Type 1 has grain size ~5 μm, essentially normal C ($\delta C^{13} = -61$ to $+23$ ‰), but heavy N of nearly constant isotopic composition ($\delta N^{15} = +295 \pm 34$ ‰) and high abundance (mean $CN^-/C^- = 0.52$). The δN^{15} value is close to the maximum values (210 and 252 ‰) of two previous samples enriched in Ne-E(L), Murray AM and AL (Tang *et al.*, 1988). The rarer Type 2 grains--4 out of 40--are only 1-2 μm in size, but have heavier C ($\delta C^{13} = +810$ to $+8000$ ‰) and much less N (~1/30) than the larger grains. The isotopic composition of this N could not yet be measured, owing to interference by nearby N-rich Type 1 grains, and since even the carbon values may be so affected, we cannot tell whether Type 2 is a single, well-defined population or a diverse mixture.

Evidently "Cα" is composite, consisting of subtypes Cα1, Cα2, etc. Thus the earlier bulk measurements must be reinterpreted. The δC^{13} value of +340 ‰ (Carr *et al.*, 1983) apparently is a mean value for the mixture, as is the Ne-E content. We do not know whether Ne-E(L) is located in Types 1, 2, or both, but since the two types seem to differ in size, it may be possible to find out.

Preliminary Raman measurements (by Brigitte Wopenka) on the most C^{13}-rich Type 2 grain did not show any lines of crystalline C (graphite, diamond), indicating that it is amorphous. A Type 1 grain disintegrated under the laser beam and could not be measured. Since crystalline graphite is stable under the beam, Type 1, too, seems to be amorphous C, perhaps a particularly labile form.

This work brings to 3 the known kinds of exotic elemental C. It is interesting that two of them, Cδ diamond and Cα1 amorphous C, have C^{12}/C^{13} ratios of 93 and 91 ±3, close to the terrestrial value of 89 but much higher than meteoritic SiC (mean = 41 ±3) or interstellar gas (43 ±4). The high solar-system ratio has been interpreted as a mixture of heavy interstellar carbon with light supernova carbon (Schramm and Olive, 1982). But now that this ratio is also showing up in diamond, amorphous C, and one type of SiC (Wopenka *et al.*, 1989), whose anomalous N, noble gases, and Si require a presolar origin, one must consider the possibility that this ratio represents a major, primary component of protosolar matter.

References. Anders E. (1988) Ch. 13.1 in: *Meteorites and the Early Solar System*, ed. J. F. Kerridge and M. S. Matthews. Tucson: Univ. Arizona Press, 927-955. Carr R. H., Wright I. P., Pillinger C. T., Lewis R. S. and Anders E. (1983) *Meteoritics* **18**, 277. Schramm D. N. and Olive K. A. (1982) *Annals N. Y. Acad. Sci.* **395**, 236-241. Tang M., Lewis R., Anders E., Grady M., Wright I. P. and Pillinger C. T. (1988) *Geochim. Cosmochim. Acta* **52**, 1221-1234. Wopenka B., Virag A., Zinner E., Amari S., Lewis R. S. and Anders E. (1989), this volume.

THE 1988/89 REMEASUREMENT OF THE TRIANGULATION NETWORK AT THE ALLAN HILLS ICEFIELD, VICTORIA LAND, ANTARCTICA. John O. Annexstad, Division of Science & Mathematics, Bemidji State University, Bemidji, MN 56601-2699 and Ludolf Schultz, Max Planck Institute fur Chemie, Mainz, FRG

The Allan Hills triangulation network, established in 1978, and remeasured in 1979(1) and 1981,(2) was revisited during the 1988/89 austral summer season. The network was measured for abalation (stake height) and horizontal and vertical ice motion using a Wild T-2 theodolite and an infrared distance meter on each leg of the system. The utilization of new instruments, the technique of braced triangulation and the 7 year lapse since the last measurements have contributed to a significant reduction in measurement errors.

Ablation measurements obtained by comparing the stake heights from the 1988/89 season to those measured in previous years show that the surface ice appears to ablate over the entire network at an average rate of 5 cm per year. There is a wide diversity in individual station rates ranging from slight accumulation to as much as 10 cm per year ablation. Station placement relative to surface topography and the prevailing wind direction appear to be significant factors.

The average rise in surface elevations along the network is rather closely balanced by the ablation of surface ice. The seven year interim between measurements results in sufficient movement of the ice field to give an elevation error that is less than the measured values. The elevation data vary from station to station showing a slight increase at some stations to deflation at others. A long term condition cannot be predicted at this time other than the suggestion that the ice in this region is probably close to a steady state condition.

Horizontal surface movement of the icefield follows almost perfectly the surface alignment of crevasse patterns. The 1978 and 1979 data, though preliminary, showed a general west to east movement of the ice sheet. A recalculation of this data and the use of the more accurate 1981 and 1988 data show that the icefield is actually moving in a more south to north direction. This is shown by Delisle and Sievers who suggest on the basis of an RES survey of ice thickness that the Allan Hills Icefield surface flow is influenced by sub-ice streams flowing from south to north.

We conclude that the RES data presented by Delisle and Sievers and the surface triangulation data from our survey are indicative of a strong S-N movement of ice with some ice dropping into the meteorite concentration zone. The majority of the ice appears to bypass the Allan Hills under the influence of the Mawson Glacier. Ice flowing in the vicinity of the Near, Middle and Far Western Icefields is probably more strongly influenced by the David Glacier outlet. We suggest that the Allan Hills Icefield is a remnant system formed by ice originating within a catchment area 100 km or less from the hills and following a path suggested by Drewry(3).

(1) Nishio, F. and Annexstad, J.O. 1980. Mem. NIPR, 17, 1-13.
(2) Schultz, L. and Annexstad, J.O. 1984. Smith. Cont. to the Earth Sciences, 26: 17-22.
(3) Drewry, D.J. 1980. Nature 287 (5779): 214-216.

LIGHT NITROGEN ASSOCIATED WITH SiC IN COLD BOKKEVELD. R.D. Ash, J.W. Arden* and C.T. Pillinger, Planetary Sciences Unit, Department of Earth Sciences, The Open University, Milton Keynes, MK7 6AA, U.K. *Department of Earth Sciences, University of Oxford, OX1 3PR, U.K.

Stepped combustion coupled with high sensitivity carbon isotope ratio measurements have proven extremely successful at detecting the presence of interstellar components in carbonaceous chondrites, since the first recognition of high $\delta^{13}C$ values by Swart *et al.* (1). Nitrogen isotope measurements made by the same technique have not enjoyed a comparable level of success although nitrogen abundance and isotope composition have been frequently made for C_δ, nanometre sized diamond (2). Thus the only measure of nitrogen isotopic abundance for the several species of silicon carbide which have been identified as interstellar grains have come from ion microprobe analysis; both high and very low $\delta^{15}N$ values have been encountered (3).

In attempting to measure the definitive $\delta^{15}N$ values for diamond in Allende, we were at pains to avoid the use of nitrogen containing reagents which might compromise the measurements (4). Thus with appropriate sample preparation techniques and high resolution stepped combustions it was possible to obtain plateau $\delta^{15}N$ values for C_δ at temperatures around 500°C (4,5); at higher temperatures there was a clear indication of lighter nitrogen (4). A sample of Cold Bokkeveld CB2C has now been prepared using similar chemical techniques to explore this observation in more detail.

The carbon release and isotope profile of Cold Bokkeveld is typical of what we have seen for other CM2 meteorites such as Murchison and Murray, with several clear cut peaks in $\delta^{13}C$ indicating a multiplicity of components. Just over 30% of the sample is carbon, the non-carbonaceous component would be attributed to spinel. The vast majority (98%) of the carbon can be accounted for by diamond which burns below 500°C. The remaining carbon has release maxima at 700°C and 1050°C; these are the temperatures generally ascribed to the components C_α and C_β. A 1.237mg sample of CB2C was taken for nitrogen isotope measurements which were made at 50°C steps over the temperature range 600 to 1300 °C; at lower temperatures the steps were either 10 or 25°C depending on the amount of nitrogen being released. Just as for carbon, 99% of the nitrogen released can be assigned to the diamond, with an average $\delta^{15}N$ value of -330.9 ± 5.8‰. Because the amounts of nitrogen from individual steps at temperatures greater than 600°C are small (<3.5 ngs) these are subject to a contribution from the system blank usually less than 1 ng/step with a $\delta^{15}N$ around 0‰. The $\delta^{15}N$ values measured above 600° range from –222 (at 600°) to –618‰ (at 1100°); applying a correction to steps where there is a peak in the amount of nitrogen released (*i.e.* 750° - 850° and 1050° to 1150°) affords $\delta^{15}N$ values of –595 and –789‰ respectively. Although the temperatures at which these $\delta^{15}N$ values are obtained are slightly greater than the peak release temperatures of C_α and C_β, the nitrogen and carbon are probably associated because an artefact in the stepped combustion analysis procedure usually means that nitrogen lags behind carbon. Assuming this interpretation is correct, then it is possible to calculate the nitrogen concentration of C_α and C_β as *ca.* 0.5 and 1.7 wt % respectively. The $\delta^{15}N$ value which we now attribute to C_β is very much in keeping with the ion probe measurements made for SiC (having a $\delta^{13}C$ of 1200 ± 200‰) which range from 0 to –900‰ with a majority between –250 and –750‰ (6). The complexity in both C and N profiles in the CB2C sample suggest that there are a number of minor interstellar components in carbonaceous chondrites still to be identified.

References:

(1) Swart, P.K., Grady, M.M., Pillinger, C.T., Lewis, R.S. and Anders, E. (1983). *Science*, **220**, 406.
(2) Ash, R.D., Grady, M.M., Wright, I.P., Pillinger, C.T., Lewis, R.S. and Anders, E. (1987). *Meteoritics*, **22**, 319.
(3) Tang, M., Anders, E. and Zinner, E. (1989). *LPSC* **XX**, 1177.
(4) Arden, J.W., Ash, R.D., Grady, M.M., Wright, I.P. and Pillinger, C.T. (1989). *LPSC* **XX**, 21.
(5) Ash, R.D., Arden, J.W., Grady, M.M., Wright, I.P. and Pillinger, C.T. (1989). *LPSC* **XX**, 26.
(6) Tang, M., Anders, E., and Zinner, E. (1988). *LPSC* **XIX**, 1177.

POSSIBLE CONSTRAINTS ON ABUNDANCE OF SHOCKED QUARTZ IN SEDIMENTARY ROCKS: D.D.Badjukov and M.A.Nazarov. Vernadsky Institute of Geochemistry and Analytical Chemistry, USSR Academy of Sciences, Moscow 117975, USSR

Quartz is abundant in the upper crust and it records prominently shock deformations. Therefore an occurrence of shocked quartz in sediments is used to identify impact events in the Earth history. When compared to the Ir record of impacts, the quartz record indicates both cometary and asteroid impacts and cannot be modified by chemical fractionation during sedimentation. However a background abundance of shocked quartz in sedimentary rocks has not been measured, and, hence, we do not know the shocked quartz content which should be considered as anomalous. For this reason we attempt to estimate the background abundance of shocked quartz.

Our calculations are based on the following assumptions. The source area for shocked quartz is the continental crust containing 20% of quartz and having a square of 1.3E18 cm^2. Production rate of impact craters (>1 km diameter) is 12E-13 km^2/y. Time of exposition of the area for impacts is taken to be 570 my because older sediments are less abundant and contain mainly components of metamorphic rocks where shocked quartz should be recrystallized.

The total mass of continental impact melt is computed to be 5.6E20 g (0.3% of the total mass of continental volcanic rocks) whereas that of crater ejecta is found to be 7.8E21 g (0.6% of the total mass of the Phanerozoic sediments). The latter is close to the mass of impacted material loaded at 10 GPa (6E21 g). The calculated total amount of shocked quartz containing planar features is 1.8E20 g. It means that the Phanerozoic sediments should contain about 0.013% of shocked quartz. However most of shocked quartz obviously resided in crater cavities and did not take part in sedimentary processes. If we adopt that only the <150 μm fraction of the ejected material was incorporated totally into the Phanerozoic sediments, and we can recognize clearly planar features in the >40 μm quartz grains, then the global mass of the 40-150 μm shocked quartz grains could be estimated to be in the range of 1.2E17-1.4E15 g. It gives an influx of these shocked quartz grains of 2E-12 - 1.7E-10 g/cm^2y into sedimentary basins. At the mean rate of sedimentation of 1.7E-3 g/cm^2y the background abundance of these shocked quartz grains should be from 1E-9 to 1E-5% that is less than 5E-4% of the total concentration of the 40-150 μm quartz grains in sedimentary rocks. The calculated mean abundance is very low and shows that the shocked quartz should be very sensitive indicator of large impact events. However it is necessary to note that local background abundances of shocked quartz should depend on environment of sedimentation and should be controlled mainly by the flux of unshocked quartz into a sedimentary basin.

TRACE-ELEMENT ZONING IN CHONDRULES AND RELICT FORSTERITE GRAINS IN SEMARKONA;

S. Bajt, E. Pernicka and **K. Traxel**, Max Planck Institut für Kernphysik, Postfach 103980, D-69 HEIDELBERG-1, West Germany

Olivine is regarded as one of the first condensation products in the solar nebula (Larimer and Anders, 1967). Some olivine aggregates may survived more or less unchanged in unequilibrated chondrites and therefore may still contain information about the conditions under which they have formed (Steele, 1986). We have measured the concentration profiles of trace elements in the concentration range of 1 - 1000 ppm in such relict forsterite grains in the unequilibrated ordinary chondrite Semarkona (LL3.0) and compared them to the spatial distribution of the same elements within chondrules. Measurements were accomplished with the Heidelberg proton microprobe using the PIXE (Proton Induced X-ray Emission) mode with a beam size of 2 x 3 μm^2 and proton energies of 2 and 3 MeV respectively. To make use of the high spatial resolution and the sensitivity of the method ultra thin sections were prepared at the Max Planck Institut für Chemie in Mainz where a new, elaborate technique was developed (Künstler, 1988).

One irregularly shaped forsterite grain of about 900 x 500 μm diameter shows enrichment of Ca, Ti, V, Cr, Mn, Fe, Ni and Zn and depletion of Mg in the outer regions of the grain. As an example concentration profiles of Mn, Ti and V are shown in **Fig.1**. Since no glass and other inclusions are present in this grain, this distribution of elements with large differences in their solid-melt distribution coefficients argues against a liquid origin. This grain probably formed by vapor condensation over a large temperature interval, since elements with condensation temperatures from ca. 1500 to 660 K are equally enriched.

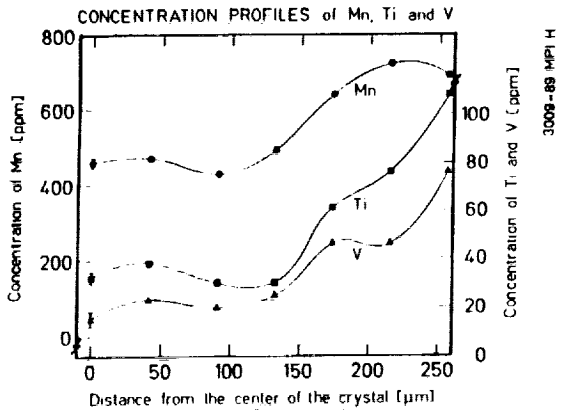

On the other hand, this grain is surrounded by grains which show signs of hydrothermal alteration (Hutchison et al., 1987). The grains are, however, not in mutual contact.

Fig.1: Compositional variation of Mn, Ti and V in a single olivine grain.

The feasibility to measure trace element profiles with spatial resolution in the μm region and sensitivities of few ppm has been demonstrated. Such measurements are therefore a further possibility to distinguish between planetary and nebular origin of chondrules and aggregates. Systematic studies are in progress.

R. Hutchison et al. (1987), Geochim. Cosmochim. Acta **51**, 1875-1882.

F. Künstler (1988), private communication.

J. W. Larimer and E. Anders (1967), Geochim. Cosmochim. Acta **31**, 1239-1270.

I. M. Steele (1986), Geochim. Cosmochim. Acta **50**, 1379-1395.

ORIGIN OF TEKTITES; V. E. Barnes, Bureau of Economic Geology, The University of Texas, Box X, University Station, Austin, TX 78713 USA

Black glassy objects collected by local residents over the years in East Texas were recognized as tektites in 1936. This discovery of the first tektite strewn-field in the western hemisphere was announced in "North American Tektites" (Barnes, 1940).

In this publication tektite literature was reviewed from the first mention of the presence of glassy objects (moldavites) along the Moldau River in central Europe (Mayer, 1788). Of the various origins suggested for these objects the prevailing view in 1940 and for some time thereafter was that they were meteorites.

However, the fact that tektites are similar in chemical composition to detrital sedimentary rocks was documented in "North American Tektites". Also that lechatelierite, identified in tektites for the first time, is fused quartz and not a segregation of silica produced during melting was demonstrated by production of lechatelierite when quartz-bearing shale was fused in a carbon arc, by identifying lechaterierite in glass produced by broken power lines that had arced through soil, and years later by fusion in a solar furnace of materials containing quartz.

Although the 1935 publication by LaCroix on the unshaped tektites of Indochina was cited in "North American Tektites", the importance of unshaped (layered) tektites was not recognized at that time. The layered deposit in Laos originally described by LaCroix could not be reached during the National Science Foundation supported tektite research in 1960. However, five other deposits, four in Thailand and one in southern Vietnam, were visited. Layered tektites and associated earth materials collected at that time were the basis for the 1962 publication by Barnes and Pitakpaivan in which it was pointed out that layered tektites had formed as puddles of melt, and that the tektites are similar in composition to associated earth materials if the changes in composition of these materials during weathering is taken into account.

The results of additional analytical work on major oxides and 26 minor elements, including REE, for both layered and splash-form tektites and associated earth materials collected in southeast Asia, were published in the Texas Journal of Science earlier this year (Barnes, 1989).

All of the tektites analyzed have REE compositions identical (within limits of analytical error) to the North American Shale Composite, confirming the origin of tektites from materials having the composition of sedimentary rocks and soils.

Layered tektites contain coesite indicating pressures in excess of 20 kilobars. They also have other properties, not present in splash-form tektites, that must be considered when speculating on the character of tne impacting bodies that produced tektites from Earth materials.

References: Barnes, V.E., 1940, U. Texas Pub. 3945, 477.
Barnes, V.E., 1989, Texas Jour. Sci., 41, 5.
Barnes, V.E. and K. Pitakpaivan, 1962, Proc. U.S. Natl. Acad. Sci., 48, 947.
LaCroix, A., 1935, Acad. Sci., Paris, C.R., 200, 2129.
Mayer, J., 1788, Böhmischen Gesell. Wiss. Abh., 1787, Prague und Dresden.

COMETS AND THE ORIGIN OF TEKTITES, Virgil E. Barnes, Bureau of Economic Geology, The University of Texas, University Station, Box X, Austin TX 78713 USA, and Virgil E. Barnes II, Physics Department, Purdue University, West Lafayette, IN 47907 USA.

Barnes (1989) postulated that layered tektites, in part coesite-bearing, found in an area 1200 km in diameter in southeast Asia, as well as the splash-form tektites found throughout the Austral-Asian tektite strewn-field, were formed by the impact of a comet arriving from the southeast. The layered tektites clearly involve melting of in situ earth materials. Present evidence is insufficient to discriminate between melting over the whole region of layered tektite occurrence or melting in several smaller areas.

What is the matter density distribution lying outside the core of a comet that would be required to produce a thickness, L, of at least one centimeter of melt over an area 1200 Km in diameter? This melt depth: (1) is chosen to be sufficient to permit flow into puddles of the thickness observed in some layered tektites, and (2) requires a melting time, from thermal diffusion, $\Delta t \simeq (L/1.4mm)^2 \simeq 50$ s, consistent with the impact time duration of a spherical coma mass distribution 1200 km in diameter, arriving at velocity v_c.

Data from the Comet Halley flyby missions indicate gas and dust releases of order $\mu_g = 20$ T/s and $\mu_d = 10$ T/s, respectively. Assuming isotropic emission at velocity v = 500 m/s, the near coma has a mass density $\rho(r) = \mu/(4\pi v r^2)$ and an areal mass density d(R) projected onto a plane normal to the comet's velocity, v_c, given by: $d(R) = \mu/(4vR) = 15/R$ (for R > core radius).

At an earth impact velocity of 42 km/s (with a possible range of 25 to 70 km/s), the areal kinetic energy density (dust + gas) of the near coma is given by:

$$D(R) = 0.5 v_c^2 d(R) = 2.2\times10^{7\pm0.5}\mu/(vR) = 1.3\times10^{9\pm0.5}/R$$

in units J/m^2, The heat energy to melt a surface layer 1 cm thick to 2500 ^oC is $D_m = 5.5\times10^7$ J/m^2. This requires $D(R) > D_m/\varepsilon_m$ where we assume an efficiency $\varepsilon_m = 0.1 - 0.01$ for delivery of coma kinetic energy to the melt. For comparison, the energy needed to compress the atmosphere to a static 20 kilobars (the minimum necessary for coesite formation) at T = 3000 ^oK is 9.2 10^9 J/m^2 (the compressed atmosphere is then 4.5 m thick).

At R = 500 km, we have $D(R) = 2.6\times10^{3\pm0.5}$ J/m^2, a factor of $2\times10^4/\varepsilon_m$ too small to accomplish the postulated surface melting. The observation that dust and gas leave comet Halley mostly in jets originating from no more than 10% of the surface area of the core is unlikely to alter this conclusion by more than a factor of ~10.

The total impact kinetic energy of a comet the mass of Halley, $E_k = 8.8\times10^{22\pm0.5}$ J is probably sufficient to melt the postulated 1200 km diameter surface area (2.8×10^{13} kg), which requires $(6\times10^{19}J)/\varepsilon_m$. However, the near coma region would have to carry a significant fraction of Halley's mass in order to fulfill the above scenario. A core capable of impacting the earth's surface and jetting melt as far as Australia also appears to be necessary. Whether other comets could have sufficient mass in the near coma is an interesting question. The parameter μ/v would need to be of order 10^6 larger than observed in the Halley flyby. The requisite parameters for a comet capable of producing the Austral-Asian tektite strewn field will be explored.

Reference: Barnes, V. E. (1989) Texas Jour. Sci., 41, 5.

THERMOLUMINESCENCE OF THE EUCRITE ASSOCIATION METEORITES; J. David Batchelor and Derek W. G. Sears, Cosmochemistry Group, Department of Chemistry and Biochemistry, University of Arkansas, Fayetteville, AR 72701 USA.

The meteorites of the eucrite-association present perhaps the most complete glimpse available of planetesimal structure and thermal his tory, as all seem to be derived from the eucrite parent body (EPB). Thermoluminescence (TL) peak shape parameters are sensitive to the thermal history of feldspathic rock (Guimon et al., 1985) and show promise of further aiding our understanding of this parent body.

Preliminary results of TL studies of eight eucrite-association meteorites are reported below. TL sensitivity trends are consistent with feldspar being the dominant phosphor. The eucrites display the highest sensitivity, the diogenites, the lowest, and the howardites lie between the two. The TL sensitivity of the howardites should prove a ready measure or the amount of eucritic material present. From previous work (Guimon et al., 1985), we know that peak temperatures of 140 C and 220 C correspond to low form and high form feldspar, respectively. Peak temperatures for the eucrites show one sample of each, while the peaks of diogenites are too small to make accurate structural assessments from. All the howardites show a low form peak, although Bholghati also shows a high form peak, indicating either clasts of different thermal histories or intermediate material. The mesosiderites show low form peaks, consistent with a long period of annealing below 500 C. Further TL studies of eucrite-association meteorites are underway.

Sample	TL Sensitivity*	Peak T (C)	Peak Width (C)
Eucrites			
Lew85303,86	554 +/- 83	209 +/- 15	188 +/- 3.5
EET79004,102	685 +/- 150	140 +/- 8	151 +/- 14
Diogenites			
ALHA84001,31	0.80 +/- 0.60	185 +/- 20	180 +/- 24
EETA79002,84	0.60 +/- 0.29	185 +/- 25	180 +/- 30
Mesosiderites			
EET87500,11	22.3 +/- 1.7	131 +/- 5.0	129 +/- 11.7
QUE86900,27	52.5 +/- 2.7	82.9 +/- 10.1	80.0 +/- 16.1
Howardites			
EET87503,3	588 +/- 150	133 +/- 15	145 +/- 14
Bholghati,28#	229 +/- 3.8	141 +/- 7	-
		220 +/- 18	-
Bholghati,29#	254 +/- 4.4	142 +/- 7.1	-
		213 +/- 19	-

* Dhajala = 1000

\# Uncertainties are for repeated measurements of a single aliquot.

This research is supported by NASA grant NAG 9-81. References:

Guimon R. K. et al. (1985) GCA 49, 1515-1524.

REFLECTION SPECTROSCOPY OF PHOBOS AND DEIMOS

Jeffrey F. Bell, P. G. Lucey, J. C. Gradie, J. C. Granahan, D. J. Tholen, J. R. Piscitelli (University of Hawaii), and L. A. Lebofsky (University of Arizona)

An intensive program of telescopic studies of the Mars satellites was carried out during the extremely favorable opposition in September-October 1988 at the University of Hawaii, using the facilities of the Mauna Kea Observatory. Special equipment for blocking the intense scattered light from Mars was employed to obtain spectra in the 0.3-1.1μm region for both Phobos and Deimos; IR data in the 1.2-3.2μm region was obtained for Deimos only.

Spectral data in the visible region indicate that both satellites have spectra very similar to C-type asteroids, as suggested by earlier data. There is a slight but significant difference between Phobos and Deimos in the shape of the ultraviolet absorption feature. This difference is well within the range seen in the Themis asteroid family, a group of C-class asteroids on similar orbits which are thought to represent fragments from a shattered parent body. The close spectral similarity of the satellites suggest that they are fragments of a single carbonaceous asteroid captured by Mars in the distant past. Smaller fragments could be responsible for the many oblique impact craters on Mars. The IR spectrum of Deimos indicates a red reflectance curve in the 1.2-2.2μm region. This is typical of the D-class asteroids rather than the C-class objects. Comparing the Deimos data with the existing asteroid data bases, we find that this unusual combination of spectral traits most closely resembles the P-class asteroid 65 Cybele, which is located at 3.4 AU from the sun in the outer reaches of the asteroid belt. P-class asteroids are most common just inside the gap between the main asteroid belt and the Trojan asteroids, suggesting that the Phobos/Deimos parent body was delivered to Mars during the cleaning out of this region.

We also attempted to directly detect water in Deimos by means of the bound-water band at 3μm, which has been observed in many dark asteroids. Our results demonstrate that this band is absent or extremely weak in Deimos (0-5% relative depth, much less than in CI or CM meteorites and comparable to the "driest" C-type asteroids). This anhydrous composition is consistent with the overall resemblance of the spectrum to that of Cybele, which has been shown to lack the hydrated-silicate band.

These results imply that Phobos and Deimos are captured asteroids from the outer asteroid belt. Several other satellites of Jupiter and Saturn also appear to be captured dark "C-class" asteroids. However, these objects are in distant, eccentric orbits of random inclinations. It is much more difficult to account for the Mars satellites in this way, since they are in close, circular orbits in the plane of Mars' equator.

TILTING URANUS IN A GIANT IMPACT; W. Benz †, W. L. Slattery ‡, and A. G. W. Cameron †, † Harvard-Smithsonian Center for Astrophysics, Cambridge, Ma 02138, USA, ‡ Los Alamos National Laboratory, Los Alamos, N.M. 87545, USA.

The large obliquity (98°) of Uranus has been discussed previously in terms of a giant collision between the planet and an object of about 1/10 its mass (Safronov 1969; Safronov and Zvyagina 1969; Harris and Ward 1982) This hypothesis has become especially attractive since giant impacts are now thought to be quite common in the early solar system (Wetherhill 1985) with some leaving signatures observable today. The origin of the Earth's Moon has been shown to be a likely outcome of a grazing collision (Benz *et al.* 1986,1987,1988), whereas the unusually high density of Mercury can be understood in terms of a more central and destructive impact (Benz *et al.* 1988). Despite being attractive and indeed very plausible, such a scenario for tilting Uranus needs to be carefully investigated. As a first step in this direction, we present in this paper results from three dimensional numerical simulations of such an event. These preliminary calculations are essentially intended to give a flavor of the dynamics of the impact considered.

The simulations made were done using our 3D Smooth Particle Hydrodynamics code (see references above) modified to include a variable smoothing length (Benz 1989). We are currently using 5000–6000 particles to model the planet and the impactor. The detailed internal structure and composition of Uranus at the time of the impact is largely unknown. If the impact occurred early in solar system history, Uranus was probably a vigorously convecting planet getting rid of its heat of accumulation. Given this assumption, Uranus was modeled as having an iron and rocky core surrounded by a mantle and atmosphere of water, and the hydrogen and helium component was ignored for these first exploratory calculations. These three major components were assumed to have the same mass ratios that they had in the solar nebula. The impactor was assumed to have a similar structure. To model the properties of these different materials we used the Ree equation of state for the water (Ree 1976), whereas for the iron and rocks (dunite) we used the equation of state from Benz *et al.* (1989). We are engaging in a program in which we will vary the mass ratio between Uranus and the impactor as well as the angular momentum and the relative velocity at infinity. Preliminary results will be presented and discussed.

Benz, W., 1989, in *Numerical Modeling of Stellar Pulsation: Problems and Prospects*, Ed. J. R. Buchler, (Dordrecht: Kluwer Academic Publishers).

Benz, W., Slattery, W. L., and Cameron, A. G. W., 1986, *Icarus*, **66**, 515.

Benz, W., Slattery, W. L., and Cameron, A. G. W., 1987, *Icarus*, **71**, 30.

Benz, W., Slattery, W. L., and Cameron, A. G. W., 1988, *Icarus*, **74**, 516.

Benz, W., Cameron, A. G. W., and Melosh, H. J., 1989, *Icarus*, in press

Harris, A. W., and Ward, W. R., 1982, *Ann. Rev. Earth and Plan. Sci.*, **12**, 61.

Ree, F., 1976, UCRL-52190, Lawrence Livermore Laboratory, Livermore, CA.

Safronov, V. S., 1969, in *Evolution of the Protoplanetary Cloud and Formation of the Earth and Planets*, Nauka Transl., Moscow. Israel Program for Scientific Translations, 1972, NASA TTF-67.

Safronov, V. S., and Zvyagina, E. V., 1969, *Icarus*, **10**, 109.

Wetherhill, G. W., 1985, *Science*, **228**, 877.

FURTHER METEORITE RECOVERIES FROM THE NULLARBOR REGION, WESTERN AUSTRALIA; A.W.R. Bevan, Department of Earth and Planetary Sciences, Western Australian Museum, Perth, WA 6000; R.A. Binns, Division of Exploration Geoscience, CSIRO, North Ryde, NSW 2113, Australia.

Large numbers of meteorites continue to be recovered from the Nullarbor Region in Western Australia. During the 1988 field season 1162 specimens were collected and accessioned into the collection at the Western Australian Museum. The bulk of the material was recovered from the strewnfields of the Camel Donga eucrite and Mundrabilla iron meteorite showers [Cleverly et al., 1986; Bevan and Binns, 1989a]. However, 71 specimens of ordinary chondrites were also collected.

To deal with the large number of new recoveries from the Nullarbor, a new system of nomenclature has been devised [Bevan and Binns, 1989a]. The system, recently approved by the Nomenclature Committee of the Meteoritical Society, currently defines a grid of 47 named areas in the Nullarbor Region. New meteorites take the name of the area in which they are found and a three digit number (e.g., Deakin 001). Further to 34 new meteorites from the Mundrabilla, Forrest, Reid and Deakin areas reported by Bevan and Binns (1989b), we have studied new recoveries from five additional named areas (Loongana, Nurina, Sleeper Camp, Camel Donga and Nyanga Lake). The recovery, classification and pairing of 32 chondritic meteorites is reported.

The new recoveries bring the total number of distinct and documented meteorites from the Nullarbor Region to 100. Preliminary statistics on the total population of Nullarbor meteorites indicate that the number of irons is below that predicted by their present day fall frequency, and that there is an unusually high percentage of rare types of stony meteorites.

BEVAN A.W.R. AND BINNS R.A. (1989a) *Meteoritics* **24**, (in press).
BEVAN A.W.R. AND BINNS R.A. (1989b) *Meteoritics* **24**, (in press).
CLEVERLY W.H., JAROSEWICH E. AND MASON B. (1986) *Meteoritics* **21**, 263-269.

COSMIC RAY INTERACTIONS IN METEORITES AND SOLAR ACTIVITY; N.Bhandari[1], G.Bonino[2] and G.Cini Castagnoli[2], 1. Physical Research Laboratory, Ahmedabad, India., 2. Istituto di Cosmogeofisica, Corso Fiume 4, Torino, Italy.

Activity levels of about 12 radionuclides ranging in half life from 16 day ^{48}V to 0.73Ma ^{26}Al have been measured in several chondrites which fell during the past two Solar cycles (Evans et al., 1982, Bhandari et al., 1989). Of these radioisotopes, three groups are useful in understanding the variation of GCR flux in the interplanetary space, which primarily occurs as a result of modulation due to solar activity. The first group consists of isotope pairs such as ^{22}Na and ^{26}Al which are produced in similar nuclear reactions in chondrites. Their ratio ie. $^{22}Na/^{26}Al$ is therefore nearly independent of the size and shape of the meteorite and shielding depth except near the surface, where solar flare effects dominate. This ratio depends slighly upon composition of the meteorite which is well understood. The residual variation, which is very prominent is due to short term (years) to long term (million years) variation of GCR flux. Comparison of the observed ratio in different meteorites and calculated ratio (Bhandari, 1981) shows a general agreement with 11 year solar cycle (Evans et al, 1982). A few cases of disagreement eg. Malakal, Innisfree and Dhajala stand out which are not due to the meteorite composition and may be related to meteorite orbits. The second group of radionuclides which are produced predominantly in spallation of iron are ^{52}Mn, ^{48}V, ^{51}Cr, ^{46}Sc and ^{54}Mn. Contributions of other target elements in these cases is small. Their relative production depends on variation of GCR flux over days to months as also on the shielding depth and size of the meteorite. Large variations in activities of these radionuclides have been observed for different chondrites. Production rates of these isotopes can not be predicted with desired accuracy at present. When better models are available, and GCR flux in the interplanetary space as a function of location and time is known, these activities can be useful in understanding orbital parameters of meteorites. The third group consists of isotopes with half life in $10\text{-}10^3$ yr range such as ^{44}Ti and ^{39}Ar. These isotopes can be useful in understanding long term cyclicity in solar activity, if it exists. The data available so far are not precise enough to ascertain long term (100 yr) periodicity of solar activity. New measurements of ^{44}Ti in Torino and other meteorites which fell during this century will be presented.

References:

Bhandari N. (1981) Proc. Ind. Acad. Sci. 90, 359-382.
Bhandari N., Bonino G., Callegari E., Cini Castagnoli G. and Queirazza G. (1989) Meteoritics 24 (in press).
Evans J.C., Reeves, J.H., Rancitelli L.A. and Bogard D.D. (1982) J.Geophys. Res. 87, 5571-5591.

GEOCHEMISTRY OF THE ROTER KAMM IMPACT CRATER, SWA/NAMIBIA.
J. Bishop[1], C. Koeberl[1,2], and W.U. Reimold[3]. [1]*Institute of Geochemistry, University of Vienna, A-1010 Vienna, Austria.* [2]*Lunar and Planetary Institute, 3303 NASA Road One, Houston, TX 77058, USA.* [3]*Schonland Research Centre, University of the Witwatersrand, P.O. Wits, Johannesburg 2050, South Africa.*

The Roter Kamm crater is located at 27° 46' S and 16° 18' E in the southern Namib Desert in SWA/Namibia. Based on morphological and geophysical studies it was suggested that this crater is an impact structure [1], which was recently confirmed by the discovery of impact breccias containing shock metamorphosed clasts [e.g., 2]. The crater has a diameter of about 2.5 km, a narrow elevated rim, and a high degree of circularity. The geology of the crater has recently been described by [2]. The impact took place in Precambrian granitic-granodioritic orthogneisses of the 1200-900 Ma old Namaqualand Metamorphic Complex that were probably overlain by Gariep metasediments (arcose/marble/graphitic schist). Arcose remnants on the rim and amphibolite xenoliths in the orthogneisses as well as quartz veins and quartz or quartz-feldspar-pegmatite intrusions are common lithologies. Allochthonous pegmatite and impact breccias are found along the crater rim. Pegmatites were probably the second most common lithology in the target area. Pseudotachylite is found along the crater rim associated with gneiss or pegmatite, or as allochthonous fragments. A large number of often bomb-shaped impact melt breccias have been found along the northern part of the rim (2), together with unusual quartz pebbles which may show signs of post-impact hydrothermal activity (3). Graphitic schist was also found in the form of small fragments on the crater rim and may have been part of the surface lithology at the time of the impact (2). The crater floor is now covered with aeolian sand deposits and large shifting sand dunes. Shock effects (planar elements and diaplectic glasses) have been discovered in quartzitic clasts in impact melt breccias. The structure of the impact melts is mostly finely crystalline (sometimes due to devitrification, otherwise because the precusor rocks was only partly melted). For a geochemical study of the target rocks and the impactites we analyzed more than 20 samples (including pseudotachylite, impact breccias, and clasts within melt breccias) for major and trace elements. We were able to determine about 40 trace elements by neutron activation analysis. Further data were provided by [2]. The target rocks in the crater area show a wide variation in major and trace element compositions. The results obtained for impact melt breccias and pseudotachylite show similar large variations in chemistry between individual samples. Gneisses, the major basement lithology, have not been a major source for most of the melt breccias. Most pseudotachylite samples could have formed from one source rock (e.g., gneissic basement, or pegmatite), others show signs of mixing. Mixing calculations show that quartz-pegmatite and quartz-feldspar pegmatites have been the main source for most melt breccias, with admixtures of schist, granite, and mafic-ultramafic components. For some melt breccias graphitic schist was a major precursor material. This is evident not only from major element analyses, but also from the rare earth element patterns. Basement rocks have typical granitic REE patterns. The pegmatite samples are similar, but in most cases have lower overall abundances because of the higher quartz content. The volatile trace elements (with the possible exception of the halogens) do not show any prominent depletion that may be assigned to impact vaporization. So far we have not been able to identify any extraterrestrial signature (e.g., Ir enrichment) in the melt breccias.

References: [1] Fudali R.F., Meteoritics **8** (1973) 245-257. [2] Reimold W.U., and Miller R.McG., Proc. 19th LPSC (1989) 711-732. [3] Koeberl C., Fredriksson K., Götzinger M., and Reimold W.U., subm. to GCA (1989).

IMPACT AND THERMAL METAMORPHISM AS FUNDAMENTAL PROCESSES IN THE EVOLUTION OF THE STANNERN, JUVINAS, JONZAC, PERAMIHO, AND MILLBILLILLIE EUCRITE PARENT BODY. Bobe K.D., Bischoff A. and Stöffler D., Institut für Planetologie, Wilhelm-Klemm-Str. 10, 4400 Münster, F.R.G.

Although the achondrites Stannern, Juvinas, Jonzac, Peramiho and Millbillillie have been classified as ordinary basaltic eucrites (1) they are texturally quite variable. The aim of this study is to identify and characterize the processes which caused episodes of brecciation and metamorphism in the evolutionary history of these meteorites. Four different processes are discernable (phase I-IV).

The primary igneous textures of these eucrites vary considerably with respect to the grain size of the main constituents and the width of exsolution lamellae in pigeonite. Therefore a wide range of cooling rates must be invoked for phase I: Crystallization from basaltic liquids. The fine-grained texture of Millbillillie can be explained by the crystallization of a magma that cooled rapidly near the surface of the parent body. Peramiho, on the other hand, can be characterized by a very coarse-grained texture with thick augite exsolution lamellae in (inverted) pigeonite. This eucrite crystallized in a deeper region of the parent body where slow cooling was possible. The textures of Stannern, Juvinas and Jonzac indicate intermediate cooling rates.

The crystallization of the magma (phase I) was followed by at least three phases (II-IV) that altered the primary igneous texture due to impact and thermal metamorphism. Based on textural observations the following processes can be distinguished. Phase II: The brecciation of the primary basaltic rocks produced either monolithological fragmental breccias or in-situ fragmented cataclastic rocks (monomict breccias) (2). Phase III: The episode of recrystallization resulted in the formation of rock units with granoblastic textures. This occurred in two steps of increasing intensity: (a) intergranular recrystallization affecting fine-grained clastic material between large relict grains and (b) intragranular recrystallization of relict grains. In the eucrite Juvinas reheating above the solidus (localized "partial" melting) took place as indicated by the presence of fine-grained subophitic textures between relict grains. Phase IV: Following recrystallization and cooling impact metamorphism again has caused fragmentation as indicated by the presence of fine-grained clastic matrix in some of these eucrites.

The described phases II-IV of impact and thermal metamorphism acted on the five eucrites analyzed in this study with variable intensity. Stannern suffered phase II-brecciation (3) which includes the formation of pseudotachylite-like veins and fine-grained rock units. The rock recrystallized due to an annealing episode (phase III) (4). Jonzac suffered in-situ (monomict) brecciation (phase II), recrystallization causing textures with fine-grained close to coarse-grained granoblastic rock units (phase III) and a late brecciation event (clastic matrix, phase IV). Millbillillie consists of two dominant rock units: areas with a fine-grained subophitic, basaltic texture, in which the interstitial pyroxene recrystallized in a fine-grained granoblastic texture, coexist with granulitic breccia units indicating an episode of recrystallization (phase III) after the formation of the fragmental rock units (phase II). Granoblastic recrystallized areas are almost missing in Peramiho. The most effective process was a shock effect, causing internal fracturing of the rock without displacement of its components (phase IV). Juvinas contains large fragments consisting of primary relicts and melt pools embedded in a clastic fine-grained matrix. After the thermal annealing that caused partial melting (phase III) Juvinas was shocked again as indicated by the severe fragmentation (phase IV).

References: (1) Basaltic Volcanism Study Project (1981) Basaltic Volcanism on the Terrestrial Planets, Pergamon Press, New York, 1286 pp. (2) Stöffler D. et al. (1979) Proc. Lunar Planet. Sci. Conf. 10th, 639-675. (3) Engelhardt W.v. (1963) Beitr. Mineral. Petrogr., 9, 65-94. (4) Hervig R. et al. (1986) Meteoritics, 21, 395-396.

PETROLOGY OF VITRIC AND BASALTIC CLASTS FROM THE BOUVANTE EUCRITE; N.Z. Boctor, R.W. Carlson, and F. Tera, Department of Terrestrial Magnetism, Carnegie Institution of Washington, Washington, D.C. 20015.

The Bouvante basaltic achondrite was classified as a monomict recrystallized eucrite that underwent brecciation rather than deformation (1), and as a dimict breccia that sampled material from two distinct but possibly related magma types (2). Petrographic and mineralogical investigations of clasts from the Bouvante eucrite revealed the presence of three distinct types, two of which have not been previously reported.

a: Vitric clasts (0.5 to > 1 cm) composed of mafic glass with rare fragments of plagioclase (An_{80-85}). The glass is compositionally heterogeneous (in wt%, FeO 15 to 25, MgO 8.6 to 9.7, CaO 9.5 to 16.8) within individual clasts. The average FeO content of the glass (19.7 wt%) is higher than that reported for the bouvante host (15.1 wt%) (3). The bulk chemical composition of the glass is similar to that reported for monomict eucrites (4). The Bouvante glass, however, is somewhat depleted in Al_2O_3 (9.6 wt%) and enriched in TiO_2 (1.34 wt%) relative to monomict eucrites (in wt%, 11.8–12.9 Al_2O_3, TiO_2 0.56 to 0.96). The Na/(Na + K) ratio of the glass (0.73 to 0.81) is lower than that of most eucrites (> 0.90). The vitric clasts display some similarities to the glassy clasts reported in polymict eucrites (5).

b: Coarse grained basaltic clasts composed of pigeonite ($Mg_{36}Fe_{60}Ca_4$ to $Mg_{37}Fe_{57}Ca_6$), augite ($Mg_{31}Fe_{44}Ca_{25}$ to $Mg_{30}Fe_{48}Ca_{22}$), and plagioclase (An_{93-78}) with minor amounts of ilmenite, chromite, troilite, and metal. The clasts show a subophitic texture and are similar in their mineralogy and mineral chemistry to the Bouvante host (1) and to lithology A described by (2). Shock metamorphic features in these clasts are represented by clouding of both plagioclase and pyroxene, kinking, deformation lamellae and mosaicism in the pyroxene.

c: Fine grained basaltic clasts (<1 cm) composed mainly of lath shaped crystals of plagioclase with subparallel orientation with interstitial pyroxene. The clasts show an intersertal texture. They differ from type B clasts by virtue of texture, abundance of plagioclase relative to pyroxene and by lack of any evidence of shock metamorphism. They also differ in their mode of occurrence, texture, and mineralogy from the plagioclase and silica-rich dioritic veins reported by (2).

The vitric clasts may have originated by localized shock melting of the Bouvante host. The minimum peak pressure required to induce such melting is in excess of 800 kbar (6). The coarse basaltic clasts are fragments of the host, produced by brecciation and the minimum peak pressure required to account for mosaicism in the pyroxene in these clasts is $\simeq$ 200 kbar. The fine grained basaltic clasts show no evidence of deformation or brecciation. They may have originated from a melt depleted in Mg and enriched in Ca and Al relative to the Bouvante host. Similar to Bereba, Bouvante gave a Pb-Pb mineral isochron age of 4.51 Ga, based on leached samples free of vitric clasts (7). Isotopic investigation of the clasts is in progress.

(1) Christophe Michel-Levy, M., M. Bourot-Denise, H. Palme, B. Spettel and H. Wänke (1987), *Bull. Mineral.* **110**, 447–458.
(2) Delaney, J.S., C. O'Neill, and M. Prinz (1984), *Lunar and Planetary Science* **XV**, 208–209.
(3) Christophe Michel-Levy, M., D.Y. Jerome, H. Palme, B. Spettel and H. Wänke (1980), *Meteoritics* **15**, 272.
(4) Basaltic Volcanism Study Project (1981), Basaltic volcanism on the terrestrial planets, New York, Pergamon, 1286 p.
(5) Delaney, J.S., M. Prinz, and H. Takeda (1984), *Proc. Lunar Sci. Conf.* **15th**, c251–c288.
(6) Schaal, R.B. and F. Horz (1977), *Proc. Lunar Sci. Conf.* **8th**, 1697–1729.
(7) Tera, F., R.W. Carlson and N.Z. Boctor (1989), *Lunar and Planet. Sci.* **XX**, 1111–1112.

PETROLOGIC AND PB ISOTOPE INVESTIGATIONS OF BINDA EUCRITE; N.Z. Boctor, F. Tera, and R.W. Carlson, Department of Terrestrial Magnetism, Carnegie Institution of Washington, Washington, D.C. 20015

We present a progress report on petrologic and isotopic investigations of the eucrite Binda. The meteorite is composed of pyroxene and plagioclase with minor amounts of chromite, ilmenite, troilite, and metal. The plagioclase in Binda (An_{92-94}) is much less abundant than in other cumulate eucrites. The pyroxene is represented by orthopyroxene ($Mg_{64}Fe_{33}Ca_3$ to $Mg_{63}Fe_{33}Ca_4$). Exsolutions of augite ($Mg_{43}Fe_{15}Ca_{42}$ to $Mg_{44}Fe_{11}Ca_{45}$) occur as lamellae and blebs in the orthopyroxene (inverted pigeonite). The pyroxenes in Binda have higher Mg/(Mg + Fe) relative to other cumulate eucrites. Pyroxene and plagioclase show a bimodal size distribution with large porphyritic crystals of both minerals occurring in nearly equigranular interlocking crystal aggregates of smaller size. Chromite has a low Ti/(Ti + Cr + Al) of 0.028, consistent with the low Ti content of Binda.

Experimental investigation (1) shows that in contrast to other cumulate eucrites, Binda's pyroxene could have equilibrated with a liquid with an Fe/(Fe + Mg) similar to that of Juvinas and Sioux County. However, the high Mg/(Mg + Fe) of Binda pyroxene suggests crystallization from a melt that is more magnesian than Sioux County. This melt was generated by an advanced degree of partial melting in the eucrite's source region and underwent a small degree of fractionation. The more iron-rich pyroxenes of Moama, Moore County and Serra de Mage would crystallize from such a melt with progressive increase in the degree of fractionation. If this hypothesis is correct, then Binda should be older than the other cumulate eucrites. Preliminary Pb isotopic investigation suggests that Binda may be older (~4.5 Ga) than the cumulate eucrites Moama and Serra de Mage (4.43 and 4.40 Ga, respectively). (2)

(1) Stolper, E. (1977), *Geochim. Cosmochim. Acta* **41**, 587-611.
(2) Tera, F., R.W. Carlson, and N.Z.Boctor (1989), *Lunar and Planet. Sci.* **XX**, 1111-1112.

TRACE MINERALS IN K-T BOUNDARY CLAYS; B.F. Bohor, E.E. Foord, and W.J. Betterton, U.S. Geological Survey, Box 25046, Denver, C O 80225

No inventory of mineral grains occurring at low abundance levels in Cretaceous-Tertiary (K-T) boundary clays has been done, although abundant quartz, feldspar, and composite grains of these minerals have been described by many workers from sites worldwide. Izett (1) mentioned seeing rare grains of zircon, garnet, epidote, and hornblende in mineral separates from K-T boundary claystones from the Raton basin. One of us has seen these same minerals, as well as ilmenite and titanomagnetite and rare magnetite, sphene, and tourmaline, in separates from the K-T claystone at Brownie Butte, MT (Bohor, unpublished data). All of these minerals can be ascribed to an acid igneous or metamorphic target rock terrane, but are not specifically diagnostic of any one rock type.

In order to eliminate the most common nonclay minerals, treatments with HCl, HNO_3, H_2SO_4, and HF were applied to clay-free separates of K-T boundary claystones from the Western Interior. We treated separate samples of the upper smectitic layer from Berwind Canyon, CO, and the lower kaolinitic layer from Brownie Butte, MT. The mineral suite recovered consisted of rutile, zircon, chromite, corundum, and tourmaline (dravite), in order of decreasing approximate abundance. These minerals were common to both layers, and the acid residues for each layer totalled 0.1 wt. % of the clay-free separates. All of these minerals can be found in acid igneous and metamorphic rocks except for the chromite, which typically occurs in basic rocks.

Some of the chromite grains reveal multiple crossed sets of planar lamellae on their etched surfaces. One of these grains was examined by X-ray diffraction. Nearly complete diffraction arcs were recorded on Debye-Scherrer films, suggesting lattice disruption. Because spinels are subject to polysynthetic twinning that could produce these arcs, Laue photographs were also taken. These showed elongated, curvilinear, streaked diffraction maxima (asterism) that rule out the presence of twinning and indicate the formation of multiple crystalline domains. Therefore, these chromite grains showing lamellae were probably subjected to deformational stress, either tectonic or shock-induced. Although we can't positively identify the origin of the stress, the multiple sets of lamellae suggest shock. Either origin indicates that the chromite grains were derived from target rocks and not from the vaporized bolide, as were other high-nickel spinels (magnesioferrite) previously described from the K-T clays and claystones (2). The chromite grains are larger than the magnesioferrite grains and do not show the skeletal morphology and high nickel content characteristic of these latter crystals.

Zunyite $[Al_{13}Si_5O_{20}(OH,F)_{18}Cl]$ and moissanite (SiC) are two trace minerals recovered from the acid residue of the kaolinitic layer at Brownie Butte. Both minerals occur very rarely in nature, and only one grain of zunyite and two grains of moissanite (40 and 65 microns) were found in this sample. Moissanite has been documented in kimberlites, but its reported occurrences in igneous, metamorphic and sedimentary rocks are not as well accepted. Carborundum is the artificial analog of moissanite and contamination is always suspect (3). If these minerals can be confirmed at other sites, they may prove valuable for identifying the target rocks.

REFERENCES: (1) Izett, G.A. (1987) USGS Open File Report 87-606, 112 p. (2) Bohor, B.F. et al. (1986/87) EPSL 81, p. 57-66. (3) Milton, C. (1985) GSA Abs. with Prog. 17, p. 665.

DISTRIBUTION OF MOLDAVITES AND THEIR STRATIGRAPHIC POSITION.
V. Bouška, Faculty of Science, Charles University, Albertov 6, Praha 2, 129 43 Czechoslovakia.

The chemical composition of the moldavites, which fell in Southern Bohemia about 14.7 My ago, is not uniform. The main differences have been preserved despite redeposition, which took place after the postdacian tectonic phase during the Pliocene and Quaternary. The moldavite occurrences can be divided into four groups: (1) Lower Sarmatan (Upper Miocene) deposits, greenish sandy to silty clays, sandy gravels and montmorillonitic clays with sculptured angular moldavites; (2) Romanian (Upper Pliocene) Formation of moldavite bearing rusty colored sandy gravels with oval, lustrous moldavites; (3) Slope loams and detritus of Pleistocene age and (4) Pleistocene sandy gravels and alluvia along present-day streams containing moldavites with a matted worn surface.

The whole moldavite strewn field can be divided into three subfields, which are geographically not completely separated. The subdivision is made on the basis of color distribution, maximum projection sphericity, lechatelierite content, bubble frequency, and chemical composition.

(a) moldavites from Radomilice (Southern Bohemia); mostly pale or bottle green, high maximum projection sphericity values, highest SiO_2 contents (83 wt%) of all moldavites, low alumina, FeO, alkalies, and low content of lechatelierite and bubbles.

(b) other occurrences in Southern Bohemia; flat shape, bottle green color, silica content around 80 wt%, abundant bubbles and lechatelierite.

(c) Moravian occurrences; mostly olive-green to brown in color, relatively high maximum projection sphericity, low lechatelierite and bubble content, average silica of 79 wt%, poorer in CaO and FeO than other groups (Bouška and Povondra, 1964; Delano et al., 1988).

The total FeO, Na_2O, Hf, Sc, REE etc. contents increase from the Radomilice over the other South Bohemian to the Moravian moldavites. The K/Na ratio decreases in the same direction. The oxygen isotopic compositions are: Radomilice: +11.42‰ $\delta^{18}O$ (n=7); South Bohemia: +11.29‰ $\delta^{18}O$ (n=12), Moravia: +11.13‰ $\delta^{18}O$ (n=5). Since changes in the distribution of large atoms (e.g., Cs, Sr, Ba) can also be observed in statistically significant trends, the parent material of the moldavites at the impact site was probably heterogeneous.

References:

Bouška V. and Povondra P. (1964), Geochim. Cosmochim. Acta **28**, 783-791.

Delano J.W., Bouška V., and Řanda Z. (1988) 2nd Intern. Conf. Natural Glasses, Prague 1987, 221-230, Charles Univ. Praha.

MINERALOGY OF NANOMETER-SIZED GRAINS IN CHONDRITIC INTERPLANETARY DUST; J. P. Bradley, McCrone Associates, Inc., 850 Pasquinelli Drive, Westmont, IL 60559, U.S.A.

Anhydrous chondritic interplanetary dust particles (IDPs) are mixtures of large (>1 μm) mineral grains, carbonaceous material, and ultra fine-grained aggregates. There are at least two types of aggregates which differ from one another in terms of grain size and mineralogy (1). A long term challenge involves determining the most likely growth environments of these aggregates but the immediate challenge is simply to identify the mineral phases, since in some cases the average grain size is <20 nm.

We have initiated an electron microscopic study of the finest grained components of anhydrous IDPs using electron microdiffraction, x-ray and energy loss spectroscopy (EELS), and lattice fringe imaging. The IDPs are first thin-sectioned using an ultramicrotome (2). Sections should be only one monolayer of crystals thick (i.e. 20-30 nm) and an electron probe with dimensions smaller than the mineral grains should be used in order to obtain the necessary spatial resolution. However, it is difficult to produce thin-sections <50 nm thick and small electron probes offer unacceptably low x-ray count rates on thin specimens. This limitation is illustrated in Figure 1 which shows Mg-Si-Fe ternary plots for two different components of IDP U219C2. The tighter clustering in (a) reflects good x-ray spatial resolution from larger (>10^2nm) grains, but the lack of clustering in (b) reflects inadequate spatial resolution from smaller (<<10^2nm) grains. EELS and microdiffraction provide alternative methods for studying small grains. EELS is useful for light element analysis and determination of oxidation states (3), while microdiffraction can be applied to grains as small as 15 nm. Both techniques offset the spatial resolution limitations of x-ray spectroscopy.

(1) J.P. Bradley, M.S. Germani, D.E. Brownlee (1989) Earth Planet Sci. Lett., in press. (2) J.P. Bradley (1988) Geochim. Cosmochim. Acta, 52, 889. (3) R.F. Egerton, Electron Energy Loss Spectroscopy in the Electron Microscope, Plenum, New York, 1986.

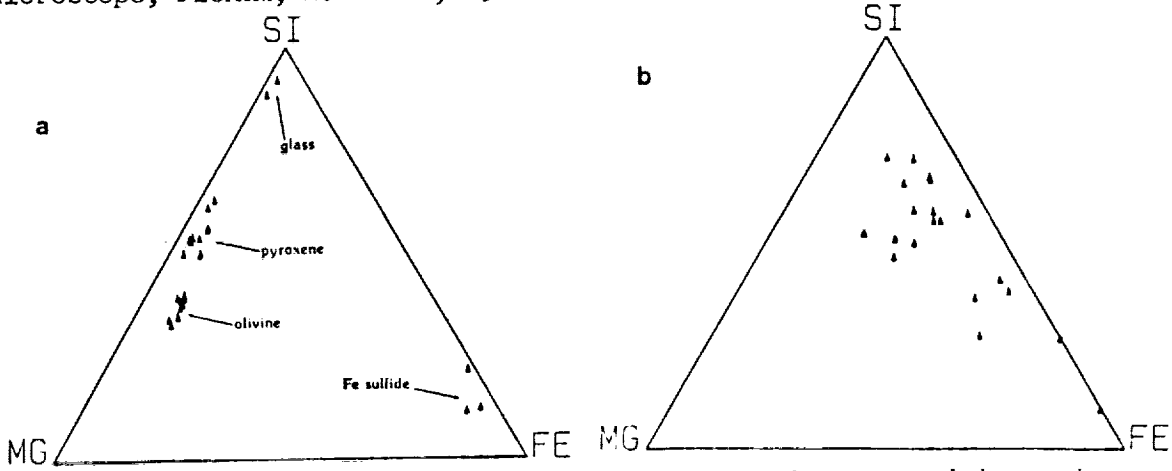

Figure 1. Ternary Mg-Si-Fe plots (atom fraction) of x-ray point count analyses of (a) a coarse-grained aggregate, and (b) a fine-grained aggregate in IDP U219C2 (section thickness 80nm).

OLIVINES RICH IN MINOR ELEMENTS FROM ORDINARY CHONDRITES

F.Brandstätter, G.Kurat, Naturhistorisches Museum , A-1014 Wien, Austria; H. Franke, Universität Jena, DDR-6900 Jena, GDR.

High minor element(ME) contents of meteoritic olivines have been considered to indicate either crystallisation from a source rich in these elements (Steele et al., 1985) or growth from the vapor phase (Steele, 1986; Kurat et al., 1987). Considering the generally very low olivine-liquid distribution coefficients for Ca, Al , and Ti (e.g. Watson, 1979; Yurimoto and Sueno, 1984) it is now commonly believed that high abundances of these elements in olivine indicate grotwh from a vapor phase. High Cr contents of olivines, however, cannot unequivocally be related to condensation because of the fairly high olivine-liquid distribution coefficient at high temperatures(Schreiber and Haskin, 1976). If present, they are, however, incompatible with metamorphic re-equilibration at T < 1000 ^{o}C. Olivines rich in MEs have been reported from carbonaceous chondrites and UOCs(op. cit.). No comparable olivine compositions are known sofar from EOCs, the presence of which , however, is predicted by the model of Kurat(1988).

We report here on the results of a search for MEs in UOCs and EOCs. Olivines from the Bjurböle(L4), Mezö-Madaras(L3), Farmington(L5), and Slavetic(H4) chondrites have routinely been analyzed by electron microprobe in order to detect ME bearing olivines, to check possible relationships between ME contents of olivine and texture of the particular constituent(chondrule, fragment etc.), and to detect some inter-element correlations which could give additional hints on the genesis of the olivines.

Our results (Table) indicate that olivines with elevated ME contents are indeed present in EOCs. In Bjurböle we found only olivines fairly poor in MEs with a marginal indication of BO being somewhat enriched in Ca and Cr as compared to PO. In Slavetic the behaviour of Ca is similar [Ca(BO) > Ca(PO)] but Ti (instead of Cr) appears to be enriched in BO as compared to PO. Relatively high contents of MEs have been encountered in Farmington BO: Cr_2O_3 and CaO average at 0.09wt.-%. Both MEs are, however, fairly variable (range 0.04-0.14 and 0.04-0.18 for CaO and Cr_2O_3, respectively). TiO_2 is also present above the detection limit but the Al_2O_3 content is low. In Mezö-Madaras olivines from unquilibrated chondrules have high ME contents whereas one equilibrated chondrule has low ME olivine. No correlations among MEs are apparent but Mn is positively correlated with iron in unequilibrated olivines.

In conclusion, there are olivines present int EOCs that have elevated ME contents with BOs tending to be richer in MEs than POs. This result supports the chondrite model proposed by Kurat(1988).

Table: Average iron and ME contents of olivines from ordinary chondrites (wt.-%).

Meteorite	CaO	Al_2O_3	TiO_2	Cr_2O_3	MnO	FeO	texture
Bjurböle	0.02	0.02	0.02	0.02	0.48	23.1	PO
	0.05	0.02	<0.02	0.07	0.44	23.1	BO
Farmington	0.06	<0.02	0.02	0.07	0.46	21.4	BO
	0.11	<0.02	0.04	0.10	0.44	21.7	BO
Mezö-Madaras	0.19	0.05	0.09	0.08	0.41	25.7	PO
	0.28	0.06	0.05	0.08	0.12	9.3	PO
	0.20	0.08	0.02	0.07	0.47	30.3	PO (platy)
	0.06	<0.02	<0.02	<0.02	0.45	21.4	BO
Slavetic	0.05	<0.02	0.09	0.06	0.45	16.0	BO
	0.02	<0.02	0.02	0.02	0.45	15.8	PO

References: Kurat G. et al.(1987) LPS XVIII, 523; Kurat G.(1988) Phil.Trans.R.Soc.Lond.A325,459; Schreiber H.D. and Haskin L.A.(1976) Proc.Lunar Sci.Conf.7th,1221; Steele I.M. et al.(1985) Nature 313, 294; Steele I.M.(1986) GCA 50,1379; Yurimoto H. and Sueno S.(1984) Geochem.J.18,85; Watson E.B.(1979) Amer.Mineral. 64,824.

CARBON-RICH AGGREGATES IN TYPE 3 ORDINARY CHONDRITES: ORIGIN AND IMPLICATIONS FOR THERMAL HISTORIES. Adrian J. Brearley, Institute of Meteoritics, Dept. of Geology, University of New Mexico, Albuquerque, New Mexico 87131, USA.

Carbon-rich aggregates are an important component of a number of type 3 ordinary chondrites (C-rich ordinary chondrites [1]). They were originally thought to consist of crystalline graphite and magnetite [2], but transmission electron microscope studies [3] have shown that they are, in fact, a fine-grained intergrowth of amorphous and poorly graphitized carbons (PGC), Fe,Ni metal and minor chromite. C-rich aggregates are a unique occurrence of carbon among chondritic meteorites and their presence places important constraints on the thermal history of type 3 ordinary chondrites. Unlike the carbon in carbonaceous chondrites, which occurs disseminated throughout the matrix, the C-rich aggregates are 50 μm to 1 mm in size and represent extremely large concentrations of carbon.

C-rich aggregates formed either by parent body processes or in the solar nebula. A possible parent body model [4] involves outgassing CO produced by a reaction such as $FeSi_{0.5}O_2$ (Fe-rich olivine) + C = Fe + $0.5SiO_2$ + CO in types 5-6 ordinary chondrites, which recondenses by the reverse reaction in type 3 material. This reaction is viable for the formation of carbon in the chondrite matrices that contain abundant Fe-rich olivine, but is not a satisfactory explanation for the formation of the C-rich aggregates. Elemental carbon could form by catalytic disproportionation of CO on Fe,Ni metal, a reaction which satisfactorily explains the association of metallic Fe,Ni with elemental C, but, in detail, is not supported by the textural characteristics of the PGC. Elemental carbons produced between 400 and 550°C by such a mechanism are filamentous and tubular PGCs, with crystalline graphite rimming Fe,Ni metal above ~450°C [5]. No filamentous carbons are observed in the aggregates and PGC rather than crystalline carbon rims the Fe,Ni grains. Thus a planetary origin does not appear to be consistent with the observations and suggests that a nebular origin is more likely.

The association of Fe,Ni metal with carbon in carbonaceous interplanetary dust particles [6] (like that in the C-rich aggregates) has been attributed to the formation of hydrocarbons by catalytic Fischer-Tropsch type (FTT) reactions in the nebula. FTT reactions appear to be a viable mechanism for the formation of the carbonaceous material in the C-rich aggregates, but the textures in the C-rich aggregates suggest that the carbonaceous material has undergone significant parent body processing. The microstructures of the PGC are typical of those produced by pyrolitic carbonization and graphitization of a hydrocarbon precursor [7] and the presence of graphitic rims around Fe,Ni grains (also observed in IDPs) suggests that catalytic graphitization has been important. Heating of PGC results in a decrease in the $d_{(002)}$ spacing from 3.60Å for the least ordered PGC to 3.354Å for crystalline graphite. Using data from terrestrial metamorphic rocks Rietmeijer and Mackinnon [8] calibrated this change in $d_{(002)}$ as a function of temperature to create a relatively sensitive cosmothermometer for extraterrestrial materials. This thermometer has been applied to PGC in the C-rich ordinary chondrites, Sharps (H3.4), ALH A77011 (LL3.5) and ALH A81024 (L3.6) and C-rich chondritic clasts from Dimmitt and Plainview. The results provide the first reliable indicator of the maximum metamorphic temperatures attained by the type 3 ordinary chondrites. The PGC in Sharps records temperatures in the range 250-375°C whereas the higher petrologic types, up to 3.6, reached temperatures of 400-500°C. These temperatures are lower than those quoted for the types 3.4-3.6 ordinary chondrites (~450-500°C) [9] and temperatures derived from the work of Sears and coworkers [10] and suggest that petrologic type 3.0-3.9 chondrites experienced a wider range of temperatures than was previously thought. In addition, the data show that these meteorites could not have accreted at temperatures higher than ~400°C or else the elemental carbon would have been present as crystalline graphite, rather than PGC. Supported by NASA grant NAG 9-30 to Klaus Keil (P.I.). References. 1) Scott, E.R.D. et al (1988) PLPSC 18, 513. 2) Scott, E.R.D. et al (1981) Nature 291, 544. 3) Brearley A.J. et al (1987) LPSC XVIII, 123. 4) Sugiura, N. et al (1986) EPSL 78,148. 5) Audier M. et al (1981) Carbon 19, 217. 6) Bradley J.P. et al (1984) Science 223 56. 7) Oberlin A. (1984) Carbon 22, 521. 8) Rietmeijer, F.J.M. and Mackinnon I.D.R. (1985) Nature 221, 1044. 9) Dodd R.T. (1981) Meteorites. Cambridge Univ. Press. 10) Sears, D.W.G. and Hasan, F.A. (1987) Surveys in Geophys. 9, 43.

MATRIX MINERALOGY OF THE BELLS CM2 CARBONACEOUS CHONDRITE AND THE IN-SITU OBSERVATION OF TITANIUM OXIDES (MAGNELI PHASES). Adrian J. Brearley, Institute of Meteoritics, University of New Mexico, Albuquerque, New Mexico 87131, USA.

The Bells meteorite is regarded as one of the most altered CM2 chondrites according to the criteria established by McSween [1]. Of all the CM2s it has one of the highest matrix to chondrule ratios (4.5) and the matrix, being Fe-poor (Fe/Si = 1.199, cf. 1.922, mean CM2) is closer to CI composition than CM [2]. The depletion in matrix Fe is due to magnetite abundances of 13-16 wt% [3,4], higher than typical CM values and similar to CIs. Such evidence led Davis and Olsen [4] to suggest that Bells has properties intermediate between CM and CI chondrites. They also argued that Bells is not as altered as the model of McSween [1] suggests.

The matrix mineralogy in Bells has been studied by transmission electron microscopy in order to elucidate the relationship between Bells and other CM2 chondrites and to determine whether Bells has suffered very extensive aqueous alteration. Bells matrix differs from that of other CM2 chondrites in lacking abundant, coarse (0.1-2μm, parallel to the c-axis) platy phyllosilicate grains. Such grains are a major component of the fine-grained matrix of other CM2s [5]. Bells matrix is dominated by amorphous or poorly crystalline material (80 vol%) which, although present in other CMs, constitutes only around 30 vol% of the matrix, significantly less than in Bells. Two distinct types of amorphous/poorly crystalline material occur in Bells. These are a) regions of ultrafine-grained phyllosilicates, 3-10nm in size, with straight, curved or cylindrical morphologies. High resolution electron microscopy has shown that crystallites of 7Å serpentine and a 14Å phase, probably chlorite, are the dominant phases. Rare crystallites with basal spacings of 9.3Å and 17Å, probably talc and tochilinite, respectively, occur mixed with the serpentine and chlorite. Magnetite, troilite and forsterite also occur. The second type of amorphous region b) consists of rare crystallites of talc (10-20nm) set in an amorphous matrix. Clearly only limited devitrification has occurred. AEM studies, although complicated by the fine-grained character of the phyllosilicates, show a range of compositions with Mg(Mg+Fe) ratios from 0.2 to 0.65. The most Fe-rich compositions contain the highest Ni and S contents (~1-3 wt%), consistent with the presence of a small component of tochilinite. Serpentine is compositionally similar to Mg-serpentine in Nogoya [6]. The amorphous component is highly Si and Al enriched and has a composition like amorphous material in a CI-type clast in the Nilpena polymict ureilite [7]. The presence of considerable amounts of an amorphous phase is difficult to reconcile with the idea that Bells has suffered very extensive alteration. Aqueous alteration, even at low temperatures, would rapidly result in the complete breakdown of such material to phyllosilicate minerals. This suggests that Bells is not as altered as has been suggested, and may, in fact, be among the least altered CM2 chondrites. In addition the absence of smectite in Bells shows that mineralogically it does not have any affinities to CI chondrites.

One of the important findings in this study is the occurrence of a single cluster of 3-4 Ti-rich grains (50-200nm) in the Bells matrix associated with amorphous Si-rich material (glass?). Electron diffraction analysis has shown that these grains are Ti oxides, (Magneli phases), which are consistent with Ti_5O_9 and Ti_8O_{15}. This is the first reported occurrence of Magneli phases in a meteorite, although they have been previously reported in chondritic IDPs [8,9,10,11]. The morphology and grain size of the Ti oxide grains in both occurrences are essentially identical. The Magneli phases in IDPs may be either nebula condensates [9] or formed at low temperatures by oxidation of Ti, possibly of interstellar origin [10]. The possibility of a presolar origin for the Ti in Bells is indicated by the presence of ^{50}Ti anomalies in matrix separates from Murchison [12]. The carrier of these isotopic anomalies may well be fine-grained Ti oxides, which are, as yet, unidentified in Murchison. Supported by NASA grant NAG 9-30 to Klaus Keil (P.I.). References: 1) McSween H.Y. (1979) GCA 43, 1761. 2) McSween H.Y. and Richardson S.M. (1977) GCA 41, 1145. 3) Watson E.E. et al. (1975) EPSL 27, 101. 4) Davis A.M. and Olsen E. (1984) LPSC XV, 190. 5) Barber D.J. (1981) GCA 49, 2149. 6) Bunch T.E. and Chang S. (1980) GCA 44, 1543. 7) Brearley, A.J. and Prinz M. (1989) LPSC XX, 103. 8). Mackinnon, I.D.R. and Rietmeijer F.J.M. (1987) Revs. in Geophys. 25, 1527. 9) Zolensky, M.E. et al, (1989) PLPSC 19, 505. 10) Rietmeijer F.J.M. and Mackinnon I.D.R. (1989) LPSC XX, 902. 11) Blake D. et al (1989) LPSC XX, 84. 12) Niemeyer S. (1985) GRL 12, 733.

BLACK CHONDRITE METEORITES: AN ANALYSIS OF FALL FREQUENCY AND THE DISTRIBUTION OF PETROLOGIC TYPES. **D.T. Britt and C.M. Pieters, Brown University, Providence, R.I. 02912.**

Introduction: Black chondrite meteorites are ordinary chondrites that are characterized by an extremely active shock history which has altered their optical properties. Although they are chemically indistinguishable from the range of normal ordinary chondrites they exhibit pervasive shock features such as brecciation, optical alteration (blackening), and low gas-retention ages [1,2,3]. The presence of these features make black chondrites invaluable samples of the effects of the space environment on ordinary chondrite material. Since shock can be a major contributor to regolith processes, black chondrites can provide insight into the optical effects of regolith processes on ordinary chondrite parent bodies. It is important to answer some of the basic questions about the fall frequency and distribution petrologic types of these optically altered meteorites to determine whether optical alteration is a major surface process on ordinary chondrite parent bodies.

Data Collection: We have initiated a program to identify and catalogue the optically altered black chondrite falls held by some of the major meteorite collections. Black chondrites are identified on the basis of three criteria. First, that the meteorite meet our functional definition of a black chondrite "any ordinary chondrite meteorite exhibiting distinctly low reflectance (≥ 0.15) in hand sample (example Farmington), or with major portions of the meteorite containing such low reflectance material (example Paragould)". Second, that there was sufficient sample mass (>5 grams) and interior exposure to make a reliable reflectance determination. Third, that terrestrial weathering and rust were minimized. In addition, since this survey focused on black chondrites only, we excluded from the study all samples that had been previously identified as gas-rich ordinary chondrites and all unequilibrated ordinary chondrites. Both of these meteorite types also contain low reflectance matrix material that would bias any selection.

Discussion and Conclusions: To date the meteorite collections of Harvard University, the Smithsonian Institution's Department of Mineral Sciences, and the USSR Academy of Sciences have been surveyed. After eliminating meteorites that did not meet the sampling criteria, a total of 339 ordinary chondrite falls were checked and a total of 48 black chondrites were identified. The statistics of the distribution of these meteorites between the petrologic types are summarized in **Table 1**. A number of surprising insights are apparent in this data. First, there are a relatively large number of black chondrites. These results suggest that black chondrites constitute about 14% of ordinary chondrite falls. If gas-rich ordinary chondrites are included, this suggests that 23 % of all ordinary chondrite falls have been optically altered by regolith or regolith-like processes. Second, black chondrites are roughly equally distributed between petrologic type. This implies that no single shock event provided a dominant proportion of black chondrites. Finally, these results show no strong trend between the metamorphic grades, suggesting that the proportion of black chondrites in each metamorphic grade is not significantly different from the proportions in all other grades. The trends of black chondrite fall frequency among petrologic and metamorphic types suggests that all ordinary chondritic material is being subjected to roughly equal levels of shock-alteration. All these factors combine to suggest that optical alteration in general, and black chondrites in particular, can be very important, both in understanding the optical effects of asteroidal regolith processes and in the search for ordinary chondrite parent bodies in the main asteroid belt.

Acknowledgments: The authors are indebted to G.J. MacPherson and T. Thomas of the Smithsonian Institution, C.A. Francis of Harvard University, and M.I. Petaev of the Meteorite Committee of the USSR Academy of Sciences for providing access to their respective meteorite collections and for their assistance during this research.

References: [1] Gaffey M.J. (1976) JGR, 81, 905-920. [2] Heymann D. (1967) Icarus, 6, 189-221. [3] Britt D.T., et al. (1989) Proc. 19th Lunar Planet. Sci. Conf., 537-545.

TABLE 1

TYPE	# CHECKED	# BLACK	PERCENTAGE
H4	32	6	18.8%
H5	66	9	13.6%
H6	41	7	17.1%
Total H	**139**	**22**	**15.8%**
L4	11	2	18.2%
L5	29	5	17.2%
L6	130	13	10.0%
Total L	**170**	**20**	**11.8%**
LL4	2	0	0.0%
LL5	8	1	12.5%
LL6	20	5	25.0%
Total LL	**30**	**6**	**20.0%**
Grand Total	**339**	**48**	**14.16%**

ON THE CORROSION OF METEORITES. V.F. Buchwald, Department of Metallurgy, Building 204, Technical University, 2800 Lyngby, Denmark.

In previous papers (Buchwald 1975, 1983) it has been shown that the decomposition of iron meteorites and of nickel iron in stony meteorites is significantly accelerated by the presence of chloride. Further it has been shown that lawrencite does not exist as a cosmic mineral (Buchwald 1977). The aggressive components in the weathering meteorite are akaganeite, β-FeOOH with about 5 wt.% Cl in the molecule, and $Fe_2(OH)_3Cl$ with about 18 wt. % Cl. It is suggested that the akaganeite, as developing in weathering meteorites, is written $\left[Fe_{15}Ni\right]\left[O_{12}(OH)_{20}\right]Cl_2OH$ (Buchwald & Clarke 1988,1989).

Under Antarctic conditions the corrosion process is slow, because diffusion is slow at low temperatures. Chlorine in snow and ice, albeit present in very low concentrations of < 10 ppm, diffuses to the metallic surfaces and cracks and depassivates the nickel iron. $Fe_2(OH)_3Cl$ and akaganeite are formed, and akaganeite by virtue of its ion-exchanging capacity acts as a storehouse for chlorine. As such it becomes a major corrosion product of the Antarctic meteorites and has a long life time.

Under temperate conditions the corrosion process is more rapid. The active corrosion front, with akaganeite, works its way into the iron nickel alloys, leaving stable oxides behind. When there is no iron left, the last akaganeite decomposes, and chlorine is set free to diffuse to new corrosion attacks elsewhere. The stable oxides are chlorine free and mainly consist of goethite, maghemite, magnetite and lepidocrocite. Hematite has only been identified in a few, special cases.

References.

Buchwald, V.F. (1975) Handbook of iron meteorites. Buchwald, V.F. (1977) Phil.Trans.R.Soc. London 286A: 453-491. Buchwald, V.F. (1983) Meteoritics 18: 272-273. Buchwald, V.F. and Clarke, R.S. (1988) Meteoritics 23: 261. Buchwald, V.F. and Clarke, R.S. (1989) American Mineralogist, May-June.

GRAVITATIONAL BODY FORCE AS A VARIABLE IN METEORITE FORMATION

P.Z. Budka, Technical Communications Unlimited, Schenectady, New York USA 12309
F.F. Milillo, Department of Mechanical Engineering, Union College, Schenectady, New York 12308

The parallel study of meteorites and Earth materials dates from at least the invention of the metallograph in the 1850s. The commonality between these fields of study has provided deeper understandings in both directions. However, with the Space Age and its impact on Materials Science, a new question fundamental to understanding the full nature of meteoritic materials must be addressed:

> What was the magnitude of the gravitational body force in effect during the formation of extraterrestrial materials, especially meteorites?

Materials processing in space experiments aboard Skylab and the Shuttle give ample testimony to the fact that materials solidified in microgravity environments (10^{-5} to 10^{-7} g) exhibit significant microstructural differences from those solidified in Earth's gravity. Likewise, solidification experiments conducted at g levels greater than that of Earth demonstrate equally significant differences.

That the question of the influence of gravitational body force has not been addressed by the vast majority of meteoriticists is evident in current meteoritics literature. That this question is fundamental to the field of meteoritics is also evident in the nature of the topics addressed by this literature.

The effect of gravitational body force during solidification and its impact on material structure, and on properties, must be considered in discussions which include any of the following:

1. Meteorite parent body formation scenarios which include a small body such as an asteroid.
2. Materials considered to have igneous origins such as eucrites, shergottites, and certain nickel-irons.
3. The presence of liquid at any point in the life of the material, regardless of how the liquid was produced.
4. Microstructural constituents such as glass, spherulites and dendrites.

It is postulated that microgravity solidification was a key factor in the generation of some meteoritic microstructural features. Thus, microgravity solidification must be considered in discussions of meteorite formation. To ignore this factor is to ignore a fundamental parameter of nature.

SAZOVICE L5 AND WESSELY H5 CHONDRITES (CZECHOSLOVAKIA) - MINERALOGY AND CLASSIFICATION. M. BUKOVANSKÁ, NATIONAL MUSEUM, 11579 PRAGUE 1, CZECHOSLOVAKIA, J. JANICKE, MAX-PLANCK-INSTITUT F. KERNPHYSIK, POSTFACH 103980, D-6900 HEIDELBERG 1, FRG, AND F. BRANDSTÄTTER, NATURHIST. MUSEUM, A-1014 VIENNA, AUSTRIA.

Based on petrological evidence, SEM-, and electron microprobe analyses the to date poorly known Czechoslovak chondrites **Sazovice** and **Wessely** were classified.

Sazovice (fall: June 1934) - After a first detailed description *[1]* and using the analyses of Kokta, the chondrite was erroneously classified as olivine-bronzite by *[2]*.

The meteorite is heavily brecciated. Barred olivine chondrules and fine-grained opx-cpx chondrules are abundant. Analyses revealed average compositions of 24.0 Fa for olivine and 20.3 Fs for orthopyroxenes. Composition of the clinopyroxenes is 48.8 En 7.38 Fs 43.8 Wo. Average composition of plagioclase is 17.9 An 76.5 Ab 5.6 Or. The feldspar analyses only partially comply the data obtained by *[3]*. The field is much wider towards anorthite.

Chromite compositions are well defined in the Ti^{4+} vs. trivalent + Mg^{2+} and are comparable to the data of the Lissa L chondrites *[4]* and Ústí nad Orlicí *[5]*. The composition of ilmenite is: $(Fe_{0.856}\ Mg_{0.128}\ Mn_{0.039})\ Ti_{0.976}\ O_{2.984}$.

Metals consist of: a) either homogeneous grains, mainly low Ni kamacite (4.17-6.8 wt.% Ni); b) or inhomogeneous taenite - tetrataenite-kamacite often intergrown with troilite. These two metal phases with the typical *perthitic* structure often show the highest Ni-content at the tetrataenite rim of the grains and very low Ni kamacite in the parts of the intergrowth. In some large grains taenite contains 36 wt.%-32 wt.% Ni. Troilite is stoichiometric.

Given a homogeneity of olivines and orthopyroxenes and well crystallized feldspars, Sazovice can be classified as an *L5* chondrite.

Wessely (*Veselí nad Moravou*, Vnorovy - syn.) fell on October 9, 1831. It was described by *[6]*. Olivine compositions were determined by *[7]*.

The meteorite contains well pronounced chondrules, barred olivines, fan-shaped opx and cpx, porphyric and fine grains of 0.5-1.8 mm. Chromite is sometimes present as well developed small chondrules.

Probe analyses revealed an average value of Fa 18.44 for olivines, Fs 16.31 for orthopyroxenes, and for clinopyroxenes En 50.43, Fs 6.08, and Wo 43.49%. One analysis of feldspar revealed Ab 81.65, Or 7.01, An 11.34%. Two types of feldspar were found: Na,K-rich and Ca,Na-rich plagioclase and glass with variable chemistry.

Chemical investigation of chromites showed two different types with a well pronounced gap in between. The large grains are high in Fe^{2+} (6.68-6.95), in Ti^{4+} (0.4-0.6), and in Cr (12.5-12.8), low in Mg^{2+}, Al^{3+}, and total of trivalent cations. A low Fe- (5.2-5.7), Ti^{4+}- (0.15-0.3), Cr- (10.4-10.7), and high Mg^{2+}-content, total of trivalent cations and Al^{3+} is observed for small chromite chondrules. Ilmenite is, on the average, composed of $(Fe_{0.788}\ Mg_{0.129}\ Mn_{0.077})\ Ti_{1.001}\ O_{3.005}$. Numerous metal analyses gave a low Ni kamacite (2.5-5.5. wt.% Ni) together with taenite (20-25 and 30-35 wt.% Ni) coexisting with troilite. Regular kamacite grains are higher in Ni (7-8%). Regular taenite has an average Ni-content of 32-35.%. Pure copper was found to be close to the very low Ni kamacite.

Wessely could be classified as *H5* chondrite. However, the very well pronounced chondrules, the presence of glass, and inhomogeneity of chromites and metals could be indicative of a lower petrologic class: *H4* .

References: [1] Z. Jaroš, *Příroda* **27**, *281, 1934.* [2] Z. Jaroš, V. Rosický, *Cas. Moravského muzea v Brně* **30**, *1-18, 1937.* [3] W.R. Van Schmus and P.H. Ribbe, *Geochim.Cosmochim. Acta* **32**, *1327-1342, 1968.* [4] M. Bukovanská, *Sborník Národního muzea v Praze, 147-167, 1986.* [5] M. Bukovanská et al., *Meteoritics* **18**, *223-240, 1983.* [6] K. v.Schreibers, A.A.R. v.Holder, *Baumgartner's Zeitschr.f.Phys.u.verw.Wiss.* **1**, *193-239, 1832.* [7] B. Mason, *Geochim.Cosmochim. Acta* **27**, *1011, 1963.*

REFRACTORY TRACE ELEMENTS IN DIFFERENT CLASSES OF ACHONDRITES BY RNAA AND INAA AND SOME NOBLE GAS DATA; Mario Burger*, Otto Eugster+ and Urs Krähenbühl*
*Laboratorium für Radiochemie, Universität Bern, Switzerland
+Physikalisches Institut, Universität Bern, Switzerland

Many trace elements are important indicators for fractionation processes. Some refractory elements are in addition important target elements for the production of noble gases by spallation reactions in meteorites.

Therefore we measured the elements Ti, Y, Zr, Ba, Hf, W and Ta by RNAA in Ca poor and Ca rich achondrites. Many of these elements are very poorly determined. Often a single value represents the average of a whole sub class of achondrites.

After acid digestion of the irradiated samples the group separations were realized by precipitation reactions. For the pure beta emitter Y the radiochemical purification was obtained on a column with HDEHP as active phase. All elements but Y were analyzed by measuring discrete gamma lines. Concentrations of the elements Na, K, Fe, Sc, Cr, Co, La, Sm and Eu were obtained by INAA for all the samples.

For many of these achondrites also noble gas analyses have recently been performed (Michel and Eugster 1989). The irradiation history for those meteorites will be given.

Table 1 : Trace elements in achondrites [ppm]

Meteorite	Class	W	Ta	Ba	Zr	Hf	Y	Ti
Yamato-7308	how	0.20	0.038	7.3	13.0	0.27	2.1	≤600
Yamato-790727	how	0.15	0.080	14.7	18.3	0.39	3.4	650
Yamato-74013	dio	0.30	≤0.01	0.32	≤1.2	0.015	0.24	≤600
Yamato-75032	dio	0.30	0.034	8.0	14.5	0.32	2.4	2000
Garland	dio	0.04	0.025	3.3	6.3	0.39	2.3	500
Millbillillie	euc	0.16	0.16	28.0	24.1	1.1	14.4	3700
Yamato-791960	euc	0.80	0.20	31.2	37.2	0.88	20.0	4000
Khor Temiki	aub	0.03	0.012	5.4	4.3	0.19	1.1	450
Goalpara	ure	0.44	0.006	4.6	0.6	0.013	0.34	≤400
Zagami	she	0.80	0.19	27.4	58.2	1.6	10.6	4600

Experimental errors: One sigma errors are ±10% for W, Ta, Ba, Zr, Hf and Y and ±10-15% for Ti.
All concentrations were calculated relative to those in the referance samples USGS standard BHVO-1.

Acknowledgement: Allocation of the Yamato samples by the National Institute of Polar Research in Tokyo is greatly acknowleged. This work was supported by the Swiss National Science Foundation.

Reference: Michel and Eugster (1989) Abstract this conference

SOURCE REGION FOR THE AUSTRALASIAN TEKTITE STREWN FIELD; Burns C. A. and Glass B. P., Geology Dept., University of Delaware, Newark, DE 19716

Most authors agree that tektites were formed by impact melting of terrestrial surface deposits; however, the source craters for the Australasian and North American tektite strewn fields have not been found. Based on petrographic, compositional, and shape data several authors have suggested that the source crater for the Australasian tektites is in the northern or northwestern end of the strewn field (e.g., Stauffer, 1978; Schnetzler et al., 1988). In particular, the heterogeneity, higher water content, and presence of relict mineral grains and coesite in the Muong Nong-type tektites from Indochina indicate that they were formed closer to the source crater than the ablated forms.

In order to help establish the location of the source crater for the Australasian tektites, we have looked at size and abundance data for Australasian microtektites from 39 sites in the Indian Ocean, Philippine Sea, and western equatorial Pacific. The greatest number/unit area were found in core sites just south of Java. Assuming that the greatest concentration is closest to the source area, we set up a random grid system to pick hypothetical source crater sites. We then did regression analyses between the distances to the hypothetical source craters and the number of microtektites/unit area to determine the location that gave the highest correlation coefficient. The best fit was for a hypothetical source region about 4-5^{o} N. Lat. and 100-102^{o} E. Long. in which the cube root of the number of microtektites/unit area varies with the inverse of the distance from the hypothetical source region. This gives an R^2 value of 0.74. This source region is southwest of the source area chosen by Stauffer (1978) based on tektite data and microtektite occurrences and the source area chosen by Schnetzler et al. (1988) based on tektite data and Seasat/Geos 3 gravity data. The source area chosen by Stauffer (1978) fits the data almost as well as the source area we identified; however, the source area defined by Schnetzler et al. (1988) does not.

Glass (1979) suggested that the Zhamanshin Crater in southern Siberia might be the source crater for the Australasian tektite strewn field. However, regressing the abundance data against the distance to the Zhamanshin crater from each core site only gives an R^2 value of 0.17. It is interesting to note, however, that the Zhamanshin Crater, the hypothetical source area defined in this study, and the Darwin Crater, which are all about the same age (i.e., $\simeq$0.7 m.y.), all fall very close to a great circle.

The size data are perplexing. The sites with the largest average size are located in the northwestern part of the strewn field in the north central Indian Ocean. We do not know how to interpret these data at this time.

Compositional data are being obtained for microtektites from seven sites to determine if the microtektites might exhibit compositional trends similar to those observed for the tektites on land. If so, the greater geographic extent of the microtektites might allow us to better define the source region.

This research was partly supported by NSF grant OCE-8314522.

References: Glass B. P. (1979) Geology, 7, 351. Schnetzler C. C., Walter L. S., and Marsh J. G. (1988) Geophys. Res. Lett., 15, 357. Stauffer, P. H. (1978) Proc. of the Third Regional Conference on Geology and Mineral Resources of Southeast Asia, P. Nutalaya (ed.), p. 285.

MINERALOGY OF THE NON-ICE MATERIAL ON CALLISTO: CLUES FROM REFLECTANCE MODELING W.M. Calvin and R.N. Clark (U.S. Geological Survey, MS 964,Box 25046, Denver, CO 80225)

In the planetary community there has been some controversy regarding the amount of water ice present in the optical surface of Callisto. In order to help resolve this controversy an extensive modeling study was undertaken. After modeling over 65 thousand combinations fairly narrow limits for the ice grain size and weight fractions were obtained (Calvin and Clark, 1988). These limits allow an inversion of the model calculations to remove this amount of ice from the observed reflectance spectrum. This results in the reflectance spectrum for the non-ice material on the surface shown in figure 1. Three broad absorption features of mineralogical origin that can be observed in this spectrum: 1) a broad absorption centered over 1μm, which is associated with both oxidation states of iron, 2) a drop in reflectance from 0.7 to 0.3μm (the "red edge") with an indication of ferric spin forbidden bands, and 3) a strong absorption from 2.8 to 4μm associated with adsorbed water.

We might expect the non-ice material to be similar to meteoritic material and after examining spectra from the meteorite classes presented by Gaffey (1976) we found that the spectral absorption bands in the Callisto non-ice material resemble those observed in the spectra of primitive carbonaceous chondrites and E6 enstatite chondrites. Closer examination revealed that the similarities to the E6 chondrites could be accounted for by terrestrial weathering products rather than truly similar mineralogies.

Among the primitive (type CM and CI) carbonaceous chondrites we found the CM meteorite Nogoya provided the best match. The spectrum of Nogoya (from Larson et al.,1979) is also shown in figure 1, but its reflectance level has been scaled to that of the Callisto non-ice material. In the meteorite spectrum the 1μm absorption, the water absorption near 3μm, and the "red edge" all closely match the Callisto material. The 1μm absorption coupled with the spin forbidden absorptions in the visible indicate both ferric and ferrous iron. Barber (1981) has discussed that the hydrous silicates present in the matrix of the CM chondrites include iron-rich serpentines and berthierines. These silicates contain both ferric and ferrous iron and are hydrated and are therefore reasonable candidates for the Callisto non-ice material.

There are two major differences between the spectra in figure 1. First, the reflectance level of the meteorite, approximately 0.06, is four times lower than the level calculated for the Callisto non-ice material. Extensive modeling has shown this cannot simply be a grain size effect. So to account for the brightness of the material on Callisto there is possibly less carbon or fewer opaque minerals than in the C-chondrites. Second, the 3μm absorption is deeper and wider in the the Callisto material. It is probable that the original band due to hydrated silicates has been augmented due to surface comminution in the presence of ice. The Callisto non-ice material, although sharing similarities to the primitive carbonaceous chondrites, appears to be distinct from them.

Calvin and Clark, 1988 *BAAS*, 20, 876. Barber, 1981, *Geochim. Cosmochim. Acta*, 45, 945. Gaffey, 1976, *J. Geophys. Res.*, 81 905. Larson, Feierberg, Fink and Smith, 1979, *Icarus*, 39, 257.

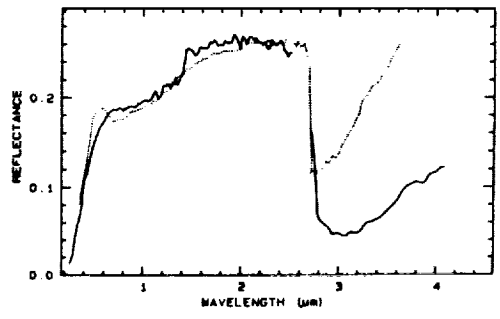

Figure 1: Reflectance of the non-ice material on Callisto (solid) and scaled reflectance of Nogoya (dotted).

HAZARDS FROM EARTH-APPROACHERS: IMPLICATIONS OF 1989 FC'S "NEAR MISS"; **C. R. Chapman**, Planetary Science Inst., 2030 E. Speedway, Tucson, AZ; **D. Morrison**, NASA Ames Research Center, Moffett Field, CA; and **E. Bowell**, Lowell Observatory, Flagstaff, AZ

The dramatic "near-miss" encounter of asteroid 1989 FC with the Earth March 23 has raised again the question of hazard posed by Earth-approaching objects. Had the object been at a very slightly different orbital longitude, its miss distance would have been only 450,000 km. Preliminary data suggests that the object may have been 200 m in diameter if it is a typical S-type, 400 m in diameter if it is a typical C-type, or even larger than these values if present discrepancies in measured magnitudes are resolved in favor of it being brighter than was first believed. The impact of such an object on the Earth would certainly have devastating local consequences. Its global consequences would also be significant, possibly large enough to threaten the existence of civilization according to the more pessimistic estimates of NASA's 1981 Snowmass Workshop (cf. Chapman and Morrison, 1989).

The consequences of impacts by asteroids and comets have not been studied in greater depth than the unpublished work of the 1981 workshop, despite advances in such related topics as the probable K-T boundary impact and nuclear winter. There have also been advances in risk assessment and, in particular, in understanding the psychological and societal responses to very large but uncommon catastrophes (e.g. Chernobyl). It is timely to reassess the issue of hazard from the perspectives of both risk assessment and the physical sciences. The latter include more thorough study of the population characteristics and the physical nature of Earth-approachers and the geological, atmospheric, climatological, and biological effects of their potential impacts onto the Earth.

The numbers of Earth-approachers are fairly well known, for sizes somewhat larger than that of 1989 FC, but our sampling of smaller objects is nearly nonexistent. Even during this exceptionally close pass, 1989 FC was nearly missed; after discovery, special efforts had to be mobilized to ensure that it was recovered during the following month so that it would not become permanently lost again. Those results indicate that the next close approach (although further away than this year) will not happen until about 2020. At most, only a few percent of objects like 1989 FC have been discovered so far. Similar close approaches with other objects like 1989 FC happen perhaps every 20 to 50 years; one in several thousand of those encounters actually hit the Earth. Thus it is important to discover these small objects, and learn as much about them as we can.

Current estimates of the numbers of Earth-approachers of various types are biased by observational circumstances. They are also biased by the physical traits of these bodies (e.g. high albedo objects are observed preferentially). Models for deriving Earth-approachers from source regions (Wetherill, 1988) suggest that most are typical main-belt asteroid fragments (including diverse compositions ranging from carbonaceous to metallic) but that about one-third are dead comets. Because of the probable differences in bulk density and cohesion of different types of Earth-approachers, their effects upon encounter with the Earth could be quite distinct.

Bibliography: C. Chapman and D. Morrison, 1989, "Cosmic Catastrophes" (Plenum, NY); G. Wetherill, 1988, Icarus, **76**, 1-18.

REE AND SOME OTHER TRACE ELEMENT DISTRIBUTIONS OF OLDHAMITE IN QINGZHEN (EH3) CHONDRITE. Yongheng Chen, Ernst Pernicka and Yangting Lin, Max-Planck-Institut für Kernphysik, D-6900 Heidelberg, F. R. G.; Daode Wang, Institute of Geochemistry, Academia Sinica, Guiyang, Guizhou, P. R. C.

The distribution of REE among enstatite chondrites has always been of interest for many researchers. Oldhamite which is one of several unusual minerals found in E-chondrites, has long been suspected of being the main REE carrier. Recently this fact was confirmed by Larimer and Ganapathy (1987) as well as Lundberg and Crozaz (1988). In this work we have determined the concentrations of REE and some other trace elements in oldhamite of Qingzhen, the most unequilibrated enstatite chondrite (EH3) so far collected in the world.

Before analysis polished sections of the meteorite were carefully examined under the microscope and minor element contents were obtained by electron microprobe analyses. Then several oldhamite grains were extracted with special tools under the microscope. Thus it was possible to obtaine single grains of oldhamite grains rather than powder samples. Until now we have extracted and analyzed by INAA three samples of rather pure oldhamite. The samples are from three different environments, namely from a metal-sulfide assemblage, an area with broken down djerfisherite ("Qingzhen reaction", El Goresy, 1985) and from the matrix. After each step of sample preparation the samples could be checked under the microscope. The samples were irradiated in quartz containers from which they were removed after irradiation in order to exclude possible interference by blanks from the quartz. The sample weights (0.5~0.8 μg) were checked by the Ca contents and the volumes of the grains ($0.2\sim0.4\times10^{-6}$cm^3).

The results obtained so far confirm that oldhamite is carrier of REE in E-chondrites. REE are enriched by factors of 110-210, 60-160 and 50-160 relative to CI respectively in all three samples. Using the bulk concentrations of REE and CaS content in Qingzhen (Wang, 1986; Kallemeyn and Wasson, 1986; Shima et al., 1983) one can calculate that the most primitive oldhamite sample from a metal-sulfide assemblage contains the entire inventory of all REE. On the contrary, the abundances of Sm and Yb are ca. 50% lower in the oldhamite sample from the matrix than in CaS from the metal-sulfide assemblage and Eu is depleted by 40% in the sample from the "Qingzhen reaction" area. Apparently they have experienced some redistribution of REE.

In contrast to E-chondrites of higher petrographic types (Larimer and Ganapathy, 1987) Sc is also enriched in all three samples (8-17×CI). This is further evidence for a high temperature origin of oldhamite. In addition and also in contrast with the literature, Cr and Zn are not enriched in the most primitive sample but rather depleted. These elements therefore may have been introduced by exchange during metamorphic processes. An interesting case is Se, which is also enriched in all samples (13-25×CI) indicating interaction with the gas phase at rather low temperatures.

El Goresy, A. (1985), *Meteoritics*, **20**, 639. **Kallemeyn, G. W. and Wasson, J. T., (1986),** *Geochim. Cosmochim. Acta*, **50**, 2153-2164. **Larimer, J. W. and Ganapathy, R., (1987),** *Earth Planet. Sci. Lett.*, **84**, 123-134. **Lundberg, L. L. and Crozaz, G., (1988),** *Meteoritics*, **23**, 285-286. **Shima, M. et al., (1983),** *Meteoritics*, **18**, 395-396. **Wang, D., (1986),** Collection of Geochemical Papers (Chinese), Beijing, p153-159.

COMPOSITION OF THREE RECENTLY FALLEN CHINESE ORDINARY CHONDRITES

Yongheng Chen and Ernst Pernicka
Max-Planck-Institut für Kernphysik, postbox 103980, D-6900 Heidelberg, F. R. G.
Daode Wang and Hou Wei
Institute of Geochemistry, Academia Sinica, Guiyang, Guizhou Province, P. R. C.

Three Chinese ordinary chondrites fallen in recent years (Wuan chondrite fell on July 31, 1986; Zaoyang chondrite fell on October 18, 1984; Zhaodong chondrite fell on October 25, 1984) were studied. Zaoyang and Zhaodong were already described petrologically (Hou Wei et al., 1986; Wang and Rubin, 1987). The contents of 21 elements (Na, Cr, Mn, Sc, Se, Zn, Br, Ni, Fe, Co, Ir, Cu, Ga, As, Au, Sb, Os, W, Re, Pt and Ru) in the magnetic fractions and 20 elements (Na, K, Ca, Sc, Cr, Mn, Fe, Co, Ni, Zn, Se, Br, La, Sm, Eu, Yb, Lu, Ir, Au and As) in the non-magnetic fractions were determined by INAA. Table 1 presents the bulk composition of each chondrite calculated from element concentrations in different phases.

The results indicate that Wuan and Zaoyang chondrites are compositionally and petrologically similar. They are classified as H6 and H5 chondrites respectively. However, the Co content (6.2mg/g) in kamacite of Wuan is higher than the upper limit of Co content (5.2mg/g) in kamacite of H-group chondrites reported up to date, which is near to the lower limit of Co content (6.5mg/g) in kamacite of L-group chondrites (Wang and Rubin, 1987; Afiattalab and Wasson 1980; Gomes and Keil, 1980). Since all other features are compatible with H chondrites, the range of Co contents in kamacite should be extended to 6.2 mg/g. Zhaodong chondrite shows the compositional features of L-group chondrites and is petrologically classified as type 4.

Table 1 Bulk compositions of three Chinese ordinary chondrites calculated from element concentrations in the magnetic and non-magnetic fractions

Contents / Samples	FeO %	FeS %	$Fe_{met.}$ %	CaO %	Na_2O %	K_2O %	MnO %	Cr_2O_3 %	Ni %	Co ppm	Ir ppm	Au ppb
Wuan	7.64	7.95	18.6	1.71	0.80	0.11	0.30	0.58	2.00	990	0.93	250
Zaoyang	6.70	8.58	17.6	1.71	0.81	0.091	0.30	0.56	1.91	910	0.88	235
Zhaodong	12.1	6.06	7.56	1.66	0.93	0.098	0.34	0.58	1.28	550	0.54	160
Contents / Samples	Sb ppb	Os ppm	Re ppm	Pt ppm	Sc ppm	Zn ppm	Se ppm	La ppb	Sm ppb	Eu ppb	Yb ppb	Lu ppb
Wuan	94	1.32	0.11	1.48	9.02	54.2	10.6	233	168	83	174	36
Zaoyang	81	1.21	0.11	1.12	8.77	51.5	11.1	298	170	76	180	29
Zhaodong	56	0.69	0.058	0.62	9.29	138	8.32	300	186	83	197	35

Aflattalab, F. and J. T. Wasson, (1980), *Geochim. Cosmochim. Acta*, **44**, 431-446.
Gomes, C. B. and K. Keil, (1980), Brazilian Stone Meteorites, 161pp.
Hou Wei et al., (1986), *Meteoritics*, **21**, 534-535.
Wang, D. and Rubin, A. E., (1987), *Meteoritics*, **22**, 97-104.

OXYGEN ISOTOPIC COMPOSITION OF LEW 86010; R.N. Clayton[1,2,3] and T.K. Mayeda[1]. [1]Enrico Fermi Institute, [2]Department of Chemistry, [3]Department of the Geophysical Sciences, all at the University of Chicago, Chicago, IL 60637, USA.

Oxygen isotope analyses were made on bulk meteorite and on pure separated plagioclase, pyroxene and olivine from LEW 86010, provided by G.W. Lugmair of U.C.S.D. Samples of Angra dos Reis were run at the same time for comparison. Results are presented in Table 1. The values of $\Delta^{17}O = \delta^{17}O - 0.52\delta^{18}O$ average -0.10, compared to -0.20 for nine eucrites (Clayton and Mayeda, 1983) and -0.21 for Angra dos Reis (Table 1). Furthermore, the mean $\delta^{18}O$ of nine eucrite whole-rocks is $+3.67 \pm 0.17$. These data confirm that LEW 86010 belongs to the HED (+ pallasites, mesosiderites and IIIAB) oxygen isotope group. LEW 86010 is indistinguishable from Angra dos Reis. An older analysis of pyroxene from Angra dos Reis gave $\delta^{18}O = 3.76$, $\delta^{17}O = 1.74$ (Clayton et al., 1976), in good agreement with the new analysis.

Analyses of separated minerals give mineral-pair isotopic fractionations, which can be used to estimate the temperature of last equilibration. The three minerals analyzed provide two independent isotopic thermometers. Temperature estimates are given in Table 2. The errors are based on ±0.2‰ uncertainties in the fractionation measurements, and assume no error in the calibration curves (Chiba et al., 1989). These thermometers are intrinsically insensitive at high temperatures, so that the errors are large. Within errors, the temperatures are concordant. The anorthite-olivine thermometer is the most precise and yields a temperature of 820 ± 80°C. For comparison, the fractionation observed for this mineral pair in lunar basalts is 0.78 ± 0.04 (three Apollo 12 basalts; Clayton et al., 1971) corresponding to 1170°C. Thus minerals in LEW 86010 record a sub-solidus equilibration at 800-900°C. The possibility of slow cooling, as indicated by mineral chemistry, has been discussed by McKay et al. (1989).

References: H. Chiba et al. (1989) (submitted to G.C.A.); R.N. Clayton et al. (1971) Proc. Lunar Planet. Sci. Conf. 2nd, 1417-1420; R.N. Clayton et al. (1976) E.P.S.L. **30**, 10-18; R.N. Clayton and T.K. Mayeda (1983) E.P.S.L. **62**, 1-6); G. McKay et al. (1989) Lunar Planet. Sci. **XX**, 675-676; M. Prinz et al. (1988) Lunar Planet. Sci. **XIX**, 949-950.

Table 1
Oxygen Isotopic Compositions of LEW 86010 and Angra dos Reis

Meteorite	Sample	$\delta^{18}O$	$\delta^{17}O$	$\Delta^{17}O$
LEW 86010	Bulk	3.55	1.70	-0.15
	Plagioclase	4.12	1.99	-0.15
	Pyroxene	3.67	1.86	-0.05
	Olivine	2.75	1.24	-0.19
	Bulk from mode*	3.58	1.76	-0.10
Angra dos Reis	Bulk	3.60	1.64	-0.23
	Pyroxene	3.61	1.67	-0.20

*Based on modal analysis of Prinz et al. (1988).

Table 2
Oxygen Isotopic Thermometry of LEW 86010

Mineral Pair	$\Delta^{18}O$	t(°C)*
Pc-Px	0.45	1040 ± 200
Px-Ol	0.92	690 ± 100
Pc-Ol	1.37	820 ± 80

*Based on calibrations of Chiba et al. (1989).

MAGNETIC PROPERTIES OF THE ESTHERVILLE MESOSIDERITE.
D.W. Collinson, Department of Physics, The University, Newcastle upon Tyne, NE1 7RU, England.

Evolutionary processes in meteorites, and magnetic fields in the early Solar System, both spatial and localized in planetary bodies, can leave their imprint in meteorites through the natural remanent magnetization (NRM) and other magnetic properties they impart to them. In the present investigation the Estherville mesosiderite has been studied to enquire whether its magnetic properties can help to resolve any of the uncertainties associated with mesosiderite history and evolution, and also indicate any magnetic fields to which it or its constituent fragments have been subjected.

The Estherville sample as received, 128g off BM 53764, British Museum, consists mainly of a very hard, compact matrix with only 5-10% by weight of large (3-10mm) iron-nickel fragments. It is strongly magnetized, with an initial NRM intensity of $1.4 \times 10^{-3} Am^2 kg^{-1}$. The NRM of individual fragments broken from the main mass, when referred to common reference axes, is scattered in direction on a scale which ranges from ~1cm down to ~1mm. Alternating field and thermal demagnetization show a range of magnetic stability among the samples and also some secondary NRM, indicating a variety of magnetic histories. Thermomagnetic analyses of matrix and iron-nickel separates show that the dominant magnetic carriers are kamacite and tetrataenite.

Anisotropy of magnetic susceptibility is significant in the matrix material, with lineation and foliation apparent. The maximum axes of the anisotropy ellipsoids of different fragments are scattered in direction when in situ in the main mass. Extracted iron-nickel masses possess reasonably stable NRMs of varying complexity, with initial NRM directions non-coherent. Tetrataenite and possibly schreibersite are present, together with dominant kamacite.

Preliminary interpretation of the above observations suggests the following. The non-coherent directions of NRM within the matrix implies the acquisition of an initial NRM by kamacite in the fragments prior to their final accumulation into the mesosiderite material, and the presence of an ambient magnetic field when the fragments were formed. If the tetrataenite carrying the primary NRM was formed from the previously magnetized kamacite during slow cooling after metamorphic heating, the maximum temperature during the latter event could not have been higher than ~700°C or the kamacite would have been remagnetized uniformly or demagnetized, according to whether or not there was an ambient magnetic field present.

The susceptibility anisotropy observations indicate the acquisition of anisotropic properties occurred before final accumulation of the meteorite. Shock and flow processes were probably important in producing foliation and lineation respectively. The scattered NRM of the iron-nickel fragments also indicates magnetization prior to emplacement, therefore favouring introduction in the solid rather than the molten form.

INFLUENCE OF BULK COMPOSITION ON OLIVINE CHONDRULE TEXTURES. Harold C. Connolly Jr., Roger H. Hewins, Geological Sciences, Rutgers University, New Brunswick, N.J. 08903

Experiments on a wide range of chondrule compositions (triangles) are shown in Figure 1, a plot of initial temperature versus molar Fe/(Fe+Mg). The squares of (1) and the closed circles of (3) are also shown. The charges show a systematic distribution of textures shown in Figure 1 as particular textural fields (GL,glass; BO, barred olivine; PO, porphyritic olivine; GO, granular olivine). The textural field boundaries are sub-parallel to the calculated equilibruim liquidus curve, which plots within the BO field. Charges show smaller, more abundant crystals and less obvious glass for lower initial temperatures, grading from PO to GO. Near liquidus heating induces rapid growth on the few remaining nuclei during cooling, producing BO. Charges heated above the BO field are quenched as glass.

The BO field represents charges with considerable textural diversity, not systematically distributed. Charges close to the liquidus are very sensitive to various chance factors. Random fluctuations in the size of the largest crystals and in the precursor mass which successfully adheres to the wire are responsible for textural irregularities in the BO field.

Transitional BO/PO textures are uncommon in nature but are observed. Synthetic BO/PO show equant crystals near the wire closure point. This could be due to excess Fe loss to the surrounding Pt wire or crystals sticking against the wire closure area, giving a higher local effective liquidus temperature and therefore, a porphyritic rather than a barred texture.

Natural chondrules show a wide range of composition and were probably generated simultaneously under very similar thermal conditions. The primary control on chondrule texture is therefore likely to be bulk composition, although variations in sphere size and precursor grain size could have had some influence.

REFERENCES (1) Bell, D.J., B.S. thesis, Rutgers University,1986 (2) Radomsky, P.M., M.S. thesis, Rutger University, 96pp.,1988. (3) Hewins, R.H., Radomsky, P.M., Connolly, H.C., Lunar Planet. Sci. XX, 412-413. (4) Connolly, H.C.,Jr., Radomsky, P.M. and Hewins, R.H. (1988) Lunar Planet. Sci. XIX, 205-206.

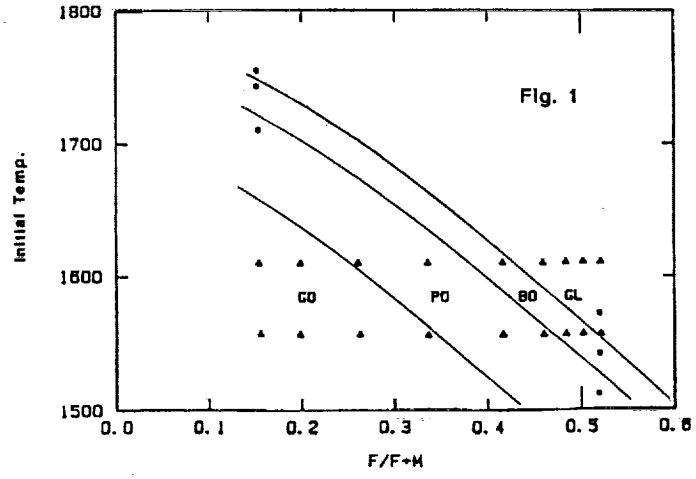

BASALTIC ACHONDRITES: DISCOVERY OF SOURCE ASTEROIDS; D.P. Cruikshank (NASA-Ames Research Ctr. and U. Hawaii), W.K. Hartmann (Planetary Sci. Inst.), D.J. Tholen and J.F. Bell (U. Hawaii), R.H. Brown (JPL)

We have found the first known Earth-approaching asteroids with spectra very similar to that of Vesta. The spectra resemble those of the howardite-eucrite-diogenite (HED) meteorites; these asteroids may deliver many HED meteorites from the asteroid belt.

The three Earth-approachers are 3551 1983 RD, 3908 1980 PA, and 1985 DO2. Our thermal flux measurements yield geometric visual albedos of the latter two averaging 0.32 ± 0.05, slightly higher than for Vesta. From these data we find diameters of 840 m, 680 m, and 3500 m, respectively. All three have deeper pyroxene bands than Vesta, suggesting coarser or absent regolith. The spectra of 3551 and 3908 are indistinguishable, and these two also have the closest orbits.

Vesta has been suggested as a parent of eucrites, but there is a puzzle of how they could be delivered from Vesta to Earth in the observed short cosmic ray exposure timescale of 10^7-10^8y (Drake, 1979). Further, the HED's appear chemically linked to pallasites, suggesting that they come from a completely disrupted parent with an interior core-mantle boundary, not just from the surface of a basaltic asteroid like Vesta (Wasson, 1985).

Our new observations resolve these problems. The asteroids have perihelia at 1.07, 1.04, and 1.22 AU, respectively. Their orbit intersections cluster near Earth's position in July and August. Strikingly, fall dates of HED's show a strong clustering at this time. Other clusters of HED fall dates suggest other undiscovered, small, basaltic achondrite Earth-approaching asteroids. That all three meteorite types share the same peak fall dates suggest that all three types may come from a single parent whose fragments have similar orbital histories.

We suggest that during disruption of a Vesta-like asteroid at least one large, HED-containing fragment was placed onto an Earth-approaching orbit. This fragment then underwent subsequent fragmentations during its passes through the belt, producing our three asteroids and probably others. Other peaks in the HED fall patterns may represent similar fragments. This evidence for the disruption of a Vesta-like body will help constrain models of asteroid evolution and asteroid-meteorite connections (see Davis et al., 1985).

Davis et al. (1985). Icarus 62, 30-53.
Drake, M.J. (1979). In Asteroids (Tucson: U. Arizona press).
Wasson, J. (1985). Meteorites (NY: W.H. Freeman).

MÖSSBAUER SPECTROSCOPY STUDY OF THE NICKEL - IRON ALLOYS IN METAL PARTICLES OF CHEROKEE SPRING LL6 CHONDRITE

J.Danon, I.Souza Azevedo and R.B.Scorzelli, Centro Brasileiro de Pesquisas Físicas - 150 Xavier Sigaud, Rio de janeiro, Brazil.

Cherokee Spring is an unbrecciated LL chondrite which has been submitted to a light shock event.

Mössbauer spectroscopy has been performed with the metal particles of the chondrite after separation from the silicates and troilite by HF treatment as described by J.Danon et al (1979). A relatively large proportion (46%)of tetrataenite has been identified from its hyperfine parameters, magnetic hyperfine field H_i=280 kOe and quadrupole splitting ΔE=0.18 $mm.s^{-1}$. A second spectrum (54%) exhibitshyperfine field H_i=322 kOe and broad linewidths. This spectrum is due to the supperposition of the spectrum from martensite (H_i=344 kOe) and that of a disordered taenite with a smaller hyperfine field.

In order to identify the nature of this disordered taenite phase further separation from martensite was performed by HCl (0.1 N) treatment of the metal particles. The Mössbauer spectrum after dissolution of martensite shows the tetrataenite phase (~ 35%) and the typical spectrum with H_i 315 kOe of a disordered taenite with 50% Ni content.

The coexistance of disordered and ordered 50-50 Ni-Fe alloys can be explained by the growth of tetrataenite in the disordered taenite with ν50% Ni content. This taenite originates by a mechanism of discontinuous precipitation in the stress areas of the meteorite, as described by Grokhovsky and Bevan (1983). We suggest that the ordering process leading to the formation of tetrataenite can be accelerated by the presence of solid state defects in the stress areas of the metal consequent to the shock event in the meteorite.

Danon,J., Scorzelli, R.B., Souza Azevedo,I. and Christophe Michel-Levy, M., 1979, Nature, 281, 469-471.

Grokhovsky, V.J. and Bevan, A.W.R., 1983, Nature, 306, 322-4.

SOLAR SYSTEM ABUNDANCES AROUND THE MAGIC PROTON TIN PEAK. J.R. De Laeter and K.J.R. Rosman and R.D. Loss, Curtin University of Technology, Perth, Western Australia, 6001.

Solar system abundance tables of the elements, which are largely based on the elemental abundance of the Cl chondrites, provide the basis for theories of nucleosynthesis and cosmochemistry. The basic processes which are involved in heavy element synthesis are the rapid-(r) and slow-(s) neutron capture processes, and the p-process, which plays an important role in the synthesis of the neutron deficient isotopes (1). The abundance N_s of an s-only process nuclide is inversely proportional to the neutron capture cross section σ (at astrophysical conditions), and directly proportional to the neutron fluence (2). Thus if σN_s is plotted as a function of mass number A, a smooth distribution is obtained, which corresponds closely to a theoretical distribution which assumes a steady neutron flow and an exponential distribution of neutron irradiations (3). The set of neutron capture cross sections (4) and solar system abundances (5) can be combined to produce Fig 1 for the mass region $100 \leq A \leq 150$.

The Maxwellian averaged capture cross section for ^{116}Sn has recently been remeasured (6) to give a value of 92 $\pm$ 5 mb (at kT = 30 kev), which is in good agreement with earlier determinations (4). This leads to a predicted abundance of 0.41 $\pm$ 0.03 (Si = 10^6 atoms) for ^{116}Sn from the σN_s versus A line of best fit, which is 26% lower than the meteoritic value. We have recently measured the abundance of tin in four carbonaceous chondrites by the mass spectrometric isotope dilution (MSID) technique to obtain a value of 3.98 (Si = 10 atoms) which is in excellent agreement with the currently accepted value (5).

Furthermore the s-only nuclide ^{110}Cd has a σN value of 50.9 (mb, Si = 10^6 atoms) as compared to the nucleosynthetic value of 41.5, based on the line of best fit as used by Beer et al. (6). Although the neutron cross section of ^{110}Cd had not recently been measured, the meteoritic value for Cd is firmly established (5) and is in good agreement with our MSID value (7). Whilst it can be argued that the meteoritic values for ^{116}Sn and ^{110}Cd can be reduced by taking into account a p-process contribution, the residual solar system abundances are still in excess of the values predicted by s-process systematics. Tin has a magic proton number, Z = 50, and the meteoritic abundances confirm the peak in this mass region.

REFERENCES (1) Burbidge, E.M. et al. (1957), Rev. Mod. Phys., 329, 547. (2) Clayton, D.D. et al. (1961), Annal. Phys., 12, 331. (3) Käppeler, F. et al. (1982), Astrophys. J., 257, 821. (4) Bao, Z.Y. and Kappeler, F.(1987), Atom. Data Nucl. Data Tables, 36, 411. (5) Anders, E. and Grevasse, N. (1989), Geochim. Cosmochim. Acta, 53, 197. (6) Beer, H. et al. (1989) Astron. Astrophys., (in press). (7) Loss, R.D. et al. (1984), Geochim. Cosmochim. Acta, 48, 1677.

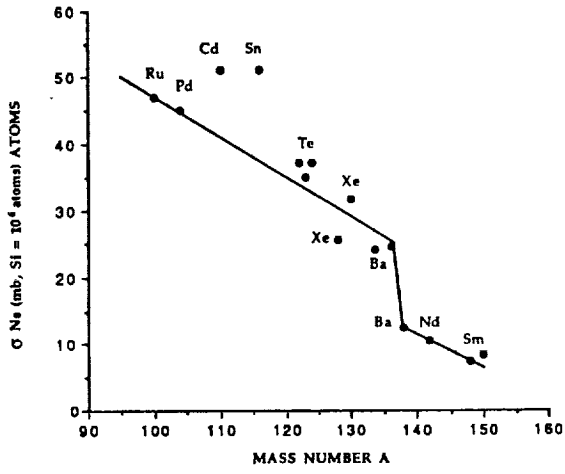

IN SITU ANALYSES OF TRACE ELEMENTS IN BASALTIC ACHONDRITE PLAGIOCLASE.

Jeremy S. **Delaney**[1] & S.R.**Sutton**[2]; (1)Dept Geology, Rutgers Univ., New Brunswick, NJ08903; (2) Dept Geophys. Sci, Univ. Chicago, Chicago, IL 60637 & Brookhaven National Lab., Upton, NY 11973

Introduction Trace element analyses of plagioclase in eucrites and mafic clasts from polymict achondrites have been made using the synchrotron X-ray fluorescence (SXRF) probe at BNL. The samples studied are from the Allan Hills (78040), Elephant Moraine (87520), and Lewis Cliff (85305, 86002, 86003, 87002, 87005, 87026)suites of Antarctic basaltic achondrites (Table 1). The elements Fe, Mn, Ni and Sr have been measured with detection limits of about 10 ppmw. Major element compositions were determined by electron microprobe.

Results Early work[1] on a few achondritic feldspars gave Fe/Mn ratios similar those of the mafic silicates but in this study we examine a systematic series of monomict and polymict samples from the achondrites. LEW85305 and EET87520 are unbrecciated eucrites with clean, well crystallized feldspar. The Fe/Mn ratios of these feldspars are however distinct (35-43 and 22-28, respectively) and are significantly different from the values for the mafic silicates (30-35 in both cases). Although the range of values (22-43) is less than for lunar samples (30 - 80), eucritic feldspars still show significant variations. In 87002, the Mg-rich eucrite (c.f. Binda), the plagioclase is packed with μm scale pyroxene inclusions that all SXRF data (beam size ≈30μm) probably reflect mixing between the true feldspar ratio and that of the pyroxene. In the polymict achondrites, feldspar has a wider range of absolute Fe concentrations (900-9000 ppm) and Fe/Mn values of the feldspar vary more than in individual monomict eucrites. Most breccias contain feldspar with generally constant Fe/Mn. (e.g. most ALHA78040 feldspars have Fe/Mn 34 - 38). In contrast, feldspar from breccia LEW87026 varies continuously from 27 to 40. In LEW86003, an augite-fayalite-silica-plag bearing lithic clast contains feldspar with Fe/Mn 37-69 coexisting with pyroxene havng ratios of 29-32 and olivine with Fe/Mn=34. The surrounding breccia and a large eucritic clast, however, have feldspar ratios of 29 -31 'coexisting' with mafics having ratios of 32 - 34. Sr concentrations range from 80 to 460 ppm. Eucritic feldspar is fairly homogeneous, as are grains in mafic clasts in polymict breccias. Feldspar in lithic clasts averages 110 - 200 ppm (fa-aug-SiO_2-plag clast in 86003 has 460 ppm). Feldspar mineral clasts (100-200ppm) fall within the range of the typical eucritic clasts

Discussion The feldspar in eucrites or mafic clasts has fairly constant Fe/Mn[3] but the observed ratios are not consistently higher or lower than the mafic silicates. The differences of Fe/Mn between the feldspar and the coexisting silicates do not, therefore, appear to reflect a simple partitioning. a Similarly, Fe/Mn ratios of lunar plagioclase are 30 - 80[2] and are much lower, in some instances, than the Fe/Mn ratios of the mafic silicates (≈80). The variability of plagioclase Fe/Mn on both the moon and the achondrite parent body appears to reflect process(es) other than the 'normal' igneous differentiation.

Possible mechanisms for differences in the ratios of the feldspar and mafic silicates include: {i} derivation from source regions with different initial ratios (possibly reflecting the time of formation); {ii} fO_2 variations during crystallization modifying substition of Fe into coexisting phases, {iii} impact induced assimilation by melts; {iv} volatilization of Mn; {v} fractionation of phases with very high Fe/Mn (metal?/spinel?/cordierite??) that radically modified the liquid Fe/Mn, Of these, {i} - {iv} are most likely to account for variability observed in the achondrites. A range of Fe/Mn ratios has been observed previously for olivine from polymict achondrites[3] and ascribed to variations in the source magmas that formed at different fO_2's. The properties of those magmas are, however, unknown since olivine is seldom in lithic clasts. The growth of feldspars in magmas from different source regions {i} is likely, but the causes of those differences are probably the result of mechanisms like {ii} fO_2 variation in the source regions or {iii} assimilation of wall rock during emplacement or impact. Reaction of melts that equilibrated in metal free environments with metal-bearing assemblages may provide a sufficient fO_2 contrast to account for the variability observed. Similarly fS_2 variation may have a comparable effect. Such mechanisms require that the oxidation state of Fe in feldspar is more sensitive to its environment than in the more Fe-rich mafics. The dependence of Fe/Mn ratios on the volatility needs to be studied by examination of the variability of similarly volatile elements in these systems. Na variations in achondritic feldspars are being examined for comaprison with Fe/Mn systematics. Fe/Mn data for mesosiderites and eucrites[1] suggest that mesosiderite plagioclase has lower Fe/Mn, perhaps because of metal reduction associated with metal - silicate equilibration but variations among achondrites are not so readily explained. Comparable Fe/Mn data for plagioclase from basaltic achondrites and many lunar rocks suggests that the basaltic achondrite planetoid and the Moon experienced similar surface, or near surface, early histories.

References: [1] Delaney, Sutton & Smith (1988) *LPSC XIX*,267-268; [2]Delaney, Sutton & Smith (1989) *LPSC XX*, 238-239; [3] Desnoyers (1982) *Geochim.Cosmochim.Acta* **46**,667-680.

METEORITES, CONCENTRATION MECHANISMS AT THE ALLAN HILLS, VICTORIA LAND, ANTARCTICA; G. Delisle and J. Sievers, Bundesanstalt für Geowissenschaften und Rohstoffe (BGR), Postfach 51 01 53, D-3000 Hannover 51, Fed. Rep. of Germany

We have constructed a subice topography map for the region between the Allan Hills and the Near Western Icefield (NWI) based on a radio echo sounding (RES)-survey in the field season 88/89. In addition, radio echo sounding data along a profile between the NWI and the Mid-Western Icefield (MWI) were gathered. 199 Meteorites, 56 on the NWI, 143 on the Allan Hills Icefield (AHI) were found.

As shown by the RES-data the AHI - an on average 300 m thick sheet of blue ice - covers a slightly westward dipping rock plateau. Likewise at the NWI, a thin (app. 100 m) sheet of blue ice rests again on a plateau with steep cliffs on both sides. The AHI and NWI are separated by a 1200 m deep depression, through which an ice stream moves from S to N. Segments of this ice stream are pushed onto the plateaus. We will present arguments showing that the amount of ice being pushed onto the plateaus is by and large balanced by losses of ice by sublimation on the blue ice fields.

Most meteorites from the AHI were found in an ice valley along the eastern boundary of the blue ice against the snow cover, which we take as strong evidence that most meteorites were windblown to their site of discovery. The more surprising was our observation that during a spell of warm weather almost 100 meteorites appeared on the flanks of the ice cliffs along the eastern side of the AHI - in areas which were searched a few days earlier with little success. We will report our observations, describe possible near ice-surface concentration mechanisms and present photographical evidence of an improvised ablation measurement suggesting an ablation rate of at least 1 cm/d at near zero temperatures.

U-Pb SYSTEMATICS IN ZIRCONS AND TITANITES, SHOCKED EXPERIMENTALLY UP TO 59.0 GPa. A.Deutsch[1], U.Schärer[2] and F.Langenhorst[1], [1]Inst. f. Planetologie, Univ. Münster, D-4400 Münster, F.R.G., [2]Univ.du Québec à Montréal, C.P.8888, Succ.A,Montréal, Canada H3C3P8.

Abraded zircons and titanite with concordant U-Pb ages were experimentally shocked up to 59.0 GPa at the Ernst-Mach-Institute (Weil/ Rhein) using the shock-wave reverberation technique (1).

X-ray and SEM investigation on the shocked zircons reveal a transition into polycrystalline grains with small, < 10 µm size domains at high pressures. The shocked titanites are characterized by lowering of the birefrigence, and increasing streakiness on Gandolfi X-ray photographs.

U-Pb dating results: Four small size fractions of **shocked zircons** yield slightly (< 3 %) discordant data (Fig. 1).No correlation between shock pressure and discordancy was observed. The discordia line defined by shocked and unshocked grains yields intercept ages of 1648 + 0.8/-0.7 and 103.8 + 79.1/-78.7 Ma (2 sigma).

Shocked **titanites** from a 59.0 GPa experiment show degrees of discordancy very similar to the zircons indicating less than 2 % of total U-Pb fractionation (Fig.2). Together with the unshocked grains they give a discordia line with intercept ages of 1642.2 + 2.6/-1.7 and 315.9 + 300.7/-294.2 Ma. Titanites shocked to 47.5 GPa plots slightly below this line.

Although errors are large on the lower intercept ages, they are statistically different from zero in both minerals. In consequence, shock-wave induced U-Pb fractionation cannot be the major cause for the up to 3% discordancy observed. Such small degrees of Pb loss are a common feature even in strongly abraded grains of Proterozoic zircons and titanite (e.g. 2).The results are in excellent agreement with U-Pb isotope systematics on highly shocked accessory phases from the Haughton impact crater (3). In the view of isotope data from naturally and experimentally shocked U-rich phases, shock-wave metamorphism is an unlikely mechanism to explain high degrees (> 90 %) of recent U-Pb fractionation in meteorites (for references and discussion see 4).

References:(1) MÜLLER WF & HORNEMANN U (1969) EPSL 7,251-264 (2) SCHÄRER U KROGH T & GOWER CT (1986) Cont Mineral Petrol 94, 438-451 (3) SCHÄRER U & DEUTSCH A, this volume (4) TERA F (1983) EPSL 63,147-166.

Fig. 1

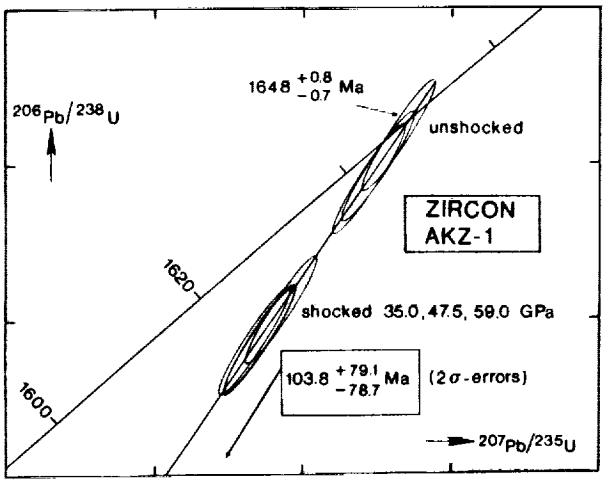

Fig. 2

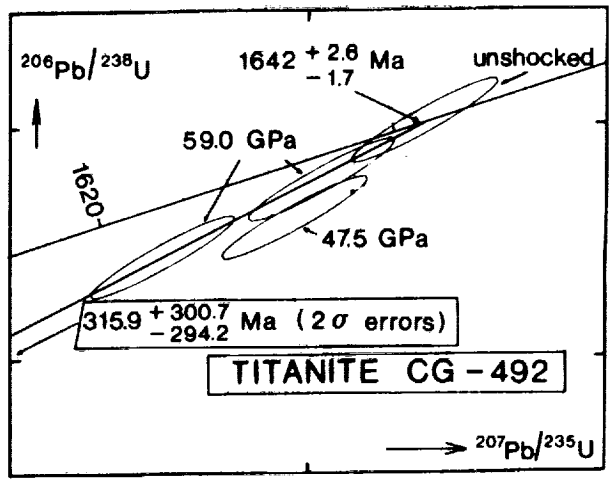

Ba and Th PARTITIONING BETWEEN IMMISCIBLE SILICATE MELTS: FURTHER EVALUATION OF THE ROLE OF SILICATE LIQUID IMMISCIBILITY IN THE PETROGENESIS OF LUNAR GRANITES; T. Dickinson and J. H. Jones, SN2, NASA Johnson Space Center, Houston, TX 77058

Silicate liquid immiscibility (SLI) has been proposed to have an important role in the petrogenesis of lunar granites by numerous workers (1,2,3,4,5). This is partially because fractional crystallization doesn't affect inter-element ratios of K, Th, Ba, and REE, but SLI can. Several inconsistencies and uncertainties remain, however, in our understanding of elemental fractionations during SLI. For example, Neal and Taylor (5) noted that there is a dichotomy between ^{Ba}D (defined as wt. % BaO in basic liquid / wt. % BaO in acidic liquid) determined by analysis of lunar basalts and those measured in laboratory experiments. In particular, ^{Ba}D determined for natural lunar immiscible melts is <1 (5), while experimentally-determined ^{Ba}D values tend to be >1 (6,7). Neal and Taylor (5) proposed that if the molar $(Na_2O+K_2O+CaO+BaO)/Al_2O_3$ ratio <1 then ^{Ba}D can be < 1 and if this ratio >1, then ^{Ba}D can be >1. Another problem is that lunar granites are enriched in Ba, U, and Th.But, based on charge density considerations, Th and U would be expected to partition strongly into the basic melt (6,8) and Ba is expected to be little affected by SLI. Precise two-liquid ^{Ba}D and ^{Th}D values need to be determined in order to further evaluate the role of SLI in the petrogenesis of lunar granites.

Our experimental charges consisted of a 50-50 mixture of the basic and acidic compositions (5), individually spiked with wt. % levels of BaO and ThO_2. The samples were placed in Fe-capsules and sealed under vacuum in fused silica tubes. Ba and Th charges were suspended in air in a Deltech furnace at 1070°C for 6 days and then quenched in water. In addition, a Ba charge was held at 1055°C for 6 days in an attempt to determine the effect of T on Ba partitioning. Charges were analyzed using a Cameca electron probe with counting times for Ba and Th of to 30 and 50 seconds, respectively. The 1055°C Ba charge produced only one glass composition (presumably acidic) and crystals. Ba and Th charges held at 1070°C consisted of basic glass coexisting with acidic glass, which contained spheres of basic glass within it, together with 5-10% crystalline phases. The acidic glass in the Ba and Th charges contained silica crystals. The acidic glass in the Th charge also contained a small ilmenite-rich region. Our ^{Ba}D value is 1.16 (± 0.16) and ^{Th}D is 6.92 (± 2.9). Our ^{Ba}D is a factor of 2 higher than that of (5), but similar to the ^{Ba}D measured in other experiments (6). However, our Ba charge had an "alkali"/Al ratio more similar to previous experiments than observed in lunar basalts. There is a considerable difference between the compositions of the two liquids in the Ba and Th charges. It is possible that incomplete separation of phases occurred in the Ba experiment, thus, giving a minimum ^{Ba}D. However, it has been shown that equilibrium liquid compositions in the system K_2O-Al_2O_3-FeO-Si_2O change with the addition of a fifth component (6). Thus, an alternative explanation for the compositional differences between the Ba and Th charges is that the field of immiscibility expands or contracts with addition of Ba or Th.

Lunar granites are extremely enriched in Ba, K, and Th relative to mare basalts and KREEP. Ba/La, Th/La and K/La ratios are a factor of 3 to 27, 4, and 13 greater in lunar granites than in mare basalts and KREEP (5). Even though the ^{Ba}D may be slightly less than or greater than one, Ba can effectively fractionate from La during SLI, because of the large difference in their D values. Ba/La ratios can change by a factor of 9-10 as a result of SLI, assuming 10% acidic liquid is formed and using D values measured in P_2O_5-bearing systems (7). Based on measured D values, Th and La should both partition into the basic melt. Th/La ratios observed in granites can be produced from those in mare basalts and KREEP by SLI, assuming 10% acidic liquid is formed, followed by 15% fractional crystallization of whitlockite. K/La ratios can increase by a factor of 45 during SLI. However, SLI, with or without whitlockite fractionation, will not elevate the absolute Ba, Th, and K abundances relative to those in mare basalts and KREEP, as observed in granite. This doesn't rule out the possibility that SLI is important in the formation of lunar granites, but does require a source extremely enriched in these elements. If it is assumed that granites are formed only by SLI, with no whitlockite fractionation, then the liquid composition prior to unmixing would have to have had Ba, La, and Th abundances at least 4 times greater than that of urKREEP (11). If whitlockite fractionation occurred after SLI, then the original liquid composition would have to have been even more enriched in Ba, La and Th, assuming mare basalt Ba/La and Th/La ratios prior to unmixing. If whitlockite fractionation preceded SLI, then again, extreme enrichments are required. In particular, Th in the liquid immediately prior to SLI would have had to have been 14 times urKREEP.

Ref. (1) Rutherford and Hess (1975), LS VI, 696-698. (2) Hess et al. (1975), PLSC 6, 895-909. (3) Rutherford et al. (1974), PLSC 5, 569-583. (4) Rutherford et al. (1976), PLSC 7, 1723-1740. (5) Neal and Taylor (1989), PLSC 19, 209-218. (6) Watson (1976), Cont. Min. Pet. 56, 119-134. (7) Ryerson and Hess (1980), GCA 42, 921-932. (8) Hess and Rutherford (1974), LS V, 328-330. (9) Bence and Albee (1968) J. Geol. 76, 382-403. (10) Longhi (1989) LS XX, 586-587. (11) Warren and Wasson (1979) Rev. Geophy. Space Phys. 17, 73-88.

A STUDY OF SURFACE CONDITIONS AND SEDIMENT ACCUMULATION IN BLOWOUT AREAS OF ROOSEVELT COUNTY, NEW MEXICO, AS EVIDENCE FOR METEORITE CONCENTRATION MECHANISMS; B.D. Dod, Dept. of Physics and Earth Sciences, Mercer University, Macon, GA, R.T. Urbanik and P.P. Sipiera, Schmitt Meteorite Research Group, Harper College, Palatine, Il.

Large numbers of meteorites have been collected from blowout and sandhill areas of eastern New Mexico, with nearly two hundred coming from Roosevelt County alone. It represents one of the most significant locations for the collection of meteorites outside of Antarctica. One reason for this can be attributed to the small amount of rock in the soil and the prevailing semi-arid climate. It is presently believed that meteorites tend to concentrate in large numbers due to a combination of slow weathering rates and possible transportation by wind and water.

In an attempt to further understand the concentration mechanisms involved, over 600 pieces of gravel were collected from a typical blowout and examined for rock type, mass, and density. These gravels range in size from 3mm to 69mm, and have a mass range from .03 grams to 66 grams. Based on that data, the present study was designed to examine possible mechanisms involved with the transport of these gravels across the blowout. By taking the broader perspective into account, it was assumed that the channel bed through which the larger gravel traveled was relatively level, with initial gravel positioning taking place within the turbulent boundary layer. That assumed, two types of drag forces would be involved in their transport. The first is skin friction, the force along the exposed surface of each particle required to rotate it above the plane of the channel bed. This rotation would be about the axis of least resistance. Once rotated, the particle is then exposed to pressure drag which can be as much as an order of magnitude greater than skin friction drag. Because the orientation of the particles within the bed are not known, a priori, an average hydraulic diameter and the surface area were determined for each piece of gravel examined. Next the Reynolds number and skin friction and pressure drag coefficients were calculated for each particle. The force that each particle was exposed to during transport was then compared to one-half of the weight of the particle which would be sufficient to rotate the particle.

Of the 350 specimens thus far examined, preliminary data indicates that an air velocity of 19.8 meters per second would be required to rotate 2/3 of the sample particles out of the plane of the channel. Once exposed to the flow of the fluid, an air velocity of approximately 6.3 meters per second is required to maintain the movement of the particle. Because there is nearly three orders of magnitude difference between the density of the air and that of water, it is readily apparent that a low velocity stream would be sufficient to transport these particles. Transportation by water has always been a possible, but unlikely, concentration mechanism for the meteorites. It is not ruled out, but wind transportation for the smaller and in situ density settling during deflation for the larger, are more probable. An additional factor may be realized from further examination of these gravels from the Ogallala Formation, with special attention given to those which have similar densities to that of stony meteorites. It is eventually hoped that the data gained here may lead to a better understanding of the concentration mechanisms present on the ice and the development of the moraines in Antarctica.

H CHONDRITE CLUSTERS AND STREAMS; R.T. Dodd, Department of Earth and Space Sciences, State University of New York at Stony Brook, N.Y. 11794, U.S.A.

H chondrites do not fall randomly throughout the year but show five statistically significant concentrations, or clusters, three of which appear in Figure 1. Two of these, No. 2 (days 240-265) and No. 3 (days 275-300), consist chiefly of H5 chondrites with diverse CRE ages, but show systematic differences in times of fall (Figure 1) and other fall parameters. These distinctions and different cosmogenic isotope relationships (Figure 2) suggest that Clusters 2 and 3 sample two coorbital streams of meteoroids, the former in orbits of high inclination and the latter in orbits of low inclination (Nyquist and McDowell, 1985). A concentration of H6 falls between Clusters 2 and 3 in Figure 1 appears to represent a third cluster (No. 5), which samples yet another stream. Isotopic data (Figure 2) weakly support the dynamic evidence for this H6 stream but are too few to establish whether H4 chondrites traveled with the other petrologic types or in one or more separate streams. It is thus unclear whether the three streams described here are petrologically homogeneous or somewhat genomict.

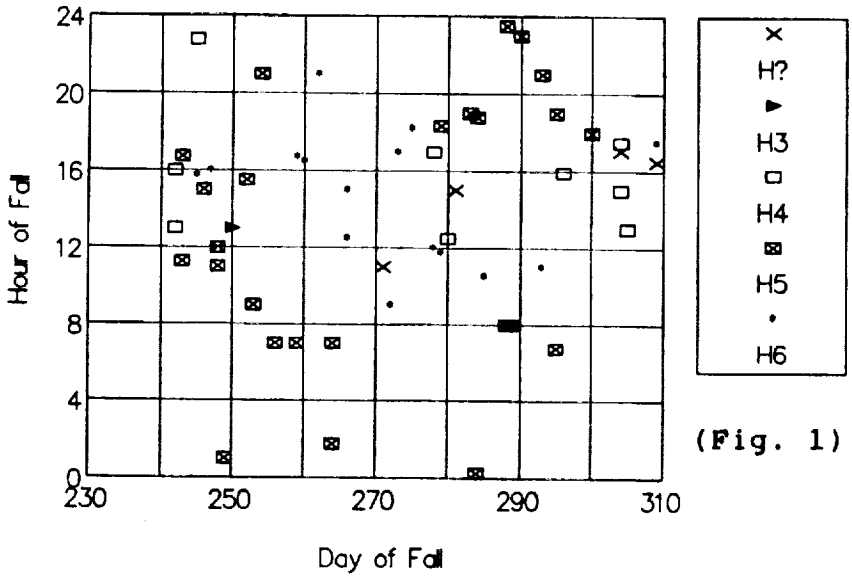

(Fig. 1)

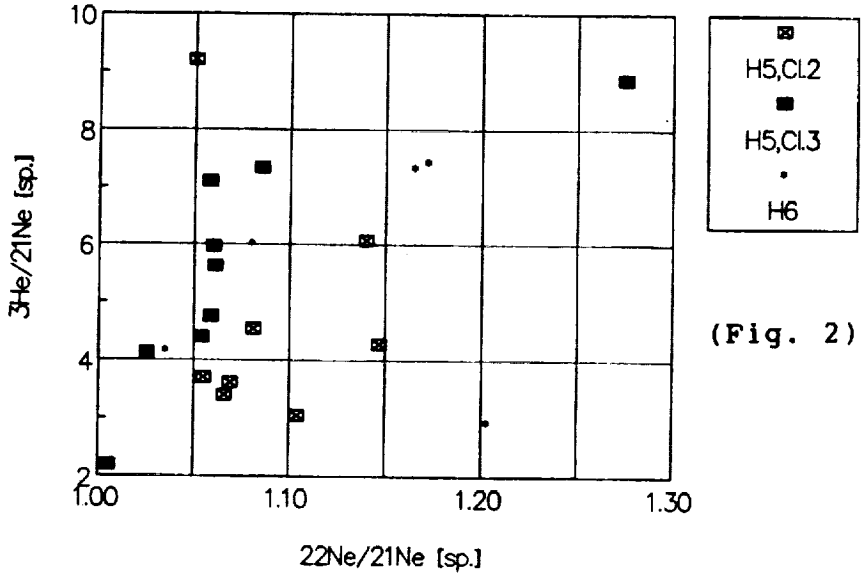

(Fig. 2)

Reference: Nyquist, L.E. and McDowell, A.F. (1985) Lunar Planetary Science XVI, 625-626.

THERMAL STATE OF THE EARLY EARTH; Michael J. Drake, Lunar and Planetary Laboratory, University of Arizona, Tucson, Arizona 85721, U.S.A.

There is a general consensus that the Earth accumulated from planetesimals and was substantially melted 4.5 Ga ago. For example, if the Moon formed in a giant impact, the mantle of the Earth and even portions of the core would be melted and, perhaps, partially vaporized. The magma ocean hypothesis developed to account for early lunar differentiation suggests similar consequences for the Earth. Phase equilibrium studies (Takahashi, 1986; Ito and Takahashi, 1987) have shown that the liquidus and solidus of a composition appropriate for the upper mantle of the Earth converge at about 170 kbar and 2000°C, an observation consistent with, although not requiring, substantial melting of the early Earth.

Surprisingly, a number of geochemical considerations conflict with this conclusion. These considerations derive from the chondritic elemental abundance ratios for many element pairs in the Earth's upper mantle. The probability that these elemental ratios will remain chondritic during large scale melting and crystallization may be tested with measured partition coefficients of plausible liquidus phases. These liquidus phases are Mg-perovskite at pressures above about 220 kbar, majorite garnet between 170 kbar and 220 kbar, and olivine at pressures below 170 kbar.

Kato *et al.* (1987, 1988a,b) have reported partition coefficients for a substantial suite of elements between Mg-perovskite and silicate liquid. Kato *et al.* find that most of the partition coefficients deviate from unity, and conclude that ratios of many refractory element pairs would deviate markedly from chondritic values with relatively small amounts (10%-30%) of fractionation of Mg-perovskite. Likewise, Kato *et al.* (1987, 1988a) and Ohtani *et al.* (1988) have shown that the ratios of many refractory element pairs will deviate markedly from chondritic values with relatively small amounts (10%-30%) of fractionation of majorite garnet.

At pressures lower than about 170 kbar, olivine is the stable liquidus phase. Agee and Walker (1988) have proposed that the high Mg/Si ratio in the upper mantle compared to CI chondrites results from mixing into the upper mantle of up to 30% olivine after solidification of a terrestrial magma ocean. McFarlane *et al.* (1989) have experimentally determined olivine/melt partition coefficients for Ni, Co, Sc, and La, elements present in the upper mantle in chondritic ratios, to test this novel proposal. They conclude that the Sc/La ratio will be unaffected by addition of 30% olivine into the upper mantle, but the Ni/Co ratio will deviate by 20-25% from chondritic.

One conclusion which is consistent with these observations is that the Earth was never significantly melted. This conclusion requires reevaluation of our models of accretion. In particular, it seems difficult to make the Moon in a giant impact. It also raises questions concerning why the much smaller Moon apparently did melt significantly. An alternative possibility is that the Earth did melt substantially but, in the ensuing magma ocean stage, crystals remained entrained in magma and did not fractionate elemental ratios from their original values (Tonks and Melosh, 1989). This possibility would resolve the paradox by eliminating the mechanism for fractionation. In either case, the high Mg/Si ratio of the upper mantle would be a primordial feature of the upper mantle. If the chondritic meteorites are indeed from the asteroid belt, as is generally assumed, then the accretional process was such that mixing between 1 AU and 2-4 AU did not occur.

References: Agee C.B. and Walker D. (1988) *Earth Planet. Sci. Lett.* **90**, 144. Kato T., Irifune T., and Ringwood A.E. (1987) *Geophys. Res. Lett.* **14**, 546. Kato T., Ringwood A.E., and Irifune T. (1988a) *Earth Planet. Sci. Lett.* **89**, 123. Kato T., Ringwood A.E., and Irifune T. (1988a) *Earth Planet. Sci. Lett.* **90**, 65. McFarlane E.A., Drake M.J., and Gasparik T. (1989) This Volume. Ohtani E., Moriyama J., and Kawabe I. (1988) *Chem. Geol.* **70**, 147. Tonks W.B. and Melosh H.J. (1989) *Lunar Planet. Sci.* **20**, 1124.

CHEMICAL CONSEQUENCES OF HIGH TEMPERATURE OXIDIZING CONDITIONS IN THE SOLAR NEBULA: DIAGNOSTIC SIGNATURES AND NEW CONSTRAINTS. Karin Ehlers and Bruce Fegley, Jr., Department of Earth, Atmospheric & Planetary Sciences, Massachusetts Institute of Technology, Cambridge, MA 02139, USA.

Introduction. Fegley and Palme(1,2) proposed that the common Mo and W depletions (relative to other refractory metals of similar volatilities) in Ca,Al-rich inclusions in carbonaceous chondrites resulted from high temperature oxidation in the solar nebula. Since their proposal, other groups (3-5) have presented additional evidence that scheelite and fayalitic rims on olivines also were formed by high temperature oxidation in the nebula. However, an opposing viewpoint has been advanced by others (6-8) who claim that oxidizing conditions at lower temperatures (presumably in planetary environments) caused many of these effects. The purpose of this work is to provide a comprehensive theoretical study of the chemical consequences of high temperature oxidizing conditions in the solar nebula in order to identify possible diagnostic signatures and new constraints. We will attempt to answer the following important questions:
(1) What unambiguous evidence (if any) shows that scheelite, Mo and W depletions, fayalitic rims on olivines, etc. are planetary (instead of nebular) products?
(2) What range of oxidizing conditions existed in the solar nebula in the high temperature regions where CAI's and their constituents formed?
(3) What mechanism was responsible for the production of high temperature oxidizing conditions in the solar nebula? Was more than one mechanism operative at a particular time and/or place in the nebula? Was an equilibrium or a non-equilibrium process involved?
Results and Discussion. Our preliminary results focus on phosphorus and the refractory metals which are both constituents of Fremdlinge(3,4,7,9-11). First, we find that possible signatures of high temperature oxidation include phosphate/silicate assemblages in Fremdlinge because at high O/H atomic ratios Fe_3P no longer condenses prior to phosphate. Second, atomic O/H ratios where loss of Os, Re, Ir, etc. will occur at "typical" temperatures of 1600 K (for CAI's) provide constraints on just how oxidizing the nebula could be. Third, carbon and nitrogen gas chemistry (e.g., CO/CO_2 and N_2/NO_x ratios) also provide potential constraints. These will be discussed in more detail at the meeting.
Acknowledgments. This work was supported by NASA Grant NAG9-108 to MIT. We thank D. Kong and A. Wandtke (both in the MIT UROP program) for their help.
References. (1) Fegley & Palme 1984 Meteoritics 19,225,(2)Fegley & Palme 1985 EPSL 72, 311, (3) Armstrong et al GCA 49, 1001, (4) Bischoff & Palme 1987 GCA 51, 2733, (5) Palme and Fegley 1987 LPS XVIII, 754, (6) Blum et al 1988 Nature 331, 405, (7) Blum et al 1989 GCA 53, 543, (8) Beckett et al 1988 GCA 52, 1479,(9) Wark 1984 Ph.D. thesis, Melbourne, (10) El Goresy et al 1979 Meteoritics 14, 390, (11) El Goresy et al 1978 Proc. 9th LPSC, 1279.

ALLENDE TE REVISITED I: PETROGRAPHIC ANATOMY AND MINERAL CHEMISTRY. A. El Goresy[1], E. Zinner[2], and C. Caillet[1,3]; [1]Max-Planck-Institut für Kernphysik, POB 103980, D-6900 Heidelberg, FRG; [2]McDonnell Center for the Space Sciences and the Physics Department, Washington University, St. Louis, MO 63130, USA; [3]Laboratoire de Petrologie Mineralogique, Universite P. et M. Curie, Paris VI, 75252 CEDEX 05, France.

TE is a petrologically complex F CAI (Dominik et al., 1978; Clayton et al., 1984) consisting of two distinct lithologies: A. An assemblage of Ca-bearing forsterite (1.22 - 1.70 CaO) and fassaite (4.2 TiO_2, 16.1 Al_2O_3). This lithology comprises more than 70% of the volume of the CAI. B. Xenoliths of spinel + fassaite and spinel + melilite (Ak_{82}). The xenoliths are located near the border of the CAI with sharp contact to lithology A. They were probably injected into lithology A while it was partially molten and after the formation of the rim layers around lithology A. Subducted rim layers of the olivine-rich lithology below several xenoliths support this interpretation. Consequently, A and B have distinct rim layers with different histories. The rimming sequence around A (older sequence) is (from inside out): Diopside (< 0.06 TiO_2, 0.63 Al_2O_3) - Fe-diopside (3.5 FeO) - pure andradite - spinel - hibonite (1.10 TiO_2, 1.25 MgO) - corundum (0.12 CaO, 0.30 FeO, 0.04 MgO). Corundum occurs only in the cores of composite grains with spinel veneers separating it from the outermost layer of hibonite. The rimming sequence around lithology B (younger sequence) is: spinel - fassaite - anorthite - spinel (13.2 FeO) - hibonite (2.68 TiO_2, 2.16 MgO). Anorthite replaced fassaite, indicating substantial loss of TiO_2 during formation of the rim. Alteration of A and B led to different assemblages: In lithology A, removal of fassaite and condensation of wollastonite + fayalitic olivine (0.03 CaO, 0.20 MnO, 11.5 FeO). In B, alteration led to removal of fassaite and to FeO enrichment in spinel. In order to document the petrologic evolution of TE, a detailed oxygen and magnesium isotopic study by ion microprobe mass spectrometry was initiated. For this purpose, various documented cores were drilled out of the polished thin section (PTS). Before drilling, the selected areas were studied in detail with the SEM and the minerals were analyzed with the electron microprobe. Cores were drilled from the interior of A, altered areas of A, interior of a lithology B xenolith, and rim layers of another xenolith. The results of the isotopic investigations are given in a companion abstract (Zinner et al., 1989).

REFERENCES: Dominik et al., (1978) *Proc. 9th Lunar Planet. Sci. Conf., 1249*; Clayton et al. (1984) *GCA* **48**, *535*; Zinner et al. (1989) *this volume.*

IS COMET HALLEY A SOLAR NEBULA CONDENSATE ? S. Engel, J.S. Lewis, and J.I. Lunine (LPL/U. of Arizona)

Comets are the best probes of the physical and chemical conditions in the outer solar nebula during planet formation despite the controversy regarding their formation environment.

The comet Halley data show high abundances in CH_4, CO_2 and NH_3 which seem at first glance inconsistent with a solar nebula origin. However, a model was developed to explain the volatile composition (CO, CH_4, CO_2, N_2, NH_3) in comet Halley as a solar nebula condensate. Assumed was a CO-N_2- dominated outer solar nebula and elemental abundances were calculated for a distance 20 AU from the sun. Mixing rates applied range from inefficient mixing to efficient mixing.

Besides calculating gas phase abundances at certain temperatures a number of other processes were included in the model: 1) a change in the elemental O to C ratio to lower values in the inner region of the nebula due to diffusive redistribution of water vapor [1], 2) surface catalyzed reactions on metal grains which lower quench temperatures [2], 3) mixing of molecular species from the inner, chemically active part of the nebula to the region of comet formation [3,4] 4) fractionation due to clathrate-hydrate formation and condensation of volatiles in the outer (colder) part of the nebula.

For a quench temperature of 700 K and roughly 10% mixing efficiency for CH_4 and CO_2 from the inner solar nebula into the CO-rich outer solar nebula the carbon composition in comet Halley can be explained with our model. Unfortunately the same scenario doesn't explain the nitrogen abundances. The N_2/NH_3 ratio measured in comet Halley is lower then the one calculated for the solar nebula. On the other hand, an interstellar origin for NH_3 seems to be possible. Icy planetesimals could have been accreted in molecular clouds that show high abundances in NH_3, CO, CO_2 and H_2CO. These cometesimals then would have been mixed with cometesimals formed in the outer solar nebula and accreted into a cometary parent body. In general this would support the view of a comet as an agglomerate.

Our results show that while some molecules (CO, CH_4, CO_2) indicate a solar nebula origin for comet Halley, others suggest contamination by interstellar material (NH_3, H_2CO). This would imply, that at least in the outer part of the nebula mixing was imperfect.

References:

[1] Stevenson D.J. and J.I. Lunine (1988) Icarus 75, 146-155.
[2] Vannice M.A. (1975) J. Catalysis 37, 146.
[3] Stevenson D.J. (1988) submitted to Astrophys. J..
[4] Prinn R.G. (1988) submitted to Astrophys. J..

SECONDARY ION MASS SPECTROMETRY OF CAPE YORK

E. U. Engström, Department of Physics,
Chalmers University of Technology, S-412 96 Gothenburg, Sweden.

Taenite, kamacite and troilite from the Agpalilik mass of the Cape York meteorite (e.g. Buchwald 1975) has been elementally mapped using imaging and analytical SIMS. The samples were analyzed using a 17 keV O_2^+ primary ion beam. Mass spectra from the selected areas were acquired in both negative and positive secondary ions.

The main interest has been focused on the elemental distribution close to the troilite phase. Furthermore, an investigation of the isotopic effect of the nickel diffusion between kamacite and taenite has been made.

1. BUCHWALD V.F. (1975) *Handbook of Iron Meteorites.* University of California Press, 1418 pp.

PELARDA FORMATION (EASTERN IBERIAN CHAINS, NE SPAIN) - CONTINUOUS DEPOSIT OF THE AZUARA IMPACT STRUCTURE; K.Ernstson, Fakultät für Geowissenschaften, Universität Würzburg, Pleicherwall 1, D-8700 Würzburg, F.R.Germany. F.Claudin, Museu de Geologia, Barcelona-08003, Spain.

The Azuara structure in northeast Spain is a complex impact structure of Lower Tertiary age with a diameter of more than 30 km (Ernstson et al., 1985, 1987; Fiebag, 1988). Recently, we identified an extended (about 12 x 2.5 km^2) and up to 200 m thick continuous deposit (Oberbeck, 1975; Morrison and Oberbeck, 1978; Hörz et al., 1983) of ejecta some 25 km distant from the center of the structure. This Pelarda Formation was described originally as a Tertiary fluvial boulder conglomerate (Carls and Monninger, 1974). Our observations show:

heavily striated pebbles and boulders - fractured and squeezed components; quartzite boulders with open fractures and offsets in the millimeter range prove plastic deformation under high confining pressure - the contribution of Buntsandstein megablocks to the Pelarda Formation - the presence of multicolored Lower Tertiary marls intimately admixed with the conglomerates - shock-metamorphic effects in quartzite components.

We conclude that the Pelarda Formation cannot be a fluvial deposit. A formation in the course of the Azuara impact event offers a reasonable alternative. Statistical analyses of the striae azimuth and the normals to locally developed bedding planes exhibit a significant correlation and coincidence with the theoretical ejection azimuth. The shock effects within the quartzite boulders suggest that the conglomeratic component of the Pelarda Formation originates from the target region as primary ejecta (Oberbeck, 1975). On the other hand, the intermixed Lower Tertiary marls are assumed to be local substrate indicating secondary cratering as a consequence of ballistic transport. Further investigations have been initiated.

References: Carls P. and Monninger W.(1974) N.Jb.Geol.Paläont.Abh., 145, 1-16. Ernstson K. et al.(1985) Earth Planet.Sci.Let., 74, 361-370. Ernstson K. et al.(1987) Meteoritics, 22, 373. Fiebag J.(1988) Diss.Univ.Würzburg, 271 p. Hörz F. et al.(1983) Rev.Geophys. Space Phys., 21, 1667-1725. Morrison R.H. and Oberbeck V.R.(1978) Proc. Lunar Planet.Conf. 9th, 3763-3785. Oberbeck V.R. (1975) Rev.Geophys. Space Phys., 13, 337-362.

C. 2

AN ALUMINIUM-RICH PYROXENE IN THE NINGQIANG CHONDRITE (CV3) REFRACTORY INCLUSIONS Hong Fang*, Xizhang Feng*, Chifang Chai*, Ziyuan Ouyang#
*Institute of High Energy Physics, Academia Sinica, P.O. Box 2732, Beijing, China; #Institute of Geochemistry Academia Sinica, Guiyang, China.

Pyroxgene is one of the mineral components of chondrite refractory inclusions. In the inclusions of the Allende meteorite, the contents of Al2O3 in pyroxenes are generally below 22 wt. percent (Grossman,1980).Here we report a unique pyroxene having extraordinarily high Al content in the refractory inclusions of the Ningqiang chondrite (CV3).

The Al-rich pyroxenes are only found in the coarse-grained and relatively large inclusions. For example,the inclusions PM010 and S4-8 (see Table 1) are the largest among the inclusions which have been studied in the meteorite ,about 6-8mm in size. The major minerals of the inclusions are melilite and spinel, other associated minerals have diopside, anorthite and hibonite. The grains of major minerals vary in size from several micron to several hundred micron. The grains of Al-rich pyroxenes are usually very small ,about < 5 micron, usually distributed in the dark fissures between the major minerals. We do not know their optical properties now. But we can determine the presence of the minerals by their bright blue luminescence, which was not found in any other minerals of the meteorite, when they were analyzed with an electron microprobe. Several electron microprobe analyses showing the ranges in compositions of pyroxenes from the two coarse-grain inclusions are given in Table 1. The results show that all of them have pyroxenes stoichiometry . The highest Al2O3 contents in some pyroxenes can reach over 49 wt. percent that is much higher than those previously reported in natural pyroxenes. An only comparable Al-rich pyroxene composition is TS8-F2-(7) in an amoeboid aggregates of Allende with 45 wt%. Al2O3 (Grossman,1975). FeO contents in S4-8-7 and S4-8-8 are relatively high to many pyroxenes of other refractory inclusions of the meteorite, and in some cases FeO are lack .The contents of TiO2 and Al2O3 seem to exhibit a negative correlation. CaO contents range from 7.46 to 25.85 wt. percent. In terms of the compositions of the pyroxene we present that it is likely a new sub-type of pyroxene which have not been well known .

Table 1. Analyses from the pyroxenes in the Ningqiang inclusions

Inclusion	PM010			S4-8			
Name	10a-2	10a-15	10ab-1*	S4-8-7	S4-8-8	S4-8-10	S4-8-18
Na2O	0.02	--	--	1.74	0.07	--	--
CaO	18.19	11.09	14.34	7.46	8.70	11.80	25.85
MgO	12.66	12.74	12.50	11.86	12.16	8.85	1.80
TiO2	3.08	--	--	0.16	0.19	--	--
SiO2	32.92	27.31	30.29	24.73	23.39	31.05	32.89
Cr2O3	0.20	--	--	0.13	0.20	--	--
Al2O3	32.11	49.29	42.86	48.43	48.39	49.30	36.82
FeO	0.10	--	--	4.41	3.80	--	0.23
Total	99.28	100.48	99.99	98.91	98.70	100.28	97.29
	Numbers of cation on the basis of 6(O)						
Si	1.1903	0.949	1.0669	0.8905	0.8588	1.0686	1.3622
Al	0.8097	1.051	0.8331	1.1094	1.1412	0.9314	0.8378
sum.	2.0000	2.000	2.0000	2.0000	2.0000	2.0000	2.0000
Ca	0.7048	0.413	0.5412	0.2878	0.3422	0.4086	1.0205
Mg	0.6824	0.660	0.6563	0.6364	0.6654	0.4539	0.1715
Al	0.5585	0.988	0.8464	0.9470	0.9537	1.0688	0.7158
Fe	0.0030			0.1329	0.1105		0.0550
Na	0.0007			0.1218	0.0049		0.0022
Ti	0.0839			0.0043	0.0053		
Cr	0.0056			0.0039	0.0057		
sum.	4.04	4.04	4.04	4.12	4.09	3.83	4.17

* The results from energy spectrometer analysis.

References Grossman L., Steele I.M. (1976) Geochim. Cosmochim. Acta 40. 149-175. Grossman L.(1980) Ann. Rev. Earth Planet Sci.8: 559-608.

PARTICULARITES OF DIAPLIETIC TRANSFORMATION OF HORBLENDE FROM PUCHEZH-KATUNK ASTROBLEM (USSR). S.P.Fedosova, L.V.Sazonova, V.I.Feldman.USSR MOSCOW STATE UNIVERSITY, GEOGRAFICAL FACULTY, USSR 119899 GPS. MOSCOW.

Horblende (Hbl) is allogenic of Puchesh-Katunk astroblem sufferred an impact at 12,0-22,0 GPa/1/. It's composion was analized on scannig microcope Camscan-4 with analizer AN-4-1000.The precise parameters were determined on Dron-ym-1. Diaplect alterations don't differ from that of Ga, St, Bi in low baric area/2/. Planar fractures spacing rises with stress increasing (up to 22GPa), quantity of altered /dark/ placesin mineral grains increases, changing of optical and x-ray characteristics is registered. Study of altered areas in grains composition shows variation which is mainly related to new formations in numerous fractures. It is seen clearly enough in slighty darkened areas in grains, whereas in completely altered grains the fractures are concealed from the observer and in this case only derivations from the primary composition noticed.It this case composition of secondary aggregates in Hbl differend. Compsition close to plagioclase are met in Hbl from altered amphybol grains plagiogneiss whereas compositions close to puroxene are typical for specimens from Hbl-Bi-gneiss and amphybolites. Amphybol composition near the fractures in unaltered parts of grains remains practically constant.Impact stress effect on x-ray mineral characteristics displays itself in reflex intensity decreasing, diffusiosity and diffraction profill asymmetry increasing and disapperances of some reflections in scanning angles 2θ-40-50 /Fe-k_α /. Lattice parameters change differently with stress increasing. The decreasing is sharpest for "c". The elementary cell volume decreases (Tabl.1.). Other x-ray reflections besides horeblende's reflections in the diagram have not been found.

Tabl.1. Alteration x-ray parameters of impact.

N deep inm	P GPa	lattice parameters a nm	b nm	c nm	Vcell	Xmg	1/h* for 2θ-0,260 nm	1/h* for 2θ-0,255 nm
627	130	0,983	1,807	0,528	0,908	60,7	0,128	0,136
		+0,0004	+00003	+0,0003				
487	126	0,985	1,804	0,528	0,908	48,7	0,200	0,190
		+0,0014	+0,0010	+0,0006				
261	183	0,982	1,806	0,525	10,902	60,14	10,187	10,270
		+0,0005	+0,0004	+0,0004				

*1/h-Half-width to altitude radio.

REFERENSE

1.S.P.Fedosova, L.V.Sazonova, V.I.Feldman. Diaplectic transformation of Horblende from Puchezh- Katunki Astroblem, USSR. 20th Lunar nd Planetary Science conference, march 13-17, 1989, N1055.

2.L.V.Sazonova,V.I.Feldman,S.P.Fedosova. Some particularites of granate transformation with impact metamorfism. Meteoritica 1987,30.

CHEMICAL MODELS OF OUTGASSING AND OXIDATION REACTIONS ON CHONDRITE PARENT BODIES. Bruce Fegley, Jr., Department of Earth, Atmospheric, and Planetary Sciences, Massachusetts Institute of Technology, Cambridge, MA 02139

I explore the chemical compositions of outgassed volatiles on chondrite parent bodies as a function of volatile content for different chondrite classes. The bulk atomic abundances of volatiles (e.g., H, C, N, S, O, P, Cl, F) for carbonaceous, ordinary, and enstatite chondrites are used as inputs for chemical equilibrium calculations with our TOP20 code. Where relevant, gas phase chemical kinetic calculations are also done. The abundances of important outgassed volatiles such as H_2O/H_2 are calculated and are then used to model possible transport and loss of trace species such as Mo, W, Re, etc. on the chondrite parent body. Possible diagnostic abundance patterns will be identified and compared to the observed abundance patterns in CAI's in chondrites. The formation conditions for phases such as scheelite, powellite, and phosphate will also be related to the abundance of outgassed volatiles as a function of temperature and pressure.

Acknowledgments. This work was supported by NASA Grant NAG9-108 to MIT.

CRYSTALLOCHEMICAL CONTROL OF DIAPLECTICAL TRANSFORMATION.

V.I.Feldman. Geological Faculty, Moscow State University, USSR 119899 GSP Moscow.

Diaplectical transformation in rock-forming minerals proceed by a to way according to crystallochemical peculiarity of minerals. There are two groups of minerals: 1) quartz, plagioclase, alkali feldspath and cordierite, wich form a diaplectic glass, and 2) biotite, staurolite, garnet and probable also amphibole, pyroxene, wich form note diaplectic glass, and undergo thermic decomposition. In last way there are make polimineral aggregate consist of aluminiterous hypersthene, spinel (hercynite or ilmenite), alkali feldspath (sanidine or albite) and small amount of glass.

The first group include tectosilicates (quartz, plagioclase, alkali feldspath) and cyclosilicate (cordierite). All this minerals have a very high level of spatial homogeneity of crystalline lattice. The second group include phyllosilicate (biotite) and other silicates, wich hawe a crystalline lattice with different degree of anisotropy. In this case shock-wave energy are distributed irregular and produce very high heating in a narrow zone (some micron only!). Here there are fusion of mineral (but the rock in a whole remain solid) and crystallization of polimineral aggregate (see above). This process was explore in detail for minerals from astroblems Popigai, Janisjarvi, Puchezh-Katunki and others.

UPPER EOCENE IMPACT EJECTA FROM DSDP SITE 612 OFF NEW JERSEY; A. Fernandes and B. P. Glass, Geology Department, University of Delaware, Newark, DE 19716

An 8 cm thick layer of tektite glass and impact ejecta has been described from Core 21, Section 5, from Deep Sea Drilling Project Site 612 taken on the upper continental slope off New Jersey (Glass, 1987; Keller et al., 1987; Thein, 1987; Bohor et al., 1988; Koeberl and Glass, 1988). Tektite fragments, up to at least 7 mm across, are abundant throughout the layer, but rock and mineral grains, showing evidence of shock metamorphism, are concentrated in the top half of the layer along with microtektites. On the other hand, spherules similar in texture and composition to upper Eocene clinopyroxene-bearing (cpx) spherules found in the Caribbean Sea and Gulf of Mexico are found in the lower half of the layer. Thus the vertical distribution of microtektites and shocked rock and mineral grains and cpx spherules indicates two separate events; but the approximately equal abundance of tektite glass throughout the entire layer indicates a single event. In order to determine if the tektite glass might be from two different events, we determined the composition of glass fragments from 10 different levels through the layer. We found no consistent difference in composition with depth that would indicate that the glass was from two different events. The glass from two adjacent samples near the top of the layer (111-112 cm and 112-113 cm) does have lower average SiO_2 and higher average Na_2O and K_2O than the average for the glass from the other depths; but there is a great amount of overlap in composition between individual glass fragments from this layer as compared with glass fragments from other layers. Much of the tektite glass has been coated with, and in some cases partly replaced with, pyrite. The greatest degree of pyritization occurs in the 111-113 cm interval. If the pyrite selectively coated and replaced the more SiO_2-rich glass fragments, then this might explain why the glass fragments from the 111-113 cm interval have slightly different average SiO_2 contents than the glass from the other levels.

In an attempt to determine the nature of the target rock from which the impact ejecta was derived, we obtained x-ray patterns for 53 rock fragments from the 250-500 μ m size fraction using a Gandolfi camera. The major minerals are coesite, quartz, glauconite, and pyrite. We believe that the pyrite and probably the glauconite are secondary minerals and were not part of the original ejecta. Glauconite, like pyrite, decreases with depth in the layer. The coesite is a shock metamorphic phase produced from the quartz. Additional minerals include sillimanite, feldspar (possibly oligoclase or bytownite), almandine garnet, and possibly hornblende. The assemblage of minerals suggests that the target material was a high grade metamorphosed argillaceous rock, or sediments derived from such a source rock. Polished thin sections are being prepared from each of the x-rayed grains for petrographic and compositional studies using a petrographic microscope, scanning electron microscope, and energy dispersive x-ray analyses.

This study was partly supported by NSF Grant OCE-8314522.

References: Glass B. P. (1987) Lunar Planetary Sci. XVIII, 328. Keller G., D'Hondt S. L., Orth C. J., Gilmore J. S., Oliver P. Q., Shoemaker E. M., and Molina E. (1987) Meteoritics, 22, 25. Thein J. (1987) Initial Repts. Deep Sea Drilling Project, 95, 565. Bohor B. F., Betterson W. J., and Foord E. G. (1988) Lunar Planetary Sci. XIX, 114. Koeberl C. and Glass B. P. (1988) Earth Planet. Sci. Lett., 87, 286.

^{41}Ca IN IRON METEORITES; D. Fink, J. Klein and R. Middleton, Dept. of Physics, University of Pennsylvania, Philadelphia, PA 19104, USA. S.Vogt and G.Herzog, Dept.of Chemistry, Rutgers University, New Brunswick, NJ 08903, USA.

As a consequence of a pure electron-capture decay mode resulting in 3.2 KeV X-rays, the detection of ^{41}Ca ($\tau_{½}\sim 1\times10^{5}$ y) by decay counting is extremely difficult. Prior to the introduction of Accelerator Mass Spectrometry (AMS) only 2 measurements of ^{41}Ca in extraterrestrial samples had been reported. First AMS measurements (Paul et al,1985 and Kubik et al,1986) in a few iron meteorites achieved a ^{41}Ca/^{40}Ca detection limit of $\sim1\times10^{-12}$, but due to low counting rates the uncertainties quoted were quite large. Recent success (Sharma et al,1987) in producing intense negative-ion molecular beams of Ca from a Cs sputter source has now reduced this limit to $<1\times10^{-15}$ (Middleton et al,1988). Building on this capability, we have initiated a program at the Univ. of Pennsylvania aimed at measuring ^{41}Ca in a wide variety of extraterrestrial materials. We report here preliminary results of the ^{41}Ca saturation activity in a set of small iron meteorite falls.

Four falls were analyzed for ^{41}Ca (dpm/kg) : Bogou (25.8±2.6) Charlotte (25.3±2.6), N'Goureyma (24.1±2.4) and Treysa (22.9±2.3). The average saturation activity is 24.5±1.3. Judging from published ^{4}He/^{21}Ne ratios (Schultz and Kruse,1983) and recovered masses, this average should be typical for small irons (radii <10 cm) in which primary GCR production of ^{41}Ca should dominate. Our result is virtually identical to that calculated by Fink et al(1987) derived using their measured Fe(p,x)^{41}Ca spallation excitation function integrated over the GCR primary flux estimated by Castagnoli and Lal (1980). From the mean ^{36}Cl saturation activity in the same 4 meteorites (Nishiizumi,1987) we obtain a ^{41}Ca/^{36}Cl production rate ratio of 1.07±0.12. The ^{41}Ca measurement by Kubik (1986) in Bogou of 6.9±1.1 dpm/kg is inconsistent with our average. Shielding cannot explain this large disagreement given that the post-atmospheric radius of Bogou is only ~7 cm.

In addition, two samples of the find Grant were analyzed : one from "bar-O", 17.2±1.9 (surface); and the other from "bar-I", 16.6±1.3 (center). The weighted mean activity in Grant measured by Fink (1987) from a depth profile study was 20±4 dpm/kg. Our measurements supplement this profile and confirm their conclusion that even at these large depths ^{41}Ca production from secondary flux is still considerable. We see a modest decrease in production from (post-atmospheric) surface to the center of at most 25% and probably less. The ^{38}Ar profile in Grant (Signer and Nier, 1960) behaves similarly. Taking the result for "bar-O" and assuming a production rate equal to the average of the small falls cited above, we calculate a terrestrial age of 51±22 ky for Grant. Given that the radius (~40cm) of Grant (Signer and Nier,1960) was probably far larger than that of the iron falls, this must be considered an upper limit for the terrestrial age.

References : Castagnoli G. and Lal D.(1980)Radiocarbon, **22**,133. Fink D. et al (1987)NIM, **B29**,275. Kubik P. et al (1986)Nature, **319**,568. Middleton R. et al(1988)Radiocarbon, in press. Nishiizumi K. (1987)Nucl. Tracks Radiat. Meas. **13**,209. Paul M. et al (1985)Meteoritics, **20**,726. Schultz L. and Kruse H.(1983)Int. Rep., MPI, Mainz. Sharma P. and Middleton R.(1987)NIM, **B29**,63. Signer P. and Nier A.(1960)JGR, **65**,2947.

143-Nd AND 146-Nd IN HNO_3- AND $HClO_4$- SOLUBLE FRACTIONS OF THE EFREMOVKA CARBONACEOUS CHONDRITE; A.V.Fisenko, S.F.Karpenko, L.F.Semjonova, A.V.Ljalikov, V.G.Spiridonov, A.K.Lavrukhina. V.I.Vernadsky Institute of Geochemistry and Analytical Chemistry, USSR Academy of Science, Moscow, USSR.

Isotopic composition of Nd in HNO_3- and $HClO_4$- soluble fractions of the HCl, HF- insoluble residues (IR) of the Efremovka chondrite are reported. The dissolution of the IR coarse-grained fraction in HNO_3 was made at 70°C for 4h. twice (EN-1 and EN-2). Residue was treated with $HClO_4$ at 140°C for 2h. twice and these solutions were taken as one (ECl-(1+2)). The IR fine-grained fraction was treated similarly with HNO_3 and $HClO_4$ (EN-3 and ECl-3) (Fisenko et al., 1987). Residue of this fraction was treated with $HClO_4$ at ~20°C for a year (ECl-4). Isotopic composition of Nd was measured on Cameca TSN 206 SA mass-spectrometer (Karpenko et al., 1984). Isotopic effects in Nd were found for 143-Nd and 146-Nd only (Table). The 143-Nd enrichment may be connected with increased concentration of Sm as compared with Nd or, as Lugmair et al. (1983) suggest, with α-decay of 147-Sm. In the first case in order that to explain the 143-Nd excess in ECl-(1+2), for example, we must consider that Sm/Nd ratio in this sample was about 1.5, which is higher than its measured value (0.3-0.4). So we consider that the Lugmair et al. hypothesis is preferable. As can be seen in Table the maximal excesses of 143-Nd were found in $HClO_4$-soluble fractions, while for Allende they were found in HNO_3-soluble fraction (Lugmair et al.,1983). Probably P,T -conditions at which surface carbonaceous films were formed on Sm-bearing grains, were different for Allende and Efremovka chondrites or these films were differently modified in the parent bodies. The excesses of 146-Nd are not supported with isotopic effects on light isotopes so we can not explain their by s-process and should study their nature in our further investigation.

Table. Values ε^x for ^{143}Nd and ^{146}Nd in etch fractions from Efremovka

Sample	Nd,ng	ε_{143}	ε_{146}
EN-1	30	-6.6 ± 8.2	+56.6 ± 10.0
EN-2	8	+47.3 ± 4.7	+9.1 ± 6.1
ECl-(1+2)	15	+393.0 ± 8.0	+21.7 ± 8.9
EN-3	6	+40.0 ± 35.0	+211.0 ± 65.0
ECl-3	5	+131.0 ± 9.0	+34.4 ± 11.0
ECl-4	3	+17.0 ± 20.0	+95.0 ± 28.0
Lab.std.	5	-0.1 ± 3.9	+5.1 ± 9.3

$\varepsilon^x = (^iR_{samp.}/^iR_{CHUR} - 1)\cdot 10^4$, where $^iR = {}^iNd/^{144}Nd$, R_{CHUR} from (Jacobsen, Wasserburg,1980).

References. Fisenko A.V. et al. (1987). Abstr.LPSL,18,p.292. Jacobsen S.B.,Wasserburg G.J. (1980) Earth and Planet. Sci.Lett.,v.50,p.139. Karpenko S.F. et al. (1984) Geochimia,N7, p.958 (in Russian). Lugmair G.W. et al. (1983) Science, v.222, p.1015.

HCl, HF - INSOLUBLE FRACTION OF THE EFREMOVKA CARBONACEOUS CHONDRITE; A.V.Fisenko, L.F.Semjonova, A.Yu.Ljul, A.K.Lavrukhina. Vernadsky Institute of Geochemistry and Analytical Chemistry, USSR Academy of Sciences, Moscow, USSR.

The content of some elements determined by INAA for samples which were obtained after of the Efremovka chondrite bulk samples (~59g and ~15g) treatment with HCl,HF at ~80°C and ~30°C respectively during 5 mounths are reported. The acid-resistant residues (ARR) consists of transparent and dull particles. Both the residues were separated into coarse - and fine-grained fractions. The coarse-grained fractions were divided by sieves into three parts with grain size of >100, 50-100 and <50 μm. The individual dull particles of >100 μm size (Ef1-Ef3) and ARR aliquots of 50-100 μm and <50 μm sizes (Ef4 and Ef5, respectively) from ~59g bulk sample, and ARR aliquot of <50 μm size (Ef6) from ~15g bulk sample were analyzed (Table). The Ef1 particle with high concentration of Ir also contain the detectable amounts of refractory siderophiles Re, Os and Ru (2.4; 21.0 and 17.0 ppm, respectively). Probably, Ef1 contain the refractory metallic inclusion (Pt-nuggest or Fremdlinge). Interestingly, Ef1 has low concentration of REE bul it enriched with Sc.

The same concentrations of REE are observed in Ef2 and Ef3, and in Ef4+Ef6 also. From this can be concluded that: 1) If Ef2 and Ef3 are polymineralic particles then the amounts of REE in their host-phases should be proportional to the masses of Ef2, Ef3 particles. Alternatively, Ef2 and Ef3 may be fragments of large particle with homogeneous distribution of REE. In these case the particle must have the inclusions, which are responsible for other content of elements in Ef2, Ef3. 2) The main amounts of REE in Ef4-Ef6 are present either in single phase and the REE concentrations in these phase did not depend from its size or in some phases and the ratio between them is constant for all fractions.

Semjonova L.F. et al. (1989). Meteoritika, 47, 105.

Table. Composition of bulk and AIR's of Efremovka (Na,Ca,Fe,Cr in %, other in ppm)

	Wt.,mg	Na	Fe	Cr	Ca	Sc	Co	Ir	Au	La	Sm	Eu	Yb	Lu
Ef1	0.17	0.14	0.70	0.09	45.7	17.3	18.0	16,5	0.05	42.20	0.03	40.60	40.4	-
Ef2	0.05	0.09	0.75	0.05	2.4	17.6	15.0	0.40	0.50	4.10	2.20	41.50	2.9	0.38
Ef3	0.08	0.23	0.90	0.08	4.0	11.0	16.0	0.30	0.40	45.50	1.90	42.00	2.8	0.35
Ef4	4.60	0.06	1.95	0.15	0.4	10.0	1.9	0.77	0.40	1.65	0.90	0.35	1.1	0.17
Ef5	2.87	0.05	1.90	0.15	0.5	8.8	2.1	0.73	0.35	1.60	0.90	0.40	1.2	0.17
Ef6	4.58	0.46	2.60	0.15	2.1	18.3	13.4	1.00	0.52	1.60	0.92	0.30	1.0	0.18
Bulk[x]	2.50	0.35	23.9	0.33	1.6	8.3	610	0.73	0.22	0.47	0.34	0.10	0.26	0.05

[x] Semjonova et al., 1989

MINOR AND TRACE ELEMENT ABUNDANCES IN EIGHT "CHONDRITIC" STRATOSPHERIC PARTICLES: EVIDENCE FOR Ni DEPLETIONS. G. J. Flynn[1] and S. R. Sutton[2], (1) Dept. of Physics, SUNY-Plattsburgh, Plattsburgh, NY, (2) Dept. of Geophysical Sciences, The Univ. of Chicago, Chicago, IL, and Brookhaven National Lab., Upton, NY.

We have determined minor and trace element compositions of seven particles classified as "C-type" (W7027-C5, U2022-G17, W7013-H17, W7013-A11, U2022-G2, U2022-B2, and U2022-C18) and an eighth particle classified as "C?" (U2001-B6) from the NASA Johnson Space Center (JSC) stratospheric particle collection. The analyses were performed using the x-ray microprobe at the National Synchrotron Light Source. The procedure has been described for our previous analyses of three other chondritic micrometeorites [1]. An increase in the synchrotron ring current and the relocation of the x-ray microprobe closer to the ring combine to increase our elemental sensitivities by about a factor of 2 over the previous analyses. For the largest particle (about 30 μm), W7027-C5, we detected most elements between S and Mo.

BROMINE: The previously reported Br enrichment [1,2] was seen in seven particles, with Br concentrations ranging from twice CI in U2022-B2 to 38 times CI in U2022-G17. Br in the eighth particle, W7013-H17, was indistinguishable from CI. Four stratospheric aluminum oxide spheres, two supplied by D. Brownlee and two from the JSC collection, were also analyzed. Upper limits on the Br concentrations in these spheres are substantially below CI. Thus, if stratospheric contamination is the source of excess Br in the chondritic particles the enrichment mechanism must be highly selective in favor of the chondritic particles.

NICKEL: Two particles exhibited substantial depletions in Ni, 0.08xCI in U2022-B2 and 0.01xCI in U2001-B6. A third chondritic particle, W7066*A4 for which the full trace element analysis is incomplete, also showed Ni at 0.05xCI. Brownlee et al. [3] have previously reported that one of 57 chondritic cosmic dust particles analyzed by EDAX had a substantial Ni depletion (0.1xCI). Previous EDAX analyses of 11 fragments of Orgueil matrix of comparable size to the cosmic dust ($\leq$ 30 μm) showed no Ni deviations by more than a factor of 3 from CI [4].

OTHER ELEMENTS: The other detected minor and trace elements are generally within a factor of two of the CI concentrations, but in detail each particle has a unique composition. Substantial deviations from CI include Y, Nb, and Mo enrichments in W7027-C5; Ca, Mn, Cu, and Zn enrichments in U2022-G17; Zn, Ga, and Se enrichments in W7015-H17; Se enrichment in W7013-A11; Cu depletion in U2022-G2; Cu, Zn, Ga, and Ge depletions and Mn enrichment in U2022-B2; Zn and Se depletions and Cu enrichment in U2022-C8; and Fe, Zn, Se, and Cr depletions and Rb, and Sr enrichments in U2001-B6.

While volatile concentrations at or above CI remain the norm, we observe particles depleted in Ni and some volatiles (eg. Zn).

REFERENCES: [1] Sutton S.R. and Flynn G. J. (1988) Proc. Lunar Planet. Sci. Conf. 18th, 607-614. [2] Van der Stap C. C. A. H. et al. (1986) LPSC XVII, 1013-1014. [3] Brownlee in Solid Particles in the Solar System, IAU Symp. 90, Reidel, 333-342. [4] Flynn G. J. et al. (1978) Proc. Lunar Planet. Sci. Conf. 9th, 1187-1208.

CHEMICAL COMPOSITION AND PROPERTIES OF COMET HALLEY DUST PARTICLES AS OBTAINED DURING VEGA MISSION;M.N.Fomenkova,E.N.Evlanov,L.M.Muknin,O.F.Prilutski,R.Z.Sagdeev,B.V.Zubkov; Space Research Institute, Academy of Sciences, Moscow, USSR

Mass-spectrometers PUMA-1,2 aboard VEGA spacecrafts (Kissel(1986)) were intended to investigate the properties and chemical composition of Halley comet dust component by means of direct measurements in the nucleus vicinity. The Puma instruments are time-of-flight dust-impact mass-analysers. A collision of a dust particle with the target at the velocity of 80 km/s results in ions formation, and mass of ions is determined from their time of flight via the ion optical system of the instrument. During the fly-by sessions more then 2000 mass-spectra were obtained by PUMA-1 and more then 500 ones were obtained by PUMA-2. Masses of studied particles are in the range $5*10^{-17}$ - 10^{-13} g. All the following conclusions were made basing on the analysis of elements' ion concentrations, assuming that ion composition is not equivalent to atomic one, but, to our mind, reflects it to significant extent.

In spectra recorded without information compression (4-5% of the total number of spectra) were found (Sagdeev(1987)) the principal elements and their isotopes: H, C, N, O, Na, Mg, Al, Si, S, Cl, Ca, Fe. The isotopic ratis are consistent with mean cosmic isotopic abundance. A significant amount of light elements (H, C, N, O) in cometary dust particles can be easily explained by the presence of organic compounds similar to observed in carbonaceous chondrites.

The large statistical material (more than 2500 mass-spectra) enables to define 4 different groups of cometary dust particles (Sagdeev(1987)):

- dust particles with light elements only (about 8%);
- dust particles, containing carbon and silicates - quasichondritic particles (75%);
- dust particles without carbon, containing silicates with hydrogen and/or sulfur (about 12%);
- other non-classified particles (about 5%).

Measured spectra contains not only peaks, identified with main elements, but also a large number of non-identified peaks uniformly distributed in time (Sagdeev(1988)). These peaks were explained as effects of very small particles impacts. Mass of these particles is several orders of magnitude less than of particles with measured spectra, but their total mass contribution in come tary dust flow can be as high as 10%.

The results of cometary dust composition measurements shows to a possible similarity of interstellar and cometary dust and can be explained by a model of cometary nuclei as aggregates of interstellar dust particles with no substancial chemical evolution.

REFERENCES

1. Kissel J., Sagdeev R.Z., Bertaux J.L. et al (1986) Nature,321,280-282.
2. Sagdeev R.Z. et al (1987) Space Researchs,25,849 (in Russian).
3. Sagdeev R.Z. et al (1987) Space Researchs,25,856 (in Russian).
4. Sagdeev R.Z. et al (1988) 27th COSPAR meet.,S.5.3.10,57.

STABLE ISOTOPE AND ABUNDANCE MEASUREMENTS OF HYDROCARBONS IN MURCHISON. I.A. Franchi[1], R.A. Exley[2], I.Gilmour[3] and C.T. Pillinger[1]. [1]Dept. of Earth Sciences, Open Univ., U.K., [2]R.A. Exley, V.G. Isotech Ltd., Cheshire, U.K., [3]Enrico Fermi Inst., Univ. of Chicago, U.S.A..

The organic compounds in the carbonaceous chondrites have been investigated for many years and by many a host of techniques, yet important problems remain unresolved, particularly as to the origin and the formation of certain classes of these intriguing materials. Stable isotopic measurement of the organic material is one of the more under-used techniques, although it is potentially of great value, particularly if applied to individual compounds.

Analyses by Yuen *et al.* (1) on the $\delta^{13}C$ value of individual volatile hydrocarbons and carboxylic acids ($\leq C_6$) from the Murchison meteorite revealed well defined trends of decreasing $\delta^{13}C$ with increasing carbon number (+9.2 to -7.9 ‰ and +22.7 to +4.5‰ respectively). These results undoubtedly indicate that the compounds are indigenous to the meteorite and that they were formed by a kinetically controlled process. The $\delta^{13}C$ of the acids being explicable in terms of carboxyl groups related to the ^{13}C enriched CO_2 trapped in the meteorite being added to a hydrocarbon chain isotopically similar to the hydrocarbons analysed. CO liberated from the meteorite on the other hand had a $\delta^{13}C$ value of -32‰, implying an isotopic fractionation in the opposite direction to that produced from laboratory simulations of Fischer-Tropsch type reactions (2).

In contrast to the volatile hydrocarbons the non-volatile hydrocarbons ($\geq C_{15}$) appear to display a trend of increasing $\delta^{13}C$ with molecular weight, from -19‰ to -25‰ (3). However, this trend is based on only five compounds (from the multitude present) and the $\delta^{13}C$ values are very similar to terrestrial values. To verify and extend this work a number of samples of different size fractions of the Murchison meteorite have been solvent extracted with mixtures of methanol and toluene and subdivided on a silica gel column to afford the saturated hydrocarbons, non-saturated hydrocarbon aromatics and polar organics.

There is no discernible variation in the distribution of the saturated hydrocarbons within the different size fractions. Initial results indicate that the non-saturated hydrocarbons are concentrated in the finer fractions, possibly at the surface of some specific, but currently unidentified, component within the meteorite. The $\delta^{13}C$ of the individual normal alkanes and the resolved aromatics is being measured on a recently designed gas-chromatograph - isotope-ratio-mass-spectrometer (GC-IRMS) system developed by V.G. Isogas Ltd. (the Isochrom II). Polar compounds are being studied by a version of stepped heating. Results of both investigations will be presented at the meeting and their significance discussed.

References:

(1) Yuen, G. *et al.* (1984). *Nature*, **307**, 252-254. (2) Lancet, M.S. and Anders, E. (1970). *Science*, **170**, 980-982. (3) Gilmour, I and Pillinger C.T. (1985). *Meteoritics*, **18**, 302.

ALLENDE CHONDRULE VS WHOLE ROCK ANALYSES; K. Fredriksson, Dept. of Mineral Sciences, Smithsonian Institution, Washington, D.C. 20560

Major and minor element analyses of 38 Allende Meteorite chondrules are compared to the bulk analysis by Jarosewich, Table 1. The individual chondrule compositions were obtained by E-probe analysis of pressed pellets of finely-ground powders (Fredriksson et al., 1982). In spite of the wide range in compositions between individual chondrules, the averages agree well with Jarosewich's "chondrule concentrate" analysis reported by Clarke et al. (1970). The Fe/Mg distribution has been discussed in some detail by Clarke et al. (1970) and Rubin and Wasson (1987). However, the Ca and Al distribution has received less attention. These element concentrations vary by a factor of 10 to 15, but the CaO/Al_2O_3 ratios only from 0.5 to 1.1, i.e. the two elements are closely correlated, as shown in Figure 1. This is similar, although even more pronounced, to the correlation in Grade 3 ordinary chondrites; in Grades 4 and 5 Al and Ca are anticorrelated (Fredriksson, 1983). Perhaps more remarkable is that the average CaO/Al_2O_3 ratio for the chondrules, 0.83, is so close to the ratio in the bulk, 0.80 (Table 1). Relations between chondrules and matrices in different chondrites will be illustrated by X,Y,Z surface plots and arguments presented for similar parent materials processed in relatively closed systems.

References:
Clarke R.S. et al.(1970) SI Contrib. to the Earth Sciences,115,p.1-53.
Fredriksson K. et al.(1982) Meteoritics,17,p.215-216.
Fredriksson K.(1983) In Chondrules and their Origin(ed.E.A. King)LPI,p.44-52.
Rubin A.E. and Wasson J.T.(1987)Geochim. et Cosmochim. Acta,51,p.1923-1937.

TABLE 1. ANALYSES OF 38 ALLENDE CHONDRULES VS BULK COMPOSITION.

	AVERAGE	CHONDRULES RANGE	SD[1]	BULK[2]
SiO_2*	41.6-	34.0-50.7	2.86	34.19
TiO_2	0.26	0.06-0.83	0.14	0.16
Al_2O_3*	3.57	0.80-10.7	1.93	3.28
Cr_2O_3	0.56	0.36-0.84	0.12	0.53
FeO	8.90	5.82-13.2	2.17	26.84
MgO	34.4-	14.0-49.3	6.41	24.62
CaO	2.89	0.69-10.0	1.63	2.64
Na_2O	0.90	0.10-3.34	0.69	0.43
K_2O	0.11	0.01-0.92	0.14	0.03
P_2O_5*	0.21	0.06-0.42	0.07	0.25
FeS	2.38	0.58-5.61	1.30	4.11
Ni	0.53	0.09-0.95	0.25	1.12
SUM	96.3-			98.20
Tot. Fe	8.43			23.58

* 32 Analyses.
1. Standard Deviation.
2. E. Jarosewich, SI Contrib. to Earth Sci. (27) p.27, 1987 (Recalculated).

Fig. 1. CaO and Al_2O_3 in 38 individual Allende chondrules. The analyses were sorted with SiO_2 generally increasing from left to right, 34 to 51%.

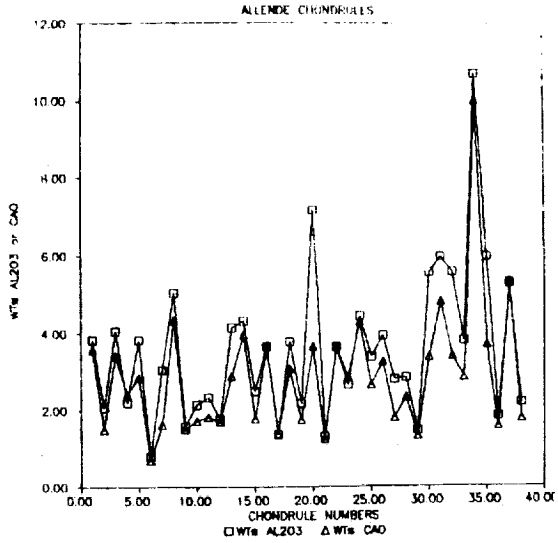

MULTI-ISOTOPIC SULFUR ISOTOPE RATIOS($\delta^{33}S, \delta^{34}S, \delta^{36}S$) IN METEORITES; Xia Gao and Mark H. Thiemens, Chemistry Dept., B-017, University of Calif., San Diego, La Jolla, Calif. 92093-0317.

There are, at present, only a few multi-isotope ratio measurements for meteoritic sulfur, specifically $\delta^{33}S, \delta^{34}S$ and $\delta^{36}S$. We have extended our sulfur isotope ratio measurement techniques to now include all three ratios. These measurements may be of particular interest, since it has been suggested that the neutron-rich isotope, ^{36}S, was produced in a different nucleosynthetic process than the other sulfur isotopes (1,2), thus, the measurement of $\delta^{36}S$, along with $\delta^{33}S$ and $\delta^{34}S$, may be a useful diagnostic probe of nucleosynthetic admixtures. Neutron-rich isotopic anomalies in the iron-group, e.g. ^{48}Ca and ^{50}Ti, are well known, and it is possible that ^{36}S is co-produced (1). Identification of a ^{36}S anomaly would be of importance in establishing both the nature of the nuclear process(es) and the subsequent chemical fate, since sulfur has a significantly different chemistry than Ti or Ca.

The chemical preparation, conversion to SF_6 by reaction with BrF_5, is the same as previously described (3), including a gas chromatographic purification procedure. Typical error for $\delta^{36}S$ associated with the mass spectrometry is ~ ± 0.2‰. The initial results are given in the Table. From the Table, as well as the measurements recently reported (3), it may be seen that the bulk meteoritic sulfur isotopic ratios are within ~ 0.5‰ ($\delta^{34}S$) of the Cañon Diablo Troilite standard. There is, for the new measurements, no indication of an isotopic anomaly for any ratio, including the $\delta^{36}S$. The mass fractionation ratio for $\delta^{36}S$ is $\delta^{36}S \cong 2\delta^{34}S$, depending upon chemistry. Further measurements, analytical refinements and higher resolution standardization are underway.

Table 1: Results of Sulfur Isotopic Ratio Measurements in Meteoritic Samples.

Sample	$\delta^{33}S$(‰)	$\delta^{34}S$(‰)	$\delta^{36}S$(‰)
Santa Rosa (Anom.)	0.09	0.14	- 0.2
Pillistifer (E6)	- 0.12	- 0.23	- 0.8
Murchison (Acid Solu.)	0.21	0.29	0.6
"	0.22	0.37	0.7
Murchison (Br_2, Acid Res.)	- 0.23	- 0.48	- 1.3

* Results are with respect to Cañon Diablo Troilite.

References:

(1) Cameron A. G. W. (1979) Astrophys. J. 230, L53-L57.
(2) Howard W., Arnett W., Clayton D. and Woosley E. (1972) Astrophys. J. 175, 201-216.
(3) Gao X. and Thiemens M. H. (1989) Lunar and Planet. Science XX, Lunar and Planet. Inst., Houston, 1221-1222.

ZINC ISOTOPIC COMPOSITION IN METEORITES ; G.Gawinowski, J.L.Birck, C.J.Allegre, Laboratoire de Geochimie et Cosmochimie,I.P.G.,4 Pl.Jussieu, 75252 Paris Cedex 05.

Isotopic anomalies in the iron peak elements (Ca,Ti,Cr,Ni) are common in the carbonaceous chondrites inclusions as well as in refractory mineral such as hibonite [1]. There is now a good convergence in the data pointing to isotopic variations related to neutron rich statistical equilibrium within massive stars. Recent investigation of Ni [2] favors the model of multiple zone mixing [3], if secondary processes did not alter the patterns of the anomalies found for the different isotopic ratios of the iron group elements. The isotopes of Zinc are a decisive test for the validity of this model [4]. For common inclusions, excesses of ^{66}Zn are expected to be about 10 to 15 ε units higher than excesses of other Zn isotopes. However Zinc is also the most volatile element of the iron group investigated so far; therefore the isotopic ratios of Zinc should yield constraints on reequilibration of inclusion-type material with solar system material of normal isotopic composition. An experimental procedure was developed to produce high precision Zn data on small size samples. The anion exhange procedure results in chemical yields higher than 99% with total blanks at a negligible level (0,5±0,2 ng) relative to samples sizes of > 500 ng. For the mass spectrometry, samples are loaded with a silica-gel emitter on a Re filament : 1 μg of Zn yields a beam of about 8.10^{-12} A at 1250 to 1400 °C during more than 6 hours. A single collector mode with field stepping was used for recording. Instrumental mass fractionation was corrected using an exponential law [5] relative to the ratio $^{68}Zn/^{64}Zn$=0,37983. Current precision for 2 μg of Zinc is 2.10^{-5} and 2.10^{-4} for $^{66}Zn/^{64}Zn$ and $^{70}Zn/^{64}Zn$ respectively; with as amount are decreased to 0,5 μg, precision degrades by a factor of 2. The mean standard is:
$^{66}Zn / ^{64}Zn = 0,569197 \pm 0,000009$ (±2σ) and $^{70}Zn / ^{64}Zn = 0,012530 \pm 0,000002$ (±2σ)
As previously noticed[4], $^{67}Zn/^{64}Zn$ is not reproductible due to some as yet unidentified interference. The scatter is in the permil range and was not significantly reduced by cold trapping. Possible interferences on the other isotopes were systematically verified and were always found to be negligible. We have investigated three types of samples previously examined for chromium isotopic systematics [6,7] : 1) C3 inclusions with four fine grained Allende pink inclusions (G1,G3,G4,G6), two coarse grained Allende white inclusions (BR1,BR9), one Allende dark inclusion. 2) whole rocks of meteorites including one C1-chondrite (Orgueil), one C2-chondrite (Murray), one C3-chondrite (Allende), one E-type chondrite (Abee). 3) Leaches which have shown very large Chromium isotopic diversity in C1; for the procedure see a companion abstract [M.Rotaru et al]. No isotopic variations higher than 1ε for $^{66}Zn/^{64}Zn$ and 2ε for $^{70}Zn/^{64}Zn$ are present in any of the analysed samples. However one of the fine inclusions gives a clearly resolved $^{66}Zn/^{64}Zn$ of 0,7±0,3ε. Other inclusions show a systematic trend towards an excess on this isotope. These data are in agreement with a previous observation [4] of an excess of 0,6ε in a fine grained inclusion. These data do not agree with the nucleosynthetic MZM NSE model [3]. There are two possibilities: 1) this model does not provide an accurate prediction of isotopic anomalies for Zn; 2) Zn may have been nucleosynthetized in amounts predicted by the model but latter processes such as alteration have rehomogeneized the exotic Zn almost completely with normal Zn. Although our data on $^{70}Zn/^{64}Zn$ are of improved precision relative to former data [4], no effect was detected; here again rehomogeneisation with normal Zn is a likely explanation. Although they have been found in low temperature products, the large ^{54}Cr isotopic effects observed in the leaches of Orgueil have no counterpart in the isotopes of Zn. Several possible processes may account for this observation: 1) the materials involved may have undergone homogeneisation of sufficient intensity to mobilize Zn but not Cr; 2) Zn is located primilary in a single mineral phase: therefore the leaching procedure is no longer able to distinguish the different nucleosynthetic components which have been present. Further investigation of other classes of meteorites and refinement of leaching techniques may help clarify these ambiguities.

REFERENCES : [1] E.K.Zinner et al. (1985) Ap.J.311, L103 . [2] J.L.Birck and G.W.Lugmair (1988) EPSL 90 .[3] D.Hartmann et al. (1985) Ap.J.297,837. [4] R.D.Loss & G.W.Lugmair (1989) LPSC XX, 588. [5] R.D.Russel et al (1978) G.C.A.42, 1075-1090 .[6] J.L.Birck & C.J.Allegre (1988) Nature 331,579. [7] M.Rotaru et al. (1989) LPSC XX, 924.

MINERALOGY OF METAMORPHOSED CARBONACEOUS CHONDRITES; Geiger T. and Bischoff A., Institut für Planetologie, Universität Münster, Wilhelm-Klemm-Str.10, 4400 Münster, FRG.

A study of the metamorphosed carbonaceous chondrites offers useful insight into the nature and the evolution of their parent bodies. Results on the bulk chemistry, the mineralogy and petrology of some type 4-6 carbonaceous chondrites have been published by Kallemeyn (1), Scott and Taylor (2), Binns et al. (3) and Geiger and Bischoff (4).

Here we report on the mineralogy of eight metamorphosed carbonaceous chondrites (see Table 1). Based on the presence of metals or magnetite these chondrites can be subdivided into an oxidized and a reduced subgroup (Table 1). Besides the existence of magnetite instead of metals the most significant differences between the oxidized and reduced subgroups are the presence of refractory siderophile element-rich particles (4) and the Ni-contents of olivine in chondrites of the oxidized subgroup (Table 1). In Karoonda, ALH82135, ALH84038 and ALH85002 0.3-0.5 wt.% NiO was found in olivine, whereas the Ni-contents in olivine of the reduced chondrite ALH84096 are below the detection limit (Table 1). We suggest that Ni diffused into olivine due to the oxidation of Ni,Fe-metals and the formation of magnetite. The Ni-concentration is homogeneously distributed in the olivine grains even in the large zoned olivines from Karoonda (4).

Zoned olivine grains were found in Coolidge and Karoonda, as mentioned before. Variations in the mineral chemistry of olivine, pyroxene and plagioclase are listed in Table 1.

In the chondrites of the oxidized subgroup various sulfide minerals occur: Pyrrhotite, pyrite, pentlandite, chalcopyrite, monosulfides (Table 1). In our view the pentlandite-pyrite intergrowth was formed from the monosulfides by exsolution during cooling (4).

The degree of brecciation is very variable among the eight chondrites. The strongest shock-induced features were found in ALH84038 and ALH82135. Mason (5) suggested pairing of ALH85002 and ALH82135. Based on different shock effects and differences in mineralogy between these chondrites, we rule out pairing of these chondrites.

References: (1) Kallemeyn G.W. (1987) Mem. Natl Inst. Polar Res., Spec. Issue, 46, 151. (2) Scott E.R.D. and Taylor G.J. (1985) Journ. Geophys. Res., 90, Supplem., C699. (3) Binns R.A. et al. (1977) Meteoritics, 12, 179. (4) Geiger T. and Bischoff A. (1989) LPS, XX, 335. (5) Mason B. (1986) Antarctic Meteorite Newsletter, 9, 3, 16.

Table 1: Preliminary data on phases and mineral compositions in eight metamorphosed carbonaceous chondrites.

	Karoonda	Mulga (west)	ALH82135	ALH84038	ALH85002	PCA82500	Coolidge	ALH84096
Reduced/Oxid.	ox	ox	ox	ox	ox	ox	red	red
Olivine (Fa)	30.7±0.7	33.3±0.8	29.4±0.7	28.6±0.6	31.1±0.6	30.7±0.7	14.6±0.7	30.4±1.0
wt.% Ni in Ol	0.5	n.a.	0.4	0.4	0.4-0.5	n.a.	n.a.	n.d.
Zoning in Ol	yes	no	no	no	no	no	yes	no
Pyroxenes* (Fs)	6-25	26-30	25-30	25-30	23-29	1-25	5-18	16-28
Plagioclase (An)	20-75	33-75	16-66	19-88	38-75	13-95	68-96	8-13
Metal(-oxide)	mag	mag	mag	mag	mag	mag	kam,taen	kam,taen
Sulfides	pyr, pent py, chalc	pent	pent, py	pent, py	pent, py mss	pyr, pent chalc	troilite	troilite
-$(Ru,Os,Ir)S_2$	yes	yes	yes	yes	yes	yes	no	no
Other opaques	$PtTe_2$	Pt,As,Ir, Fe-alloy						
Brecciation	no	weak	severe	severe	distinct	strong	weak	distinct
Chondrule relicts	yes	yes	yes	yes	yes	yes	yes	yes

Abbreviations: ox = oxidized; red = reduced; n.a.= not analyzed; n.d.= below detection limit; Ol = olivine; Fa = fayalite; Fs = ferrosilite; An = anorthite; mag = magnetite; kam = kamacite; taen = taenite; pyr = pyrrhotite; py = pyrite; chalc = chalcopyrite; mss = monosulfides; *) low-Ca-pyroxenes.

RESONANCE IONIZATION MASS SPECTROMETRY OF METEORITIC XENON.
J D Gilmour, S M Hewett, I C Lyon, M R Stringer and G Turner, Geology Department, University of Manchester, UK.

We have developed a time-of-flight mass spectrometer with a resonance ionization ion source to analyse meteoritic xenon. The required excitation wavelength (249.6nm) [2] is produced by a laser system consisting of several components. Firstly a Nd:YAG laser produces 1064nm radiation which is frequency doubled and used to pump a dye laser. Output from this is frequency doubled and mixed with residual radiation from the pump laser yielding 2.5mJ of 249.6nm radiation with a bandwidth of $0.2cm^{-1}$. This light is selected by a prism and focused into the ionization region of a time-of-flight mass spectrometer.

Theory predicts that our mass spectrometer should have an effective volume of ionization of approximately $0.5mm^3$. Experimentally measured values are highly dependent on operating conditions but the best results are comparable with this value. Our mass spectrometer has a volume of 200cc, implying a lifetime against detection for a xenon atom of the order of 10 hours. This will be greatly improved by a new ion source incorporating an atom buncher [1] that is presently under construction.

The ions are detected by a chevron pair of microchannel plates which, when combined with standard time focusing techniques, give a pulse of fwhm 14ns, yielding a mass resolution of 350 with a flight tube of only 50cm. Abundances are extracted by fitting a series of numerically defined peak shapes to the spectrum. Isotope abundances from a $10^{-12}cm^3$ xenon sample extracted from an aliquot of air are in good agreement with standard values.

We have used our spectrometer to obtain mass spectra from samples of $10^{-13}cm^3$ of air and have also done stepped heating experiments on Allende chondrules. These have shown the well known Xe^{129} anomaly [3] produced by the decay of I^{129}. We are now analysing xenon released by stepped heating and stepped combustion of acid residues of carbonaceous chondrites. We hope to present these results at the conference.

References

[1] G.S.Hurst, M.G.Payne, R.C.Phillips, J.W.T.Dabbs and B.E.Lehmann. *Journal of Applied Physics*, **55**:1278–1284, 1984

[2] M.G.Payne, C.H.Chen, G.S.Hurst, S.D.Kramer, W.R.Garrett and M.Pindzola. *Chemical Physics Letters* **79**:142–148, 1981

[3] J.H.Reynolds. *Physics Review Letters*, **4**:8–10 , 1960

Variable $^{196}Hg/^{202}Hg$ Ratio in Meteorites

P.S. GOEL and A.N. Thakur

Department of Chemistry, Indian Inst. Tech. Kanpur, India

We have continued our earlier work (Goel and Thakur, 1987) on measurements of isotopic ratio of $^{196}Hg/^{202}Hg$ in meteorites and AIRIMS (acid-insoluble residues of iron meteorites), by radiochemical neutron activation. Some selected results are given in Table 1.

Table 1: $^{196}Hg/^{203}Hg$ Ratios in Some Meteoritic Samples

Sample	Temperature	Hg ppb	Hg ng	R/R^+
IRONS				
Bogou	RT-100	30	31	1.38 ± 0.12
	100-200	67	69	1.46 ± 0.04
Huizopa	RT-100	16	31	1.0 ± 0.12
	100-200	171	325	1.0 ± 0.04
	200-300	10	20	1.12 ± 0.07
	300-400	14	27	1.10 ± 0.10
AIRIMS				
Sikhote Alin	RT-400	3000	153	1.0 ± 0.03
Inclusion	RT-400	4000	32	0.53 ± 0.1
	RT-500	1030	108	0.93 ± 0.05
nm 150-300 μm	150-200	6780	172	1.10 ± 0.06
Campo del Cielo	RT-100	2350	155	1.26 ± 0.05
	100-200	5540	365	0.93 ± 0.05
STONES				
Allende	RT-150	976	138	0.38 ± 0.02
	150-250	189	80	1.54 ± 0.08
	RT-500	2313	1972	1.02 ± 0.02

RT: Room Temperature, R/R^+: Hg(196)/Hg(202) ratio relative to the monitor value.

We have permormed many control experiments which establish the reliability of the technique. Our data show that:

(i) Most samples give normal isotopic ratios
(ii) Anomalous isotopic ratios are frequently found in step wise heating of a sample.
(iii) Both positive and negative deviation from the normal ratio are seen.
(iv) As yet it is not possible to pin down the phases which carry isotopically anomalous Hg.

Goel P.S. and Thakur A.N. (1987) Meteoritics, 22, 389 (abstract).
Thakur A.N. and Goel P.S. (1989) Earth and Planet. Sci Letters (under publication).

U-PB STUDY OF PHOSPHATES IN CHONDRITES; C.Göpel, G.Manhès & C.J.Allègre, Laboratoire Géochimie et Cosmochimie, I.P.G, 4 place Jussieu, 75252 Paris, Cedex 5, France

The isotopic Pb compositions measured in fragments of chondrites show a wide spread with $^{206}Pb/^{204}Pb$ ratios ranging from 9.5 to 130. Chondrites of all groups yield a Pb-Pb age of 4.55 ± 0.02 Æ. Two points have to be emphasized:

- All fragments are characterised by an excess of radiogenic Pb in respect to the measured U concentrations. This open system behaviour of U-Pb does not allow to validate the Pb-Pb model ages of these fragments within the analytical precision, typically in the order of a few to 10 million years.

- We do not know if the Pb-Pb age defined by the fragments of the metamorphosed chondrites corresponds to the formation of this material or whether it dates postmetamorphic closure of the U-Pb system during cooling.

The U-Pb study of phosphates, an accessory mineral in chondrites, offers two advantages:

- Phosphates are enriched in U (0.1-2 ppm) compared to the bulk rock (10-15 ppb) and contain today Pb with a radiogenic isotopic composition. This allows age determinations with precisions in the order of a few million years.

- Phosphates are secondary mineral phases, produced during metamorphism. Thus the determination of the closure time of this mineral phase allows to precise the period of metamorphism.

Until today only one analyses of phosphates from chondrites (LL6 St.Severin) has been published (Manhès et al.,1978; Chen & Wasserburg, 1981). The U-Pb system is concordant, the Pb-Pb age corresponds to 4.551 ±0.003 Æ and is similar to the Pb-Pb age of chondrites.

We report U-Pb analyses of phosphates separated from chondrites. The first meteorites we studied are L5 KNYAHINYA and L5 HOMESTEAD. In both cases is the U-Pb system concordant.

The U concentration of the phosphates separated from KNYAHINYA is ≈160 ppb. The measured Pb isotopic composition is radiogenic ($^{206}Pb/^{204}Pb$ =290) and defines a Pb-Pb age of 4.5330 ± 0.0008 Æ. This age is significantly lower than the Pb-Pb model age determined on fragments which show less radiogenic Pb isotopic compositions (80< $^{206}Pb/^{204}Pb$ >116, Pb-Pb- model age: 4.55 Æ; Unruh, 1982).

The higher U-concentration (900 ppb) of the phosphates separated from HOMESTEAD leds to an even more radiogenic Pb isotopic composition ($^{206}Pb/^{204}Pb_{mes}$ =1320). Again the Pb-Pb age of 4.5142 ±0.0006 Æ is significantly lower than the model age of fragments (4.55- 4.56 Æ), characterized by less radiogenic Pb isotopic compositions (45< $^{206}Pb/^{204}Pb$ <126). The observed age differences will be discussed.

Chen, J . H. & Wasserburg, G. J.(1981) Earth Planet. Sci. Lett. 52,1-15

Mahnès, G.; Minster, J. .F; Allègre, C.J.(1978) Earth Planet.Sci.Lett.39, 14-24

Unruh, D. M.(1982) Earth Planet.Sci.Lett. 58, 75-94

CARBON AND NITROGEN STABLE ISOTOPE ANALYSES OF TWO LUNAR METEORITES. Monica M. Grady and C. T. Pillinger, Planetary Science Unit, Dept. of Earth Sciences, The Open University, Walton Hall, Milton Keynes, MK7 6AA, U.K.

Currently, there are six meteorites known to originate on the moon, all of which have been collected from Antarctica. Three of them (Y 82192, Y 82193 and Y 86032) are believed to be paired (1), hence there are samples of four separate lunar meteorites, derived from at least three discrete craters (2). In composition, the lunar meteorites are anorthositic breccias, comparable to highland regolith breccias; they extend the types of lunar material now available for study. Stable isotope analysis of lunar samples has unravelled, to a certain extent, the somewhat complex post-accretionary history of the moon, from its early volatile degassing, through to its bombardment by meteoritic debris, the solar wind and cosmic rays. A stable isotope study of lunar meteorites from outside the relatively restricted surface area sampled by the Apollo and Luna missions might provide a new angle on the volatile inventory of the moon.

Two lunar meteorites were analyzed for carbon and nitrogen; results are summarized in the table. The total carbon contents are much higher than comparable lunar regolith breccias (12-198 ppm; 3,4), or indeed soils. Summed $\delta^{13}C$ are, however, within the range of $\delta^{13}C$ exhibited by lunar breccias (3,4). Three distinct maxima occur in the carbon yield histogram, over the temperature ranges given in the table. The T < 450°C material is most likely to be terrestrial contamination, whereas the higher temperature components could be indigenous. A fourth component of probable spallogenic origin is indicated only by the isotopic composition above 1150°C, and occurs in minor abundances. ALHA 81005 is richer in this component than Y 86032, in keeping with the known relative cosmic ray exposure ages of the two samples.

Total nitrogen data are also given below. Both [N] and $\delta^{15}N$ are within the range reported for lunar breccias (4 - 70 ppm; $\delta^{15}N$ *ca.* –65 to +74‰; refs. 5-7). As for carbon, there are several nitrogen-bearing components present, with variable isotopic composition. ALHA 81005 again evinces the greater influence of spallogenic nitrogen (as indicated by a higher $\delta^{15}N$ value) in the 1200°C step than does Y 86032. There is also little evidence in either meteorite for isotopically light ancient solar-wind nitrogen.

Both samples are different from returned lunar materials, particularly in carbon systematics. It is possible that volatile elements may have been added from the projectile during the impact which excavated the samples.

References: (1) Takeda, H. *et al.* (1988). *13th Symp. Ant. Met.* 9-11; (2) Warren, P.H. *et al.* (1989). *EPSL.* **91**, 245-260; (3) Kaplan, I.R. *et al.* (1970). *Proc. Ap. 11 Conf.* 1317-1329; (4) Petrowski, C. *et al.* (1974). *P5thLC.* 1939-1948; (5) Becker, R.H. & Clayton, R.N. (1975). *PLSC6th.* 2131-2149; (6) Fourcade, S. & Clayton, R.N. (1984) *EPSL.* **68**, 7-18; (7) Kaplan, I.R. *et al.* (1976). *PLSC7th.* 481-492.

Temp. °C	ALHA 81005 [C] ppm	$\delta^{13}C$ ‰	[N] ppm	$\delta^{15}N$ ‰	Y 86032 [C] ppm	$\delta^{13}C$ ‰	[N] ppm	$\delta^{15}N$ ‰
< 450	576	–25.5			292	–28.4		
550-700	102	–23.3			86	–22.1		
900-1100	226	–26.1			131	–28.2		
Total	1055	–23.9	53	+29.1	612	–26.7	31	+7.7

H-CHONDRITES: EXPOSURE AGES AND THERMAL EVENTS ON PARENT BODIES.

Thomas Graf and Kurt Marti, Dept. of Chemistry, B-017, Univ. of Calif., San Diego, La Jolla, CA92093

Clusterings of meteorite exposure ages are generally interpreted as evidence for collisions in space and of meteorite parent body break-ups [1-6]. Some authors infer evidence for fragmentation and reassembly of asteroids [7,8]. We report results of a reevaluation of exposure ages of H-chondrites based on as far as possible shielding corrected production rates of ^{3}He, ^{21}Ne, and ^{38}Ar. The exposure ages obtained for the H6 group were already reported [9].

First, we briefly discuss the criteria for subdividing the exposure age data into classes A, B, and C (for details see [9]): For class A data at least 3 quantities are required to compute averages: agreement of all 3 exposure ages or agreement of 2 shielding corrected exposure ages and arguments which may account for the disagreement of the third age (e.g. loss of ^{3}He indicated by $^{4}He < 1000 \times 10^{-8}$ cm^3 STP/g, or a large abundance of the trapped component). At least 2 quantities are required to qualify for class B, and all other samples belong to class C. We believe that the 1σ uncertainty of class A ages is about 10%. We make the following observations:

1) The well known broad peak of exposure ages between 3-8 Ma is resolved into 2 peaks with maxima at about 4.0 Ma and 6.5 Ma, respectively. The frequency of cases in the 4.0 Ma peak relative to the 6.5 Ma peak decreases with decreasing petrographic type.

2) A cluster of exposure ages is observed between 10-16 Ma. The relative frequency of occurrence decreases with increasing petrographic type.

3) Table 1 gives the percentage of meteorites which show loss of radiogenic ^{40}Ar (indicated by $^{40}Ar < 4200 \times 10^{-8}$ cm^3 STP/g) for several exposure age intervals and shows that the frequency of meteorites showing gas losses is not uniformly distributed with time. Further, the exposure age distribution of meteorites with gas loss is different for the different petrographic types. Except in a few cases, the loss of radiogenic ^{40}Ar is not correlated with loss of cosmic-ray produced ^{3}He, indicating that the loss of ^{40}Ar occurred on the parent bodies and suggesting varying magnitudes of the corresponding heat pulses.

4) The average $^{22}Ne/^{21}Ne$ ratio of meteorites with exposure ages <3 Ma is 1.08. This ratio is systematically lower than the average $^{22}Ne/^{21}Ne = 1.10$ of meteorites in the 6.5 Ma peak which is close to the total average. Because meteorites with low exposure ages are widely used for the calibration of production rates, it is important to notice, that the low $^{22}Ne/^{21}Ne$ ratios may sometimes indicate complex irradiation histories (e.g. preirradiation in a 2π geometry as in the case of the well documented Jilin H5 chondrite).

We will discuss the differences in the histograms for the various types of H-chondrites, the inferred thermal histories and implications regarding parent body structure.

Table 1: Percentage of meteorites with $^{40}Ar < 4200 \times 10^{-8}$ cm^3 STP/g

Exp. Age [Ma]	0-3	3-4.5	4.5-8	8-10	10-16	>16
H4	57 (7)	75 (4)	60 (25)	0 (2)	50 (10)	20 (10)
H5	17 (6)	29 (7)	57 (37)	0 (2)	55 (11)	24 (21)
H6	83 (6)	17 (6)	25 (8)	0 (4)	0 (7)	8 (13)

The number of chondrites evaluated in each interval is given in parantheses

References: (1) Anders, E. (1964) Space Sci. Rev. 3, 583-714. (2) Hintenberger, H., König, H., Schultz, L. and Wänke, H. (1964) Z. Naturforsch., 19A, 327-341. (3) Eberhardt, P. and Geiss, J. (1964) in: Isotopic and Cosmic Chemistry (eds H. Craig, S. L. Miller, and G. J. Wasserburg), 452-470. (4) Wänke, H. (1966) Fortschr. Chem. Forsch., 7, 322-408. (5) Tannenbaum, A.S. (1967) Earth Planet. Sci. Lett., 2, 33-35. (6) Schultz, L. and Crabb, J. (1981) Geochim. Cosmochim. Acta, 45, 2151-2160. (7) Taylor, G. J., Maggiore, P., Scott, E. R. D., Rubin, A. E. and Keil, K. (1987) Icarus, 69, 1-13. (8) Lipschutz, M. E., Gaffey, M. J. and Pellas, P. (1989) submitted to Asteroids II. (9) Graf, Th., and Marti, K. (1989) Lunar Planet. Sci. XX, 353-354.

IMPACT MELT ROCKS FROM NEW QUEBEC CRATER; R. Grieve[1], P. Robertson[1], M. Bouchard[2], C. Orth[3], M. Attrep[3] and R. Bottomley[4], 1.GSC, Canada; 2.U. Montreal, Canada,3.Los Alamos Lab., U.S.A., 4.U. Toronto, Canada

Introduction. The impact origin of New Quebec crater was until recently based on circumstantial evidence. In 1962, a fist-sized float sample of vesicular impact melt rock containing shocked mineral clasts was recovered from inside the rim. (1). A second ~ 5g sample from 3 km to the NNW on the shore of Lac Laflamme was described in 1986(2). In 1988, twenty one impact melt samples were discovered in an outwash channel near Lac Laflamme. The total collected weighed ~ 1500 g, with the largest sample being ~ 650 g.

Petrography. The impact melt samples have a glassy to cryptocrystalline matrix with minute granular oxides. The matrix composition, as determined by microprobe analyses, is basically quartzo-feldspathic, with the averages for two samples being: 61.4-71.1 SiO_2, 23.3-13.9 Al_2O3, 1.0-2.8 FeO, 0.8-5.5 CaO, 4.0-6.9 Na_2O, 1.6-6.2 K_2O. Feldspar microlites, up to 0.6 mm, have compositions ranging from Ab_{49} An_{46} Or_5 to Ab_{62} An_{33} Or_5. Pyroxene laths, up to 0.5 mm, have compositions ranging from En_{54} Fs_{42} Wo_4 to En_{70} Fs_{27} Wo_3. No high-Ca pyroxene was encountered (2). Mineral clasts, 5-20% of the samples, are generally limited to feldspar and quartz, some with planar features and ballen texture, after cristobalite. Flow texture around clasts is observed in some samples.

Chemistry. The average bulk composition of the melt samples is within the range of target rock compositions (Table 1). A similar correspondence occurs for trace elements but with enrichments in Co, Ni, Cr, and Ir in the melt rocks (Table 2). Further analysis on one sample indicates additional enrichments in Os (2.2 ppb), Pt (8.1 ppb) and Au (2.3 ppb). A chondritic body is favored by the high Cr and siderophiles but the data are insufficient to assign a class.

Age. A conventional Ar^{39}-Ar^{40} spectrum on the previous sample (1) has a U-shape. Based on previous work with melt rocks, the minimum in the U represents a maximum age of 1.3 m.y. for the event (3). The most recent samples are currently being dated with the Ar^{39}-Ar^{40} laser technique.

Origin. The textural character of the melt rocks differs from ejecta bombs and melt bodies within the interior breccia lens at simple craters. They most likely originated as small melt bodies deposited in fractures in the upper crater wall and owe their present location to fluvial glacial transportation.

Composition of lithologies from New Quebec

Table 1

	I	II	III
SiO_2	59.8-72.0	63.2	68.6
TiO_2	0.19-0.93	0.71	0.42
Al_2O_3	13.7-17.6	15.8	15.8
Fe_2O_3	1.1-3.0	1.7	2.1
FeO	0.8-3.5	3.8	4.0
MnO	0.03-0.09	0.10	0.06
MgO	0.56-2.30	2.08	1.8
CaO	0.75-4.20	3.11	3.2
Na_2O	3.7-4.9	3.9	3.7
K_2O	1.8-4.0	3.0	0.8

I. Range of 3 target rocks. II. Av. 3 melt rocks collected in 1988. III. Melt rock from (1)

Table 2

	I	II	III
Be, ppm	12-16	16	---
Co	4-13	25	12
Cu	11-14	22	---
La	16-140	87	52
Ni	0-37	230	79
V	17-63	64	70
Vb	0.0-2.1	1.2	<2
Zn	21-120	73	27
Cr	5-69	97	52
Ir, ppb	0.001-0.05	1.40	0.68

I, II, III as in Table 1. Ir in I and II, and all elements in III by neutron activation. Other elements in 1 are by emission spectroscopy.

References. (1) Currie, K.A. (1966) GSC Bull. 150, (2) Marvin, U.B. et al. (1988) Meteoritics, 23, 287-288, (3) Bottomley, R.J. and York, D. (1989) LPSCXX, 101-102.

WATER AND THE THERMAL EVOLUTION OF CARBONACEOUS CHONDRITE PARENT BODIES, Robert E. Grimm, Department of Geological Sciences, Southern Methodist University, Dallas, TX 75275, and Harry Y. McSween, Jr., Department of Geological Sciences, University of Tennessee, Knoxville, TN 37996.

Many carbonaceous chondrites have been aqueously altered within their parent bodies, although such alteration has not been quantitatively related to a thermal driving mechanism. We have modelled the thermal evolution of carbonaceous chondrites to constrain the size of the heat source and parent objects and to investigate the effect of water on thermal state. The models are based on the assumptions that ice and anhydrous silicates are the original nebular condensation products [1] and that the principal heat source is ^{26}Al.

Two classes of hypotheses can account for alteration of chondrite matrix materials: alteration in asteroid interiors, with later residence in regoliths; or contemporaneous alteration and brecciation in regoliths. Since deep sampling of asteroidal interiors requires catastrophic disruption, altered samples under the former model should be representative of the interior. Alteration temperatures for CM (25°C) and CI (150°C), as well as water:rock ratios, are given by oxygen isotopic data [2]. These constraints do not apply to unsampled interiors under the regolith-alteration model. We further assume alteration temperatures represent peak temperatures experienced by these meteorites.

Interior-alteration model. We find that initial $^{26}Al/^{27}Al$ ratios up to several parts per million are allowed for CI parent bodies a few hundred km in diameter containing 10% to 40% ice by volume. Calculations for CO chondrites, which are anhydrous but have higher peak temperatures, give similar bounds on initial ^{26}Al; these limits are also comparable to those inferred for ordinary chondrites [3,4]. We suggest that the fusion heat of ice, the high heat capacity of water, and the ability of circulating water to enhance rates of heat loss may all significantly contribute to thermal buffering of primordial heat sources for carbonaceous chondrite parent bodies. Hydrothermal circulation can cause the time-integrated water:rock ratio for some samples to be large and therefore qualitatively satisfy oxygen isotopic constraints. CM chondrites require $^{26}Al/^{27}Al$ ratios a factor of 2-3 lower than CI, and model objects of this group do not develop the hydrothermal circulation and hence cannot satisfy implied water:rock ratios unless the initial composition is >50% ice by volume. For both groups, the large temperature excursions and rapid exhaustion of water caused by explicitly including alteration reactions require that water was gradually introduced into reaction sites.

Regolith-alteration model. The release of water occurs readily in interior-alteration models because of the insulating effects of overlying rock. In cold surface regoliths, however, supplying liquid is more difficult. Water may be introduced into the regolith by internal heating in three ways: by direct melting of local ice, which may lead to H_2O circulation and replenishment from below, by venting of liquid or vapor along fractures caused by failure under high pore pressure, or by vapor diffusion through existing pores and cracks. Under different initial conditions, each of these mechanisms can supply water to within a few km of the surface.

Regolith alteration can also resolve some of the inconsistencies found under the interior-alteration model. Water can be introduced to the regolith from below in great quantities by venting or vapor diffusion, but probably at irregular intervals. Condensation there would provide a low-temperature environment for aqueous alteration, and removal of reaction heat is more easily accomplished from a near-surface location. Local melting of ice still fails to satisfy observed water:rock ratios, unless hydrothermal circulation extends into the regolith.

We have also investigated impact melting of ice as the thermal driving mechanism for regolith alteration, and have found that impacts can provide sufficient heat only after parent bodies have accreted and encounter velocities have been increased by gravitational interactions with Jupiter. Moreover, late-accreting planetesimals must be ice-rich in order to deliver the required water volumes.

References. [1] R.G. Prinn and B. Fegley; in Origin and Evolution of Planetary and Satellite Atmospheres (eds. S. Atreya et al.), Univ. Ariz. Press., in press, 1988; [2] R.N. Clayton and T.K. Mayeda, *EPSL, 67*, 151, 1984; [3] I.D. Hutcheon et al., *LPSC XIX*, 523, 1988; [4] M. Miyamoto et al., *PLPSC, 12B*, 1145, 1981.

THE STRUCTURE PECULIARITIES OF TAENITE PARTICLES AND TWO STAGES OF ITS THERMAL HISTORY IN OKHANSK H4 METEORITE

V.I.Grokhovsky, Physico-technical Dep., S.M.Kirov
Urals Polytechnical Institute, Sverdlovsk, 620002, USSR

Metal in two polished sections of the OKHANSK chondrite was investigated in detail with a microscope and an electron microprobe. The large kamacite particles and zoned taenite grains (25-29 wt.% Ni in the centre) were described earlier. We report new data for small γ-Fe, Ni particles and coexistent phases from ordinary chondrite matrix. Two types of particles have been observed among a variety of metal microstructures.

1. The complex assemblages of several Fe,Ni phases, troilite and copper. Tetrataenite with up to 0.47 wt.% Cu in solution is a dominant Fe,Ni phase. Separate copper grains are met in tetrataenite. The morphology of the clear taenite regions copies the shape of the troilite grains contained in it, which presumes their determinative history in solid state. A peculiar Ni distribution is observed in the zones taenite. The diffusion gradient of Ni is revealed from the surface of metal particles only and is not observed at the internal phase boundaries. Further, a great amount of distinctly expressed interfaces "tetrataenite - X-phase Fe,Ni". The X-phase with 25-29 wt.% Ni reveals the domain-type structure and corresponds to the hypothetic Fe_3Ni phase in composition.

2. The small particles of polycrystalline taenite with many μm-sized chromdiopside (27 wt.% MgO, 16 CaO, 59 SiO_2, 8 Cr_2O_3). We suggest that these type of microstructure may have formed by decomposition of supersaturated solid solution.

The two types of taenite particles are the extreme cases. There exist different combinations of these types, for example, diopside precipitates in taenite-troilite assamblages.

The structure peculiarities indicate the existence of two stages in thermal history of small metal particles from matrix in OKHANSK chondrite:

- the rapid supercooling at temperatures of 1100-600°C (polycrystalline taenite, the taenite-troilite morphology, X- Fe, Ni, chromdiopside precipitate);
- the prolonged Ni saturation of the surface at 300-400°C.

These data confirm the hypothesis of the formation of individual metal particles before accretion and their independent thermal history.

Asteroid core crystallization by inwards growth

Henning Haack, Institute of Geophysics, Haraldsgade 6, 2200 Copenhagen N, Denmark

Most of the iron meteorite groups have formed from a well mixed liquid in a central core of the iron meteorite parent bodies. Mixing of the liquid seems to require that the core crystallized from the inside out [1]. Diffusion in the liquid during crystallization might have been important at low cooling rates whereas solid state diffusion was of minor importance in case of plane front growth [2].

Even though the melting point of the liquid is higher at the center of the core due to the higher pressure, it is still difficult to explain why the crystallization should commence at the warm center of the core. Albeit the pressure effect is small even in a large parent body, it constitutes the only real difference between core center and core surface capable of influencing the commencement of crystallization. In a parent body with a radius of 100 km, the difference in pressure between the center and the surface of the core is ca. 0.15 kbar. The melting point of iron increases with 3.0 K/kbar [3] and the difference in melting point of iron between the center and the surface of the core is thus less than ca. 0.5 K. Thermal models of iron meteorite parent bodies indicates a temperature difference between the center and the surface of the core of 5 K [4]. In these models the center of the core is 4.5 K above the melting point when the rim of the core begins to crystallize.

In this work a new 2-D numerical model is presented simulating outside-in crystallization with irregular dendrites growing deep into the core from the rim. The irregular surface of the dendrites may cause trapping of P-rich immiscible liquid at a late stage in the crystallization process [5]. Plane front growth is not possible in the outside-in mode due to the concentration of light sulphurrich liquid below the growing solid front. Even at very high temperature gradients small scale experiments show that the growth front tend to become irregular [6]. Small perturbations in growth rate of the solid will be enhanced due to the upward migration of the light sulphurrich liquid. The sulphur will migrate upwards and concentrate in cavities at the solid-liquid interface. Sulphur lowers the melting point and will thus delay the crystallization process. The deepest regions of the solid front will therefore grow from a liquid of less sulphur. The growth at the deepest parts of the solid front is controlled by the temperature gradient in the core and the upward migration rate of the sulphurrich liquid.

It is found that plane front growth in an inwards crystallizing core is impossible if the sulphur content exceeds 0.02 wt%. Several iron meteorite parent bodies had sulphur contents in excess of 0.02 wt% [7] and it is thus likely that buoyancy effects were responsible for the mixing of the liquid in many of the iron meteorite parent bodies.

[1] Esbensen et al (1982) GCA 46, pp. 1913-1920.
[2] Jones and Drake (1983) GCA 47, pp. 1199-1209.
[3] McLachlan and Ehlers (1971) JGR 76, pp. 2780-2789.
[4] Haack et al (1989) Submitted to JGR
[5] Malvin et al (1984) GCA 48, pp.785-804.
[6] Sellamuthu and Goldstein (1983) Proc. Lunar Planet. Sci. Conf. 14th in J. Geophys. Res., 88, pp. B343-B352
[7] Willis and Goldstein (1982) Proc. Lunar Planet. Sci. Conf. 13th in J. Geophys. Res., 87, pp. A435-A445

Elemental Abundances of Trapped Noble Gases in Primitive Meteorites Determined by Isotope Dilution; B. Hagee, T. Bernatowicz and F. Podosek. McDonnell Center for the Space Sciences, Washington University, St. Louis MO 63130 USA.

Trapped noble gases in meteorites -- those which are not attributable to *in situ* nuclear effects or to exposure to solar wind -- occur in a characteristic pattern of relative elemental abundances designated the "planetary" pattern: in comparison with solar abundance ratios, there is a progressively greater depletion of the lighter gases relative to the heavier gases. No quantitative model has been advanced which satisfactorily explains the absolute and relative elemental abundances. The planetary noble gas "component" is nevertheless an important cosmochemical concept, *e.g.* it is frequently assumed that the initial noble gas inventory of the terrestrial planets has "planetary" composition.

Previous noble gas elemental abundances for meteorites have been acquired by the "peak height comparison" method, *i.e.* obtaining an instrumental sensitivity by analysis of standards and applying this sensitivity in analysis of samples. Such data are typically quoted with uncertainties around 20% or more and are also potentially subject to larger systematic errors. We have reexamined trapped noble gas abundances in a variety of meteorites using isotope dilution; this technique is more precise (uncertainties of a few percent) than peak height comparison and also more robust in that it is insensitive to possible systematic errors such as pressure dependent sensitivity. Gases were extracted from bulk samples (100-300mg) by RF induction heating and equilibrated with a mixed noble gas spike. Normal procedures were used for cleanup and mass spectrometry. Results for the heavy gases are illustrated in Fig. 1.

Although the relative abundances do not vary by more than about a factor of two for ordinary and carbonaceous chondrites, there are clearly real variations in the elemental composition of planetary gas, and these variations are not readily interpretable in one-parameter models, *e.g.* mixing of two components. As noted by Mazor *et. al.* (1970), the largest variations are in the relative abundances of Ne. This is plausibly attributed to different carrier phases for Ne (and He) and for the heavier gases (Ming and Anders, 1988). Even for the heavier gases, however, the observations preclude such simple models as attributing gas abundance variations to variable proportions of a single carrier.

References: **Crabb** and **Anders** (1981) *Geochim. Cosmochim. Acta* **45**, 2443; **Ming** and **Anders** (1988) *Geochim. Cosmochim. Acta* **52**, 1245; **Mazor, Heymann** and **Anders** (1970) *Geochim. Cosmochim. Acta* **34**, 781.

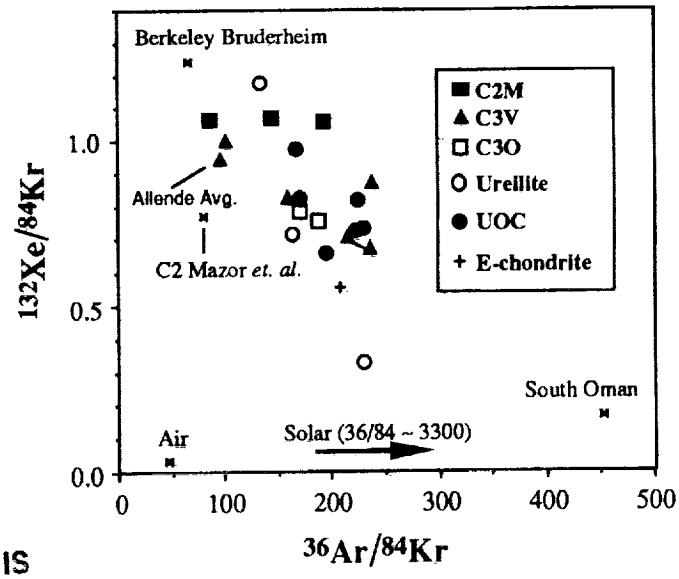

Fig. 1: Xe-Kr & Ar-Kr elemental ratios for various classes of meteorites: note legend. One sigma errors are about the size of the symbols. Allende Avg. is an average of six analyses. Standard compositions are plotted for reference. Note the C2 Mazor *et. al.* value often used as a standard planetary composition is significantly different from our data (although within its 30% error this value overlaps ours). Crabb and Anders (1981) describe South Oman (E4) as rich in a "sub-solar" component with distinct elemental ratios.

METEORITIC ZIRCON REVISITED: A NEW SEPARATION FROM TOLUCA

Charles L. Harper, mail code SN2, NASA Johnson Space Center, Houston, TX., 77058, U.S.A.

In 1895 Laspeyres and Kaiser reported an acid dissolution separation of ~73 micrograms of zircon from 585 grams of Toluca 'Rostrinde' (rust), produced by corrosion in the humid storage environment of the mineralogical museum in Bonn (1). The credibility of this claim to have discovered authentic meteoritic zircon, compromised as it was by the possibility of contamination, was later confirmed by Marvin and Klein (2) in an examination of several interior silicate and rutile bearing graphite-troilite nodules (3), one of which yielded two colorless euhedral crystals similar in size and morphology to those described by Laspeyres and Kaiser. As a supply of 'primordial' meteoritic zircon is desirable for isotopic investigations, a new effort was made to obtain a separate from this 4.55Byr old (4) type IA iron meteorite.

From a 6.56 Kg whole specimen provided by Elbert King, a 1071 gram slice was cut and, after extensive exterior cleaning, dissolved in dilute HCl and aqua regia baths, yielding ~30 grams of insoluble residue, which was then ground, sieved, and processed by heavy liquid and magnetic separation techniques in zircon-free environments. Examinations of the 74-149μ and 44-74μ nonmagnetic heavy mineral sieve fractions have thus far produced *one* zircon: a clear colorless euhedral specimen, 95μ by 46μ, possessing a type S4-5 morphology according to the classification of Pupin (5), and similar to the type L4 and ~S4 specimens shown in figures 1 and 2 of Laspeyres and Kaiser (1895). As the size of the new specimen is only slightly larger than the mesh of the smallest sieve, it seems likely that further crystals are present in the sub-44μ fines.

With the Winonaites, Lodranites, Brachina, Enon and type IIICD silicate inclusions, type IAB silicates represent an early era of non- to minimally-evolved 'primitive achondrite' melt formation events (6), and characteristically possess chondritic ^{129}I-^{129}Xe formation ages and undisturbed ^{40}Ar-^{39}Ar step-heating plateau spectra (7).

The presence of ~100μ zircons in type IA silicates --and surprisingly also in H chondrites (8)--encourages the prospects for the determination of a reliable fine-scale chronology for these earliest differentiation events as determined by single crystal analytical techniques in the $^{235/238}U$-$^{207/206}Pb$ systematics. A progress report will be given on these efforts.

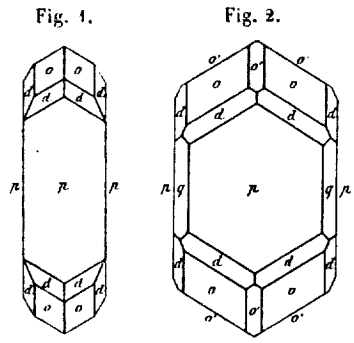

[Laspeyres and Kaiser, 1895]

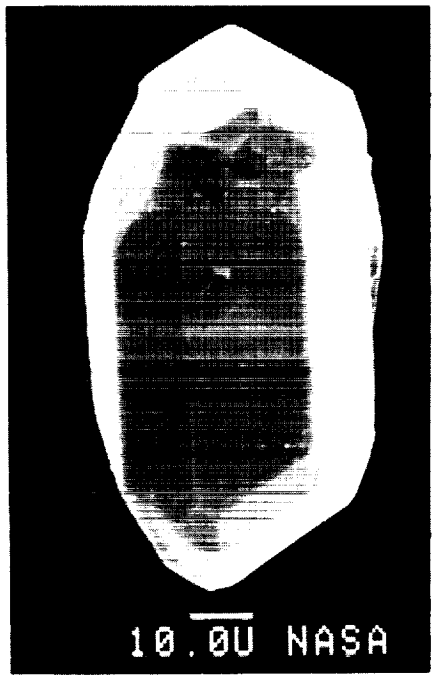

References: (1) Laspeyres H. and Kaiser E. (1895) *Zeitschr. f. Krystallogr.*, **24**, 485-493; Laspeyres H. (1897) *ibid.*, **27**, 586-600. (2) Marvin U. B. and Klein C. Jr. (1964) *Science*, **146**, 919-920; Frondel C. and Klein, C. Jr. (1965) *ibid.*, **149**, 742-744. (3) El Goresy A. (1965) *Geochim. Cosmochim. Acta*, **29**, 1131-1151. (4) Burnett D. S. and Wasserburg G. J. (1967) *Earth Planet. Sci. Lett.*, **2**, 397-408; Bogard D. et al., (1967) *ibid.*, **3**, 275-283; Gopel C. et al., (1985) *Geochim. Cosmochim. Acta*, **49**, 1681-1695. (5) Pupin J. P. (1980) *Contrib. Mineral. Petrol.*, **73**, 207-220. (6) Wasson et al., (1980) *Zeitschr. f. Naturforsch.*, **35a**, 781-795; Prinz et al., (1983) *Lunar Planet. Sci.*, **XIV**, 616-617; Kracher A. (1985) *Proc. 15th Lunar Planet. Sci. Conf.*, (J.G.R., **90** suppl., C689-698). (7) Niemeyer S. (1979) *Geochim. Cosmochim. Acta*, **43**, 843-860 and 1829-1840. (8) Ramdor P. (1967) Neues Jb. Miner. Mh., **2/3**, 90-92; ----(1973) *The Opaque Minerals in Stony Meteorites*. Elsevier, p. 88.

"ASTEROID" 2060 CHIRON: BLURRING THE DISTINCTION BETWEEN ASTEROIDS AND COMETS; William K. Hartmann (Planetary Sci. Inst.), D.J. Tholen and Karen J. Meech (Inst. Astronomy, U. of Hawaii), D.P. Cruikshank (NASA-Ames Research Ctr.)

In 1988 we recognized anomalous brightening of "asteroid" Chiron beyond its predicted magnitude (Tholen et al., 1988). Bowell, et al. (1988) confirmed our results. From our earlier observations we find that the anomalous brightening started in mid-1987 when Chiron was 13.0 AU from the Sun. (Activity has been observed for Comet Bowell as far as 13.6 AU; Meech and Jewitt, 1987).

Chiron brightened fairly steadily for some 23 months, until about 1989 January, when it was about 1.1 magnitude brighter in absolute magnitude (i.e. corrected for distance and phase angle) than in the mid-80's (Hartmann et al., 1989). According to our latest observations, Chiron faded in the interval 1989 January-April.

Our colorimetric observations show that Chiron's spectrum remained flat, characteristic of class C, during the brightening. The VJHK colors and the poorly determined albedo of .06 to .20 (Lebofsky et al., 1984) are consistent with a C-like object with slightly higher than average albedo and slightly bluer than average color.

Our hypothesis of cometary activity was strengthened by Lowell Observatory data (Bus et al., 1988), which show the rotational lightcurve amplitude dropping in half as the brightness doubled. This behavior (Nov. 1989) would apply if a rotating nucleus had ejected a coma. Meech and Belton (1989) first detected a coma on 1989 April 10.

Chiron is cataloged as an asteroid, but it is now exhibiting cometary behavior. It is a uniquely large comet, at diameter roughly 180 km, and its behavior reveals that we have much yet to learn about small interplanetary bodies. Better understanding of comet nucleus properties (which resemble certain black asteroids) may clarify the types of meteorites, if any, that can be delivered by comets.

Bowell, E., B. Bus, B. Skiff, and C. Cunningham (1988). IAU Circ. 4579.
Bus, S.J., E. Bowell, and L.M. French (1988). IAU Circular 4684.
Hartmann, W.K., D. Tholen, K. Meech, and D. Cruikshank (1989). Submitted to Icarus.
Lebofsky, L., D. Tholen, G. Rieke, and M. Lebofsky (1984). Icarus 60, 532-537.
Meech, K.J. and M. Belton (1989). IAU Circ. 4770.
Meech, K. and D. Jewitt (1987). Nature **328**. 506-509.
Tholen, D., W. Hartmann, and D. Cruikshank (1988). IAU Circ. 4554.

IN SITU DETERMINATION OF VOLATILES IN CM2 CHONDRITES. C.P. Hartmetz and E.K. Gibson Jr., SN2, Planetary Sciences Branch, NASA-JSC, Houston, TX 77058.

Five CM2 chondrites, Bells, Murchison, LEW87022, EET83355, and EET83389 were examined for *in situ* volatile elements (H, C, N, O, and S) and molecules. Analyses of freshly broken interior surfaces were performed at the 30-50μ scale using a laser microprobe/ quadrupole mass spectrometer technique (1). A minimum of 45 analyses were performed on the five meteorites and each distinct phase was analyzed at least 8 times. The variety of phases analyzed included: fine-grain matrix, fine and coarse grained inclusions (both reddish and white), porphyritic chondrules, chondrules with "matrix-like" rims, and olivine clasts.

Major volatile elements and molecules released include: C, O, S, OH, H_2O, C_2H_2 (minor CN), CO (C_2H_4 and minor N_2), O_2 (minor S), H_2S, CO_2, COS, CS_2, undersaturated hydrocarbon fragments (m/z=13, 15, 26, 39, etc.), and aromatic hydrocarbons (m/z=78 and 91). The largest amount of total volatiles were released from Bells, then Murchison and EET83389, followed by LEW87022 and EET83355 (these samples contained a factor of 1.65 and 1.7 less total volatiles than Bells). Bells released high quantities of H_2O (5 times Murchison and 12 times EET83355). It appears that Bells contains more H_2O than Orgueil (~21.2%) (2,3). Ubiquitous sulfide-related components (S, H_2S, COS, and CS_2) were released from almost all areas in these meteorites. Bells released the largest quantities of sulfide components followed closely by EET83389, Murchison, and LEW87022, with EET83355 releasing an order of magnitude less sulfide-related species than Bells. LEW87022 released components related to sulfates (i.e. large releases of SO and SO_2) that were heterogeneously distributed in the sample. We interpret the heterogeneous distribution as terrestrial fluids flowing through cracks and oxidizing sulfide. Sulfates were previously identified on Antarctic meteorites (4). Phases within the 5 CM2 meteorites were found to have low total volatile abundances, suggesting a high-temperature volatile-poor formation component (5). Dark chondrules in Murchison (6) were one such volatile-poor phase along with chondrules in Bells and EET83389, and an olivine clast in LEW87022. Low volatiles released from the olivine clast are in direct contrast to an olivine clast in Allende that was the most volatile-rich phase found in Allende (6). This must be a function of the formation environment of the olivine. In many terrestrial cases, olivines are known to trap volatiles upon formation (7).

References: (1) Gibson, E.K., Jr. and R.H. Carr (1989) In New Frontiers in Stable Isotope Research: Laser Probes, Ion Probes, and Small Sample Analysis (in press). (2) Böstrom and K. Fredriksson (1966) Smithsonian Misc. Collect., 151, 1-39. (3) Hartmetz, C.P. et al. (1989) In LPS XX, 381-382. (4) Marvin, U.B. and K. Motylewski (1980) In LPS XI, 669-670. (5) Anders, E. (1964) Space Sci. Rev., 3, 583-714. (6) Hartmetz, C.P. et al. (submitted) Geochim. Cosmochim. Acta. (7) Roedder, E. (1984) Fluid Inclusions, In Reviews in Minerology, 12, (ed. P.H. Ribbe) MSA, Washington, D.C.

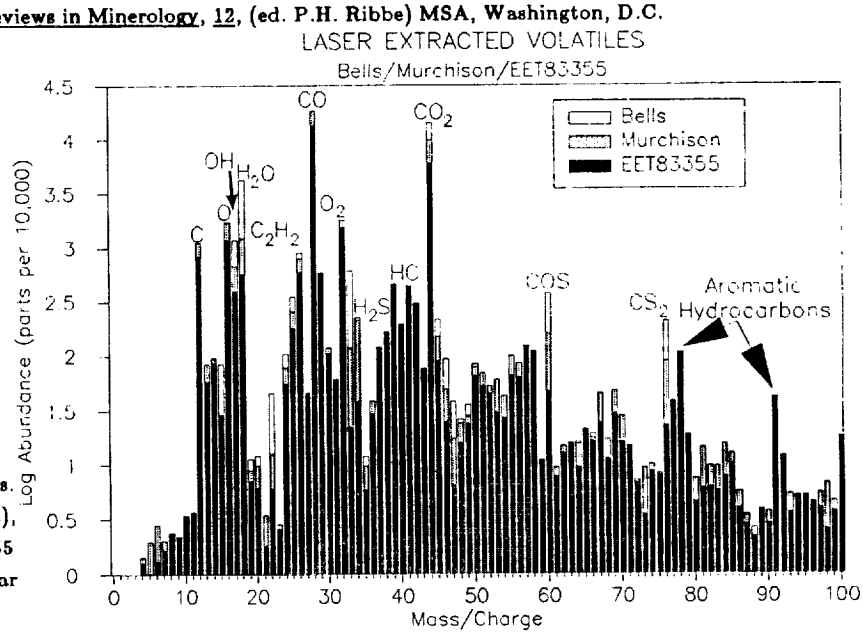

Figure 1. Plot of relative abundance vs. mass over charge fo Bells (unfilled bars), Murchison (shaded bars), and EET83355 (filled bars). The top of each type of bar represents the mean relative abundance.

TOTAL CARBON AND SULFUR ABUNDANCES IN ANTARCTIC CARBONACEOUS CHONDRITES, ORDINARY CHONDRITES, AND EUCRITES. C.P. Hartmetz, E.K. Gibson Jr., and R.A. Socki*, SN2 Planetary Sciences Branch, NASA-JSC, Houston, TX 77058. *LESCO.

Total carbon and sulfur abundances have been determined in 43 Antarctic meteorites and one terrestrial alteration product found on an H5 chondrite using published techniques (1,2). Carbon and sulfur abundances are reported in Table 1. Comparison of the carbon abundances from Antarctic meteorites (3,4) and falls (5) indicate that within each group, Antarctic meteorites have generally lower carbon contents. For example, 15 Antarctic L-group chondrites contain a median carbon abundance of 0.023% in comparison to a median value of 0.105% for non-Antarctic L-group falls (5). Carbonaceous chondrites are particularly depleted in carbon, except for LEW85332 (C3O) which has higher than average C3 (fall) carbon abundance. A study of the interior and exterior of Antarctic meteorites (4) indicates carbon is leached to the meteorite's surface. Carbonate weathering products have been observed on the surfaces of these meteorites. Perhaps, once the carbon reaches the surface, wind removes the carbonate or carbonaceous material. It is also possible that falls are contaminated during storage by atmospheric carbon.

White weathering products found on the exterior of LEW85320 (H5) are carbon-rich (8.8%), the same percentage of carbon is in $MgCO_3 \cdot 3H_2O$ (nesquehonite) which is the weathering product on this sample (6). Sulfur abundance (0.85%) is probably contamination from the bulk meteorite.

Sulfur abundances for Antarctic ordinary chondrites tended to be slightly higher than previously observed for falls (5). Mean values for 10 Antarctic H-chondrites were 2.59% S vs 2.00% S for 73 non-Antarctic H-chondrites (5). Mean values for 15 Antarctic L-chondrites were 2.88% S vs. 2.17% S for 115 non-Antarctic L-chondrites (5). These differences are not considered significant because they are within the range for L-group chondrites except for GEO85701, EET83273, and LEW86018 which were >2σ outside the range of falls. One might expect sulfur loss due to weathering, however no significant sulfur loss has been observed despite the presence of sulfates on the surface of some Antarctic meteorites (7). Occasionally the small sample sizes that are provided may introduce bias (e.g. ALH84086 (LL3) which contained 10.8% sulfur). LL3 chondrites are known to have heterogeneous compositions on a small scale and our sample undoubtedly contained significant amounts of sulfide.

References: (1) Moore, C.B. et al. (1970) Proc. Apollo 11th Lunar Sci. Conf., 1375-1382. (2) Gibson, E.K., Jr. and G.W. Moore (1974) Proc. 5th LPSC., 1823-1837. (3) Gibson, E.K. Jr. and Yanai, K. (1979) Proc. 10th LPSC, 1045-1051. (4) Gibson, E.K. Jr. and F.F. Andrawes (1980) Proc. 11th LPSC, 1223-1234. (5) Moore, C.B. (1971) In Handbook of Elemental Abundances in Meteorites, (ed. B. Mason) Gordon and Breach, N.Y., 81-91 and 137-142. (6) Jull, A.J.T. et al. (1988) Science, 242, 417-419. (7) Marvin, U.B. and Motylewski, K. (1980) In LPS XI, 669-670.

Table 1. Total carbon and sulfur abundances of Antarctic meteorites.

Sample Name	Type	C Content (wt%)	S Content (wt%)	Sample Name	Type	C Content (wt%)	S Content (wt%)
GRO85208,8	L6	0.011±0.001	2.62±0.02	LEW86018,9	L3	0.308±0.003	3.25±0.07
GEO85701,7	L6	0.021±0.001	3.49±0.01	ALH85062,7	L3	0.03±0.01	2.6±0.1
GRO85204,8	L6	0.0226±0 0003	2.64±0.01	ALH85045,8	L3	0.0278±0.0009	3.1±0.2
EET83273,3	LL6	0.0085±0.0004	3.38±0.07	ALH84120,6	L3	0.023±0.001	2.62±0.07
DOM85503,7	L6	0.0207±0.0008	3.3±0.2	EET83399,10	L3	0.236±0.004	2.7±0.2
ALH85029,8	L6	0.0136±0.0005	2.9±0.2	EET87526,12	C4	0.0070±0.0008	1.9±0.1
ALH85026,7	L6	0.0194±0.0001	3.0±0.1	EET83311,6	C4	0.04±0.03	1.98±0.03
EET83238,5	L6	0.008±0.001	3.05±0.08	ALH84096,7	C4	0.012±0.001	2.74±0.05
RKPA80201,8	H6	0.025±0.002	2.7±0.1	ALH85002,5	C4	0.0065±0.0001	1.86±0.06
RKPA80202,7	L6	0.021±0.002	2.9±0.1	ALH85003,6	C3O	0.090±0.002	2.41±0.08
ALH80105,7	L6	0.031±0.001	2.2±0.2	LEW85332,5	C3O	0.69±0.01	2.7±0.1
LEW86371,6	H5	0.051±0.009	2.54±0.08	MAC87300,13†	C2	0.88±0.01	2.67±0.07
LEW86083,6	H5	0.083±0.004	2.58±0.04	LEW87022,9	C2	1.750±0.004	4.17±0.04
ALH86603,4	H5	0.0315±0.0006	2.65±0.02	EET87522,14	C2	1.6±0.2	4.92±0.01
LEW85318,7	H5	0.101±0.002	2.47±0.02	EET83389,6	C2	1.8±0.1	2.86±0.05
ALH84155,3	H5	0.0194±0 0007	2.5±0.1	EET83355,6†	C2	0.88±0.03	3.09±0.07
ALH85033,7	L4	0.039±0.005	2.7±0.2	LEW85311,8	C2	1.9075±0.0003	4.07±0.07
ALH84084,4	H4	0.021±0.002	2.49±0 03	LEW85303,55	Eu	0.010±0.001	0.27±0.02
ALH80106,7	H4	0.067±0.002	2.7±0.1	LEW85300,37	Eu	0.010±0.001	0.405±0.003
ALH84059,7	H4	0.078±0.001	2.5±0.3	ALH85001,6	Eu	0.011±0.001	0.20±0.04
ALH80128,6	H4	0.037±0.001	2.8±0.1	LEW85320,*	H5	8.8±0.2	0.85±0.05
ALH84086,6	LL3	0.025±0.002	10.80±0.03				

* Average values from two splits (LEW85320,15 and 39) of what is an terrestrial alteration product.
† Two samples were identified incorrectly as type C2, they are C3V (Zolensky and Lipschutz, personal comm.).

THE SEARCH FOR EXTRATERRESTRIAL MATERIAL IN SEDIMENT FROM A LAKE ALONG THE MARGIN OF THE LEWIS CLIFF ICE TONGUE, EAST VICTORIA LAND, ANTARCTICA

Ralph Harvey, Department of Geology and Planetary Sciences, University of Pittsburgh, Pittsburgh, PA 15260.

During the 1987-88 ANSMET field season several small lakes were discovered along the terminal end of the Lewis Cliff ice tongue (LCIT) in the Beardmore glacier region of East Victoria Land, Antarctica (84°17'S, 161°05'E). These lakes vary in size and depth, are partially surrounded by morainal material, and are ice-bottomed. A thin (<2 cm) coating of sediment covers the bottom of some lakes. The largest lake was roughly 350 m^2, with an estimated maximum depth of 1 meter. Since the LCIT has a high density of meteorites on its surface, it was hoped that these lakes would be traps of concentrated extraterrestrial material analogous to the blue lakes of Greenland as investigated by Maurette, et. al. (1986). With this in mind, approximately 1 kilogram of sediment was collected from the largest lake and returned for analysis.

The sediment consists predominantly of fine-grained (<2 μm) clay (mixed illite, smectite and kaolinite) and a small fraction of larger (10-200 μm) lithic material consisting of glass shards, well rounded quartz, gypsum and calcite grains, and larger fragments of limestone and coal. Examination of the sediment with a stereo binocular microscope revealed the occasional presence of small (20-80μm) spherical particles. 9 spheres were recovered from approximately 250 g. of sediment. These specimens were removed for SEM and electron microprobe analysis.

On the basis of SEM and EDX analysis two spheres were shown to be terrestrial contaminants. Of the remaining particles, 6 were of a common type with some affinities to alkaline volcanic glass found previously in dust bands within the LCIT (Koeberl, et. al., 1988). However, preliminary electron microprobe analysis results are inconclusive as to their true composition and origin. Preliminary analysis of the remaining particle (a hollow sphere) indicates that it is composed of magnetite. The presence of significant Ni or Mg was not detected in the particles, making it unlikely that any are of extraterrestrial origin.

Conclusions. While the lakes seem a likely source of extraterrestrial material preliminary sampling has not revealed particles of definite extraterrestrial origin. Unlike the Greenland blue ice lakes, the LCIT lakes contain a predominant amount of terrestrially derived sediment with strong morainal affinities. The resulting dilution of any "cosmic" placer deposit makes it a less interesting source of extraterrestrial material. Other reasons for lack of success may include poor sampling, trapping of material in the short streambed between the lake and the ice tongue, or the true absence of small extraterrestrial particles in the ice. More careful sampling is planned for future ANSMET field seasons, while the existing sample is available for further study.

Acknowledgements My thanks to R. Witkowski, G. Cooke, and J. Wagstaff for their help. This work was supported by NSF grant DPP 83-14496 to W.A. Cassidy.

References

Koeberl, C., Yanai, K., Cassidy, W.A., and Schutt, J.A. (1988) Proc. NIPR Symp. Antarct. Meteorites, *1*, 291-309.

Maurette, M., Hammer, C., Brownlee, D.E., Reeh, N, and Thomsen, H.H. (1986) Science, *233*, 869-872.

CORRELATED ISOTOPIC MASS FRACTIONATION OF OXYGEN, MAGNESIUM AND SILICON IN FORSTERITE EVAPORATION RESIDUES; A. Hashimoto, Harvard-Smithsonian Center for Astrophysics, Cambridge, MA; A. M. Davis, R. N. Clayton and T. K. Mayeda, University of Chicago, Chicago, IL

Isotopic mass fractionations of O, Mg and Si in calcium-, aluminum-rich inclusions (CAI) in carbonaceous chondrites are correlated [1]. Since the degree of mass fractionation can be large and equilibrium fractionation of isotopes between solid and gas at high temperatures is small, it has been proposed that large fractionations occur through the kinetic isotope effect. We have reproduced this effect in the laboratory by evaporating forsterite under vacuum.

Solid forsterite was evaporated at 1750°C and liquid forsterite at 1900°C in vacuum ($<10^{-6}$ torr). Experimental run products ranged from 15.6 to 84.4% evaporated. The duration of the experiments was 1 to 6 hours for solid forsterite and 20 to 64 minutes for liquid forsterite. For each residue O and Si isotopes were measured in bulk by isotope ratio mass spectrometry and Mg isotopes were measured on a polished section by ion microprobe. Solid forsterite evaporated congruently and liquid forsterite evaporated nearly congruently, as the residue from the latter contains only a small amount of glass (65-67 wt% SiO_2).

Remarkably little isotopic mass fractionation was observed in the solid forsterite residue: $\Delta^{18}O$, $\Delta^{26}Mg$ and $\Delta^{30}Si$ were enriched by less than 2‰ in even the most heavily evaporated residue (77.7% evaporated). An ion microprobe traverse across one residue showed a $\Delta^{26}Mg$ enrichment of 5-10 ‰ in the outer 10 μm. Liquid forsterite residues have much larger effects (Fig.). The curve passing through the Mg points is a fractionation trajectory determined from the Rayleigh equation: $R = f^{\alpha-1}$, where $R = \frac{(^{26}Mg/^{24}Mg)_{residue}}{(^{26}Mg/^{24}Mg)_{initial}}$ and $\alpha = \frac{(^{26}Mg/^{24}Mg)_{gas}}{(^{26}Mg/^{24}Mg)_{solid}}$ and f is the fraction remaining. Similar curves were calculated for Si and O. α for each isotope ratio (Fig.) was determined by linear regression of ln R *vs.* ln f.

Kinetic evaporation experiments suggest that forsterite evaporates to form the gas phase species Mg, SiO_2 and O (or O_2) [2]. In kinetically-controlled evaporation, isotopic mass fractionation depends only on the masses of the evaporating species and the magnitude can be calculated: for $SiO_{2(g)}$, $\alpha = \sqrt{60/62} = 0.9837$. The experimentally determined α for $SiO_{2(g)}$ is slightly closer to 1 (Fig.), indicating that a heavier molecule is also evaporating. Similarly, calculated α's for Mg (0.9607) and the mean of O_2 and SiO_2 (0.9769) are slightly lower than observed values for Mg and O, respectively (Fig.).

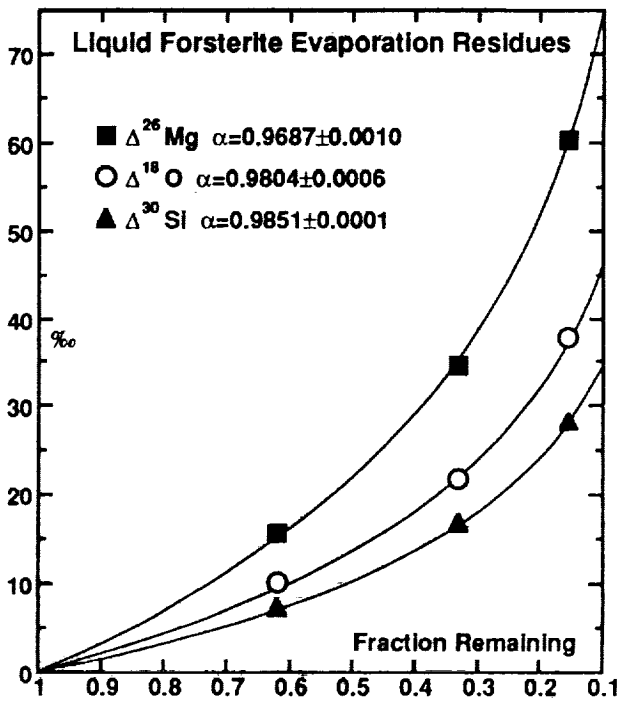

These results imply that it is necessary to melt CAI to obtain large isotopic mass fractionation effects during evaporation. The results obtained here appear to be directly applicable to CAI: in the forsterite residues, $\Delta^{26}Mg/\Delta^{30}Si$ = 2.08 and in CAI this ratio is 2.15 [1]. The first gas evaporated from an isotopically normal residue has $\Delta^{30}Si$ = -14.9 ‰ and $\Delta^{26}Mg$ = -31.3 ‰. No CAI lighter than this has been found [1]. If FUN CAI formed from an unfractionated reservoir, the most fractionated CAI (B7H10, $\Delta^{26}Mg$ = 76‰ [3]) formed after 90% of its material was evaporated.

References: [1] R. N. Clayton *et al.* (1988) *Phil. Trans. Royal Soc. London* A325, 483. [2] A. Hashimoto (1989) *LPS XX*, 385. [3] C. A. Brigham *et al.* (1988) *LPS XIX*, 132.

EFFECTS OF MELTING ON EVAPORATION KINETICS; A. Hashimoto, B.B. Holmberg, and J.A. Wood, Harvard-Smithsonian Center for Astrophysics, Cambridge, MA 02138, USA.

Understanding the kinetics of evaporation and condensation will provide the key to answering two questions: (1) Are chondrite components condensates or evaporation residues? (2) Did they form near equilibrium or far from it? One direct approach is to determine separately the evaporation and condensation rates of various planet-forming oxides. To eliminate the effect of vapor recondensation,we have measured the evaporation rates (J_L) of solid oxides at various temperatures *in a vacuum*. Each of these can be compared to J_e, the equilibrium incident rate at which molecules would impinge on the solid surface from a vapor in equilibrium with it, which can be calculated from its equilibrium vapor pressure [1].

The ratio J_L/J_e, termed the *evaporation coefficient* α_v, cannot exceed unity because at equilibrium the evaporation rate cannot exceed the recondensation rate, by definition. In situations where kinetic effects are unimportant, α_v should tend to unity.

Hashimoto [2] found that kinetic effects are important in the evaporation of MgO (periclase), SiO_2 (cristobalite) and Mg_2SiO_4 (forsterite), as indicated by their very small α_v's (~0.15, 0.01 and 0.1, respectively). He also observed that forsterite evaporates congruently in a vacuum. MgO and SiO_2 are major components of most chondrules and CAI's, and all chondrules and some CAI's are of molten origin. A fundamental question, then, is whether the kinetic effects observed for solids also apply at temperatures above their melting points. To answer this, we have investigated evaporation kinetics of molten forsterite, and additionally of Al_2O_3 and $CaAl_4O_7$ in both the solid and liquid states.

Forsterite liquid evaporated nearly stoichiometrically, with a trace of SiO_2-rich glass found only in the most highly evaporated residues. This contrasts with equilibrium calculations, which indicate that the vapor should be richer in Si than forsterite stoichiometry. α_v's were found to be ~0.2 for the MgO component and ~0.1 for SiO_2, similar to those of solid forsterite. As in the case of solid forsterite [2], if the hypothetical reaction mechanism ($Mg_2SiO_4 \rightarrow 2Mg(g) + SiO_2(g) + 2O(g)$) is considered, α_v^- becomes ~0.8, again almost unity. (α_v^- is used to distinguish the coefficient for this hypothetical system from the normal α_v.) This suggests that the evaporation mechanism does not change on melting.

Pure Al_2O_3 showed α_v~0.35 both for solid and liquid. Burns [3] observed α_v~0.3 for the solid, but 1.0 for liquid. The cause of this discrepancy is unknown. When a hypothetical reaction mechanism ($Al_2O_3 \rightarrow 2AlO(g) + O(g)$) is adopted in calculating J_e, α_v^-=0.9 for the solid and 1.0 for the liquid result, suggesting that Al_2O_3 evaporates directly to AlO(g) which subsequently decomposes to stable Al(g). $CaAl_4O_7$ in the molten state became more aluminous by preferred evaporation of Ca. After crystallization, one sample contained skeletal hibonite and the other skeletal corundum in fine-grained groundmasses of Ca-rich phases. $\alpha_v \simeq 1.0$ for CaO component (*cf.* 1.0 for pure solid CaO), and $\alpha_v \simeq 0.5$ for the Al_2O_3 component (slightly larger than that of pure Al_2O_3). Evaporation of solid $CaAl_4O_7$ produced a thin (~10 μm) veneer of hibonite overlaying residual $CaAl_4O_7$, indicating preferred Ca evaporation.

From these observations, it is concluded that basically the same kinetic effects exist during evaporation from both solid and liquid states. Other oxide systems will be investigated.

REFERENCES: [1] Langmuir, I. (1913) *Phys. Rev. 2*, 329-342. [2] Hashimoto, A. (1989) *LPS XX*, 385-386. [3] Burns, R.P. (1966) *J. Chem. Phys. 44*, 3307-3319.

LARGE METAL NODULES IN MESOSIDERITES; Jamshid Hassanzadeh, Alan E. Rubin and John T. Wasson, Institute of Geophysics and Planetary Physics, University of California, Los Angeles, CA 90024

The remarkable mixture of subequal amounts of metal and basaltic and pyroxenitic silicates in mesosiderites seems to require the accretion of a core-like metal mass produced in one asteroid onto the surface of another asteroid; our INAA data on 11 large mesosiderite metal nodules show that the accreted metal mass had a composition similar to the mean IIIAB iron-meteorite core. The similarity of the siderophile compositional pattern to mean IIIAB irons, the very limited compositional range, the inferred large projectile/target ratio, and the electrical interconnectedness of mesosiderite metal indicate that the bulk of the metal was molten when accreted.

Mesosiderites have previously been divided into plagioclase- and tridymite-rich subgroup A and orthopyroxene-rich subgroup B on the basis of modal silicate mineralogy. The same subgroups can be defined by metal compositions; Au, As and Ni are higher, and W and Cr are lower in subgroup A than in subgroup B. A plausible model is that subgroup A best preserves the regolithic silicate and accreted core compositions; subgroup B was formed from a mixture of this material with a minor amount of accreted core-mantle materials consisting of olivine and refractory, Ni-poor metal. The covariation of Ga, Re, Ir and Pt may reflect fractionations during impact heating events.

Reckling Peak A79015 is an anomalous mesosiderite consisting of extremely heterogeneous mixtures of silicate and metal. It is strongly depleted in refractory siderophiles and slightly enriched in volatile siderophiles. This composition could have been produced either by impact-induced heating and fractionation (as observed for large metal nodules in H chondrites) or by fractional crystallization of metal different in composition from that in the other mesosiderites.

NEW CHEMICAL CONSTRAINTS ON THE ORIGIN OF AUBRITES

C.F. Heavilon[1], M. Wheelock[2], K. Keil[2], M.M. Strait[3], G. Crozaz[1]. [1]Department of Earth and Planetary Sciences and McDonnell Center for the Space Sciences, Washington University, St. Louis, MO 63130. [2]Department of Geology and Institute of Meteoritics, University of New Mexico, Albuquerque, NM 87131. [3]Department of Chemistry, Alma College, Alma, MI 48801.

Among aubrites, Shallowater is unique because it is the only one with an unbrecciated igneous texture (Foshag, 1940). It contains 80% large orthoenstatite crystals and 20% of an assemblage of clinoenstatite, forsterite, plagioclase, metal and troilite, found as inclusions in and interstitial to the orthoenstatite. This assemblage appears xenolithic and, according to Keil (1988) and Keil *et al.* (1989), Shallowater formed by breakup, mixing and reassembly of two asteroidal objects. We measured trace element concentrations of the xenolithic phases and host enstatite, by in-situ ion microprobe analysis, in order to (1) test this model and (2) identify REE carriers in aubrites.

Electron microprobe analyses show that forsterite, orthoenstatite and clinoenstatite are virtually iron-free, with <0.1% (by weight) FeO. Orthoenstatite generally has <0.1% CaO, but contains CaO-enriched "hotspots" with up to 0.5% CaO. Clinoenstatite has 0.4 - 0.5% CaO. Feldspar is quite variable, ranging from 8.3 - 10.2% Na_2O, 0.06 - 4.4% CaO and 0.4 - 2.5% K_2O.

REE are below detection limits (<10 ppb) in olivine, clinoenstatite and orthoenstatite, indicating that they crystallized from highly REE-depleted melts. Relative abundances of Ca, Mn and Ti are enriched in clinoenstatite over orthoenstatite by more than a factor of 10 and Zn by a factor of 3. Smaller enrichments of Sc, V, Cr and Zr are also observed. Trace element abundances of the Ca "hotspots" are similar to those in clinoenstatite, consistent with the proposal of Keil *et al.* (1989) that they represent partially-digested, xenolithic clinoenstatite grains which served as nuclei for crystallization of the host enstatite magma.

REE patterns were obtained from four feldspar grains, spanning the range in CaO content. Eu increases with CaO, reaching a maximum of about 6 x CI. La ranges from below detection to 0.1 x CI, and CI chondrite-normalized La / Nd is about 8. HREE concentrations are below detection in all grains. Whole rock REE patterns for Shallowater (Keil *et al.*, 1989) range from La = 0.1 - 0.4 x CI and exhibit a positive Eu anomaly at ~ 0.5 x CI. REE abundances (including Eu) in plagioclase are too low to account for the bulk of the REE in Shallowater. At least one other REE carrier is required.

Oldhamite, the major REE host in enstatite chondrites (Lundberg and Crozaz, 1988), is a good candidate (Strait, 1983). Trace amounts of oldhamite have been reported in Shallowater (Keil *et al.*, 1989), but none was found in our sections. However, we analysed two oldhamite grains in Bishopville and found nearly flat REE patterns at about 100 x CI, with a slight negative Eu anomaly. In addition, large (up to 500 microns) weathered areas, resembling weathered oldhamite (Okada *et al.*, 1981), show Ca and REE signals similar to those of the analysed oldhamite; this indicates that weathering of oldhamite was not accompanied by extensive leaching of these elements. If Bishopville oldhamite is representative of aubrites, we can conclude that 0.3 - 0.4 modal % oldhamite may have existed in Shallowater, and that its weathering products are now the carriers of a significant portion of the REE.

Foshag, W.F. (1940) Amer. Mineral. **25**, 779-786.
Keil, K. (1988) Meteoritics **23**, 278-279.
Keil, K. *et al.* (1989) Geochim. Cosmochim. Acta (submitted).
Lundberg, L. and Crozaz, G. (1988) Meteoritics **23**, 285-286.
Okada, A. *et al.* (1981) Meteoritics **16**, 141-152.
Strait, M.M. (1983) Ph.D. Thesis, Ariz. State Univ., 172pp.

DOUBTS ON METEORITES AS COSMIC RAY PROBES. G. HEUSSER, MAX-PLANCK-INSTITUT FÜR KERNPHYSIK, P.O.BOX 103 980, D-6900 HEIDELBERG, F.R. GERMANY

The complex irradiation history of the *Jilin* chondrite revealed how important it is to investigate all possible cosmogenic products. Short-lived radionuclides are as important as stable noble gases to deciphering the irradiation conditions of meteorites.

Two out of the three recently measured chondrites *Ybbsitz*, *Guizhou*, and *Trebbin* are suspected to have no single-stage irradiation histories. Information on cosmic irradiation ages deduced from only one of the pairs $^{26}Al/^{21}Ne$ or $^{53}Mn/^{21}Ne$ can be quite incorrect if a two-stage irradiation history was experienced by the meteorite. Figure 1 depicts the variation of the ratios of the irradiation ages from both pairs in dependence of the duration of the second stage. The curves denote two extreme cases, where the first stage irradiation occurred with heavy shielding (lower curve) and with very moderate shielding (upper curve). Most investigations on cosmic ray constancy have compared irradiation ages from these or similar pairs of cosmogenic nuclides. If further complete investigations of fresh falls confirm the high frequency of complex irradiation history, then meteorites would loose their quality as poor man's space probes.

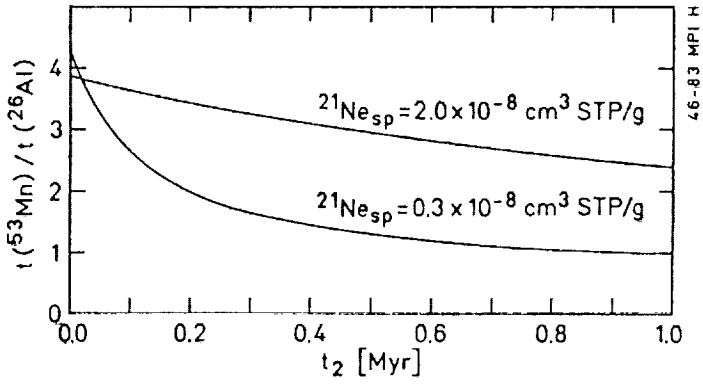

Figure 1

HG ANOMALIES AT THE K/T BOUNDARY: EVIDENCE FOR ACID RAIN?

A.R. Hildebrand and W.V. Boynton, Dept. of Planetary Sciences, Univ. of Arizona, Tucson AZ 85721

In 1982, Lewis et al. (1) suggested that acid rain would be a consequence of a large impact that may have terminated the Cretaceous Period; sufficient acid rain would cause mortality and extinctions, possibly being the dominant K/T extinction mechanism instead of the oft-discussed darkness and cold scenario. Prinn and Fegley (2) suggested that acid rain should produce a geochemical signature of normally immobile but acid-rain leachable elements, such as Hg, in sediments and carbonate shells from near-shore marine K/T boundaries. We have discovered anomalous amounts of Hg at several K/T boundary localities.

We found no Hg to our detection limit of ~50 ppb in bulk samples from the middle shelf marine environment represented by the Brazos River K/T locality, but we have found a sub-ppm Hg anomaly at three widely-spaced nonmarine K/T boundary localities: Dogie Creek, Wyoming; Raton, New Mexico, and Police Island, Northwest Territories, Canada. The boundary clay layers are separated from the typically overlying coal seam by a mudstone at Raton and Dogie Creek establishing the occurrence of the Hg anomaly independent of the coal, although some Hg has apparently been geochemically mobilized to the reducing environment of the coal. Other chalcophile elements (e.g. As, Sb, and Se) show evidence of similar geochemical mobilization. Nonmarine sites, rather than marine sites, may record a truer geochemical picture of such an acid-rain episode, since the ocean would dilute continental leachates and oceanic processes might prevent rapid deposition.

Both the ejecta and fireball layers have many associated elemental anomalies which are from different sources. Secondary geochemical processes have affected many elements at all K/T sites, necessitating care in drawing interpretations. The major elements (e.g. Na, Mg, K, Ca, Al, Si, and Fe) may be depleted or enriched in the boundary layers and are variable from site to site. We feel their abundance reflects only the various end-products produced by the pervasive alteration of the layers, making them useless as indicators of provenance. Siderophile elements (e.g. Ru, Rh, Pd, Os, Ir, Pt, Au, Co, and Ni) are present in chondritic ratios implying derivation from a chondritic projectile. Rhenium, which is in excess relative to the other siderophiles, may have been derived from impact-induced volcanism (3). Incompatible lithophile elements (REE, Rb, Sr, Cs, Zr, Ba, Hf, Ta, W and Th) show varying degrees of depletion in the layers, indicating oceanic crust and mantle, not a continent, were the target of the impact (4). However, Sc, V, Cr and Ti, four more-compatible lithophile elements, are enriched in the boundary layers (e.g. 5). The enhancement of these elements implies the presence of a mantle component, consistent with an oceanic provenance. (However, we note the Cr may be derived, at least in part, from the projectile.) Chalcophile elements (e.g. As, Sb, Se, Cu, Zn, Mo and Ga) are anomalous in both marine and nonmarine sections (e.g. 6), thus eliminating the possibility of a seawater provenance for the chalcophiles and establishing the chalcophile anomaly as a primary signal of the K/T boundary event. We have suggested (7) that the As, Sb and Se anomalies may have been produced by mantle outgassing on the basis of their similarity to mantle ratios. All the chalcophile elements may have a mantle outgassing provenance or may have been mobilized by acid-rain leaching (or some combination thereof).

Impact-produced acid rain may have left a chemical fingerprint at the K/T boundary in the form of Hg (and other chalcophile element) anomalies. The acid rain may have been the dominant extinction mechanism, at least for marine organisms, at the K/T boundary. The observed Hg anomaly may support those advocating heavy metal poisoning as a K/T extinction mechanism (e.g. 2). This evidence for an acid rain pulse also buttresses the suggestion of Retallak et al. (8) that the "bone gap" of the western U.S. is due to dissolution of bones at and near the soil surface.

REFERENCES: (1) Lewis, J.S., Watkins, G.H., Hartman, H. and Prinn, R.G., 1982, Silver, L.T., and Schultz, P.H., eds., G.S.A. Special Paper 190, p. 215-221, (2) Prinn, R.G. and Fegley, B., 1987, E.P.S.L., v. 83, p. 1-15, (3) Hildebrand, A.R., Boynton, W.V. and Zoller, W.H., 1984, Meteoritics, v. 4, p. 239-240, (4) Hildebrand, A.R. and Boynton, W.V., 1987, L.P.S.C., v. XVIII, p. 427-428, (5) Gilmore, J.S., Knight, J.D., Orth, C.J., Pillmore, C.L. and Tschudy, R.H., 1984, Nature, v. 307, p. 224-228, (6) Hildebrand, A.R. and Wolbach, W.S., 1989, L.P.S.C., v. XX: 414-415, (7) Hildebrand, A.R. and Boynton, W.V., 1989, Proceedings of the 2nd Snowbird meeting (submitted), (8) Retallak, G.D., Leahy, G.D., Spoon, M.D., 1987, Geology, v. 15, p. 1090-1093

NITROGEN ISOTOPES IN SINOITE GRAINS FROM THE YILMIA ENSTATITE CHONDRITE;

P.Hoppe and J.Geiss, Physikalisches Institut, University of Bern, CH-3012 Bern, Switzerland
A. El Goresy, MPI Kernphysik, P.O.Box 103980, D-6900 Heidelberg, FRG

Some of the E6-chondrites, like Yilmia, are characterized by the occurence of the mineral Sinoite (Si_2N_2O) which has neither been found in terrestrial samples nor in other meteorite classes. Sinoite was discovered in the Jajh deh Kot Lalu enstatite chondrite by Andersen et al. (1964). Enstatite chondrites have a relative high nitrogen content (several hundred ppm) and compared to other chondrites a "light" nitrogen composition. This covers a range of $\delta^{15}N_{Air}$ = -25°/oo to -45°/oo (Kung and Clayton, 1978).

The aim of this work was to measure the isotopic composition of nitrogen in different Sinoite grains from Yilmia. Recently made N-isotopic measurements on interstellar SiC grains (Tang et al., 1988) yielded large isotopic anomalies ($\delta^{15}N$=-850°/oo to +3200°/oo) and a nitrogen component in the solar nebulae having a large isotopic anomaly ("LPN", $\delta^{15}N \leq -500$°/oo) has been postulated (Geiss and Bochsler, 1982). However, due to the thermal history of E6-chondrites, the size of the Sinoite grains (≈100 μm) and N-isotopic measurements on enstatite chondrites (which in part contain Sinoite) it seemed unlikely to find such large isotopic anomalies in these Sinoite grains.

The isotopic measurements were made with an ion probe (modified CAMECA IMS 3f) on a thin section of Yilmia, using the N^+ ion. The Sinoite grains were microscopically identified. The results are shown in figure 1. We used synthetic Si_3N_4 as isotopic standard, accordingly the $\delta^{15}N$ values of Sinoite are related at the present time to the N-composition of Si_3N_4. The nitrogen isotopic composition of Si_3N_4 should be close to that of air (deviation: a few °/oo), if isotopic equilibrium was approximately achieved in the high temperature production of Si_3N_4. An additional uncertainty results from the fact that the standard and Sinoite are different in chemistry and mineralogy. Such a "matrix effect" can lead to a systematic error for the $\delta^{15}N$ values in the order of about 1%. In spite of this uncertainties the following conclusions can be made:

1)There is no variation of isotopic composition between single grains within the given limits of error.

2)The average isotopic composition of Sinoite yields $\delta^{15}N_{Si3N4}$ = -27±3°/oo. Hence no significant isotopic anomalies have been found. The agreement of this result with the bulk N-isotopic composition of enstatite chondrites seems to be relatively good but the above given uncertainties should be considered.

To eliminate the uncertainty due to the "matrix effect" we are trying to obtain synthetic Sinoite or if not available to synthesize it ourselves.

Acknowledgements

We thank F. Bühler and B. Perny for discussions. This work was supported by the Swiss National Science Foundation.

References

Geiss J. and Bochsler P. (1982). Geochimica et Cosmochemica Acta, **46**, 529-548. **Andersen C.A., Keil K. and Mason B.** (1964). Science, **146**, 256-257. **Kung C.C. and Clayton R.N.** (1978). Earth and Planetary Science Letters, **38**, 421-435. **Tang M., Anders E. and Zinner E.** (1988). Lunar and Planetary Science, **19**, 1177-1178.

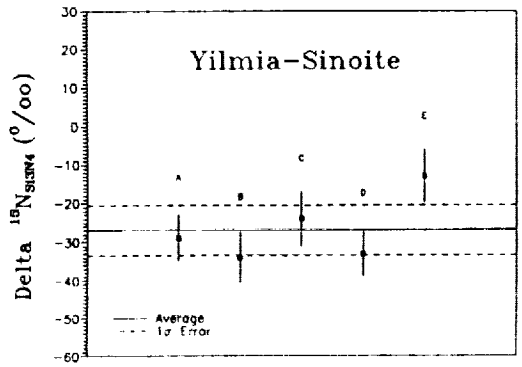

Figure 1

Shown are preliminary $\delta^{15}N$ values of 5 single Sinoite grains related to the N-composition of synthetic Si_3N_4. In addition the average (solid line) of all grains and the mean 1σ-error (dashed line) of single grains are given. The N-isotopic composition of the Si_3N_4 should be close to that of air. There is a systematic uncertainty in the order of about 1% for the $\delta^{15}N$ values of all grains (see text).

INTERSTELLAR DIAMONDS AND SiC FROM TYPE 3 ORDINARY CHONDRITES.

Gary R. Huss and Roy S. Lewis
Enrico Fermi Institute, Univ. of Chicago, Chicago, IL 60637-1433 USA

We have isolated interstellar diamonds (Cδ) from Ragland (LL3.4), ALHA 77214 (L3.2), and Dimmitt (H3.9?). Cδ diamonds have now been reported in varying concentrations from CI, CM2, CV3, LL3, L3, H3, and E4 chondrites and noble-gas data strongly suggest their presence in CO3 chondrites. Interstellar diamonds were apparently incorporated into all classes of primitive chondrites.

Cδ in Ragland, ALHA77214, and Dimmitt is essentially identical to that in Allende in physical behavior and in Ne, Kr, and Xe contents and compositions (except for differences in ^{21}Ne and ^{129}Xe which probably reflect variations in cosmic-ray exposure and ^{129}I in the host meteorites). The noble-gas characteristics are summarized in Table 1. Stepped pyrolysis data for Cδ from Allende [1], Ragland, and ALHA77214 show a remarkably similar isotopic structure. However, these samples lack the characteristic low-temperature 'planetary' component found in Cδ from CM2 chondrites [2].

Recovered amounts of Cδ were 70 ppm in Ragland, 29 ppm in ALHA77214, and 0.5 ppm in Dimmitt. Estimates of the true Cδ abundances for these meteorites may increase slightly (significantly for ALHA77214) as yields are better constrained. Abundance data for other meteorites can be estimated from yields of recovered Cδ [2,3,4] or, now that the noble gas contents and compositions in Cδ are more precisely known, somewhat less reliably from noble-gas data for etched HF,HCl residues [5,6,7]. Cδ abundances seem to vary with compositional group, as shown by the values (ppm) for the most primitive type 3 chondrites: CV3 (300-450), CO3 (150-300), LL3.2-4 (50-150). If Cδ is in the matrix, then matrix abundances of Cδ are rather similar for these classes. L3 and H3 chondrites appear to have increasingly less Cδ, down to 0.5 ppm in Dimmitt, but we cannot yet separate intrinsic differences from possible metamorphic effects. Within CO3 and LL3 chondrites, Cδ content seems to decrease with increasing subtype, e.g., from Kainsaz to Lance to Ornans, or from Bishunpur (LL3.1-2), Krymka (LL3.0-3), Chainpur (LL3.2-4), and Ragland (LL3.4) to Parnallee (LL3.6-9), which has almost no Cδ.

A sample of Ragland HF,HCl residue, etched to remove 'planetary' noble gases, was analyzed by stepped pyrolysis. Ne-E(H) was clearly detected, corresponding to $\approx$0.5 ppm SiC (its supposed carrier) in Ragland. Previous data on etched residues [7] also show hints of Ne-E in Bishunpur, Krymka, and Chainpur, which, if due to Ne-E(H), would correspond to 1-5 ppm SiC. Interstellar SiC has now been isolated or inferred from CI, CM2, CV3, and type 3 ordinary chondrites. It may be that SiC was as widely distributed in the early solar system as was Cδ.

Table 1: Noble gases in Cδ from Allende and type 3 ordinary chondrites.

^{20}Ne	^{84}Kr	^{132}Xe	20	82	86	124	130	134	136
(10^{-8} ccSTP/gr)			22	84	84	132	132	132	132
9500	13.5	25.0	8.44	.171	.347	.00782	.1560	.594	.648
±500	.5	.5	.04	5	9	15	5	10	11

[1] Lewis and Anders (1988) LPSC XIX, 679-680. [2] Tang and Anders (1988) GCA, 52, 1235-1244, 1245-1254. [3] Lewis et al. (1987) Nature, 326, 160-162. [4] Ash et al. (1989) Talk given at 20th Lun. Plan. Sci. Conf., Houston. [5] Matsuda et al. (1980) GCA, 44, 1861-1874. [6] Alaerts et al. (1979) GCA, 43, 1421-1423. [7] Alaerts et al. (1979) GCA, 43, 1399-1415.

TRACE ELEMENTS IN THE FUN INCLUSION C-1: ABSENCE OF Ce AND W ANOMALIES; I. D. Hutcheon[1], H. Palme[2], A. Kennedy[1] and B. Spettel[2]. 1. Div. Geol. & Planet. Sci., Caltech, Pasadena, CA 91125. 2. Max-Planck-Institut, Mainz, FRG.

FUN inclusions are characterized by large mass-dependent isotope fractionation for O, Mg and Si and nonlinear isotope anomalies. The FUN inclusion C-1 is regarded as chemically anomalous due to a large negative Ce anomaly [1]. C-1 is one of two CAI with a Ce anomaly and the Ce depletion may indicate formation of C-1 in a highly oxidizing environment [2]. We determined trace elements in a bulk sample of C-1 and in individual minerals using INAA and SIMS. (Fig. 1) Bulk C-1 is uniformly enriched in refractory lithophile and refractory siderophile elements with an average chondrite-normalized enrichment factor (E_{ch}) of ~26. Two exceptions are V, which is depleted (E_{ch}~0.6), and Mo ($E_{ch}\lesssim 4$). In contrast to previous results [1,3], Ce and W are not depleted in bulk C-1. The chondrite-normalized abundance of Ce (25.8) is slightly higher than that of La (24.6), while E_{ch} for W (22.2) is the same as for Ir (22.1) and Re (22.7) and very similar to Os (24.7). Analyses of fassaite, melilite and anorthite separated from the bulk sample reveal striking differences in La, Ce and W abundances between the bulk CAI and individual minerals. Refractory metal contents of the separates are high, comparable to the bulk, but W and Mo are absent. La and Ce in silicates are 2 to 10 times lower than in the bulk CAI and all 3 phases exhibit negative Ce anomalies. The anomaly is not constant; La/Ce is 1.2-1.5 in fassaite, ~3 in melilite and 3.7 in anorthite. Fassaite and melilite exhibit complementary REE patterns characteristic of igneous partitioning. Fassaite is LREE-depleted with a negative Eu anomaly; E_{ch} increases from ~10 for La to ~50 for Lu. Melilite and anorthite contain lower REE and are LREE-enriched with positive Eu anomalies; E_{ch} for anorthite and the most enriched melilite decrease from ~12 for La to <1 for Lu. REE abundances in melilite decrease with increasing Åk content, in agreement with experiments [4]; E_{ch} (La) decreases from ~12 for Åk 45 to ~2.5 for Åk 68.

Our results show that C-1 is not depleted in Ce or W. The Ce anomaly reported by [1] most plausibly reflects non-representative sampling and indicates that oxygen fugacities based on trace element abundances in CAI must be viewed cautiously. We find no evidence for formation in an oxidizing environment and suggest C-1 formed at normal solar fO_2. Refractory metals condensed as alloys of cosmic composition and the precursor CAI received the full complement of refractory lithophiles and siderophiles. During melting and subsolidus oxidation, La, Ce and W were redistributed within the CAI, while Mo was lost. The low abundances of Ce, La and W in the major minerals indicate La and Ce were segregated from other REE, while oxidized W was lost from metal nuggets. The present sites are unknown, but the presence of celsian, pyrochlore and Nb-perovskite suggests substantial trace element redistribution in C-1. Comparison of refractory siderophile abundances in C-1 with experimental results [5] suggests that the fO_2 during metamorphism was between the Fe-FeO buffer, where no Mo is lost, and the Ni-NiO buffer, where Re is lost.

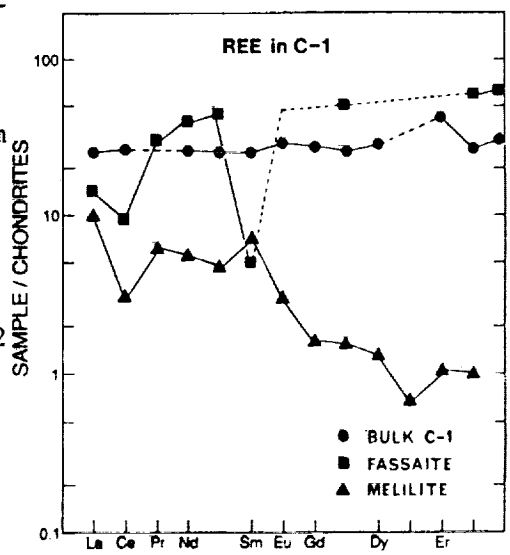

[1] R.Conard (1976) M.S. Thesis, Oregon State U.; [2] W.V. Boynton (1978) LPS IX, 120; [3] D.Wark (1983) Ph.D. Thesis, Un. of Melbourne; [4] J.R.Beckett et al. (1989) GCA, in press; [5] A.V.Köhler, pers. comm. (#674).

ARE CHONDRITES PRIMITIVE? A PAPER FOR DISCUSSION

R. Hutchison, Mineralogy Department, British Museum (Natural History), London SW7 5BD, UK

With few exceptions (1,2,3), the chondrites have recently been viewed as primitive objects whose origin is linked with processes that occurred in a protosolar nebula. Anders, Wasson, and Wood, with their co-workers, argue strongly that the chemistry and mineralogy of chondrites were determined by nebular condensation (4,5,6). A nebular origin for the chondrites requires that they accreted cold, then were metamorphosed to varying degrees. Planetary processes affected chondrites only at a later stage, for example in the production of gas-rich regolith breccias.

More recently it was recognized that the mineral assemblages of CI, CM and other carbonaceous chondrites were controlled to some extent by hydrous alteration on their parent bodies (7,8). So, although the chemical composition of C chondrites may be primary and primitive, this is not true of much of their mineralogy.

All three groups of ordinary chondrites have members that contain clasts or clast-chondrules of igneous rock, some of which have fractionated rare earth element patterns testifying to a planetary origin (9,10). Long-lived and/or short-lived radioisotopic systematics indicate that some planetary clasts are as old as chondrules. Thus, we cannot argue that the ordinary chondrites are older than differentiated bodies. We know that grains of presolar origin are present in chondrites (11), hence they must be mixtures of presolar and planetary materials. The question is one of degree.

In the ordinary chondrites the ratio of presolar and nebular material to planetary material may lie in the range from 99:1 to 1:99, the latter being favoured by the author. Early impacts on a planetary (distinct from asteroidal) scale, with a tiny spike of unaccreted dust, may have led to the origin of chondrules and chondrites.

(1) H C Urey, JGR 64, 1721-1737 (1959). (2) K Fredriksson, in Meteorite Research (Ed. P M Millman) Reidel, 155-165 (1969). (3) J V Smith, Mineralog. Mag. 43, 1-89 (1979). (4) J W Morgan et al., GCA 49, 247-259 (1985). (5) J T Wasson and G W Kallemeyn, Phil. Trans. R. Soc. Lond. A325, 535-544 (1988). (6) J A Wood and G E Morfill, in Meteorites and the origin of the solar system (Eds. J F Kerridge and M S Matthews) University of Arizona, 329-347 (1988). (7) S W Richardson, Meteoritics 13, 141-159 (1978). (8) D J Barber, Clay Minerals 20, 415-454 (1985). (9) R Hutchison et al., EPSL 90, 105-118 (1988). (10) I D Hutcheon and R Hutchison, Nature 337, 238-241 (1989). (11) C M O'D Alexander et al., Lunar Planet. Sci. XX, 7-8 (1989).

OXYGEN ISOTOPIC COMPOSITIONS OF MURCHISON REFRACTORY INCLUSIONS; T.R. Ireland and E.K. Zinner, Physics Dept. and McDonnell Center for the Space Sciences, Washington University, St. Louis, MO 63130, U.S.A.

We report O-isotopic compositions in 14 inclusions, composed of hibonite, spinel, and perovskite, from the Murchison CM2 chondrite. The hibonite-bearing inclusions comprise three groups (Ireland, 1988; Ireland *et al.*, 1989): 4 platy hibonite crystal fragments (PLACs), 7 spinel-hibonite grains (SHIBs) and 2 HAL-type hibonite inclusions. Grain 7-A52 is composed of spinel and perovskite.

Mean O-isotopic compositions of PLACs, SHIBs, and 7-A52, lie within error of the Allende-mixing-line with a range of ^{16}O excesses from +4 to +6% (analyses with normal rim material excluded). This is consistent with previous analyses of 8 PLAC-type hibonites (Fahey *et al.*, 1987). Spinel and hibonite have the same O-isotopic compositions in individual SHIBs, and no differences are apparent between PLACs and SHIBs despite the differences in morphology, hibonite chemistry, and Ca, Ti, and Mg isotopic systematics.

In contrast, 7-404 and 7-971 have FUN O-isotopic systematics being enriched in ^{16}O as well as having mass-fractionation effects. All data points from 4 fragments of each inclusion have been plotted, including those with rim material; those from 7-404 extend up to the mixing line of HAL (Lee *et al.*, 1980), while 7-971 shows less overall fractionation. FUN O-systematics have been interpreted as due to a mass-fractionation event, such as distillation, which enriches the heavy isotopes relative to the initial ^{16}O-enriched reservoir. Isotopically-heavy Ca and Ti have also been measured from these inclusions (Ireland *et al.*, 1989). The range in O-mass-fractionation from each inclusion is beyond that expected from the reproducibility of the Burma spinel standard, as well as the scatter of the PLACs and SHIBs, and suggests that these inclusions were not completely molten during the distillation event.

References: **Fahey *et al.*** (1987) *Ap. J.* **323**, L91; **Ireland** (1988) *Geochim. Cosmochim. Acta* **52**, 2827; **Ireland *et al.*** (1989) *LPSC XX*, 442; **Lee *et al.*** (1980) *Geophys. Res. Lett.* **7**, 493.

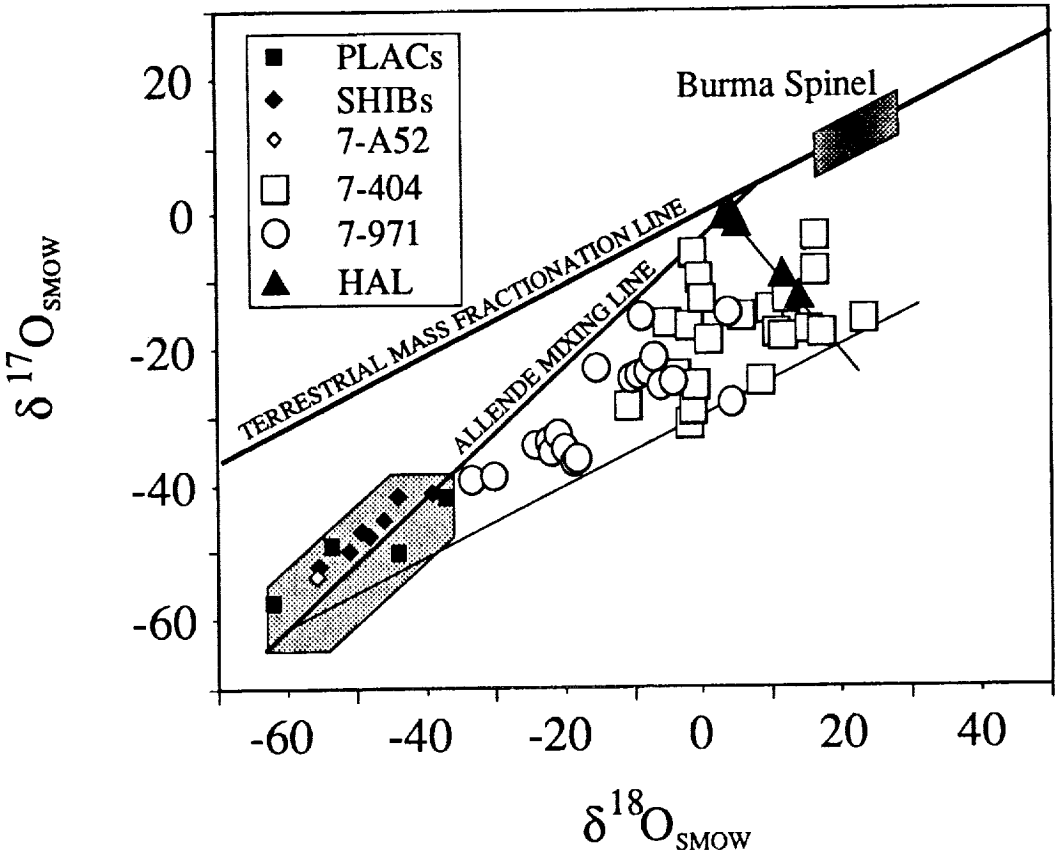

PALEOMAGNETIC AND ROCK MAGNETIC EXAMINATION OF THE NATURAL REMANENT MAGNETIZATION OF SUEVITE DEPOSITS AT RIES CRATER, WEST GERMANY; D.A. Iseri, J.W. Geissman, H.E. Newsom (1), G.Graup (2), (1) Dept. of Geology, University of New Mexico, Albuquerque, NM, 87131, USA, (2) Zum Romergrund 50, D-6501 Worrstadt, West Germany.

INTRODUCTION: Recent interest in impact produced formations and deposits, fueled by controversy concerning the origin of the Cretaceous-Tertiary boundary clay layer [1] and other impact ejecta, has inspired our research into the mechanisms of formation of suevite breccia deposits. Key problems include the initial temperature of the suevite, and the origin of the clays and other alteration phases, such as maghemite, which may bear on the origin of the Martian soil [2]. The suevite located at the Ries Crater in West Germany is well preserved [3], and provides a unique opportunity for new detailed investigations.

RESULTS: The magnetization of ejected suevite breccias at the Ries crater was examined in detail to determine if any significant variations in natural remanent magnetization direction exist, and to characterize the phases which carry the remanence. Magnetization variation was studied in vertical section and at various sites. Physical separation of several types of clasts which possibly carry the natural remanent magnetization (NRM) was performed to investigate important carriers of the NRM and their genesis. Azimuthally oriented core was collected along vertical sections and very dense sampling intervals (2-10cm spacing) at the Altenburg, Aumuhle, Otting, and Polsingen suevite localities at the Ries crater. Individual breccia inclusions (glass and highly shocked crystalline basement material) were also cored. The magnetization of the core was measured in a low magnetic field room using a superconducting rock magnetometer. The natural remanent magnetization of 540 specimens from all localities was found to be ($D = 188.6^0$, $I = -60.8^0$, $\alpha 95 = 0.78^0$) in excellent agreement with Pohl [4], but with significantly smaller uncertainties.

Examination of the magnetic response of individual clasts of material, separated from the bulk suevite, to thermal and alternating field demagnetization as well as DC field saturation and demagnetization has shown significant differences among clasts. Demagnetization behavior of unaltered glass and highly shocked (stage III) crystalline inclusions indicates a very homogeneous size/shape population of principally single domain low-Ti titanomagnetite grains.

Maghemite formation during low temperature oxidation of titanomagnetite is also indicated. The maghemite, however, records the same magnetic direction as Ti magnetite, which recorded the magnetic direction when the suevite was at high temperature. This result strongly suggests that the low temperature alteration of the suevite, including clay formation [5], occurred due to hydrothermal alteration ($<130^0$ C) shortly after the emplacement of the suevite, and not because of weathering under ambient conditions since crater formation, 15 my ago.

Significant variations in magnetic properties with stratigraphic height occur at Aumuhle. The lower red zone 6, appears to contain more titaniferous and or finer grained magnetite than all other suevite. This layer appears to be petrologically related to the upper sorted suevite layer of the Nordlingen (1973) drill hole and may represent very early ejecta. If this is the case, traces of the impactor, may be found in these deposits.

The melt rich suevite at the Polsingen locality is the only material found to contain hematite as a dominant carrier of the NRM, as well as titanomagnetite. Hematite probably formed during high temperature oxidation of the melt rich suevite along vesicles.

CONCLUSIONS: The remarkable consistency in magnetic directions from different suevite constituents and different outcrops suggests that after deposition, the suevite deposits were all significantly above 540^0 C following thermal equilibration. These results suggest that the thermal differences between suevite and coherent melt sheets may be less than previously assumed. Identical magnetization directions recorded by phases formed at high and low temperatures strongly indicates that low temperature ($<130^0$ C) hydrothermal alteration of the suevite occurred immediately after emplacement of the suevite, and not during weathering over an extended period of time since the formation of the crater. The fine scale differences in magnetic mineralogy of the various suevite deposits may have implications for models of ejecta formation and interpretation of ejecta deposits in future studies.

REFERENCES: [1]. Alvarez, W., et al.(1988), abstr., in Proc. of Global Catastrophes in Earth History, Snowbird, Utah, U.S.A., Oct. 1988, 1. [2] Newsom, H.E. (1980) Icarus, 44, 207-216 [3] Engelhardt, W. v., and Graup, G.(1984), Geol. Rundschau, 73, 447-481. [4]. Pohl, J. et al. (1977) in Impact and Explosion Cratering, 343-404, Pergamon, New York. [5] Newsom, H.E. et al. (1986) J. Geophys. Res. 91, E239-E251.

RELATIONSHIP BETWEEN AUSTRAL-ASIAN TEKTITE STREWN-FIELD AND ZHAMANSHIN CRATER: CLUE TO THE ORIGIN OF TEKTITES;

E.P.Izokh, Inst. Geol. a. Geoph., Novosibirsk, USSR

Both objects are located along the same trajectory. The properties and ages of tektites are about the same (2). In both regions, as well as in Australia, the well known tektite age-paradox is established: the radiogenic age tektite-glasses is 0.4-1.0 m.y. and more, while the time of fall to the Earth is quite recent - less than 0.01 m.y. (1,3). The latter is based on the ^{14}C-age of charcoal, on the age of the river low-terraces, the palinological data, etc.

In Vietnam the loess in the tektite-bearing layer enriched with Ir, Ru, Os, Rh, Pd. Thus the replacement of tektites cannot have occured. A similar geochemical anomaly has been discovered in the layer synchronous to the impact event not only in the vicinity, but as far as 150-250 km NE of the Zhamanshin crater.

The age-paradox is the direct evidence of the tektite extraterrestrial origin. There are some other age-paradox occurences: the findings of tektites of various ages within the same layer (4); the annihling of fission-tracks as a result of sharp heating during the flight through the Earth atmosphere (6); great difference between the ages of Zhamanshin tektites and impactites (5). The latter are argued (7,8).

A hypothesis of tektite comet delivery to the Earth has been advanced (1). According to it some ice-blocks (comet-fragments) having a steep trajectory give rise to impact craters like Zhamanshin, while the ones having a sloping or skipping trajectory bring about band-like "Tektite showers".

1. Izokh E. Meteoritika, 1983, N 42; 1985, N 44. 2. Izokh E. Petrochemistry of the target rocks, impactites and tektites of Zhamanshin astrobleme, Novosibirsk, 1986. 3. Izokh E. 4-5. Kashkarov L. 6. Korotkova N. 7. Kolesnikov E. 8. Storzer D. 3-8: abstr. 2d Intern.Confer.Natur.Glasses, Prague, 1987.

PB-SR-ND ISOTOPIC EVOLUTION ON MARS AND EARTH

Emil Jagoutz Max-Planck-Institut für Chemie, Saarstrasse 23, D6500 Mainz F.R.Germany

A new chemical procedure for the isotopic analysis of EETA 79001 has been developed. This new method allows Sr, Nd, and Pb isotopes from the same dissolution to be measured. In SNC meteorites plagioclase is the host phase for Sr and Pb and results in low Rb/Sr and U/Pb ratios. The Sr/Nd ratio reflecting the whitlockite/maskelynite ratio seems to independent of the amount of cumulus minerals. In order to evaluate mixing relations, the age corrected isotopic initial ratios are used. A single stage model age evolution was applied to extrapolate the Nakhla source to match the shergottite ages. The range of isotope compositions observed in the five SNC meteorites can be explained by the mixing of three reservoirs. Multidimensional factor analysis indicates that the data do form a two dimensional array (i.e. a plane), similar to the the case of terrestrial oceanic basalts From the Pb isotope data, but also indicated by the Sr isotope data, it is clear that these three reservoirs on Mars were isolated for more than 4 Ga, possibly during an early differentiation (e.g., accretion, core-mantle differentiation) of Mars. On Earth, however, the three reservoirs could originate from a common reservoir at much later time, perhaps between 1 and 2 Ga. It is apparent that the isotopic variation on Mars is larger than in the terrestrial mantle. The two dashed lines indicate different cosmic fractionation trends, with both the C1 and C 2-3 trend linked at an achondritic point having a very radiogenic Pb and unradiogenic Sr isotopic composition. Assuming that U/Sr ratio and Sm/Nd ratio in both planets are chondritic their pronounced isotopic difference must be caused by different Rb/Pb ratios in the accreting materials (Jagoutz, 1986). It is noteworthy in this context that the Si/Mg ratio of the Earth (Jagoutz et al. 1979) and in C 2-3 chondrites are also lower than in C1 and ordinary chondrites. The isotopic systematics of Mars and Earth suggeste that Mars accreted from ordinary chondrites, while the Earth may have accreted from material which falls along a cosmochemical fractionation trend from C1 to C2, C3, CV chondrites to the Earth

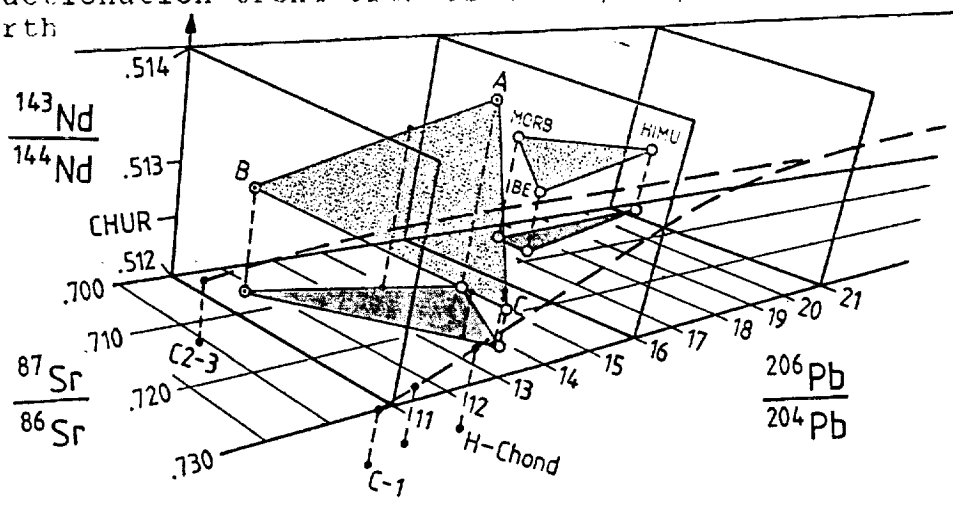

HALLEY'S GRAINS, INTERPLANETARY AND INTERSTELLAR DUST. E.K. Jessberger, Max-Planck-Institut für Kernphysik, P.O. Box 103980, 6900 Heidelberg, FRG

Three years after the missions to Halley and with the new knowledge of the chemical and isotopic composition of cometary grains, one can now investigate their relationship to interstellar matter identified in meteorites [1] and also their inferred [2] relationship to interplanetary dust particles (IDPs).

Halley's grains are a complex mixture of two principal particle types [3,4]: CHON [5] and SILICATES [6]. The overall proportions are such that the abundances of C, N, and O (relative to Mg) approach solar abundances identifying Halley's grains as less fractionated than even CI chondrites [6]. Enrichments of volatile elements have also been reported to occur in chondritic, porous IDPs which have C > 2 wt.%. Among the elements enriched relative to CI-chondrites are Br, Ga, and Zn [7-9]. These findings have recently been confirmed by combined PIXES and SYXFA studies of two IDPs [10]. Although Br, Ga, and Zn are not accessible from the mass spectra taken at Halley, the common enrichment of volatile elements relative to CI-abundances points to a genetic link between Halley's dust and some IDPs.

The Fe/(Fe+Mg) distribution for Halley's dust, which in previous analyses peaked at about zero and then extended with low abundances up to one [6, 11,12] indicating lack of chemical equilibrium as also found in anhydrous IDPs [12,13], from a new evaluation of 854 compressed PUMA-1 mass spectra [14] is almost evenly distributed over the whole range.

Densities of six IDPs range from 0.4 to 3.4 g/cc [9] and are independent of the chemical composition of the particles. A new analysis of the densities of about 200 Halley particles measured by PUMA-1 revealed a bimodal density distribution related to grain chemistry [15].

In interstellar SiC $^{12}C/^{13}C$ ranges from 11 to 159 [1]. It has been suggested [1] that even higher values than the present maximum of 159, encountered in an SiC-aggregate, should exist in individual minerals. Cometary 12/13-intensity ratios span from 1 to 5100. Lower than normal (=90) values may be due to interference from $^{12}CH^+$ at mass 13, while high values, for which reasons to be artifacts are not easily envisioned, could be true $^{12}C/^{13}C$. The particle with the maximum 12/13 ratio has CI-like abundances of O, Si, Ca, Fe, and Ni (within a factor of two, relative to Mg) and excesses of C (40*CI), N (16*CI), and S (4*CI).

References: [1] T. Ming et al., (1989): Interstellar SiC in meteorites: implications and origin. submitted to Nature; [2] D.E. Brownlee (1985) Ann. Rev. Earth Planet. Sci. 13, 147; [3] J. Kissel et al. (1986) Nature 321, 280; [4] J. Kissel et al. (1986) Nature 321, 336; [5] J. Kissel, F.R. Krueger (1987) Nature 326, 755; [6] E.K. Jessberger et al., (1988) Nature 332, 691; [7] C.C.A.H. van der Stap et al., (1986) LPSC XVII, 1013; [8] G.J. Flynn, S.R. Sutton (1987) LPSC XVIII, 296; [9] M.E. Zolensky et al., (1989) LPSC XX, 1255; [10] R. Wallenwein et al., (1989) LPSC XX, 1171; [11] D. Brownlee et al., (1987) LPSC XVIII, 133; [12] M.E. Lawler et al., (1989) Icarus, in press; [13] J.P. Bradley (1988) GCA 52, 889; [14] M. Solc et al., (1989) Sulden-Workshop, April 17-21, 1989; [15] F.R. Krueger et al., (1989) Sulden-Workshop, April 17-21, 1989.

MAGNETITE IN SILICATE INCLUSIONS IN THE BOCAIUVA IRON: FORMATION BY REACTION OF CO3 CHONDRITIC SILICATES AND METAL; Craig A. Johnson[1], M. Prinz[1], and M. K. Weisberg[1,2], (1)Amer. Museum of Natural History, New York, NY 10024, (2)Brooklyn College (CUNY), Brooklyn, NY 11201

Bocaiuva is a silicate inclusion-bearing iron meteorite that differs from the silicate inclusion-bearing iron groups IAB and IIE in the composition of the metal, the mineral assemblage in the inclusions, and the oxygen isotopic composition of the silicates [1-4]. Of particular significance is the occurrence of magnetite in the inclusions which was first noted in [3]. The magnetite has implications for the oxidation state of the Bocaiuva meteorite, and for the origin of the silicates which, on the basis of oxygen isotopes [4], appear to be derived from a CO3 chondrite-like source.

Olivine and pyroxene in the inclusions is coarse, equigranular and homogeneous in composition (Fo_{92}, Wo_3En_{90}, $Wo_{42}En_{54}$) [3,4], and they appear to have recrystallized and equilibrated at high temperature. Pyroxene Ca-(Mg,Fe) exchange thermometry [5] yields T in the range 1150-1250°C. Other phases in the inclusions, however, grew by reaction of the silicates, sulfides and metal during cooling of the meteorite (or during a reheating event). Small chromite grains occur only on the margins of the inclusions at silicate/metal and silicate/sulfide grain boundaries. The chromites are heterogeneous within individual grains and from grain to grain. They vary widely in Al_2O_3 (2-10 wt%), FeO (17-20 wt%) and MgO (7-11 wt%), but olivine-spinel Fe-Mg exchange thermometry [6] consistently yields T=600-700°C. The chromites apparently grew at a T substantially below the last equilibration of the pyroxene, and in Fe-Mg exchange equilibrium with olivine and pyroxene. The wide variation in Al_2O_3 signifies that equilibrium with respect to Al was maintained only locally; Al levels in chromite were probably controlled by proximity to plagioclase grains. The strong influence of X_{Al} in chromite on $K_D^{Fe\text{-}Mg}$(olivine-chromite) resulted in the observed variation in FeO and MgO. In addition, pentlandite, which is stable only below ~610°C, appears to have formed by reaction of kamacite and FeS. Finally, magnetite grains occur at metal/silicate grain boundaries and, more commonly, within the inclusions. They are nearly pure, often associated with pentlandite, and appear (along with pentlandite) to be products of the breakdown of metal+FeS assemblages, also below ~610°C.

The composition of the silicates and the occurrence of magnetite in Bocaiuva are consistent with the meteorite having cooled along an fO_2-T path controlled by metal-silicate reactions starting with relatively oxidized, perhaps CO3 chondrite-like, silicate material. The fO_2-T curve defined by the Bocaiuva olivine+pyroxene+metal assemblage (formulation of [7]) corresponds very closely with the curve defined by the reaction: $3Fe + 2O_2 = Fe_3O_4$ at T below ~527°C (e.g. [8]). Thus, the silicate compositions are approximately what one would expect for minerals that followed an fO_2-T path which ultimately stabilized magnetite on cooling. The lack of graphite in the assemblage is permissive evidence that C-CO-CO_2 reactions did not buffer fO_2 in the meteorite [9]. If elemental C ever existed in the assemblage, it was completely oxidized and the oxidation state of the meteorite was subsequently controlled by reactions between metal, pyroxene and olivine. The data indicate that Bocaiuva silicates formed at or above 1150-1250°C, that they were mixed with metal prior to the time that the meteorite cooled through the 600-700°C T range (chromite formation), and that magnetite and pentlandite formed subsequently below ~610°C. These types of reactions and their capacity to buffer fO_2 may have relevance for other metal-silicate assemblages with little or no C.

References: [1] Araujo S. I. et al. (1983) Meteoritics 18, 261, [2] Curvello W. S. et al. (1983) Meteoritics 18, 285-286, [3] Desnoyers C. et al. (1985) Meteoritics 20, 113-124, [4] Malvin D. J. et al. (1985) Meteoritics 20, 259-273, [5] Lindsley D. H. and Andersen D. J. (1983) Proc. Lunar Planet. Sci. Conf. 13th, A887-A906, [6] Engi M. (1983) Am. J. Sci. 283A, 29-71, [7] Johnson M. C. (1986) Geochim. Cosmochim. Acta 50, 1497-1502, [8] McMahon B. M. and Haggerty S. E. (1980) Proc. Lunar Planet. Sci. Conf. 11th, 1003-1025, [9] Brett R. and Sato M. (1984) Geochim. Cosmochim. Acta 48, 111-120.

SIDEROPHILE TRACE ELEMENT PARTITIONING IN THE Fe-Ni-C SYSTEM: PRELIMINARY RESULTS WITH APPLICATION TO UREILITE PETROGENESIS. J. H. Jones* and C.A. Goodrich§. *SN2, NASA Johnson Space Center, Houston, TX 77058. §Lunar and Planetary Laboratory, University of Arizona, Tucson AZ 85721.

Siderophile element abundances of ureilites exhibit complex patterns which most likely are attributable to either metal-silicate fractionations [1] or to volatility-related processes [2]. To evaluate the nature and magnitude of (solid metal/liquid metal) fractionations, experiments have been performed to determine trace element partition coefficients ($D_{sm/lm}$) in the Fe-Ni-C system. The results can be compared to D values in the Fe-Ni-S system used by [1] to model ureilites. Preliminary results of these studies are reported below.

Experimental. Charges containing Fe, Ni and C were spiked with ~1 wt.% of either Ge, Au, or Ir_2O_3. The Fe/Ni ratio of these charges was ~10:1. Experimental charges were placed in alumina crucibles and sealed in silica tubing under vacuum [3]. Charges were suspended in a Deltech furnace for 1-2 weeks, depending on the temperature, at either 1200 or 1300°C. After quenching, samples were mounted in epoxy, polished and analyzed using the electron microprobe. At this time we have not actually analyzed for C. Following Willis and Goldstein [4], we have used the Fe-C phase diagram to estimate the carbon content of our liquids.

Results. Equilibration appears to require longer times than in the Fe-Ni-S system. Heterogeneities may persist on a week timescale. This observation is qualitatively consistent with tracer diffusion studies, which indicate that diffusion in solid Fe-metal becomes more sluggish as C is added to the carbon-free system [5]. Consequently, the results given below are preliminary. Some analyses of crystal cores, which appeared to have not equilibrated with coexisting liquid, have been excluded.

As the eutectic of the Fe-Ni-C system is approached, $D_{sm/lm}$ values for Ni, Au, Ge and Ir increase. As temperature decreases from 1500°C to 1200°C, ^{Ni}D increases by a factor of 1.8, ^{Au}D increases by a factor of 4.5, ^{Ge}D increases by a factor of 3.2, and ^{Ir}D increases by a factor of 5.4. These changes in partitioning behavior are qualitatively similar to those observed in the Fe-Ni-S and Fe-Ni-P systems, but the absolute magnitudes of the changes are not necessarily commensurate. For example, the magnitudes of the changes in ^{Ni}D and ^{Au}D are very similar in both the Fe-Ni-S and the Fe-Ni-C systems; but changes in ^{Ge}D and ^{Ir}D are much smaller than in the Fe-Ni-S system. ^{Ge}D increases to only about 1/3 of its maximum value in the Fe-Ni-S system and ^{Ir}D changes by only ~1/8 as much as in the Fe-Ni-S system. Thus, while the effects of C on Ni and Au partitioning mimic those of S, the effect of C on Ge and Ir is much weaker. These results are qualitatively consistent with the reconnaissance experiments of [4] although our D values tend to be slightly larger at a given C concentration.

Implications for ureilites. In their analysis of siderophile element abundances in ureilites, Goodrich et al. [1] found that the abundances of a variety of siderophile elements in ureilites could be predicted if D values in the Fe-Ni-S system could be extrapolated to the C-rich metals of ureilites. The results here indicate that the correspondence between the Fe-Ni-C and Fe-Ni-S systems is far from exact. Even so, abundances of these elements in Kenna, relative to CI, still correlate well with $D_{sm/lm}$. Using the new Fe-Ni-C data in the ureilite model of [1] results in only minor changes. There is essentially no difference in the model for Golpara and the changes to the model fit for Kenna are minor. If the Kenna model is modified so that Ir fits exactly, the fit to Ni is somewhat improved, the fit to Au is somewhat worsened and the fit to Ge remains unchanged. Solid metal-liquid metal fractionation remains a viable model for understanding the siderophile element abundances and fractionations observed in ureilites.

References. [1] Goodrich et al. (1987) *G.C.A.* **51**, 2255-2273. [2] Wasson et al. (1976) *G.C.A.* **40**, 1449-1458. [3] Jones and Drake (1983) *G.C.A.* **47**, 1199-1209. [4] Willis and Goldstein (1982) *Proc. LPSC 13th.*, A435-A445. [5] Askill (1970) *Tracer Diffusion Data for Metals, Alloys, and Simple Oxides.* pp. 107.

EXPERIMENTAL DEVITRIFICATION OF CHONDRULE MESOSTASIS: IMPLICATIONS FOR THE THERMAL HISTORY OF CHONDRULES. Rhian H. Jones and Sabine Ullmann, Institute of Meteoritics, Department of Geology, University of New Mexico, Albuquerque, New Mexico 87131, USA.

Chondrule mesostases in unequilibrated chondrites contain a high proportion of glass, resulting from rapid cooling of the chondrule droplet. In chondrites of higher petrologic type devitrification has taken place, and no glass remains in type 5 and 6 chondrites. We have begun an experimental study which will investigate the kinetics of devitrification, in order to place constraints on the temperatures and times of metamorphic processes. We will also investigate the mineral assemblages obtained, and the textural relationships, for comparison with natural examples. Annealing experiments on type 3 ordinary chondrites carried out by Guimon et al. (1985, 1988) showed changes in TL properties which were attributed to crystallization of feldspar during devitrification of chondrule mesostasis.

Preliminary experiments have been carried out using a synthetic composition corresponding to the composition of mesostasis in type IA porphyritic olivine chondrules in Semarkona (LL3.0) (Jones and Scott, 1989). [SiO_2=59, Al_2O_3=18, CaO=17, MgO=5, Na_2O=1 wt%.] Minor elements, including Fe, with concentrations <1wt% in the natural analogues, have been omitted in the experiments carried out so far. Starting materials with a variety of textures were prepared by carrying out runs at different cooling rates from above the liquidus. Quenched material, and samples cooled at 1000°C/hr, consisted entirely of glass. Cooling rates of 300 and 100°C/hr resulted in glass beads, with some crystals nucleating on the Pt wire loop which held the charge. Slower cooling at 50 and 10°C/hr resulted in charges which contained more than 50 vol% plagioclase, occurring as long laths, evenly distributed throughout the sample. Interstitial glass in these samples contained some dendritic material, indicating that some devitrification occurred during the cooling time.

Annealing experiments at 900°C for 1, 2, and 3 days, and at 800°C for 3 and 7 days have been carried out, using 2mm chips of starting material. *Quenched glass starting material*: A fine dendritic devitrification front nucleated around the edge of the sample, with an average width which varied with time and T as shown in Fig. 1. After 3 days at 900°C nucleation had occurred at numerous sites throughout the sample, which consisted entirely of spherulitic crystallites with an average diameter of 25μm. Growth of these spherulites impeded growth of the devitrification front at the edge of the charge. *1000°C/hr starting material*: Although the starting material was glass, devitrification behavior differed from that observed in the quenched material. Annealed samples contained wide regions (150-500μm) with coarse devitrification textures, which grew from the edge of the sample, in addition to a dendritic front of similar width to that observed in the quenched material. The slower cooled sample apparently shows an enhanced ease of heterogeneous nucleation.

Conclusions: Results from the experiments at different cooling rates are consistent with cooling at around 1000°C/hr, for type IA chondrules that contain significant proportions of glass. Devitrification takes place in times of the order of days at 800-900°C. The ambient temperature of the solar nebula must therefore have been much lower, for glass to be preserved. Further experiments will enable an estimation of devitrification rates at lower temperatures, and will compare devitrification rates in types IA and II chondrule mesostases.

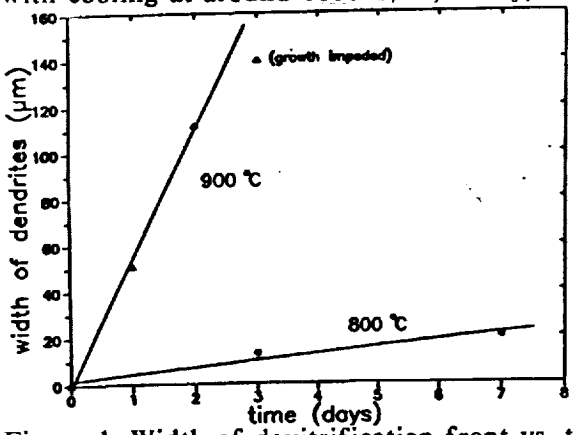

Figure 1. Width of devitrification front vs. time, for quenched glass starting material.

References: Guimon et al. (1985) GCA, 49, 1515-1524; Guimon et al. (1988) GCA, 52, 119-127; Jones and Scott (1989) Proc. 19th LPSC, LPI, Houston.

This work was supported by NASA Grant NAG9-30, P.I. Klaus Keil (RHJ) and the DAAD (SU).

MID-IR REFLECTANCE SPECTRA OF CARBONACEOUS CHONDRITES: APPLICATIONS TO LOW-ALBEDO ASTEROIDS; T.D. Jones, Central Intelligence Agency. Address: 3592 Plum Dale Dr., Fairfax, VA 22033. L.A. Lebofsky and J.S. Lewis, Lunar and Planetary Laboratory, University of Arizona, Tucson, AZ 85721.

Low-albedo asteroids (Tholen classes C,B,F,G,P, and D) are spectrally similar to carbonaceous chondrites; these objects probably preserve relatively pristine materials related to those which formed the terrestrial planets. The carbonaceous meteorites are probable samples of such asteroids: here we present diffuse reflectance spectra of 16 carbonaceous chondrites (CI, CM, CO, CV) and a variety of mineral analogs. The measurements directly supported a mid-IR reflectance survey (Jones et al. 1989) aimed at determining the distribution of hydrated silicates on asteroid surfaces (Jones et al. 1989).

Our spectra span a 2.4-25 μm range (4600-400 cm^{-1}, 4 cm^{-1} resolution) and include the following meteorites: **CI** -- Orgueil, Alais, and Ivuna; **CM** -- Murchison, Murray, and Cold Bokkeveld; **CO** -- Ornans, Ina, Warrenton, Lance, Felix, ALH 83108, and ALH A77003; **CV** -- Allende, Vigarano; and **CO/CV** -- Karoonda. Samples were ground and sieved to $\leq$ 75 μm, mildly heated to drive off adsorbed H_2O, and sealed in dry air until measurement (Jones 1988). Dr. J.W. Salisbury (USGS Reston) furnished the Nicolet spectrometer (Salisbury et al. 1987). The spectra are available from the authors as ASCII text files.

The major carbonaceous chondrite class were readily identifiable via their characteristic 3-μm H_2O band depths (cf. Pang et al. 1982; Miyamoto 1987), a distinct advantage over reflectance spectra at visual/near-IR wavelengths. We supplemented the meteorite data with a variety of low-albedo analogs, both to span gaps in meteorite mineralogy and aid in analysis of asteroid spectra. The analogs used the organic-rich kerogen residue from the Murchison CM chondrite as the opaque component (Alaerts et al. 1980; Jones 1988); the silicate end-members were terrestrial serpentine and olivine. The analog series showed that the 3-μm hydrated silicate band is very difficult to suppress, even with high concentrations (~50%) of meteoritic kerogen. Thus, an asteroid spectrum without a 3-μm band indicates hydrated silicates are indeed absent, not merely masked by *in situ* organic material.

To explore possible asteroid/meteorite associations, we compared the lab spectra to those from over 40 low-albedo asteroids (Jones 1988). 1 Ceres has no spectral match among the carbonaceous chondrites, but a 40%/60% CI/CV areal combination comes closest to reproducing its 3-μm band depth, suggesting a surface H_2O content of about 5 wt.%. 2 Pallas' spectrum closely resembles a 40%/60% CM/CV areal mixture, with an H_2O abundance of roughly 2 wt.%. Our range of meteorite spectra is clearly smaller than the variations seen among just a few low-albedo asteroids: we plan to obtain a wider range of analog spectra to better span gaps in meteorite composition, and especially to understand the spectra of the outer belt P and D classes (Lebofsky et al. 1989).

REFERENCES: Alaerts, L., Lewis, R.S., Matsuda, J., and Anders, E. (1980) Ann. Rev. Earth Planet. Sci. **16**, 273. Jones, T.D. (1988) PhD dissertation, Univ. of Arizona. Jones, T.D., Lebofsky, L.A., Lewis, J.S., and Marley, M. S. (1989) Icarus, in press. Lebofsky, L.A., Jones, T.D., Owensby, P.D., Feierberg, M.A., and Consolmagno, G.J. (1989) Icarus, in press. Miyamoto, M. (1987) Icarus **70**, 146. Pang, K.D., Chun, S.F.S., Ajello, J.M., Nansheng, Z., and Minji, L. (1982) Nature **295**, 43. Salisbury, J.W., Walter, L.S., and Vergo, N. (1987) U.S. Geological Survey Open-File Report 87-263. Reston, VA.

COMPOSITIONAL STUDIES OF TYPES 4-6 CARBONACEOUS CHONDRITES. G. W. Kallemeyn, University of California, Los Angeles, CA 90024.

Seven carbonaceous chondrites of petrologic types 4-6 that were recently returned from the Elephant Moraine and Lewis Cliff regions of Antarctica are currently being studied by INAA. There are five chondrites classified as type 4 (EET87507, EET87514, EET87519, EET87529 and EET87529), one as type 5 (EET87860) and one as type 6. The five type 4 carbonaceous chondrites are probably paired as they are small fragments (23-88 g.) collected in the same general area. Preliminary compositional data is available for all of the chondrites, except EET87529. The INAA study for that sample as well as for the replicates of some of the other samples is currently underway. This study significantly adds to our data set of six previously studied carbonaceous chondrites of types 4-5 (ALH82135, ALH84038, EET83311, Karoonda, LEW86258 and PCA82500).

CI-normalized refractory lithophile element abundances tend to be intermediate between abundance ratios of CO (~1.12) and CV (~1.35) group falls. Characteristic ratios of refractory and volatile lithophile and other non-siderophile elements, e.g., Zn/Mn and Al/Mn, also tend to fall intermediate between CO and CV ratios. The lithophile data show occasional outliers, but no chondrite yields consistently strange values. Siderophile element ratios (e.g., Ir/Ni, Au/Ni, Ir/Au, Sb/Au) show considerably more scatter than lithophile element data, and are especially more varied than the relatively tight ranges shown by CV and CO group falls. The siderophile element, Au, shows a considerable range of values (~110-180 ng/g) as compared to CO (~175-190) or CV (~135-150), which does not seem to clearly correlate with either petrologic type or extent of weathering.

The five 'paired' chondrites from Elephant Moraine show a surprising large amount of scatter in their data, especially siderophile elements. This is probably due at least in part to differences in weathering. Two of the samples, EET87507 and EET87519, show significant loss of Ni, and to a lesser extent loss of Co relative to Fe as compared to the other samples, a pattern noted in analyses of other chondrite finds, both Antarctic and non-Antarctic.

It would appear that all of the type 4-6 carbonaceous chondrites studied thus far could be related, at least as a clan with compositional characteristics intermediate between the CM-CO and CV clans. Compositional (and petrographic) data previously supported the possible grouping of ALH82135, ALH84038, EET83311 and Karoonda into their own group, and to that one might now also add EET87860, LEW87009 and taken as a whole, the Elephant Moraine set (EET87507, EET87514, EET87519 and EET87526).

^{40}Ar-^{39}Ar AGE AND NOBLE GASES OF A H-CHONDRITIC CLAST IN A SHOCKED L6-CHONDRITE FROM ANTARCTICA; I. Kaneoka, Earthquake Research Institute, University of Tokyo, Bunkyo-ku, Tokyo 113, Japan, N. Takaoka, Faculty of Science, Yamagata University, Yamagata 990,Japan, and K. Yanai, National Institute of Polar Research, Itabashi-ku, Tokyo 173, Japan.

Yamato-75097(Y-75097)(L6) chondrite has been known to include some unique inclusions, which are classified into H-chondritic group on the basis of oxygen isotope studies(Prinz et al.,1984). Mineral compositions of the clasts in this meteorite are reported to be rather similar to but substantially different in details from Brachina(Yanai et al.,1983). Further, REE patterns in these clasts are also different from Brachina(Nakamura et al.,1984). As an example for a meteorite with clasts of different group, the L6 chondrite Barwell has been reported(Hutchison et al.,1988). Although Barwell is reported to have been unshocked, Y-75097 shows some evidences of shock effects (Yanai et al.1983). In this respect, this meteorite would give us a good example to evaluate the effect of a shock on the degassing from a meteorite and its inclusions. For this purpose, ^{40}Ar-^{39}Ar age and noble gas isotopes were examined for a clast of the Y-75097. For the host meteorite, noble gas compositions(Takaoka et al.,1981) and ^{40}Ar-^{39}Ar age studies(Kaneoka et al., 1988) have been made and present results are compared with those data.

The result of ^{40}Ar-^{39}Ar ages with step-wise heating procedure indicates a U-shaped pattern in the ^{40}Ar-^{39}Ar age diagram, suggesting a degassing event at around 480Ma. Such a pattern and the estimated degassing age are similar to those of the host meteorite(Kaneoka et al.,1988). However, in the higher temperature fractions of more than 1200°C, much higher ^{40}Ar-^{39}Ar ages were observed in the clast, suggesting the incorporation of inherited radiogenic ^{40}Ar due to the shock. Such cases have been reported for Lunar samples which show some shock effects(e.g.,Kirsten et al.,1972). Such a high age has not been observed in the host meteorite(Kaneoka et al.,1988).

For an aliquot of the clast, noble gas isotopes were examined in the two temperature fractions(600°C, 1650°C). Most noble gases were degassed in the 1650°C fraction including the lighter ones. He and Ne are mostly cosmogenic, while the xenon isotopes show a rather high $^{129}Xe/^{132}Xe$ ratio of about 30, implying a very high $^{129}I/Xe$ ratio in the source materials of the clast.

References

Hutchison, R., Williams, C. T., Din, V. K., Clayton, R. N., Kirshbaum, C., Paul. R. L. and Lipschutz, M. E. (1988) Earth Planet. Sci. Lett., 90, 105.

Kaneoka, I., Takaoka, N. and Yanai, K.(1988) Proc. NIPR Symp. Antarct. Meteorites, 1, 206.

Kirsten, T., Deubner, J. Horn, P., Kaneoka, I., Kiko, J., Schaeffer, O. A. and Thio, S. K. (1972) Proc. Third Lunar Sci. Conf., Suppl.3, 1865.

Nakamura, N., Yanai, K. and Matsumoto, Y. (1984) Meteoritics, 19, 278.

Prinz, M., Nehru, C. E., Weisberg, M. K., Delaney, J. S., Yanai, K. and Kojima, H. (1984) Meteoritics, 19, 292.

Takaoka, N., Saito, K., Ohba, Y. and Nagao, K. (1981) Mem. Natl Inst. Polar Res., Spec. Issue No.20, 264.

Yanai, K., Matsumoto, Y. and Kojima, H. (1983) Mem. Natl Inst. Polar Res., Spec. Issue No.30, 29.

THE PROJECTILE RECONSTRUCTION BY THE METEORITE MATTER IN THE IMPACTITES. I.G.Kapustkina. Geological Faculty, Moscow State University, USSR 119899 GSP Moscow.

In the small craters, such as Henbury, Meteor, where the fragments of the meteorite are preserved, the pair ratios of the indicator elements (Ir, Ni, Co, Cr) in the melts and in the parent meteorites are different (fig.1). This discrepancy may be grater in larger craters because of fractionation of the meteorite matter (1). But the absence of the projectile fragments in these craters doesn't permit to check this supposition. Therefore we believe in many cases we may determine the projectile type (iron or stony meteorite) and sometimes the class (chondrite or achondrite) on the basis of the enrichment of the melts by the dispersed meteorite material. More detailed determination is above the limits of the accuracy of our studies and knowledge. Thus, low enrichment of the massive glasses of the impact crater Elgygytgyn by the scattered meteorite matter surely demonstrates the projectile achondrite nature. But the pair ratios of the indicator elements give different answers to this question (tabl.1).

Relations between Fe, Ni, Co in the iron spheres of the craters Meteor, Wabar, Henbury don't correspond to the relations in the parent meteorites. Fractionation of the meteorite matter is undoubtedly observed in these separations. In the craters Ries, Rochechouart, Ternovskoy the Fe-Cr-Ni veinlets and particles are found. For these craters the unconformity of the progectile evaluation on the basis of the indicator elements relations in these separations and in the melts are observed. We believe that the metallic spherules, veinlets, particles are the partly changed meteorite material. Consequently we may determine the projectile by these separations only as the addition to the investigation of dispersed meteorite matter in the impact melts.

References: (1) Kapustkina I.G., Feldman V.I. Geochimical International, (1988), N 11, p.1547-1557

Fig.1. Diagram Ni-Cr for the different meteorites.

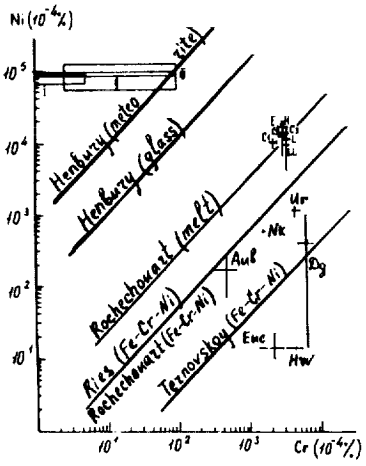

Tabl.1. Estimation of the meteorite.

Ratio	Ratio value	Propose meteorite
	ELGYGYTGYN	
Ni/Cr	$2,7 \cdot 10^{-1}$	Aubrite, ureilite
Ni/Co	2,3	Aubrite, eucrite, howardite
Ni/Ir	$3,8 \cdot 10^4$	Aubrite, diogenite, LL, E4, I, IIIa
Cr/Co	8,5	Aubrite, LL
Cr/Ir	$1,4 \cdot 10^5$	Aubrite
Co/Ir	$1,7 \cdot 10^4$	Howardite, IIIab
	BOLTYSHSKIY	
Ni/Cr	2,5	L, C
Cr/Ir	$4,7 \cdot 10^4$	Aubrite, eucrite
Ni/Ir	$1,2 \cdot 10^5$	Diogenite, IIIa

TRACK STUDY OF PESYANOE ACHONDRITE RADIATION HISTORY; L.L.Kashkarov, L.I.Genaeva. Vernadsky Institute of Geochemistry and Analytical Chemistry, USSR Academy of Sciences, Moscow, USSR.

We studied the nuclear particle tracks in gas-rich Pesyanoe achondrite in order to get the data about the regolith stage on the parent body surface. Solar composition of the gas (Shultz and Kruse, 1983) is evidence of irradiation of this meteorite by solar wind ions. We have studied two samples of the Pesyanoe (No217 and No753). Weight of each sample was about ~0.5 grams. So the each sample was the "point" indicator of the track parameters in the definite part of the meteorite body. Grains of enstatite were selected from achondrite after crushing of samples. The results of track measurements are presented in Fig.1. We can see identical distribution of grains for both samples. Track densities (ρ) in enstatite crystals cover the wide interval of values (more than three orders of magnitude). There are three groups of crystals with different ρ values. We assume that maximum of N in interval 5.10^5-2.10^6 cm^{-2} due to VH-nuclei of galactic cosmic rays. Crystals with $\rho > 5.10^6$ cm^{-2} were irradiated at different depths of the regolith and on its surface ($\rho \geq 10^8$ cm^{-2}). Four crystals among all studied (N=201) have clear track density gradient. The part of crystals irradiated on surface of regolith equal to about 10%. Therefore these samples of meteorite in comparison with lunar regolith are objects with average dose of irradiation (Price et al., 1975). It is needed to indicate that dispersion of ρ values for Norton County achondrite, which has not traces of the solar wind irradiation (Shultz and Kruse, 1983), is not more than ten times and depends only on depth of sample localisation in the preatmospheric meteorite body (Kashkarov and Genaeva, 1989).

Kashkarov L.L. and Genaeva L.I. (1989) Lunar and Planet. Sci.Conf. XIX
Price P.B. et al. (1975) Proc. 6th LPSC, p.3453.
Shultz L. and Kruse H. (1983) Helium, neon, argon in meteorites. A data complication. Mainz.

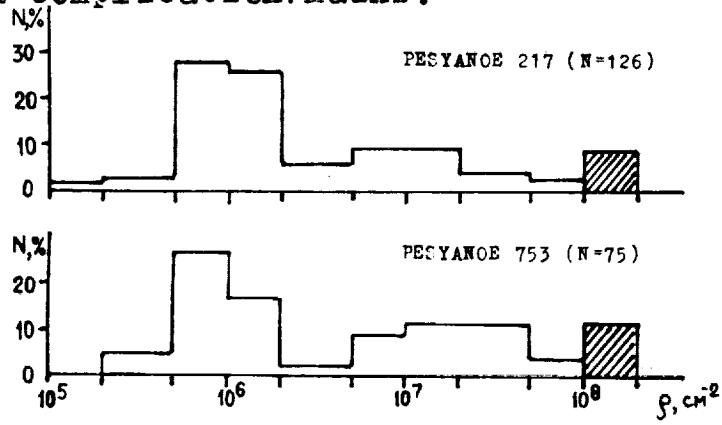

RADIATION AND THERMAL HISTORY FOR THE ORDINARY CHONDRITES SARATOV L4 AND ELENOVKA L5: THERMOLUMINESCENCE STUDY FOR CHONDRULES; Kashkarov L.L., Kashkarova V.G. Vernadsky Institute of Geochemistry and Analytical Chemistry of USSR Academy of Sciences, Moscow, USSR.

Chondrules from two ordinary chondrites Saratov L4 and Elenovka L5 have been studied by thermoluminescence (TL) method, which is one of the most effective and sensitive mode of checking for the meteorite thermal history (McKeever et al.,1979; Sears et al.,1983).

The results of TL measuring for 30 chondrule samples and separate mineral grains excluded from these chondrules are presented in fig.1.The following interpretation of data can be made.(1) It is seen correlation (fig.1A,B)between TL intensity in low (LT), $T \lesssim 230\,^{\circ}C$ and high temperature (HT) regions of the TL glow curves for Elenovka chondrules. This correlation is about the same for natural (TL_{nat}) and artificial (TL_{art}), induced by γ-radiation of ^{60}Co.On this basis we can to assume the presence in this chondrite of the two chondrule types indicated as (a,b) and differing each other by the chondrule mesostasis TL phosphors.However thermal history for these chondrules is identical.At that time it is not observed any chondrule grouping by this TL parameters for Saratov L4 chondrite. (2) TL_{nat} intensity (fig.1C) spreads over 10^3-fold range for Elenovka chondrules and only one order of magnitude for Saratov. (3) Distribution of TL_{nat} glow curve peak temperature (T_{peak})(fig.1C) and the full width of the peak at half its maximum intensity ($\Delta T_{1/2}$)(fig.1D) also indicate that the Elenovka chondrules are subdivided at least into two distinct groups.In addition it is possible to suppose that obtained TL parameters for two investigated chondrites are due to their different metamorphic histories.

McKeever S.W.S.et al.,(1979), Meteoritics 14, 29.
Sears D.W.G. et al.,(1983), J.Geoph.Res.,Suppl. 1,88,B301.

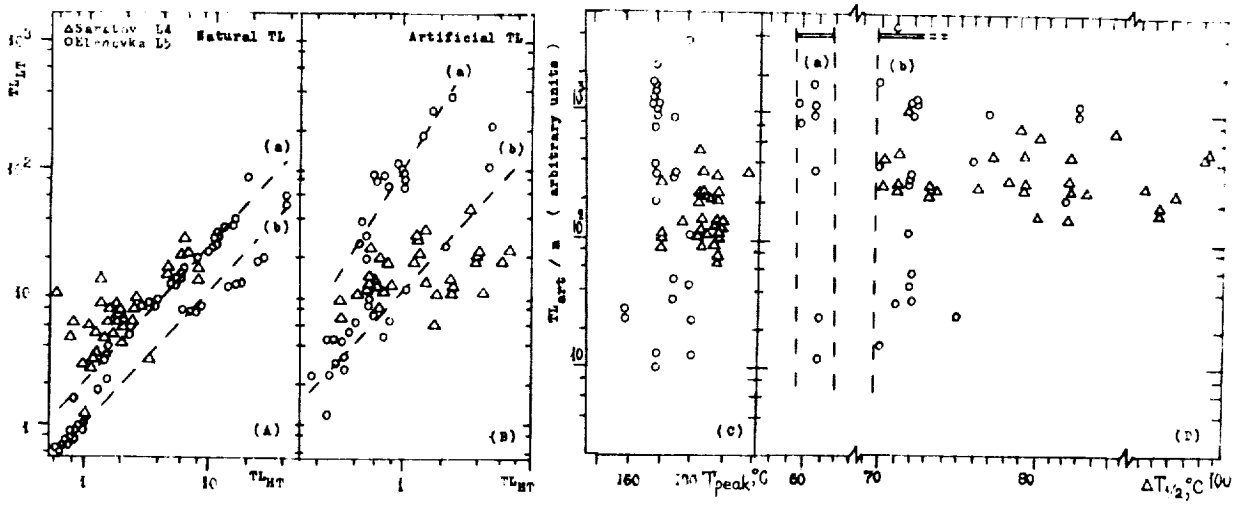

ACCRETION OF ORDINARY CHONDRITES ON DATA OF TRACK STUDIES. Kashkarov L.L.,Korotkova N.N.,Skripnik A.Ya,Lavrukhina A.K. Vernadsky Inst.of Geochemistry and analytical Chemistry of USSR Acad. of Sciences, Moscow,USSR.

The silicate mineral grain aggregates entered into gas rich chondrites during accretion can provide a unique source of information about the pre-compaction environment conditions and radiation of primitive matter (e.g.Goswami et al.,1984).

The paper presents the results of pre-accretion track study of olivines from Nikol'skoe L4-5 and Elenovka L5 ordinary chondrites containing no solar gases.Firstly the chondrules and crystals from Nikol'skoe were selected by a special method taking into account the accretion structure (Skripnik,1988). The method allowed to localize the regions enriched in pre-irradiated chondrules (Korotkova et al., 1988).From the one revealed structure ~2x6 cm in size~400 crystals and ~112 chondrules have been studied.Track have been found in 32 of 72 chondrules containing large(~50μm) olivine crystals.Each chondrule contains a few olivine grains with ρ_{VH}~10^6-10^7cm^{-2}.The revealed localization can be interpreted as accretionary shell containing the admixture of chondrules with another radiation and/or thermal history.The possible influence of accretion process on tracks was elucidated by comparison of chondrule and matrix olivine crystals from Elenovka L5.Track densities (ρ)measured in 372 matrix grains and in 320 grains from 46 chondrules (fig.1)indicate clear difference between the percentage of crystals with $\rho > 1\cdot10^6$ cm^{-2}:~5%and ~30% for chondrules and matrix respectively.The part of grains with $\rho \lesssim 10^5$cm^{-2}in chondrules (~85%)is twice more than that in matrix.Only ~0,5% of crystals with $\rho \lesssim 10^7$ cm^{-2} and absence of track density gradients have been recognized in both chondrules and matrix.

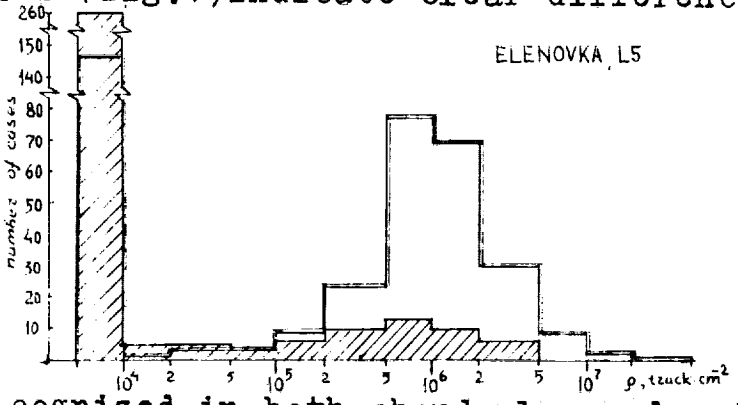

Thus we obtained the preliminary confirmation of reality of primary accretion structure in Nikol'skoe L4-5 chondrite.The clear difference between track characteristics in chondrule and matrix crystals of Elenovka L5 chondrite can be due to higher degree of thermal influence on chondrule precursor.

References.1.Goswami J.N.et al.,Space Sci.Rev.,1984,37, 111--159. 2.Skripnik A.Ya.,LPS XIX,1988,1091-1092; ibid., 1093--1094. 3. Korotkova N.N.,ibid., 641-642.

BORON ABUNDANCES IN BULK FRAGMENTS AND SEPARATED PHASES OF ALLENDE. Bradly D. Keck, University of Missouri Research Reactor, Columbia MO 65211, USA.

Boron analyses of chondrites and chondrules are relatively few in number and, often, plagued with terrestrial or laboratory contamination. The most reliable method seems to be the use of Prompt Gamma Neutron Activation Analysis (PGNAA) using fresh interior samples meticulously kept free of contamination (Curtis et. al., 1980; Curtis and Gladney, 1985). Boron is a moderately volatile element, having a condensation temperature of approximately 750 K (Cameron et. al., 1973), which should be depleted in chondrules. Consequently, when calculating the cosmic abundance of B it seems necessary to consider the chondrule content of a given meteorite class and correct the observed boron values for the presumably depleted chondrules (Anders and Ebihara, 1982). Where attempts have been made to measure the B content of separated chondrules directly using PGNAA, however, no such depletion is apparent (Curtis et. al., 1980). In fact, measurements of the boron content of the chondrules of Allende indicate boron concentrations nominally 15 times higher than that observed in the bulk fractions of Allende. Analyses of such small individual samples may be treated with some suspicion and further data is needed to resolve the chondrule B content experimentally.

Observations of C2M chondrites exhibit an inverse relationship of B to Na (Curtis and Gladney, 1985). These authors have suggested that this relationship is the result of low temperature hydrous alteration of an initially homogeneous mixture. The persistence of such a relationship in Allende would perhaps indicate similar processes, though class differences would have to be considered.

In the present experiment, I attempt to gain some direct insight into the distribution of B in a 200 g individual of Allende which was recovered only seven days after the fall (Clarke, personal communication). Using the instrument and techniques described by Hanna et. al. (1980), I am in the process of measuring both bulk and separated chondrule enriched and chondrule depleted fractions of the meteorite for B, Na and Si content. In this manner it may be possible to directly ascertain the chondrule B content. Additionally, the relationships of B and Na in both bulk fragments and these separates can be determined.

Acknowledgements. The provision of sample material by the Smithsonian Institution and the excellent cooperation of Roy Clarke are greatly appreciated. Valuable advice regarding the PGNAA instrument has been provided by Michael Glascock. This work is supported with MURR in house funds, for which the author is grateful.

References.

Anders E. and Ebihara M. (1982) Geochim. Cosmochim. Acta 46, 2363 - 2380.

Cameron, A. G. W., Colgate, S. A. and Grossman, L. (1973) Nature 243, 204 - 207.

Curtis D. B. and Gladney, E. S. (1985) Earth and Planet. Sci. Lett. 75, 311 - 320.

Curtis D. B., Gladney E. S. and Jurney, E. (1980) Geochim. Cosmochim. Acta 44, 1945 - 1954.

Hanna, A. G., Brugger, R. M. and Glascock, M. D. (1981) Nuclear Instruments and Methods 188, 619 - 627.

AQUEOUS ALTERATION OF THE KABA CV3 CARBONACEOUS CHONDRITE; Lindsay. P. Keller and Peter. R. Buseck, Departments of Geology and Chemistry, Arizona State University, Tempe, AZ, USA 85287

Kaba is a primitive member of the oxidized subgroup of the CV3 chondrites (McSween, 1977; Peck, 1984). Recent work on Kaba has focussed on the refractory inclusions (Fegley and Post, 1985; Holmén and Wood, 1987; Liu and Schmitt, 1987, 1988); other than the study by Peck, little is known about the mineralogy of Kaba matrix and chondrules. We are particularly interested in the reports of high- and low-Al phyllosilicates ("HAP" and "LAP") in inclusions and matrix (Fegley and Post, 1985). Our results from a transmission electron microscope (TEM) study of Kaba show that matrix and chondrules have undergone aqueous alteration that resulted in the formation of trioctahedral smectite from glass in chondrules and from olivine in matrix.

Phyllosilicates in Kaba chondrules are coarse grained, occurring in micrometer-sized bundles of subparallel packets. High-resolution (HRTEM) images show basal fringe spacings of 1 to 1.2 nm that are characteristic of smectite-group phyllosilicates. Energy-dispersive, x-ray spectroscopy (EDS) analyses show that the smectite is rich in Mg and poor in Al, corresponding to saponite. EDS analyses also show small peaks of Fe, Ni, and S, suggesting the presence of pentlandite or pyrrhotite mixed with the smectite.

Matrix phyllosilicates occur in three forms: 1) discrete, coarse-grained clusters (< 700 nm in diameter); 2) lamellar replacements of olivine; and 3) fine-grained packets of phyllosilicates between olivine grains. HRTEM images show that all three forms have 1- to 1.2-nm basal fringe spacings. Only the clusters are large enough to obtain EDS analyses; they are chemically similar to the smectite in chondrules. The lamellar replacements are generally <5 nm wide, although they can be as wide as 50 nm; they are similar to the planar zones filled with saponite described from the Mokoia CV3 chondrite by Tomeoka and Buseck (1986). The fine-grained packets are bent (deformed) in appearance and contain numerous terminated layers (apparent edge dislocations) and stacking faults.

The matrix of Kaba bears a striking resemblance to matrix in the Mokoia CV3 chondrite; each has undergone a similar alteration process to form essentially the same hydrated assemblages. There are, however, subtle differences. We have not observed the intimate intergrowth of magnetite and ferrihydrite with smectite as observed in Mokoia (Tomeoka and Buseck, 1986). Rather, we observe discrete grains of magnetite throughout Kaba matrix suggesting that oxidation did not play as great a role in the alteration of Kaba as it did in Mokoia.

Because both chondrules and matrix are altered, we believe the hydration occurred on the Kaba parent body after accretion. Based upon the similarities to terrestrial iddingsite, the smectite in Kaba probably formed at low temperatures. The presence of smectite in Kaba rather than the serpentines that occur in CO3 chondrites (Keller and Buseck, 1988) also suggests low temperatures for the alteration.

The formation of smectite from matrix olivine requires a source of Al, alkalis, and H_2O, and a sink for Fe. The Fe was probably incorporated in magnetite. Al and alkalis may have been mobilized from aluminous phases (such as feldspars or glass), provided that the fluid phase had a high pH.

Acknowledgements. This work was supported by NASA grant NAG 9-59. We thank R. A. Schmitt for providing a sample of Kaba. Electron microscopy was performed at the Facility for High-Resolution Electron Microscopy in the Center for Solid State Science at Arizona State University.

References: Fegley, B. and Post J. E. (1985) *Earth Planet. Sci. Lett.* **75**, 297-310; Holmén, B. A. and Wood, J. A. (1987) *Meteoritics* **22**, 413; Keller, L. P. and Buseck, P. R. (1988) *Lunar Planet. Sci. XIX*, 595-596; Liu, Y. G. and Schmitt, R. A. (1987) *Lunar Planet. Sci. XVIII*, 560-561; Liu, Y. G. and Schmitt, R. A. (1988) *Lunar Planet. Sci. XIX*, 684-685; McSween, H. Y. (1977) *Geochim. Cosmochim. Acta* **41**, 1777-1790; Peck, J. A. (1984) *Lunar Planet. Sci. XV*, 635-636; Tomeoka K. and Buseck, P. R. (1986) *Meteoritics* **21**, 526.

MODELLING THE EVOLUTION OF N AND $^{15}N/^{14}N$ IN THE LUNAR REGOLITH

J.F.Kerridge, Inst. of Geophysics, UCLA, Los Angeles, CA 90024
P.Bochsler & J.Geiss, Physikalisches Institut, Universitat Bern
CH-3012 Bern, Switzerland

Attempts to explain the long-term increase of $^{15}N/^{14}N$ in the lunar regolith as the result of either nuclear reactions or mass-dependent fractionation have been shown to be unsuccessful [Kerridge 1980;Geiss & Bochsler 1982]. Consequently, several models have been advanced that invoke mixing of solar N with N from some hypothetical non-solar reservoir. Because present observations yield values for lunar-regolith $^{15}N/^{14}N$ from more than 20% below the terrestrial value to more than 20% above it [Clayton & Thiemens 1980;Becker 1989], the end-member compositions in any proposed mixing model must lie at or outside those limits. The present solar-wind value is unknown, so the solar component in such a model can, in principle, lie at either end of the mixing trend. Although $^{15}N/^{14}N$ values both heavier and lighter than the extreme lunar values have been observed occasionally in meteorites [Anders 1988], the hypothetical non-solar component is generally taken to be ^{14}N- rather than ^{15}N-rich. Suggested sources for such ^{14}N-rich N have included the lunar interior [Becker & Clayton 1975], planetary nebulae [Ray & Heymann 1980], interstellar grains in meteorites [Norris et al. 1983] and the upper reaches of the terrestrial atmosphere [Geiss & Bochsler 1989].

Although mixing models can qualitatively explain the increase in lunar-regolith $^{15}N/^{14}N$, it has not been explicitly demonstrated whether they are quantitatively consistent with lunar N systematics. In order to address this question, we are evaluating a series of numerical models designed to illustrate the evolution of N and $^{15}N/^{14}N$ by two-component mixing on the lunar surface. Preliminary results suggest that the broad features of the dependence of N content on maturity and of $^{15}N/^{14}N$ on antiquity can be reproduced. Further, more rigorous, testing should reveal whether or not such a model can explain more subtle details in the observational record.

Anders E. [1988] Meteorites and the Early Solar System, p.927.
Becker R.H. [1989] Lunar Planet.Sci. XX, p.54.
Becker R.H. & Clayton R.N. [1975] Proc.Lunar Sci.Conf.6th. p.2131
Clayton R.N. & Thiemens M.H. [1980] The Ancient Sun, p.463.
Geiss J. & Bochsler P. [1982] Geochim.Cosmochim.Acta 46, 529.
Geiss J. & Bochsler P. [1989] The Sun in Time, in preparation.
Kerridge J.F. [1980] The Ancient Sun, p.475.
Norris S.J. et al. [1983] Meteoritics 18, 366.
Ray J. & Heymann D. [1980] The Ancient Sun, p.491.

DISCOVERY OF E-CHONDRITE ASSEMBLAGES AND SILICA-BEARING OBJECTS IN ALH85085: - LINK BETWEEN E- AND C-CHONDRITES. M. KIMURA AND A. EL GORESY; MPI KERNPHYSIK P.O. BOX 103980, 6900 HEIDELBERG, FRG.

We report the discovery of a suite of minerals in ALH85085 typical of E-chondrites. The new suite consists of schreibersite (Ni 5.5-18.9%), a new Fe-Cr-phosphide (Fe 46.5-51.7, Ni 4.2-4.6, Cr 20.8-22.2%), a new Fe-silicide (Fe 58.2, Ni 19.2, P 7.7, Si 12.5%), Mn-free vanadian daubreelite (V 0-1.2%), and alabandite (Mn 24.9-30.7, Fe 23.4-33.6, Cr 0.1-4.0, Mg <0.2%). High-Si FeNi metal (Si 1.8-10.8%) was also found associated with these minerals. These findings are in accord with the discovery of osbornite [1-3]. However, our discovery established a link of this meteorite to presumably EL-chondrites.

In addition we also discovered at least 31 silica-bearing objects similar to those reported from ordinary chondrites [4]. They consist of 2 major assemblages; 1) Ca-poor pyroxene (Fs_{5-55}) + silica ± FeNi metal and 2) Fe-rich olivine (Fa_{45-80}) + silica ± FeNi metal. Other phases include a member of the ilmenite-geikielite-pyrophanite series (FeO 11.9-42.9, MnO 4.7-18.9, MgO 0-10.2%), chromite (MgO 0-8.1, Al_2O_3 0-17.0, TiO_2 0-4.7%), rutile, Mg-rich armalcolite (TiO_2 76.8-78.9, FeO 3.7-6.3, MgO 9.4-11.6%), a member of the enstatite-rhodonite series $(Mn_{0.3},Mg_{0.7})SiO_3$, magnetite (NiO 0-10.3%), and the assemblage nickeliferous pentlandite (Ni 34.0%) + heazelwoodite (Ni 69.0%) + FeNi metal (Ni 49.1%).

We also found at least 47 CAIs and their fragments, 5-70 μm in size. The mineral constituents are hibonite (TiO_2 1.5-3.1, MgO 0.7-2.0%), $CaAl_4O_7$ (TiO_2 <0.5, MgO <0.3%), spinel (TiO_2 0.1-0.5, Cr_2O_3 0.1-0.4, V_2O_3 <0.3%), perovskite and melilite (Geh_{98-71}) with Ca-pyroxene (TiO_2 0.05-14.9, Al_2O_3 2.4-42.4, MgO 1.9-19.0%) and rare Ca-Al-rich glass. A characteristic feature is the low Mg- and Ti-contents in hibonite and pure compositions of the $CaAl_4O_7$. Refractory siderophile elements or their alloys were never encountered in any of the inclusions. CAIs in ALH85085 were classified into melilite-rich (like type A CAI), spinel-hibonite inclusions, and igneous spherules rarely with $CaAl_4O_7$ [5]. Every inclusion contains spinel, hibonite or $CaAl_4O_7$. We found 17 CAIs bearing hibonite and/or spinel. They show similar mineralogy to type A or spinel-hibonite inclusions. We find a complete petrographic suite covering intermediate compositions between these two types of CAIs. Only one inclusion contains similar mineral assemblage and melilite (Geh_{71}) to type B CAI. Another unique 17 $CaAl_4O_7$-bearing inclusions are also encountered. $CaAl_4O_7$ occurs not only in igneous spherules, but also in melilite- and spinel-rich CAIs. In each case hibonite and $CaAl_4O_7$ are surrounded by spinel, melilite and/or pyroxene. Melilite and/or pyroxene abundantly occur as rims around CAIs.

Although oxygen isotope study classify ALH85085 as anomalous CR chondrite [6], the present investigation is not consistent with such classification. Especially, the presence of EL-chondritic assemblages and silica-bearing objects advocates for an early mixing process in the solar nebula. Simple condensation process cannot explain such a mineralogy. Therefore, the constituents of ALH85085 probably originated from various reservoirs of the solar nebula with highly contrasting fO_2, namely reservoirs where C-, O- and E-chondrites formed.

References: [1] Scott E.R.D. (1988) *EPSL* **91**, 1., [2] Weisberg M.K. *et al.* (1988) *EPSL* **91**, 19., [3] Bischoff A. *et al.* (1989) *LPS* **XX**, 80., [4] Brigham C.A. *et al.* (1986) *GCA* **80**, 1655., [5] Grossman J.N. *et al.* (1988) *EPSL* **91**, 33., [6] Clayton R.N. and Mayeda T.K. (1989) *LPS* **XX**, 169.

SCR PRODUCED ^{41}Ca IN LUNAR BASALT 74275; J. Klein[1], D. Fink[1], G.F. Herzog[2], E. Pierazzo[3], R. Middleton[1], and S. Vogt[2]. 1) Dept. Physics, Univ. Pennsylvania, Phila., PA 19104; 2) Dept. Chemistry, Rutgers Univ., New Brunswick, NJ 08903. 3) Dipart. di Fisica, Univ. di Padova, Italy

The concentrations of certain cosmogenic radionuclides in the topmost few millimeters of lunar samples (Reedy, 1980) provide a measure of the average fluxes of solar cosmic rays (SCRs) over time intervals comparable to their half-lives. Reedy,*et al.* (1989) compile such analyses for numerous isotopes. A comparison of the results for the shortest- (^{22}Na, ^{55}Fe, and ^{14}C) and longest-lived (^{36}Cl and ^{26}Al) isotopes suggests that the average integral flux of SCRs (E>30 MeV) may have been four times greater during the past 10^4 a than during the previous 10^6 a. Although several cosmogenic isotopes have half-lives in the gap between ^{14}C and ^{36}Cl, at present only ^{41}Ca (ca. 10^5 a) and ^{81}Kr (2×10^5 a) can be measured with sufficient sensitivity to make their detection in lunar samples feasible.

The exploratory experiments described here were undertaken 1) to obtain a ^{41}Ca profile for a lunar rock, and 2) to see whether SCR-derived ^{41}Ca could be identified from the shape of the profile. Identification was a concern because ^{41}Ca is produced not only by SCR-induced spallation of medium-Z elements such as Ti, but also by high-energy spallation induced by galactic cosmic rays (GCRs) of high-Z metals principally Fe, and by thermal-neutron capture by ^{40}Ca. Calculations furnished little guidance on the relative magnitude of the SCR contribution because the important cross-sections — specifically those for the production of ^{41}Ca from 0-150 MeV protons on Ti and possibly the heavier isotopes of Ca — are largely unknown. We concluded that the most direct way to test the utility of ^{41}Ca as a SCR flux monitor was to make measurements of the surface concentration of ^{41}Ca in a high-Ti lunar rock. We report the ^{41}Ca contents of 4 samples taken from the top 4 cm of the titanium-rich lunar basalt 74275.

Vogt (1988) describes the chemical methods used to separate Ca as CaO from the four 30-mg samples analyzed. To each sample we added approximately 20 mg of natural Ca carrier. The two-step reduction of CaO to CaH_2 is given by Sharma and Middleton (1987). Pending our own determinations, we have assumed a stable Ca content of 7.4% (Duncan,*et al.*, 1974; Rose,*et al.*, 1975) in all samples. The measured ^{41}Ca/^{40}Ca ratios ranged from 15.1×10^{-14} to 4.0×10^{-14}. Two blanks prepared from pure CaO gave ^{41}Ca/^{40}Ca ratios of 0.7×10^{-14} and 4.6×10^{-14}, the latter the complete chemical blank for the lunar samples, probably overestimates the blank level: It was reduced just after the highest-level samples ($\sim8\times10^{-12}$) and probably suffered an atypically large degree of contamination; accordingly, we used $(2.3\pm2.3)\times10^{-14}$ for the blank correction. Figure 1 shows the profile of ^{41}Ca over the top 10 g·cm^{-2} of 74275. Clearly evident is the decrease in concentration of ^{41}Ca by more than a factor of two, similar to the ^{26}Al profile previously measured in the same rock by Klein,*et al.* (1988). This decrease can only be explained if the SCR production accounts for at least 50% of the surface production. To convert the ^{41}Ca contents into a SCR flux, it will be necessary to determine accurately the low-energy cross sections from Ti, and also to know more accurately the half-life of ^{41}Ca.

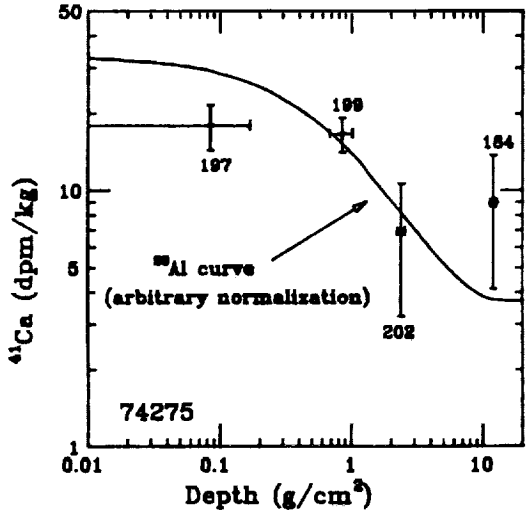

References:

Duncan A.R. *et al.* (1974) *Proc. 5th Lunar Conf.*, 1147-1157.

Klein J. *et al.* (1988) *Lunar Planet. Sci. 19*, 609-610.

Reedy R.C. (1980) in: *Conf. Ancient Sun*, ed. Pepin, R.O., Pergamon Press, 365-386.

Reedy R.C. *et al.* (1989) *Lunar Planet. Sci. 20*, 890-891.

Rose H.J. *et al.* (1975) *Proc. Lunar Sci. Conf., 6th*, 1363-1373.

Sharma P. and Middleton R. (1987) *Nucl. Inst. and Methods* **B29**, 63-66.

Vogt S. and Herpers U. (1988) *Fres. Z. Anal. Chem.* **331**, 186-188.

COMPARISON OF OLIVINE COMPOSITIONS IN IDPs AND CHONDRITE MATRICES.

W. Klöck[1], K.L. Thomas[2], D.S. McKay[1], M.E. Zolensky[1]
[1]SN14, NASA/JSC, Houston, TX, 77058; [2]Lockheed, 2400 Nasa Rd.1, Houston, TX , 77058

Zolensky (1) showed that the bulk compositions of matrices and chondrule rims in CM2 meteorites are essentially identical. It is not clear if chondrule rims are the precursor material of CM2 matrix material. Comparing mineral compositions in chondrule rims and matrices might help us to find genetic relationships between chondrule rims and matrices.

Rim and matrix olivines

Olivine compositions in rims and matrices (one each) of three CM2 meteorites (Murchison, Murray, EET 83226) are shown in Fig. 1 along with rim and matrix olivine data for Vigarano (CV3). The compositions of chondrule-rim olivines in CM2 meteorites extend to higher Fe/Fe+Mg values compared to matrix olivines. Chondrule rims as well as matrices contain a significant fraction of forsterites with Fa values in the range of 0.1 to 2.5. This is in contrast to olivine compositions in Vigarano matrix and chondrule rims. The average olivine compositions in both materials are centered at about Fa 50 and no forsterites are present. Hydrous alteration of CM2 matrices under oxidizing conditions might be a possible way to preferentially destroy iron-rich olivines but leave magnesium-rich olivines unaffected.

LIME olivines in CM2 meteorites

The MnO contents of CM2 forsterites are plotted versus FeO contents in Fig. 2. Most of the data (filled squares) plot at a FeO/MnO ratio of about 1.0. Semarkona (LL3.0) meteorite matrix also contains this type of low-iron manganese-enriched (LIME) olivines (2); although not shown on the graph, they plot in the same area as CM2 forsterites. In addition, we found LIME forsterites in a number of chondritic interplanetary dust particles. IDP data are indicated by the hatched field in Fig. 2. The distinct chemical signature of these LIME olivines seems to support a related origin of these phases in CM2 matrices, chondrule rims, and Semarkona matrix, as well as in IDPs.

There are at least two possibilities to explain the formation of Mn-rich forsterites: reduction of initially FeO-and MnO-rich olivines, or condensation of Mn into forsterite in the solar nebula. The first possibility is unlikely because none of these forsterites contains any detectable iron inclusions. The second possibility, condensation from a solar gas, may be a better explanation. Forsterite is the first major silicate phase to condense from a cooling gas of solar composition. Iron condenses as metal at similarly high temperatures, but Mn, which is not stable as metal in the solar nebula, condenses at about 1100 K as Mn_2SiO_4 in solid solution in forsterite. The decoupling of Mn and Fe during condensation processes thus provides an effective means for the formation of Mn-rich forsterites.

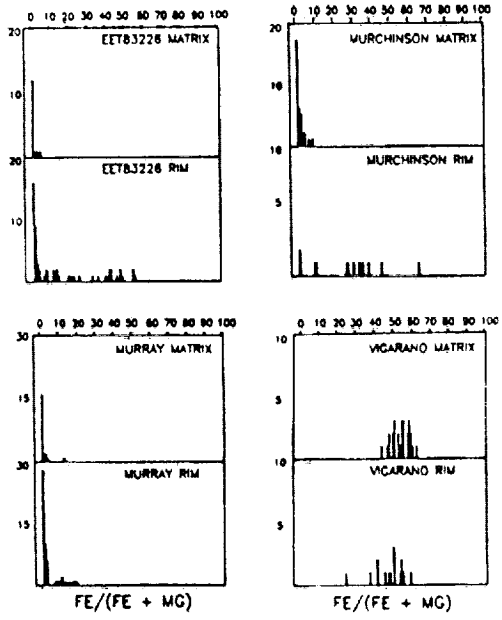

Fig. 1

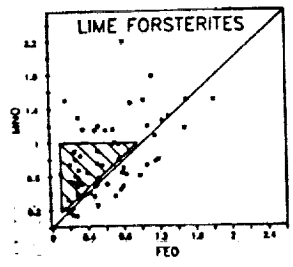

Fig. 2

References: (1) Zolensky M.E. et al. (1989), LPSC XX, 1249-1250, (2) Klöck W. et al. (1989), LPSC XX, 522-523.

GEOCHEMISTRY AND AGE OF IVORY COAST TEKTITES. Christian Koeberl[1,2], Richard J. Bottomley[3], Billy P. Glass[4], Dieter Storzer[5], and Derek York[3]. [1]*Institute of Geochemistry, University of Vienna, Dr.-Karl-Lueger-Ring 1, A-1010 Vienna, Austria.* [2]*Lunar and Planetary Institute, 3303 NASA Road One, Houston, TX 77058, USA.* [3]*Department of Physics, University of Toronto, Toronto, Canada M5S 1A7.* [4]*Department of Geology, University of Delaware, Newark, DE 19716, USA.* [5]*Laboratoire de Mineralogie, Museum, 61 Rue Buffon, F-75005 Paris, France.*

Ivory Coast tektites have been known since more than 50 years, but due to the limited number of samples available, not many studies have been reported until about 20 years ago. Since then, several studies of major and trace element chemistry, isotopic composition, and K-Ar and fission track ages have been published. Most data (except major element analyses) have been obtained for only a very limited number of specimens. Ivory Coast tektites are very rarely found *in situ*. They occur in an area of small geographical extent in a weathered zone of micaceous schist and granitic rocks of the Precambrian Upper Birrimian system and in alluvial gravel. The discovery of microtektites in drill cores, taken from deep sea sediments off the coast of West Africa, has considerably increased the area of the Ivory Coast tektite strewn field (e.g., [1]). On the basis isotopic and age studies the Bosumtwi crater in Ghana, which is located about 300 km east of the tektite strewn field, has been identified as the most probable source crater for the Ivory Coast tektites. The crater has a diameter of about 10.5 km (but may be even larger than that), and is mostly filled with a lake. Recent Rb-Sr and Sm-Nd isotopic studies [2] and chemical analyses of Bosumtwi impact glasses [3] strongly support the theory of a common impact origin of the Bosumtwi crater and the Ivory Coast tektites. In order to provide a modern and more complete data base for Ivory Coast tektites, we have analyzed up to 11 specimens for major elements and possible inclusions (by electron microprobe analysis), trace elements (by neutron activation analysis), and water content (IR spectrometry). In addition, their fission track and ^{40}Ar-^{39}Ar ages have been determined. Several microtektites have been analyzed individually for their major and trace element composition and Ar-Ar age. The results from our study show that Ivory Coast tektites are very homogeneous and do not show significant chemical variations between individual samples or even within one sample. Rare earth element abundances are particularly useful for relating target rocks with impact melts. Previously only very few analyses of lower precision have been available. Our analyses show that Ivory Coast tektites and microtektites have very similar chondrite-normalized REE patterns and show little variation between individual samples. The negative Eu anomaly is not very pronounced. The REE patterns in the tektites are very similar to the ones observed in Bosumtwi impact glass [3]. Other trace element contents agree with previously reported data (e.g., [4,5]). The trace element concentrations in the microtektites are very similar to tektites and material from the Bosumtwi crater. Our results show that the water content of Ivory Coast tektites (which has not been measured before) is as low as in tektites from other strewn fields. At this time the fission track and ^{40}Ar-^{39}Ar and fission track age determinations are still in progress. Our data are in agreement with an origin of Ivory Coast tektites and microtektites from the Bosumtwi impact event.

References: [1] Glass B.P. and Zwart P.A. (1979) EPSL 43, 336-342. [2] Shaw H.F. and Wasserburg G.J. (1982) EPSL 60, 155-177. [3] Jones W.B. (1985) Geochim. Cosmochim. Acta 49, 2569-2576. [4] Schnetzler C.C., Philpotts J.A., and Thomas H.H. (1967) Geochim. Cosmochim. Acta 31, 1987-1993. [5] Cuttitta F., Carron M.K., and Annell C.S. (1972) Geochim. Cosmochim. Acta 36, 1297-1309.

COOLING HISTORY OF IAB-SILICATE INCLUSIONS AND RELATED CHONDRITIC METEORITES

T. Köhler, H.Palme and G. Brey
Max-Planck-Institut für Chemie, D-6500 Mainz, Saarstr. 23, F.R. Germany

Solubility of Ca in olivine in equilibrium with cpx is dependent on temperature and pressure. This thermobarometer was recently calibrated and successfully applied to peridotitic upper mantle rocks (Köhler, 1989). Extrapolation to low pressures allows the application as a thermometer to meteorites.

Several meteorites, such as Acapulco, Winona, Mt. Morris and Pontlyfni, which are sometimes called "Winonaites", are chondritic (i.e. primitive) in composition, but lack chondrules. Silicate inclusions of IAB-irons are in many respects very similar to these stones. Olivine and cpx compositions are comparable to those of upper mantle rocks.

We, therefore, have applied the Ca-ol/cpx thermometer to these meteorites. Ca-contents of separated olivine grains from Acapulco and Pontlyfni and from silicate inclusions of Landes and El Taco were determined by electron microprobe. Typical results for a Landes olivine grain are shown in the figure. The grain is strongly zoned in Ca (and Cr) with much lower contents at the rims. The observed Ca-content in the center corresponds to a temperature of 668°C, more than 300°C below the peak metamorphic temperature of this meteorite, derived from the two-pyroxene thermometer (Brey et. al, in prep.). For the rim of this olivine grain a formal temperature of 462°C is calculated (see fig). Results for the other meteorites are comparable to those of Landes. The parallel zoning profiles of Ca and Cr indicate similar diffusion coefficients for both elements in olivine. In addition, the temperature dependence of the solubility of Cr in olivine must be similar to that of Ca.

Besides the disequilibria in distribution of Ca and Cr between olivine and pyroxene, there are several reports of disequilibrium distribution of Fe^{2+} (which has a similar diffusion coefficient to Ca) in IAB silicate inclusions. Fayalite contents of olivines are significantly below ferrosilite contents of pyroxenes. The lower Fe^{2+} in olivine probably does not reflect cooling itself but lowering of fO_2 during cooling, possibly caused by oxidation of Phosphide to Phosphate.

Calculations are in progress to model the cooling rates of these meteorites and compare them to cooling rates obtained by other methods. Similar peak temperatures and cooling rates for silicate inclusions in iron meteorites and chondritic meteorites would imply similar thermal histories for the parent bodies of both types of meteorites.

The contents of volatile elements (including planetary rare gases) in "Winonaites" and IAB-silicate inclusions are higher than those of all types of ordinary chondrites (Palme et al., 1981). The high metamorphic temperatures and the comparatively slow cooling rate shows that heating of a chondritic parent body to the Fe-FeS-eutectic does not necessarily imply loss of volatiles.

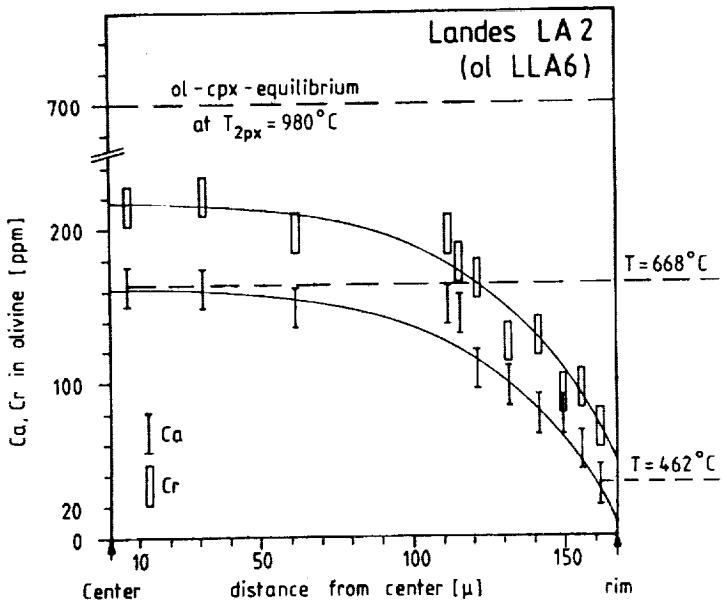

Brey, G.P., Köhler, T. and Nickel, K.G. (in preparation).
Köhler, T., Dissertation, Mainz 1989.
Palme, H. et al. (1981), Geochim. Cosmochim. Acta 45, 727-752.

CONDENSATION OR EVAPORATION: THE ORIGIN OF MODERATELY VOLATILE ELEMENTS IN CHONDRITIC METEORITES.

A.-V. Köhler, H. Palme[1], T. Geiger[2] and K. Müller[3]
[1]Max-Planck-Institut für Chemie, Saarstraße 23, D-6500 Mainz, FRG. [2]Institute of Mineralogy, University of Münster, Correnssstr. 24, D-4400 Münster, FRG. [3]Institute of Mineralogy, University of Tübingen, Wilhelmstr. 56, D-7400 Tübingen, FRG.

Most groups of chondritic meteorites have lower contents of moderately volatile elements (e.g. Au, Ga, Na, K, Cu, Zn, Se) than CI-chondrites. They have either not acquired the full share of these elements during condensation or have lost them later during thermal metamorphism or by some more severe heating episodes, such as chondrule formation. The purpose of this study is to find out to what extent heating of originally CI-material has contributed to establishing the presently observed abundance pattern of moderately volatile elements in chondritic meteorites.
We have performed heating experiments on primitive meteorites, primarily Allende, to shed light on the process that caused depletion of volatiles. All experiments were made under controlled oxygen fugacity. Residues were analysed by INAA-techniques. Texture and mineralogy of the residues are being investigated with the SEM. Temperatures were between 1050°C and 1255°C. Run times about 4 days, in most cases.
Heating experiments in closed quartz vials with solid state buffers (from $Cr-Cr_2O_3$ to $Fe_3O_4-Fe_2O_3$) and a cold trap produced large losses of Na and K; up to 90 % of Na was lost at 1150°C (4 days). Experiments in an open system with fO_2 controlled by $CO-CO_2$ mixtures gave only moderate losses of Na (max. 50 %) under otherwise similar conditions. Evidently quartz acts as a sink for some elements and results of this type of experiments must be viewed with caution.
An absolute upper fO_2 limit for processing of chondritic material is obtained from Re-abundances (1). At Ni-NiO, Re begins to volatilize (resulting in higher than chondritic Ir/Re ratios) in both types of experiments. Since chondrites have constant Ir/Re-ratios their parent material can never have been exposed to an fO_2 corresponding to Ni-NiO at elevated temperatures.
A similar constraint is obtained from the loss of Au and As. At the Ni-NiO buffer both elements become more volatile than Na, K, and Ga in open system experiments. In bulk chondrites Au and As abundances are in all cases higher than those of Ga, Zn and Se, and in most cases higher than Na and K. At very high oxygen fugacities (air) Zn is not lost even at 1255°C under the conditions of the experiments.
At reducing conditions losses of Zn and Se (compared to Au, As, Ga) produced in the experiments are in all cases higher than those observed in CM, CV and ordinary chondrites.
Loss of Mn, which is significant in carbonaceous chondrites, was not observed in the experiments, perhaps because Mn is concentrated in coarse olivine grains, compared to Na and K, which are primarily contained in fine grained Al-silicates. Prolonged heating would only amplify the difference. SEM-measurements show indeed strong zonation of Ni in olivine. If, however, during condensation major differencies in grain size are absent, Mn may behave similarly volatile as Au or the alkali-elements.
It therefore appears that depletion patterns of moderately volatile elements in chondritic meteorites primarily reflect nebular processes, such as, for example, continuous removal of volatiles during condensation, perhaps by settling of dust as originally envisioned by Wasson (2). This could also explain the low but constant abundance level of the highly volatile elements observed in unequilibrated chondritic meteorites.
References: (1) Koehler, A.-V. & Palme, H. (1988) **LPSC 19**: 627-628. (2) Wasson, J.T. & Chou, C.-L. (1974) **Meteoritics Vol.9**, No.1: 69-84.

ORIGIN OF PCP: Hideyasu Kojima and Keizo Yanai, Department of Meteorites, National Institute of Polar Research, 9-10, Kaga 1-chome, Itabashi-ku, Tokyo 173, Japan

PCP is one of constituents of CM carbonaceous chondrite. and is considered as secondary material which was produced by aqueous alteration in a parent body(1, 2). On the other hand, chondrules, inclusions and their fragments of Yamato-74662 and Yamato-791198 have well developed rims. These rims consist mainly of fine phyllosilicates, pyrrhotites and Fe-Ni metals. No PCP is included in rims. PCP is mainly situated out side of rims. This textural feature indicate that PCP situated out side of rims are not altered materials derived from metals and sulphides in chondrules, inclusions and rims, but PCP accretes to rims after rim formation around chondrules, inclusions and their fragments prior to parent body formation.

The chemical compositions of PCP in the CM chondrites which were altered to various degrees are plotted on the two different lines on the Si-Mg-Fe diagram. One is a tie-line between FESON and cronstedtite. The other is a line between Mg-serpentine and 75% cronstedtite on FESON-cronstedtite tie -line. PCP on former line are observed in relatively weakly altered CM chondrites and PCP on latter line are in heavily altered ones.

These facts lead following conclusions.

1. FESON reacted with Si-rich material to form cronstedtite prior to parent formation. However this reaction did not proceed completely, FESON was preserved in weakly altered CM chondrites. It is not clean that the FESON is a low-temperature condensation product or alteration product of precursor materials in the nebula.
2. Cronstedtite reacted with SiO_2 and MgO that released from low-Ca pyroxene and olivine to form Fe-serpentine in the stage of aqueous alteration on the parent body.

1) Bunch and Chang (1980) Geochim. Cosmochim. Acta 44, 1543-1577. 2) Tomeoka and Buseck (1985) Geochim. Cosmochim. Acta 49, 2149-2163.

SEARCH FOR DISPERSED TUNGUSKA METEORITE MATTER. E.M.Kolesnikov, Geology Faculty of Moscow State University, 119899 Moscow, USSR.

Mass of Tunguska cosmic body(TCB) is supposed to be $\sim 10^6$ tons, therefore search for traces of dispersed TCB matter should be a success. The Academy of Sci.expeditions(1961-1962)found the 20-1000μm cosmic magnetic spherules in Tunguska area soils. Their cosmic character has been confirmed by Ganapathy(1983)and Nazarov et al.(1983). However it is difficult to prove that these spherules are TCB matter because analogue ones can be found in soils everywhere. Sphagnum fuxum peat from which "catastrophe" layer(CL)may be isolated seems to be more appropriate object. Kolesnikov et al.(1977)have shown that there are often 30-80μm silicate spherules in CL. Their composition differ from larger spherules from soils(Glass,1969) and peat(Dolgov et al., 1973) .

The most probable hypothesis of TCB nature is a cometary one. According to "Vega" and "Giotto" missions the mean size of dust particles is~0,1μm with a large C content in some of them. Nobody has ever tried to search for such small particles in the Tunguska area. NAA of peat have shown a sharp increase of content of a number of elements in CL at one site(Golenetskii et al.,1977 ,Kolesnikov,1980) ,while at the other one only Ir increase being determined(Korina et al.,1987) . Presence of abiogenic cometary carbon in CL must have been possibly fixed in $^{12}C/^{13}C$ study(Kolesnikov,1984) . These results correlate with decrease of ^{14}C activity in CL(L'vov,1984) and in "catastrophe" tree rings(Firsov et al.,1984) . It is necessary to search for sites enriched with cosmic matter at catastrophe area and look for methods to isolate ultrasmall cometary dust particles from peat.

References: Ganapathy R.(1983),Science,v.220,N4602,p.1158-1161.
Glass B.P.(1969),Science,v.164,N 3879,p.547-549.
Golenetskii S.P.,Stepanok V.V.,Kolesnikov E.M.(1977),Geochimia, N 11,p.1635-1645(Russian).
Dolgov Yu.A.,Vasil'ev N.V.,Sugurova N.A.,Lavrent'ev Yu.G.,Grisin Yu.A.,L'vov Yu.A.(1973),Meteoritika,N 32,p.147-149(Russian
Firsov L.V.,Juravlev V.K.,Panichev V.A.(1984),In:Meteorite investigations in Siberia,Nauka,Novosibirsk,p.67-77(Russian)
Kolesnikov E.M.,Lyul A.Yu.,Ivanova G.M.(1977),Astr.Vestn.,v.11, N 4,p.209-218(Russian).
Kolesnikov E.M.(1980),In:Interaction of meteoritic matter with the Earth,Nauka,Novosibirsk,p.87-102(Russian).
Kolesnikov E.M.(1984),In:Meteorite investigations in Siberia, Nauka,Novosibirsk,p.49-63(Russian).
Korina M.I.,Nazarov M.A.,Barsukova L.D.,Suponeva I.V.,Kolesov G.M.,Kolesnikov E.M.(1987),Proc.Lunar Planet.Sci.Conf.18th, p.501-502.
Nazarov M.A.,Korina M.I.,Kolesov G.M.,Vasil'ev N.V.,Kolesnikov E.M.(1983),Proc.Lunar Planet.Sci.Conf.14th,p.548-549.
L'vov Yu.A.(1984),In:Meteorite investigations in Siberia,Nauka, Novosibirsk,p.83-88(Russian).

STUDIES ON CHEMICAL SPECIATION OF ANOMALOUS IRIDIUM AT CRETACEOUS-TERTIARY BOUNDARY Kong Ping Chai Chifang (Institute of High Energy Physics, Academia Sinica, P.O.Box 2732, Beijing, China)

During recent years, much attention has been paid in the sources of the anomalous iridium found globally widespread in Cretaceous-Tertiary (K-T) boundary (Alvarez, et al., 1980; Chai, 1988; Chai and Kong, 1988). In the present study, interest is turned to focus on the mechanism rather than the discovery of the Ir enrichment, that is, which origin of the anomalous iridium is plausible, extraterrestrial, volcanogenic or other sources? Even though much succeeding research has been catalyzed, no imperative evidence either for or against any hypotheses has yet been given. Recent research on kerogen extracted from K-T boundary clay seems to shed some new light on this problem. Schmitz, et al. (1988) reported that the concentration of Ir in kerogen leaching from two K-T boundary clays may reach 1100 ppb (Stevns Klint, Denmark) and 1500 ppb (Caravaca, Spain). Thus, the imperative problem is whether the anomalous iridium is originated from biomass extinction or vice versa? Wells, et al. (1988) reported that typical marine biological materials are low in Ir (range <4-80ppt) and believed marine organisms can be rejected as a source of Ir to K-T boundary layer sediment.

Our research is focused on the chemical speciation study of the anomalous iridium in K-T boundary samples. We separated geological samples into six components (carbonate, metal, sulfide, oxide, silicate and acid-resistant residue) by a selective chemical dissolution procedure and analyzed the element distribution patterns in each phase. The results of K-T boundary samples (Fish Clay from Stevns Klint, Denmark, and Montana, USA) were carefully analyzed and compared with those of meteorites (Ning Qiang, Bao Xian, Sui Zhou) and ultrabasic rock from SRTH. Our results showed that up to 50% Ir in K-T boundary samples were present in residue phase but little in sulfide phase. The Ir distribution pattern disfavors the hypotheses of geochemical enrichment and volcanogenesis of the anomalous iridium. Some detailed research were carried out in the residue phase of K-T boundary samples. The results of X-ray diffraction showed the existence of beaverite and pyrite in marine K-T boundary samples. Light element analysis in marine K-T boundary sample (Fish Clay) told us, its concentration of C, H, N could reach 35%, 2.5%, 3.8%, respectively, which component is regarded as insoluble kerogen. Whereas in continental K-T boundary sample (Montana) the concentration of C, H, N were 4.0%, 2.0%, <0.30%, respectively. It is obvious that the Ir enrichment did not necessarily associate with kerogen, namely having a biological precursor. So our conclusion is if the anomalous Ir did originate from a single source, the Ir existed in Kerogen should have a primitive precursor, say, most likely extraterrestrial material. The Ir enrichment in kerogen probably occurred after deposition as a result of Ir redistribution within the sediments.

REFERENCES: Alvarez,L.W.,Alvarez,W.,Asaro, F. and Michel, H.V. Science 208(1980) 1095; Chai,C.F. Isotopenpraxis 24(1988) 257; Chai,C.F. and Kong,P. Meteoritics 23(1988) 263; Schmitz,B., Andersson,P. and Dahl,J. Geochim. Cosmochim. Acta 52(1988) 229; Wells,M.C., Boothe,P.N.and Presley, B.J. Geochim. Cosmochim. Acta. 52(1988) 1737.

* This work is supported by National Natural Science Foundation of China (NSFC).

FAYALITE-BEARING EUCRITES AND THE ORIGINS OF HED MAGMAS:
Jean M. Kozul and Roger H. Hewins, Dept. of Geological Sciences, Rutgers University, New Brunswick, N.J. 08903, USA

The relative importance of partial melting, fractional crystallization, and perhaps other processes, have not been clearly resolved for the HED basalt suite. The rare appearance of ferroan olivine in these rocks is a potential constraint on their evolutionary history. The LEW 85300, 85302 & 85303 polymict eucrites contain magnesian, common eucritic and two kinds of fayalite-bearing rock. One variety is only slightly more Fe-rich than common eucrites and contains Fa83 granules on grain boundaries and in veins in pigeonite. This fayalite may possibly have formed by solid state reactions. The other variety is seen in 85303,67 and ,30 and is distinctly more Fe-rich and is rich in incompatible elements (IE), with 23% FeO and REE 30X chondrites (1). Since it contains primary fayalite (Fa88) along with augite (En21Wo40) and plagioclase (An83), it is considered here in terms of HED basalt evolution.

LEW 85303,30 plots very close to the peritectic point where pigeonite is replaced by fayalitic olivine plus a silica phase in a projection from An onto Sil-Fo-Fa. There are two ways in which such liquids can arise. Fractionation of HED Mg-basalt or common eucrite pushes liquids across the pigeonite+plagioclase field until silica saturation is achieved; subsequent crystallization of pigeonite+plagioclase+tridymite moves liquids down to the point where pigeonite is replaced by fayalite. With this origin, there should be eucrites saturated with silica plotting at the eutectic in Sil-Ol-Pl projections but these rocks have not been sampled yet. Liquids saturated in fayalitic olivine could also arise as primary magmas by partial melting of plagioclase peridotite or olivine norite with intermediate to high Fe/Mg ratio.

Both phase equilibration and fractionation calculations require at least 50% crystallization (of pigeonite, plagioclase and tridymite with minor augite and ilmenite) to produce liquids saturated with fayalitic olivine from common eucrites. Fractionation calculations generate adequate REE concentrations for the daughter liquids only if the parent is IE-rich, e.g. Stannern. Thus even if 85303,30 is not a primary magma, at least two magma types are represented in the samples because the other clasts are IE-poor and resemble the common eucrites.

A fractionation origin for the fayalite-bearing rocks is plausible provided that silica-saturated liquids can be found. If they are not found, a primary magma origin would be more plausible.

Reference (1) Mittlefehldt D.W. and Lindstrom M.M. (1988) Lunar Planet. Sci. XIX, 790-791.

CHEMICAL MEMORY IN CHONDRULES OF PRECURSOR DUST WITH FRACTIONATED COMPOSITIONS -- David A. Kring and William V. Boynton, Lunar and Planetary Laboratory, University of Arizona, Tucson, AZ 85721.

Refractory inclusions and ferromagnesian chondrules may differ in part because they formed from aggregates of dust with dissimilar bulk compositions which had somehow become fractionated in the solar nebula. However, the fractionation of the precursor material was apparently incomplete, because many objects exist with properties intermediate to CAIs and ferromagnesian chondrules. For example, some amoeboid olivine aggregates have fractionated isotopes and REE patterns indicative of CAIs [Clayton *et al.* (1985), Grossman *et al.* (1979)], yet consist of the same minerals as ferromagnesian chondrules. Also, both plagioclase-rich chondrules [Sheng *et al.* (1988), Kring and Holmén (1988)] and fassaite-rich chondrules [Bischoff and Keil (1984)] are more siliceous than Type C inclusions, but less so than ferromagnesian chondrules.

We have begun a study of the REE abundances in chondrules with neutron activation techniques to determine the nature of their refractory precursor components, how these components were fractionated between different chondrules, and to see if they resemble precursor components previously identified in CAI. Our initial sampling of 10 Allende chondrules includes POP, BO, and BOP chondrules, a Ca-rich chondrule consisting of olivine, enstatite, pigeonite, and abundant feldspathic mesostasis, and a Ca,Al-rich chondrule containing spinel, plagioclase, fassaite, and olivine. Both the Ca-rich and the Ca,Al-rich chondrules have negative Eu and Yb anomalies similar to those of Group III CAIs. These anomalies cannot have been produced by igneous processes, but must be a record of solid/gas processes involving precursor dust that formed in reducing conditions [Boynton (1978)]. In addition, the HREE are enriched relative to the LREE in the Ca,Al-rich chondrule. Preliminary results also indicate that several of the BO, BOP, and POP chondrules may have negative Ce anomalies, which are characteristic of oxidizing conditions (O/H > solar, Boynton (1978)). Such oxidizing conditions may be those in which a precursor dust component formed, or those in which the chondrules formed since they are rich in FeO (~Fa2) suggesting an O/H ratio in the gas ~20-40 times greater than the solar ratio.

The fractionated REE patterns observed indicate the REE were not homogeneously distributed among the precursor components of chondrules. This is a result, in part, of solid/gas fractionation of the REE during condensation and evaporation processes that produced the precursor dust. The patterns observed could also be the result of igneous (solid/liquid) fractionation processes if a component in the precursor aggregates were fragments of older chondrules or any other once-molten material. The Ca-rich and Ca,Al-rich chondrules, which have bulk compositions and mineral assemblages intermediate between refractory inclusions (Types A, B, and C) and ferromagnesian chondrules, had precursor material with similar fractionated REE abundances to those previously identified in refractory inclusions; thus some of the precursor dust of chondrules and refractory inclusions may have come from the same reservoir, or from different reservoirs that experienced similar processes.

References: [1] Bischoff, A. and Keil, K. (1984) *GCA 48*, 693. [2] Boynton, W.V. (1978) *LPS IX*, 120. [3] Clayton, R.N. *et al.* (1985) *Protostars and Planets II*, D.C. Black and M.S. Matthews (eds.), University of Arizona Press, 755. [4] Grossman, L. *et al.* (1979) *GCA 43*, 817. [5] D.A. Kring and B.A. Holmén (1988) *Meteoritics 23*, 282. [6] Sheng, Y.J. *et al.* (1988) *LPS XIX*, 1075.

HEAT SOURCE FOR THE MELTING OF CAI IN THE SOLAR NEBULA --
D.A. Kring, W.V. Boynton, A. Yarn, N. Jest, Lunar and Planetary Laboratory, University of Arizona, Tucson, AZ 85721.

The mechanism which produced the high-temperature (>1500K) environment in the solar nebula where CAI were melted and partially vaporized has remained an enigma. Among the heat sources that have been postulated are nebular lightning [Whipple (1966)], impact melting [Kieffer (1975)], aerodynamic drag as interstellar dust accreted into the nebula [Wood (1984)], intense radiation from an active sun [Wasserburg and Papanastassiou (1982)] or nebular flares [Levy and Araki (1989)], and snowplowing shocks produced by nebular flares. Unfortunately, it is not yet clear if any of these mechanisms can satisfy all the constraints imposed by the textures and chemistry of CAI; none are widely accepted.

One of the curious features of CAI is the presence of refractory platinum metal nuggets (RPM, Wark and Lovering (1976)) which have much higher melting and vaporization temperatures than the CAI in which they reside, and thus appear to predate CAI and to have remained solid when CAI formed. Recent work by Fleischmann and Pons (1989) and Jones *et al.* (1989) has indicated that lattice sites in the types of metals found in RPM nuggets, especially Pd, can easily accommodate hydrogen. Because the spacing between lattice sites in these metals is so small, the probability of fusion *via* tunneling becomes large; one consequence of fusion is the generation of heat [Fleischmann and Pons (1989)]. We suggest that RPM nuggets, which when in the nebula were sitting in a hydrogen bath (a gas of solar composition), could have absorbed H and D, promoting fusion, and thus melting any aggregates of dust to which they accreted, forming CAI. A typical RPM nugget is ~2 μm in diameter, which with a density of about 12 g/cm^3, has ~5 x 10^{10} lattice sites, all of which could be filled with H and D. If the absorption of H and D into these lattice sites was controlled by the rate at which hydrogen molecules collided with RPM nuggets, then the lattice sites of a RPM nugget in a gas of solar composition with a total pressure of 10^{-3} atm would become filled with H and D in ~10^{-3} seconds. If on the other hand the absorption of H and D is limited to the rate at which hydrogen molecules diffuse into RPM (~10^{-7} cm^2/s, Fleischmann and Pons (1989)), then the lattice sites of such nuggets would have been filled in ~0.1 seconds.

These calculations illustrate the ease in which RPM nuggets in the nebula would have become saturated with H and D. Once fusion had commenced in the RPM nuggets and any aggregates of material that surrounded them had been melted, the molten and finally crystalline CAI would have effectively shielded the RPM nuggets from the hydrogen gas, removing the fuel source for the fusion reaction. Thus hydrogen fusion would have ceased in the RPM nuggets once their initial supply of hydrogen became small, allowing the CAI to cool and solidify.

References: [1] Fleischmann, M. and Pons, S. (1989) *J. Electroanalytical Chem.*, submitted. [2] Jones, S.E. *et al.* (1989) *Nature*, submitted. [3] Kieffer, S.W. (1975) *Science 189*, 333. [4] Levy, E.H. and Araki, S. (1989) *Icarus*, in press. [5] Wark, D.A. and Lovering, J.F. (1976) *Lunar Science VII*, 912. [6] Wasserburg, G.J. and Papanastassiou, D.A. (1982) *Essays in Nuclear Astrophysics*, C.A. Barnes *et al.* (eds.), Cambridge University Press, 77. [7] Whipple, F.L. (1966) *Science 153*, 54. [8] Wood, J.A. (1984) *EPSL 70*, 11.

PRIMITIVE OLIVINES WITH HIGH TRACE ELEMENT CONTENTS IN ALLENDE-AF AGGREGATES; G.Kurat, Naturhistorisches Museum, A-1014 Wien, Austria; E.Zinner, Washington University, St.Louis, MO 63130, USA; H.Palme, Max-Planck-Institut für Chemie, D-6500 Mainz, FRG

An unusual chondritic rock fragment (All-AF) from the Allende CV3 chondrite has recently been described (Palme et al., 1985; Kurat et al., 1987). All-AF mainly consists of olivine-rich aggregates and has a bulk composition similar to that of bulk Allende. The olivine is rich in FeO (Fa 26-40) and unusual in several respects: it is poorly crystallized (low Δ), occurs in fluffy stacks of platelets (commonly 5x15 μm) which form aggregates up to ~1 mm in diameter, and is rich in minor elements (Al_2O_3 0.5-2.5 wt.%, CaO 0.2%, TiO_2 0.02-0.15%, Na_2O around 0.1%). These features led to the conclusion that the olivines in All-AF formed by condensation and escaped the sintering and partial melting experienced by aggregates and chondrules of other chondritic rocks.

The high Al-contents of All-AF olivine made us suspect that it may be rich in trace elements normally not present in olivine. We selected an aggregate with a fairly coarse-grained proto-BO center for measurements of the distribution of refractory trace elements by ion microprobe spectrometry following the procedure of Zinner and Crozaz (1986). Analyzed were a bulk portion (average of a large area) and olivine-rich areas. We also succeeded in identifying trace-element-rich mobilisates associated with the olivines.

The results (Figure) show that the bulk aggregate is rich in refractory trace elements and grossly unfractionated, as is the olivine whose RTE abundances are a factor 3-4 lower. In addition to common RTE the olivine contains large amounts of Be (5xCI), Li (1xCI) and B (3.5xCI). Surprising are the very high contents of Zr and Nb (about 2xLREE). Small, fine-grained, Ca-rich areas associated with the olivine are substantially enriched above the bulk in trace elements and are interpreted as local partial mobilisates derived from the olivine. Less refractory elements (V,Cr,Li) have abundances decreasing with increasing volatility. Surprising is the high abundance of Li a good portion of which appears to reside in olivine.

In conclusion, the All-AF olivines are indeed primitive condensates which originally held the major share of the refractory trace elements. Some mobilization of trace elements did take place presumably during the metasomatic event which added FeO to the originally forsteritic olivines and during which Ca together with some mobile incompatible elements moved to the crystal surface. This study confirms our previous conclusion that All-AF consists of aggregates (proto-chondrules) of primitive condensates.

References: Kurat G. et al. (1987) LPS XVIII, 523; Palme H. et al. (1985) LPS XVI, 645; Zinner,E. and Crozaz G.(1986) Int.J.Mass.Spectr. and Ion Processes 69, 17.

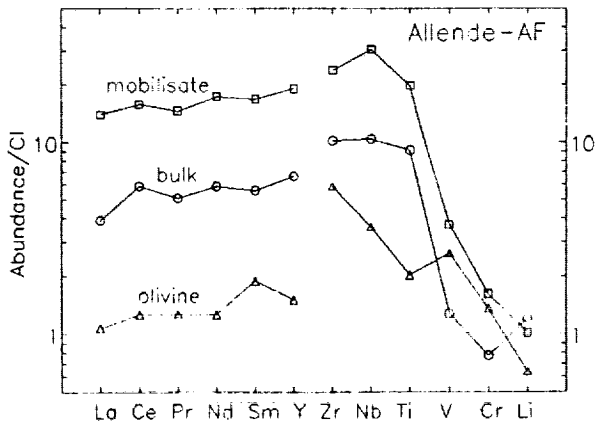

Figure: CI-normalized trace element abundances in olivine, a bulk portion, and a Ca-rich mobilisate of an aggregate in All-AF.

GRAPH-THEORETICAL INDICES PROBING COSMOCHEMICAL EFFICACITY: CYANOPOLYYNES AS TRACERS; Bruno Lang and Tomasz Grochowski, Warsaw University, Department of Chemistry, Zwirki i Wigury 101, 02-089 Warsaw, Poland.

Cyanopolyynes (cyanoacetylenes) of general formula $H-(C\equiv C)_n-CN$ were found abundant enough to be used for astrophysical molecular diagnostics. With n triple-bonded C≡C pairs the members of this homologous series differ in decreasing length of the linear carbon chain . We applied them for scaling the cosmochemical efficacity. To evaluate the change in local cosmochemical synthesis we assigned to them numerical values of topological indices i.e. graph-theoretical invariants [Hansen and Jurs, 1988; Randic et al. 1988].

From numerous topological indices as offered we selected: (i) the spectra i.e. eigenvalues of matrices of interatomic distances in molecules (Table 1), (ii) the Randić path one molecular connectivity index, $^1\chi$, defined as

$$^1\chi = \sum_k (1/mn)^{1/2}$$

where k covers all path of length one in a molecule, while m, n are valencies of points contained in these paths, (iii) indices obtained by applying information theory to chemical graphs [Basak et al., 1988], (iv) index of molecular complexity bridging information theory and group theory [Bertz, 1981] defined as

$$C(\eta) = 2\,\eta\,\log_2(\eta) - \sum \eta_i \log_2(\eta_i)$$

where η_i are connections per atom set i.

In Fig. 1 the values for indices are shown plotted against n, beginning from n=0 for hydrocyanic acid HCN, while tabulated in Table 2.

Table 1

	Eigenvalues										
n=1	5.16	-0.59	-1.16	-3.41							
n=3	21.82	-0.64	-0.71	-0.80	-0.91	-1.57	-4.09	-13.10			
n=6	49.57	-0.64	-0.68	-0.69	-0.70	-0.86	-0.86	-1.32	-2.43	-4.03	-8.44	-28.93

Figure 1

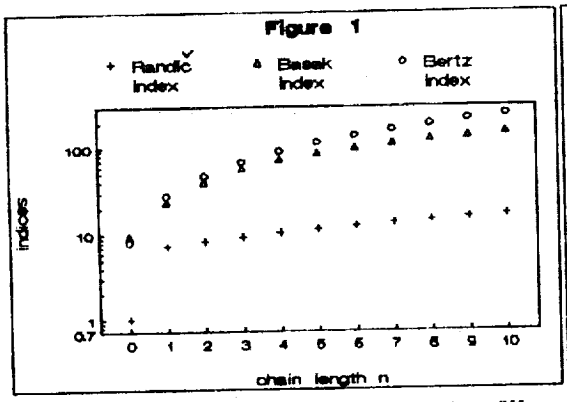

Table 2

Chain length n	Randić index	Basak index	Bertz index
0	1.00	9.51	8.00
1	7.18	23.22	27.25
2	8.18	39.30	46.53
3	9.18	57.06	67.47
4	10.18	71.36	89.86
5	11.18	84.60	113.47
6	12.18	97.56	138.15
7	13.18	110.44	163.76
8	14.18	123.37	190.20
9	15.18	136.37	217.37
10	16.18	149.48	245.22

The observed characteristic n-values for diffuse and dense molecular clouds, [Duley and Williams, 1984], stellar envelopes and planetary nebulae are from n=5 to n=0. For cometary matter n=0 has been reported but n>1 suggested. For Titan's atmosphere n=1 and n=0 is reported. For the Allende carbonaceous chondrite CV3 cyanopolyynes n=1 and n=0 are belived to occur.

REFERENCES: Basak S., Magnuson V., Niemi G. and Regal R.(1988) Discrete Appl.Mathem. 19, 17-44. Bertz S.(1981) J.Amer.Chem.Soc. 103, 3599-3601. Duley W. and Williams D.(1984) Mon.Not.Rastr.Soc. 211, 97-103. Hansen P. and Jurs P.(1988) J.Chem.Educ. 65, 574-580. Randić M., Hansen P. and Jurs P.(1988) J.Chem.Inform.Comp.Sci. 28, 60-68.

EXPERIMENTALLY SHOCKED PLAGIOCLASE: CHANGES OF REFRACTIVE INDICES AND OPTIC AXIAL ANGLE IN THE 10-30 GPa RANGE. F. Langenhorst, Institut für Planetologie, Universität Münster, D-4400 Münster, Germany

The optical properties of tectosilicates have been most widely used for shock wave barometry of naturally shocked rocks (1,2). Most data on experimentally shocked feldspars are restricted to diaplectic glasses (3,4). Up to now no reliable high precision optical data of feldspars exist for pressures below about 30 GPa where feldspars are still crystalline.

In this study samples of experimentally shocked single crystals of oligoclase (An_{21}) and sanidine (Or_{86}), and polycrystalline bytownite (An_{78}) previously studied by Ostertag (3), were analyzed optically. The shock recovery experiments were performed on disks (11 mm in diameter, 0.65 mm thick) cut parallel to the {100} face of the single crystals using a high-explosive plane wave generator and steel sample containers (3) at the Ernst-Mach-Institut, Weil a. Rh.. Peak pressures achieved by the shock reverberation technique were 10.5, 14, 18, 22, 26, and 28 GPa. The pressure accuracy is $\leq 3\%$. The refractive indices n_x, n_y and n_z, the birefringence, and the optic axial angle $2V_x$ were determined by means of the Medenbach microrefractometer spindle stage (5). The error of this most accurate immersion method is ± 0.0005 for refractive indices and $\pm 0.5^\circ$ for optic axial angle of shocked crystals.

Results of the spindle stage measurements can be summarized as follows. The three principal refractive indices of oligoclase and bytownite change most drastically in the 22 to 28 GPa range. It is remarkable that n_x first increases and then decreases with increasing shock pressure whereas n_z decreases steadily. In spite of this, the birefringence ($n_z - n_x$) which is 0.0116 (bytownite) and 0.0085 (oligoclase) for unshocked crystals decreases continuously above about 10 GPa until the isotropic state is reached at 26 GPa (bytownite) and 28 GPa (oligoclase). The optic axial angle changes from 0 to 22 GPa only moderately for oligoclase and bytownite where $2V_x$ increases with by only about 3° (from 85° to 88°) and 2° (from 87° to 89°), respectively. Sanidine displays a much stronger change of $2V_x$ with pressure: 13°(D) at zero pressure and 40°(D) at 22 GPa. Moreover, a distinct, so far unknown decrease of the wavelength dispersion of the optic axial angle of sanidine has been recorded with increasing pressure from 10 to 22 GPa. The difference of $2V_x$ between the wavelengths of 486 nm (F) and 656 nm (C) drops from ca. 6° to 1°.

The observed shock-induced changes of optical parameters of feldspars demonstrate that the optical indicatrix of feldspar crystals is affected by shock pressures above about 10 GPa which marks the onset of the plastic regime of the Hugoniot curve (6). Obviously, shock states of this regime are required for any permanent change of the crystal structure.

REFERENCES: (1) Stöffler, D. (1974) Fortschr. Miner. 51, 256. (2) Stöffler, D. et al. (1988) in Kerridge, J.F. and Matthews, M.S. (eds.) Meteorites and the Early Solar System, University of Arizona Press, Tucson, 166. (3) Ostertag, R., (1983), J. Geophys. Res. 88, 364. (4) Stöffler, D. (1984) J. Non-Cryst. Solids, 67, 465. (5) Medenbach, O. (1985) Forstschr. Mineral. 63, 111. (6) Ahrens, T.J. et al. (1969) J.-Geophys. Res. 74, 2727.

THE OXYGEN ISOTOPIC COMPOSITION AND THE ^{40}Ar-^{39}Ar AGE OF THE KAINSAZ CO CHONDRULES. A.K.Lavrukhina, V.I.Ustinov, M.M.Fugzan, G.V.Baryshnikova, and Yu.A.Shukolyukov. V.I. Vernadsky Institute of Geochemistry and Analytical Chemistry of USSR Academy of Sciences, Moscow, USSR

The unique Kainsaz CO chondrite is differed from other carbonaceous chondrites by absence of thermal metamorphism indicators (Kashkarov et al., 1984), and by high contents of chondrules, Fe,Ni-phase and graphitic carbon (Vdovykin, 1974). The absolute deviation of $\delta^{17}O$ and $\delta^{18}O$ values is equal to $\pm$ (0.1-0.15)‰. The chondrules of d>800 μm are positively droplet chondrules. The fraction of other size are mixtures of droplet and lithic chondrules. The data of table show the increase of $\delta^{17}O$ and $\delta^{18}O$ values for great size droplet chondrules. The impoverishment of these chondrules in nucleogenic ^{16}O can be understood best of all by model of their formation by means of stucking together small chondrules and matrix that is strongly depleted in cosmogenic ^{16}O. Kainsaz CO chondrules lie on the $\delta^{17}O$-$\delta^{18}O$ plot higher than chondrules and CAI of Allende CV and Murchison CM chondrites. It witnesses about various nature of chondrule precursors for these chondrites.

Table. $\delta^{17}O$ and $\delta^{18}O$ values relative to SMOW, ‰

Chondrule size, μm	Mass mg	$\delta^{17}O$	$\delta^{18}O$
149 < d < 210	12	-3.8	-1.3
210 < d < 260	12	-3.5	-1.3
260 < d < 350	16	-3.8	-1.2
350 < d < 520	10	-3.5	-1.8
520 < d < 800	12	-3.7	-0.9
d > 800	10	-2.0	-0.3

For ^{40}Ar-^{39}Ar age determination the chondrules of 520< d < 800 μm, silicate phases of d < 100 μm and d=100-200 μm poored in chondrules, and the bulk probe of 250 < d < 800 μm were selected. Histograms of stepwise realization of ^{40}Ar from all investigated samples have the minimum at t=1100°C, and from the silicate phase of d <100 μm it observed at t=1000-1200°C. It is obvious that chondrules and silicate phases contain some high temperature mineral phases which are not able to retain noble gases. Presense of analogous minima on the curves of Xe realization obtained by stepwise heating of HF,HCl-resistant residues of the same silicate phases and bulk probe (Shukolyukov et al., 1985) can witness about that. The ^{40}Ar-^{39}Ar ages determinated according to ^{39}Ar contents in the $\leq$1100°C gas fractions are equal to (3.96$\pm$0.01)AE for chondrules and 4.0AE for silicate phases of Kainsaz CO chondrite. The ^{40}Ar-^{39}Ar age values for chondrules of other chemical group chondrites are higher ($\lesssim$4.6AE). It witnesses that process of chondrule genesis was highly long.

References. Kashkarov L.L. et al. (1984) Abstracts XIX Conf. on meteoritics and cosmochemistry, p.53.
Shukolyukov Yu.A. et al. (1985) Meteoritika, 44, p.64.
Vdovykin G.P. (1974) Meteorites. Nauka, 181 p.

The Nature of Low Albedo Asteroids from 3-μm Multi-Color Photometry and Spectrophotometry Larry A. Lebofsky[1] and Thomas D. Jones[1,2], Lunar and Planetary Laboratory, Univ. of Arizona, Tucson, AZ USA.

In order to understand the compositional distribution of asteroids, we rely upon theories of the origin and evolution of the solar system and on telescopic observations of the asteroids. In the latter case, we must depend heavily on the taxonomic classification of asteroids and their implied relationship to meteorites [1,2,3]. Unfortunately, the taxonomic classes are determined solely from observed parameters and do not in and of themselves involve any compositional determination. For example, can we assume that a D-class asteroid in the middle of the main belt at 2.9 AU is compositionally similar to a Trojan asteroid at 5.2 AU?

Our major emphasis over the last few years has been on the determination of the composition of low albedo asteroids. These asteroids have been assumed to be unaltered and are thought by some to represent the raw materials from which terrestrial planets formed and so are important to our understanding of the origin and evolution of the Solar System.

There now exists a body of data at much higher resolution and over a greater spectral range (out to 2.5 μm) [4]. Also, we now have 1- to 4-μm observations of over 40 low albedo asteroids [5,6]. These observations span all low-albedo taxonomic classes (C, D, F, G, P, and T). Several (*e.g.*, the C asteroids) of these classes appear to be spectrally analogous to chemically primitive, volatile-rich carbonaceous meteorites. Others (*e.g.*, the D asteroids) appear to be compositionally 'ultraprimitive' and thus are presumed to be more volatile-rich than the mainbelt C asteroids. Therefore, it had been presumed that these outer belt and Trojan asteroids should show a larger volatile content (*i.e.*, hydrated silicates and organics) than the Cs. However, from our recent observations, we find that most of them do not show the spectral signature of hydrated silicates.

This is consistent with the scenario that in the outer part of the asteroid belt the kinetics of the nebula-solid reactions were too slow for chemical equilibrium to be attained. Under these conditions, all the asteroid belt started out as a mixture of ice and anhydrous rock. Asteroids in the inner part of the belt may have undergone moderate heating, resulting in the melting of some of this ice and subsequent aqueous alteration; those in the outer belt were not so heated, and instead lost their water to gradual sublimation over the age of the solar system.

This work was supported by NASA Grants NSG-7114 and NAGW-1146. References: [1] Tholen (1984) Ph.D. Dissertation, U. of AZ. [2] Gradie and Tedesco (1982) *Science* **216,** 1404–1407. [3] Tedesco *et al.* (1989) Astron. J. **87,** 580–606. [4] Bell *et al.*, in preparation. [5] Jones (1988) Ph.D Dissertation, U. of AZ. [6] Lebofsky *et al.* (1989) *Icarus*, in press.

---

[1] Visiting astronomer at the Infrared Telescope Facility which is operated by the University of Hawaii under contract to the NASA

[1,2] Present address: Central Intellegence Agency

PETROLOGY OF THREE UNDESCRIBED HUNGARIAN CHONDRITES: KISVARSANY, MIKE AND OFEHERTO. G.R. Levi-Donati and Martin Prinz. Inst. Tec. Ind. di Stato "A. Volta", 06100 Perugia, Italy. Dept. Mineral Sciences, Amer. Museum Nat. Hist., New York, NY 10024, USA.

The Catalogue of Meteorites (1985) does not report any petrologic classification for three chondrites which were recovered at different times and places in Hungary. They are KISVARSANY (May 24, 1914), a shower of at least thirty stones; MIKE (May 3, 1944), a fall of several stones, four of which were recovered; and OFEHERTO (July 25, 1900), one stone only, weighing 3.75 kg.

As it is not possible, at present, to obtain material from the Hungarian Museums, we studied a polished thin section of KISVARSANY from the National Museum of Natural History, Smithsonian Institution (No. 6000-1), and polished thin sections from the American Museum of Natural History of MIKE (No. 4093-1) and OFEHERTO (No. 4102-1).

Modal data for each chondrite were determined by an automated electron microprobe technique and the modal abundances and mineral compositions are typical of L-group ordinary chondrites. The meteorites consist mainly of olivine and orthopyroxene, with lesser clinopyroxene, and plagioclase; accessory minerals include chromite, metallic FeNi and troilite. Olivine compositions are: KISVARSANY, Fo_{76}; MIKE, Fo_{76}; OFEHERTO, Fo_{77}. Coexisting pyroxene is equilibrated with the olivine, and plagioclase is typically albitic. The textures are highly recrystallized with poorly defined chondrules. Thus, all three stones are L6 chondrites. Nevertheless, some features such as the thickness of the fusion crust, cracking and fracturing in KISVARSANY, and veining in OFEHERTO, are indicative of similar, but not identical histories.

NOBLE GAS COMPONENTS IN KRYMKA (LL3.0); K.L. Levsky, Leningrad University, U.S.S.R; U. Ott and F. Begemann, Max-Planck-Inst. für Chemie, Saarstraße 23, D-6500 Mainz, F.R.G.

We have studied trapped noble gases in Krymka (LL3.0) by a combination of chemical etching and stepwise pyrolysis/combustion for noble gas release. Krymka appeared of special interest because -a) Xe isotopic systematics in the study by Alaerts et al. (1) seemed to indicate a ratio of the exotic Xe components L-Xe/H-Xe lower than that observed in carbonaceous or other ordinary chondrites (2) and -b) since it is one of the most primitive ordinary chondrites (3,4) the occurrence of additional isotopically anomalous phases in it appeared likely. Samples studied include a HF/HCl resistant residue before (R10) and after (R11) etching with HNO_3 (80°C; 17 hrs.), and a residue resistant to HF/HCl, $HClO_4$ (~175°C, ~5 hrs.) and H_3PO_4 (~185°C, 0.75 hrs.). After a first pyrolysis at 630°C, the latter was combusted in nine temperature steps from 400°C to 1200°C.

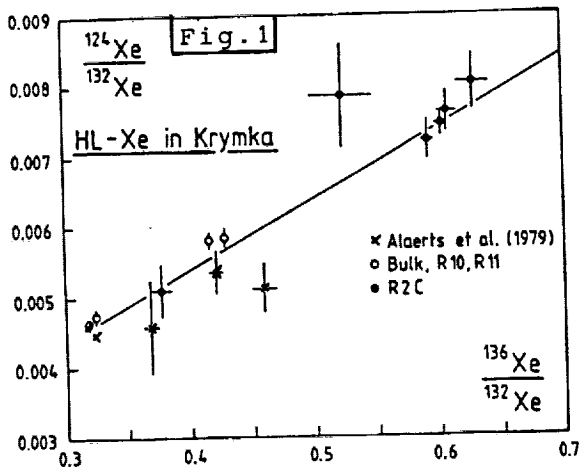

Relevant results concerning the first point are shown in Fig.1. Unlike the results of (1), our data points, if anything, plot above, not below the mixing line between AVCC and HL-Xe in C3V Allende (5), hence our data do not confirm a low L-Xe/H-Xe ratio for Krymka. In fact, since the R2C data points extend almost to the putative endmember composition of H-Xe ($^{136}Xe/^{132}Xe$=0.678; ref.6), any deviation from the carbonaceous chondrite H/L-Xe ratio can be minor only.

Ne-E(H) and s-Xe (7) were observed in the higher temperature combustion steps, with the most extreme compositions encountered at 1100°C. Ne released at this temperature had $^{20}Ne/^{22}Ne$=0.47 and $^{21}/^{22}Ne$=0.05. In the case of Xe, non-s isotopes were indistinguishable from blank, with *measured* $^{130}Xe/^{132}Xe$=0.26 and *measured* $^{136}Xe/^{132}Xe$=0.21. Abundances of the exotic components in R2C per gram of bulk Krymka are: 1.0×10^{-11} cc/g (Ne-E(H)), 2.2×10^{-12} ($^{136}Xe_H$) and 5×10^{-15} cc/g ($^{130}Xe_s$), approx. 2 orders of magnitude lower than in, e.g., C2M Murray (6; their HL-Xe composition was also used in our decompositon of Xe components). They occur, however, in similar abundance ratios: $^{22}Ne(H)/^{130}Xe_s$ and $^{136}Xe_{HL}/^{130}Xe_s$ in Krymka R2C are ~2000 and ~430, resp., which compares with ~1100 and 112 in Murray (6).

References: (1) Alaerts et al. (1979) GCA 43, 1399. (2) Anders E. (1981) Proc. R. Soc. Lond. A374, 207. (3) Sears D.W. et al. (1980) Nature 287, 791. (4) Anders E. and Zadnik M.G. (1985) GCA 49, 1281. (5) Frick U. (1977) Proc. Lin. Sci. Conf 8th., 273. (6) Tang M. and Anders E. (1988) GCA 52, 1235. (7) Anders E. (1987) Phil. Trans. R. Soc. Lond. A323, 287.

MULTIPLE STELLAR SOURCES OF s-PROCESS KRYPTON

Roy S. Lewis and Sachiko Amari
Enrico Fermi Institute, University of Chicago, Chicago, IL 60637-1433, USA.

Ott *et al.* (1988a) have shown that meteoritic Kr-S, unlike Xe-S, has variable isotopic composition, implying several different kinds of *s*-process. In a 5-step combustion/pyrolysis run on Murchison residue CFOc, they found large variations in isotopes 80 and 86, which lie at branch points of the *s*-process and thus are sensitive to stellar temperature and neutron density. To study these variations in greater detail, we analyzed by stepped pyrolysis 3 rather pure (>90%) SiC fractions from Murchison, of the following nominal grain sizes: LQB 0.05-0.15 μ, LQC 0.15-0.3 μ, LQD 0.3-0.5 μ, as well as Murray CF (0.03-0.2 μ, ~8% SiC) from Tang and Anders (1988a), but reprocessed to remove Cδ.

A plot of 83/82 vs 84/82 resembles that of Ott *et al.*, being linear and covering the same range. The analogous plots for isotopes 80 and 86 again deviate from linearity, but variations in 86/82 exceed those seen by Ott *et al.* The highest values imply *a neutron capture time of Kr^{85} comparable to its 10.8 yr half-life.* Interestingly, the 86/82 ratios increase monotonically with grain size, as does the Kr^{82}/Xe_S^{130} ratio, whereas the 80/82 ratios reach a minimum for the middle fraction. *Apparently differences in s-process conditions in the parent star(s) are somehow reflected in the circumstellar shell, causing correlated differences in the size distribution of SiC.* Since substantial isotopic differences show up even among our narrow, imperfectly separated size cuts, it appears that the original size distributions are sharply peaked, like the log-normal distribution of the SiC carrier of Xe-S (Tang and Anders, 1988a).

It was not feasible to determine the composition of the Kr-S components. Ott *et al.* found that 4 of their 5 points were collinear on a Kr^{84}/Kr^{82} vs Xe^{136}/Kr^{82} plot (implying a binary mixture of *s*-process and trapped gas), and assumed that the y-intercept gave a universal 82/84 ratio for all types of Kr-S. However, 5 of our 9 points (including all 1400° fractions) lie off the above mixing line, as did Ott's 1080° point. *This suggests that either the "trapped" component or the 82/84 ratio of Kr-S is variable.* Xenon plots confirm that the trapped component in our samples resembles a somewhat variable mixture of Xe-P and Xe-HL (Tang and Anders, 1988b), presumably accompanied by a Kr complement of similar pedigree. However, stepped combustion data on 3 parent or sibling samples of LQB to LQD suggest that the Xe-HL-like component does not come from a Cδ diamond impurity, but from SiC or another phase of similar combustibility. Some way will have to be found to reduce the contribution of this component or to correct for it.

Our data confirm the increase of Kr^{86}/Kr^{82} with Ne_E^{22}/Xe_S^{130} first noted by Ott *et al.* (1988b), but since it parallels an increase in grain size, we consider it fortuitous. Kr^{86}/Kr^{82} increases with grain size due to correlated changes in *s*-process and condensation conditions, whereas Ne_E^{22}/Xe_S^{130} increases with grain size because the Xe-S carrier has a much smaller grain size than does the Ne-E(H) carrier (Tang and Anders, 1988a; Tang *et al.*, 1988).

Clearly, meteoritic SiC contains a well-preserved isotopic record from a remarkable variety of sources, but to disentangle this record, the SiC must either be studied grain by grain (Tang *et al.*, 1989) or in fractions separated by size or other properties.

References. Ott U., Begemann F., Yang J., and Epstein S. (1988a) *Nature* **332**, 700-702. Ott U., Begemann F., Yang J., and Epstein S. (1988b) *Lunar Planet. Sci.* **19**, 895-896. Tang M. and Anders E. (1988a) *Geochim. Cosmochim. Acta* **52**, 1235-1244. Tang M. and Anders E. (1988b) *Geochim. Cosmochim. Acta* **52**, 1245-1254. Tang M., Anders E., and Zinner E. (1988) *Lunar Planet. Sci.* **19**, 1177-1178. Tang M., Anders, E., Hoppe P., and Zinner E. (1989) *Nature*, in press.

EVIDENCE FOR DIFFERENT AND COMPLEX THERMAL HISTORIES OF INDIVIDUAL AGGREGATES IN SOME EH CHONDRITES. Y.T. LIN[1], A. EL GORESY[1], Z. OUYANG[2] AND D. WANG[2]. [1]MAX-PLANCK-INSTITUT FÜR KERNPHYSIK, SAUPFERCHECKWEG 1, 6900 HEIDELBERG 1, FRG; [2]INSTITUTE OF GEOCHEMISTRY, ACADEMIA SINICA, GUIYANG, PRC.

We report the discovery of three different types of zoning profiles in niningerite grains in various metal-sulfide spherules, metal-rich aggregates and niningerite silicate fragments in *Qingzhen* and *Yamato-691* EH chondrites. The three zoning types occur in different aggregates in the same meteorite.

(1) A normal zoning trend in niningerite grains associated with silicates and no troilite. The FeS-content decreases from core to rim from 16.5-17.5 mole% to 14.5-15.5 mole%. The MgS-content displays an inverse behavior (64.5-65.5 mole% to 67.5-71.5 mole%). The zoning profile is quite flat in the core and descends steeply in a narrow rim. This trend is found in *Qingzhen* and reflects presumably primordial zoning as fixed during condensation of niningerite.

(2) Reverse zoning in niningerite in contact with troilite. This zoning was first described by [1]. FeS-content decreases from core to rim from 11.0-14.0 mole% to 15.5-18.3 mole% in *Yamato-691* and from 14.5-17.0 mole% to 18.5-21.5 mole% in *Qingzhen*.

(3) Normal zoning in niningerite bordered by troilite. This type is found only in *Yamato-691*. FeS-content decreases from 16.3 mole% to 14.0-14.4 mole% from core to the rim adjacent to troilite. This profile was produced by equilibration of niningerite and troilite upon cooling.

The presence of both normal and reverse zoning in niningerites in different fragments of the same meteorite indicates that (1) these zoning features predated the accretion in the meteorite parent body, (2) the reverse zoning was not produced during a thermal event of the meteorite parent bodies because this thermal event would have erased the normal zoning profiles, (3) the late stage thermal episodes in the *Yamato-691* and *Qingzhen* parent bodies were not insense enough to erase the normal zoning profiles in the niningerite-troilite assemblages. The results rather argue for individual complex thermal histories of the metal-sulfide objects predating the accretion event. These events do not exclude the possibility of a thermal episode affecting aggregates in the protobody followed by disaggregation and reaccretion in a second parent body.

REFERENCES: [1] K. Ehlers and A. El Goresy (1988): Normal and reverse zoning in niningerite: a novel key parameter to the thermal histories of EH-Chondrites. *Geochim. Cosmochim. Acta* **52**, 877-887.

EUROPIUM ANOMALY PRODUCED BY SULFIDE SEPARATION AND IMPLICATIONS FOR THE FORMATION OF ENSTATITE ACHONDRITES (AUBRITES)

K.Lodders, H.Palme, Max-Planck-Institut für Chemie, Saarstr.23, 6500 Mainz, FRG

Several authors suggested that enstatite achondrites (aubrites) are produced by igneous processes from enstatite chondrites [1,2]. Sulfide and metal separation on the enstatite chondrite parent body are required to account for the depletion of chalcophile and siderophile elements in aubrites. To explain the negative Eu anomaly commonly observed in aubrites, fractionation of plagioclase is genarally invoked. The results of our sulfide/silicate REE partition coefficients indicate that this may not be necessary.

REE partition coefficients were determined between iron sulfide liquid and REE doped tholeiitic basalt melt. Samples were equilibrated at 1210°C in evacuated sealed quartz tubes. After melting samples were quenched and phases were separately analyzed by INAA. Oxygen and sulfur fugacities were calculated from the observed phase compositions.

Preliminary results are shown in Fig. 1. Partition coefficients smoothly decrease from light to heavy REE, except for Eu, which has a sulfide /silicate partition coefficient significantly above those of the other REE. The pattern closely resembles that of plagioclase/melt partition coefficents [6]. In addition to the REE, partition coefficents for several other elements (e.g. Mn, Cr, Na, K) were determined under the same conditions. These data may be used to model the origin of aubrites in a qualitative way. In Fig. 2 CI-normalized data on aubrites are plotted and compared to enstatite chondrites. The simultaneous decrease of light REE and Cr, Mn, Na and K in various samples may be accomplished by sulfide fractionation alone. Numerical calculations are premature since the absolute values of the REE partition coefficients are too low. Experiments under more reducing conditions appropriate for aubrite formation are expected to yield higher partition coefficients. Such experiments are in progress.

Fig. 1

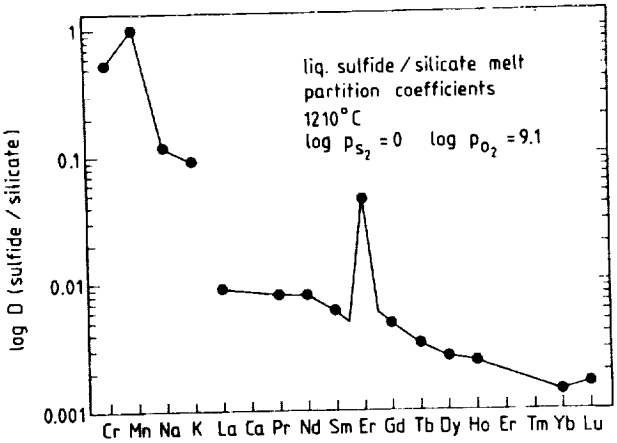

Fig.2

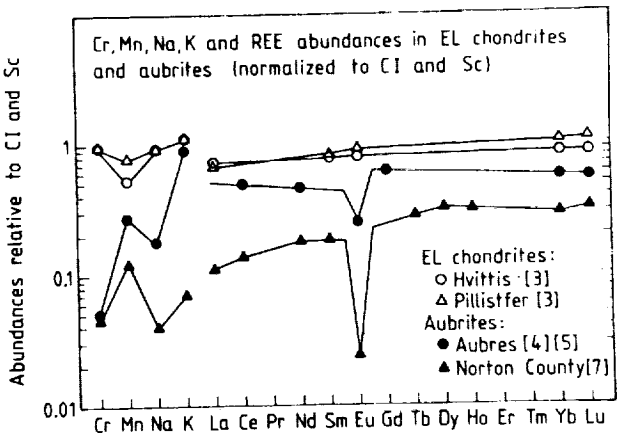

[1] T.R.Watters, M.Prinz, PLPSC 10th(1979)1073
[2] A.Okada et al., Meteoritics 23(1988)59
[3] G.W.Kallemeyn, J.T.Wasson, GCA 50(1986)2153
[4] A.J.Easton, Meteoritics 20(1985)571
[5] R.Wolf et al., GCA 47(1983)2257
[6] G.A.McKay, D.F.Weill, PLPSC 8th(1977)2339
[7] B.Spettel, Mainz, pers.comm.

LIMITS ON CHONDRULE FORMATION PROCESSES IMPOSED BY DYNAMIC CRYSTALLIZATION EXPERIMENTS

G. E. Lofgren, SN-2, NASA Johnson Space Center, Houston, TX 77058

Over the last several years numerous studies of the dynamic crystallization properties of a variety of chondrule melts have begun to give us a clearer picture of the formation conditions for chondrules (1,2,3,4,5). The experiments define some conditions uniquely and confirm conditions realized by other lines of investigation. The uniquely defined parameters include cooling rate, melting temperature, and melting time which combine to give the total duration of the chondrule forming event. Cooling rates in the range 100 to 3000°C/hr are capable of producing the observed textures. These cooling rates require the immediate environment to be denser that typical solar nebula (6). While the existence of previously crystalline material has been demonstrated by direct observation (7), the experiments establish that its presence is necessary for the formation of the bulk of the chondrules, those with porphyritic textures. Textures controlled by heterogeneous nucleation do not correlate readily with cooling rate (8). It is the need to preserve crystalline nuclei which limits the melting temperatures to the range 1450 to 1650°C for times ranging from a few minutes to a few hours (times are mostly likely less than one hour). This range of temperatures reflects a variation both in composition of the bulk chondrules and in the grain size of the precursor material. Combining the times for melting and cooling to near solidus temperatures gives a total event time of a few minutes to a couple hours. The short, near liquidus, melting times are also necessary to retain volatile elements in chondrules. Times of a few minutes are short enough to retain most of, e.g., sodium, but if the times exceed an hour, volatilization will be extensive unless there is a commensurate increase in the vapor pressure of volatile. The need to eliminate olivine zoning, which is unavoidable during crystallization, suggests that subsolidus cooling must be slow enough to allow homogenization of olivine. The duration of the actual heating event need be only a few minutes, and presumably heating must cease so cooling can begin.

The results of experiments have also allowed us to eliminate some of the existing models for chondrule formation. The direct condensation of liquids does not provide the preexisting crystalline materials necessary for the formation of the porphyritic chondrules. The controlled heating required to keep the temperature within a limited interval of melting renders the lighting model unlikely, although the short heating times suggest a transient event of comparable duration. There are models which appear to fulfill the requirement of transient heating, but none have gained universal acceptance because of other difficulties (6). The source of the preexisting crystalline material necessary to form chondrules is likely interstellar dust. The the report by Kurat (9) of fluffy aggregates in Allende as precursors which, if melted, could form chondrules deserves attention. It would be difficult for dust particles to spontaneously come together as part of the chondrule forming process, but if the dust has already agglomerated into fluffy masses, then melting and formation of chondrules is easier. Much of the heterogeneity between chondrules would then be related to the formation of these aggregates which could have a much longer and more complex history.

REFERENCES: (1) Tsuchiyama et al., 1981, EPSL 48, 155. (2) Hewins et al., 1981, LPSC 12B, 1123. (3) Planner and Keil, 1982, GCA 46, 317. (4) Lofgren and Russel, 1986, GCA 50, 1715. (5) Lofgren, 1989, GCA 53, 461. (6) Wood, 1988, Ann. Rev. Earth Planet. Sci. 16, 53. (7) Nagahara, 1983, In Chondrules and their Origins, ed. E.A. King, 211. (8) Lofgren, 1983, J. Petrol. 24, 229. (9) Kurat and Palme, 1989, LPSC XX, 552.

DIRECT MEASUREMENT OF OXYGEN-ISOTOPE RATIOS IN INDIVIDUAL MINERAL GRAINS OF REFRACTORY INCLUSIONS BY MEANS OF SECONDARY ION MASS SPECTROMETRY;
J.C. Lorin, G. Slodzian and R. Dennebouy, Laboratoire de Physique des Solides, Université Paris-Sud, 91405-Orsay, France.

A study of the fine-scale distribution of oxygen-isotope abundances in refractory inclusions of CV3 carbonaceous chondrites has been undertaken by means of high resolution and high transmission secondary ion mass spectrometry. *In situ* oxygen-isotope ratios determinations are carried out on spot areas (8 μm) of polished sections by means of a prototype instrument (1) based upon the Cameca SMI-300 ion analyzer, using Cs^+ primary ions ($\Phi = 10^{14} cm^{-2} s^{-1}$) and O^- secondary ions. Self-regulated electrostatic charge compensation is ensured by means of low-energy electrons brought close to the sample surface, the objective lens acting as an electrostatic mirror with respect to an auxiliary electron beam (2). Separation of analytical ions from interfering molecular ions is effected at high mass resolution: interfering $^{16}OH^-$ contributes less than 2×10^{-5} its own intensity to the measured $^{17}O^-$ intensity. Accurate and rapid selection of analytical ions is achieved by means of an electrostatic peak-switching system (1). A minor effect on the secondary ions energy-bandwidth brought about by this procedure is corrected for by an appropriate modulation of the voltage(s) of the electrostatic prism. Value of the magnetic field, regulated with a NMR probe, is kept constant to within one part per million. Optimum detection efficiency, regardless of the mass of the isotope, is ensured by the high energy of impact (∿10 keV) of the secondary ions onto the electron multiplier first dynode. The relative precision (1 σ) obtained in these conditions on the $^{18}O/^{16}O$ and $^{17}O/^{16}O$ ratios by sputtering a sample thickness of 2 μm is 5×10^{-4} and 1.1×10^{-3}, respectively, as expected from counting statistics alone. Sensitivity is high: the useful yield (O^- detected per sputtered O atom) ranges, depending upon the mineral species, between 0.5 and 1.0%. Isotopic discrimination is modest (5×10^{-3} per amu), favouring the light isotopes. In contradistinction with what is observed for positive ions (3), no variation of the isotopic discrimination with the energy bandwidth of the secondary ions is observed.

In the present study oxygen-isotope abundances have been determined in the different mineral phases of refractory inclusions of types A,B and C (as labelled according to the classification of Grossman (4) modified by Wark(5)) from the Allende and Leoville meteorites. The analysis of melilite, pyroxene and spinel in these inclusions beautifully confirms the observations made on the same type of material by R.N. Clayton and coworkers (6). The agreement is remarkable, considering that these authors have analyzed mineral separates numbering millions of grains, and of far-reaching consequence. In addition, secondary ion mass spectrometry makes it possible to extend these observations to refractory inclusions of a small size and to mineral phases not heretofore analyzed.

References:
(1) Slodzian, G. *et al.* (1984) in *SIMS IV* (eds. A. Benninghoven *et al.*), pp. 153-157, Springer-Verlag, Berlin. (2) Slodzian, G. *et al.* (1985) in *SIMS V* (eds. A. Benninghoven *et al.*), pp. 158-160, Springer-Verlag, Berlin. (3) Lorin J.C. *et al.* (1982) in *SIMS III* (eds. A. Benninghoven *et al.*), pp. 140-150, Springer-Verlag, Berlin. (4) Grossman, L. (1972) *Geochim. Cosmochim. Acta,* 36, 597. (5) Wark, D.A. (1987) *Geochim. Cosmochim. Acta,* 51, 221. (6) Clayton, R.N. *et al.* (1977) *Earth Planet. Sci. Lett.,* 34, 209.

ISOTOPIC AND MINOR ELEMENTS SIGNATURE OF COARSE-GRAINED MICROMETEORITES FROM GREENLAND BLUE ICE LAKES; J.C. Lorin and M. Christophe-Michel Lévy, Laboratoire de Minéralogie-Cristallographie, Université Pierre et Marie Curie, 75230-Paris, France; G. Slodzian and R. Dennebouy, Laboratoire de Physique des Solides, Université Paris-Sud, 91405-Orsay, France; M. Bourot-Denise, Laboratoire de Minéralogie, Muséum National d'Histoire Naturelle, 75005-Paris, France.

Micrometeorites are usually sorted out in deep-sea sediments by their magnetic properties and in Greenland and Antartic ice by their "chondritic" composition coupled with their more or less molten aspect. This leaves cosmic grains with a non-chondritic composition unaccounted and does not prevent confusion with terrestrial analogues. More reliable criteria would be the presence of spallogenic radionuclides, spallogenic and implanted noble gases, oxygen of a non-terrestrial isotopic composition, high irridium contents, etc. Mineral chemistry is also a powerful tool for identifying extraterrestrial matter, as shown by a recent study (1) in which possible relationships of coarse-grained micrometeorites with known meteorite groups, namely ordinary and carbonaceous chondrites, are evidenced by the fayalite content of olivine and the ferrosilite content of the pyroxene. The present study which couples oxygen-isotopes abundances and minor-elements concentrations has been carried out on coarse-grained micrometeorites in the size range 100-200 μm collected in Greenland blue ice lakes by M. Maurette and co-workers (2). Polished sections of these particles have been analyzed with the electron microprobe for minor elements content determination in the main mineral phases and with a modified Cameca SMI-300 ion-analyzer for oxygen-isotopes ratios determination on spot areas (8 μm) of selected mineral grains.

Oxygen isotopic composition appears to provide an excellent diagnosis of an extraterrestrial origin. On a three-isotopes correlation diagram the relative deviations from SMOW of the $^{18}O/^{16}O$ and $^{17}O/^{16}O$ isotope ratios plot, as a rule, away from the terrestrial mass-fractionation line and, within experimental uncertainties, right upon the CV3 mixing-line (3). No obvious correlation exists between oxygen isotopic composition and fayalite content of the olivine in which it is measured. Samples CG-27 and CG-28 with contrasted Fa contents (50 and 2, respectively) have closely similar oxygen isotope compositions. Minor elements content of main mineral phases indicate that coarse-grained micrometeorites are akin to, but not identical with, known meteorite groups. Some of them have a non-chondritic composition, such as the one in which a manganoan and chromian pyroxene is associated with a feldspar-rich glass: the MnO content of this object is however close to that of some IDP, and close also to that of rare mineral grains in unequilibrated ordinary chondrites. Iron-rich olivines such as found in CG-27, with "normal" minor elements content, may belong to the same batch of olivines commonly found in carbonaceous chondrites as isolated crystals. CG-27, where the olivine is associated with augite, chromite and albitic glass, may perhaps represent a tiny fragment of the parental rock from which stems this olivine population.

References:
(1) Robin, E. *et al.* (1989) *Earth Planet. Sci. Lett.*, submitted.
(2) Maurette, M. *et al.* (1986) *Science*, 233, 869
(3) Clayton, R.N. *et al.* (1977) *Earth Planet. Sci. Lett.*, 34, 209

THE OXYGEN OF RUSTY ORNANS; J.C. Lorin and G. Slodzian, Laboratoire de Physique des Solides, Université Paris-Sud, 91405-Orsay, France; M. Christophe-Michel Lévy, Laboratoire de Minéralogie-Cristallographie, Université Pierre et Marie Curie, 75230-Paris, France; G. Kurat, Naturhistorisches Museum, A-1014 Wien, Austria; H. Palme, Max-Planck-Institut für Chemie, Saarstrasse 23, D-6500 Mainz, F.R. Germany.

"Rusty Ornans" consists of mm-sized "rusty" fragments which have been found on broken surfaces of the Ornans carbonaceous chondrite (C3O) in the course of a neutron activation analysis (1). These fragments are characterized by marked enrichments in the light rare earths and by an exceptional mineralogy: corundum, tourmalin, iron-titanium oxides, pyroxene and olivine coexist along with a host of minor mineral phases. In order to ascertain the origin of this remarkable material we have undertaken a study of the oxygen composition of the constituent mineral phases by means of secondary ion mass spectrometry. Isotopic measurements have been made *in situ* on spot areas 8 μm in diameter on a polished section of a 2 mm fragment by means of a prototype instrument (2) based upon a Cameca SMI-300 ion-analyzer, using the same analytical conditions as described in a companion paper (3). Oxygen composition of corundum is, expressed as per mil deviations from SMOW, $^{18}\delta = +10.7 \pm 0.6$ and $^{17}\delta = +4.3 \pm 1.4$ (1σ). The remarkable fact is that it plots, on a three-isotope correlation diagram, right upon the intersection of the terrestrial mass-fractionation line and the CV3 mixing line (4). This particular isotope composition along with the high abundance of corundum in "Rusty Ornans" might help understand the intriguing fact that the isotopic composition of bulk "Rusty Ornans" oxygen, as measured by gas-phase mass-spectrometry (5), appears to be shifted with respect to bulk Ornans oxygen (6) towards terrestrial oxygen *with a shift directed along the CV3 mixing line*. Elucidation of the origin of this enigmatic mineral assemblage must await analysis of other mineral phases. These additional data will be reported at the meeting.

References:

(1) Kurat, G. *et al.* (1981) *Meteoritics*, 16, 343
(2) Slodzian, G. *et al.* (1984) in *SIMS IV* (eds. A. Benninghoven *et al.*), pp. 153-157, Springer-Verlag, Berlin.
(3) Lorin, J.C., Slodzian, G. and Dennebouy, R., this meeting.
(4) Clayton, R.N. *et al.* (1977) *Earth Planet. Sci. Lett.*, 34, 209
(5) Clayton, R.N., written personal communication, 1982.
(6) Clayton, R.N. and Mayeda, T.K. (1984) *Earth Planet. Sci. Lett.*, 67, 151

ON THE DISTRIBUTION OF ZINC ISOTOPE ANOMALIES WITHIN ALLENDE CAIs.

R.D. Loss and G.W. Lugmair, Scripps Inst. of Ocean., University of California, San Diego, Jolla. CA 92093 - 0212.

The discovery of excess ^{66}Zn ($^{66}Zn^*$) in Allende CAIs, reported earlier this year (1), confirmed the prediction (2) that these anomalies should exist along with those of other neutron rich isotopes of "iron peak" (IP) elements. These results revealed: 1) $^{66}Zn^*$ is present in a fine grained inclusion; this type of CAI is thought to be more thermally altered than coarse grained CAIs. 2) In contrast, the only coarse grained inclusion measured appeared to have normal $^{66}Zn/^{64}Zn$ in the HF-HCl soluble portion. The experimental uncertainty, however, is very large due to the very low Zn concentration and amount of sample available. 3) $^{66}Zn^*$ (<1 ϵ) are significantly smaller than excesses for Ca and Ti in the same samples and at least an order of magnitude smaller than predicted by the MZM model of Hartmann *et al.* (2). The simplest explanation for the latter may be related to the high volatility of Zn relative to the other IP elements. This fact could lead to dilution of $^{66}Zn^*$ during formation and/or subsequent thermal alteration of CAIs. If indeed volatility accounts for the lower than expected effect perhaps larger $^{66}Zn^*$ could be trapped by some of the more refractory components within CAIs which are also capable of retaining Zn during thermal processing.

To address this possibility we measured the Zn isotopic abundances in two CAI components: i) HF-HCl soluble or silicate fraction and ii) the remaining residue which consists primarily of spinel and represents typically 10-15%, by weight, of the total CAI sample analyzed. Zinc abundances in each of the components are given in the table below. The higher abundance of Zn in the residues are consistent with high levels of Zn in CAI spinels reported by Kornaki and Wood (3).

To enable comparisons to be made with a more refractory element, isotopic measurements of Ti in both components were also performed. The results so far indicate that the Ti is in isotopic equilibrium between the residues and the acid soluble fractions. The Zn data for the same samples (see table below) show that no large ^{66}Zn or ^{70}Zn anomalies are present in the residues. Only coarse grained CAI CGWI exhibits some evidence of $^{66}Zn^*$ heterogeneity although the values for both fractions still agree within experimental uncertainty. Therefore, based on the present results, one cannot exclude the existence of differences in $^{66}Zn^*$ between the HF-HCl soluble and residue portions of at least the CGWI sample. However the fine grained inclusion appears to have homogeneous $^{66}Zn^*$ distributed between both components.

References: (1) Loss, R.D. and Lugmair, G.W. LPSC XX, (1989).
(2) Hartmann, D.,Woosley, S.E. and El Eid, M.F. Ap.J. **297** (1985).
(3) Kornaki, A.S. and Wood, J.A. GCA **49** (1985).

Sample/Type		Zn Conc (ppm)	ϵ 66/64	ϵ 70/64
CGWI (Coarse grained)	acid sol.	54	0.16 ± 0.71	-2.5 ± 17.9
	residue	125	1.29 ± 0.44	9.0 ± 11.4
75-1 (Coarse grained)	acid sol.	27	0.52 ± 0.25	-1.6 ± 8.2
	residue	150	0.53 ± 0.14	1.2 ± 10.6
FGPI (Fine Grd. Pink)	acid sol.	1176	0.62 ± 0.29	2.1 ± 8.0
	residue	2810	0.43 ± 0.13	1.3 ± 4.9

CATHODOLUMINESCENCE PROPERTIES OF ST MARY'S COUNTY, A TYPE 3.3 ORDINARY CHONDRITE, COMPARED WITH OTHER TYPE 3 ORDINARY CHONDRITES

Lu Jie, John M. DeHart and Derek W.G. Sears, Cosmochemistry Group, Dept.of Chem.& Biochem., Univ.of Arkansas, Fayetteville, AR72701

The type 3 ordinary chondrites have experienced a considerable range of secondary alteration. It is clear that from 3.3 to 3.9, thermal metamorphism has been the major secondary process, but the lower types may have also suffered aqueous alteration [1,2]. The most "primitive" ordinary chondrites should be those which have experienced least metamorphism and least aqueous alteration. In this case, it is at least arguable that the 3.3 ordinary chondrites should be the materials most closely resembling the primary nebular materials. St Mary's County meteorite is an important ordinary chondrite in this connection, since its TL measurements indicate that it is type 3.3. However, it has received little attention, the only publication dealing specifically with this meteorite is the description by Noonan et al.[4]. We have carried out a study of the CL petrography of St Mary's County and compared it with similar studies of other type 3 ordinary chondrites.

Our previous work has shown that the cathodoluminescence (CL) properties of type 3 ordinary chondrites vary systematically with the degree of metamorphism experienced [5-7]. St Mary's County share a lot of properties in terms of luminescent materials and variety of luminescent colors with the previously studied primitive type 3 chondrites, but also have important differences in both numbers and type of luminescing materials. They all have relatively low level CL, and the matrix in St. Mary's is comparable to the matrix in Krymka, which is virtually nonluminescent. The luminescent types of mesostases appear to be intermediate between the most primitive (i.e. Semarkona and Krymka) and the intermediate categories of petrologic subtype. 61.3% of the chondrules emit blue luminescence, 16% emit dull red/purple light and 18% are nonluminescent. The olivine composition data of ref.4 are also consistent with St Mary's County being intermidiate between Krymka (3.1) and ALHA77214 (3.4). Other luminescent types are observed, but are only minor in their mode of occurrence (dull blue 3.3% and yellow 1.3%). St. Mary's County also possess a particular chondrule association only previously observed in Chainpur [5]. These chondrules have very large red luminescing grains rimming chondrules with bright blue luminescing mesostases and other more interior grains that are nonluminescent. These are not observed type 3 ordinary chondrites of lower or higher petrologic types.

St Mary's County therefore has all the CL and TL properties expected for a type 3.3 ordinary chondrite. It is hoped that this will provide further insight into mineralogic and petrologic changes accompaying very low levels of metamorphism and of any possible role aqueous alteration may have played in their history.

References: 1.Hutchison et al, (1987) G.C.A. 51: 1875-1882. 2. Guiman et al, (1987) G.C.A. in press. 3. Sears et al, (1988) in " Meteorites and the Early Solar System", J.F. Kerridge and M.S. Mathews(ed.), Univ. of Ariz.,(1988), 3-31. 4. Noonan et al, (1977), Smithson. Contrib. Earth Sci., No.19, 96-103. 5. DeHart et al, (1987) L.P.S. XVIII, 225-226. 6. DeHart et al,(1988) L.P.S. XIX, 259-256. 7. DeHart et al, (1989) G.C.A. submitted.

Support: NASA grant NAG 9-81

ISOTOPIC EVOLUTION AND AGE OF ANGRITE LEW 86010.

G.W. Lugmair and S.J.G. Galer, Scripps Inst. of Ocean., Univ. of California, San Diego, La Jolla, CA 92093-0212.

We will summarize and discuss results of an extensive Rb-Sr, Sm-Nd and Pb isotopic investigation of the unique Antarctic Angrite LEW 86010 (LEW) [1].

Mineral separations performed on a homogenized bulk sample (+75-125 μm) resulted in high purity separates of plagioclase (Pl), olivine + kirschsteinite (Ol), and core (PxLt) and rim (PxDk) pyroxene. Machine and inter-laboratory biases render it difficult to decipher detailed relative initial Rb-Sr systematics of early Solar System objects. To facilitate this comparison, various low Rb/Sr ratio samples were measured concurrently with LEW: small chips of predominantly Px were used from Angra dos Reis (ADOR), and a Pl fraction from the cumulate eucrite Moore County (MC). Multiple analyses were made to assess machine external reproducibility. These Rb-Sr studies show that the initial $^{87}Sr/^{86}Sr$ isotope ratios of all mineral fractions of LEW, ADOR Px, and MC Pl, calculated for an assumed age of 4.55 Ga, are indistinguishable within the uncertainties of measurement. The resulting best estimate for the initial $^{87}Sr/^{86}Sr$ ratio is 0.698970 ± 15 (2σ, external) for the Angrite Parent Body relative to 0.710263 ± 5 (2σ, mean of 18 runs) for the NBS-987 standard. This is only marginally higher than that of Allende CAIs [2], but is somewhat more representative of differentiated Solar System objects. An internal Rb-Sr isochron for LEW cannot be obtained because of the very low Rb/Sr in all mineral phases. Sm-Nd measurements are still in progress at the time of writing; preliminary data so far obtained indicate that the Sm-Nd age of LEW is within error of ADOR (4.55±0.04 Ga), measured twelve years ago at UCSD [3].

Pb isotopic compositions were measured in LEW total rock (unwashed) and the high purity mineral separates (washed). Acid washing removed >97% of the total Pb (~6-11 ppm equiv.) in each instance. All of the leachates and the unwashed total rock are isotopically indistinguishable from modern terrestrial Pb. Only the washed Plag, PxLt and PxDk are uncontaminated in this way and sufficiently radiogenic to constrain the age of LEW. The most radiogenic Pb was found in the PxDk ($^{206}Pb/^{204}Pb$ 285.7) which has a Pb model age of 4.555 Ga; the PxDk-Plag pair yield an 'isochron' age of 4.557 Ga. These ages appear to be consistent with the Pb model ages of ~4.552 Ga obtained for ADOR [4] (and amended Pb data in [5]) although inter-laboratory biases etc. render errors difficult to quantify absolutely.

In summary, the Rb-Sr, Sm-Nd and Pb isotopic data as it presently stands do not preclude isotopic consanguinity among the two Angrites ADOR and LEW 86010.

[1] Mason B. (1987) *Antarct. Meteor. Newsl.* 10, 2. [2] Gray C.M. *et al.* (1973) *Icarus* 20, 213-239. [3] Lugmair G.W. and Marti K. (1977) *Earth Planet. Sci. Lett.* 35, 273-284. [4] Chen J.H. and Wasserburg G.J. (1981) *Earth Planet. Sci. Lett.* 52, 1-15. [5] Wasserburg G.J. *et al.* (1977) *Earth Planet. Sci. Lett.* 35, 294-316.

RARE EARTH ELEMENTS AND CALCIUM ISOTOPES IN THE OLDHAMITE OF UNEQUILIBRATED ENSTATITE CHONDRITES; Laura L. Lundberg[1], Ghislaine Crozaz[1], Ernst Zinner[1] and Ahmed El Goresy[2]; (1) McDonnell Center for the Space Sciences, Washington University, St. Louis, MO 63130 USA; (2) Max-Planck-Institut für Kernphysik, 6900 Heidelberg 1, FRG

Our previous *in situ* ion microprobe rare earth element (REE) determinations (Lundberg and Crozaz, 1988) in oldhamite (CaS) from Indarch (EH4)and Jajh deh Kot Lalu (EL6) confirmed that this mineral is the major REE carrier in enstatite chondrites. In these meteorites, if oldhamite is a high temperature condensate (Larimer and Bartholomay, 1979) analogous to the hibonite and perovskite found in the more oxidized carbonaceous chondrites, it also may be a carrier of isotopic anomalies. For this reason, we started a correlated study of REE abundances, Ca isotopic compositions and mineral associations of oldhamite in unequilibrated enstatite chondrites. Data for Qingzhen (EH3) are reported here.

Oldhamite is found: 1) as individual grains sometimes associated with niningerite or intergrown with troilite, 2) in metal-sulfide spherules, and 3) in chondrules, as inclusions in enstatite or associated with troilite between silicate grains (El Goresy *et al.*, 1988). Figure 1 shows typical examples of the four distinct REE patterns obtained in this study. Pattern A is relatively flat (La ~70-90×C1) sometimes with a small positive Yb anomaly. It was observed in oldhamite intergrown or associated with troilite and in an oldhamite between silicate grains in a chondrule. Pattern B is also relatively flat with a more pronounced positive Yb anomaly but the LREE are enriched (~60-100×C1) over the HREE (~40-70×C1). It was found in oldhamite in metal-troilite spherules, in oldhamite associated with troilite and in oldhamite in contact with niningerite. Pattern C is similar to Pattern B but there is also a positive Eu anomaly. However, the overall REE abundances are lower in C (LREE ~30-50×C1, HREE ~10-25×C1) than in B. Pattern C was found only in individual grains of oldhamite. Pattern D, observed in two oldhamite grains from a chondrule, has very large positive Eu and Yb anomalies and otherwise low REE abundances (~2-25×C1). Of nine oldhamites, six have normal Ca isotopic compositions. However, three show substantial depletions at mass 48. Delta ^{48}Ca values of -9.4±1.9‰, -5.9±1.9‰, and -6.1±1.8‰ (2σ errors) were found, respectively, 1) in an oldhamite grain in contact with niningerite, 2) in oldhamite associated with troilite and 3) in oldhamite intergrown with troilite. The first two grains have type C REE patterns. The third grain has a type B REE profile. The Ca isotopic anomalies exhibited by oldhamite grains show that inhomogeneities also existed in the region of the solar nebula where enstatite chondrites formed and that oldhamites have indeed a primitive origin.

El Goresy *et al.* (1988) *Proc. NIPR Symp. Antarct. Meteorites* 1, 65-101; Larimer J.W. and Bartholomay M. (1979) *Geochim. Cosmochim. Acta* 43, 1455-1466; Lundberg L.L. and Crozaz G. (1988) *Meteoritics* 23, 285-286.

Figure 1

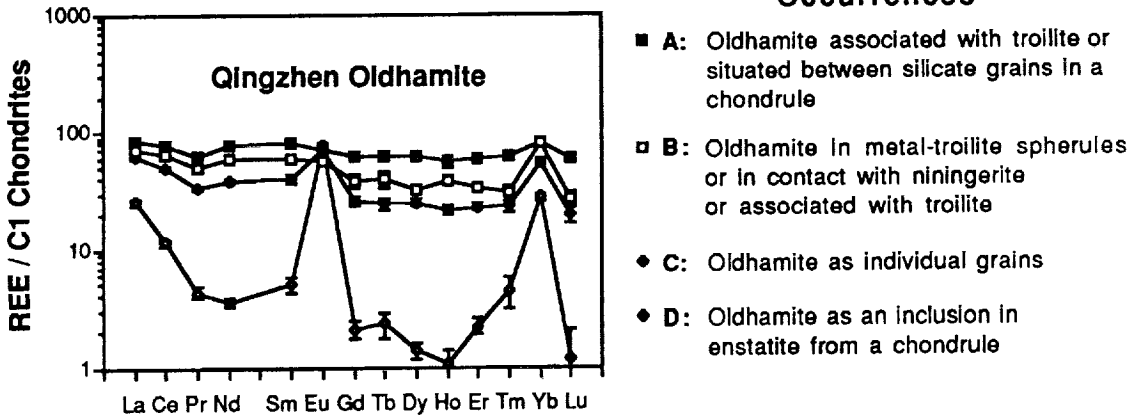

CHRONOLOGY OF CHEMICAL CHANGE IN THE ORGUEIL CI CHONDRITE BASED ON SR ISOTOPE SYSTEMATICS; J.D. Macdougall and G.W. Lugmair, Scripps Institution of Oceanography, La Jolla, USA

It is well known that the CI meteorites contain a substantial water-soluble component, at least partly in well-defined veins. This observation, together with other details of the mineralogy and petrography of these meteorites, have led to the suggestion that one or more periods of aqueous activity occurred on the parent body of the CI meteorites. An important question is the timing of these events. In earlier work (Macdougall et al., 1984) we reported low $^{87}Sr/^{86}Sr$ ratios in carbonate separates from Orgueil, and concluded that at least some carbonates were precipitated from aqueous solutions within approximately 100Ma of meteorite formation. In the interim, we have developed improved documentation methods and more efficient running techniques for Sr isotopic ratio measurements, permitting precise $^{87}Sr/^{86}Sr$ values to be measured on mineralogically characterized samples containing as little as a few ng of Sr. Currently such measurements are being made on separated "dolomite", breunnerite and various sulfate samples from Orgueil. Because these phases contain negligible amounts of Rb, the time of their isolation from the whole meteorite chemical system, which has high Rb/Sr, is accurately determined by their Sr isotopic ratios. The new data confirm that Ca-Mg carbonates contain very primitive Sr and must have crystallized very early, within 50Ma of the formation of the meteorite. Measurements presently in progress are focussing on the question of whether or not breunnerite crystallization occurred slightly later, as is hinted at in our earlier data (Macdougall et al., 1984).

In addition to the work discussed above, we have conducted a series of leaching experiments designed to complement the carbonate and sulfate measurements. These experiments produced surprising results. Two approximately 100 mg fragments of Orgueil were leached sequentially in pure water for 44 hours, 0.5N HCl for approximately an hour and 2N HCl for several hours. Results for each of the two samples were similar. The water leaches contained large amounts of Sr (equivalent to about 2.7 ppm out of a total of approximately 7.8 ppm in the meteorite) with extremely radiogenic isotopic ratios (0.8189 and 0.8123). Although considerable Rb was also found in the water leaches, the measured Rb/Sr is much too low to account for the Sr isotopic ratio over the age of Orgueil; model ages for the leach component are on the order of 7 Ga. This is consistent with our earlier finding that sulfate vein material contains unsupported radiogenic Sr, and provides evidence for very recent chemical mobility of Rb and Sr. The 0.5N HCl leach contained even larger amounts of Sr than the water leach (equivalent to about 4 ppm) but with a less radiogenic isotopic ratio (0.7356) probably in part reflecting dissolution of carbonates. The 0.5N HCl leach contained much less Sr (equivalent to 0.3 ppm) which is also less radiogenic (.7433) than the water leach. Thus the bulk of modern Sr in Orgueil is easily mobilized by water or weakly acidic solutions.

REFERENCE: Macdougall J.D. Lugmair G.W. and Kerridge J.F. (1984) Nature 307, 249-251.

REFRACTORY INCLUSIONS IN THE UNIQUE CHONDRITE ALH85085; G. J. MacPherson, Smithsonian Institution, Washington, D. C., A. M. Davis, University of Chicago, Chicago, IL and J. N. Grossman, U. S. Geological Survey, Reston, VA

The unique carbonaceous chondrite ALH85085 has a high abundance of tiny (<110 μm) Ca-, Al-rich inclusions (CAI), some of which are unusual types rarely seen in any other chondrites; a surprising number contain $CaAl_4O_7$; most are unaltered. We have studied five of these CAI in detail using SEM and ion microprobe techniques.

The most distinctive CAI are microporphyritic spherules containing euhedral hibonite crystals enclosed in glass ± melilite ± $CaAl_4O_7$ ± perovskite ± fassaite ± spinel. In bulk composition these spherules are Al-rich and Si-, Mg-poor relative to coarse-grained CV3 CAI. **F101** (22.5% SiO_2, 41.6% Al_2O_3, 27.7% CaO, 4.8% MgO, 3.2% TiO_2, 1.0% FeO), representative of this class, consists of hibonite, glass, spinel, pyroxene and perovskite. This CAI has no detectable excess ^{26}Mg despite high Al/Mg ratios. Neither **F101** nor any of the other CAI studied here showed evidence for mass fractionation of magnesium ($\Delta^{25}Mg<5‰$). The bulk rare earth element (REE) pattern is fractionated, with heavy (H) REE depleted relative to light (L) REE, positive Tm,Yb and Eu anomalies, and LREE themselves fractionated according to volatility (La,Nd<Pr<Ce,Sm). Zr, Y and Sc are low, ~1xC1; Nb is highly enriched, ~86xC1. Similar patterns were seen in one hibonite and three perovskite grains from Murchison [2]. The REE patterns are similar to those of group II CAI seen in other chondrites and probably formed in a similar way; however, the initial condensation and removal of the ultrarefractory component proceeded to lower temperatures than in the normal group II case, such that not only were highly refractory HREE almost completely removed but also the somewhat less refractory LREE were partially removed. Condensation of the remaining gas also proceeded to lower temperatures than in group II, allowing Eu and Yb to completely condense. **F123** is a 20 μm-diameter spherule consisting of tiny hibonite blades and trace interstitial glass (?) surrounding a perovskite core. It has no excess ^{26}Mg despite high Al/Mg ratios. The REE pattern resembles that in **F101**. **F105** is a representative of a group of irregularly-shaped melilite-rich CAI; it contains melilite ($Åk_{10-20}$), $CaAl_4O_7$, perovskite, spinel and a rim of aluminous diopside. Portions of the melilite and $CaAl_4O_7$ have ^{26}Mg excesses consistent with *in situ* decay of ^{26}Al and $^{26}Al/^{27}Al$ ~$5x10^{-5}$, but some places show no consistent excesses and may have been disturbed after ^{26}Al decay. REE are relatively uniformly enriched in melilite at 2-10xC1 except for Eu (15-20xC1); such a pattern is expected if the REE partitioned between the melilite and another phase. **F102** is a hibonite-rich CAI with minor spinel and a rim of melilite, anorthite (secondary after melilite) and aluminous diopside. ^{26}Mg excesses correlated with $^{27}Al/^{24}Mg$ are consistent with $^{26}Al/^{27}Al$ ~$5x10^{-5}$. Hibonite has a group II REE pattern, with LREE 20-30xC1, HREE depleted down to 2-10xC1 and Tm at 20xC1. **F119** is a 110 μm broken fragment consisting only of fassaite, spinel and forsterite (1.4% CaO); it resembles forsterite-bearing Type B CAI from CV3 chondrites. Fassaite is uniformly enriched in REE and many other refractory elements by ~20xC1. The flat REE pattern and lack of Eu anomaly suggest that fassaite is the only carrier of refractory lithophiles in this CAI.

The two melilite-bearing CAI (**F102, F105**) are the only ones with evidence of extinct ^{26}Al; their presence argues against a model [3] in which ALH85085 formed by impact processes on an evolved parent body, since there is no evidence for ^{26}Al in any differentiated meteorite. Two hibonite spherules (**F101, F123**), like a similar object in Lancé [4], show no evidence for extinct ^{26}Al. In spite of their Al-rich character relative to many CV3 CAI, many CAI in ALH85085 are less refractory in their trace element composition; most appear to have formed originally by condensation after prior condensation and removal of the ultrarefractory components. Their closest analogues in this sense are the group II CAI in CV3 chondrites.

References: [1] J. N. Grossman *et al.* (1988) *EPSL* **91**, 33-54. [2] T. R. Ireland *et al.* (1988) *GCA* **52**, 2827-2840. [3] J. T. Wasson (1988) *LPS XIX*, 1240-1241. [4] A. J. Fahey (1988) Ph.D. Thesis, Washington Univ.

TEMPERATURE CONDITIONS IN THE PREPLANETARY DISK, IMPLICATION FOR METEORITES AND PLANETS; A.B.Makalkin, Schmidt Institute of Physics of the Earth USSR Acad.Sci., B.Gruzinskaya 10, 123810 Moscow, USSR; V.A.Dorofeyeva, Vernadsky Institute of Geochemistry and Analytical Chemistry USSR Acad.Sci., Kosygin str., 117975 Moscow, USSR

Temperature distribution within the preplanetary disk (the solar nebula) depends on the internal heat source - viscous dissipation (usually considered as the only source) and the external heat source. At the disk formation phase (the accretion phase of collapse) the external source is radiation at the shock front at the surface of the core of the protosun and the neighboring part of the disk. This radiation is absorbed and reradiated in infrared in the accretion envelope around the core. A significant part of the disk ($R \lesssim 5$-7 AU) is immersed in the optically thick part of the envelope and is substantially heated by its radiation (Makalkin, 1987). The next phase of disk evolution begins after the end of envelope accretion onto the core and the disk. It is the phase of viscous evolution of the disk. The external source of disk heating during this phase is the solar radiation incident at a small angle upon the surface of the disk. This source is much weaker than the internal source - viscous dissipation (Makalkin, Dorofeyeva, 1989).

The results of our calculations of the temperature at the midplane of the disk are sketched in the Figure. Curve 1 represents the maximum temperatures reached near the end of the disk formation phase. Curves 2, 3 and 4 show the temperatures at the phase of viscous evolution of the disk at 10^5 yr (after the beginning of the phase), $2 \cdot 10^5$ yr and 10^6 yr respectively. Crossed bars denote the temperatures in the cosmochemical model of Lewis (1974). Slope of the curves agrees with Lewis data.

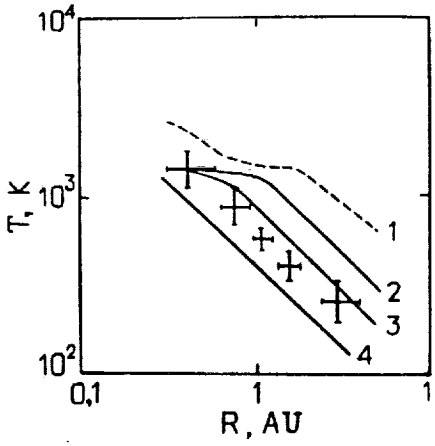

Temperatures of sublimation of magnesian silicates and iron had been probably never reached in the disk at $R > 2$ AU on timescales of 10^5-10^6 yr (though could be reached on much shorter timescales). Refractory material which had experienced condensation could come from the inner zone. During accretion of chondrite parent asteroids at 3 AU temperature would decrease from 500 K to lower than 200 K within 10^6 yr. As the timescale for accretion at any moment is lower than that for cooling of planetesimals, their interiors during the whole accretion period would at least maintain the initial temperature (if other heat sources are excluded) which corresponds to near 10^5 yr period (curve 2), when 1-10 km-sized bodies had formed.

REFERENCES: Lewis J.S.(1974) Science, 186, 440-443.
Makalkin A.B.(1987) Astron.vestnik (Solar Syst.Res.), 21, 324-
Makalkin A.B. and Dorofeyeva V.A.(1989) In Planetary Cosmogony and Earth Science (ed.V.A.Magnitsky), pp.46-88. Moscow: Nauka.

IR/AU RATIO -- INDICATOR OF ORIGIN OF GEOLOGICAL EVENT

Mao Xueying, Chai Chifang, Ma Jianguo, Institute of High Energy Physics, Academia Sinica, (P.O.Box 2732,Beijing,China)

The Ir/Au ratio can be used as a criterion to judge extraterrestrial or terrestrial materials (Palme, 1982; Chai ,1988). Here we summarized the abundance ratios of Ir/Au in the geological boundaries in order to decipher the origin of anomalous iridium at the boundary layers. The data obtained in our laboratory are listed in the Table 1 in the order of geological time.

It is evident that only the Ir/Au ratios of the Cretaceous-Tertiary boundary layers are close to the extraterrstrial value (3.3), no matter where the K/T boundary samples are taken from. The global average Ir/Au ratio is 0.0N. On the contrary , all other geological boundaries have much lower Ir/Au ratios. According to the data available, The ratios are 0.03; 0.06 (Pℭ / ℭ), 0.03 (O/S), 0.03 (D/C), 0.25 (F/F), 0.01-0.22 (P/T) respectively. These results only favour the extraterrstrial origin of anomalous iridium at the K/T boundary, but disfavour other geological boundaries. Although the volcanic ash at Kilauea, Hawaii, contained extremely high Ir aboundace (~600 ppm), its Ir/Au roughly ranges from 0.01 to 0.1 (Crowe, et al. 1987; Olmez, et al. 1986), far from the solar one. Thus, in the view of correlation between Ir and Au, the volcanogenic origin of Ir anomaly at the K/T boundary is not valid.

Using a newly-developed step-by-step chemical dissolution procedure, we detemined the Ir/Au ratios in different mineral fractions i.e. carbonate, Fe-Ni, sulfide, oxide, silicate, and HF-insoluble residue of the Fish clay, Stevns Klint, Denmark. It is interesting that the Ir/Au ratios at the fractions of Fe-Ni and residue are the same as the ratio of the bulk rock (~3), but other fractions have large discrepancy. Our experimental results suggest that Ir at K/T boundary layer may consist of two parts. One is extraterrestrial, while the other is post-depositional enrichment.

Table 1 The Ir/Au ratios in the geological boundaries

Boundary	section	Ir (ppb)	Au (ppb)	Ir/Au
Pℭ/ ℭ	Mei Shu Chen	0.053	1.69	0.03
	Mai Di Ping	0.097	1.67	0.06
O / S	Yi Chang	0.640	21.8	0.03
D / C	Wu Xuan	0.156	5.3	0.03
F / F	Ma An San	0.087	0.35	0.25
P / T	Chang Xing	0.04-0.6	2.7	0.01-0.22
K / T	Contessa(3)*	4.78	1.66	2.88
	DINO(5)*	33.0	9.67	3.41
	Stevns Klint(9)*	37.78	8.74	4.32

* The number in parenthesis means the number of sample analysis.

REFERENCES: Palme,H.,(1982) Geol. Soc. Amer., Spec. Pap., pp. 223-233; Chai,C.F.,(1988) Isotopenpraxis Vol.24 No.7 p 257-277; Crowe, B., et al., (1987) J. Geophysical Research, Vol.92 No.B13, p 13708-13714; Olmez, I., et al.,(1986) J. Geophysical Research, Vol.91 No.B1, p 653-663,

GENETIC RELATIONS BETWEEN HONDRULES AND MATRIX IN HONDRITE SARATOV; A.A.Marakushev, L.B.Granovsky, N.G.Zinovyeva, O.B.Mitreikina; USSR, Moscow, Moscow State University, Geological Department, Petrography chair.

Magmatic nature of hondrite and general scheme of its formation (fig.1) are defined by results of microprobe analysis of its phases, their structural and textural relations. The hondrite was formed in two steps: (A) in depth at high fluidal pressure conditions; (B) at magmatic eruption into parental planet body surface. These steps are established by composition gap in clinopyroxenes, which enteres in (A) normal slow crystallization reactional series Ol-Opx-Cpx and (B) association with volcanic glass (as sceletic crystals). It is liquid immiscibility which caused in magma separation into silicate hondrules and enriched in iron matrix. It manifests itself not only in silicate drops (hondrules) in matrix, but also in metallic drops in hondrules. Olivine crystals grouring at this boundaries is seen both inward and outward, which reflects equilibrium relations between hondric and matrix melts at early stages (A). However, the liquid state of the matrix metallic phase is detected also after final solidification of hondrules, which are partly crushed and cemented with matrix material.

Second type of strictly magmatic differentiation is expressed by separation of hondric melt into two melts: pyroxen-olivinic (1) and olivine-pyroxenic (2). Their genetic relations are exposed in "hondrule in hondrule" structure (fig.2). Hondrules 1 occupies inner position and hondrules 2 outer position in such double hondrules structures. Hondrules 1 and 2 have the identical composition of the same name minerals, which determines the equilibrium between them at deep-seated crystallization (A). However, this equilibrium was broken down at the stage (B), as residual glasses compositions (1 and 2 types) are substantially different.

Fig.1. The "hondrule in hondrule" structure. 1-inner olivinic hondrule, 2-outer olivine-pyroxenic hondrule.

Fig.2. Petrochemical diagram of chondrite Saratov. 1-average composition of the chondrite(L); 2-compositionof the silicate matrix(M1); 3-composition of the metallic matrix(M2); 4-olivine hondrules(1 type); 5-olivine-pyroxenic hondrules(2 type).

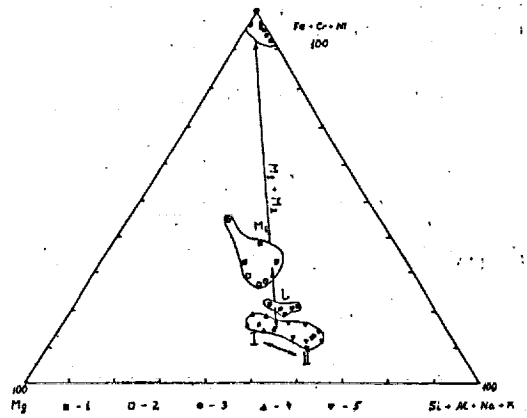

XENON IN CHONDRITIC METAL; K. Marti[1], J. S. Kim[1], B. Lavielle[1,2], P. Pellas[3] and C. Perron[3], [1]Chem. Dept., B-017, Univ. of Calif., San Diego, La Jolla, Calif., 92093-0317, [2]CENBG, 33170 Gradignan, France, [3]Museum National d' Histoire Naturelle Mineralogie, 61, Rue de Buffon, Paris 5e, France, 75005.

We have reported evidence for a new xenon component (FVM-Xe) in metal grains of the H4 chondrites Forest Vale and Ste. Marguerite (1). We extend this study to other H-chondrites. A search for the carrier(s) of the FVM-Xe is carried out, and possible relationships to other solar system reservoirs are evaluated.

Xenon isotopic systematics in the pyrolysis steps above 600° are similar for the investigated two H4 chondrites, but strikingly different for the H6 chondrite Estacado. The ^{132}Xe concentrations measured in the latter are very low ($\sim 4 \times 10^{-14} cm^3 STP\ g^{-1}$) in the 800-1200°C steps and no evidence for FVM-Xe is observed. About 70% of the Estacado Xe ($\sim 90 \times 10^{-14} cm^3 STP\ g^{-1}$) is released in the melt step and reveals an isotopic signature which is close to FVC-Xe. A fission Xe component due to ^{244}Pu is observed in H4 metal, but appears to be lacking in Estacado. In Estacado metal, a radiogenic ^{40}Ar component ($1.0 \times 10^{-7} cm^3 STP\ g^{-1}$) is observed in the melt step but, contrary to the ^{40}Ar release pattern in H4 metal, very little ^{40}Ar is observed in the 800-1200° steps. Spallation ^{38}Ar, which is produced in the metal phase, is observed in all temperature steps.

Metal grains in FV (and in other H4 chondrites as well) are of very irregular shapes. Most of them are found to contain inclusions of what we called type I (2). These inclusions are a few μm in size, and the largest ones are 20-30 μm. The most abundant mineral is low-Ca pyroxene, with 17.5% ferrosilite. The metal grains bearing inclusions are more abundant in H3 than in H4; they are rare in H5. A second type of inclusion is present only in some of the metal grains. These are very small (< 1 μm), very numerous, and apparently of a rounded shape. Because of their small size, chemical analyses are difficult.

We discuss now possible relationships to solar system Xe components. First, FVM may represent a xenon reservoir which already contains a ^{244}Pu-derived fission component. Second, there is the possibility that ^{248}Cm fission fragments recoiled into metal grains or precursors thereof during the presolar history of the metal. Third, we may consider the possible presence of a neutron-induced fission component due to ^{235}U. In this case, the inferred trapped component is consistent with solar-type Xe (3). Finally, we consider the possibility that FVM-Xe represents a distinct solar system or presolar component that was incorporated at an early stage in the history of metal grains. Indications of a grain-size dependence, as well as the release characteristics, favor a near-surface location of FVM-Xe. Further studies on grain-size fractions of Dhajala (H3) metal are in progress.

References: (1) Marti K., Kim J. S., Lavielle B., Pellas P. and Perron C. (1989) Lunar and Planet. Science XX, Lunar and Planet. Inst., Houston, 618-619, (2) Perron C., Bourot-Denise M., Pellas P., Marti K., Kim J. S. and Lavielle B. (1989) Lunar and Planet. Science XX, Lunar and Planet. Inst., Houston, 838-839, (3) Marti K., Kim J. S., Lavielle B., Pellas P. and Perron C. (1989) Z. Naturforschg. (in press).

GRANOBLASTIC LUNAR "DUNITES" REVISITED; Ursula B. Marvin, Beth B. Holmberg, Harvard-Smithsonian Center for Astrophysics, Cambridge, MA 02138, and Marilyn M. Lindstrom, NASA Johnson Space Center, Houston, TX 77058.

Clasts consisting almost entirely of polygonal olivine grains are rare constituents of lunar highland samples. We have analyzed three such clasts in Apollo 15 breccias 15295 and 15445 and have concluded that they are rock fragments from a deep-seated source in the lunar crust.

The clasts are roughly oval with long axes ranging from 1.25 to 4 mm. Within the clasts, the individual olivine grains vary in size from about 30 to 110 μm and occur in a wide array of optical orientations. Electron microprobe analyses show strong similarities and subtle differences between the clasts. All of them consist of 99% olivine that is strikingly uniform in composition. The olivine of Clast A in thin section 15295,40 runs Fo_{88-89} with 0.07 wt.% CaO; that of Clast B in 15445,147 is Fo_{88-89} with 0.13 wt.% CaO; and that of Clast C in 15445,135 is Fo_{87-88} with 0.15 wt.% CaO. In all clasts, some of the minute interstices between the olivine grains contain bytownite ($An_{73-83}Ab_{16-22}Or_{<0-5}$). Clast A contains several small (15-25 μm) clots consisting of augites ($En_{46-53}Fs_{5-6}Wo_{41-48}$) and thin, curving crystallites of chromian spinel $(Fe_{0.63}Mg_{0.37})(Cr_{0.83}Al_{0.15}Ti_{0.02})_2O_4$. Clast B, in contrast, contains neither augite nor chromian spinel, but has sparse grains, <12 μm across, of low-Ca pyroxenes ($En_{77-83}Fs_{12-16}Wo_{2-7}$). We ascribe the granoblastic olivine textures to subsolidus annealing, which clearly took place before aggregation of the clasts into the breccia matrixes. The latter contain an abundance of olivine fragments that are richer in FeO (Fo_{70-76}) and show no trace of polygonization. We assume that the disordered patches of pyroxene and chromian spinel record a post-metamorphic shock event that affected Clast A, in section 15295,40, but not Clasts B or C in sections 15445,147 and ,135.

Additional phases in all of the clasts include minute (2-10 μm) grains of FeS and metals. Most of the metals are angular grains of $Fe_{47-48}Ni_{49-50}Co_{2.8-3.0}$. One compound grain, 8 μm across, in Clast A, consists of Ni-Co-rich metal embedded in FeS which, in turn, includes an angular patch of a Ti-rich phase (probably ilmenite) that is too small to analyze quantitatively. A lustrous 15-μm metal, isolated within the olivine of Clast B, consists of several irregular grains of brass, containing about 50 wt.% each of copper and zinc plus 1-2 wt.% Fe. The location and shapes of the grains and composition of the metal argue against the brass being a contaminant. Our samples contain no detectable tin, unlike the small grains of lunar brass in which Gay *et al.*, (1970), reported 0.3-5% Sn. The origin of lunar brass remains unexplained.

Granoblastic olivine clasts, including Clast B in 15445,147, have been reported previously (e.g. Ryder and Bower, 1977; Steele *et al.*, 1977), but no descriptions or analyses of their accessory minerals have been published. The possible origin of these clasts as deep-seated "dunites" was dismissed by Wilshire and Jackson (1972) who regarded them, along with granoblastic "anorthosites" and "pyroxenites," simply as recrystallized mineral grains. We advocate a metamorphic rather than a cumulate origin for our small "dunite" clasts, which may, indeed, represent single grains of olivine. However, their Mg-rich compositions and the high Ni-Co content of their Fe metals groups them with dunite 72415 (Albee *et al.*, 1974) and certain spinel troctolites (e.g. Prinz *et al.*, 1973) that are universally regarded as deep crustal rocks. The extreme rarity of granoblastic olivine clasts also suggests a deep source; if this texture were easily formed in olivines by shock or by annealing in hot ejecta blankets, it should be observed much more commonly than it is in the lunar samples. For these reasons, we propose to add granoblastic olivine clasts to the small number of lithologies now generally accepted as originating in a deep layer of the lunar crust.

References: Albee, A.L., Chodos, A.A., Dymek, R.F., Gancarz, A.J., Goldman, D.S., Papanastassiou, D.A., Wasserburg, G.J. (1974) *Lunar Science V*:3-5. Gay, P., Bancroft, G.M., Brown, M.G.,(1970), Proc. Lunar Sci. Conf. **1**:481-187. Prinz, M, Dowty, E, Keil, K, Bunch, T.E.,(1973), *Science* **179**:74-76. Ryder, G. and Bower, J.F. (1977), *Proc. Lunar Sci. Conf.* 8th **2**:1895-1923. Steele, I.M, Irving, A.J., Smith, J.V.,(1977), Proc. Lunar Sci. Conf. 8th:**1**:1925-1941. Wilshire, H G and Jackson, E.D. (1972), *EPSL* **16**:396-400.

STRUCTURAL FEATURES OF GIANT ASTROBLEMES. V.L. Masaitis, All-Union Scientific Research Institute, Leningrad 199026, USSR.

Little attention has been given to individual structural elements of impact craters and their combinations that originated during successive phases of the formation of very large craters. Deformation of target rocks (and fractures) could nearly transect the complete continental crust. Three well preserved astroblemes - Popigai (100 km diameter), Puchezh-Katunki (80 km), and Kara (65 km) were studied in detail. They formed in subaerial (Popigai) and subaqueous (Kara and Puchezh-Katunki) settings in areas of folded Paleozoic and Mesozoic sediments lying horizontally on the crystalline basement. The Popigai crater is thought to have been formed by a projectile similar to ordinary chondrites, whereas Kara and Puchezh-Katunki may have been formed by cometary projectiles. As a result of the giant impacts complex multi-order structural forms were created by processes that are not well understood.

During the compression phase a concentric structural zonation (vaporization, melting, brecciation) forms in the target rocks. The zonation is governed by the form of the shock wave. The outer zones, which contain fractures, overthrusts, folds, etc., are only party preserved. The excavation is accompanied by the formation of a structural ring uplift, zones of radial plastic flowage, systems of radial trenches at the bottom of the transient crater, and deep fissures filled with rock fragments and impact melts. The radial trenches create the polygonal outlines of some astroblemes (Popigai, Kara, Manicouagan). In the case of a layered target structure the excavation is more intense in the rocks with lower densities. This may lead to two cavities of differing diameter. In the early phases the rebounding of the transient cavity is responsible for the growth of the central uplift and rupture trenches. The central uplift may collapse to create breccias that are sometimes cemented by impact melts. Target rocks beneath the crater in areas of a steep geothermal gradient may become plastic or melt as a result of additional shock heating. Subsequently intrusive bodies (Sudbury) or a dome with tilted walls (Vredefort) may form.

The craters are then filled by ballistically ejected materials. This leads to accumulative structures, primarily of sheet or lenticular form. The inner structure of the rock mass formed by breccias and impactites is determined by the proportions of disrupted and melted rocks and the degree of homogenization of the material. Different radial elements of the inner structure caused by ejecta which originated in the crater filling stage were observed at Popigai, Puchezh-Katunki, and Kara. Early crater modifications may be accompanied by rock-slides from the crater rim. The cooling and crystallization of the impact melt may lead to a vertical zonation. The final stages of early modification may consist of the uplift of the apparent crater bottom and formation of ring-concentric and radial fissures (which are filled by rock debris, such as clastic dikes in suevites at Kara).

The analysis of peculiarities of the inner crater structure permits the detailed reconstruction of the characteristic formation mechanism of giant craters. The primary structures may be considerably altered during successive cratering phases. The investigation of these giant craters and their characteristic features are important for remote sensing studies of impact craters on other planets.

XENON ISOTOPE PRODUCTION CROSS-SECTIONS FROM BA-TARGETS BY PROTONS IN THE 12 TO 45 MeV ENERGY RANGE.

K.J.Mathew(1),M.N.Rao(1),R.Michel(2),and K.Precsher(3);
(1)Physical Research Laboratory,Ahemedabad,India.(2)ZfS, University of Hannover , F.R.G. (3) Abteilung Nuklearchemie, University of Cologne ,F.R.G.(*).

For the study of solar cosmic ray(SCR)proton effects in extra-terrestrial samples ,Xe isotopes produced from Ba-targets by low energy protons may provide a new window . So far no experimental cross-sections are available for Xe isotopes production from Ba targets by low energy protons ,except for an isolated measurement by Kaiser(1977) at 38 MeV.In the present study thin target excitation functions for Ba-Xe system for proton energies from 12 to 45 MeV were determined using stacked foil technique at JULIC cyclotron of IKP/KFA Juelich(FRG).
Ba glass discs were used as targets for irradiation.To minimize the uncertainities of the proton energy due to energy straggling three different stacks were used to degrade the proton energy from 44 to 34 MeV, from 34 to 20 MeV and 22 to 12 MeV.After the irradiated targets have sufficiently cooled the stable Xe isotopes were measured at PRL and University of Cologne using standard massspec.procedures.
For different Xe isotopes the production cross- sections as a function of energy from 12 to 45 MeV are determined. There is good agreement between PRL and Cologne measurements. The isotopes 129,131 and 132 show relatively increased production (sevaral millibarns)at low energies compared to other Xe isotopes 126,128 and 130.In contrast Kaiser(1977) found very low values for Xe -129 and Xe-132 production cross-sections from Ba at 38 MeV proton energy. Using the hybrid model calculations following the Alice Livermore 87 code (Michel et al .1982) we estimate an average SCR production rate for Xe-132 of 8×10^{-15} ccSTP per ppm Ba per my. for lunar soils for J(E>10 MeV)= 100 $p.cm^{-2}.\ sec^{-1}$. at about 0 to 0.5 $g.cm^{-2}$ depth . Further we have determined the isotopic excesses of Xe-129 and Xe-132 in lunar soils 14148 and 69921 (feldspar fractions) after accounting for the GCR production of these isotopes .The Xe-132 SCR production rates obtained in this study are used to estimate the surface exposure ages of these soil grains in lunar regolith .

Kaiser W.A.(1977) Phil.Trans. Royal Soc.London A,285, 337 .
Michel R.,Brinkmann G. and Stueck R. (1982) E.P.S.L. 59, 33; erratum 64(1983)1974.

C-3

VOLATILE ELEMENT GEOCHEMISTRY OF TARGET ROCKS AND IMPACT GLASSES AT THE ZHAMANSHIN CRATER (USSR) AND OTHER IMPACT CRATERS.
Dietmar Matthies[1], Alfred Sauerer[1], and Christian Koeberl[2,3]. [1]*Mineralogisch-Petrographisches Institut, University of Munich, Theresienstrasse 41, D-8000 Munich 2, West Germany.* [2]*Institute of Geochemistry, University of Vienna, A-1010 Vienna, Austria.* [3]*Lunar and Planetary Institute, 3303 NASA Road One, Houston, TX 77058, USA.*

Volatile elements are of key importance in the study of impact craters, impact materials, and physico-chemical processes during large-scale meteorite impacts. Tektites and impact glasses are depleted in volatile elements (and water) compared to their terrestrial source rocks (which have commonly been sediments). Muong Nong type tektites are less depleted in volatile elements than normal splash-form tektites. They also contain slightly more water than splash form tektites [1]. The enrichment factor of volatile elements (abundances in Muong Nong type tektites/splash form tektites) varies between about 2 and 40 for different elements. The halogens do not show consistent behavior. Cl and Br show much higher enrichments than F. Muong Nong type tektites are of great importance in understanding certain physico-chemical processes which take place during the impact. Impact glasses from the Zhamanshin impact structure (most notably the Si-rich zhamanshinites) are very similar in appearance, structure, and chemistry to Muong Nong type tektites. Because of the proven impact origin of the Zhamanshin crater and of the glasses and breccias that are found in the structure, the study of the impactites and their related target rocks may provide an interesting model case (although of somewhat smaller size) for the processes during the formation of tektites.

The Zhamanshin impact structure is situated in a semi-arid region in Khazakstan (USSR) and has a rather complex geological setting. The diameter of the crater was originally thought to be about 6.5 km, but recent remote sensing studies have shown that it may be as large as 13 km [2]. The bedrocks comprise Paleozoic metamorphic crystalline rocks, including Upper Paleozoic volcanic-sedimentary series, and some ultrabasic dikes. The impactites found at the crater include Si-rich zhamanshinites (which are very similar to Muong Nong type tektites), Si-poor zhamanshinites (which often show andesitic composition), blue zhamanshinites (which are closely related to Si-rich zhamanshinites), and irghizites [3,4]. Irghizites are small, Si-rich, of irregular (wire, rope, or droplet) shape, and are in some respects similar to tektites. The Si-rich zhamanshinites have a layered structure and show clear signs of of glass flow. Some samples contain more or less intact relict pieces of sedimentary precursor rocks embedded in normal glass. In order to better constrain the behavior of some volatile elements in the impact process, and because of the scarcity of data available in the literature, we analyzed the F and B content of a large number of different target rocks, Si-rich zhamanshinites, Si-poor zhamanshinites, and irghizites. Irghizites have the lowest F and B content of all impactites, about 100 and 30 ppm, respectively. Si-rich zhamanshinites show a range of about 70-290 ppm F and a B content of about 55 ppm, while Si-poor zhamanshinites have higher contents of both elements (190-280 ppm F, 70-150 ppm B). The target rocks cover the whole range: 130-770 ppm F (one marble sample contains 66 ppm F) and 7-130 ppm B). Mixing models show that the chemistry of the impactites can be successfully reproduced by mixtures of different country rocks, most notably Paleogene clays, shales, andesites, and quartzites, with partial loss of volatiles during the impact. Data from other impact craters give similar results.

References: [1] Koeberl C. and Beran A. (1988) Proc. 18th LPSC, 403-408. [2] Garvin J.B. et al. (1989) subm. to Proc. Conf. Global Catastrophes in the Geological Record. [3] Koeberl C and Fredriksson K. (1986) EPSL 78, 80-88. [4] Koeberl C. (1988) Geochim.Cosmochim.Acta 52, 779-784.

HIGH RESOLUTION ELECTRON MICROSCOPE STUDIES OF "CAP-PRUDHOMME" UNMELTED MICROMETEORITES. PRELIMINARY COMPARISONS WITH STRATOSPHERIC IDPs AND PRIMITIVE METEORITES. M.Maurette, Centre de Spectrométrie Nucléaire et de Spectrométrie de Masse, Batiment 108, 91405 Campus-Orsay, France. J.P.Bradley, McCrone Associate Inc., 850 Pasquinelli Drive, Westmont, IL 60559. C.Jouret, Laboratoire d'Optique Electronique, BP 4347, 31055 Toulouse, France. P.Veyssieres, Laboratoire d'Etude des Microstructures, ONERA, BP 72, 92322 Chatillon-sous-Bagneux.

A large number of unmelted chondritic micrometeorites have been extracted from 100 tons of artificially melted blue ice, near Cap-Prudhomme in Antarctica (1). We present a preliminary comparison of such "Cap-Prudhomme" micrometeorites (CPMMs) with both stratospheric IDPs and primitive meteorites (Orgueil; Allais; Murchinson).

Both ultramicrotomed sections (on thin membranes), and micron-size crushed grains directly stuck to gold and/or platinum electron microscope grids without membrane, have been investigated with several high voltage analytical electron microscopes. The following studies have been launched: high resolution imaging up to magnification of 500,000X (400 KV analytical electron microscope at ONERA); measurements of C/O atomic ratios in crushed grains (scale of 0.2μm^3), with the electron spectrometer of the 1 MV microscope at Toulouse; point-count chemical analyses (scale of $10^{-3}\mu m^3$) with the 200 KV microscope at McCrone Associate; in-situ pyrolisis up to 1000°C with the reaction chamber of a 3 MV microscope at Toulouse.

Comparison with stratospheric IDPs previously analyzed at McCrone Associate (2,3), and primitive meteorites allow the following inferences: (1) The fine grained "amorphous" matrix of about 20% of the ~200μm-size CPMMs show C/O ratios higher than those measured in the corresponding material of primitive meteorites; (2) The distribution of the C-Rich phases is rather homogeneous in both the CPMMs and the primitive meteorites; (3) Cluster analysis of Si-Mg-Fe ternary diagrams indicate that the C-rich CPMMs are different from the major classes of IDPs, as they show a much tighter clustering of data points and higher Fe contents; (4) Besides the few mineral species usually quoted in the litterature the CPMMs contains a striking variety of nanophase minerals, yielding spectacular electron diffraction patterns, which have not been observed yet in primitive meteorites; (5) These nanophases seem to be concentrated in the "amorphous" components found in all objects, that keeps a complex structure up to the highest magnifications.

REFERENCES: (1) Maurette, M., Pourchet, M., Bonny, Ph., de Angelis, M., Siry, P. (1989) Lunar Planet.Sci. XX, 644-645; (2) Bradley, J.P. (1988) Geochim.Cosmochim.Acta 52, 889-900; (3) Bradley, J.P., Germany, M.S., Brownlee, D.E. (1988) Lunar Planet.Sci. XIX, 126-127.

INTERNAL OXYGEN ISOTOPE VARIATIONS IN TWO UNEQUILIBRATED CHONDRITES; T.K. Mayeda,[1] R.N. Clayton[1,2,3] and A. Sodonis[1]. [1]Enrico Fermi Institute, [2]Department of Chemistry, [3]Department of the Geophysical Sciences, all at the University of Chicago, Chicago, IL 60637, USA.

Deakin 001 is a weathered unequilibrated chondrite found in the Nullarbor Plain of Australia. It is exceptional in the high iron content of its olivine and pyroxene (Fa 28.1, Fs 21.8) (Bevan and Binns, 1989). Its whole-rock oxygen isotopic composition is unique ($\delta^{18}O = 8.3$, $\delta^{17}O = 5.2$). The $\Delta^{17}O$ value of 0.9 is intermediate between those of equilibrated H chondrites (0.7) and L chondrites (1.1), but it is fractionated by about 4‰ in $\delta^{18}O$ relative to ordinary chondrites. The meteorite was separated into seven density fractions in order to search for unusual components. Their oxygen isotopic compositions fall along a mass-dependent fractionation line covering a range of 7.5 in $\delta^{18}O$ (Fig. 1). There is a monotonic relation between density and $\delta^{18}O$, the highest density fractions being the lowest in $\delta^{18}O$. The range of compositions does not appear to be a terrestrial weathering effect since neither end of the array approaches the terrestrial line. If the ^{18}O fractionation of 5.5‰ between heaviest and lightest samples in Deakin 001 is interpreted as an equilibrium fractionation between oligoclase and olivine, the implied equilibration temperature is about 400°C (Chiba et al., 1989).

Since a similar analysis of separated density fractions of unequilibrated chondrites had not been done, we analyzed six density fractions of the Mezö-Madaras (L3) chondrite, covering the same density range (Fig. 2). The data points fall exactly on the ^{16}O-mixing trend previously observed for separated chondrules from UOC (Clayton et al., 1983), except that the lowest-density fraction (<2.85 g cm^{-3}) lies about 2‰ farther up the line than any whole chondrule. This fraction, consisting primarily of plagioclase and glass, demonstrates for the first time a mineralogical control of oxygen isotope mixing in the UOC. The implication is that the more easily exchanged phases move *up* the mixing line, in conflict with previous conclusions, based on chondrule size, that exchange causes compositions to move *down* the line.

Deakin 001 and Mezö-Madaras clearly have different internal variations of oxygen isotopic composition. Deakin 001 is an apparently unique meteorite, and it is important to determine in future whether its pattern is intrinsic to the meteorite or is due to some kind of terrestrial process.

References: A.W. Bevan and R.A. Binns (1989) Meteoritics (in press); H. Chiba et al. (1989) (submitted to G.C.A.); R.N. Clayton et al. (1983) in "Chondrules and their Origins".

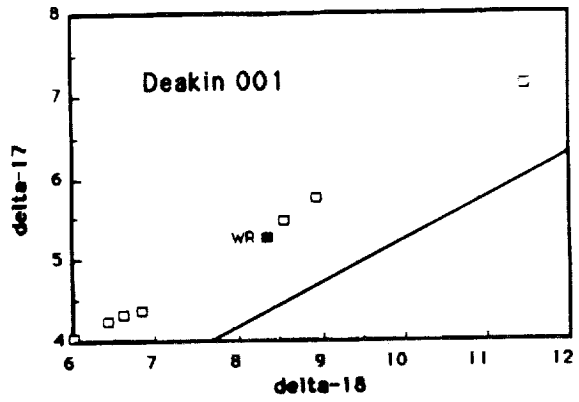

Fig. 1. Isotopic compositions of density fractions and whole-rock from Deakin 001. Terrestrial fractionation line shown for reference.

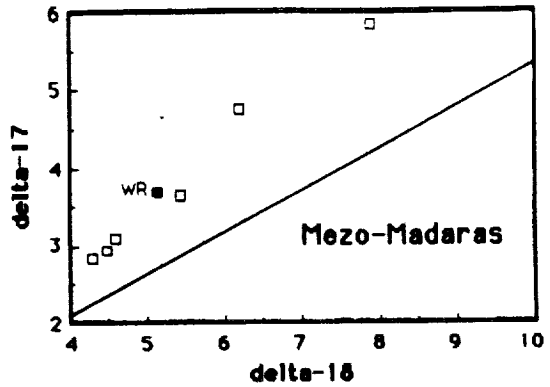

Fig. 2 Isotopic compositions of density fractions and whole-rock from Mezö-Madaras (L3). Terrestrial fractionation line shown for reference.

COSMOGENIC HELIUM AND VOLATILE-RICH MANTLE FLUID IN SIERRA LEONE DIAMONDS; P. McConville and J. H. Reynolds, Department of Physics, University of California, Berkeley, CA 94720

Clear fragments of a large alluvial diamond from Sierra Leone were pulverized, harshly washed in acids, and separated into two aliquots for noble gas analysis. The replicate analyses agreed well, showing 35×10^{-12} ccSTP/g of ^{3}He, a high value, and a $^{3}He/^{4}He$ ratio 246 times the atmospheric value, strongly supporting the cosmogenic hypothesis of Lal *et al.*,[a] although a shallow burial history of 35 m.y. duration is required. The concentrations of ^{36}Ar, ^{84}Kr, and ^{132}Xe were high, suggesting shock implantation of atmospheric noble gases during the crushing. To test this hypothesis, another Sierra Leone alluvial stone was separated into "uncrushed", "crushed in air", and "crushed in pure N_2" aliquots. As expected, the sample crushed in air contained more trapped noble gases. Unexpectedly the second stone belongs to a distinct population of diamonds (mostly cubic diamonds from Zaire at present) containing much radiogenic $^{40*}Ar$. We suspect that such stones are those found to be rich in submicrometer inclusions[b] and in parentless $^{40*}Ar$.[c] They (see Table for noble gas signatures) appear to sample a volatile-rich fluid in the upper mantle as do MORB glasses and the CO_2-rich well gas[d] from Harding County, New Mexico.

Table. Sampling (?) of upper mantle, volatile-bearing fluids

Sample	$^{3}He/^{4}He$	$^{129}Xe/^{131}Xe$	$^{136}Xe/^{132}Xe$	$^{40*}Ar/^{4}He$
	Normalized to Atmospheric Values			
Average of 5 to 6 $^{40*}Ar$-rich Zaire cubic diamonds[e]	4.6 (σ=2.2)	1.09 (σ=0.05)	1.08 (σ=0.026)	1.6 (σ=0.6)
$^{40*}Ar$-rich milky white, cloudy diamond, Brazil (Sample BCD)[f]	<10.1	1.14±0.09	1.29±0.09	1.2±0.35
$^{40*}Ar$-rich sample L#6, this work	10.8±0.2	1.07±0.025	1.15±0.05	1.6±0.2
CO_2 well gas[g]	3.1±0.3	1.084±0.003	1.102±0.0025	2.0±0.6
MORB glass, compiled values[d,h]	8.7	1.02-1.16	1.034-1.171	0.08-0.33 (0.65-2.7)[i]

[a]Lal D., Nishiizumi K., Klein J., Middleton R., and Craig H. (1987) Nature, 328, 139. [b]Navon O., Hutcheon I. D., Rossman G. R., and Wasserburg, G. J. (1988) Nature, 335, 784. [c]Ozima M., Zashu S., Takigami Y., and Turner G. (1989) Nature, 337, 226; Turner G. and Burgess R. (1989) Lunar and Planet. Sci. XX, 1140. [d]Staudacher T. (1987) Nature, 325, 605. [e]Ozima M., Zashu S., Mattey D. P., and Pillinger C. T. (1985) Geochem. J., 19, 127; Ozima M. and Zashu S. (1988) Geochim. Cosmochim. Acta, 52, 19. [f]Honda M., Reynolds J. H., Roedder E., and Epstein S. (1987) J. Geophys. Res., 92, 12507. [g]Phinney D., Tennyson J., and Frick U. (1978) J. Geophys. Res., 83, 2313. [h]Tolstikhin I. (in press) Geochim. Cosmochim. Acta. [i]Corrected for solubility fractionation, see Lux G. (1987) Geochim. Cosmochim. Acta, 51, 1549.

MINERAL/MELT PARTITIONING AND THE EARLY THERMAL HISTORY OF THE EARTH; Elisabeth A. McFarlane and Michael J. Drake, Lunar and Planetary Laboratory, University of Arizona, Tucson, AZ 85721, Tibor Gasparik, Department of Earth and Space Sciences, SUNY Stony Brook, NY 11794-2100.

Introduction: Drake [1] has reviewed the question of whether or not the Earth was substantially molten immediately following accretion. In particular, Agee and Walker [2] have determined experimentally that olivine becomes neutrally buoyant in a melt representative of upper mantle composition at about 80 kbars. This observation has led them to propose that the high Mg/Si ratio in the upper mantle results from mixing into the upper mantle of up to 30% olivine after solidification of a terrestrial magma ocean. This proposal may be tested against olivine/melt partition coefficients for elements present in the upper mantle in chondritic ratios [1]. If the elements in a pair have sufficiently different partition coefficient values, their chondritic ratios may be used to limit possible olivine addition into the upper mantle. This contribution focuses on the partitioning of Ni, Co, Sc, and La between olivine and natural basaltic melt at 1800°C and 75 kbars.

Procedures and Results: Aliquots of ground KLB-1 (~100 mg) were doped with 1-2 wt. % each of Ni, Co, and Sc, loaded into graphite capsules, placed inside a lanthanum chromite sleeve (which serves as the furnace) and into a standard MgO octagon pressure medium. The entire assembly was inserted into a uniaxial-split sphere cubic anvil pressure apparatus (USSA-2000). Charges were compressed to 75 kbars and heated to 1800°C for approximately one hour. Charges were quenched by turning off power to the furnace. During the experiments, La and Cr from the furnace contaminated the charges. Successful run products typically consist of a subsolidus assemblage of olivine, orthopyroxene, clinopyroxene, spinel, and probably garnet at the cold end, and silicate melt containing quench crystals of olivine at the hot end. Analysis was by electron microprobe using standard techniques. Homogeneity of phase compositions in the same region of the charge may indicate an approach to local equilibrium. Olivine/melt partition coefficients (D) at 75 kbars and 1800°C, rounded to one significant figure are D(Ni) = 2, D(Co) = 1, D(Sc) = 0.1, and D(La) < 0.007.

Conclusions: The low value of D(Sc) indicates that chondritic Sc/REE ratios do not constrain olivine addition to the upper mantle, contrary to the conclusions of [1]. The Ni/Co ratio, however, is an indicator of olivine accumulation, and is 20-25% higher than its initial value for a 30% addition of olivine to the upper mantle. The implication of these experiments and those of Kato *et al.* [3,4,5] is that the Earth did not undergo extensive fractionation during and immediately following accretion. One possibility is that the Earth did not become substantially molten. If so, the accretional process must have delivered gravitational potential energy more slowly than current theory predicts, and an origin of the Moon in a giant impact would be unlikely. Alternatively, if the Earth was indeed substantially molten, then it is possible that minerals were entrained in magma and were unable to segregate [6]. In either case, the high Mg/Si ratio in the Earth relative to most classes of chondrites would be intrinsic to the Earth, implying that the accretional process did not mix material between 1 AU and 2-4 AU where most chondritic meteorites are presumed to originate.

References: [1] Drake, M.J. (1989) *Zeitschrift für Naturforschung* (submitted); this volume. [2] Agee, C.B. and Walker D. (1988) *Earth. Planet. Sci. Lett.* **90**, 144-156. [3] Kato, T., Irifune, T., and Ringwood, A.E. (1987) *Geophys. Res. Lett.* **14**, 546-549. [4] Kato, T., Ringwood, A.E., and Irifune, T. (1988a) *Earth. Planet. Sci. Lett.* **89**, 123-145. [5] Kato, T., Ringwood, A.E., and Irifune, T. (1988b) *Earth. Planet. Sci. Lett.* **90**, 65-68. [6] Tonks, W.B. and Melosh, H.J. (1988) *Lunar Planet. Sci. XX*, 1124-1125.

COOLING HISTORY OF ANGRITE LEW 86010. G. McKay (SN4, NASA-JSC, Houston, TX 77058, USA), M. Miyamoto (Dept. of Pure and Applied Sci., Univ. of Tokyo, Komaba, Tokyo 153), and H. Takeda, Mineralogical Inst., Faculty of Sci. Univ. of Tokyo, Hongo, Tokyo 113, Japan)

Antarctic angrite LEW 86010 has many chemical and mineralogical characteristics which suggest it is closely related to Angra dos Reis (ADOR) [e.g.,1-5]. However, despite their similarities, these meteorites have had very different thermal histories. Olivines and pyroxenes in ADOR are nearly homogeneous [6], suggesting very slow cooling or extensive subsolidus equilibration. In contrast, LEW 86010 pyroxenes are extensively zoned in both major and trace elements [2-4]. On the other hand, olivines in LEW 86010 are nearly homogeneous, suggesting that cooling of this sample was slow enough to homogenize olivines, but too fast to homogenize pyroxenes.

The presence of exsolution lamellae of kirschsteinite in LEW 86010 olivines [1-5] and associated diffusion gradients at the host-lamellae interfaces [2] suggests it may be possible to quantify the cooling rate of this sample. The kirschsteinite lamellae range up to 20 μm in width, while the spacings between them are typically a few hundred μm. Slight but distinct gradients in Fe, Mg, and Ca are present in both olivine and kirschsteinite adjacent to the host-lamellae interfaces and were undoubtedly formed by diffusion during exsolution [2]. Microprobe profiles illustrating typical gradients across two such lamellae are shown in Fig. 1. We have studied Ca gradients in the host olivine to estimate cooling rates and burial depths for LEW 86010. The method is similar to that in our previous studies [7,8]. We assume that the initial profile is a step function (i.e., olivine Ca content is locally homogeneous at onset of lamellae formation). As time passes, Ca ions move from olivine into to the growing kirschsteinite lamellae, and therefore Ca zoning is produced in olivine. We use the diffusion coefficient of Ca in olivine parallel to the *c* direction [9], because the lamellae are parallel to (001) [3]. We estimate an initial exsolution temperature of 1000°C based on the chemical compositions of kirschsteinite and olivine [2,3] and determinations of the solvus by [10]. A Cooling rate of 1.5°C/year gives the best fit for the observed CaO zoning profile (Fig. 2). This cooling rate corresponds to a burial depth of about 60m under solid rock (thermal diffusivity = 0.004 cm^2/s), or a few meters under regolith material. At this cooling rate, any primary Fe/Mg zoning in olivine will be homogenized, but zoning in pyroxene will not be, in agreement with observation [2,3].

References: [1] Mason (1987) *Antarctic Meteorite Newsletter* 10, no. 2. [2] McKay *et al.* (1988) *Lunar and Planetary Science XIX*, 762. [3] Prinz *et al.* (1988) *Lunar and Planetary Science XIX*, 949. [4] Crozaz *et al.* (1988) *Lunar and Planetary Science XIX*, 231. [5] Mittlefehldt *et al.* (1989) *Lunar and Planetary Science XX*, 701. [6] Prinz *et al.* (1977) *EPSL* 35, 317. [7] Miyamoto *et al.* (1986) *J. Geophys. Res.* 91, 12804. [8] Miyamoto *et al.* (1985) *Proc. 16th Lunar Planet. Sci. Conf.*, D116. [9] Morioka (1981) *Geochimica et Cosmochimica Acta* 45, 1573. [10] Davidson and Mukhopadhyay (1984) *Contr. Min. Pet.* 86, 256.

Fig. 1

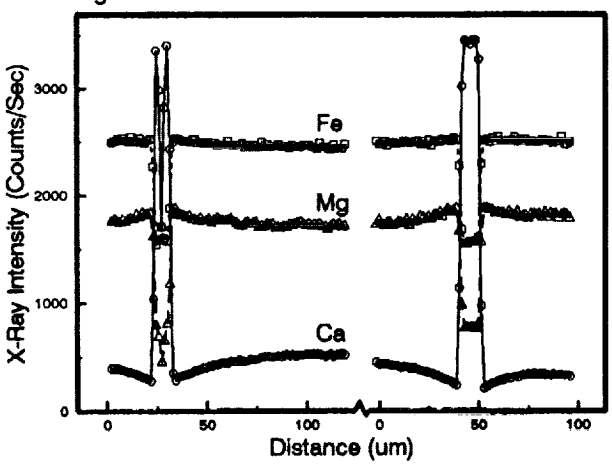

Fig. 2

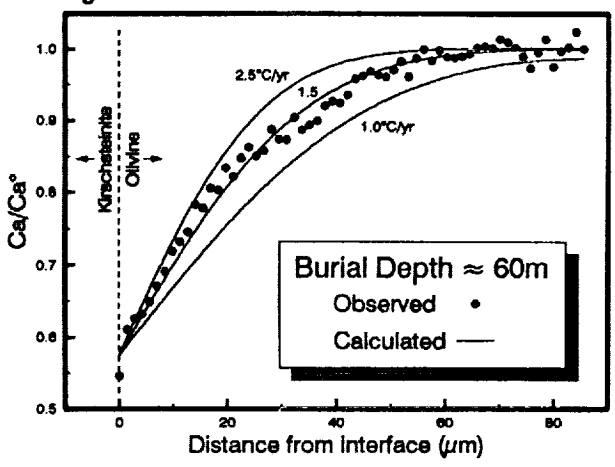

ON THE ABSENCE OF PRESSURE EFFECTS IN METAMORPHOSED ORDINARY CHONDRITES. Harry Y. McSween, Jr. and Allan D. Patchen, Department of Geological Sciences, University of Tennessee, Knoxville, TN 37996, USA.

Distinguishing between onion-shell and rubble-pile models for chondrite parent bodies is difficult, because pressure effects in asteroidal bodies are so small (pressures are typically in the kbar range even near the centers of such objects). However, Heyse (1978) measured a Tschermak's (Al) substitution in LL chondrite orthopyroxenes, which he suggested indicated a pressure gradient that correlated with temperature. This is an important conclusion, because it constitutes the only reported pressure effect in metamorphosed ordinary chondrites. We have analyzed pyroxenes 12 LL chondrites of varying petrologic type and find no evidence for pressure-dependent substitutions.

Equilibration temperatures for LL group chondrites, measured from two-pyroxene geothermometry using the calibration of Lindsley (1983), give a consistent pattern: type 3 (1340-1180°C), type 4 (1225-900), type 5 (1100-910), type 6 (1020-910), type 7 (1155). Temperatures for low petrologic types reflect igneous crystallization, progressively overprinted by attempts to equilibrate to metamorphic temperatures that are only realized in types 6 and 7. These calculated temperatures are based on the compositions of clinopyroxenes, which are more sensitive than coexisting orthopyroxenes to temperature changes, and they bear little relationship to the compositions of coexisting orthopyroxenes. Thus orthopyroxene wollastonite contents probably cannot be used as measures progressive equilibration temperatures, as was done is Heyse's study. Even if we accept the idea that orthopyroxene wollastonite contents reflect metamorphic equilibration, their Al contents show no correlation. Al_2O_3 contents in orthopyroxenes are low, typically < 0.5 weight percent. However, we are confident that our analyses are accurate because molar Al correlates with molar Cr+Ti-Na (equal to the minimum tetrahedral Al necessary for charge balance). The absence of a correlation between Al and either equilibration temperature or orthopyroxene wollastonite content does not support the contention that there is an observable pressure effect in metamorphosed chondrites.

These new data do not necessarily offer support for the rubble-pile model for chondrite parent bodies, but they o negate the only reported instance of correlated pressure and temperature effects in chondritic meteorites. The failure of types 4 and 5 LL chondrites to equilibrate to metamorphic temperatures also suggests that kinetics, rather than varying temperatures, may have played a major role in establishing the properties of the various petrologic types.

Heyse J.V. (1978) The metamorphic history of LL-group ordinary chondrites. Earth Planet. Sci. Lett. 40, 265-381.

Lindsley D.H. (1983) Pyroxene thermometry. Amer. Mineral. 68, 477-493.

GEOCHEMICAL STUDIES OF MUONG NONG TYPE INDOCHINITES AND POSSIBLE MUONG NONG TYPE MOLDAVITES. Thomas Meisel[1], Christian Koeberl[1], and Jaromir Jedlicka[2]. [1]Institute of Geochemisty, University of Vienna, A-1010 Vienna, Austria. [2]Geological Survey, 79376 Zlaté Hory, Czechoslovakia.

Muong Nong type tektites are of key importance in the investigation of tektite formation. We have studied the major and trace element geochemistry of selected Muong Nong type indochinites and possible Muong Nong type tektites from the moldavite strewn field. Muong Nong type tektites have been found almost exclusively in the Australasian tektite strewn field, more specifically, in Laos, Thailand, Cambodia, and Vietnam (all in the Indochina sub-strewn field). Muong Nong type tektites are distinguished from normal (splash-form) tektites by the following physical characteristics: blocky, chunky shape; larger overall weight; layered structure; a higher content of volatile elements; and greater internal variations of major and trace elements compared to normal splash-form tektites [1,2]. Previous searches for Muong Nong type tektites in strewn fields other than the Australasian one have been inconclusive [3]. Only recently, possible Muong Nong type (or layered) tektites have been reported from the North American and Moldavite strewn fields [4,5].

We have studied several moldavites classified by one of us (JJ) as being of Muong Nong type according to observable criteria such as layering and structures. We attempted to confirm the petrological classification through geochemical analyses of five of these samples; however, our data indicate that these are geochemically indiscernible from typical moldavites - i.e. we observed no evidence of considerably higher concentrations of volatile elements or significant inhomogeneities.

Our study also involved the analysis of a moldavite chip from Jakule (CSSR) which was formerly analyzed and classified as a Muong Nong type tektite [5]. Our data exhibit higher volatile trace element contents which support the Muong Nong type tektite classification. Some elemental deviations from the former study were observed; however, these may be due to inhomogeneities in the Jakule specimens. Examination of additional samples similar to the Jakule specimen from this region is necessary to conclusively confirm the existence of Muong Nong type moldavites. In addition, geochemical investigations of the light-colored vesicular inhomogeneities in a Muong Nong type indochinite (kindly provided by D. Futrell, [6]) were performed. Three possible origins of the vesicular white glass are possible: incomplete mixing of target materials, incomplete incorporation of materials at the deposition site, or reaction product formation during ejection.

References: [1] Koeberl, C. (1986) Ann. Rev. Earth Planet. Sci. **14**, 323-350. [2] Koeberl, C. 1987, 2nd Int. Conf. Natural Glasses, Prague, 371-377. [3] Koeberl, C. (1986) Proc. 17th LPSC, JGR **91**, E253-E258. [4] Wittke, H., and Barnes, V.E. (1988) Meteoritics **23**, 311. [5] Glass, B.P., et al. (1989) Lunar Planet. Sci. **XX**, 341-342. [6] Futrell, D.S. (1988) Lunar Planet. Sci. **XIX**, 365-366.

INTERACTION OF Fe,Ni-METAL WITH PREPLANETARY NEBULA GASES (H_2O,H_2S,CO,CO_2): PHYSICOCHEMICAL ASPECT; R.A.Mendybaev, N.S.Kuyunko, A.K.Lavrukhina. Vernadsky Institute of Geochemistry and Analytical Chemistry, USSR Academy of Sciences, Moscow, USSR.

The isolated inclusions and clasts rich in carbon have been discovered in the unequilibrated ordinary chondrites and ordinary-chondrite regolith breccias (Scott et al. 1981). The first investigations of the mineralogy of these aggregates have showed the main minerals to be graphite and magnetite. However, more detail study (Scott et al., 1988) allowed to establish that the graphite phase is highly disordered (poorly graphitized carbon) and usually associate with Fe,Ni-metal in the examined aggregates. Small amounts of magnetite, carbides, sulphides, chromite are also observed. These aggregates have been believed to be formed by low temperature oxidation of Fe,Ni-metal with the gas phase of the PPN.

In the present work we attempted to analyse the interaction of Fe,Ni-metal with the PPN gases taking into account thermodynamics and kinetics of the reactions. Carbon, carbides and magnetite formation can takes place at $T \leq 450$ K according to reactions of Fe,Ni-metal with carbon-bearing gases (CO, CO_2) of the PPN. However, at higher temperatures ($T \simeq 680$ K) troilite should be formed due to reaction of metal with H_2S. Low abundances of troilite in the carbon-rich aggregates may be assumed to result from the low rate of sulphurization process. We compared the rates of these reactions and concluded that there is no any kinetic constraints on the sulphurization of the metal. The CO and CO_2 concentrations higher than equilibrium values may be expected in the PPN owing to kinetic constraints on the hydrogenation of CO (Lewis,Prinn,1980; Mendybaev et al.,1985) and carbon gasification by water vapour (Mendybaev et al.,1989). In this case interaction of Fe,Ni-metal with CO should take place at higher temperatures and the formation of carbon-metal-magnetite and carbon-metal-carbide assemblages are possible.

Alternative mechanism for the formation of these assemblages is decomposition of the metal carbonyls. In these processes metal and CO are formed and their interaction result to carbon, oxides and carbides. The carbonyl formation can take place at shock events in the PPN and during the parent bodies formation stage. It should be noted that most of the meteorites with carbon-rich inclusions and clasts are either regolith breccias or shocked chondrites.

Scott E.R.D. et al.(1981) Nature, v.291, p.544.
Scott E.R.D. et al.(1988) Proc.XVIII LPS, p.513.
Lewis J.S., Prinn R.G.(1980) Astrophys.J., v.238, p.357.
Mendybaev R.A. et al.,(1985) Geokhimija, No 8, p.1206.
Mendybaev R.A. et al. (1989) Geokhimija, No 4, p.467.

FORMATION OF ACCRETIONARY DUST MANTLES IN THE SOLAR NEBULA AS CONFIRMED BY NOBLE GAS DATA OF CM-CHONDRITES; Metzler, K. and Bischoff, A., Institut für Planetologie, Münster, FRG

Most CM-chondrites are breccias (1,2), in some of which solar wind implanted noble gases were measured (3). The majority of CM-chondrites contain *pristine fragments* representing the texture of the pristine CM parent body(ies) (2,4). The most characteristic features of these fragments are the fine grained accretionary dark rims, surrounding all coarse grained components (e.g. chondrules, fragments, CAIs, PCP-rich units). Metzler and Bischoff (2) suggest that these so-called *accretionary dust mantles (ADMs)* were formed in a dust-rich environment of the solar nebula prior to parent body formation. Since dust-rich nebula regions should be opaque to the solar wind, the ADMs should be free of solar wind implanted noble gases. Besides the pristine fragments the CM-chondrites contain a *clastic matrix* due to impact-induced cataclasis of primary CM rocks. These clastic matrices could be the dominant carriers of the solar wind implanted noble gases similar to the dark portions of the ordinary chondrite regolith breccias (5). Using the data compilation of Schultz and Kruse (3) and unpublished data of Nagao for Y-791198 and Y-74662, the solar wind Ne-contents for several CM-chondrites were calculated (Fig.1). These values represent the mean of all available Ne-measurements for the respective CM-chondrites, listed in (3). We also determined the modal abundance of pristine fragments in all studied CM-chondrites by point counting methods. In Fig.1 the solar wind Ne-contents are plotted against the modal abundances of pristine fragments. Some important facts become evident:

1) CM-chondrites that basically consist of the pristine fragments (representing primary unbrecciated CM rocks) do not contain any solar wind implanted noble gases (Y-791198, Y-74662), because they do not have clastic matrices. Therefore, pristine fragments also have to be free of these gases.

2) A few CM-chondrites containing only a small percentage of pristine fragments and abundant clastic matrix (Bells, Essebi) exhibit negligible solar wind implanted noble gas contents. These breccias, probably formed on the meteorite parent body(ies), were not exposed to the solar wind.

3) The CM-chondrites Murray, Murchison, Cold Bokkeveld and Nogoya contain variable abundances of pristine fragments and variable contents of solar wind implanted noble gases. These breccias suffered distinct degrees of brecciation on a planetary surface and were exposed to the solar wind to various extent.

CONCLUSIONS: Only those CM-meteorites with impact-induced, fine grained clastic matrices contain solar wind implanted noble gases. These matrices are the carriers of solar wind gases. The absence of these gases in Y-791198 and Y-74662 that entirely consist of pristine fragments indicates, that the internal structure of these fragments *is really pristine*, and not the product of regolith processes. Since the accretionary dust mantles are a main constituent of all pristine fragments (42-60 Vol%, (2)), they also have to be free of solar wind gases. This is a clear confirmation of the *solar nebula origin of accretionary dust mantles* and points against their formation in a regolith on a planetary surface.

References: (1) McSween (1987),GCA 51, 2469; (2) Metzler and Bischoff(1989),LPS XX, 689; (3) Schultz and Kruse (1983,1986), MPI f. Chemie, Mainz. (4) Metzler et al. (1988), LPS XIX, 772; (5) Bischoff et al. (1983), EPSL 60, 1

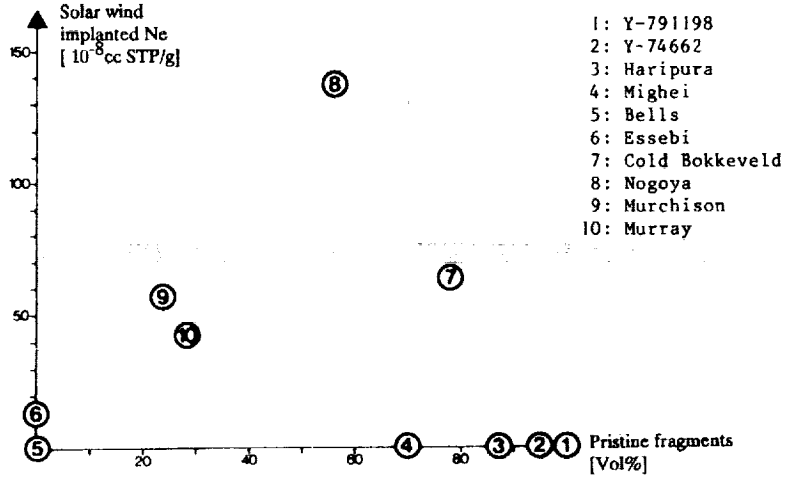

Fig.1

COSMIC-RAY EXPOSURE AGES OF HOWARDITES, EUCRITES, AND DIOGENITES; Th. Michel and O. Eugster, Physikalisches Institut, University of Bern, CH-3012 Bern, Switzerland

Two howardites, one eucrite, one diogenite, and one achondrite, being chemically intermediate between howardites and diogenites, were studied with the purpose of determining their cosmic-ray exposure age based on stable noble gas isotopes and time of fall on the Antarctic ice, using ^{81}Kr. Furthermore, we started dating recently fallen achondrites using the ^{81}Kr-Kr method with the aim of determining the ^{3}He, ^{21}Ne, ^{38}Ar, ^{83}Kr, and ^{126}Xe production rates of HED's. Table 1 gives the He, Ne, and Ar data obtained so far.

Table 1: Cosmogenic and trapped noble gases, and cosmic-ray exposure ages (preliminary data)

		Cosmogenic				Trapped					
Meteorite	Class	^{3}He	^{21}Ne	^{38}Ar	^{22}Ne	^{20}Ne	^{36}Ar	T^{3}	T^{21}	T^{38}	Ave.
		10^{-8} cm^3 STP/g			^{21}Ne	10^{-8}cm^{3}STP/g		Ma			
Yamato-7308	how	29	5.2*	1.07	1.17*	6.3	0.49	18	19	13	17
Yamato-790727	how	1.63	4.3	1.04	1.25	26	2.3	1.0	16	14	15†
Yamato-791960	euc	12.2	2.2*	1.25	1.22*	1.5	0.45	7.7	11.0	9.6	9.4
Millbillillie 20 mg	euc	21.6	4.9	3.6	1.19	0.02	0.26	14	25	27	26†
Millbillillie 30 mg	euc	22.6	5.0	3.4	1.18	0.02	0.13	14	25	26	26†
Yamato-74013	dio(A)	74	18	1.16*	1.08	1.0	0.10	47	51	43	47
Yamato-75032	dio(B)	38	6.9	1.19*	1.12	0.50	0.17	24	26	22	24

Experimental errors: Cosmogenic abundances ∿ 6%, ratio ∿ 2%, trapped abundances for howardites ∿ 15%, trapped abundances for others > 100%, exposure ages ∿ 25% (mainly from production rates), * errors considerably larger, † without T^{3}.

^{3}He and ^{21}Ne are essentially purely cosmogenic. In eucrites and diogenites also ^{38}Ar is almost purely cosmogenic. Howardites contain a small contribution of trapped solar wind Ne and Ar, supporting the hypothesis that they constitute regolith material of the HED parent body. In the following discussion the ages, calculated with preliminary production rates, will be compared with those obtained from the ^{21}Ne and ^{38}Ar data of HED's compiled by Schultz and Kruse (1983) using average production rates for the respective class. The exposure ages of the two howardites are quite similar and within the range observed for the meteorites of this class. It appears that most of ^{3}He in Yamato-790727 was lost by diffusion. The age of the Yamato-791960 eucrite falls into the clustering regions at about 10 Ma, whereas that of Millbillillie into the 25 - 30 Ma peak of the eucrite class. The age of the Yamato-74013 diogenite is very high compared to that of other diogenites except for Yamato-692. This diogenite yielded results for cosmogenic ^{3}He, ^{21}Ne, ^{38}Ar, and $^{22}Ne/^{21}Ne$ (Shima et al., 1973) differing by 6% or less compared with Yamato-74013. The latter two diogenites may be paired. Finally, Yamato-75032, classified as diogenite, is chemically intermediate between diogenites and howardites (Takeda and Mori, 1985; Schultz, 1986; Burger and Krähenbühl, 1989). Assuming corresponding production rates concordant results for T^{3}, T^{21}, and T^{38} are obtained. Yamato-75032, thus, fills the gap between diogenites and howardites.

Acknowledgements - Allocation of the valuable samples by the National Institute of Polar Research in Tokyo is greatly acknowledged. We thank P. Guggisberg, M. Zuber, and B. Aebersold for their assistance. This work was supported by the Swiss National Science Foundation.

References - BURGER and KRAEHENBUEHL (1989) Personal communication. SCHULTZ L. (1986) Mem. Natl. Inst. Polar Res., Spec. Issue 41, 319-327. SCHULTZ L. and KRUSE H. (1983) Max-Planck-Institut für Chemie (Otto-Hahn-Institut) Mainz, and supplement 1986. SHIMA M., SHIMA M., and HINTERBERGER H. (1973) Earth Planet. Sci. Lett. 19, 246-249. TAKEDA H. and MORI H. (1985) J. Geophys. Res., 90, Supplement, C636-C648.

WEATHERING IN ANTARCTIC METEORITES: AN INAA-SEM STUDY

David W. Mittlefehldt[1] and Marilyn M. Lindstrom[2] 1. Lockheed ESCO, C23, 2400 Nasa Rd 1; 2. SN2, NASA/Johnson Space Center, Houston, TX 77058.

The Antarctic ice fields represent an invaluable source of meteorite samples for probing the secrets of the solar system. However, their high terrestrial residence ages (1), their blatant as well as more subtle (2) weathering effects and the occurrence of evaporites on many samples (3) show that interpretations of compositional data need to be cautiously applied. We have initiated an INAA-SEM study of weathering effects on interior, exterior and evaporite samples of Antarctic meteorites. Herein we report our preliminary results, concentrating on H chondrites and eucrites.

H chondrites. We have performed INAA on samples of weathering class B H5 chondrites EET82603 and LEW85320, and of weathering class C H4 chondrite AHLA77225. Preliminary INAA data for the evaporite samples are normalized to Sc as a refractory element expected to be relatively immobile in H chondrites. The low Sc content of the evaporites (0.02-0.07x interior) supports this assumption. Compared to interior samples or mean H4-6 chondrites, the evaporites exhibit high element/Sc ratios for Na, K, Rb, Cs, La, Ce, Sm and Br. There is a systematic increase in alkali element/Sc ratio with atomic number with Na/Sc ~10x, K/Sc ~50x, Rb/Sc ~150x and Cs/Sc ~ 500x mean H4-6. The evaporites are LREE enriched with La/Sm ratios 2-5x cosmic. Siderophile elements and Cr are generally depleted relative to Sc with mean ratios of; Fe/Sc ~0.12x, Co/Sc ~ 0.31x, Ni/Sc ~0.16x and Cr/Sc ~0.09x interior. Iridium is an exception to this with Ir/Sc ~3.5x the interior ratio. Evaluation of the consequences of evaporite formation on meteorites is difficult because the source of the elements in the salts and the concentrations of trace elements in the solutions from which they crystallized are unknown. If the salts represent material leached from the chondrites, then clearly, Cs and Rb concentrations should be treated with caution, even for weathering class B stones.

Eucrites. Four eucrites were investigated: ALHA76005, ALHA78040, EETA79004 and EETA79005. EETA79004 is weathering class B and the rest belong to class A, although the weathering classification scheme may not be appropriate for achondrites. We find no differences between interior and exterior samples of EETA79005 that cannot be due to sampling effects. EETA79004 exterior is enriched in K ~3.3x the interior and depleted in Ce ~0.6x the interior. The REE pattern for EETA79005 exterior is typical of eucrites except for the Ce depletion, with Ce/La ~0.5x cosmic. Both ALHA76005 and ALHA78040 show REE depletions in the exterior samples compared to the interior. The exterior samples exhibit positive Eu anomalies and positive Ce anomalies. An exception to this is the dark gray weathering rind on ALHA78040 which has no Ce anomaly, but is otherwise similar to the other exterior sample. The interior sample of ALHA76005 appears to be typical of eucrites, while ALHA78040 interior has a slight positive Ce anomaly. The REE patterns of the exterior samples of the ALHA eucrites are similar to the "Eu-rich rocks" of (4), which we suggested might be a result of weathering.

Preliminary SEM study of some of the eucrites has revealed gypsum, a probable calcium carbonate phase, a phase or phases rich in S, Cl and K, and "rust" developed on and/or in the exterior samples. Based on qualitative EDS spectra, the dark gray weathering rind appears to be a thin veneer of a silica-rich material. We have yet to find any of these phases except for rust in the interior samples. However, our SEM studies are incomplete.

References: (1) Freundel et al. (1986) GCA 50, 2663; (2) Gooding (1986) GCA 50, 2215; (3) Velbel (1988) Meteoritics 23, 151; (4) Mittlefehldt and Lindstrom (1988) LPS XIX, 790.

VARIOUS FORMATION PROCESSES OF THE K-T BOUNDARY SAMPLES FROM DENSITY VARIATION OF QUARTZ MINERALS

Yasunori MIURA
Faculty of Science, Yamaguchi University, Yamaguchi, 753, Japan.

Formation processes of the 4 Cretaceous-Tertiary (K-T) boundary samples from Japan, Italy, Denmark and Tunisia are discussed on density-variation of the quartz mineral, compared with those of 2 terrestrial impact craters and of 5 terrestrial metamorphic, volcanic and plutonic rocks by using standard α-quartz of rock-crystal.

Deviations of the calculated density (Δd) from the standard quartz are summarized as follows. 1) The progressive changes of quartz mineral are considered to be one of the best indicator of the formation process of the host rocks than the higher-density silica minerals or glass. 2) Negative values of the deviation (i.e. lower density) indicate the higher-temperature type silica minerals of β-type quartz (-5.0 %) and tridymite (-14.7 %). Positive values of the deviation (i.e. higher density) indicate the higher-pressure type silica minerals of coesite (+9.7 %) and stishovite (+61.9 %). 3) Quartz minerals of the terrestrial metamorphic rocks show positive Δd values (+0.03 to +0.09 %), though volcanic sedimentary rocks show various data from -0.06 to 0.22 (%). 4) Quartz minerals from the Barringer crater have larger positive values (+0.09 to +0.49 %), though quartz from the melt rocks of the Manicouagan impact crater shows negative values (-0.11 to +0.01%). 5) The K-T boundary samples show various Δd values; that is, mixed data of Japan (-0.18 to -0.12 %; +0.23 to +0.59 %), positive data of Tunisia (+0.63%), negative value of Italy (-0.06 %), and positive value of Denmark (+0.12 %).

Typical quartz minerals formed by impact process are found in Tunisia sample (and also in Denmark one), though the quartz from the Italy K-T boundary sample shows temperature-dependent effect caused by impact melt and/or volcanic melt. The Japanese K/T boundary samples are mixed samples of temperature- and pressure-dependent events.

Although there are two major explanations of the various K-T boundary events in the world (i.e. extraterrestrial impact and terrestrial volcanic events)[1,2,3], it is important to find the real simple K-T boundary samples which include relict or memory of the first events without major terrestrial products and mixtures.

References:
1) Miura Y.(1986): LPSC XVII, 555-556.
2) Miura Y., Shibuya G., Imai M., Takaoka N. and Saito T. (1988): Global Catastrophes in Earth History, 124-125.
3) Miura Y. and Imai M. (1989): 14 th Symp. NIPR Antartic Meteorites (NIPR, Tokyo), (in press).

NEW APPROACHES TO THE CHINGUETTI METEORITE PROBLEM

Prof.Th.MONOD - Mus.Nat.Hist.Nat. 43 rue Cuvier - F 75005 Paris

For many years, after the Lacroix's publication (1924) on the possible existence of both a small meteorite (4,5 kg) bea= ring the number 1291 in the Paris Collection, and another one of great size (40 x 100 m) in the Adrar desert of Mauritania, several field researches and inquiries among local smiths have been conducted, all of them entirely unsuccessful.

In spite of a short episode (1932) when Captain Ripert was himself once again interviewed, nothing happened and, time pas= sing, the whole problem was practically forgotten.

A report by Jacques Gallouédec, dated 1980, had announced the discovery of a semi-circular structure in the Meghalleg Akle, in the south-east of Chinguetti.

In 1932, Captain Ripert had mentioned himself that the me= teorite was probably situated south-east instead south-west of Chinguetti.

A careful study of all available documents (e.g.: the Chin= guetti meteorite files of IFAN's Archives in Dakar) showed that the whole inquiry had to be resumed again starting from scratch.

After two expeditions in the south-east of Chinguetti, with camels (1987 - 1988), following results have been obtained: the place visited by Captain Ripert in 1916 has been identified with the guelb " Aouinet N'Cher" (20°10'30"N-12°28'24"W), Ripert had said " 45 kilometers south-west of Chinguetti and west of Aouinet wells"; in fact it was 35 kilometers south-south-west of Chinguetti as the crow flies, south-west of the wells.

The " Aouinet guelb" measures about 40 m high, exactly the height given by Captain Ripert for his meteorite.

The " Aouinet guelb" is only made of sandstones at the bot= tom and quartzite for the rest of it.

As the guelb was supposed by Captain Ripert to represent a gigantic meteorite, it becomes obvious that the story origina= ted in a misinterpretation of that rock's nature.

However, a last problem has to be mentioned: why was Cap= tain Ripert taken from Chinguetti to the Aouinet rock? Certain= ly not to show him the small block discovered by chance on the spot.

As Captain Ripert had spoken of the possible interest of local smiths for his supposed meteoritic iron and, as frag= ments of iron ore had been lately discovered (december 1988) at the foot of the Aouinet hill, it seems very likely that it was either some lateritic bed or remains of ancient iron works that where shown to Captain Ripert.

Is it even sure that the small meteoritic block was resting in its original place when discovered by Captain Ripert?

As the possible existence of a giant meteorite in the Adrar region seems still to be accepted by many astronomers or geo= chemists, it is important to inform the scientific community of the latest development of the question.

PRELIMINARY STUDY OF CHAVES HOWARDITE. J.Fernando Monteiro. Departamento de Geociências, UTAD, 5000 Vila Real, Portugal.

The Chaves meteorite fell on May 3, 1925 at about midday (local time) in the small village of Vilarelho da Raia, situated 8 Km north of Chaves town (Portugal). The fall was accompanied by two very strong explosion sounds followed by a noise resembling that of a cannon fire. Three fragments were recovered by the local authorities with total mass of 2945 g. This meteorite was briefly described by Jérémine (1) and Mason et al. (2) who show that it is a typical polymict breccia.

All stones have a shiny dark brownwish-black crust, which is fissured, and present areas of striated crust. In the broken surfaces, where the samples are void of fusion crust, light to dark gray interior material is exposed. In addition to a light grey groundmass containing angular fragments varying from white to greenish and sometimes grey, the meteorite shows ophitic fragments, which are up to 9 mm long.

In thin section Chaves is a complex breccia with a clear regolithic texture. It consists mainly of fragments of single minerals, pyroxene (orthopyroxene and pigeonite) and plagioclase, with several pyroxene fragments up to 2 mm. Both the breccia fragments and the groundmass show the effects of strain, being shottered, and showing undulatory extinction. Dark brown glass and devitrified glass are very common and they are intimately associated with cristalline grains of plagioclase and pyroxene. Turbid glass shows sometimes crystalline needles of pyroxene. Some ancient thin sections present fragments of comminuted orthopyroxene with an igneous granular texture. Others enclaves are halocrystalline pyroxene plagioclase aggregates, and vary considerably in texture from coarse-grained gabbroic to fine-grained basaltic types. Microprobe analyses show that the pyroxene consists largely of orthopyroxene with lesser amount of pigeonite. Pyroxene have a range of compositions from Wo_2 En_{78} Fs_{18} to Wo_5 En_{37} Fs_{58} . The more magnesian pyroxenes all have low Ca contents but the more Fe-rich varieties range from Wo_4 En_{38} Fs_{58} to Wo_{24} En_{38} Fs_{38} . Feldspars, generally twinned, ranges in composition from $Or_{0.6}$ Ab_6 An_{94} to $Or_{0.6}$ Ab_{12} An_{87} with more sodic grains in some of the volcanic clasts. Some silica minerals,quartz and tridymite, were observed in thin section and, during electron microprobe work, many small complex intergrowths between plagioclase and pyroxene crystals were found to contain very high silica. Quartz is always associated with pyroxene, recrystallized pyroxene , glass and magnetite. At least 70% of the opaque minerals in the section studied is troilite, which occur frequently as fine intergrowths with pyroxene. Chromite, ilmenite and some grains of Fe-Ni metal was encountered. No olivine was found. The Chaves meteorite is a typical howardite.

References: (1) Jérémine, E. (1954) Bol. Soc. Geol. Port., 11, 127-138. (2) Mason, B. et al. (1979) Smithson. Contrib. Earth Sci. 22, 27-45.

HYDROGEN IN THE INMAN ORDINARY CHONDRITE. A.D.Morse, I.P.Wright and C.T.Pillinger, Planetary Sciences Unit, Open University, Milton Keynes. MK7 6AA. UK.

The large deuterium enrichment of carbonaceous chondrites has been attributed to the organics in these meteorites (1,2). Some of the most primitive ordinary chondrites (petrologic type 3.0 to 3.4) also show large deuterium enrichments (3), with those that have been affected least by metamorphism tending to have the greatest deuterium enrichments. By analogy with the carbonaceous chondrites the D enrichment could be due to a similar organic phase (4).

The carbon and nitrogen analyses of acid residues from unequilibrated ordinary chondrites such as Semarkona and Bishunpur show broad similarities (in terms of components and isotopic compositions) to the carbonaceous chondrites (5). Of the ordinary chondrites Semarkona has the highest δD enrichment measured, δD = +5740‰ and the second highest $\delta^{15}N$ ratio measured in acid residue of +195‰. The meteorite with the greatest ^{15}N enrichment was Inman $\delta^{15}N$ = +256‰. Inman is a type L3.4 ordinary chondrite, found in 1966 with a mass of 7.25 kg and is highly weathered. Carbon analysis has shown that as much as 18.5% of its carbon in an acid insoluble phase. If the nitrogen and hydrogen enrichments are part of an organic phase and coupled, then Inman would be expected to have a very high deuterium enrichment. This would make it an ideal meteorite to study for the deuterium enriched organics due to its high amount of acid resistant material and its greater availability. However it is a highly weathered find so the possibility of a large amount of terrestrial contamination needs to be evaluated.

Using stepped combustion/pyrolysis of small samples the simultaneous water and carbon release profiles were measured. For comparison with Inman, Chainpur has also been analysed; this type LL 3.4 ordinary chondrite is relatively available and has a reasonably high deuterium content (6). Terrestrial organic material (Green River Shale) has also been studied in order to assess the behaviour of organic matter (kerogen) during stepped heating.

The stepped combustion and pyrolysis of ~5mg samples of Chainpur showed complex release profiles for hydrogen and carbon. One of the carbon components pyrolysed between 450 and 700°C, was accompanied by a simultaneous hydrogen release and had an H/C ratio of about 1.8. During combustion the carbon was released at a lower temperature in a much narrower peak (400 to 550°C) and there was no simultaneous hydrogen release. By comparison with the Green River Shale the component could be organic. The hydrogen in the Green River Shale sample combusted at a lower temperature than the carbon and in Chainpur the 'organic' hydrogen was probably masked by silicate water.

During stepped combustion and pyrolysis of Inman the carbon release profiles were similar to that of Chainpur, although the 'organic' component was much larger in Inman, especially during pyrolysis, possibly due to oxygen supplied by iron oxides. However the hydrogen release profiles during both combustion and pyrolysis were very similar, had similar yields and appeared to consist of only one component. Most of the water, 1035 ppm, was released from Inman below 300°C with δD = -90‰, possibly terrestrial contamination. Above 300°C there was 597 ppm water with the δD decreasing to -135‰ and no indication of a deuterium-rich component There was little evidence of a hydrogen peak corresponding to the organic carbon peak during pyrolysis of Inman and the H/C ratio between 450 and 700°C was less than 0.6. In an attempt to remove silicate water that could be obscuring the 'organic' component a sample was first pyrolysed at 300°C for 72 hours. The water yield above 300°C was reduced to only 72 ppm, but still had a δD of -135‰.

Thus it appears that the organic phase in Inman contains little hydrogen and does not have a high deuterium enrichment. These observations are consistent with most of the hydrogen being contained in silicate water with δD = -135‰, and can probably be accounted for by terrestrial weathering. However, it is not impossible that the results could be explained by cracking of the organics with hydrogen and methane not being collected during pyrolysis. During combustion the organic hydrogen release occurs at a lower temperature and is obscured by the silicate water, as in the Chainpur combustion. This will be evaluated by analysis of acid residues of Inman from which the silicate water has been removed.

References (1) Y.Kolodny *et al.* (1980) *Earth Planet. Sci. Lett.* **46** 149-158. (2) J.Yang and S.Epstein (1983) *GCA* **47** 2199-2216. (3) McNaughton *et al.* (1983) *Proc 13 LPSC* A297-A302. (4) Alexander *et al.* (1989) *Lun.Plan.Sci* **XX** 7. (5) Alexander *et al.* (1988) *Lun.Plan.Sci* **XIX** 5. (6) Robert *et al.* (1987) *GCA* **51** 1787-1805.

Unusual distribution of N and Li in Ambapur Nagla

S.V.S.MURTY[1] and P.S.GOEL[2]
1. Physical Research Laboratory, Ahmedabad-380 009, India.
2. Dept. of Chemistry, I.I.T. Kanpur, Kanpur-208 016, India.

Nitrogen occurs mostly in organic form in carbonaceous chondrites and in inorganic form in enstatite chondrites. In both these classes of meteorites nitrogen is present upto several hundred ppm. In the ordinary chondrites, nitrogen contents are in the range of 10-40 ppm and no specific N-carrying phase has been identified for these meteorites (Murty et al. 1983a). Li, on the other hand has an uniform abundance of 1-2 ppm in all classes of chondritic meteorites (Murty et al 1983b).

In an effort to identify N-rich phases in ordinary chondrites, we analysed nitrogen in density separates and grain size fractions of several meteorites. Since our RNAA approach allows us to study N and Li simultaneously (Shukla et al 1978) we studied Li also in all these meteorites. Here we present the results from Ambapur Nagla (H5) showing unusual enrichments of both N, Li in some grain size fractions.

Both N, Li are in normal abundance in the bulk sample as well as chondrules of Ambapur Nagla. But in grain size fractions separated into magnetic and nonmagnetic portions, N shows an enrichment with decreasing grain size in both magnetic and nonmagnetic fractions, while Li shows a similar effect in the magnetic fraction only. In the $<38\ \mu m$ magnetic fraction where the highest enrichments are observed, N is as high as 1000 ppm and Li goes upto 160 ppm. Surface contamination due to atmospheric nitrogen is ruled out by the results of our etching experiments (Murty et al 1983a). No ordinarty chondrite has ever shown such high N-contents and no chondritic material is known to contain such high Li contents. We are currently looking at the isotopic composition of nitrogen in Ambapur Nagla to identify its plausible source.

References:

Murty S.V.S., Shukla P.N. and Goel P.S. (1983a) Geochemical J.17 165
Murty S.V.S., Shukla P.N. and Goel P.S. (1983b) Meteoritics 18 123.
Shukla P.N., Kothari B.K. and Goel P.S. (1978) Anal. Chim. Acta 96 259.

EARLY OUTGASSING OF THE EARTH AND MARS:

Donald S. Musselwhite, Michael J. Drake and Timothy D. Swindle (Lunar and Planetary Laboratory, University of Arizona, Tucson, AZ 85721)

Introduction: Allègre *et al.* [1] proposed a two-layer mantle to explain excess ^{129}Xe found in upper mantle-derived materials on Earth: the upper mantle degassed early in Earth history while ^{129}I was still alive, thereby enhancing its I/Xe ratio. The residual ^{129}I in the upper mantle decayed to ^{129}Xe ($t_{1/2}$ = 17 m.y.), enhancing its $^{129}Xe/^{130}Xe$ ratio. The lower mantle is undegassed and, therefore, has a low I/Xe ratio and thus a low $^{129}Xe/^{130}Xe$ ratio. Ozima *et al.* [2] suggested that the excess ^{129}Xe in MORBs originated in a reservoir of different composition that accreted earlier than the atmospheric source region.

Model [1] implicitly assumes (with no experimental basis) that Xe is less compatible than I in order to fractionate I from Xe. Mineral/melt partitioning studies on Xe [3,4] show that it is not as incompatible as previously thought. We have determined experimentally upper limits on mineral/melt partition coefficients for I, D(I), at 1 bar [5] ($D(I)^{di/melt} \leq 0.003$, $D(I)^{an/melt} \leq 0.015$, and $D(I)^{fo/melt} \leq 0.035$). Only upper limits are available because I is below detection in the crystals. High pressure partitioning experiments are under way in order to rectify this problem and to obtain spinel/melt and garnet/melt partitioning data. However, from the available data, it is clear that I and Xe cannot be significantly fractionated during partial melting of the mantle. Furthermore, since both I and Xe have low solubilities in silicate melts at 1 bar, both will be outgassed upon eruption. These facts cast doubt on the early outgassing model of [1].

Earth Outgassing Model: Since the excess ^{129}Xe found in the Earth's upper mantle ($^{129}Xe/^{132}Xe$ = 1.01 for MORBs, cf. $^{129}Xe/^{132}Xe$ = 0.988 for OIBs and $^{129}Xe/^{132}Xe$ = 0.98 for Earth's atmosphere [6]) is most likely the result of ^{129}I decay, the problem of fractionating I from Xe remains. Therefore, we propose a model for fractionating I from Xe which makes use of the extreme differences in solubilities of I and Xe in water [7]. (1) Condensation and accretion occur from 4.55 Ga to 4.45 Ga. (2) By 4.45 Ga accretion ceases and liquid water is stable at the Earth's surface [8]. (3) Erupted mantle-derived melts outgas I and Xe. (4) Iodine, being highly soluble in water, goes into solution and is rapidly incorporated into the crust. Xenon, with an extremely low water solubility, is partitioned into the atmosphere. (5) ^{129}I, now residing in the crust, decays to ^{129}Xe and is subsequently reincorporated into the now volatile depleted MORB source by crustal recycling. Although the abundance of ^{129}I drops by a factor of 100 in the 10^8 years between solar nebula formation and the incorporation of I into the crust, the extreme fractionation of I from Xe due to their extreme differences in H_2O solubilities and a relatively high I/Xe ratio in the primordial mantle can account for the ^{129}Xe excess seen in MORBs today.

Mars Outgassing Model: A similar model can explain $^{129}Xe/^{132}Xe$ values for Mars ($^{129}Xe/^{132}Xe$ = 2.5 - atmosphere [9], $^{129}Xe/^{132}Xe$ = 1.0 to 1.5 - SNC source [6]) as follows. Steps (1) to (4) are the same as the Earth model. (5) Calculations of [10] show that atmospheric blowoff from late heavy bombardment is significant for Mars but not for Earth and that impact erosion will diminish the martian atmosphere to nearly its present level by about 4.0 Ga. Xenon partitioned into the atmosphere escapes into space by this blowoff. Water (containing dissolved I) not directly involved in impact will remain standing. (6) As with the Earth model, ^{129}I in the martian crust decays to ^{129}Xe, but is not recycled into the mantle. (7) ^{129}Xe in the crust is released over geologic time into the now diminished atmosphere. This model is consistent with ^{40}Ar enrichment in the martian atmosphere which requires release of ^{40}Ar over geologic time.

References: [1] Allègre *et al.* (1983) *Nature* **303**, 762-766. [2] Ozima *et al.* (1985) *Nature* **315**, 471-474. [3] Hiagon and Ozima (1986) *GCA* **50**, 2045-2057. [4] Broadhurst *et al.* (1988) *LPS* **XIX**, 138–139. [5] Musselwhite *et al.* (1989) *LPS* **XX**, 748-749. [6] Dreibus and Wänke (1987) *Icarus* **71**, 225-240. [7] *Lange's Handbook of Chemistry*, Dean ed., McGraw-Hill, New York, 1979. [8] Matsui and Abe (1986) *Nature* **322**, 526-528. [9] Anders and Owen (1977) *Science* **198**, 453-465. [10] Melosh and Vickery (1989) *Nature* **338**, 487-489.

DYNAMIC VAPORIZATION EXPERIMENTS IN THE SYSTEM FORSTERITE-ANORTHITE AND ITS IMPLICATION FOR THE ORIGIN OF CAIS AND CHONDRULES; H. Nagahara and I. Kushiro, Geol. Inst., Univ. Tokyo, Hongo, Tokyo 113, Japan.

A mixture of forsterite and anorthite was heated at high temperatures and low pressures and compositional and mineralogical changes of the residues were studied. The starting material is a 1:1 mixture of synthesized forsterite and natural anorthite with sizes of 25-63um. About seven mgs of the starting material was put in a graphite capsule and held in a furnace in a vacuum chamber. They were heated at 1300 to 1500°C and the total pressure was kept at $(1\text{-}5)\times10^{-1}$ torr with hydrogen gas for 2 to 72 hrs.

The results are as follows: (1) The residue heated at 1290°C for 7 hrs showed no visible change but forsterite and anorthite were sintered. (2) The residues heated at 1300°C, which is below the liquidus temperature of the system (1320°C at 1atm), melted to form a liquid and crystallized spinel, and the amount of liquid increased with time. The residue of a short run showed a similar appearance to that of the 1290°C experiment, which consists of forsterite and anorthite with a minor amount of interstitial liquid. The residue of a longer experiment shows different appearance, which consists of porphyritic large forsterite and small (several to 20 um) spinel in glass matrix with a thin spinel rim. Small euhedral spinel grains completely surround the charge, which is similar to the spinel rim of some CAIs. (3) The residues heated at 1330°C, which is above the solidus temperature, also melted to form liquid and spinel. The mineral assemblage and texture of residues of different duration experiments except for the longest experiments (72hrs) are essentially the same as those of the long experiment at 1300°C with porphyritic large forsterite and small spinel in glass matrix. Difference from 1300°C experiments is absence of clear spinel rim; spinel is almost homogeneously distributed in the charge with weak concentration near the surface. The residue of the longest experiments is different from others in that it lacks forsterite phenocrysts and spinel rim is totally absent. (4) The residue heated at 1500°C for 3 hrs, which is above the liquidus temperature of the system, totally melted to loose Si and Mg and changed to aggregates of calcium-dialuminate ($CaAl_4O_7$), which is a characteristic mineral in a group of CAIs, especially in Murchison. The charge heated at 1500°C for 7 hrs was lost by vaporization.

The chemical composition of liquid changes with heating temperature and time. The liquid formed at 1300°C for 2 hrs is very rich in CaO (about 30wt%) and poor in Al_2O_3 (10%) and MgO (10 %), which is far from the eutectic composition of forsterite-anorthite system (43% SiO_2, 26% Al_2O_3, 16% MgO, and 15% CaO). The SiO_2 and CaO contents increase and Al_2O_3 and MgO contents decrease with increasing duration. This may be due to melting of anorthite component and subsequent spinel crystallization. The compositional change of liquids observed at 1330°C is different from that of lower temperature experiments. The liquid of 2-hour experiment is rich in Al_2O_3 (22%) and MgO (17%) and poor in CaO (15%); SiO_2, Al_2O_3, and MgO contents decrease and CaO content increases with duration. The liquid formed at 1330°C for 72 hrs has composition similar to that formed at 1300°C for 72 hrs. These results show that the bulk composition of the system changes with time by partial vaporization of Si, Al, and Mg which resulted in relative enrichment of Ca in the residue.

Although the composition of the present system may not be directly applicable, compositional and textural variations observed in the present experiments give important clues on the origin of chondrules and CAIs. Intensive vaporization of components with simultaneous crystallization largely changes bulk composition of the system and mineral assemblage with time even below the vaporus temperature of the system.

SPHALERITE COMPOSITIONS IN METEORITES: A DILEMMA OF AN ORIGINALLY PROMISING COSMOBAROMETER; H.-J. Nagel, Y.T. Lin, A. El Goresy, Max-Planck-Institut für Kernphysik, 6900 Heidelberg, West-Germany

The FeS-content of meteoritic sphalerites could be an important clue to the P-T-conditions in the solar nebula and in the parent bodies [1, 2, 3]. However, this is only valid if the meteoritic sphalerites are strict members of the binary system ZnS-FeS.

Our detailed studies indicate that sphalerites are quite complex in composition. In the Qingzhen meteorite they show a broad range in composition in the various clasts. The number and concentration of minor constituents depend on the assemblage in which sphalerite occurs. Sphalerites coexisting with perryite are high in Ni (1-4 mole% NiS) and are barren of schreibersite inclusions. In contrast, sphalerites without perryite are low in Ni (< 1 mole% NiS) and abundently contain schreibersite spherules. In SEM using a BSE-detector, sphalerites usually display dark and bright domains. Dark areas have usually low totals, a sulfur/metal ratio greater than unity, high Ga-contents (1-2 mole% GaS) and are low in Zn (36-38 mole% ZnS). Analyses of bright areas reveal satisfactory totals, sulfur/metal ratios are almost unity, the Ga-content is low (< 1 mole% GaS) and the Zn-content is high (40-42 mole% ZnS).

In addition to Zn, Fe and S, sphalerite contains Mn and Mg as major elements. A large number of minor elements including Cu, Ga, Ni, Cr, Ca, Na and K was also detected in the Qingzhen sphalerites. Under these conditions it becomese difficult to estimate the thermodynamic and kinetic properties of sphalerites in such a multicomponent system. Specifically the effect of these elements on the cosmo-barometer is unknown and the reliability of the calculated parameters becomes questionable.

A comparison of the Mn-contents in the sphalerite-niningerite pairs in Indarch, Qingzhen and Yamato 6901 reveals consistent increase in the MnS-contents from Yamato 6901 (2-4 mole% in Sph, 5 mole% in Nin), Indarch (5 mole% in Sph, 7-10 mole% in Nin) to Qingzhen (4-9 mole% in Sph, 13-16 mole% in Nin) (see also [4]). This is another evidence for decreasing oxygen fugacities from Yamato 6901, Indarch to Qingzhen.

[1] Hutchison, Scott, GCA, 47 (1983) 101
[2] Kissin, GCA (1989) in press
[3] El Goresy, Ehlers, GCA, (1989) in press
[4] Ehlers, El Goresy, GCA, 52 (1988) 877

GEOLOGY, GEOCHEMISTRY AND GEOCHRONOLOGY OF THE KARA IMPACT STRUCTURE; M.A.Nazarov (1), D.D.Badjukov (1), E.M.Kolesnikov (2), L.D.Barsukova (1), and G.M.Kolesov (1).
(1)Vernadsky Inst. of Geochemistry and Analyt. Chemistry, USSR Academy of Sciences, Moscow 117975; (2)Geological Faculty of Moscow State University, Moscow 119899, USSR

The Kara impact structure is supposed to associate with the K/T boundary event. In order to test the possible association we are studying geology, geochemistry and geochronology of the structure. Here we report some results of the investigation.

The structure is situated at the Kara Sea shore and consists of two adjacent craters, the Kara crater and the Ust-Kara crater. The structure is heavily eroded. An original diameter of the Kara crater is computed to be 65 km as a minimum. The size of the Ust-Kara crater situated mainly underwater is unknown. Estimated diameters of the crater are 25, 75 or 160km. Both craters are excavated mostly in Permian sediments represented by shales and sandstones. When compared to the upper crust the Permian rocks are higher in Fe, Mg, Cr, Ni, Ti, V, Sc, Ir, and poorer in Si, Na, K, REE. Approximately, the Kara target composition can be modelled by mixing of upper crust and tholeiitic basalt components. Sources for the basalt material could be the Ural and Pai-Khoi mountains. The crater cavities are filled with suevite breccias and impact melts which are overlain by recent sediments. The impactites are very similar in chemistry to the Permian rocks. No extraterrestrial material has yet been identified in the impactites by geochemical and mineralogical methods.

Paleontological data indicate that the Kara structure can be of the K/T age and cannot be older than the Campanian/Maastrichtian transition. Whole-rock K-Ar isochrone for the Kara impact melts yields an age of 65.6+/-0.6 (1 6) my that is consistent with the K/T boundary age. Results of paleomagnetism studies are compatible with the K/T age of the structure but do not prove it. 39Ar-40Ar researches give a Campanian/Maastrichtian age of 75 my for the Kara event. However the interpretation of the 39Ar-40Ar data is disputable. Age determinations by Rb-Sr and fission track techniques are in progress. Stratigraphical position of the Kara ejecta is currently being studied in the Yamal Peninsula sedimentary sequence.

In general, we can conclude that the Kara structure was formed in the interval of 65-75 my ago. At the same time the K/T event took place and ejected also a continental material. A probability of formation of two and more continental craters different in their ages and bigger than 65 km is about 0.1 at the normal rate of cratering. Therefore there is a probability of 0.9 that the Kara and K/T impacts are simultaneous or the production rate of impacts at the end of Cretaceous was higher. In the both cases the study supports the impact scenario of the K/T mass extinction.

CHARACTERIZATION OF A PURE urKREEP SIGNATURE BY IDENTIFYING THE "DREGS" OF THE LUNAR MAGMA OCEAN Clive R. NEAL and Lawrence A. TAYLOR, Dept. of Geological Sciences, University of Tennessee, Knoxville, TN 37996 USA.

The derivation of **"urKREEP"** (primeval, pristine KREEP) from the Lunar Magma Ocean (LMO) after ≅ 99% crystallization has been hypothesized by Warren & Wasson (1979) and Warren (1985). However, a pure, unadulterated urKREEP composition has never been identified, but KREEPy components have (Neal et al., 1988; Neal & Taylor, 1989a). Generation of such a residual is within the realm of silicate liquid immiscibility (SLI), which splits urKREEP into K- and REEP-Fractions. The KREEPy components are manifest as: granite (K); high-K glass in basaltic mesostases (K); evolved phosphates in primitive highland lithologies (REEP); quartz ferrotroctolite in soils (REEP); high-Fe glass in basaltic mesostases (REEP). Viscosity differences between K- and REEP-Fractions (30000 & ≅ 12 poise, resp.) allow separation: the "REEP-Frac" migrates upward, the viscous "K-Frac" is basically static.

Using experimental evidence for immiscible melt proportions (e.g., Hess et al., 1975) the K- and REEP-Fractions may be recombined to recreate an urKREEP composition. Major and trace element compositions for the K- and REEP-Fractions are derived from the components above using the method of Neal & Taylor (1989a). Results demonstrate that the calculated urKREEP REE compositions are more LREE-enriched, contain a deeper negative Eu anomaly and greater REE abundances than in high-K KREEP (Warren & Wasson, 1979; Warren, 1988). As high-K KREEP falls below this defined range, it is probably a diluted form of urKREEP. Furthermore, the ferrobasaltic nature produces a low MG# (2-3) of our urKREEP compositions, which is more consistent with urKREEP being a residual product of extreme fractionation than the MG# of 64 from high-K KREEP. Sample **14001,28.3** contains evidence of SLI (Morris et al., 1988) and REE abundances (and profile) similar to our calculated urKREEP range. **This sample may be the first pure, unadulterated urKREEP specimen recorded in the lunar sample return.**

Another way of estimating the urKREEP composition is by back calculation using an average lunar granite and liquid-liquid Kd's (see Neal & Taylor, 1989b for $D_{b/a}$ values). The major element composition of this calculated urKREEP is similar to that reported above, being generally ferrobasaltic. The urKREEP REE profile thus calculated is concave-upward. This is probably due to phosphate removal required in lunar granite petrogenesis (e.g., Warren et al., 1983). Whether this occurred before or after SLI is unclear. It is feasible that the melt thus calculated represents urKREEP minus whitlockite/apatite, and that calculated above represents urKREEP *in toto*.

CONCLUSIONS - 1) KREEP, as seen at the surface of the Moon, **is not a rock type but a chemical signature** - it is a diluted form of urKREEP; 2) Extreme fractionation of the LMO allows portions of the urKREEP residual to undergo SLI; 3) The resulting K- and REEP-Fractions form real lunar components and can be used to estimate the composition of urKREEP. Results demonstrate that the major elements are more representative of a residual magma after fractional crystallization, and the REE exhibit a deeper negative Eu anomaly, have higher abundances, and are more LREE-enriched than high-K KREEP.

REFERENCES: Hess et al. (1975) PLSC 6, 895-909; Morris et al. (1988) Apollo 14 Workshop, 43-45; Neal et al. (1988) LPS XIX, 831-832; Neal & Taylor (1989a) GCA 53, 529-541; Neal & Taylor (1989b) PLPSC 19, 209-218; Warren (1985) Ann. Rev Earth Planet. Sci. 13, 201-240; Warren (1988) Apollo 14 Workshop, 106-110; Warren & Wasson (1979) Rev. Geophys. Sp. Phys. 17, 73-88; Warren et al. (1983) EPSL 64, 175-185.

NITROGEN ISOTOPE VARIATION IN IRON METEORITES. N.J. Neal, I.A. Franchi and C.T. Pillinger, Planetary Sciences Unit, Department of Earth Sciences, The Open University, Milton Keynes, England, MK7 6AA.

Preliminary studies of the nitrogen isotopic systematics in iron meteorites revealed a large range in nitrogen isotopic compositions from –96 to +156‰ (Prombo and Clayton, 1983; Franchi *et al.*, 1987). However, it was noted that the irons could be divided into four isotopically distinct "families": (1) –96 to –74‰, groups IC, IIAB, IIIAB and IIIE; (2) –66 to –43‰, groups IAB and IIICD; (3) –16 to +46‰, groups IID, IIE, IIF, IIIF, IVA and IVB; (4) +125 to +156‰, group IIC. The range in $\delta^{15}N$ values from individual groups generally being considerably smaller than that of its family. As each meteorite group is believed to be from a separate parent body this indicates that the effects of parent body processes are slight in comparison with the total range in $\delta^{15}N$ values and that the variation between the four families is the result of a primary fractionation event within the condensing solar nebula. The mechanism(s) producing this range in $\delta^{15}N$ values is as yet unresolved, although both isotopic heterogeneity and fractionation processes may have contributed to the effect. To study this problem better definition of the variation in $\delta^{15}N$ between groups within the "families" of iron meteorite groups is required, particularly in defining the full range of the less studied groups which should establish whether any primary fractionation of the nitrogen has occurred within individual families. The initial work of Franchi *et al.* (1987) revealed some variation within the "family" of iron meteorite groups with the lowest $\delta^{15}N$ values (around –80‰), i.e. groups IC, IIAB, IIIE and IIIAB.

A further 18 iron meteorites have now been prepared for nitrogen isotopic analyses. Initial results indicate that the ranges in $\delta^{15}N$ values from the smaller groups (IC and IIAB) are larger than originally defined, and therefore comparable with the ranges obtained from the more popular groups (IAB's and IIIAB's). If this is so then any evidence for $\delta^{15}N$ variation within this family has either been obliterated by secondary processing or was never present, in which case the parent bodies of the iron meteorite groups within the families must have formed from an initially homogenous nitrogen reservoir. Such a conclusion has interesting implications for nitrogen isotopic variation observed within meteorites in general. Sufficient data was available from the earlier work to conclude that there were differences in the way $\delta^{15}N$ value varied with the composition in the groups IAB and IIIAB, the main non-magmatic and magmatic groups, (Franchi *et al.* 1987). However, due to the paucity of data it is impossible to establish whether such trends are present in the other 11 groups. Although the new data reveals larger ranges in $\delta^{15}N$ value in groups IC and IIAB there appears to be a lack of any systematic co-variation between nitrogen and the bulk chemistry.

References:

Franchi, I.A., *et al.* (1987), *Meteoritics*, **22**, 379-380.
Prombo, C.A. and Clayton (1983), *Meteoritics*, **18**, 377-379

CHONDRULES IN EH3 CHONDRITES C.E. Nehru [1,2], M. Prinz [2] and MK. Weisberg [1,2]
(1) Dept. of Geology, Brooklyn College, CUNY, Brooklyn, N.Y. 11210
(2) Dept. of Mineral Sciences, Amer. Museum Nat. Hist. New York, NY 10024.

The EH3 group is the most unequilibrated among the enstatite chondrites. Detailed data on some aspects of these chondrules from a few meteorites and a general summary are available in literature (see Grossman et. al., 1988). Chondrules are common in this group and much less common, rare or absent in the recrystallized groups. This is a progress report of our ongoing study of chondrule populations from different chondritic groups and is based on mineralogical, petrological and bulk chemical data on more than one hundred chondrules from five EH3 meteorites.

Petrography Most of the major textural varieties of chondrules present in ordinary chondrites are also present in the EH3 group. The proportions of the different chondrule varieties are also similar to those in OC. The chondrule sizes in EH3 chondrites are similar but somewhat smaller compared to their counterparts in other chondrites (c.f. Rubin and Grossman, 1987). Among the textural varieties pyroxene porphyritic chondrules are the most common (over 50%). Pyroxene-olivine porphyritic, granular olivine porphyritic are much less abundant. Among the non-porphyritic varieties radial pyroxene chondrules are the most abundant variety. Minor quantities of cryptocrystalline and glassy chondrule are also present. Barred olivine variety is extremely rare or absent. Several chondrules show relict dusty olivine grains. The glassy chondrules exhibit strain textures similar to those observed in OC chondrules.

Euhedral to anhedral grains of olivine and polysynthetically twinned clinoenstatite, are common as phenocrysts. Interstitial glass, cryptocrystalline material or finer grained mineral grains are common in the chondrule matrix. The radial pyroxene chondrules are made up of clinoenstatite blades. Mineral compositions are uniform in individual chondrules but vary from chondrule to chondrule. The olivine and pyroxene compositions are variable in the same range of FeO contents as those in the rest of the meteorite. Feldspathics glass (variable in composition). and silica are also present. Kamacite, taenite, troilite, schriebersite, oldhamite, daubreelite, djerfisherite, and niningerite also occur as accessory minerals in some of the chondrules. Modally EH3 chondrules are pyroxene-rich (about 75 vol %); olivine is lower (average about 20 %) but in some chondrules it is as high as 64 %. Feldspathic glass and silica are usually about 10%. Others are generally in very small quantities.

Discussion The mineralogical and chemical variations among chondrules from different meteorite groups are known to bear general resemblances to their corresponding host condrite groups. The major components of the chondrules and the host chondrites are few and the variations between the chondrule populations could be accounted for by the same processes that caused the variations between the host chondrite groups. The EH3 chondrule oxygen isotopic data are very close to those of OC chondrules and these two groups show little overlap with the CV and CO groups. This indicates that the EH3 chondrules sampled precursors akin to those sampled by OC chondrules. However, the conditions of formation of the two populations are different in terms of iron oxidation as shown by the mineral-chemical data of EH3 contrasted with OC chondrules. Details of systematic variations, or the lack of them, between chondrules from different groups need to be considered further.

References

Grossman, J. N. Rubin: A. E., Nagahara H and King E. A. (1988). In Meteorites and Early Solar System Ed. J. F. Kerridge and M. S. Matthews Univ. Arizona Press. p.680-696. Rubin, A. E. and Grossman, J. N., (1987) Meteorites v. 22, p. 493-494.

W, Sb AND As DEPLETIONS IN THE POMOZDINO EUCRITE AND ANGRA DOS REIS;

H.E. Newsom[#], K.W. Sims[#*] and E.S. Gladney[*,#] Dept. of Geology and Institute of Meteoritics, Univ. of New Mexico, Albuquerque, NM 87131, [*] Los Alamos National Laboratory, Health and Environ. Chem. MS k484, Los Alamos, NM 87545.

INTRODUCTION: The depletion of siderophile elements due to core formation has been well established for several planets, including the Earth, Moon and the eucrite parent body [1,2,3]. Jones et al. [4] have suggested that the parent body of Angra dos Reis may also exhibit evidence of siderophile depletions. We have used a radiochemical epithermal neutron activation analysis technique [5] to determine the abundances of W, Sb and As in the unusual Mg-rich eucrite Pomozdino and the fassaite pyroxenite Angra dos Reis (AdoR). The results of preliminary analyses are: AdoR, 360 ppb W ± 6%, 210 ppb Sb ± 15%, 180 ppb As ± 8%; Pomozdino, 380 ppb W ± 40%, 65 ppb Sb ± 40%, 86 ppb As ± 25%. We hope to have improved analyses, including Mo, in the near future, as well as metal/silicate partition coefficients for As and Sb.

DISCUSSION: The incompatible behavior of W during igneous events on the eucrite parent body has been discussed by [1], and is evident from the correlation between W and La in Fig. 1. Both Pomozdino and AdoR are less depleted in W by a factor of two compared to the incompatible-enriched Bouvante eucrite.

Data for the volatile elements Sb and As are more difficult to interpret due to variability in some samples, such as Juvinas and Stannern (Fig. 2). This variability has been attributed to volatile redistribution by [1]. A similar problem could explain the difference between the high value for our analysis of AdoR and the 9 ppb value from the Chicago lab (Fig. 2) [4]. However, our Sb value, which implys a lesser siderophile depletion for AdoR compared to the eucrites, is consistent with the W and As depletions. The trends for Sb (Fig. 2) and As, excluding the most enriched values for Juvinas and Stannern, also suggest the incompatible behavior of Sb and As during igneous events on the eucrite parent body, consistent with their terrestrial behavior [5]. Pomozdino is also less depleted than Bouvante by a factor of 2 for Sb and As, similar to W.

CONCLUSIONS: Pomozdino may not be a normal eucrite in terms of siderophile depletion. Ibitira is an unusual eucrite that may also be less depleted in many siderophile elements including W (Fig. 1), Sb? (Fig. 2), Co [1], and Mo [2]. The difference in depletions may be due to different conditions during core formation on the same or multiple parent bodies.

AdoR shows significant depletions of the refractory siderophile element W, consistent with core formation on the angrite parent body [4]. Measurement of siderophile elements in the other angrite LEW 86010, which is not so enriched in incompatible elements, may provide useful trends for modelling siderophile element depletions in terms of metal content and other conditions during core formation.

Refs.: [1] Palme and Rammensee (1981) Proc. Lunar Planet. Sci. Conf. 12B, 949-964. [2] Newsom (1985) Proc. Lunar Planet. Sci. Conf. 15, J. Geophys. Res. 90, C613-C617. [3] Hewins and Newsom (1988) in Meteorites and the Early Solar System, 73-101. [4] Jones et al. (1988) Meteoritics 23, 276-277. [5] Sims et al. (1989) in Workshop on the Archean Mantle, L.P.I., 38-40. Support: NASA grant NAG 9-30 (K. Keil), NSF grant EAR 8804070 (Newsom) and the D.O.E. Samples provided by the USSR Academy of Science, and Ed Olsen via Alan Treiman.

Figure 1 Data from [1] and this work.

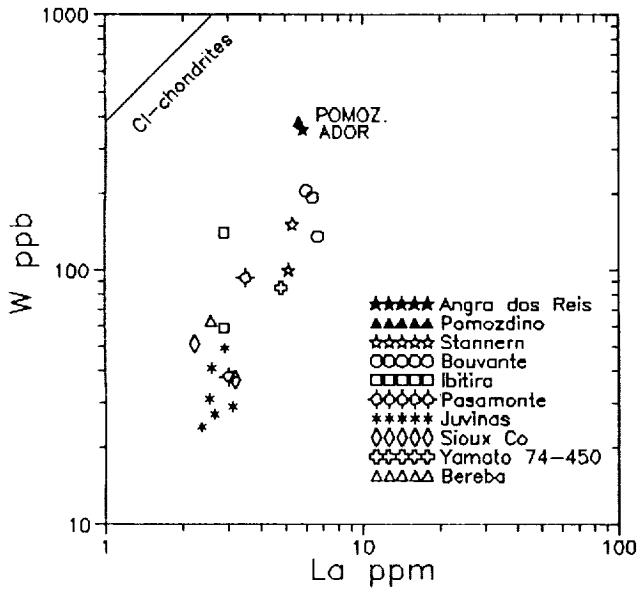

Figure 2 Data from [1] and this work.

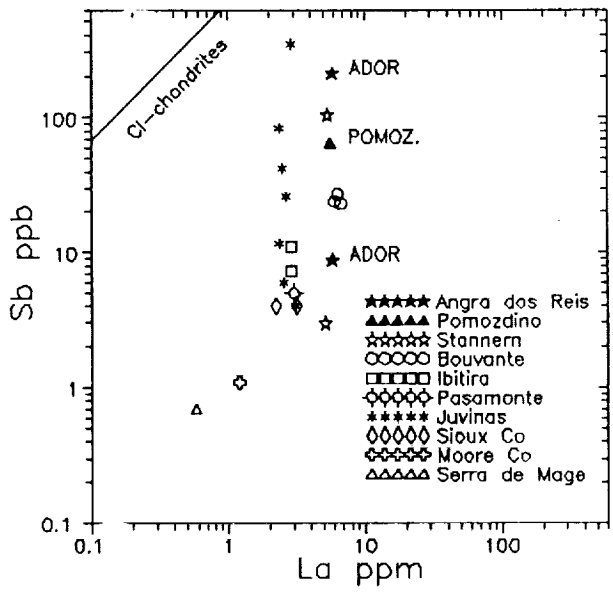

Extended Regolith Histories or An Active Early Sun: Another Piece of the Puzzle.

R. H. Nichols, Jr., C. M. Hohenberg, C. T. Olinger *McDonnell Center for the Space Sciences, Physics Department, Washington University, St. Louis, MO 63130 USA*
J. N. Goswami, *Physical Research Laboratory, Navarangpura, Ahmedabad 380 009, India*

A very large body of data has been gathered on the pre-compaction irradiation of meteoritic breccias. Caffee et al. [1] discovered a correlation between the presence of tracks, revealed by acid etching, and pre-compaction spallation neon. Concentrations of neon in these grains were too high to be easily explained assuming GCR irradiation using constraints on compaction and regolith models available at the time. With an admittedly small data set they also found that samples without tracks did not have detectable excesses of spallation neon. These observations, in conjunction with the similarity in ranges between solar protons and high energy solar flares led them to conclude that an active early (T-Tauri) phase of the sun was suggested by the data [2].

Further work, analyzing grains individually, extended the requirement of pre-compaction irradiation, and found that the overlap between the track-rich grains and track-free grains was indeed very small [3,4]. Grains classified as track-free generally displayed no polished surface abnormalities after etching. A subset of grains not classified in either bin contain no solar flare or GCR tracks, but the grains do contain minor surface pits after etching, possibly due to damage from spallation recoil of the target nucleus.

Interestingly, early results suggest that the grains which display only spallation recoil tracks bridge the gap between the two earlier catagories. Some of these have GCR model ages comparable to the early results on track rich grains obtained by Caffee et al. The importance of this observation comes from the fact that up to now the overlap between track-rich and track-free grains was considered insignificant, and possibly non-existant. Such a near perfect correlation was difficult to understand in any model without resorting to ad hoc arguments [1,5,6]. The continuum now seen not only in the age distribution of track rich grains, but in track free grains as well, allows for more palatable models. Concentrations of neon in individual grains still represent tremendous exposures (extreme in either duration or flux or both) which must be explained. However, the data no longer requires a model where grains are either exposed to both track-producing particles and spallation producing particles or exposed to neither.

The present data demand a model which allows for a few grains to be exposed near the surface of the parent body long enough to get track damage from VVH nuclei, but for a short time on a spallation production time scale; other particles that never reached close enough to the surface to be irradiated by VVH nuclei, but close enough for secondary protons/neutrons to produce spallation; some grains that received irradiation by both suites of particles; and a majority of grains that never saw either during their parent body residence.

The jury is clearly still out on whether a T-tauri irradiation or extended regolith exposure (or both) is required, but this is a new and potentially important piece of the puzzle.

References: [1] Caffee, M. W. *et al.* (1983), *J. Geophys. Res.* **88**, B267. [2] Caffee, M. W. (1986), Ph.D. Thesis, Washington University. [3] Olinger, C. T. *et al.* (1988), *Meteoritics* **23**, 295. [4] Nichols, R. H. *et al.* (1989), Lun. Planet. Sci. XX, 786. [5] Weiler, R. *et al.* (in press), GCA. [6] Pedroni, A. *et al.*, Lun. Planet Sci. XIX, 913.

Re-Os DATING OF IIIAB AND SILICATE-BEARING IRON METEORITES;
S. Niemeyer, D. Gerlach, and G.P. Russ III, Lawrence Livermore National Laboratory, P.O. Box 808, Livermore, CA 94550

The development of Re-Os dating techniques provides a means for directly dating metal and sulfide phases in meteorites. The purpose of this study is to address the issue of metal-silicate fractionation in the early solar system. We focus initially on the IAB iron meteorites because of their chondritic affinities, e.g. most siderophile trace elements have relative abundances similar to "cosmic" ratios, and the silicate inclusions are chondritic in mineralogy and bulk composition. ^{40}Ar-^{39}Ar dating of IAB silicates have plateau ages ranging from 4.50 to 4.57 Ga (Niemeyer, 1979). However, the recent laboratory measurement of the ^{187}Re half-life (Lindner et al., 1989) coupled with earlier Re-Os measurements of iron meteorites (Luck and Allegre, 1983; Walker and Morgan, 1989) indicate an age of 4.15 Ga for all the analyzed irons.

We have developed techniques for Re and Os separation from 0.1-1.0 g iron samples with typically 90% yields. Os concentrations and $^{187}Os/^{188}Os$ ratios are determined in a single analysis by adding a ^{192}Os spike. Measurements are made with an ICP-MS using similar techniques for Os isotopic compositions as in the half-life work, whereas Re is currently analyzed using the nebulization mode. Typical precisions at the 95% confidence level are 1% for the $^{187}Os/^{188}Os$ ratios (for several ng of Os), as well as for Re and Os abundances. Analyses have been completed for two IAB iron meteorites. The $^{187}Os/^{188}Os$ ratio for Pitts is 0.1239 $\pm$ .0012 (2-sigma) and for Woodbine is 0.1275 $\pm$ .0012, but in contrast to expectations, Woodbine with the more radiogenic Os has a lower Re/Os ratio (both Re/Os ratios fall within the range for the the cosmic ratio). This non-correlation was also observed by Walker and Morgan (1989) for some carbonaceous and unequilibrated ordinary chondrites. Thus within each suite, i.e. primitive stony meteorites and IAB irons, meteorites have either different initial Os isotopic ratios, different Re-Os closure ages, or both.

Because of the discordancy of these two IAB meteorites, we will next attempt to obtain internal isochrons for individual IAB meteorites. Once we complete our calibration of the ^{192}Os spike against the same natural Os standard used for the half-life determination, we will then be able to calculate Re-Os ages which will be nearly independent of any error in the Os normal. Data will also be obtained from IIIAB iron meteorites because they represent metal samples which clearly are the product of planetary fractional crystallization. The comparison of Re-Os systematics for IAB and IIIAB iron meteorites should provide insight into the relative time-scales of metal-silicate fractionation in chondritic-like materials and the formation of planetary iron cores.

Lindner M., Leich D.A., Russ G.P., Bazan J.M., and Borg R.J. (1989) Geochim. Cosmochim. Acta, in press.
Luck J.-M. and Allegre C.J. (1983) Nature 302, 130.
Niemeyer S. (1979) Geochim. Cosmochim. Acta 43, 1829.
Walker R.J. and Morgan J.W. (1989) Nature 243, 519.

COSMOGENIC RADIONUCLIDES IN INDIVIDUAL COSMIC PARTICLES;

K. Nishiizumi, J. R. Arnold, Department of Chemistry, B-017, University of California, San Diego, La Jolla, CA 92093, D. Fink, J. Klein, R. Middleton, Department of Physics, University of Pennsylvania, Philadelphia, PA 19104-3859, D. E. Brownlee, Department of Astronomy, University of Washington, Seattle, WA 98195, M. Maurette, Laboratoire René Bernas, Orsay, France.

As new sources of spherules and extraterrestrial fragments in the sub-millimeter range are developed in Greenland and the Antarctic (Maurette et al., 1987; Maurette and Brownlee, 1989), it becomes more interesting than ever to understand their nature and origin. Raisbeck and colleagues (Raisbeck et al., 1983) showed that the pattern of cosmogenic radionuclides in a representative suite of large deep sea spherules conformed to that expected for fused meteoroids whose masses were of the same order as those of the recovered spherules. That is, a wide range of activities was seen, showing clear evidence of SCR (solar cosmic rays) effects in some cases, and of low total GCR (galactic cosmic rays) production (shorter life) in others.

Two questions seem to us important at this stage. First, since spall droplets from larger meteoroids must occur, what is their proportion and how may they be identified? Second, what is the distribution of micrometeoroid lifetimes? Note that calculated ages (Dohnanyi, 1978; Grün et al., 1985) seem to be much shorter than those corresponding to the measurements of Raisbeck et al, (1983) and Nishiizumi (1983).

We have measured the content of ^{10}Be and ^{26}Al in a collection of individual large deep-sea spherules (20-200 μg) from the Pacific Ocean (Brownlee et al., 1979; Murrell et al., 1980) and in extraterrestrial fragments from Greenland ice (Maurette et al., 1987). ^{26}Al activities in these spherules seem to fall into two groups. Many spherules contain high ^{26}Al, up to ~270 dpm/kg, which is produced by SCR bombardment of the small objects in space. On the other hand, a significant number of spherules contain 30-50 dpm ^{26}Al/kg, similar to chondritic values. The observed ^{10}Be contents are about 10 dpm/kg or less as expected, since ^{10}Be is not produced by SCR. ^{10}Be content can be used to estimate exposure time in space. The chondritic level values of ^{26}Al and the corresponding ^{10}Be values suggest that this population of spherules may have received GCR bombardment in objects of sufficient size to produce saturation levels of these nuclides (Reedy, 1987) comparable to those familiar to meteoriticists, say >5 cm. The implications of this will be discussed, along with suggested further experiments.

References

Brownlee, D. E., et al. (1979) Lunar Planet. Sci. **X**, 157-158.
Dohnanyi, J. S. (1978) in Cosmic Dust (Wiley) 527-605.
Grün, E., et al. (1985) Icarus **62**, 244-272.
Maurette, M., et al. (1987) Nature **328**, 699-702.
Maurette, M. and Brownlee, D. E. (1989) Lunar Planet. Sci. **XX**, 636-637.
Murrell, M. T., et al. (1980) Geochim. Cosmochim. Acta **44**, 2067-2074.
Nishiizumi, K. (1983) Earth Planet. Sci. Lett. **63**, 223-228.
Raisbeck, G. M., et al. (1983) Lunar Planet. Sci. **XIV**, 622-623.
Reedy, R. C. (1987) Proc. 17th Lunar Planet. Sci. Conf., J. Geophys. Res. **92**, E697- E702.

^{129}I DEPTH PROFILES IN CORES FROM JILIN AND THE MOON : K. Nishiizumi, P. W. Kubik*, P. Sharma* and J. R. Arnold, Department of Chemistry, B-017, University of California, San Diego, La Jolla, CA92093, *Nuclear Structure Research Lab, University of Rochester, Rochester, NY14627

Activity vs. depth profiles of cosmic ray produced ^{129}I (half life = 1.57×10^7 yr) were measured in bulk samples from two cores in the Jilin chondrite and in soil from lunar cores 12028 and 60009/10. The AMS (accelerator mass spectrometry) measurements of ^{129}I were carried out using the University of Rochester MP tandem van de Graaff accelerator [1, 2].

Jilin : ^{129}I was measured in two cores, A and B. Cores A (64.8 cm) and B (105 cm) were drilled perpendicular and parallel, respectively, to the surface of the 2π first stage irradiation [3]. The depth of core B from the surface during the 2π irradiation was at least 85 cm, and both cores intersected at the geometric center of the body during the second stage irradiation [3]. Figure 1 shows ^{129}I activities in core A. The horizontal axis indicates distance from one end of the core (A-37) which is estimated to have been about 250 g/cm^2 depth from the surface during the 2π irradiation. The main target element for production of cosmogenic ^{129}I in meteorites is Te. It is produced by both ^{130}Te(n, 2nβ)^{129}I and ^{128}Te(n,γβ)^{129}I reactions [2]. We do not know the Te concentrations in our specific samples. However assuming a homogeneous Te content of 570 ± 150 ppb [4] and an 8 My first stage irradiation [e. g. 5], the production rate of ^{129}I can be calculated to be 0.95 - 2.1 atom/min g Te. These values are higher than those previously determined for Abee, Allende,and Dhajala [2] as expected, since the large preatmospheric size of Jilin means more low energy neutrons. The maximum production of ^{129}I in core A is seen at about 300 g/cm^2 depth from the surface of the 2π irradiation. This depth is somewhat greater than the location of the maximum production of the (n,γ) product ^{60}Co in lunar cores [6]. It is puzzling that the ^{129}I activities near the ends of core B are higher than at the center, since the entire length of core B was exposed to cosmic rays at the same depth except for the very short, 0.4 My, second stage irradiation.

Lunar cores : Figure 2 shows ^{129}I in double drive tubes 12028 and 60009/10. The surface gardening depths are less than 20 g/cm^2 and 10 g/cm^2, respectively, based on the ^{53}Mn profiles [7]. The ^{129}I profile doesn't show evidence of gardening at 23 g/cm^2 in 60010. Low ^{129}I at 30 g/cm^2 in 12028 indicates a small amount of contamination by the unique soil from unit VI which is located just above the sample measured [8] and whose Ba content is very low [9]. Since the lunar concentrations of Te and Cs are very small, the main target element for the production of ^{129}I in lunar samples is Ba ,with a small amount of production from La and Ce. The production rates of ^{129}I in the cores are calculated to be 2.8 - 4.5 atom/min g Ba using published chemical compositions [9, 10, 11]. The ^{129}I activities decrease with increasing depth below 60 g/cm^2. Lack of various cross sections for production of ^{129}I prevents calculation of the Reedy-Arnold theoretical profiles [12]. More detailed ^{129}I measurements will extend the study of lunar surface mixing to a few tens of millions of years.

References : [1] Elmore, D. et al., (1980) Nature 286, 138-140;[2] Nishiizumi, K. et al., (1983) Nature 305, 611-612;[3] Ouyang, Z. et al., (1987) Scientia Sinica, 30, 885-896;[4] Sakuragi, Y. and Lipschutz, M. E. (1985) EPSL, 72, 299-303;[5] Honda, M. et al., (1982) EPSL, 57, 101-109;[6] Wahlen, M. et al., (1973) EPSL, 19, 315-320;[7] Nishiizumi, K. et al., (1979) EPSL, 44, 409-419;[8] Duke, M. B. and Nagle, J. S. (1976) Lunar Core Catalog, JSC 09252;[9] Schnetzler, C. C. and Philpotts, J. A. (1971) PLSC 2nd, 1101-1122;[10] Ali, M. Z. and Ehmann, W. D. (1976) PLSC 7th, 241-258;[11] Ali, M. Z. and Ehmann, W. D. (1977) PLSC 8th, 2967-2981;[12] Reedy, R. C. and Arnold, J. R. (1972) JGR, 77, 537-555.

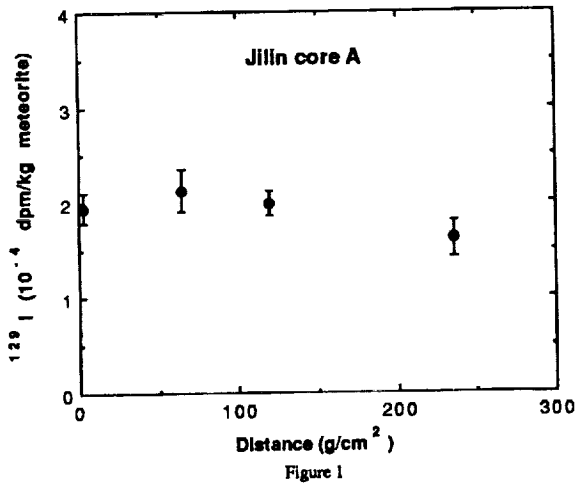

Figure 1

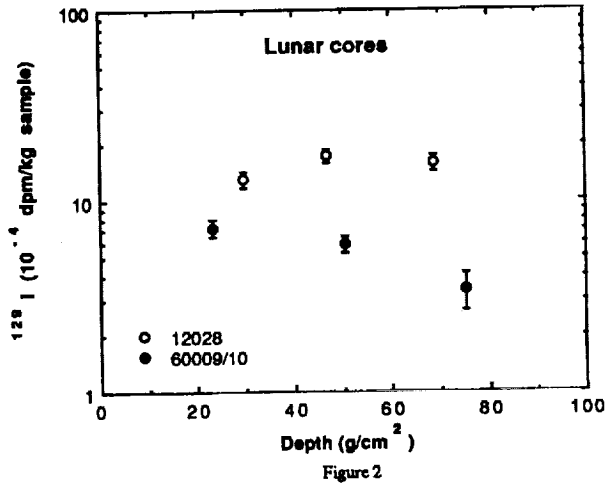

Figure 2

Student paper, Grant application

STOCHASTIC EVOLUTION OF ASTEROIDS TO PRODUCE THE ORDINARY CHONDRITES; M. C. NOLAN AND R. GREENBERG, Lunar and Planetary Laboratory, University of Arizona, Tucson, AZ 85721 USA.

Introduction. The asteroids have been widely argued to be the sources of most of the meteorites that fall on the Earth. This presents the issue of connecting specific meteorites with specific parent asteroids, or with classes of asteroids. The difficulty is that the most common type of meteorites (ordinary chondrites) do not appear to be derived from the most available asteroids (Gaffey, 1986). There are also the puzzling data on meteorites recovered from Antarctica, which indicate that the "average" properties of meteorites may have changed measurably over the last 100,000 years, an implausible timescale for the asteroid belt as a whole.

Perhaps the observed population of meteorites is not representative of the population of asteroids, but is instead a result of stochastic collisions of asteroids that deliver to the Earth predominantly products of a single (or a few) large asteroid(s). In this case, most of the meteorites we see would be derived from a very small number of parent bodies; so that most of our meteorites would be the product not of a mean population of asteroids but a few random ones, and cannot be expected to represent the asteroid belt as a whole, except over a period of time much longer than we are able to sample.

Methods. Our preliminary model for the collision behavior of the asteroids which are in orbits en route to the Earth works by "painting" all of the larger asteroids (parent bodies) a different "color" so that their collisional products can be followed, and allowing the system to evolve collisionally. Thus we can determine whether meteoroids are predominantly one color and thus fragments of a particular parent body. For a range of reasonable input parameters relating to the size distributions of asteroids and their collisional lifetimes, single parent bodies are able to contribute from 1 to 4 % of the total meteoroid population, with one to four parent bodies being recognizable at any one time. As the model progresses in time, different colors predominate, as new parent bodies begin generating meteorites and old ones lose importance over millions to billions of years.

Results. The simple model has shown that meteorites are not a uniform sample of the asteroid belt, or even of the dynamical regions in the belt which can put asteroids into Earth-crossing orbits, but rather that stochastic collisions allow single asteroidal parent bodies to produce a significant fraction of the meteorites. The ordinary chondrites however form more than 80 % of the known meteorites, a result not predicted by the simple model as a stochastic variation. We plan to expand the current model into one which, in addition to collisional breakup, includes the known mechanisms for migration of asteroid orbits from the asteroid belt (such as the resonances with Jupiter's orbit), as well as the related loss processes. The effects can reasonably be expected to further reduce the sampled population, and thus significantly increase the observed stochastic variations.

M. J. Gaffey (1986) *Icarus* 66, 468–486.

PETROLOGY OF SULFIDES AND FE-Ni METAL FROM KHOR TEMIKI AUBRITE. Th. Ntaflos[1], K. Keil[2] and H. E. Newsom[2]. [1]BVA-Arsenal, Geotechnisches Institut, Wien, Austria. [2]Institute of Meteoritics , University of New Mexico, Albuquerque, NM 87131

The Khor Temiki aubrite is a regolith breccia with highly variable REE contents (1,2). Newsom et al. (2) studied numerous clasts (dark and light) and found that the dark clasts have variable REE contents, probably attributable to variable oldhamite contents. They conclude that probably the dark clasts are not the basaltic complement of the aubritic pyroxenites as suggested by (1). Further studies show that Khor Temiki contains material from at least two different sources that may or may not have formed in the same parent body.

Results: Khor Temiki consist mainly of enstatite with little olivine, diopside or plagioclase. Opaque phases enclosed by enstatite or embedded in the matrix, are troilite, kamacite, oldhamite, daubreelite, alabandite, djerfisherite and osbornite. Coarse grained enstatite up to 2 mm are rich in micron-sized vesicles. Many vesicles contain sulfides, like troilite, djerfisherite or Fe-Ni metal occupying less than 20 vol% of the vesicle area. These vesicles found, by SEM procedures, appear to be largely empty and are probably the same as those described by (3).

The silicates are compositionally homogeneous. Kamacite and troilite are highly variable in Si, Ni and Ti, Fe, Cr contents, respectively. The Si concentrations within kamacite range between <.02 and 1.81 wt% and the Ni concentrations between 0.10 and 5.2 wt%. There is no correlation between kamacite grain size and Si or Ni concentration. Likewise, there is no correlation between Ni concentration and whether the kamacite is enclosed by silicates or not.. Like kamacite, troilite is highly variable in composition. Ti content varies between <.02 and 14.3 wt%. A compositional gap between 5.7 and 8.2 wt% Ti provides two populations: one with low Ti content up to 5.7 wt% and one with high Ti from 8.2 to 14.3 wt %. Osbornite appears to be pure (α)TiN.

Discussion:The presence of at least two populations of troilite (high and low Ti content), the high and low Si content in kamacite, the high variability of the REE concentrations of the different clasts suggest mixing of at least two lithologies, i.e. metal and sulfides from one source with metal and sulfides from yet another source.

A magmatic origin for the enstatite achondrites, as opposed to a condensation origin, is supported by our observation of vesicles in the enstatite which are now largely empty, but which also contain small amounts of metallic Fe-Ni or sulfides similar to vesicles observed in many terrestrial magmatic environments (3).

References: (1) Wolf et al. (1983) GCA, 47, 2257, (2) Newsom et al. (1986) Meteoritics, 21, 469, [3] Roeder E., (1981) Bull. Mineral. 104, 339

^{147}Sm-^{143}Nd AGE AND INITIAL $^{146}Sm/^{144}Sm$ RATIO OF AN EUCRITE CLAST IN THE BHOLGHATI HOWARDITE. L. E. Nyquist[1], H. Wiesmann[2], B. M. Bansal[2], and C.-Y. Shih[2]. [1]NASA Johnson Space Center, Houston, TX 77058, [2]Lockheed Engineering and Science Co., Houston, TX 77058.

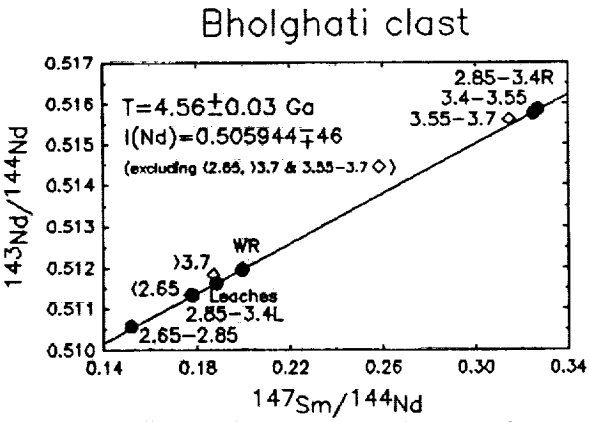

Figure 1. Sm-Nd internal isochron for the large eucrite clast from the Bholghati howardite.

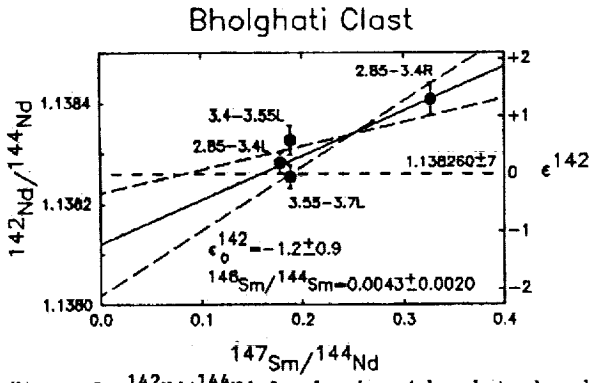

Figure 2. $^{142}Nd/^{144}Nd$ for leaches (phosphates) and the residue of the 2.85-3.4 g/cm^3 fraction.

^{147}Sm-^{143}Nd Age: Major mineral phases severely disturbed in the Rb-Sr system of the Bholghati clast (>3.7 g/cm^3 ilmenite, 3.55-3.7 g/cm^3 pyroxene; (1)) are also slightly disturbed in the Sm-Nd system (Figure 1). The remaining analyses yield a well-defined isochron corresponding to an age of 4.56±0.03 Ga and initial $^{143}Nd/^{144}Nd$ = 0.505944±46 normalized to $^{146}Nd/^{144}Nd$ = 0.72414 (equivalent to $^{148}Nd/^{144}Nd$ = 0.24308). The initial $^{143}Nd/^{144}Nd$ value is ~1 ϵ-unit higher than the CHUR value (2) although we measure the CIT nNdβ standard about 0.8 ϵ-units lower than the CIT value (3). These discrepancies are under investigation.

Initial $^{146}Sm/^{144}Sm$ Ratio: The antiquity of the clast suggests that variations in $^{142}Nd/^{144}Nd$ due to the *in situ* decay of ^{146}Sm should be observable. Precise measurements of $^{142}Nd/^{144}Nd$ require simultaneous monitoring of the Ce background which was done only for our later analyses; i.e., the three leaches and the leach residue of the 2.85-3.4 g/cm^3 fraction. $^{142}Nd/^{144}Nd$ ratios of the three leach fractions are close to those measured for the isotopic standard, whereas the 2.85-3.4 g/cm^3 leach residue shows an excess of ^{142}Nd (Figure 2). An initial $^{146}Sm/^{144}Sm$ ratio of 0.0043±0.0020 is obtained from the correlation of $^{142}Nd/^{144}Nd$ and $^{144}Sm/^{144}Nd$. This value agrees well with values for Juvinas (4), Moama (2), and Allende (5), but is lower than that for Ibitira (6). The Bholghati value also agrees well with the value reported for Angra Dos Reis by (7), but is lower than that reported by (2). The (ϵ_o^{142}, $^{146}Sm/^{144}Sm$) parameters of the Bholghati clast are nearly identical to those of Moama (2) implying an age of ~4.46 Ga for the correlation between ϵ_o^{142} and $^{146}Sm/^{144}Sm$ presented in (6).

Discussion: Both the ^{147}Sm-^{143}Nd and ^{146}Sm-^{142}Nd chronometers show the Bholghati clast to be ≥4.46 Ga old. The two chronometers are concordant for $^{146}Sm/^{144}Sm$ ~0.0045 in the early solar system as inferred by (5) from measurement of recoil Nd in a carbon-chromite fraction of Allende. The disturbances apparent in the isotopic systems suggest that caution be exercised in interpreting these results.

References: (1) Nyquist L.E. et al. (1989) Lunar Planet. Sci. XX, 798-799. (2) Jacobsen S.B. and Wasserburg G.J. (1984) EPSL 67, 137-150. (3) Wasserburg G.J. et al. (1981) GCA 45, 2311-2323. (4) Lugmair G.W. et al. (1975) EPSL 27, 79-84. (5) Lugmair G.W. et al. (1975) Science 222, 1015-1018. (6) Prinzhofer et al. (1989) Lunar Planet. Sci. XX, 872-873. (7) Lugmair G.W. and Marti K. (1977) EPSL 35, 273-284.

ORIENTATION AND PLANE OF POLISH OF OCTAHEDRITES-METHOD II

R. E. Ogilvie, Dept. of Mat. Sci., MIT, Cambridge, MA 02139

To determine the orientation and plane of polish of octahedrites by METHOD I, it was necessary to have four traces visible on the plane of polish. However, this is not always possible. Therefore, METHOD-II was developed which requires only three traces. As before, a reference plane is selected and designated as the $(11\bar{1})$ plane. The angles must be selected so that $\theta > \eta < \phi$ (see Figure 1).

With the conditions as defined, the $[11\bar{1}]$ pole must lie on the central north-south meridian of the stereographic projection. It is assumed that it lies south of center, which means that it can be on the back side of the projection. Therefore, the $[\bar{1}\bar{1}1]$ pole will be to the north. The [111] pole will lie nearest to the center. The other {111} poles will have a position as illustrated in Figure 2.

In the two spherical triangles shown in Figure 2, $A = 180-\theta$, $B = 180-\phi$, $N = 109.47°$, and $q + p = 120°$. From the conditions set forth, q and p will have values between 30° and 90°. The program steps from 30° to 90° calculating γ_1 and γ_2 ; when $\gamma_1 - \gamma_2$ changes sign, a solution has been passed. The program then determines the correct q to evaluate γ. The following equations are used for this procedure:

$$\sin(\gamma_1 - M_1) = \text{ctn } A \tan q \sin M_1$$
$$M_1 = 180 + \tan^{-1}(\cos q \tan N)$$

$$\sin(\gamma_2 - M_2) = \text{ctn } B \tan p \sin M_2$$
$$M_2 = 180 + \tan^{-1}(\cos p \tan N)$$

$$\cos\alpha = \cos N \cos\gamma + \sin N \sin\gamma \cos q$$
$$\cos\beta = \cos N \cos\gamma + \sin N \sin\gamma \cos p$$

With this procedure, it is possible that more than one solution will be obtained. The angle ϵ is evaluated for each and if the (111) trace is visible the correct solution can be determined. It must be remembered that the (111) trace may be visible but cannot be measured accurately. If the (111) trace is not visible, then a second surface must be prepared to measure one of the three angles α, β, or γ.

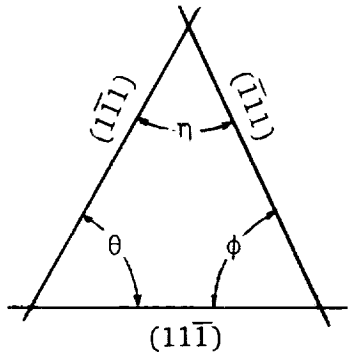

Fig. 1. {111} Traces

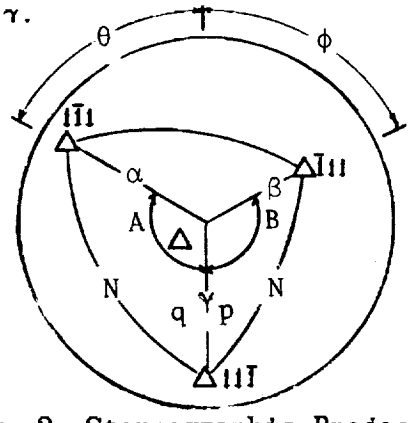

Fig. 2. Stereographic Projection

ORIENTATION AND PLANE OF POLISH OF OCTAHEDRITES-METHOD I

R. E. Ogilvie and J. Chang, Dept. of Mat.Sci., MIT, Cambridge, MA 02139

There have been many approaches to determine the orientation and plane of polish of octahedrites. They include the very complicated method of Drazin and Otte (1963) and the very easy to use tables of Buchwald (1968).

Two new methods have been developed to determine the orientation and plane of polish. METHOD I is described here. This method requires that traces of four octahedral planes are visible. The first step is to select one of the traces as the reference plane and designated as the $(11\bar{1})$ plane. It is necessary that $\theta > \eta < \phi$ (see Figure 1). With the traces defined as in Figure 1, the following equations can be determined:

$$r_1 = \begin{vmatrix} i & j & k \\ h & k & l \\ 1 & 1 & \bar{1} \end{vmatrix}, \quad r_2 = \begin{vmatrix} i & j & k \\ 1 & \bar{1} & 1 \\ h & k & l \end{vmatrix}, \quad r_3 = \begin{vmatrix} i & j & k \\ h & k & l \\ \bar{1} & 1 & 1 \end{vmatrix}, \quad r_4 = \begin{vmatrix} i & j & k \\ h & k & l \\ 1 & 1 & 1 \end{vmatrix}$$

$$\tan\theta = \frac{r_1 \times r_2}{r_1 \cdot r_2}, \quad \tan\phi = \frac{r_1 \times r_3}{r_1 \cdot r_3}, \quad \tan\epsilon = \frac{r_1 \times r_4}{r_1 \cdot r_4}, \quad \tan\eta = \frac{r_2 \times r_3}{r_2 \cdot r_3}$$

where i,j,k are unit vectors, r_1 , r_2 , r_3 are vectors parallel to the traces on the plane of polish, and h,k,l are the Miller indices of the plane of polish. If we employ the direction cosines for h,k,l, the following equations can be evaluated:

$$\tan\theta = \frac{k+l}{h^2+kl}, \quad \tan\phi = \frac{h+l}{k^2+hl}, \quad \tan\epsilon = \frac{h-k}{l^2-hk}, \quad \tan\eta = \frac{h+k}{l^2+hk}$$

The first three tan functions can be solved by Newton's method of successive approximations to determine h,k,l. The program also determines the angles of the $\langle 111 \rangle$ poles with respect to the [hkl] pole of the plane of polish.

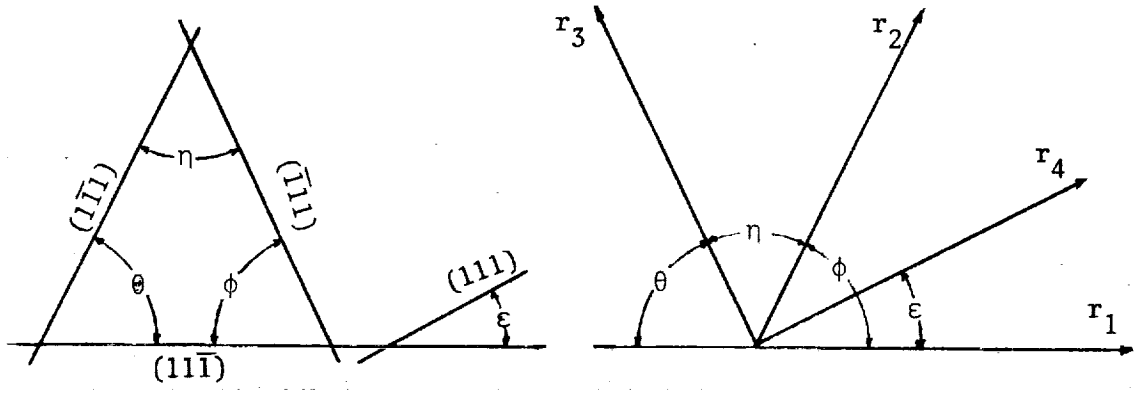

Fig. 1. Traces of the (111) planes on the plane of polish.

Buchwald, V.F., 1968 THE AUSTENITE-FERRITE TRANSFORMATION
Drazin, M.P. and Otte, H.M., 1963 phys. stat. sol. 3, 824

NOBLE GAS MEASUREMENTS OF EXTRATERRESTRIAL PARTICLES FROM ANTARCTIC SEDIMENT; C. T. Olinger, R. M. Walker, C. M. Hohenberg, McDonnell Center for the Space Sciences and Physics Department, Washington University, St. Louis, MO 63130 USA. M. Maurette, Laboratory Rene Bernes, University of Paris, Orsay, France.

Several particles found in Antarctic glacial sediment have been measured to determine their neon concentrations and isotopic compositions. Similar to our earlier study on particles from Greenland sediment [1], the results confirm an extraterrestrial origin for many of these ~100 micron particles. Results also suggest that some particles survive entry with limited heating and that some were exposed as micrometeoroids, and are not ablation products of larger meteorites.

Large numbers of micrometeorites have been collected from approximately 100 tons of blue ice near Cape Prudhomme, Antarctica [2] . Twenty-nine of these were mounted in acrylic plugs (mount AWU01) and polished to allow internal characterization using SEM-EDS techniques. Following documentation of micrographs and spectra, the acrylic plugs were dissolved in a stream of acetone, after which the freed particles were retrieved, individually weighed and 24 were mounted in aluminum sample holders for Ne analyses by laser extraction techniques[3].

Ne data establishes the extraterrestrial origin of 9 of these samples, each of which have a roughly chondritic elemental spectrum. The trapped neon component is usually dominated by an SEP composition defined by Wieler *et al.* [4] (see Fig. 1). Error bars on particle 14 prevent an absolute identification of origin based on composition. However, the neon concentration is significantly higher than terrestrial sediments [5], suggestive of extraterrestrial origin. All other particles in this study had gas amounts near blank level, or large corrections at ^{22}Ne due to doubly charged CO_2, preventing identification based upon neon alone. Some of these showed obvious signs of melting and thus degassing, possibly from atmospheric entry, while others had elemental spectra similar to terrestrial debris.

Of the particles shown here, three are especially noteworthy. Particles 13 and 19 are euhedral, yet have neon concentrations orders of magnitude higher than their gas-rich meteorite analogues. This would suggest at least these particles were exposed as individual micrometeoroids. They are not ablation products, and are not significantly degassed during atmospheric entry. Particle 9 has a high gas concentration, yet appears totally melted. Therefore, either the melt structure is due to pre-entry processes as shown to occur by Hanchang *et al.* [6], or its heat/quench cycle during entry was very rapid, preventing degassing as G. Turner has observed in some fusion crust samples [personal comm.].

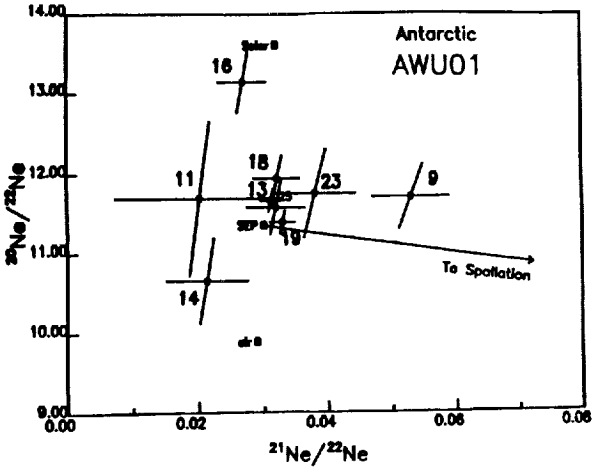

Figure 1. Neon isotopic structure of particles from AWU01 with measurable neon.

REFERENCES: [1] Maurette, M., *et al* . (1989), *Lunar Planet. Sci.* XX, 640-641. [2] Maurette, M., *et al.* (1989), *Lunar Planet. Sci.*, XX, 644-645. [3] Olinger, C. *et al.* (1988), *Meteoritics* 23, 295. [4] Wieler, R. *et al* (1986), *GCA* 50, 1997-2017. [5] Ozima, M., Podosek, F. (1983), Noble Gas Geochemistry, Cambridge Univ. Press. [6] Hanchang, P., Zhenkun, L. (1989), *Lunar Planet. Sci.*, XX, 836-837.

CORRELATION BETWEEN PLAGIOCLASE CRYSTAL MORPHOLOGY AND COOLING KINETIC OF BOLTYSH ASTROBLEME IMPACT MELT (USSR).
A.O.Orlova, L.V.Sazonova, V.I.Feldman. Geological Faculty, Moscow State University, USSR 119899 GSP Moscow.

Melted impactites of Boltysh Astrobleme have been formed in place of granites and granito-gneisses of Archaean fundament of Russian Plate. Plagioclases of impactites characterized by some morphological and chemical features (1). There are the tabular crystals and the tabular in the core of the crystal with the transformation forms to the skeletal growth at the exterior parts of crystals (fig.1). The gradual alternation of chemical contents along the tabular crystal surface reflects the local equilibrium at crystal-melt range. The main crystallographic forms of this growth stage crystals are as follows: (010),(110),(100). The tabular-skeletal morphological transformation is accompanished by the abrupt leap in plagioclase chemistry. The skeletal parts of crystals are characterized by the increasing of K-content. This may be connected with the change of local equilibrium on the crystal-melt surface. The growth rate exceeds the diffusion rate of the necessary components (Ca and Na). The lack of Ca and Na is compensated in plagioclase crystal structure by K (1)

The above mentioned features reflect the increasing of melt viscosity, the fall of its temperature, the leap in supersaturation of melt and the increasing of crystal growth rates. These factors lead to the formation of the following crystallographic forms inside the space ranged by skeletal forms: {110}, {130}, {101}, {201}, {111}, {021}. The 010 , however, preserves as the main habit form of such crystals.

REFERENCES: (1) Sazonova L.V., Korotaeva N.N. - Meteoritika, 1989, N 48. (In Russian).

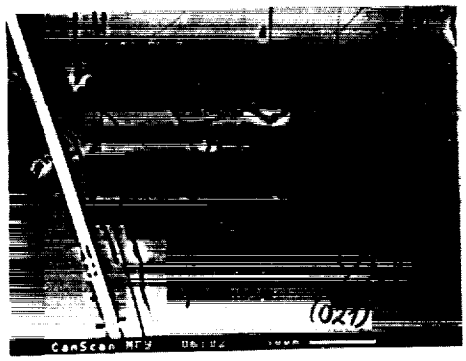

Fig.1

CORRELATED ISOTOPIC ANOMALIES OF XE AND BA IN MURCHISON;

U. Ott, K. Kallas, S. Schmitt-Strecker and F. Begemann, Max-Planck-Institut für Chemie, Saarstraße 23, D-6500 Mainz, F.R.G.

A wealth of data exists on isotopic variations of Xe in primitive meteorites (e.g. [1] and references therein). Some unresolved questions such as the nature of the trapping processes and the nuclear origin of HL-Xe, however, may require the search for correlated isotopic variations in neighboring elements [2].

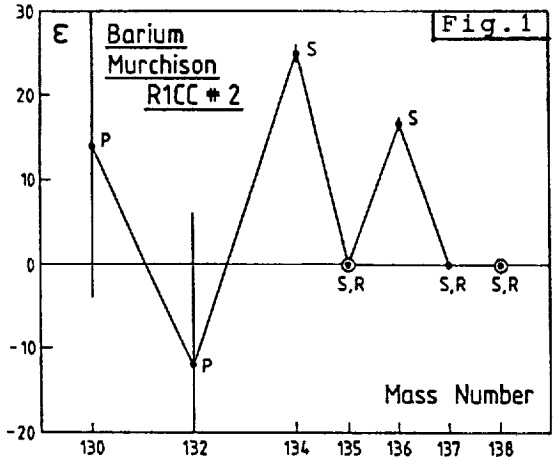

We have analyzed for its Ba isotopic composition a residue from C2M Murchison (R1CC), resistant to HF/HCl, $HClO_4$ (~195°) and H_3PO_4 (~180°C), which is expected to contain Ne-E(H), s-Xe and Xe-HL [3]. Analyses were done using the direct loading technique. Results from one run (No.2) are shown in Fig.1; $^{135}Ba/^{138}Ba$ = 0.091940 was used as internal standard for fractionation correction [2,4]. In this representation, clear excesses of ~20 ε-units show up at the s-only isotopes ^{134}Ba and ^{136}Ba.

Comparison of the s-Ba excess (Ba abundance in R1CC ~100 ppm (wt.) as determined by ion probe) with the amount of s-Xe in a similar sample (Murchison CFP [5]) implies that trapping of the s-process component was chemically highly selective, with a fractionation factor Ba/Xe on the order of several thousand.

Addition of s-process Ba will have altered $^{135}Ba/^{138}Ba$, so that a fractionation correction based on this ratio is not correct. A better choice may be the ratio of the s-only isotopes $^{134}Ba/^{136}Ba$, provided that the extra s-contributions here do not differ in composition from average solar system s-material, an assumption consistent with the Xe data [5,6,7]. In this normalization all isotopes with non-s contributions show deficits (R1CC No.2 in ε-units: 135: -21±1, 137: -12.5±1.3, 138: -8.4±1.9). The relative size of the deficits at masses 135 and 137 argues for an s-contribution distinctly different from average solar system s-matter or an excess at ^{135}Ba from another source.

References: [1] Anders E. (1988) In: Meteorites and the Early Solar System, p. 927ff. University of Arizona Press. [2] Lewis R.S et al. (1983) Science 222, 1013. [3] Tang M. and Anders E. GCA 52, 1235. [4] McCulloch M.T. and Wasserburg G.J. (1978) Ap. J. 220, L15. [5] Ott U. et al. (1985) Meteoritics 20, 722. [6] Ott U. et al. (1988) Nature 332, 700. [7] Tang M. and Anders E. (1988) GCA 52, 1245.

LOSS OF TUNGSTEN FROM REFRACTORY METAL CONDENSATES BY HIGH-TEMPERATURE OXIDATION.

H. Palme, A. V. Köhler, B. Spettel and I. D. Hutcheon*
Max-Planck-Institut für Chemie, Saarstrasse 23, D-65 Mainz, F. R. G.
*Div. Geol. & Planet. Sci., Caltech, Pasadena, CA 91125, U. S. A.

We recently reported bulk chemical analyses of seven metal-sulfide grains with high concentrations of refractory metals (Re, Ir, Os etc.). These grains had been seperated from the EGG-6, Ca,Al-Allende inclusion (1). A smooth dependance of CI-normalized refractory metal abundances from condensation temperatures was found, strongly suggesting that the grains formed by condensation from a solar gas. However, W-contents were much lower in these grains than expected. One possibilty, condensation under more oxidizing conditions than those normally assumed for the solar nebula can be excluded, since this would imply a simultaneous depletion in Mo (2). Bulk samples of Egg-6 show no depletion of W. Analyses of inclusion material adjacent to the metal-sulfide assemblages showed large excesses of W (see Fig. 1). The analyses of the largest "Fremdling" of EGG-6, Zelda (3) showed a similar excess (45 ppm W) with a W/Ir ratio of 3.7, compared to the CI-ratio of 0.19 and a ratio of 0.0036 in bulk Zelda. Tungsten was quantitatively removed from the inclusion and deposited, presumably as WO_3 in the silicates, surrounding the metal-sulfide assemblages. A considerable increase in oxygen fugacity is required to account for the oxidation of W (4). Oxidized Fe and V, presumably formed by oxidation of metal, are found in silicates surrounding metal-sulfide assemblages and as major constituents of the interior of the assemblages, while oxidized W is absent. This probably indicates that W was oxidized to gaseous WO_3. Other metal-oxide assemblages in CAIs contain oxidized W and Mo in the interior (4).

The model envisioned here is supported by the results of simulation experiments. W is readily lost from artificially produced refractory metal alloys, but as soon as the metal is surrounded by silicate W is trapped within silicates (5). Fig. 2 shows results of such experiments at the NI-NiO buffer. Loss of W in Egg-6 must have occurred at lower oxygen fugacities, since at the Ni-NiO buffer loss of Re is observed. (6).

Our results show that, even under extreme conditions, W is not lost from bulk inclusions, reinforcing the conclusions of (2), that low W and Mo in bulk inclusions reflect enhanced oxygen fugacities during condensation.

Lit.:(1) H. Palme et al.(1989) LPSC XX, 814;(2) B. Fegley, H. Palme (1985) EPSL 72, 311;(3) J. T. Armstrong et al.(1987) GCA 51, 3155;(4) A. Bischoff, H. Palme (1987) GCA 51, 2733;(5) A. V. Köhler et al.(1988) LPSC XIX, 627;(7) A. V. Köhler et al. (this volume).

Fig. 1 ↓

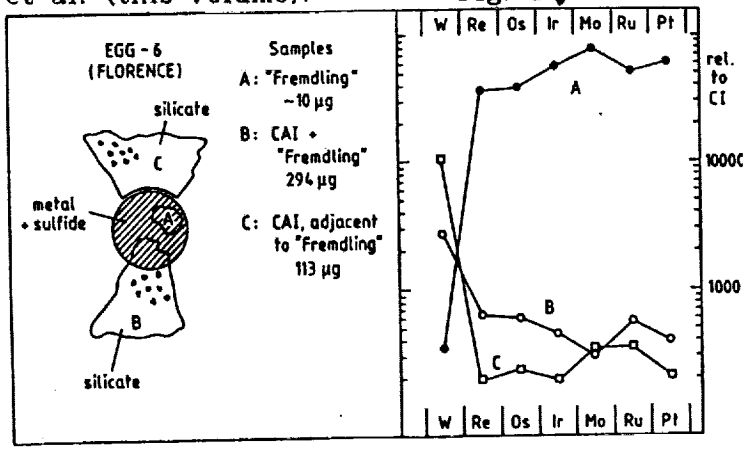

Fig. 2 ↓

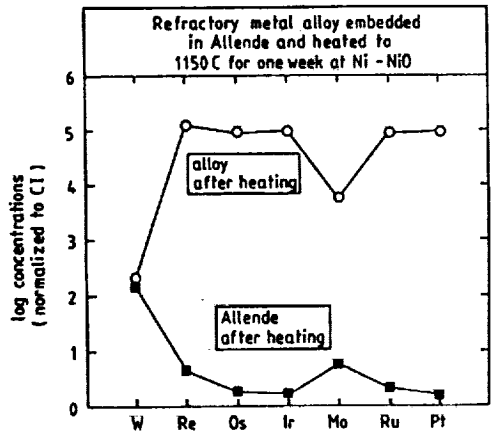

PHOTOGRAPHS FROM GEOSTATIONARY SATELLITES INDICATE THE POSSIBLE EXISTENCE OF A HUGE 300 KM IMPACT CRATER IN THE BOHEMIAN REGION OF CZECHOSLOVAKIA

Michael D. Papagiannis, Dept. of Astronomy, Boston U., Boston, MA 02215, USA

In 1983, in an image of Europe obtained from geosynchronous orbit by the weather satellite Meteosat, I noticed for the first time an oval feature that looks like a huge impact crater. It encircles most of western Czechoslovakia, i.e., roughly the region called the Bohemian Massif, and its dimensions are about 300 km E-W and 250 km N-S. It is worth mentioning here that when Galileo made his pioneering observations of the Moon with the first astronomical telescope, he wrote that the large lunar craters reminded him "of a region like Bohemia" (Drake, 1957).

In 1986 I showed the data I had collected on this region to Dr. F. El-Baz and in 1988 we presented them in 2 scientific meetings (Papagiannis & El-Baz, 1988). It is true that geologically the Bohemian Massif is a very complex region, with a wide range of ages. Topographically, though, it shows concentric elevated and depressed rings, centered near Prague (Praha), that support the impact possibility. So does too the recent work of S. Vrana (1987, 1988), of which I was told by Dr. Koeberl at the 1988 AGU meeting. S. Vrana has presented evidence that a large (46 km) region, inside and near the southern rim of the much larger oval structure, is actually an impact area about 200 or more million years old. It seems appropriate, therefore, to examine more carefully the whole oval region, because if indeed it were proven to be a huge impact crater, it would become one of the largest known on Earth.

FIGURE. The Bohemian 300 km oval structure, as seen in a space photograph obtained by the Meteosat weather satellite of ESA from a geostationary orbit.

REFERENCES

Drake S. (1957) Ed. Discoveries and Opinions of Galileo, p. 36. Doubleday.

Papagiannis M. D. and El-Baz F. (1988), Abstract, EOS, 69, 44, p. 1293.

Papagiannis M. D. and EL-Baz F. (1988), Abstract, Bull. AAS, 20, 4, p. 1043.

Vrana S. (1987), Geol. Rundschau 76, pp. 505-526.

Vrana S. (1988), Abstract, Lunar & Planetary Science XIX, pp. 1222-1223.

A MODEST PROPOSAL FOR CARBONACEOUS CHONDRITE CLASSIFICATION IN LIGHT OF THE ANTARCTIC SAMPLES; R. L. Paul* and M. E. Lipschutz, Dept. of Chemistry, Purdue Univ., W. Lafayette, IN 47907. (*Now at Dept. of Chemistry, San Jose State Univ., San Jose, CA 95192)

Classification schemes for carbonaceous chondrites, particularly those of types 1 and 2, had been straightforward until now, unambiguously summarizing a meteorite's petrographic characteristics, oxygen isotopic composition and labile (volatile/mobile) trace element pattern. The C1 (=CI), C2 (=CM) classification is well-known, simple and evocative of the chondrites' properties.

Two recent consortia to study 4 carbonaceous chondrites from Queen Maud Land - Yamato (Y) 82042, 82162 and 86720 and Belgica (B) 7904 - produced data indicating a more complicated situation. The ensemble of properties of the Antarctic samples are unlike that of the non-Antarctic carbonaceous chondrites. For example, our RNAA measurements of the trace elements Ag, Au, Bi, Cd, Co, Cs, Ga, In, Rb, Sb, Se, Te, Tl, U and Zn indicate patterns like those of C1 (for Y-82162) and C2 (for B-7904 and Y-86720) chondrites, modified by thermal metamorphism at 600-700°C. In addition, the petrographic type indicated by trace element patterns of these 3 and the unmodified C2 pattern for Y-82042 differ from classifications that would be made based upon petrography and/or oxygen isotopic composition ([1] and references therein).

We propose a classification involving

$$\text{Chemical Type}\ \begin{matrix}\text{Oxygen Isotopes}\\ \text{Petrography}\end{matrix}\ \text{Labile Trace Elements.}$$

By this scheme, B-7904 and Y-82042, 82162 and 86720 are, respectively, $C_M^{I}2^*$, $C_I^{M}2$, $C_Y^{I}1^*$ and $C_M^{I}2^*$, respectively, with the * indicating thermal metamorphism in a parent body. A meteorite like Murchison could still be classed as a C2, C2M or CM, or, according to the above, as a $C_M^{M}2$.

Reference

[1] Paul R. L. and Lipschutz M. E. (1989) Labile trace elements in some Antarctic carbonaceous chondrites: Antarctic and non-Antarctic meteorite comparisons. Z. Naturf. submitted.

THE ISOTOPIC FRACTIONATION EFFECTS OF THERMAL UNIMOLECULAR DECOMPOSITION OF OZONE; Mi-Ae Park, Seon Mi Hong, and Jongmann Yang, Department of Physics, Ewha Womans University, Seoul 120-750, Korea

Clayton et al.(1) discovered an exotic oxygen isotope pattern which seems to imply that there was a pure O^{16} component when carbonaceous meteorites formed. Since then the component was regarded as a nucleosynthetic product. Chemical origin has been constantly seeked by several groups (2-5) and non-mass dependent chemical isotope effect was observed during the production of ozone by the discharge of oxygen gas(3-5). Several mechanisms have been proposed to explain such anomalous chemical isotope patterns(3-8).

We calculated the rate constant of the thermal decomposition reaction ($O_3+M \rightarrow O+O_2+M$) of various ozone isotopomers by RRKM theory of unimolecular reactions. The range of temperatures was 20-373K and the range of pressures was 10^{-6}-10^{7} torr. The quantum statistical RRKM theory gave us several interesting isotope patterns, which can be compared with the experimental discharge isotope data even though the actal physical processes were different.

The fall-off curves are obtained. The isotopic fractionation effects are affected by molecular symmetry, mass, and vibrational frequencies of ozone molecules. The primary isotope effect increases markedly as temperature decreases for all pressure range (normal isotope effect) because of the difference in critical energies of ozone isotopomers. In case of the secondary isotope effect, there is a relatively weak temperature dependence. For example, the δ values between $^{50}O_3$(18..16-16) and $^{48}O_3$(16..16-16) are -31‰ at 300K and -138‰ at 100K for 1 torr ozone pressure. The δ values between $^{50}O_3$(16..16-18) and $^{48}O_3$(16..16-16) are 21‰ at 300K and 10‰ at 100K for 1 torr. Antisymmetric isotopomers such as $^{51}O_3$(16..17-18) have strong isotope effects bigger than a factor of two at high pressures ($\geq 10^5$ torr) for all temperatures.

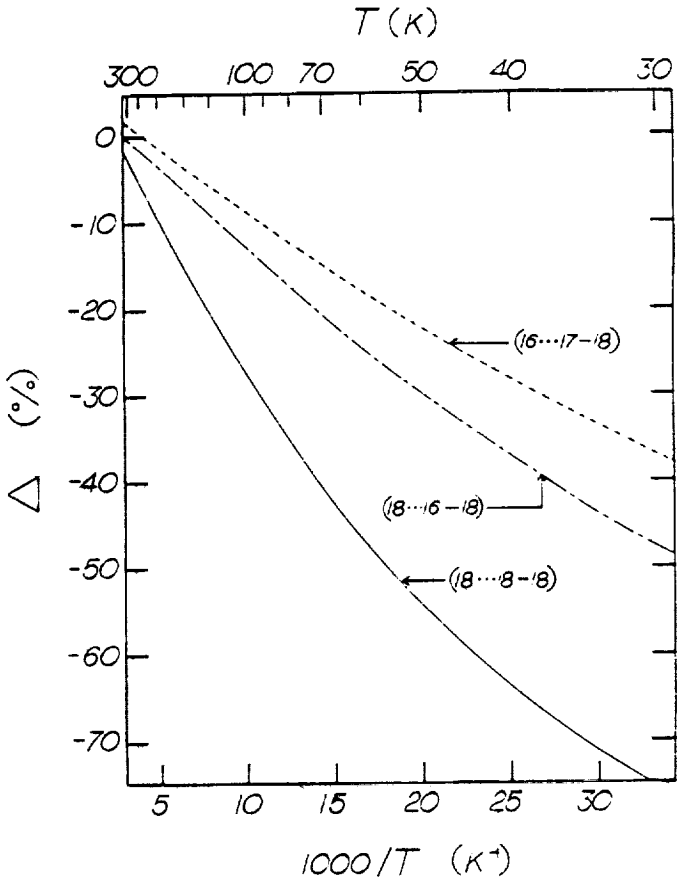

References:

(1) Clayton, R.N. et al.(1973) Science 182, 485-488.
(2) Arrhenius, G. et al.(1979) Ap. Space Sci. 65, 297-307.
(3) Thiemens, M. H. and Heidenreich, J. E. III(1983) Science 219, 1073-1075.
(4) Yang, J. and Epstein, S.(1987a) Geochim. Cosmochim. Acta 51, 2011-2017.
(5) Yang, J. and Epstein, S.(1987b) Geochim. Cosmochim. Acta 51, 2019-2024.
(6) Navon, O. and Wasserburg, G. J. (1985) Earth Planet. Sci. Lett. 73, 1-16.
(7) Heidenreich, J. E. III and Thiemens, M. H.(1986) J. Chem. Phys. 84, 2129-2136.
(8) Park, M. and Yang, J.(1987) In Abstracts for the 55th Annual Korean Physical Society Meeting, 232.

Strewn-fields of Imilac and Vaca Muerta

H.Pedersen Apartado 161, E 38700 Santa Cruz de La Palma, Spain
H.Lindgren ESO, Casilla 19001, Santiago 19, Chile
C.Canut de Bon Universidad de La Serena, La Serena, Chile

The strewn-fields of the Chilean stony-iron meteorites Imilac (pallasite) and Vaca Muerta (mesosiderite) are investigated. Both meteorites split in the atmosphere, producing primary strewn-fields. The largest fragment of each shower disintegrated upon hitting ground, thereby giving rise to secondary strewn-fields.

The Imilac fireball probably arrived from SW, contrary to the supposition by former students of that meteorite. The >8 km long primary strewn-field contained at least 10 large fragments, most of which were found during recent years. However, there is published evidence that also the 198-kg fragment in London, and the 95-kg mass, of which most is in Copiapo, belong to the primary strewn-field. Tens of thousands of fragments, up to and possibly exceeding 325 gram were produced by the impact of the largest fragment. They scattered over an area 1000 meter long, NE of the impact-point. This is the hitherto recognized find-area for all material. The fragmentation is examined, using field-studies, as well as information currently being obtained from numerous public and private collections. This will allow us to determine approximate (N,log(m))-curves for the primary and secondary masses. The curves are followed in logarithmic steps of two, from 10 mg to 200 kg.

Vaca Muerta produced 59 impacts, of which 51 are recent finds. All were probably found at the location of fall. A precise map has been constructed of the 11-km long primary strewn-field. The fireball arrived from East, more precisely azimuth 112 degrees. Evidence is found of attempted commercial exploitation of some of the (thereby) disturbed masses, and it also seems likely that local indians have had knowledge of the biggest mass, i.e. the one which produced the 40-m long secondary strewn-field. Undisturbed material was found in a rare state of conservation. With more than 1200 kg recovered Vaca Muerta is the largest of all known mesosiderites.

SPALLATION RECOIL TRACKS AND FISSION TRACKS IN CHONDRITIC MERRILLITES.

P. Pellas, C. Fiéni and C. Perron, URA 286, M.N.H.N.,61 rue Buffon, 75005 Paris, France.

To retrace early thermal histories of OCs by the Pu fission track method important corrections may have to be applied to track data of merrillites (MRL). These corrections were not taken into account in the past (1) for two reasons : I) most of the OCs studied were selected according to their rather short (7 Ma peak) exposure ages and high shielding, to decrease the cosmic-ray track background ; II) the spallation track production rate (STPR) obtained on lunar and meteoritic MRLs by SEM were estimated to be $\sim$1 track/cm^2.a (2,3), or 1.7 tr/cm^2.a by optical microscopy (4). These rather low values of STPR would have led to small or negligible corrections for short exposures and were therefore neglected (1). Recently however, it has been found that a large fraction ($\sim$50%) of tracks (SEM data) observed in Forest Vale (H4) MRLs must be attributed to spallation tracks produced during the very long exposure ($\sim$80 Ma) of this object. This was based on a calibration of the proton induced STPR ($\sim$4 tracks/cm^2.a) carried out at CERN (5).

Here we want to point out that appropriate corrections may be done on MRLs through a simple laboratory annealing procedure that allows to obtain sound fission track data. Track density reduction of F. Vale MRLs ($\rho_{tot} = 7.9 + 0.5\times10^8$/cm^2) was studied by isochronal (1h) annealing of 15-30 crystals (from one location) at various temperature steps from 225 to 430°C. The results are displayed in Fig. 1 (squares: the line is to guide the eyes), together with those obtained on Estacado (H6) MRLs (full dots) by Mold et al. (6). F.Vale MRLs present a sharp track density decrease ($\sim$40%) at 250-260°C, followed by a plateau at 260-275°. A subsequent decrease is observed above 275°. Then the track density reduction with increasing temperatures adopts a sigmoidal shape. In Estacado, the track density reduction shows a different behavior, starting at 325°C, with no evidence of track density decrease at lower temperature (space exposure: $\sim$5 Ma). The different behavior of the two samples could be accounted for by their early thermal and late irradiation histories: 1) F.Vale has cooled very fast (5) and its fission tracks are not thermally affected; it has also a long space exposure. The total track density contains essentially two components: thermally unaffected spallation and fission tracks. The spallation tracks are almost totally erased at a temperature of 290°C while the fading of fission tracks has hardly started. Estacado MRLs show no evidence of spallation tracks and the fading of fission tracks starts at higher temperature ($\sim$330°C), probably due to the early slow cooling that has thermally affected a large fraction of Pu fission tracks, leaving the most (thermally) resistent part of the latter. From the curve of Fig.1 a Pu content of $\sim$45ppb (corresponding to a fission track density of 3.5×10^8/cm^2) is obtained for F.Vale MRLs, in rather good agreement with fission xenon data (5). The STPR obtained throuh this annealing experiment of F.Vale MRLs is 5.3 tracks/a, also in good accord with the CERN proton irradiation results. In conclusion, annealing of chondritic merrillites at a temperature of 290°C (1h) seems to completely erase spallation tracks preserving, however, the fission track component.

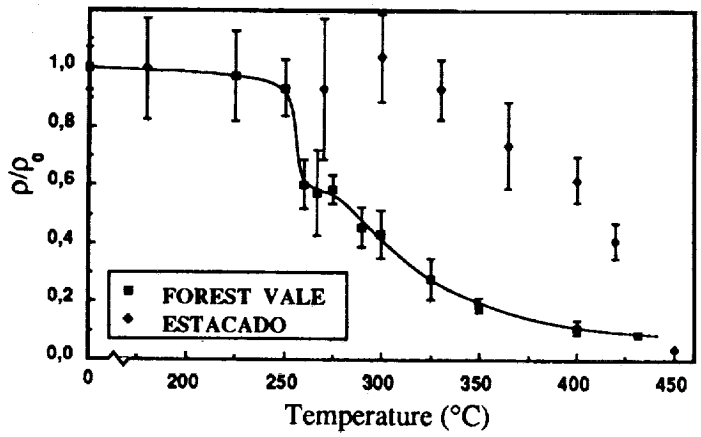

Fig.1

Ref. (1)Pellas and Storzer (1981) Proc. Roy. Soc. A374, 253. (2) Seitz (1971) Ph.D.Thesis, Washington Univ. St. Louis. (3) Crozaz et al.(1972) Proc. 3th Lun. Sci. Conf.,1623. (4) Crozaz and Tasker (1981) C.C.A. 45, 2037. (5) Lavielle et al. (1989) Meteoritics, to be published. (6) Mold et al. (1984) Nucl. Tracks 9, 119.

MEASUREMENT OF THE ANNUAL FLUX OF COSMIC DUST IN DEEP-SEA SEDIMENTS. Peng Hanchang[1] and Lui Zhenkun[2]. [1]First Institute of Oceanography, State Oceanic Administration, P.O. Box 98, Qingdao, China. [2]Institute of Hunan Coloured Metallurgical, Huangtulin, China.

Numerous investigators have studied the annual flux rate of cosmic dust onto the earth. Various methods have been applied, yielding different results (e.g., [1]). We studied cosmic spherules in deep-sea sediments from Northern Pacific sites in an area of several hundred square kilometers (6-13° N, 166-167° W) [2]. In addition, we also measured the annual cosmic dust flux rate in deep-sea sediments. The cosmic dust content in sediments of 20 North Pacific stations is given in Table 1.

Based on the cosmic dust content of the sediment we calculated the annual cosmic dust flux M_y. The following basic parameters were used in the calculation: (1) sedimentation rate U; (2) thickness of layers h; (3) area of dredger S_g; (4) surface area of the earth S_e; (5) weight of ooze sample O_m; (6) weight of wet sediment used for analysis M_a; (7) total weight of cosmic particles in the wet sediment N_m. The general formula used is:

$$M_y = (N_m \cdot O_m \cdot U \cdot S_e)/(M_a \cdot S_g \cdot h \cdot 1000) = 73.44\,(N_m/M_a).$$

The fluxes that have been determined at the individual stations are similar to each other, ranging from hundreds to thousands of tons per year and are in accordance with results obtained by previous investigators using the same methodology [1].

Sample #	*Sedim. wt.[g]*	*#grains*	*Cosmic Dust wt.[ug]*	*wt.[ug/g]*	*Flux [t/a]*
M2	*4230*	*219*	*29900*	*7.07*	*5191*
M6	*385*	*27*	*3600*	*9.35*	*6867*
M8	*1205*	*24*	*3300*	*2.74*	*2011*
M10	*907*	*7*	*1000*	*1.10*	*810*
M11	*1718*	*29*	*3900*	*2.27*	*1667*
M15	*562*	*4*	*400*	*0.71*	*523*
M27	*2850*	*61*	*8600*	*3.02*	*2216*
M0	*1140*	*41*	*5500*	*4.82*	*3543*
N2	*1576*	*8*	*1100*	*0.70*	*5.13*
N3	*1936*	*17*	*2400*	*1.24*	*910*
N4	*855*	*29*	*4100*	*4.80*	*3522*
N11	*386*	*14*	*2000*	*5.18*	*3805*
N12	*176*	*1*	*200*	*1.14*	*584*
N13	*1250*	*23*	*3200*	*2.56*	*1880*
N15	*1877*	*51*	*7100*	*3.78*	*2778*
N17	*991*	*7*	*1000*	*1.01*	*741*
N20	*1174*	*32*	*4500*	*3.83*	*2815*
N26	*1732*	*66*	*9300*	*5.37*	*3943*
N39	*1372*	*10*	*1400*	*1.02*	*749*
N41	*500*	*12*	*1600*	*3.20*	*2350*
Ave.	*1341*	*34.1*	*4700*	*3.25*	*2461*

Table 1. Abundance of cosmic dust (>60 um) in deep sea sediments and annual flux

References: [1] Shima, M. (1978) The birth of stars and cosmic dust, Yuchuan Univ.Publ.,Japan, 78-80. [2] Peng H. and Lu K. (1986) Chin.J.Ocean.Limnol. 4, 286-292.

THE RESULTS OF CALIBRATING METEORITIC OLIVINE CRYSTALS WITH ^{238}U NUCLEI AT THE BEVALAC ACCELERATOR. V.P. Perelygin, S.G. Stetsenko, O. Otgonsuren*, R.I. Petrova, and G.G. Bankova. Joint Institute for Nuclear Research (Dubna), P.O. Box 79, 10100 Moscow, USSR (*State Pedagogical Institute, Ulaanbaatar, Mongolia).

We present preliminary results of studies on the origin of fossil tracks due to Z>50 nuclei in meteoritic olivine crystals from the Marjalahti and Eagle Station pallasites. Olivine crystals are an example of a threshold solid state track recorder. As shown previously [1], the etchable track length is an unique parameter, allowing the determination of the atomic number Z of the trapped nucleus. The method for revealing the tracks has been described before [1]. It eliminates earlier disadvantages (e.g., the problem of different track lengths due to different registration times for nuclei of the same Z). The annealing procedure chosen here (430 +/- 1°C for 32 h) changes the threshold from Z=22 to Z=50. Under these conditions the ^{132}Xe track length was 26.5 +/- 2.5 μm. The track length spectrum (Fig. 1a) shows groups between 120-140 and 190-220 μm, which are attributed to cosmic ray nuclei from Pt-Pb and Th-U, respectively. One long track (365 μm) may have been produced from a Z>110 nucleus. In later studies [2] other long tracks have been measured, but so far it was not possible to identify their origin. One of the tracks may have been due to a Xe nucleus. To clarify these questions, meteoritic olivine crystals have been calibrated with 30 MeV/n and 70 MeV/n U-238 ions (25° and 10° incidence angles) at the Bevalac accelerator. The crystals were annealed and etched according to [1,2]. The results of ^{238}U track length measurements of 100 crystals are given in Fig. 1c, showing good correlation with the fossil tracks (Fig. 1a). This is strengthened by annealing studies (Fig. 2a,b) of ^{208}Pb and ^{238}U tracks. The longest ^{238}U tracks need further investigation. We conclude that the etchable track lengths are much longer (by a factor of about 1.3-1.6) along the crystal planes and axis than at a random orientation. Based on our investigations we further conclude that: 1. The fossil tracks [1] are due to Th-U nuclei of galactic origin, and 2. Analyzing fossil cosmic ray tracks (from Z>50) in meteoritic crystals leads to a new experimental basis for qualitative results with higher sensitivity.

Acknowledgements: We thank Prof.G.Flerow, Y.Oganessian, and Ter-Akopian for discussions and G.P.Knyazeva for measurements.

References: [1] V.P.Perelygin and S.G.Stetsenko (1980) JETP Pisma, 32, 622. [2] V.P. Perelygin et al. (1985) JINR Comm. E 7-85-245, Dubna.

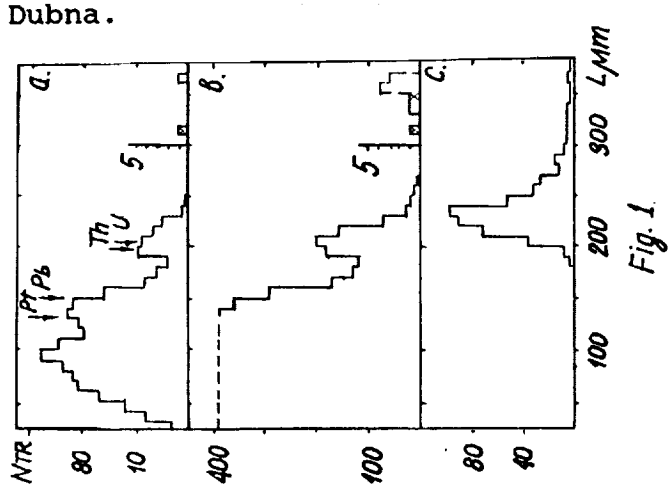

Fig. 1

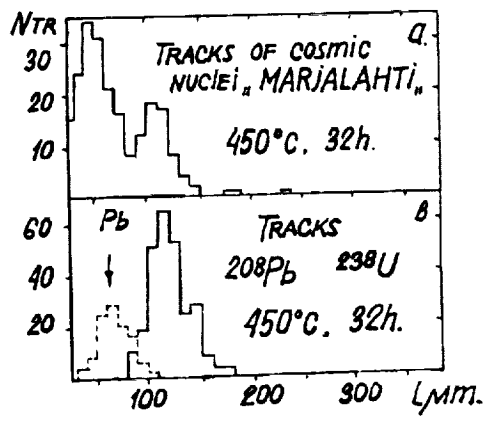

Fig. 2

COMPOSITION AND INTERRELATIONSHIP OF CHONDRULES, LITHIC FRAGMENTS AND FINE-GRAINED MATRIX FROM CHAINPUR (LL-3). E. PERNICKA, S. BAJT, AND K. TRAXEL, MAX-PLANCK-INSTITUT FÜR KERNPHYSIK, POSTBOX 103980, D-6900 HEIDELBERG, F.R.G.; G. KURAT AND F. BRANDSTÄTTER, NATURHIST. MUSEUM, A-1014 VIENNA, AUSTRIA

Chondrules, various types of inclusions, and fine-grained matrix comprise the major petrographic components of unequilibrated ordinary chondrites. In an attempt to learn more about the interrelationships of these materials we analyzed 25 chondrules, 15 chondrule-sized lithic fragments and 6 different grain-size fractions of matrix material chemically and petrographically. Analytical methods employed included INAA, electron microprobe and proton-induced X-ray excitation (PIXE).

The chondrules have PO or POP, RP, and BO textures (terminology after[1]) in decreasing abundance with a few unusual textures, such as radiating olivine, skeletal olivine in glassy matrix or radiating olivine-pyroxene with little matrix and abundant pore space. The lithic fragments are dominated by PO and POP textures (72%) followed by GO and GOP textures. One fragment consists of porphyritic pyroxene.

The major silicate minerals are generally rich in minor elements such as Ca, Al, Ti, Cr, and Mn. Olivines show a range in Fa content from 0.5 to 43 mole %. Two distinct populations can be distinguished: A rare Mg-rich variety with "blue forsterites"[2], a common type with low contents of Al_2O_3 and TiO_2 but relatively high abundances of CaO, Cr_2O_3, and MnO. Refractory elements are correlated with Cr and anticorrelated with Mn and Fe.

Kamacite shows wide variations of Co content between 0.08 and 2.1%. Low-Co kamacite is always found in spheroids entirely enclosed in silicates while high-Co kamacite is usually present as irregular grains in chondrule rims and most lithic fragments as reported previously[3,4]. Interestingly, Ge is also depleted in low-Co kamacite (< 10 μg/g) but not in high-Co kamacite (62-130 μg/g). Since the Ni/Co ratio of low-Co kamacite ranges up to the CI ratio, we infer that this kamacite is a primitive component which could have formed by condensation at relatively high temperatures and reducing conditions. The very low Ge content supports this view. Apparently, this metal was shielded by silicates from further exchange with the gas phase and other metallic phases at lower temperatures, while common metal clearly did so. This is evident from the higher abundances of volatile siderophile elements and equilibration between taenite and kamacite.

Chondrules and lithic fragments clearly differ in their Na/Sc-ratios. Most chondrules have Na/Sc>CI but all fragments have Na/Sc<CI. Fragments are generally depleted in volatile incompatible elements. The mass balance is obtained by the finest matrix fractions, which are enriched in these elements. Since chondrules and lithic fragments apparently have both experienced a high temperature event, chondrule formation may be tightly controlled by the bulk chemical composition.

Finally, the fine-grained matrix samples have Co/Ni-ratios>CI and are enriched in Ir relative to Ni. Their composition is incompatible with suggestions that matrix could form a chondrule or rim precursor material.

References

1. J.L. Gooding and K. Keil (1980), *Meteoritics* **16**, 17-43. *2.* I.M. Steele (1986), *Geochim.Cosmochim. Acta* **50**, 1379-1395. *3.* F. Affiatalab and J.T. Wasson (1980), *Geochim.Cosmochim. Acta* **44**, 431-446. *4.* E. Pernicka *et al.* (1985), *Meteoritics* **20**, 729.

THE ROLE OF CVD IN THE PRODUCTION OF INTERSTELLAR GRAINS. C.T. Pillinger, R.D. Ash, Planetary Sciences Unit, Department of Earth Sciences, The Open University and J.W. Arden, Department of Earth Sciences, University of Oxford.

Diamond is a metastable phase in comparison to graphite, therefore its recognition in meteorites in the past has been attributed to a shock origin: graphite being converted to diamond by collisions between asteroidal sized objects or violent impacts by large meteorites on Earth. Clearly diamond cannot be a secondary phase in primitive meteorites, such as carbonaceous chondrites, which show little evidence of shock, hence the supposition that it is a form of interstellar grain pre-existing before incorporation into the host. It is suggested that the diamond grew in the environment surrounding an evolved star by a process akin to chemical vapour deposition (CVD). Many variations in CVD technique for making diamond in the laboratory have been investigated but they all have certain features in common: (i) the carbon source (virtually any hydrocarbon) is present in *ca.* 1% abundance in hydrogen; (ii) the substrate for collecting diamond produced must have the diamond structure or contain elements capable of producing it, and (iii) some means of generating a plasma. Some experiments can lead to the production of material with a distinct lack of crystal structure; such products have been given the name diamond-like carbons because they possess many of the desirable properties of diamond. Sometimes this alternative substance contains large amounts of hydrogen so that it then becomes known as diamond-like hydrocarbon.

The exact mechanism for CVD diamond production is unknown but certain important facets of the process are appreciated: (i) diamond growth is not spontaneous, it requires some kind of seed; the identification of SiC together with diamond even when a substrate does not contain Si is highly suspicious; (ii) hydrogen radicals are involved in continuous exchange with the free tetrahedral sites of the growing diamond creating activity and eliminating graphite (and other forms of carbon) which would block diamond production; (iii) substrates are almost always in the temperature regime 900-1000°C; lower temperatures give a product but of inferior quality.

Finding situations in the vicinity of evolved stars, interstellar clouds or even the early solar system where hydrogen is abundant relative to carbon (or other elements) and plasma conditions similar to those required for CVD is very easy. Thus, it would not be difficult to arrive at the combination of circumstances where diamond was produced. It is interesting to note that wherever we have looked in meteorites diamond and silicon carbide co-occur, the latter being the minor partner; this may be fortuitous or, like in the CVD situation, SiC is the seed. There is very little evidence for graphite but there are a number of unidentified components carrying isotopic anomalies in meteorites which could be the equivalent of diamond-like materials; likewise all the meteorites which host interstellar grains contain copious amounts of amorphous or macromolecular carbon. Furthermore, samples rich in diamond are amongst those where D/H ratio is high and it is well accepted that the D/H carrier in meteorites may only be a small fractionation of total carbonaceous matter. The continuous exchange of hydrogen with the diamond surface affords the perfect situation for large scale isotopic fractionation.

Isotopic effects in plasmas are almost a complete mystery with no information whatsoever about those occurring during diamond CVD. Results from the step combustion analysis of samples produced by CVD will be presented at the meeting.

THE PORT ORFORD METEORITE HOAX. Howard Plotkin (1), Vagn F. Buchwald (2), and Roy S. Clarke, Jr. (3); (1) Department of History of Medicine and Science, University of Western Ontario, London, Canada N6A 5C1, (2) Department of Metallurgy, The Technical University, Lyngby, Denmark, (3) Department of Mineral Sciences, Smithsonian Institution, Washington, D.C. 20560, U.S.A.

John Evans, a contract explorer for the U.S. government claimed to have found a 10 ton pallasite near Port Orford, Oregon in 1856. Discovery was first announced by C.T. Jackson shortly after he received a small pallasite specimen from Evans (Smithsonian #617, Vienna A662) for analysis and without comment in 1859. Jackson's inquiries led Evans to describe a large mass, high on a scenic slope of Bald Mt, overlooking the Pacific. The site, he claimed, could easily be relocated, and Evans would be pleased to undertake its transport to the Smithsonian in Washington. With astonishing speed, an aggressive campaign by natural history societies, interested government officials and private individuals was mounted to lobby Congress and concerned government agencies to produce the necessary funding. Momentum built but was abruptly dissipated with the firing on Fort Sumter April 12, 1861. Evans, a man of 49, died the following day of a mild pneumonia, and the country's thoughts turned to preparations for civil war. In the early 1900s interest in the meteorite was revived by journalistic accounts. Within a few years irresponsible reporting created the myth of a large "lost" meteorite with a gigantic reward assured, a myth that has troubled government officials and enticed thousands of inexperienced outdoorsmen into the inaccessible Siskiyou National Forest. Field searches by one of us (HP), Smithsonian representatives, and others have produced no trace of the meteorite and have cast serious doubt on the Evans story.

The assumption that Evans had high standards of professional and personal conduct has undergirded the myth. Reexamination of known documents and retrieval of previously unused materials show this assumption to be wrong. Evans had no professional training, and his field work and specimen collection was useful exploration but casual and certainly not insightful science. His ethical conduct is open to serious question, and he was overwhelmed with a sense of impending doom brought on by a crushing load of professional and personal debt amassed through mismanagement of government funds and land speculation. A small pallasite specimen that he obtained in 1858 offered a ray of hope and led to an elaborate hoax that was to have resulted in Congress appropriating the necessary funds to solve his manifold problems. Death terminated Evans involvement but left a legacy that continues to exploit the public and harass officials.

Metallographic and chemical data pair Port Orford and Imilac, a meteorite that was already widely distributed. It is fusion crusted, part of a small individual from a pallasite that broke up in the atmosphere and corroded under arid conditions. It is a somewhat atypical Imilac specimen based on chemical trends and mineralogical observations.

CONSEQUENCES OF A GIANT IMPACT EXAMPLIFIED AT CRETACEOUS/ TERTIARY BOUNDARIES IN AUSTRIA

Preisinger A., Inst.f.Mineralogie, Kristallographie und Strukturchemie, TU-Wien, A-1060 Vienna, Austria

Three independent high-resolution stratigraphic methods (bio-, magneto- and event-stratigraphy) are used to determine the time structure of the K/T event and the post event sequence at two Austrian boundary sites (Elendgraben, Gosau and Knappengraben, Gams). A detailed mapping of the lithostratigraphy of these K/T sections, which are 100 km apart, shows that hemipelagic deposits are interbedded by turbidites. The Maastrichtian hemipelagic deposits consist of 70% and 65% biogenic calcium carbonate respectively. Because of dilution with "fallout" at the K/T boundary the $CaCO_3$ content reaches a minimum there. Quantitative analyses of minerals (i.e. quartz and shocked quartz) and trace elements (i.e. Ir, Cr) across the K/T boundary show anomalies in millimeter scale and permit an optimal time resolution of approximately one year for the "fallout" of the material rain from the atmosphere. In hemipelagic sediments we can distinguish between the direct "fallout" as well as transported and redeposited "fallout" ("redeposition"). Careful sedimentological analyses as well as pollen and spores analyses show that the diluted fossil zone after the impact is caused by terrigeneous current flows, which originated in consequence of a giant tsunami. The time required for the depostion of this post event sequence is about 4000-5000 years.

Preisinger A., Zobetz E., Gratz A.J., Lahodynsky R., Becke M., Mauritsch H.J., Eder G., Grass F., Rögl F., Stradner H., Surenian R.: Nature 322(1986)794-799

Eder G., Preisinger A.: Naturwiss. 74(1987)35-37

Preisinger A. "Erdgeschichtliche Katastrophen", Verlag Österr. Akad.d.Wiss., Wien(1987)17-19

Stradner H., Eder G., Grass F., Lahodynsky R., Mauritsch H.J., Preisinger A., Rögl F., Surenian R., Zeissl W., Zobetz E.: Terra cognita 7(1987)212

Preisinger A., Stradner H., Mauritsch H.J.: 2nd Snowbird Conference, USA (1988)143-144 (abstract)

MICROTEKTITES IN MUONG NONG TEKTITES; E. Preuss, Saint-Privat-Str. 14, D-8000 Munich 80, FRG; J. Pohl, Institut für Allgemeine und Angewandte Geophysik, Theresienstr. 41, D-8000 Munich 2, FRG.

11 Muong Nong Indochinites and 1 Muong Nong type Moldavite have been investigated. "The Muong Nong Tektites are the result of the welding of microtektites" (O'Keefe 1969). Etching with hydrofluoric acid reveals the grain boundaries of the microtektites as narrow grooves. The form of the microtektites varies from flat, round lenticules with a thickness of 5 to 20 microns to long spindles. We assume that the microtektites were blown in into depressions on the ground (like snowdrift in a snowstorm) by the hot gases coming from the impact site. The temperature at the time of deposition was still very high, which explains the formation of the elongated spindles. Other types of deformation and welding of the originally spherical microtektites have not been observed by the authors, but they can not be excluded. The orientation of the spindles corresponds to the macroscopic texture of the Muong Nong tektites. If the Muong Nong tektites were deposited at high temperature on the ground, they probably acquired their remanent magnetization (de Gasparis 1973) during cooling in the Earth' magnetic field, which allows to determine the original orientation of the tektites on the ground. This information, combined with the knowledge of the recovery site and the lineation direction of the microtektites, may eventually allow to determine the direction from the recovery locality to the impact site. References: O'Keefe, J. A. (1969), J. Geophys. Res. 74, 6795-6804; de Gasparis, A. A. (1973), Magnetic properties of tektites and impact glasses. Ph. D. Thesis, University of Pittsburgh, 173 p.

CHONDRULES IN THE B7904 CI2 CHONDRITE. M. Prinz[1], M. K. Weisberg[1,2], R. Han[1,3], M. E. Zolensky[4]. (1) Amer. Mus. Nat. Hist., NY, NY 10024 (2) Brooklyn College, (CUNY), Brooklyn, NY 11201 (3) City College (CUNY), NY, NY 10031 (4) NASA-Johnson Space Center, Houston, TX 77058.

CI2 chondrites are a new type of primitive chondrite and three such chondrites have been found by the Japanese in Antarctica. They are the subject of a consortium led by Prof. Y. Ikeda, of which this is a part. Clayton and Mayeda [1] have shown that they have oxygen isotopic compositions near CI1 chondrites. Of the three, Y82162 contains no chondrules, Y86720 has chondrules nearly completely altered by phyllosilicates, and B7904 has olivine and pyroxene bearing chondrules with some alteration to phyllosilicates. Since B7904 are the least altered chondrules they are the objects of this study. They are most analogous to CM2 chondrules and thus a set of chondrules from the Murchison CM2 chondrite was studied for comparison. Texturally, B7904 chondrules make up about 20% of the chondrite, although the area studied is relatively small. They are generally small and similar in size to CM2 chondrules, although one layered chondrule is 3mm across. They are usually round, but many are irregular. B7904 contains type I and II chondrules. Type I chondrules have granular, porphyritic and barred olivine textures, whereas type II chondrules are usually porphyritic. Chondrules appear to be aggregational, and many contain post-aggregational melt components. Chondrules are usually surrounded by a dark, fine-grained rim resulting in an overall rounded shape, regardless of the irregular core interior. Chondrules contain massive phyllosilicate-rich areas, studied by Zolensky et al. [2], but only type I chondrules contain abundant small (~10 μm) brown microspherules (or "brown balls"), which are especially abundant in the outer margins of the chondrules. They appear to have accreted onto, and into, the type I chondrules. In addition, type I chondrules contain small "black balls," which are magnetite-pyrrhotite-pentlandite-phosphate-rich assemblages, analogous to the OA's (opaque assemblages) of Blum et al. [3] These are in the interior of chondrules, often in circular patterns. Mineralogically, Type I chondrules contain mainly Mg-rich olivine ($Fo_{99.5}$) (opx and cpx are rare) and phyllosilicates mixed with minor phases. The olivine/phyllosilicate ratio is highly variable. Phyllosilicates are mainly antigorite, ferroan antigorite and clinochlore [2], and the brown balls have similar compositions. Feldspathic components are rare. One chondrule contains a micron-sized grain of zircon. Type II chondrules contain mainly zoned olivine (Fo_{88-34}). Zoning is sometimes irregular, with increasing and decreasing Fe toward the margins. Large grains are often Mg-rich, increasing in Fe towards the margins, and surrounded by smaller ol grains similar in composition to the Fe-rich marginal ol. Zoning appears to be the result of nebular solid-gas diffusion, not igneous processes. Pyroxene is rare, but some chondrules contain opx only (En_{76-55}). Some type II chondrules display extreme enrichments in apatite (up to 8.2% P_2O_5), whereas some contain no apatite, and others are intermediate. Small euhedral crystals of chromite are found in all type II chondrules. Phyllosilicates are similar to those in type I chondrules. Comparison with CM2 Chondrites. B7904 type I and II chondrules have some similarities to chondrules in the Murchison CM2 chondrite, but there are important differences which clearly distinguish them. Murchison type I chondrules have a wider range of olivine compositions, and coexisting opx and cpx is more common; the phyllosilicates are generally more Fe-rich. Type II chondrules in Murchison have more coexisting pyroxene, and contain little or no phosphates. Bulk compositions of type I and II chondrules in B7904 and Murchison show significant differences. Murchison chondrules (I and II) are highly depleted in volatiles (Na, K, P, S) compared to B7904 chondrules. B7904 chondrules have more phyllosilicates than Murchison chondrules. One type II chondrule in Murchison contains a large euhedral type I olivine crystal, indicative of the aggregational nature of most of the chondrules in both meteorites. Thus, B7904 chondrules are unique to the CI2 chondrites and represent a new type of primitive component sampled by the carbonaceous chondrites.

REFERENCES: [1] Clayton, R.N. and Mayeda, T.K. (1989) LPSCXX, 169-170. [2] Zolensky, M.E., Barrett, R., Prinz, M. (1989) Mineralogy and Petrology of Y86720 and B7904. 14th Symp. Antarctic Meteorites, Tokyo. [3] Blum, J.D. et al., (1989) GCA 53, 543-556.

TITANIUM ISOTOPES IN ALLENDE INCLUSIONS. C. A. Prombo[1,2], L. E. Nyquist[2], and H. Wiesmann[3]. 1. Nat. Res. Coun. Assoc. 2.SN2, NASA/JSC, Houston TX 77058. 3.Lockheed, 2400 Nasa Rd. 1, Houston 77058.

Titanium isotope data for CAIs [1-5] give a suggestion that ^{50}Ti effects in fine grained [fg] aggregates are larger than those in coarse grained CAIs. To pursue this suggestion and to try to determine if chemical factors are involved, we are analyzing a suite of fg CAIs sampled from Allende slabs graciously provided by Elbert King and the Houston Museum of Natural Science.

Titanium was extracted using a plastic AG 1 X 4 anion exchange column and HF-HCl. Our analyses are for Ti^+ ions in the double filament, static multi-collection mode. The Ti standard was provided courtesy of S. Niemeyer. For both standards and samples, isobaric interferences on $^{50}Ti^+$ were observed from $^{50}Cr^+$; they were corrected using the $^{52}Cr^+$ intensity measured during the scan at the start and end of each analysis. Rare interferences from Ca and V were negligible. Typically, 2 μg of Ti are loaded on a Re filament, although we have included some standard runs using 6 μg. In the figures 2 μg standard runs have labels that begin with 2, e.g. 2-1, whereas labels for 6 μg loads begin with 6. Normalization is to $^{48}Ti/^{46}Ti = 9.21251$ [1]. Our means of the Ti standard with 95% confidence limits ($2\sigma_p$) are $^{47}Ti/^{46}Ti = 0.914980 \pm 0.000031$, $^{49}Ti/^{46}Ti = 0.685904 \pm 0.000052$ and $^{50}Ti/^{46}Ti = 0.667696 \pm 0.000064$. There are no significant differences between the results for the 2 and 6 μg runs. Results for the standard analyses are shown in Figures 1-3 expressed as ε units relative to the above means.

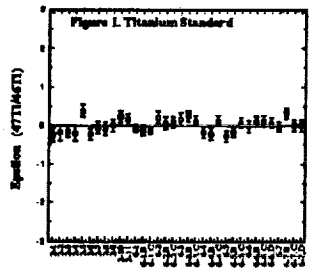

For our running technique, we have found that the exponential law does not adequately correct for mass fractionation. We have derived an empirical "modified power law" which for $^{50}Ti/^{46}Ti$ becomes

$$(^{50}Ti/^{46}Ti)_T / (^{50}Ti/^{46}Ti)_M = [(^{48}Ti/^{46}Ti)_T / (^{48}Ti/^{46}Ti)_M]^{\alpha}$$ where

$$\alpha = [(50 - 46) * (1 - (50 - 46)/\beta 46)]/[(48 - 46) * (1 - (48 - 46)/\beta 46)]$$

and similarly for other ratios. Here T stands for the "true" and M for the measured ratios. The parameter β was determined by fitting the formula to the observed variation of $^{i}Ti/^{46}Ti$ with $^{48}Ti/^{46}Ti$ for the normalization value of $(^{48}Ti/^{46}Ti)_T$.

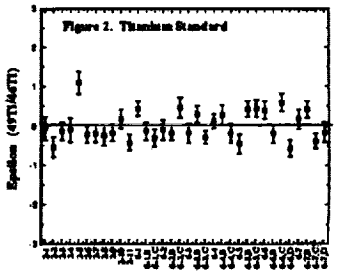

We analyzed 11 mg of the fg white CAI CPLN 13b1 and 9 mg of the dark inclusion EKPB 5a1. Titanium isotope compositions are reported in Table 1 in ε units relative to the laboratory standard with 2 σ uncertainties from the mass spectrometer analyses. External reproducibilities ($2\sigma_p$) for $^{47}Ti/^{46}Ti$, $^{49}Ti/^{46}Ti$ and $^{50}Ti/^{46}Ti$ are 0.34, 0.76 and 0.96 ε units, respectively, as determined from the means of analyses of the laboratory standard. Uncertainties on the mean are $2\sigma_p/(n)^{1/2}$ for samples. The CAI exhibits a ^{50}Ti effect of +9.1 ε units, which is unremarkable and on the low side of observed values for Allende fg CAIs [1,2,4,5,] Deficits of ^{47}Ti are common; this deficit of 0.7 ε units is also unremarkable. Effects on ^{49}Ti are rare in C3V CAIs; 13b1 exhibits a hint of an effect on ^{49}Ti. We will seek to confirm the ^{49}Ti effect with additional measurements. Niemeyer [3] reported the only other Ti isotope analyses of a dark inclusion; his ^{50}Ti effect for an Efremovka dark inclusion is within error of our 3.4 ε unit ^{50}Ti effect for 5a1. Figure 4 shows ε ($^{50}Ti/^{46}Ti$) for the inclusions and for a terrestrial basalt relative to 0.667696. References: 1.Ap.J. 240, L73-7., 2.EPSL 53, 211-5., 3.GCA 52, 2941-54. 4. LPS XVII, 685-6. 5.LPS XVIII, 804-5.

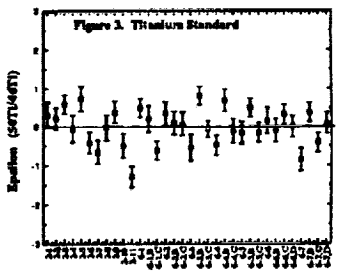

Table 1. Titanium isotope compositions of Allende inclusions

	ε (47/46)	ε (49/46)	ε (50/46)
CPLN13b1,1	-0.8 ± 0.3	+1.6 ± 0.4	+9.0 ± 0.6
CPLN13b1,2	-0.6 ± 0.2	+1.3 ± 0.3	+9.1 ± 0.3
Mean	-0.7 ± 0.2	+1.4 ± 0.5	+9.1 ± 0.7
PBEK5a1,1	-0.5 ± 1.0	-0.4 ± 0.9	+2.7 ± 0.9
PBEK5a1,2	+0.2 ± 0.2	+0.2 ± 0.3	+3.5 ± 0.3
Mean	+0.2± 0.2	+0.1 ± 0.5	+3.4 ± 0.7

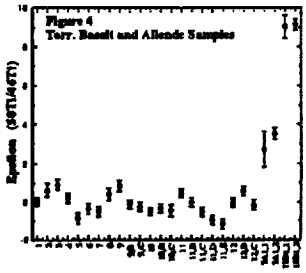

COSMIC RAY EXPOSURE AGES OF COSMIC SPHERULES

G.M. Raisbeck and F. Yiou

IN2P3 - Centre de Spectrométrie Nucléaire et de Spectrométrie de Masse
Bât. 108 - 91405 Campus ORSAY - FRANCE

For the past several years we have been measuring the cosmogenic isotopes ^{10}Be and ^{26}Al in melted (cosmic spherules) and unmelted microparticles collected from deep sea and Greenland ice sediments (Raisbeck et al 1985, Raisbeck and Yiou, 1987). These measurements have led us to the following conclusions: (i) a large fraction of these objects can indeed be unambiguously identified as extraterrestrial (ii) most of these objects have been irradiated in interplanetary space as small (<1cm) objects -ie they are true "micrometeorites" (iii) the cosmic ray exposure times of these objects is typically 10^5-10^6 years. The second conclusion above led us to hypothesize that a significant fraction of these micrometeorites are probably cometary in origin, since most meteors in this size range are known to have cometary like orbits. A further possible test of this hypothesis is to look at the distribution of exposure ages of these particles. Sanford(1986) has pointed out that small particles of asteroidal origin reaching the earth are expected to have a rather narrow band of exposure ages, equal to the time necessary for them to spiral into 1 A.U. by the Poynting Robertson effect. Particles of cometary origin, on the other hand, are expected to have a broad distribution of exposure ages, determined essentially by the wide variety of orbits and probability of being captured by the earth. We show below ^{10}Be concentrations measured recently in 21 deep sea cosmic spherules, and the corresponding exposure ages as estimated by the procedure described in Raisbeck et al (1985). One notes first of all that the exposure ages are considerably shorter than those of normal chondritic meteorites, thus supporting our previous interpretation that these objects are indeed not ablation products from such classic meteorites. Secondly one sees that the distribution of exposure ages is large, thus also supporting the interpretation of a cometary origin. Finally one should note that the exposure ages are considerably larger than those predicted theoretically (cf. Dohnanyi, 1978). This may indicate either some inadequacy in the model calculations, or an indication that the interplanetary dust complex is not in secular equilibrium. We discuss in another paper at this meeting a possible method of studying this last hypothesis.

We thank D. Brownlee and K. Yamakoshi for providing the spherules.

Dohnanyi J.S. (1978) in "Cosmic Dust", McDonnell J.A.M. (ed.) pp. 527-605 Wiley. Raisbeck G.M. et al. (1985) in "Properties and interactions of interplanetary dust", Giese R.H. and Lamy P. (eds.) pp. 169-174, D. Reidel. Raisbeck G.M. and Yiou F. (1987) Meteoritics 22, 485. Sanford S.A. (1986) Meteoritics 21, 501.

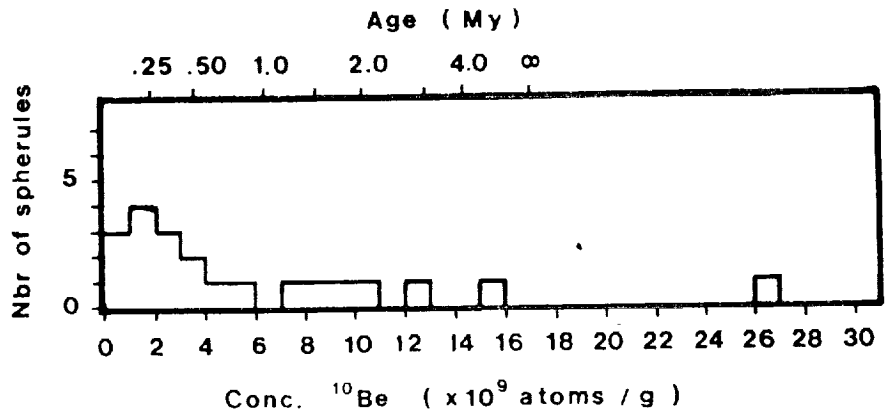

SOLAR FLARE TRACKS AND NEUTRON CAPTURE EFFECTS IN THE CARBONACEOUS GAS-RICH METEORITE MURCHISON, R. S. Rajan, Jet Propulsion Laboratory, California Institute of Technology, Pasadena, CA 91109, and G. W. Lugmair, Scripps Institute of Oceanography, University of California at San Diego, La Jolla, CA 92093

Over the last two years, we have reported evidence for precompaction neutron capture effects in SM-149 from two gas-rich meteorites, Kapoeta and Fayetteville (1). We have also measured solar flare track characteristics in these samples and looked for possible correlations between them. Our results suggest that there is no apparent correlation and that irradiation on the parent body regolith of ≥30 Myr is adequate to explain the data and that a T-Tauri scenario as suggested by Caffee et al. (2) is not warranted at this time.

We have extended our line of research to the gas-rich carbonaceous chondrites. It has been known for some time that irradiation features on the gas-rich carbonaceous chondrites are distinctly different from other gas-rich meteorites and suggest a different irradiation environment for them. We have chosen Murchison for our initial study, since it was also known to contain large amounts of precompaction spallation neon. Our results are summarized in Table 1. The quoted uncertainties refer to 2σ errors.

TABLE 1
SOLAR FLARE TRACKS AND NEUTRON CAPTURE EFFECTS

Sample	Weight (mg)	$^{150}Sm/^{149}Sm$	Relative Excess (ϵ Units)*	Abundance of Track-rich Grains (%)
Terrestrial STD	—	0.53398 ± 2	≡ 0	
Murchison				
Me 2682-11a	45	0.53405 ± 5		2.1
Me 2682-11b	45	0.53410 ± 7		2.1
Average		0.53407 ± 5	1.8 ± 0.9	

* One ϵ unit refers to 1 part in 10^4.

We have identified small, but statistically significant neutron capture effects in Sm-149 in Murchison. The effects are comparable to those previously observed in Kapoeta and Fayetteville. Such small effects can be easily understood in terms of regolith activity on the parent body and does not require invoking of an irradiation during an early T-Tauri phase to explain the precompaction effects.

REFERENCES

1) Rajan and Lugmair (1987). *LPSC XVIII*, 818.

2) Caffee *et al.* (1983). J. Geophys. Res., B-267

SOLAR-PROTON-PRODUCED ^{81}Kr IN LUNAR ROCKS.*

R. C. Reedy,[1] K. Marti,[2] and **B. Lavielle.[3]** (1) Earth & Space Sciences Division, Los Alamos National Laboratory, Los Alamos, NM 87545; (2) Department of Chemistry, B-017, University of California, San Diego, La Jolla, CA 92093-0317; (3) Centre d'Études Nucléaires de Bordeaux-Gradignan, Le Haut Vigneau, F-33170 Gradignan, France.

Cosmogenic nuclides in the outer centimeter of lunar samples have allowed us to determine the fluxes of solar cosmic rays (SCR) over the past $\sim 10^7$ years (1). Much still needs to be done to utilize, confirm, or extend existing measurements (2). The solar-proton fluxes averaged over the last ~1-Ma (1 Ma = 10^6 years) are fairly well determined (e.g., 3), although the fluxes above 10 MeV and the proton spectral shape are still somewhat uncertain (1,4). There are considerable uncertainties in average fluxes over the last ~5–500 ka (2). Four radionuclides cover this period: 5730-a ^{14}C, 0.1-Ma ^{41}Ca, 0.21-Ma ^{81}Kr, and 0.30-Ma ^{36}Cl. The solar-proton fluxes previously reported for ^{14}C and ^{81}Kr (1) are much higher than those averaged over ~1 Ma. There is a need for additional measurements of these radionuclides in lunar samples and of cross sections for their production (2) to check previously reported results.

The earlier ^{81}Kr results of Yaniv *et al.* (5) were for samples from rock 12002. Here we present new measurements for solar-proton-produced Kr isotopes in lunar rock 68815, taken from the top of a boulder near 2-Ma-old South Ray Crater. Sampling details for 68815 can be found in (3). Krypton isotopes were measured in pieces of the surface layer and three subsurface chips of 68815 by static mass spectrometry with peak switching techniques. Concentrations (in units of 10^{-12}cm^{3}STP/g) of cosmogenic ^{81}Kr ranged from 0.33 ± 0.06 in the top 0.5 mm to 0.19 ± 0.03, 0.16 ± 0.02, and 0.140 ± 0.012 at depths of 8–11, 12–15, and ≈18 mm, respectively, clearly showing a strong SCR signature.

New cross sections based on (6–8) were used to unfold these measurements. However, measured cross sections at proton energies near the reaction thresholds (the most important ones) are missing. As there are no good ^{81}Kr measurements for 68815 samples well shielded from solar protons, we treated the GCR production rate as an adjustable parameter along with the erosion rate and the parameters for the solar protons. The best match is with no erosion, an integral flux above 10 MeV of 145 protons/(cm^2 s), and R_o = 85 MV. These flux parameters are similar to those that can fit the ~1 Ma measurements (4). The parameters for other matches are less reasonable, e.g., GCR rates too low. Even the GCR rate used here is on the low end of the expected range. More details are in (9).

Yaniv *et al.* (5) reported a hard spectral shape ($R_o \approx 150$ MV) for their ^{81}Kr results for 12002, but such a hard spectral shape is not consistent with our measurements for ^{81}Kr in 68815 (as it would require an unreasonably low GCR rate). The ^{81}Kr data for 12002 need to be re-examined to see if they can be matched with softer spectra. We prefer not to give any fluxes based on ^{81}Kr until production cross sections are measured at low proton energies and there are additional ^{81}Kr measurements in lunar rocks in which the target elements for cosmogenic krypton (e.g., strontium and zirconium) are well determined.

References: (1) Reedy R. C. (1980) *Proc. Conf. Ancient Sun*, p. 365. (2) Reedy R. C. *et al.* (1989) *Lunar Planet. Sci. XX*, 890. (3) Kohl C. P. *et al.* (1978) *Proc. Lunar Planet. Sci. Conf. 9th*, p. 2299. (4) Nishiizumi K. *et al.* (1988) *Proc. Lunar Planet. Sci. Conf. 18th*, p. 79. (5) Yaniv A. *et al.* (1980) *Lunar and Planetary Science XI*, 1291. (6) Regnier S. *et al.* (1982) *Phys. Rev. C* **26**, 931. (7) Lavielle B. and Regnier S. (1984) *J. Physique* **45**, 981. (8) Lavielle B. (1987) Thesis, Univ. Bordeaux I. (9) Reedy R. C. and Marti K. in *The Sun in Time*, submitted 4/89. * Research supported by NASA. Los Alamos work done under the auspices of US DOE.

CARBONACEOUS FRAGMENTS IN THE BHOLGHATI HOWARDITE; A.M. Reid, and P.C. Buchanan, Geosciences, University of Houston, Houston, TX 77204, R.A. Barrett, Lockheed Engineering and Sciences Co., Houston, TX 77058, and M.E. Zolensky, NASA, Johnson Space Center, Houston, TX 77058

The Bholghati howardite is a regolith breccia with angular clasts of mineral and lithic fragments derived from a series of related igneous rocks, ranging from diogenite to eucrite. Dispersed throughout the breccia are small (1-2mm) dark clasts of material that resembles carbonaceous chondrites. We have separated 30 of these small carbonaceous clasts for study. The majority are mixtures of silicates, Fe-Ni sulphides, and fine-grained dark matrix, similar to CM carbonaceous chondrites. The silicates form aggregates, some chondrule-like but mostly irregular, of low Fe olivine (~1 wt. % FeO), low Fe, low Ca pyroxene (also ~1 wt. % FeO, much of it twinned clinoenstatite), with minor high Ca pyroxene and rare Fe-Ni inclusions. The matrix, largely Mg-Fe phyllosilicates, is heterogeneous with a bulk composition (Table 1) comparable to CM chondrites (Fig. 1) but with lower Mg contents (Fig. 2).

One of the dark clasts has a single angular forsterite grain in a fine matrix that also contains pyrrhotite and pentlandite, framboidal and spherulitic magnetites, and some grains of calcium carbonate. Texturally, mineralogically, and compositionally (Figs. 1 and 2) this clast resembles a CI chondrite.

Many howardite regolith breccias are known to contain carbonaceous clasts. In the Bholghati breccia we note 1) that most clasts resemble but are not identical to CM chondrites, and 2) that more than one type of carbonaceous material has been added to the regolith.

Table 1. Major Element Compositions of Bholghati Carbonaceous Clast Matrices

SiO_2	27.4	25.2	26.8	29.3	28.3	30.2	29.4	29.8	28.5	29.8	30.5	35.2
Al_2O_3	2.6	3.0	2.9	2.5	2.4	2.6	2.5	2.5	2.6	2.4	2.5	3.2
FeO	33.8	40.3	36.5	31.7	33.5	32.7	32.3	33.1	32.7	31.64	29.8	19.1
MgO	15.8	14.1	14.6	17.3	15.9	17.7	18.1	17.7	16.7	1.8.1	18.4	20.0
CaO	.6	.8	.3	1.0	.6	.6	.8	.6	1.0	1.0	.6	.4
Na_2O	.7	1.0	.7	.4	.3	.6	.6	.6	.5	.7	.5	n.d.
SO_3	14.8	13.4	9.9	10.0	8.1	8.6	9.9	9.2	10.1	8.8	8.8	12.5

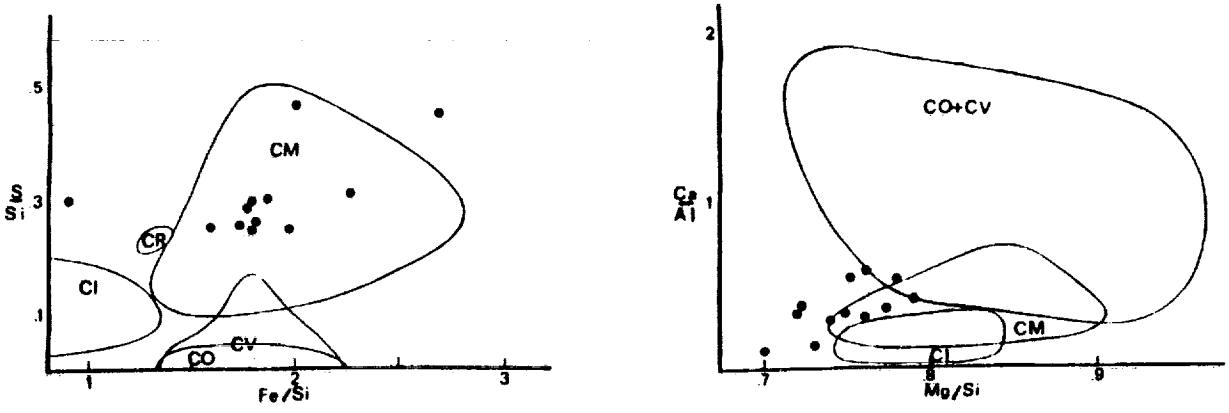

Figures 1 and 2. Matrix compositions for carbonaceous clasts, compared with fields for carbonaceous chondrites (chondrite data from McSween and Richardson, 1977).

RELECTIONS ON MINERAL LOCI OF ELEMENTS IN INTERPLANETARY DUST PARTICLES: EXTRATERRESTRIAL SULFUR IN THE LOWER STRATOSPHERE.

Frans J. M. Rietmeijer, Department of Geology, University of New Mexico, Albuquerque, NM 87131, U.S.A.

Chondritic interplanetary dust particles [IDPs] are small-sized (<~50 μm) micrometeorites originating from undifferentiated Solar System bodies such as short-period comets and asteroids and chondritic IDPs represent the least altered Solar System materials currently available for analyses[1-3]. Two important trends in chondritic IDP research include observations of (1) volatile trace element abundances in excess of these abundances in carbonaceous chondrites[4-7] and which indicate an emerging trend of volatile element enhancements in chondritic IDPs as a function of elemental condensation temperature[6,8] and (2) small-scale textural heterogeneity of minerals that contain volatile elements, such as $BaSO_4$ [barite][1,9] and oxides of bismuth[1] and tin[8]. In another development, trace element data are used to calculate the micrometeorite component of halogens and sulfur in the lower stratosphere[10]. These calculations assume that (1) micrometeorite volatile elements occur in CI-abundances and (2) volatiles are released as a result of atmospheric entry flash-heating[10]. In a study of extra-terrestrial F, S, Cl, Br and I in the lower stratosphere, calculated fractional masses of halogens are close to observed values but for sulfur the calculated fractional mass [1.5×10^{-9} g] is in excess of the observed value [5×10^{-10} g][10]. The mineralogical sites for halogens in chondritic IDPs are not known but it is plausible that these elements reside in highly volatile mineral phases which may be completely vaporised during flash-heating on atmospheric entry.

SULFUR In chondritic IDPs sulfur occurs in sulfides[1,2] and carbonaceous material[11]. Release of sulfur from the host mineral during flash-heating is a function of (1) evaporisation kinetics of the host mineral, (2) grain size of the host mineral and (2) textural relationships of the host mineral(s) in the parent IDP. For example, sulfides occur as (1) micron-sized euhedral single crystals and (2) submicron crystals embedded in a matrix of carbonaceous material[11,12] or layer silicates[12,13]. It is conceivable that the matrix protects a fraction of sulfides from vaporisation during flash-heating[14]. Sulfur release from carbonaceous material is difficult to assess but gas phase pyrolysis and carbon graphitisation are thermally activated kinetic processes with reaction times in excess of minutes[15,16]. This timescale seems prohibitive to extensive loss of sulfur from carbonaceous materials in IDPs during flash heating at T > 800 °C [cf. ref. 10].

To calculate the fractions of sulfur in sulfides and carbonaceous material ($S_{total} = S_{sulfides} + S_{carbon}$), I use average C/Si and S/Si ratios in chondritic IDPs[17] [C/Si= 1.86 and S/Si= 0.38] and I assume a C/S ratio for carbonaceous material in these IDPs similar to this ratio in mantled comet Halley dust grains[18] [C/S= 11.3]. Thus, S_{carbon} in an average chondritic IDP becomes 0.16 and $S_{sulfides}$ = 0.22. This latter represents 58% of the total sulfur content. Thus, the calculated fractional mass of sulfur in the lower stratospheric that derives from sulfides in chondritic IDPs becomes 8.7×10^{-10} g which is 1.7% greater than the observed value. The difference between calculated and observed fractional masses of sulfur decreases further if the layer silicate or carbonaceous matrix protects some fraction of sulfides from vaporisation. This example shows that meaningful use of chemical data for chondritic IDPs depends on a complete understanding of the host mineral(s) for the elements under consideration.

REFERENCES. 1. Mackinnon IDR & Rietmeijer FJM (1987) Rev. Geophys. 25, 1527-1553; 2. Bradley et al (1988) In MESS (JF Kerridge & MS Matthews, eds), 861-895; 3. Brownlee DE (1985) Ann. Rev. Earth Planet. Sci. 13, 147-173; 4. Vis RD et al (1987) Nucl. Instr. Methods Phys. Res. B22, 380-385; 5. Wallenwein R et al (1989) LPS20, 1171-1172; 6. Sutton SR & and Flynn GJ (1988) Proc18th LPSC, 607-614; 7. Zolensky et al (1989) LPS20, 1255-1256; 8. Rietmeijer FJM (1989) Meteoritics 24, in press; 9. Rietmeijer FJM & Mackinnon IDR (1984) Meteoritics 19, 301; 10. Sutton SR & Flynn GJ (1988) LPS19, 1154-1155; 11. Rietmeijer FJM (1989) Proc19th LPSC, 513-521; 12. Bradley JP (1988) GCA 52, 889-900; 13. Blake DF et al (1988) Proc18th LPSC, 615-622; 14 Sandford SA (1986) LPS17, 754-755; 15. Fitzer E et al (1971) In Chem. Phys. Carbon 7 (Walker PL ed), 237-383; 16. Fischbach DB (1971) In Chem. Phys. Carbon 7 (Walker PL ed), 1-105; 17. Schramm LS et al (1989) Meteoritics 24, in press; 18. Jessberger EK et al (1988) Nature 332, 691-695.

This work is supported by NASA Grant NAG-9-160.

A NITROGEN ISOTOPE ANOMALY AT THE K-T BOUNDARY.

François ROBERT, Agnès REJOU-MICHEL & Marc JAVOY.
Laboratoire de Géochimie des Isotopes Stables; IPGP and Université Paris VII, 75251 PARIS CEDEX 05, FRANCE.

Large isotope variations linked to major geo-biological events have been reported in the literature. Following this approach, the carbon and nitrogen concentrations and isotope compositions of carbonates and acid resistant organic matter were determined in the marine Cretaceous-Tertiary boundary sampled in Sopelana (North of Spain). As it is common for such geological boundaries [1,2], a marked decrease in $\delta^{13}C$ was found in the carbonates ($\Delta^{13}C = 2.1‰$). This change is associated with a slight but clearly resolved increase in $\delta^{13}C$ of the acid resistant organic matter ($\Delta^{13}C = 1.1‰$). This anti-corelation has been observed at other geological sites and is attributed to the kerogen fraction [3] (and not to the elemental carbon or soot which are also concentrated in acid residues). The interpretation for this heavy kerogen supports the idea of a drastic decrease in the marine bioproductivity: The input of marine dead plankton whose heavy isotopic composition is preserved in the sediment by a rapid burial, yields an increase in the organic $\delta^{13}C$. However opposite correlations are also reported at the K/T boundary [4] and it is unclear if the present anti-correlation represents a local rather than a global effect.

All the samples below and above the boundary exhibit $\delta^{15}N$ values lying between +5 and +9‰. Such isotopic compositions can be attributed to well preserved marine organic matter [5]. At the boundary (40cm thick) a ^{15}N enrichment is observed with $\delta^{15}N$ values up to +22‰. The isotopic variations are correlated with a marked increase in the N/C ratio. Since a variation of 15‰ in the isotopic composition of the atmospheric nitrogen is precluded, the change in $\delta^{15}N$ is related to the conditions of formation of this organic matter. Such conditions may be illustrated by the high $\delta^{15}N$ values observed in the marine organic matter of the Scheldt estuary. In this case Mariotti et al. [6] have found $\delta^{15}N$ values in the autochtonous phytoplankton similar to those found in the present case. They explain such a ^{15}N enrichment by the large kinetic isotope fractionation between NH_4^+ and NO_3^- occuring in strongly anoxic conditions (with $\delta^{15}N$ values up to +30‰ in NH_4^+). The phytoplankton reflects mainly the isotopic composition of NH_4^+ and exhibits $\delta^{15}N$ values up to +25‰. By analogy with this unique known natural occurence of such high $\delta^{15}N$ values, the following interpretation could be imagined for the conditions of the organic matter formation at the boundary : The change in $\delta^{15}N$ is related to the appearance of anoxic conditions at the water surface. Therefore the disappearance of the organic carbon suggested to interpret the carbon isotopic data would be related to a decrease in free oxygen. At this locality, the nitrogen anomaly would provide a clear evidence for a drastic change in the redox conditions of the sea-water. The extent of the $\delta^{15}N$ anomaly to a global scale, should be investigated in order to test the assumption of a global change in the atmospheric oxygen concentration.

References: [1] Magaritz *et al.* (1983) *Earth Planet. Sci. Lett.* **66**, p.111-124. [2] Magaritz & Turner (1982) *Nature* **297**, p. 389-390. [3] Wolbach et al., *Meteoritics*, 22, p. 531-532. [4] Schimmelmann et al., Earth & Planet. Sci. Lett. 68, p. 392-398. [5] Halbout *et al.* (1988) *Chem. Geology* **70**, p. 119. [6] Mariotti *et al.* (1984) *Geochim. Cosmochim. Acta* **48**, p. 549-555.

Pseudotachylite and Mylolisthenite. Jehan Rondot. Astrobleme Exploration, 1111 Amiens, Sainte-Foy (Québec) Canada G1W 4C8

"The name pseudotachylyte (now pseudotachylite) has been adopted in recognition of the fact that these rocks have a great similarity to tachylyte ..." [1], in particular its dark color and intrusive aspect. The name mylolisthenite, from "mulon" to mill and "olistanein" to slide, has been introduced to distinguish a special type of autochthonous breccia different from pseudotachylite and from allochthonous breccia filling fractures in the bottom of the astroblemes [2]. Unlike the pseudotachylite, the mylolisthenite are pale grey, green or red and are found in sedimentary as well as in crystalline rocks.

Tectonic pseudotachylite, found in small quantities in crystaline rocks along some major fault and thrust planes, has been the object of a lot of descriptions and studies [3,4,5 etc.]. The complex network of black, aphanitic or glassy veins is filled with partly fused rock with crystalline powder. Pseudotachylite found in highly deformed rocks is itself rarely deformed [6] and it is formed in a single episode of slip [7]. It is a product of earthquake faulting in the brittle zone of rock deformation, [8,9]. Pseudotachylite has also been found in great circular structures: Vredefort where the name originally came from [1,10] and Sudbury where it is called Sudbury breccia [11-12]. Here it appears not only in complex network of black centimetric veins, but also in irregular or tabular bodies up to a few meters thick and often with subrounded fragments. In both structures we found other types of light coloured breccia which do not look as tachylyte.

The mylolistenite, as indicated by its name, contain powder of crushed rocks in the fragments and in the matrix and show several indications of movement in differents directions, e.g. slickensides on the fragments, pieces of rock coming from some distance, crushed fragments of differents color or grain size, irregular crushed contact with wall-rock etc... The relative motions are best seen in astrobleme where there is contrast of litology as in Charlevoix, Carswell, Manicouagan, Siljan etc. [13]. Unlike pseudodachylite, mylolisthenite has no fused matrix, even if we can find melted rock in fragments [14]. Mylolisthenite are decimeters to meters in thickness which represent a great volume of crushed minerals and therefore of volatiles. Hydrothermal alterations are common and some dykes show vesicles. As pseudotachylite the mylolisthenite is the last deformed rock of an event and in both cases the chemical composition is not very different from that of the neighbouring rocks.

It is proposed here to limit the use of the term pseudotachylite for the autochthonous breccia with dark aphanitic or glassy, partly melted rock as a matrix and use mylolisthenite for autochtonous irregular bodies or dykes with fragments of breccia and a matrix of breccia, with or without hydrothermal alteration. References: [1] Shand (1916) J. geol. Soc. London 72, 198-231. [2] Rondot (1971) Meteoritics 6 307-308. [3] Francis (1972) Comments Earth Sci. Geophys. 3, 35-53. [4] Wenk and Weiss (1982) Tectonophysics 84, 329-341. [5] Philpotts (1954) Am. J.Sci. 262, 1008. [6] Macaudière and Brown (1982) J. Struct. geol. 1, 395-406. [7] Grocott (1981) J. Struct. geol. 3 169-178. [8] Gibson (1975) Geophysic J.R. astro Soc. 43, 775-794. [9] Gibson (1977) J. geol. Soc. London 133, 191-213. [10] Wilshire (1971) J. Geol. 79 195-206. [11] Dietz (1964) J. Geol. 72. 412-434. [12] Dressler et al. (1984), Ontario Geol. Surv. Spec. Vol. 1, 39-68. [13] Rondot (1975) U. Uppsala N.S. Bul. Geol. 6 85-92, (1983) U. Clermont Fd. France Ann. Sci. 75. [14] Reimold et al. (1987) J. Geophys. Res. 92, E737-E748.

CR ISOTOPIC DIVERSITY IN CARBONACEOUS CHONDRITES; M. Rotaru, J.L. Birck and C.J. Allègre, Laboratoire de Géochimie, IPG, 4 Place Jussieu, 75252 Paris Cedex 05

The most significant non linear isotopic effects for iron group elements, have so far been found in refractory inclusions of C3 chondrites or similar materials like hibonites in C2s. We report here a chromium isotopic investigation of the mineral phases of the bulk meteorites. Bulk powdered samples of carbonaceous chondrites were submitted to a leaching procedure involving increasing strength: dilute acids for leach 1, 2, 3 & HF + strong acid for leach 4 & 5.

Results: the data are normalized for instrumental fractionation to the terrestrial $^{52}Cr/^{50}Cr$ ratio. The most significative results show very large isotopic effects in C1 and C2's. For all samples, effects on ^{53}Cr are close to normal. Isotopic variations on this isotope are probably related to the decay of ^{53}Mn in the early Solar System materials [2]. The following discussion will focus on isotope ^{54}Cr which shows the largest effects.

Two samples of the C1: Orgueil were analysed. Dilute acid leaches shows systematic deficits (1) between 5 and 15 ε. At the reverse very large ^{54}Cr excesses close to 1% are present in the silicate fraction (leach 4).

Two C2's Murchison and Murray were analysed: they display deficits of about 15 ε in the weak acid leachate[1] and excesses of similar magnitude in the silicate fraction. The same procedure applied to the C3 Allende gives results close to normal isotopic composition.

As a general observation for the iron group, it is the first evidence in non refractory materials of isotopic anomalies which display magnitudes comparable to FUN inclusion.

The smaller effects in C2's than in C1 and the near absence of effect in the C3:Allende is probably related to more complete isotopic reequilibration with higher degree of metamorphism.

A number of important implications follow from the data:

- In C1 an C2's the most significant fractions do not have normal isotopic composition: therefore, if the bulk happens to be close to normal it is only because the different (1) components have been mixed in the adequate porportions to produce the normal composition. We may see here a general feature of the solar system: it is known that the solar system is a mixture of numerous nucleosynthetic contributions: as C1s are thought to be good representative of solar system composition, this is the first direct evidence of mixing of different nucleosynthetic components present at the microscopic scale within a planetary body to produce normal matter at a larger scale.
- Considering the isotopic pattern for leach 4 of Orgueil, this fraction could result from mixing of normal Cr with very pure ^{54}Cr (99,5 %). This is similar to PSI inclusions[3] where a similar component is missing. This component constituted by almost pure ^{54}Cr represents a strong constraint for the nucleosynthetic processes at the origin of these isotopic anomalies.
- The Cr isotopic ratios of non-FUN inclusions in C3s are closer to normal than the leaches of Orgueil: they appear to be more processed materials than the fractions found in C1's.

In conclusion, very large chromium isotopic differences have survived in the phases of C1 and C2 matrix. The investigation of the extent of this isotopic diversity in Cr and in other elements will help to clarify the exact nature of these primitive compnents of the solar system.

REFERENCES: 1) Rotaru M. et al. (1989) LPSC XX, 924. 2) Birck J.L. & Allègre C.J. (1988) Nature 331, 579. 3) Papanastassiou D.A. & Brigham C.A. (1988) LPSC XIX, 899. 4) Papanastassiou D.A. (1986) Ap. J. Lett., 308, L27.

	LEACH N° 2		LEACH N° 4		LEACH N° 5	
	53Cr/52Cr	54Cr/52Cr	53Cr/52Cr	54Cr/52Cr	53Cr/52Cr	54Cr/52Cr
ORGUEIL	0,30 ±0,31	-15,66 ±0,67	-0,62 ±0,15	92,58 ±0,32	-1,45 ±0,16	23,12 ±0,32
ORG Dupl.	0,87 ±0,18	-5,26 ±0,43	-0,21 ±0,26	101,43 ±0,43	-0,97 ±0,23	53,3 ±0,53
MURCHISON	0,70 ±0,24	-13,99 ±0,50	0,04 ±0,16	15,03 ±0,35	-0,52 ±0,33	27,41 ±0,67
MURRAY	0,78 ±0,16	-17,63 ±0,35	0,22 ±0,17	15,38 ±0,43	-0,27 ±0,16	27,69 ±0,39
ALLENDE	1,90 ±0,35	-0,04 ±0,64	0,59 ±0,33	1,69 ±0,64	-0,57±0,41	2,6±0,80

OXYGEN ISOTOPES IN SEPARATED COMPONENTS OF CI AND CM CHONDRITES; M.W. Rowe,[1] R.N. Clayton,[2] and T.K. Mayeda. Enrico Fermi Institute, University of Chicago, Chicago, IL 60637. [1]Permanent Address: Department of Chemistry, Texas A&M University, College Station, TX. [2]Also: Departments of Chemistry and of the Geophysical Sciences.

Oxygen isotopes are useful to seek genetic relationships between carbonaceous chondrites whose oxygen isotopic compositions are distinctive for each class; but no clear genetic relationship has been seen between them [1]. We examined the oxygen isotopes in separated magnetite, matrix, chondrules, and an olivine/pyroxene concentrate, as well as in whole rock samples, from some CI and CM chondrites.

The oxygen isotopic compositions of magnetite separated from the Ivuna and Orgueil CI and the Essebi CM2 chondrites differ from all other meteoritic values. In particular, three analyses of magnetite from Orgueil and one each from Ivuna and Essebi all lie very close to a slope-1/2 line on the three isotope graph, about 1.8 $\delta^{17}O$ units higher than the terrestrial mass fractionation line. This indicates that this magnetite has a common origin, suggesting that the magnetite is the oxidation product of previously existing iron-sulfur species by aqueous alteration [2-4]. This conclusion is strengthened by the recent observation of the CI, Yamato-82162 [5] that shows evidence of only a low degree of aqueous alteration, and has magnetite much lower and iron sulfides much higher in abundance than in other CI chondrites. That all the magnetite analyses lie on the slope-1/2 line points to water that had a single oxygen isotopic composition during magnetite formation. In all cases the magnetite and phyllosilicates fall on different fractionation lines, indicating that water of different isotopic compositions was present for formation of the two mineral types. Once the magnetite was formed, its oxygen isotopic composition would not exchange further [6] as water continued to react to produce the matrix minerals, the water oxygen isotopic composition presumably becoming continuously more ^{16}O-rich during this process. The data are inconsistent with production of the magnetite and phyllosilicates by aqueous alteration of olivine [7].

Two of three Essebi chondrules fall on the line defined on the three isotope plot by CV chondrules [8], neither slope-1/2 nor 1. This implies a common origin of these CM2 chondrules from Essebi and the CV3 chondrules. Thus Essebi's magnetite seems to have a common origin with that in CI chondrites while its chondrules are related to those in CV chondrules. The third Essebi chondrule lies on the slope-1 line of the Allende inclusions.

References: [1] Clayton, R.N. and T.K. Mayeda, 1989. LPS 20, 169-170; [2] Herndon, J.M. et al., 1975. Nature 253, 516-518; [3] Hyman, M. and M.W. Rowe, 1986. J. Trace Microprobe Tech. 3, 275-302; [4] Kerridge, J.H. et al., 1979. Science 205, 395-397; [5] Tomeoka et al., 1989. Proc. 13th Antarctic Met. Sym.; [6] Clayton, R.N. et al., 1986. E.P.S.L. 79, 235-240; [7] Jeffrey, P.M. and E. Anders, 1970. GCA 34, 1175-1198; [8] Clayton, R.N. et al., 1983. In Chondrules and Their Origins, ed. E.A. King, LPI, Houston, 37-43.

AN OLIVINE-MICROCHONDRULE-BEARING CLAST IN KRYMKA AND THE ORIGIN OF MICROCHONDRULES; Alan E. Rubin and John T. Wasson, Institute of Geophysics and Planetary Physics, University of California, Los Angeles, CA 90024, USA.

Microchondrules occur as the principal chondrule size in unique meteorite ALH85085, and as the predominant or exclusive chondrule size in unequilibrated clasts from several OCs. Three such microchondrule-bearing clasts have been previously described, including one in Piancaldoli (LL3.4) containing 0.25-64-μm-size RP chondrules, one in Rio Negro (L regolith breccia) containing 5-74-μm-size RP and POP chondrules, and one in Mezö-Madaras (L3.7) containing 2-150-μm-size pyroxene- and silica-rich chondrules. A fourth microchondrule- bearing clast occurs in Krymka (LL3.1). This 150x200-μm-size clast consists of 20 vol.% 6-31-μm-size olivine microchondrules (with barred and granular textures) and 80 vol.% fine-grained silicate matrix material.

We offer three mechanisms for forming microchondrules:

(1) Impact splash formation. Chondrule-like crystalline spherules occur in howardites, the lunar regolith, and suevite; all of these objects were produced by impact-melting and concomitant splattering of surficial materials. Microchondrules may have been formed by a similar process. There is some evidence that microchondrules tend to consist of aggregates of closely related siblings: e.g., the RP microchondrules in the Piancaldoli clast show far less interchondrule compositional variability than normal-size RP chondrules. Hence, microchondrules in this clast may have been produced simultaneously during impact-melting of the same aggregate of precursor material. During such impact events, numerous melt droplets may have been entrained in jets, propelled from the impact point and incorporated into matrix material.

(2) Nebular droplet disruption. Microchondrules may have formed in the nebula from normal-size chondrule precursor droplets by collisional disruption and spattering. The small interchondrule compositional variability of the RP microchondrules in Piancaldoli is readily accounted for by this mechanism.

(3) Nebular sorting by size and type. Chondrule size varies with chondrite group; even within an individual chondrite group, chondrule size can vary from one meteorite to another. Such inter- and intra-group differences have been attributed to aerodynamic size-sorting in the nebula. Maximum chondrule size may also be a function of the intensity of the heat source. Such processes could have resulted in certain nebular regions containing only microchondrules. Furthermore, different chondrite groups contain different proportions of chondrule textural types, and it is conceivable that certain nebular regions contained chondrules predominantly of one textural type.

Although all three mechanisms are probably responsible for forming some microchondrules, each has potential problems forming microchondrule-bearing clasts. (1) Impact-melting of OC whole-rocks should form products similar in composition to the silicate portions of the target; thus, it seems difficult for impact-melting to form the RP microchondrules in the Piancaldoli clast unless a pyroxenitic target is invoked; such material is rare in OCs. (2) Although droplet-disruption in the nebula can produce microchondrules, these objects should spread apart rapidly; it seems unlikely that groups of them would be trapped in small clast-size clumps. (3) There is evidence from several chondrite groups that the smallest chondrules are predominantly RP; thus, nebular size-sorting could potentially yield regions with abundant tiny RP chondrules. However, there is currently no evidence that in some nebular regions the smallest chondrules were predominantly olivine-rich, as in the Krymka clast. Perhaps these different microchondrule-bearing clasts were formed by different mechanisms.

AGES OF LUNAR IMPACT MELTS AND LUNAR BOMBARDMENT. **G. Ryder, Lunar and Planetary Institute, 3303 Nasa Rd. 1, Houston, TX 77058.**

The Moon has been subject to severe cratering over some period of time following creation of a solid crust capable of preserving the record. The absolute ages of specific cratering events are best determined by radiogenic isotope analyses of impact melts produced during the cratering; the most unambiguous results are obtained on coarser, clast-free impact melts. In an impact, only a small amount of target material (less than 5%) is melted (or nearly melted) and its radiogenic clocks reset. Most of the ejecta is merely brecciated and mixed, and both the ejection and deposition are accomplished at temperatures too low to reset radiogenic isotopes. This means that an impact melt on the Moon, once created, retains the radiogenic age of its cratering origin unless it is once again included by chance in the small part of a target that gets remelted.

If the Moon had undergone a heavy post-accretional (or late-accretional) bombardment from 4.5 to 3.9 Ga ago, as is widely believed and extrapolated to the other terrestrial planets, then the lunar highlands should contain a high proportion of impact melt, as shown by Lange and Ahrens (1979). The actual proportion found, which is certainly less than 30% and possibly as low as 10%, is inconsistent with postulated heavy bombardments. If there had been an early heavy bombardment, then many of the impact melts should show correspondingly old ages, because later impacting is inefficient in resetting them; many should have survived a declining bombardment, no matter how severe. Only conversion of most rocks to impact melt could eradicate old ages, and this conversion did not happen. The lunar sample record, with Apollo, Luna, and lunar meteorite data, is clear that there are no collected impact melts that have been unambiguously dated at older than 3.92 Ga. The only claimed group of older impact melts are very fine-grained with more than 50% tiny plagioclase clasts, and were dated with Ar-Ar whole-rock techniques; efficient degassing in their creation is dubious. All rocks with ages older than 3.92 are igneous rocks or cataclasized samples for which the date cannot be demonstrated to reflect an impact event. One exception is a granulite, which represents an ancient breccia.

The lack of old ages is not a function of collecting bias, and does not represent the influence of one or even a few impact events; the range in compositions and small but real differences in ages demonstrates this. The lunar record of impact melts is quite clear in showing the existence of a severe impacting cataclysm in the period 3.92-3.83(??) period, as suggested by Tera et al. (1974). Other features of the lunar sample record are consistent with this cataclysm. Those who deny this cataclysm do so by ignoring the lunar sample record, a tangible inheritance of the Apollo program, not by using it. The lunar record and its correct or incorrect extrapolation to the rest of the inner solar system is of profound importance in planetology; it behooves us to question our understanding of it, not blindly accept the fiats of others derived from less-testable foundations.

References: Lange M. and Ahrens T. (1979) Proc. Lunar Sci. Conf. 10th, 2707-2725. Tera F. et al. (1974) Earth Planet. Sci. Lett. 22, 1-21.

ZONED AND EXSOLVED COMPLEX PYROXENES IN EVOLVED HIGHLANDS ROCKS FROM THE APENNINE FRONT. G. Ryder[1] and R. Martinez[2] ([1]Lunar and Planetary Institute, 3303 Nasa Rd 1, Houston, TX 77058. [2]Lockheed Emsco, 2400 Nasa Rd. 1, Houston, TX 77058).

Three cataclastic coarse fines samples from Station 7 on the Apennine Front have mineral compositions and assemblages similar to those of the quartz-monzodiorite (QMD) clasts in a Station 6a boulder, including iron-rich pyroxenes and silica-potash feldspar intergrowths. The original grain sizes appear to have been more than 1 mm.

Fe-augite and Fe-pigeonite coexist in complex intergrowths (e.g. Fig. 1) that also characterize QMD, and some evolved rocks of the Palisades sill (Walker, 1969). All pyroxenes have exsolved, with lamellae less than 10 microns thick. The exsolution in almost all instances occurs in only one direction in any sub-grain. In one preserved patch in 15434,12, the lamellae do not maintain a constant direction across the aggregate, but rather the aggregate is a series of sub-grains (Fig. 1).

The high-Ca pyroxenes have a regular range of compositions over nearly 20 mol% Fs (Fig.2). The low-Ca pyroxenes show a smaller but still significant range. The most Mg-pyroxenes do not appear to touch low-Ca pyroxenes. The most iron-rich grains coexist with fayalite. The aggregate shown in Fig. 1 has a range of no more than 3 or 4 mol% in its high-Ca pyroxene, but the cataclasized patch of pyroxenes adjoining it includes the magnesian varieties. Grains in the QMD show less than about 3 mol% Fs variation, but differences among grains appear to be up to about 10 or 15 mol% (e.g. Takeda et al. 1981). The bulk pyroxene solvus indicates crystallization temperatures of the order of 1030+/-10°C, consistent with evolved KREEP basalt crystallization (Hess et al., 1989); the lamellae compositions suggest continued diffusion over at least a few tens of microns down to 900°C. However, their thermal history is quite different from Apollo 15 KREEP basalts, and the age of the QMD (4.35 Ga; Compston et al. 1984) makes these samples a continuing enigma in lunar evolution. The range of compositions of the pyroxenes, their petrographic features, and their exsolution suggest crystallization in a shallow sill-like feature.

Fig. 1

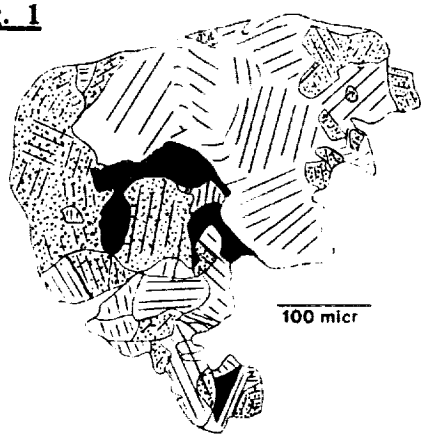

Fig. 2

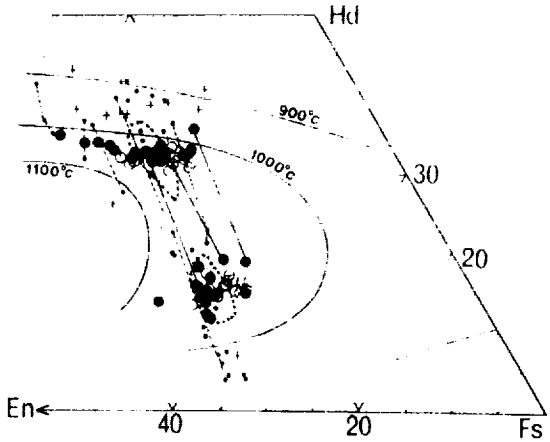

Fig. 1 Map of a complex grain in 15434,12,138. Black is plagioclase, stippled is pigeonite, white is augite. Straight lines show direction of exsolution lamellae.
Fig. 2 Microprobe analyses of pyroxenes. Examples of tie-lines between adjacent pyroxenes are shown. Large symbols are bulk analyses, small are point analyses. Black is 15434,12; open is 15434,14; crosses are 15434,10. Fields enclosed with tiny crosses are our new analyses of QMD 15405,57.

References: Compston W. et al. (1984) LPS XV, 182-183. Hess P. et al. (1989) LPS XX, 408-409. Takeda H. et al. (1981) PLPSC 12th, 1297-1313. Walker K. (1969) Geol. Soc. Am. Spec. Paper 111, 178 pp.

PROBLEMS OF ORIGIN OF ASTEROIDS AND COMETS. V.S.Safronov. O.Schmidt Institute of Physics of the Earth,USSR Ac.Sci.Moscow

Asteroids. In 50-ties physico-chemical study of meteorites by H.Urey led him to the conclusion that these bodies had been formed from asteroidal size bodies.At the same time O.Schmidt suggested that the formation of a normal planet in the asteroidal zone (AZ) had been prevented by Jupiter's perturbatios.Theory of formation of the asteroid belt should answer two main questions: (1) How random velocities of the asteroid zone bodies (AZB) at an early stage became so high to prevent further growth? With the present velocities of 5km/s practically all collisions lead to disruption. (2) How to remove from AZ more than 99.9% of the initial mass of solid matter which exceeded the mass of the Earth? The study of accumulation of bodies in the Jupiter's zone (JZB) has shown (1) that when protoJupiter reached a few tenths of the Earth's mass,eccentricities of JZB orbits became large and they penetrated into AZ. It has been suggested that these JZB being much larger than AZB (due to high fraction of volatiles) sweeped most AZB from AZ at collisions and increased their random velocities at close encounters. Later it has been estimated that only about a half of the total mass of AZB could be removed by JZB (2). In the model of a runaway growth of planet embryos with very small random velocities v of bodies (parameter $\theta \sim v^{-4}$ is about 10^3), Jupiter can form during 10^6 yr, but other JZB grow slower. Due to small v they reach AZ essentially later and sweep out AZB less effectively. Hence moderate values of θ are preferable: ~20-30 in JZ and 10-15 in AZ. More rapid growth of JZB relative to AZB can be provided only at higher surface density of condensate in JZ $\sigma_p \sim 15\text{-}20$ g/cm^2 and therefore at a more slow decrease of the density of gas in the solar nebula (SN) than is usually assumed. To solve the question (2) an additional mechanism of removal of AZB is needed. The scanning of resonances through the AZ during a dissipation of gas from SN (3) needs a loss of mass nearly that of the sun. In the more preferred SN model of small mass ($\lesssim 0.1\ M_\odot$) another mechanism of resonance scanning through AZ could exist - a variation of the Jupiter's distance from the sun at the stages when Jupiter accreted the gas and when it ejected bodies from the solar system.

Comets. At the final stage of accumulation many preplanetary bodies were expelled from the solar system and into outer Oort cometary cloud (R > 20000a.u.) by gravitational perturbations of giant planets. Due to "recoil" effect which decreased the distances of the planets from the sun the expelled mass could not be large: $\lesssim 10^2 m_\oplus$. Formation of comets in situ in the model of small mass SN is possible at distances R not more than several hundreds of a.u., their total mass being $< 10^3 m_\oplus$.

REFERENCES:(1) Safronov V.S.(1969) Evolution of the protoplanetary cloud and formation of the Earth and the planets.Moscow, Nauka; NASA TTF-677(1972).(2)Safronov V.S.(1979).In:Asteroids, Ed.T.Gehrels,Univ.Ariz.Press,pp.975-991.(3)Cameron A.G.W.&Pine M.(1973)Icarus 18,377-406.

APPLICATIONS OF STATISTICS TO ANTARCTIC, NON-ANTARCTIC DIFFERENCES.
Stephen M. Samuels, Dept. of Statistics, Purdue University, W. Lafayette, IN 47907 USA

Linear Discriminant Analysis and Logistic Regression [Afifi and Clark (1984) and Flury and Riedwyl (1988)] effectively distinguish between Antarctic and non-Antarctic H or L Chondrites solely on the basis of their trace element compositions. This is true both overall and for strongly shocked L4-6 chondrites. As with any statistical analysis of this kind, we conclude only that the data *support* one hypothesis (the hypothesis of a difference), and are *inconsistent* with another (the hypothesis of no difference). Our statistical argument says nothing whatsoever about the *causes* (if any) of such differences.

Numerous analyses have been performed and will be reported on. These are based on the data in Dennison and Lipschutz (1987), Huston and Lipschutz (1984), Kaczarel, Dodd and Lipschutz (1989), Lingner, Huston, Hutson, and Lipschutz (1987), Neal, Dodd, Jarosewich and Lipschutz (1981), and Walsh and Lipschutz (1982).

For example, when the 11 shocked Antarctic L4-6 chondrites in Kaczarel, Dodd and Lipschutz (1989) were compared with the 18 shocked non-Antarctic L4-6 chondrites (for which data was available for all 13 trace elements) in Huston and Lipschutz (1984), the Discriminant Function values had very slight overlap and the significance level was .0062, indicating that identical multivariate normal populations have only about one chance in 160 of looking as different from each other as do these two groups of samples. Logistic Regression (using SAS PROC LOGIST) on the same two groups of shocked L4-6 chondrites correctly classified all the samples, assigning probabilities (of "belonging to the Antarctic population") 0.995 or greater to each of the 11 Antarctic samples, and 0.0002 or less to each of the 18 non-Antarctic samples.

Validation Runs are necessary, in both Discrimination Analysis and Logistic Regression, to avoid giving too rosy a picture. In such runs, part of the data (the training cases) are used to generate a discriminant function or a logistic regression function, which is then applied to the rest of the data (the validation cases). A high rate of correct classifications of these validation cases reinforces the argument for a real statistical difference between Antarctic and non-Antarctic meteorites. For the shocked L4-6 chondrites cited above, repeated runs with 20% (randomly selected) validation cases resulted in over 80% correct classification by both methods.

REFERENCES

Afifi A. A. and Clark V. (1984) *Computer-Aided Multivariate Analysis,* 245-306.

Dennison J. E. and Lipschutz M. E. (1987) *Geochim. Cosmochim. Acta* **51**, 741-754.

Flury B. and Riedwyl H. (1988) *Multivariate Statistics: A Practical Approach,* 88-123.

Huston T. J. and Lipschutz M. E. (1984) *Geochim. Cosmochim. Acta* **48**, 1319-1329.

Kaczaral P. W., Dodd R. T. and Lipschutz M. E. (1989) *Geochim. Cosmochim. Acta* **53**, 491-501.

Lingner D. W., Huston T. J., Hutson M. and Lipschutz M. E. (1987) *Geochim. Cosmochim. Acta* **51**, 727-739.

Neal C. W., Dodd R. T., Jarosewich E. and Lipschutz M. E. (1981) *Geochim. Cosmochim. Acta* **45**, 891-898.

Walsh T. M. and Lipschutz M. E. (1982) *Geochim. Cosmochim. Acta* **46**, 2491-2500.

CHEMICAL DIAPLECTIC CHANGES OF PLAGIOCLASES FROM IMPACTITES (POPIGAI AND PUCHEZH-KATUNK ASTROBLEMES,USSR)

L.V.Sazonova,N.N.Korotaeva, USSR,Moscow, Moscow State University, Geological Department, Petrography chair.

PLagioclases (Pl) from target impacted rocks have been studied by the method of microprobe analyses (Popigai and Puchezh-Katunk Astroblemes). Chemical composition of Pl does not change at the average rock pressure of 20 GPa. Na content decrease has been observed only in the smallest fusion zones appearing in planar features (fig.1). Weak but observable Na diffusion has been noted in maskelynite (30 GPa) (fig.2). Na diffusion intensity increases sharply when separate fused regions in maskelynite appear due to non-homogeneous shock wave distribution and local heating of the substance K is brought into the fused regions (table). At higher shock pressures and residual temperatures Ca begins to diffuse. It is either removed or redistributed in the grain (table). The greater part of the grain is fused, the more intensite the alkali redistribution processes become (up to the complete removal of Na) (fig.3). Pl shock fusion usually begins by a definite twinning system (fig.3). With pressure increase fusion part of Pl grains increases.

Fig.2 - Popigai 1-3; Pychezh-Katunk 4-6; 1,4 - target Pl; 2,5 - maskelynite; 3-6 - fused Pl.

Fig.3 - Pl fusion by a definite twinning system.

Table.

Alkali content in Reference to the Mineral Formula.

	Popigai				Puchezh-Katunk			
	Ca	Na	K		Ca	Na	K	
Target Pl	0.27	0.70	0.02	0.99	0.42	0.55	0.02	0.99
Diaplactic glass	0.28	0.58	0.04	0.90	0.43	0.42	0.01	0.85
	0.25	0.67	0.04	0.96	0.43	0.45	0.02	0.90
Fused glass	0.30	0.23	0.11	0.64	0.53	0.12	0.16	0.81
	0.30	0.23	0.11	0.64	0.33	0.16	0.07	0.55

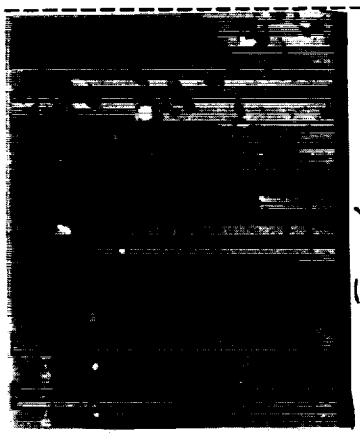

Fig. 1

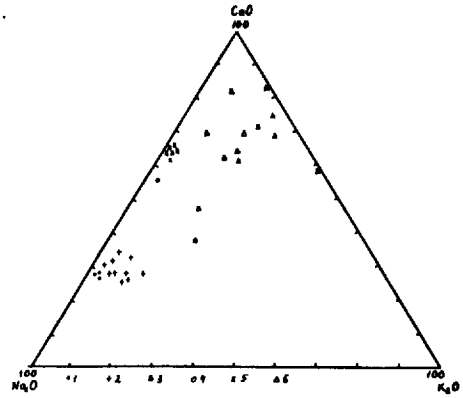

Fig. 2

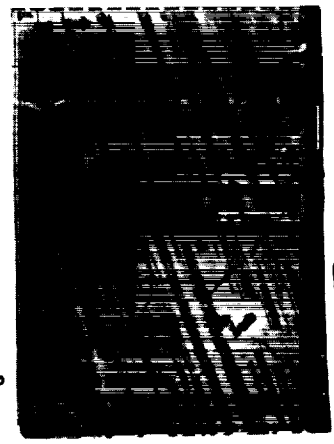

Fig. 3

ORIGINAL PAGE
BLACK AND WHITE PHOTOGRAPH

Rb-Sr AND U-Pb SYSTEMATICS IN HIGHLY SHOCKED MINERALS: HAUGHTON IMPACT STRUCTURE, ARCTIC CANADA. U. Schärer, Université du Québec à Montréal, C.P. 8888, Succ. A., Montréal, Canada H3C 3P8. A. Deutsch, Institut für Planetologie, Wilhelm-Klemm-Straße 10, D-4400 Münster, F.R.G.

Response of isotope systems to shock-wave metamorphism in minerals was studied on a crystalline rock fragment, shocked to ~50 GPa of the polymict breccia from the 23 Ma old (1, 2) Haughton impact crater. For comparison age dating was also performed on unshocked counterparts, sampled in the crystalline basement at Sverdrup Inlet about 100 E of the crater. There, last major chemical fractionation occurred at 1.9 Ga, as substantiated by a U-Pb monazite age of 1903.3 ± 0.5 Ma (2σ) and a Sm-Nd WR-garnet age of 1894 ± 28 Ma. WR-biotite from the same rock indicate that the Rb-Sr system closed slightly later, at 1859 ± 19 Ma.

The analyzed gneiss fragment of shock stage III consists of diaplectic quartz-glass, vesiculated alkali-feldspar-glass, biotite (partly converted into glass and decomposition products) and, as a noticeable feature, of mm-wide veins and layers of gypsum. Preserved primary minerals such as sillimanite, and accessory zircon and monazite display shock-induced fractures.

Rb-Sr measurements on WR, total- and leached biotite, K-feldspar-glass as well as gypsum show these phases in isotopic disequilibrium. Biotite suffered strong depletion in K, Rb and to a lesser degree Sr, taken up by K-feldspar-glass, which shows complementary enrichment in these elements. A preferential loss of radiogenic Sr from biotite into K-feldspar-glass produces meaningless isochron ages of 1784 ± 17 Ma for biotite, and an absurdly old age for K-feldspar-glass (> 2.8 Ga).

In contrast to the unshocked accessory minerals, zircon and monazite from the shocked gneiss were not abraded prior to analyses (3) in order to preserve maximal degrees of U-Pb perturbations. The zircons analyzed show a significant scatter in the Concordia diagram yielding U-Pb ages around 2.0 Ga, and minimum ages in excess to 2.2 Ga. The scatter of the data is due essentially to inherited components, and the discordancy pattern does not reveal any significant fractionation which could be ascribed to the Miocene impact-metamorphism. Monazite from the same rock defines a regression line with Concordia intercepts at 1928.2 ± 2.1/-2.0 Ma and 277.5 ± 35.1/-35.0 Ma. Maximal degree of discordancy in monazite reaches ca. 10% of relative Pb loss. The least discordant grain shows a relative Pb loss of ca. 4%, being identical to degrees observed in unshocked, abraded grains. This observation, and the fact that the lower intercept age of the regression line is more than 200 Ma older than the impact event leads to the conclusion, that shock-wave metamorphism, which generated an isotopic disequilibrium in the Rb-Sr system, and a nearly total resetting of the K-Ar system in biotites (pers. com. Stephan and Jessberger) did not cause any significant U-Pb fractionation in zircons and monazites. Maximal fractionation during impact cannot exceed 1 to 2% of total U-Pb fractionation observed.

These results are consistent with data from shock recovery experiments on the same type of minerals, confirming that U-Pb systems in U-rich phases such as zircon, monazite and titanite remain unaffected by shock-pressures up to 59 GPa (Deutsch et al., this volume). Our observations do not support the suggestion by (4) that "isotopic disturbance" found by ion-probe U-Pb analyses on lunar zircons corresponds to a cratering event, i.e. that lower intercept ages of highly shocked accessory minerals have real age significance.

REFERENCES: (1) Jessberger, E.K. (1988) Meteoritics 23, 233-234. (2) Omar, G., Johnson, L.J., Hickey, L.J., Robertson, P.B., Dawson, M.R. and Barnosky, C.W. (1987) Science 237, 1603-1605. (3) Krogh, T.E. (1982) Geochim. Cosmochim. Acta 46, 637-649. (4) Meyer, C., Williams, I.S. and Compston, W. (1989) Lunar and Planetary Science XX, 691-692.

MT. WEGENER, A NEW ANTARCTIC IRON METEORITE; L. Schultz, B. Spettel and H. W. Weber, Max-Planck-Institut für Chemie, D-6500 Mainz FRG; H.-Ch. Höfle, Niedersächsisches Landesamt für Bodenforschung, D-3000 Hannover FRG; V. Buchwald, Technical University of Denmark, DK-2800 Lyngby; K. Bremer and U. Herpers, Universität Köln, D-5000 Köln FRG; J. Neubauer and K. G. Heumann, Universität Regensburg, D-8400 Regensburg FRG.

In 1988 an iron meteorite of 3480 gm weight was discovered in the South-Eastern part of the Shackleton Range on top of Mount Wegener (longitude 23°35'W, latitude 80°42'S, altitude 1540 m). The plateau on top of Mt. Wegener lies 150 to 350 m above the glacier surface; the mica shists present exhibit strong weathering effects which are mainly caused by wind action and frost shattering.

The exterior of the meteorite - we propose the name Mt. Wegener - is corroded and the surface shows a faint relief, displaying the Widmanstätten structure. Corrosion products are minerals like akaganeite, maghemite and goethite. Mt. Wegener is a medium octahedrite with a kamacite bandwidth of 1.1 $\pm$ .1 mm. With a Ni-content of 8.1 % (Ga: 20.9 ppm; Ge: 33 ppm; Ir: 3.96 ppm) this iron belongs to group IIIA. Heavy cosmic shocks have transformed the kamacite to shock-hatched ϵ-structures and have brecciated the rhabdite and schreibersite inclusions. These shock structures are partly annealed and partially recrystallized.

Both, the corroded exterior as well as material from a crack of the interior contain high concentrations of halogens (up to 400 ppm Cl; .65 ppm Br and 7 ppm I) which are interpreted as terrestrial contamination.

The cosmogenic noble gas record indicates low shielding ($^{4}He/^{21}Ne$ = 250). Concentrations are consistent with an exposure age of about 650 Ma, typical for IIIA irons. From the ^{10}Be content of 4.5 $\pm$ .2 dpm/kg an upper limit for the terrestrial age of 415000 a is calculated. This value is lower than those of other Antarctic irons found on rock surfaces. It is an lower limit for the time since the ice has completely overrun the Shakleton Range for the last time.

CHONDRULES IN CO3 CHONDRITES - KEYS TO UNLOCKING THEIR NEBULAR AND ASTEROIDAL SECRETS;

Edward R.D. Scott and Rhian H. Jones, Institute of Meteoritics, Department of Geology, University of New Mexico, Albuquerque, NM 87131, USA

We have analyzed olivines and low-Ca pyroxenes in type IA and type II porphyritic chondrules in ten CO3 chondrites to help distinguish primary igneous zoning from zoning caused by nebular alteration or asteroidal metamorphic processes. From this work, earlier studies of CO3 metamorphism [1, 2] and a comparison of CO3 and ordinary type 3 chondrite features, we assign the following petrologic subtypes: Colony, ALH A77307: 3.0; Kainsaz: 3.1; Felix: 3.2; ALH 82101, Ornans: 3.3; Lancé, ALH A77029: 3.4; ALH A77003: 3.5; Warrenton: 3.6; Isna: 3.7. Type 3.0 chondrites show only igneous zoning, types 3.1 to 3.7 show increasing degrees of metamorphism.

Results. Through the Colony-Isna sequence, mean concentrations of Fe in chondrule olivines increase, and Ca and Cr concentrations decrease: 1 to 22% FeO, 0.25 to 0.15% CaO, 0.4 to 0.2% Cr_2O_3 in type IA chondrules, and 28 to 33% FeO, 0.25 to 0.10% CaO, 0.4 to 0.05% Cr_2O_3 in type II chondrules (all wt.%). Low-Ca pyroxenes in type IA chondrules increase in FeO, 0.7 to 3%, through this sequence. Silicate compositions and zoning profiles in type IA chondrules in Colony and ALH A77307 closely resemble those of Semarkona (LL3.0) [3, 4]. Olivines in type IA chondrules in A77307 and Semarkona have respectively 1.3 ± 1.0 and 1.0 ± 0.5% FeO, 0.25 ± 0.05 and 0.31 ± 0.12 % CaO, and 0.42 ± 0.03 and 0.37 ± 0.25% Cr_2O_3 ($\pm 1\sigma$ of mean compositions of individual chondrules). Low-Ca pyroxenes in type IA chondrules in A77307 and Semarkona have respectively 1.2 ± 0.2 and 1.2 ± 0.5% FeO. However, olivines in type II chondrules in A77307 are richer in FeO (28 ± 1 vs 15 ± 2%) and CaO (0.25 ± 0.11 vs. 0.13 ± 0.03%) than those in Semarkona.

Discussion. Similarities between silicate compositions and zoning in type IA chondrules in Colony and ALH A77307 and those in Semarkona [3] and our studies of type II chondrules in Semarkona [4] suggest that Colony and A77307 are type 3.0 and that the compositions of their chondrule silicates reflect closed-system crystallization with no subsequent metamorphic alteration. Compositions of chondrule silicates in type 3.1-3.7 CO chondrites are entirely consistent with metamorphic exchange between chondrules like those in Colony and A77307 and an FeO-rich matrix (Fa 70?). Olivine crystals in type IA chondrules of CO3.1 to CO3.7 chondrites show significant enrichments of FeO at their rims and along cracks. Examples of core-rim ranges in individual olivine crystals are as follows: 4-12% FeO in Lancé (3.4), 3-22% FeO in ALH A77003 (3.5) and 22-31% FeO in Isna (3.7). Enrichments of FeO in type IA pyroxenes are smaller, consistent with lower diffusion rates, e.g. a core-rim range of 2-8% FeO in an Isna crystal. The resemblance of these metamorphic changes to those observed in type 3.0-4 LL chondrites [5] and the slow metallographic cooling rates derived for two CO3 chondrites [6] suggest that CO3 chondrites were metamorphosed in an asteroid. The general similarity in the metamorphic features of chondrules in Parnallee (LL3.6) and Warrenton suggests that Warrenton is a type 3.6. The subtypes that we assign to the CO3 chondrites are close to those that can be derived from the thermoluminescence sensitivity (130° C peak) [2], and the criteria for ordinary chondrites. However, we do not imply that, for example, an LL3.6 and a CO3.6 have identical time-temperature histories, only that the levels of metamorphism shown by their silicates are comparable. In view of evidence for brecciation after metamorphism in CO3 chondrites [7], the subtypes only indicate the mean level of metamorphism of the constituents. However, unlike most type 3 ordinary chondrites, each CO3 chondrite appears to contain material from only one metamorphic grade.

The secondary FeO enrichments we find on olivine rims and along cracks in CO3 chondrites appear to be distinct from those reported in type I chondrules in CV3 chondrites, which have been attributed to nebular condensation of fayalite [8, 9]. Rims on CO3 chondrules are not enriched in Al, Cr and Ti to the levels observed in CV3 rims. However, it is possible that some of the red luminescing, FeO-rich rims on forsterite that Steele [10] attributed to crystallization from an FeO-rich liquid may have formed during metamorphic exchange, as described above.

References: [1] McSween H.Y. Jr. (1977) Geochim. Cosmochim. Acta 41, 477. [2] Keck B.D. and Sears D.W.G. (1987) ibid 51, 3013. [3] Jones R.H. and Scott E.R.D. (1989) Proc. 19th Lunar Planet. Sci. Conf. 523. [4] Jones R.H. (1989) Lunar Planet. Sci. XX 481. [5] McCoy T.J. et al. (1989) ibid, 654. [6] Wood J.A. (1967) Icarus 6, 1. [7] Van Schmus W.R. (1969) in "Meteorite Research" ed. P.M. Millman, pp. 480. [8] Peck J.A. and Wood J.A. (1987) Geochim. Cosmochim. Acta 51, 1503. [9] Hua X. et al. (1988) ibid 52, 1389. [10] Steele I.M. (1986) ibid 50, 1379. Supported by NASA grant NAG 9-30 (K. Keil P.I.).

CHONDRULE MESOSTASIS CATHODOLUMINESCENCE AND COMPOSITION: IMPLICATIONS FOR (1) METAMORPHISM AND AQUEOUS ALTERATION IN LOW TYPE 3 ORDINARY CHONDRITES AND (2) SELECTION EFFECTS IN CHONDRULE STUDIES. Derek W.G. Sears and John M. DeHart, Cosmochemistry Group, Department of Chemistry and Biochemistry, University of Arkansas, Fayetteville, AR 72701.

Evidence for aqueous alteration in type 3.0-3.2 ordinary chondrites are observations of calcite and smectite in Semarkona (1,2). 'Consistent' and relevant observations are that (i) water released by step-wise heating has extreme deuterium enrichments (3); (ii) hydrothermal annealing treatments cause 10-fold decreases in TL sensitivity (4); and (iii) there is a weak inverse correlation between deuterium enrichment and TL sensitivity for individual Semarkona chondrules (5).

In terms of mesostasis CL and composition there are two types of chondrule in Semarkona (6), one whose mesostasis luminesces brightly and is plagioclase normative (type A, 60% of chondrules, generally type I of refs. 7,8), and one which does not luminesce and is quartz/orthoclase normative (type B, 40% of chondrules, generally type II). Compositional data make it clear that these two chondrule types are not related to each other through aqueous processes, but represent differences in chondrule formation conditions (peak temperatures and post-formational cooling rates); differences in formation location might also be involved. Ref. 9 used olivine data to come to a similar conclusion. This being so, what can be learned from the TL sensitivity/deuterium data?

The compositional difference between the two chondrule mesostasis types is best demonstrated on CaO-Na_2O plots. As Fig. 1 shows, while 60% of the chondrules observed in thin section are type A, only < 12% of the chondrules physically separated for isotopic work are of this type. (The 12% figure may be overestimated, since some CAI may be included.) It seems unlikely that a selection effect is present in the thin section data, since these studies were systematic in nature and the same results found independently in three other meteorites. Rather, it seems that type A chondrules are less capable, than type B, of surviving the gentle disaggregation necessary for physical separation. Thus it is only type B chondrules that are represented in the data responsible for the deuterium-TL sensitivity trend. We conclude that (1) while aqueous alteration is not the process responsible for the major variations in chondrule properties, it may be playing a secondary role (i.e. causing variations in TL sensitivity within the types A and B); (2) studies based on chondrules separated from type 3 ordinary chondrites by handpicking are not dealing with representative samples.

1 Nagahara (1984) GCA 48, 2581. 2 Hutchison et al (1988) GCA 51, 1875. 3 McNaughton et al (1981) Nature 294, 639. 4 Guimon et al (1988) GCA 52, 119. 5 Sears et al (1988) LPS XIX 1051. 6 DeHart et al (1989) GCA submitted. 7 McSween (1977) GCA 41, 477. 8 Scott and Taylor (1983) Proc. 14th LPSC B275. 9 Jones and Scott (1989) Proc. 19th LPSC 523. Supported by NASA grant NAG 9-81.

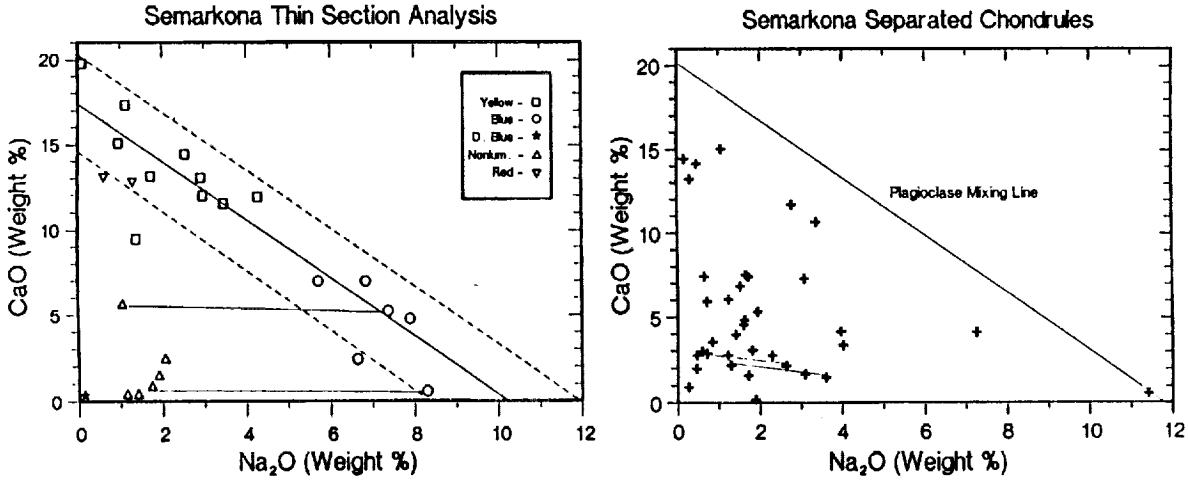

Fig. 1. CaO vs Na_2O for the mesostasis of chondrules in the Semarkona type 3.0 ordinary chondrite. Left, data obtained from a thin section (6); right, data obtained for physically separated chondrules (5).

LUNAR BORON, SAMARIUM, GADOLINIUM CORRELATIONS

D.M. Shaw, T.A. Middleton, P.A. Smith, Department of Geology, McMaster University, Hamilton, Ontario, Canada L8S 4M1.

Lunar samples provide material for study of B in a (presumed) dry environment. This gives a reference pattern to compare terrestrial fractionations. Our previous report (Shaw and Middleton, 1987) is now extended by analysis of an additional 53 samples representing all the major lunar rock types.

The rocks were analysed by prompt gamma activation analysis, which gives sensitive and precise concentrations for B, and simultaneously permits analyses for Sm and Gd.

The preliminary results may be summarised as follows:-

	n	B ppm	Sm ppm	Gd ppm
Basalts excluding Apollo 14	26	0.62-5.7	3.1-20.5	4.0-27.0
Apollo 14 rocks, except for two basalts	8	>18	>23	>28
Granulites and anorthosites	6	nd-2.1	nd-3.1	nd-3.4

Boron shows a marked positive correlation with Sm and Gd, which indicates that, in the absence of water, B behaves as an incompatible element. It is a member of the KREEP group of elements, being concentrated in the more exotic products of lunar magmatic differentiation.

The mineralogical location of B in these rocks is not yet resolved.

References

Shaw, D.M. and Middleton, T.A. (1987) Proc. 18th LPSC, p.912-913.

ABOUT THE NATURE OF "ATMOSPHERELIKE" XENON IN METEORITES. Yu.A.Shukolyukov, Vernadsky Institute of Geochemistry and Analytical Chemistry, Moscow, USSR.

An "atmospherelike" xenon with the excess of 132Xe, 131Xe, 134Xe, 136Xe realitively to 130Xe in comparison with the solar or AVCC-Xe can be found out in chondrites. For example in L5-6 Tsarev chondrite: 136Xe:134Xe:132Xe:131Xe:130Xe:129Xe:128Xe: 126Xe:124Xe= 2,40:2,87:7.24:5,62:100:7,65:0,427:0,021:0,021. The same exsesses are also in Xe from the Earth atmosphere. But this effect can not be explained by the isotope mass-fractionation or by the addition of fission products of known nuclei.

Qualitatively similar xenon anomaly we have found out in several earth samples, where two simultaneous processes took place-generation of xenon isotopes by fission and geochemical migration. Anomalous xenon is found out in the samples from the Oklo deposit (Republic of Gabon), which was "the natural nuclear reactor", in ultradispersed mineralization in sands (pitchblendes) and in the sample from the epicenter of the first atomic explosion in Alomogordo, New Mexico, USA. In the last sample isotopic shifts are giant: 136Xe:134Xe:132Xe:131Xe=1.00:14,5:76,3:85,9. It is possible, that there is exsisting a process in nature, which leads to the appearance of anomalous Xe: β^-- radioactive progenitors of xenon stable isotopes are migrating - members of the radioactive chaines of fission fragments. They are concentrated in the separate mineral phases due to their different geochemical properties and at last they transform into the stable isotopes of xenon with the anomalous ratios. Just the same process could have taken place in the hot particles on the early evolution stages of the protoplanetary cloud, when 238U, 235U, 244 Pu fission and simultaneous migration of xenon progenitors took place. The absence of the "atmospherelike" krypton in chondrites can be explained by the very small yield of krypton during the fission.

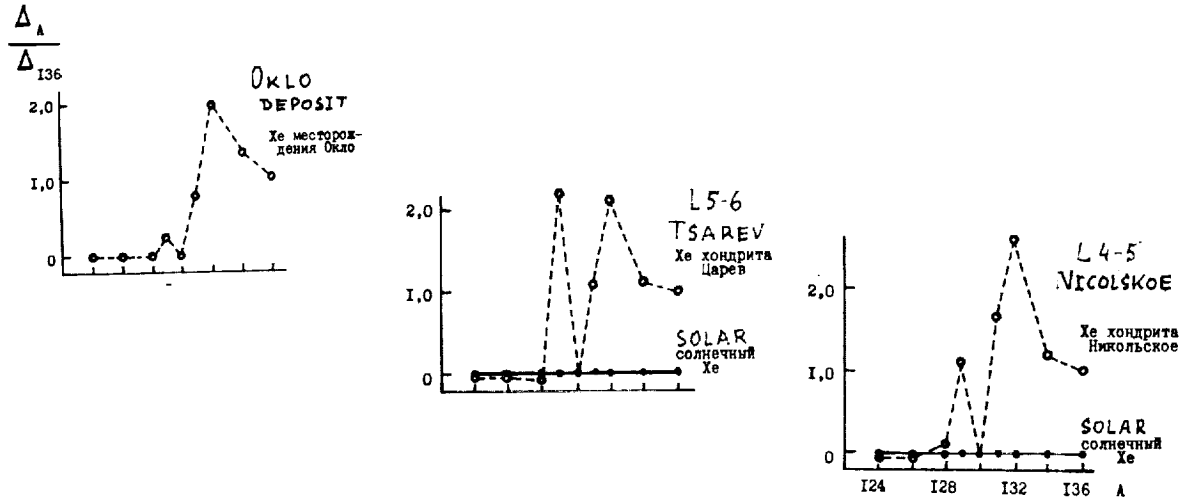

COMPARATIVE PETROLOGY OF LUNAR REGOLITH BRECCIAS AND SOILS, AND IMPLICATIONS FOR THE HOWARDITE PARENT BODY REGOLITH; S.B. Simon, Institute for the Study of Mineral Deposits, S.D. School of Mines and Technology, Rapid City, SD 57701. Present Address: Dept. of Geophysical Sciences, University of Chicago, Chicago, IL 60637

Lunar regolith breccias are rocks formed by compaction and lithification of the lunar regolith, itself an impact-derived debris blanket. By virtue of their lithification they are essentially "closed" to the addition of new material, whereas present-day regoliths and soils (the <1 mm regolith fraction) continue to change; they can lose and gain material as a result of meteorite impacts, and they become more "mature" with continued exposure (at the surface) to micrometeorite impacts. This study of regolith breccia-soil suites from each of the Apollo sites demonstrates that because soils evolve and regolith breccias do not, comparison of breccias and soils from the same site can show how the regolith at that site changed since the formation of the breccias, if the breccias were formed locally.

A relationship observed at all the Apollo sites is that the regolith breccias contain fewer fused soil particles (agglutinates and regolith breccias) than the present-day soils. Agglutinates form only at the surface, and increase in abundance with increasing surface residence time of a soil. The low agglutinate abundances recorded in the breccias indicate that the breccias formed from relatively freshly exposed regolith compared to most of the present-day soils that have been sampled.

Unlike soil-derived particles, other components such as non-local rock types and volcanic glasses that are no longer being added to the regolith tend to decrease in abundance over time, as they are mixed in and diluted or made into agglutinates. The Apollo 11 breccias contain a group of glasses that is now very rare in the soil; Apollo 16 soils contain glasses not found in some of the Apollo 16 breccias, indicating that addition of the glasses to the regolith occurred after formation of breccias. The Apollo 14 samples show evidence of dilution of one glass type and addition of another glass type in the soil after breccia formation. Thus, in some cases, regolith breccias can help us determine the sequence of addition of regolith components.

Comparison with soil samples shows that most of the breccias were formed near where they were collected. These breccia-soil suites reveal site-specific characteristics related to the local geology. An exception is the Apollo 12 suite, in which at least three and possibly six of the eleven samples studied were not formed from the regolith now present at the site.

Finally, lunar regolith breccia-soil relationships can be used to infer properties of the regoliths of the parent body(ies) of meteoritic regolith breccias, rocks known as howardites. If the analogy is valid, then the howardite parent body probably has a regolith similar to that represented by lunar regolith breccias: abundant mineral and lithic fragments, and a maturity less than that of lunar soils but greater than that of howardites. This is consistent with models of asteroidal regoliths.

BLEACHED CHONDRULES AND THE DIAGENETIC HISTORIES OF ORDINARY CHONDRITE PARENT BODIES: William R. Skinner, Department of Geology, Oberlin College, Oberlin, OH 44074; Harry Y. McSween, Jr., and Allan D. Patchen, Department of Geological Sciences, University of Tennessee, Knoxville, TN 37996.

"Bleached chondrules" have margins or internal fractures that have been lightened in color by some leaching process. Leaching has been previously described by Kurat (1969) and Christophe Michel-Levy (1976) for radial pyroxene chondrules in Tieschitz. We confirm their observations of leached margins and crack boundaries, the removal of a feldspathic component (alkalies, alumina, and calcium), and the development of porosity in the affected regions. Our study extends these observations to include radial pyroxene, cryptocrystalline, and glassy chondrules in H, L, and LL chondrites of petrologic types 3.0 through 6. We also relate this phenomenon to a specific period of parent body history.

Bleaching was an early, parent-body process. The overclose packing of most ordinary chondrites was produced during compaction, forming a fitted fabric of chondrules, fragments, and matrix (Skinner, 1989). Bleached rims follow chondrule outlines modified by compaction, indicating that they are post-compaction features. On the other hand, Semarkona and Krymka are essentially unmetamorphosed, yet both contain bleached chondrules. Bleaching thus occurred after compaction but before subsequent peak metamorphism. This interpretation is consistent with the view that accretion and compaction occurred at low temperatures (Skinner, 1989). Furthermore, the kinds of chondrules affected as well as the patterns of alteration seem to be similar for all ordinary chondrites, suggesting that bleaching occurred in all of them under similar conditions of temperature and volatile content.

Parent bodies of H, L, and LL chondrites had similar early histories consisting of distinct, transitional stages: 1) accretion, 2) diagenesis (including compaction and lithification followed by bleaching of selected chondrules), 3) metamorphism or all but a few chondrites, and 4) post-metamorphic cooling under essentially volatile-free conditions. During the diagenetic period low temperatures and the presence of a fluid phase seem to be required to produce compactional fabrics (Skinner, 1989) and the subsequent bleaching described here. Diagenesis is an important developmental stage for chondritic meteorites and is just being recognized. It's effects on chemical and isotopic systems has yet to be evaluated. Volatiles associated with diagenesis may have been derived locally or from deeper regions undergoing metamorphism within the parent bodies. In any case, it appears that ordinary chondrites evolved in parent-body settings characterized by chemical mobility prior to the onset of high metamorphic temperatures. Alteration by circulating volatiles may have been widespread during this period (Hutchison, et al., 1987).

Support: Oberlin College and BP America (W.R. Skinner) and NASA grant NAG9-58 to H.Y. McSween, Jr.

References:

Christophe Michel-Levy M. (1976), Earth Planet Sci. Lett. 30, 143-150.

Hutchison R., Alexander C.M.O. and Barber D.J. (1987) Geochim. Cosmochim. Acta 51, 1875-1882.

Kurat G. (1969) in Meteorite Research (ed. Peter M. Millman), pp. 185-190, D. Reidel Publ. Co., Holland.

Skinner W.R. (1989) (abstract) Lunar Planet. Sci. 20, 1020-1021.

HAVE DIFFERENT PARTS OF ALLENDE SAMPLED COMPOSITIONALLY DIFFERENT CHONDRULES?

B. Spettel, H. Palme and G. Kurat*
Max-Planck-Institut für Chemie, D-65 Mainz, F.R.Germany; *Naturhistorisches Museum, Postfach 417, A-1014 Vienna, Austria.

We have analysed 24 chondrules from the Allende meteorite by INAA-techniques (including 4 chondrules previously described (1)). Thin sections for petrographic characterization are presently prepared. Chondrules span a range in mass from 1.13 to 167 mg. There is no apparent dependence of composition on size.
In the Fig. we compare the average chondrule composition of this study with results of an earlier study of 20 chondrules by Rubin and Wasson (2). Both data sets are normalized to bulk Allende. Standard deviations of the mean are indicated.
Our average total Fe-content (6.27%) is half of that of R&W (13.13%). Refractory element contents are a factor of 2 higher in our suite, 24 ppm Sc vs. 12.7 ppm of the R&W sample. Ni and Co follow the Fe trend, while Na and K are enriched in our sample along with the refractories. There is no obvious sample bias that would explain these differencies. The R&W chondrule suite has 13 chondrules with coarse-grained rims, compositionally similar to matrix (i.e. high Fe, Ni, Co). However, the mean composition of chondrules with coarse-grained rims (analysed after rim removal) and those without rims is the same.
Presently, we cannot exclude the possibility that chondrules of different parts of Allende have different compositions.
This could imply a close genetic relationship between chondrules and matrix. A lower Fe content in chondrules must be compensated by higher Fe in other Allende components, primarily matrix, considering that chondrules make up about 40 % of Allende and assuming a constant bulk composition of Allende.
Major conclusions of our study are:
1.) Our chondrules span the whole range in refractory element contents, from matrix to CAI. This indicates that basically the same process is responsible for melting of CAIs and chondrules.
2.) Our data indicate the possibilty that different parts of Allende contain different populations of chondrules.
2.) Chondrules and matrix are complementary in composition, indicating a common reservoir.
3.) Our new data and earlier findings by other authors exclude the possibility that Allende chondrules were made from Allende matrix and vice versa.

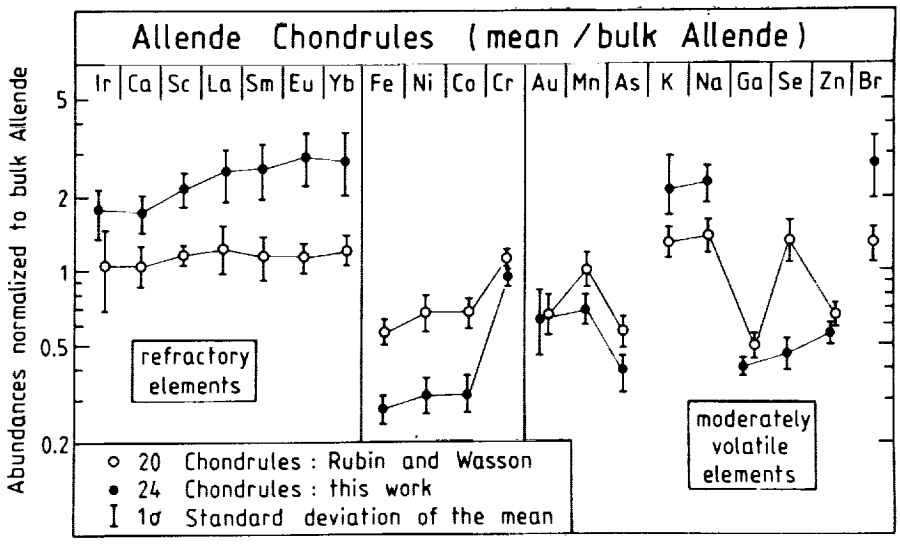

Lit.:(1) Kurat G. et al.(1985) LPSC XVI 471; (2) Rubin A. and Wasson J.T.(1987) GCA 51, 1923.

TRACE ELEMENT ANALYSIS OF UREILITE METEORITES: A PROGRESS REPORT

A.H. Spitz[1], Joaquin Ruiz[2] and William V. Boynton[1]. [1]Lunar and Planetary Laboratory; University of Arizona; Tucson, AZ 85721. [2]Department of Geosciences; University of Arizona; Tucson, AZ 85721.

We have used instrumental and radiochemical neutron activation (NAA) analysis to determine Sc, Cr, Fe, Co, Ni, As, REE, W, Re, Os, Ir and Au for bulk samples of PCA82506 and ALHA78019. In addition, we are comparing residue and leachate products using HCl to those using HNO_3. HNO_3 leachates of PCA82506, ALHA78019 and Kenna have also been examined qualitatively using inductively coupled plasma source spectrometry (ICP-MS). This abstract reports on the preliminary results obtained with the NAA acid comparison experiment and with the ICP-MS for bulk samples of Hajmah, LEW85328, and PCA82506.

RESULTS

Bulk samples of ALHA78019, the most iron-rich ureilite, and PCA82506 were analysed using NAA. In addition, splits of PCA82506 were taken to do acid-leaching. The bulk samples of ALHA78019 and PCA82506 display similar results to previously analysed ureilites: refractory siderophiles (Re, Os, W and Ir) are well correlated and all siderophiles (including volatiles such as Co, Ni, Ga and Au) have similar CI chondrite normalized abundances. REE patterns (Ureilite/CI chondrite) display subdued v-shaped patterns with the characteristic LREE enrichment and HREE enrichment (1,2,3). Comparison of the HNO_3 and HCL leachates and residues reveals that the acid leaching is due more to mechanical than to chemical causes: the residues and leachates of the two different acids have similar element abundance ratios.
Preliminary ICP-MS results indicate that elements in the ppm range, such as Sc, Co, Zn and refractory siderophiles can be determined with relative ease. The ppb levels of rare-earth elements makes their detection more problematic.

DISCUSSION

The abundance ratios determined for ALHA78019 and PCA82506 hold no surprises: they are similar for both siderophile and rare-earth element to other ureilite meteorites. The leaching experiment on PCA82506 was somewhat surprising in that the two different acids, to which different minerals are susceptible, produced similar results: residues' and leachates' abundances with respect to bulk values behaved in similar fashion. This does indicate, however, that care must be taken in the use of acids to clean ureilite samples - such cleaning may, in fact, affect the abundance determinations.

ICP-MS is a recently developed analytical tool with which little work on geological or meteoritical samples has been done. We are, therefore, developing new procedures to apply this powerful tool. Such adjustments are particularly critical for ureilites because of the low concentrations of elements such as the rare earths.

REFERENCES

(1) Boynton W.V., Starzyk P.M. and Schmitt R.A. (1976) GCA 40, 1439-1447. (2) Spitz A.H and Boynton W.V. (1986) Meteoritics 21, p.515-516. (3) Spitz A.H. and Boynton W.V. (1988) Meteoritics 23, p. 302-303.

ION MICROPROBE MEASUREMENTS OF NITROGEN ISOTOPIC VARIATIONS IN INDIVIDUAL IDPs; F.J. Stadermann, R.M. Walker, and E. Zinner, McDonnell Center for the Space Sciences and Physics Department, Washington University, St. Louis, Missouri 63130, USA.

We report N and C isotopic measurements on individual interplanetary dust particles (IDPs). Measurements were made with a CAMECA IMS 3F ion microprobe at high MRP ($M/\Delta M \approx 6500$) using a Cs^+ primary beam and negative secondary ions [1]. We analyzed 24 different IDPs which had previously been characterized by SEM-EDX, FTIR transmission, Raman microprobe, and/or D/H isotopic measurements. All samples had already been identified as being extraterrestrial by one or more of these techniques. Depending on how much material of the particles was left after preceding analyses, we were able to measure C and N isotopes in up to 7 different fragments of a single particle.

No ^{13}C enrichments were observed among the measured IDPs. The lowest $^{13}C/^{12}C$ ratios are only slightly smaller than the lower limit of the range of the terrestrial ratios [2], with no $\delta^{13}C_{PDB}$ values significantly below -60 ‰. The variations among different fragments of a given particle are small, i.e. all IDPs seem to be homogeneous with respect to their C isotopic composition.

N isotopes are measured as CN^- ions and thus can be measured only in carbonaceous phases. Although a quantitative estimate of the N concentrations cannot be given at this time, we note that CN^-/C^- ratios in the IDPs were comparable to those measured in the 1-hydroxy-benzotriazole-hydrate standard (N concentration 27.5 wt%), indicative of high N concentrations, probably in organic compounds. In contrast to the essentially normal C isotopic compositions, 10 of the IDPs exhibit heavy N ($\delta^{15}N$ up to 442 ‰ relative to air) and large intra-particle variations of the N isotopic composition. The rest of the analyzed particles fall within the terrestrial range of $\delta^{15}N$ from -8 ‰ to 20 ‰ [3]. Fig. 1 shows the results of the N isotopic measurements for the 6 most ^{15}N-enriched IDPs with error bars representing standard errors of the mean. From particle "Santa Fe" 4 different fragments have been measured; their $\delta^{15}N$ values range from (61 ± 11) ‰ to (442 ± 29) ‰.

Because of the initial selection criteria, most of the analyzed IDPs have a "chondritic" major element composition. However, one of the IDPs containing heavy N, St. Elizabeth, is a FSN-type (Fe-S-Ni containing) particle. The IR-class has been determinated for only 3 of the 6 most ^{15}N-enriched IDPs: Santa Fe and Cedarcreek are pyroxene class particles while Calrissian mainly consists of layer lattice silicates and carbonates. All ^{15}N-enriched IDPs are also enriched in D, although there is no quantitative correlation between these enrichments and several high D-enriched particles show no N anomalies. There is no correlation between $\delta^{15}N$ and $\delta^{13}C$.

At this point no firm conclusions can be drawn regarding the origin of the ^{15}N enrichments in IDPs. The enrichments measured here are probably carried by organic material, in contrast to the most ^{15}N-rich components found in meteorites (ranging up to $\delta^{15}N \approx 3200$ ‰) which are carried by more refractory phases [4,5]. The heaviest N component so far found in organic meteoritic material (in Inman residues) has a $\delta^{15}N$ value of 256 ‰ [6]. It has been argued that the D enrichments in IDPs originated in molecular clouds by ion-molecule reactions [7]. While such a mechanism cannot be completely excluded for N, fractionation effects are expected to be much smaller than for H [8].

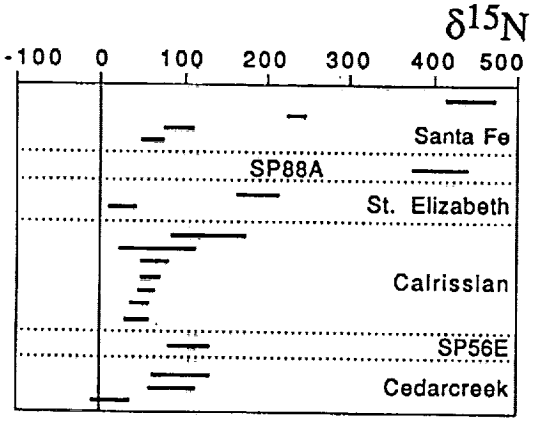

References: [1] Zinner E. et al. (1987) Nature 330, 730; [2] Faure G. (1986) Principles of Isotope Geology. Wiley, 2nd ed., 589pp.; [3] Geiss J. and Bochsler P. (1981) GCA 46, 529; [4] Franchi I.A. et al. (1986) Nature 323, 138; [5] Tang M. et al. (1988) LPSC XIX, 1177; [6] Alexander C.M.O. et al. (1989) LPSC XX, 7; [7] McKeegan K.D. et al. (1985) GCA 49, 1971; [8] Zinner E. (1988) in: Kerridge J.F. and Matthews M.S. (eds.) Meteorites in the Early Solar System. Univ. of Arizona Press, 956;

Figure 1: Isotopic composition of 6 IDPs with heavy N.

SHOCK-INDUCED DISTURBANCE OF THE K-AR SYSTEM - A COMPARISON BETWEEN EXPERIMENTAL AND NATURAL SHOCK; Thomas Stephan and Elmar K. Jessberger, Max-Planck-Institut für Kernphysik, P. O. Box 103980, 6900 Heidelberg, FRG.

In continuing to study the effects of shock metamorphism on the K-Ar clock, samples from the Haughton impact crater with different shock stages were investigated to compare the results with ^{40}Ar-^{39}Ar data of experimentally shocked samples (Stephan and Jessberger, 1988).

The Haughton impact structure (Devon Island, Canada) with a well defined ^{40}Ar-^{39}Ar age of 23.4 ± 1.0 Ma (Jessberger, 1988) has a much older basement (~ 1.7 Ga, Deutsch, 1988), so the gap between crystallisation and impact is very large.

We investigated mineral separates - biotite and feldspar-quartz - with shock stages 0 (unshocked), I, II, and III, respectively. An unshocked biotite yielded a plateau age of 1749 ± 10 Ma (Fig. 1). At shock stage III pressures up to 60 GPa are expected. The K-Ar system of the heavily shocked sample was not completely reset by the impact. The plateau age of 31.7 ± 1.4 Ma for the biotite separate (Fig. 2) has no chronological significance although a well defined ^{40}Ar-^{39}Ar plateau was observed. The ^{40}Ar-^{39}Ar age of 23.4 ± 1.0 Ma has been obtained from a glass sample which was totally molten by the impact. For the feldspar-quartz separates highly disturbed age spectra were observed for all shock stages which might be due to diffusive loss of radiogenic argon even in the unshocked material.

In addition to our study on experimentally shocked samples, where also only a partly loss of radiogenic argon due to shock was observed, these results show that if the ^{40}Ar-^{39}Ar technique is to be applied to the dating of a cratering event, then either melt rocks, glass, or samples, whose K-bearing phases have demonstrably been molten, should be selected. Heavily shocked samples may deliver mixing ages with no chronological importance (cp. Bogard *et al.*, 1988).

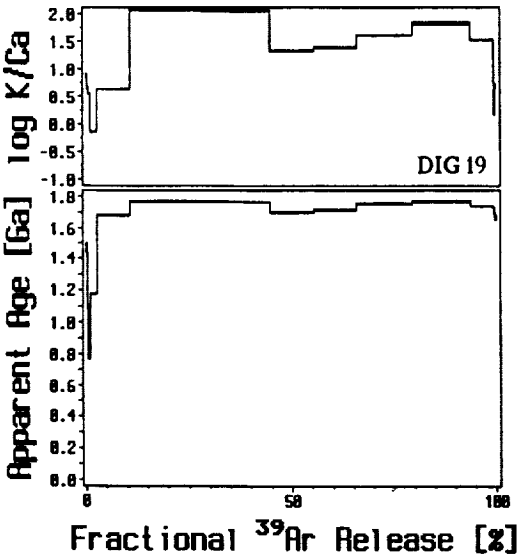

Fig. 1. K/Ca and ^{40}Ar-^{39}Ar age spectrum of an unshocked biotite sample (DIG 19) from the Haughton impact structure.

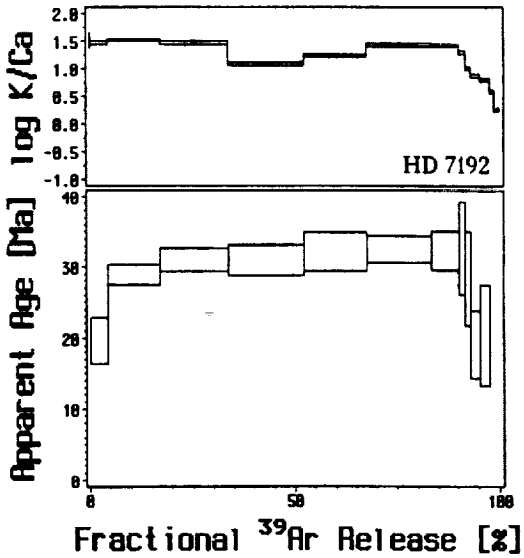

Fig. 2. K/Ca and age spectrum of the heavily shocked (stage III) biotite sample HD 7192.

References: Bogard D., Hörz F. and Stöffler D. (1988) *Geochim. Cosmochim. Acta* **52**, 2639 - 2649. Deutsch A. (1988) *Naturwissenschaften* **75**, 355-357. Jessberger E. K. (1988) *Meteoritics* **23**, 233-234. Stephan T. and Jessberger E. K. (1988) *Meteoritics* **23**, 303 - 304.

ON CANONICAL INTERPRETATIONS OF LUNAR HIGHLAND ROCK AGES: LATE CATACLYSM OR INTENSE EARLY BOMBARDMENT? D. Stöffler[1], E.K. Jessberger[2], and S. Lingner[1], [1] Institut für Planetologie, Universität Münster, D-4400 Münster, [2] Max-Planck-Institut für Kernphysik, D-6900 Heidelberg.

The knowledge of the absolute ages of the major lunar multi-ring basins is crucial to the understanding of the cratering rate of the early moon and its geological evolution. Two opposing main concepts received most attention: (a) late terminal cataclysm at about 3.9 AE (1) and (b) intense early bombardment until about 3.8 AE (2). Both views achieved a canonical status at different times in the past 15 years. More recently, a "smooth" decline of the cratering rate was more generally preferred over the earlier "cataclysm" concept (3, 4, 5).

In a recent assessment of the problem, Ryder (6, 7) argues in favor of a revival of the late cataclysm concept. He infers a late cataclysm of possibly less than 0.05 AE duration from the lack of impact melt rocks older than 3.92 AE. This view prompts us to point out a number of facts and conclusions opposing a straightforward revival of the cataclysm concept (see also arguments in (8, 9). The following points can be made: (a) The observed range of reliable ages of impact melt rocks is not 3.85 to 3.92 AE (7) but 3.75 to 4.14 AE (10, 11, 12); (b) The ^{40}Ar- ^{39}Ar-ages of some old ($>$ 4 AE) feldspathic fragment-laden impact melt breccias of Apollo 16 as well as of young ($<$3.8 AE) Apollo 14 melt breccias are true crystallization ages because of perfect plateaux (10, 13, 14); (c) The abundance of impact melt lithologies in the highlands is not only 10-20% (7) but ranges from 44 to 70% at Apollo 14 and 16 (11, 15); (d) "Well-defined" ages of the Orientale, Imbrium, Serenitatis and Nectaris basins (7) do not exist; the disagreement of published ages for these basins and their uncertainties are distinct (16, 17, 18, 19, 20, 21, 22); (e) The measured differences of crater frequencies on the ejecta blankets of Imbrian and older basins (22) are difficult to reconcile with a single late cataclysm.

We argue that the survival of 4.6 - 3.9 AE old igneous plutonic rocks (23) and the lack of impact melt rocks older than 4.15 AE must not necessarily reflect an early epoch of extremely reduced impact rate. We present the following alternative views. All Apollo highland sites are heavily dominated by the Imbrium ejecta blanket. Only at Apollo 16 and 17, also Nectaris and Serenitatis ejecta are present. These deposits contain basin ejecta sensu stricto and local pre-Imbrian or pre-Nectarian surface rocks (24). The latter must contain a high concentration of impact melt rock clasts because impact melts are only formed at the surface. In contrast, basin ejecta are dominated by more deep seated rocks, e.g. plutonic igneous lithologies (besides some melt ejecta). The age ranges and the compositions of impact melt lithologies at Apollo 14 (3.75 - 3.95 AE (12)), Apollo 16 (3.74-4.14 AE (8, 11)) and Apollo 17 (3.83-3.96 AE (22)) reveal differences of the Imbrium and Nectaris ejecta deposits. The oldest age group (3.96-4.14 AE), only found in the Descartes region, is most probably related to pre-Nectarian impact melt formations at the Nectaris site. The lack of impact melts older than 4.15 AE can be explained by an intense early bombardment (non-cataclysmic model A of (3)) which prior to 4.2 AE "pulverized" and remelted older highland rocks to a depth of 1 - 5 km where all pre-Nectarian melt sheets were concentrated. Therefore, impact melt rocks survive only at later times whereas the $>$4.2 AE old plutonic rocks are preserved because they were brought to the surface from greater depths by late basin impact events. The cut-off at 3.95 AE for the Apollo 14 and 17 impact melt ages may be explained by the special target situation at the Imbrium site where pre-Imbrian crust had been removed by earlier very large basin impacts (e.g. Procellarum and Insularum basins (22, 25)). This explains not only the observed impact melt ages but also the lack of Fe-anorthosite and of old pristine igneous rocks (23) at the Apollo 14 site (9).

The absolute ages of the basins mentioned above remain uncertain. We have argued in favor of a 3.77 - 3.75 AE age of Imbrium (8). The ages of Serenitatis and Nectaris must be in the 3.83 to 3.96 AE range if we accept the feldspathic fragment-laden impact melt breccias (3.96 - 4.14 AE) as pre-Nectarian rocks. However, Nectaris could still be as young as 3.85 AE if all melt rocks of North Ray, Apollo 16, were pre-Nectarian. Consequently, about 30 pre-Nectarian basins (22) were formed within 440 to 550 million years since 4.4 AE, and about 12 post-Nectaris basins fall into a time period of 110 to 210 million years.

REFERENCES: (1) Tera, F. & G.J. Wasserburg (1974) Proc. Lunar Sci. Conf. 5th, 1571-1599. (2) Hartmann, W.K. (1975) Icarus 24, 181-187. (3) Hartmann, W.K. (1980) Proc. Conf. Lunar Highlands Crust, 155-171. (4) Taylor, S.R. (1982) Planetary Science: A lunar perspective, Plenum Press, N.Y. (5) Wilhelms, D.E. (1984) Moon, in: The Geology of Terrestrial Planets, NASA SP-469, 107-206. (6) Ryder, G. (1988) Workshop on Moon and Transition: Apollo 14, KREEP, and Evolved Lunar Rocks, 71-74. (7) Ryder, G. (1989) Lunar Planet. Sci. Conf. XX, 934-935. (8) Deutsch, A. & D. Stöffler (1987) Geochim. Cosmochim. Acta 51, 1951-1964. (9) Stöffler, D. et al. (1988) Workshop on Moon in Transition: Apollo 14, KREEP, and Evolved Lunar Rocks, 101-104. (10) Maurer, P.P. et al. (1978) Geochim. Cosmochim. Acta 42, 1687-1720. (11) Stöffler, D. et al. (1985) Proc. Lunar Planet. Sci. Conf. 15th, C449-C506. (12) Stadermann, F.J. et al. (1988) Workshop on Moon in Transition: Apollo 14, KREEP, and Evolved Lunar Rocks, 105. (13) Wacker, K. (1984) Dipl. thesis, Universität Heidelberg. (14) Heusser, E. (1985) Dipl.thesis, Max-Planck-Institut für Kernphysik, Heidelberg. (15) Lingner, S. et al. (1988) Workshop on Moon in Transition: Apollo 14, KREEP, and Evolved Lunar Rocks, 23-26. (16) Schaeffer, G.A. & O.A. Schaeffer (1977) Proc. Lunar Sci. Conf. 8th, 2253-2300. (17) Jessberger, E.K. et al. (1977) Lunar Planet. Sci. XIII, 511-513. (18) Jessberger, E.K. et al. (1978) Proc. Lunar Planet. Sci. Conf. 9th, 841-854. (19) James, O.B. (1981) Proc. Lunar Planet. Sci. Conf. 12th, 209-233. (20) Spudis, P.D. & G. Ryder (1981) Proc. Lunar Planet. Sci. Conf. 12th, 133-148. (21) Spudis, P.D. & G. Ryder (1985) Trans. Am. Geophys. Union 66, 724. (22) Wilhelms. D.E. (1987) The Geologic History of the Moon, U.S. Geol. Survey, Prof. Paper 1348, pp. 301. (23) Shih, C.-Y. et al. (1989) Lunar Planet. Sci. Conf. XX, 1004-1005. (24) Oberbeck, V.R. (1975) Rev. Geophys. Space Phys. 13, 337-362. (25) Spudis, P.D. et al. (1987) Proc. Lunar Planet. Sci. Conf. 18th, 155-168.

SHOCK-INDUCED DISTURBANCE OF THE K-AR SYSTEM - A COMPARISON BETWEEN EXPERIMENTAL AND NATURAL SHOCK; **Thomas Stephan and Elmar K. Jessberger,** Max-Planck-Institut für Kernphysik, P. O. Box 103980, 6900 Heidelberg, FRG.

In continuing to study the effects of shock metamorphism on the K-Ar clock, samples from the Haughton impact crater with different shock stages were investigated to compare the results with ^{40}Ar-^{39}Ar data of experimentally shocked samples (Stephan and Jessberger, 1988).

The Haughton impact structure (Devon Island, Canada) with a well defined ^{40}Ar-^{39}Ar age of 23.4 ± 1.0 Ma (Jessberger, 1988) has a much older basement (~ 1.7 Ga, Deutsch, 1988), so the gap between crystallisation and impact is very large.

We investigated mineral separates - biotite and feldspar-quartz - with shock stages 0 (unshocked), I, II, and III, respectively. An unshocked biotite yielded a plateau age of 1749 ± 10 Ma (Fig. 1). At shock stage III pressures up to 60 GPa are expected. The K-Ar system of the heavily shocked sample was not completely reset by the impact. The plateau age of 31.7 ± 1.4 Ma for the biotite separate (Fig. 2) has no chronological significance although a well defined ^{40}Ar-^{39}Ar plateau was observed. The ^{40}Ar-^{39}Ar age of 23.4 ± 1.0 Ma has been obtained from a glass sample which was totally molten by the impact. For the feldspar-quartz separates highly disturbed age spectra were observed for all shock stages which might be due to diffusive loss of radiogenic argon even in the unshocked material.

In addition to our study on experimentally shocked samples, where also only a partly loss of radiogenic argon due to shock was observed, these results show that if the ^{40}Ar-^{39}Ar technique is to be applied to the dating of a cratering event, then either melt rocks, glass, or samples, whose K-bearing phases have demonstrably been molten, should be selected. Heavily shocked samples may deliver mixing ages with no chronological importance (cp. Bogard *et al.*, 1988).

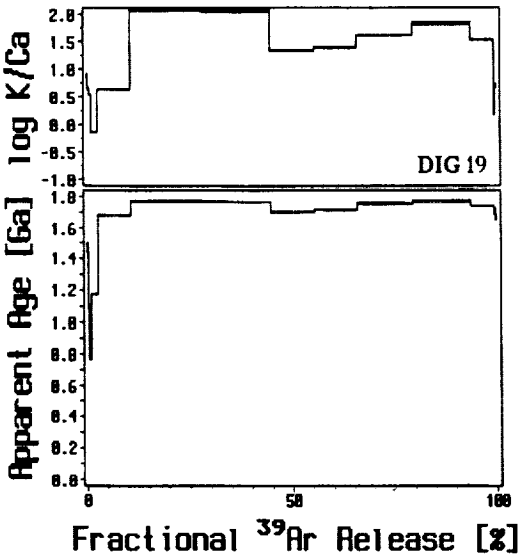

Fig. 1. K/Ca and ^{40}Ar-^{39}Ar age spectrum of an unshocked biotite sample (DIG 19) from the Haughton impact structure.

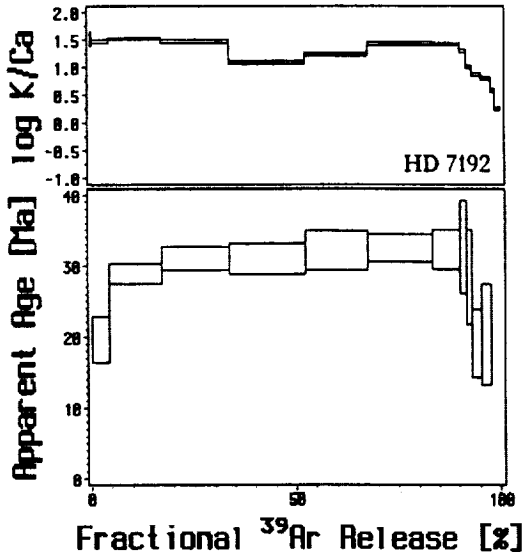

Fig. 2. K/Ca and age spectrum of the heavily shocked (stage III) biotite sample HD 7192.

References: Bogard D., Hörz F. and Stöffler D. (1988) *Geochim. Cosmochim. Acta* **52,** 2639 - 2649. Deutsch A. (1988) *Naturwissenschaften* **75,** 355-357. Jessberger E. K. (1988) *Meteoritics* **23,** 233-234. Stephan T. and Jessberger E. K. (1988) *Meteoritics* **23,** 303 - 304.

ON CANONICAL INTERPRETATIONS OF LUNAR HIGHLAND ROCK AGES: LATE CATACLYSM OR INTENSE EARLY BOMBARDMENT? D. Stöffler[1], E.K. Jessberger[2], and S. Lingner[1], [1] Institut für Planetologie, Universität Münster, D-4400 Münster,[2] Max-Planck-Institut für Kernphysik, D-6900 Heidelberg.

The knowledge of the absolute ages of the major lunar multi-ring basins is crucial to the understanding of the cratering rate of the early moon and its geological evolution. Two opposing main concepts received most attention: (a) late terminal cataclysm at about 3.9 AE (1) and (b) intense early bombardment until about 3.8 AE (2). Both views achieved a canonical status at different times in the past 15 years. More recently, a "smooth" decline of the cratering rate was more generally preferred over the earlier "cataclysm" concept (3, 4, 5).

In a recent assessment of the problem, Ryder (6, 7) argues in favor of a revival of the late cataclysm concept. He infers a late cataclysm of possibly less than 0.05 AE duration from the lack of impact melt rocks older than 3.92 AE. This view prompts us to point out a number of facts and conclusions opposing a straightforward revival of the cataclysm concept (see also arguments in (8, 9). The following points can be made: (a) The observed range of reliable ages of impact melt rocks is not 3.85 to 3.92 AE (7) but 3.75 to 4.14 AE (10, 11, 12); (b) The ^{40}Ar- ^{39}Ar-ages of some old (> 4 AE) feldspathic fragment-laden impact melt breccias of Apollo 16 as well as of young (< 3.8 AE) Apollo 14 melt breccias are true crystallization ages because of perfect plateaux (10, 13, 14); (c) The abundance of impact melt lithologies in the highlands is not only 10-20% (7) but ranges from 44 to 70% at Apollo 14 and 16 (11, 15); (d) "Well-defined" ages of the Orientale, Imbrium, Serenitatis and Nectaris basins (7) do not exist; the disagreement of published ages for these basins and their uncertainties are distinct (16, 17, 18, 19, 20, 21, 22); (e) The measured differences of crater frequencies on the ejecta blankets of Imbrian and older basins (22) are difficult to reconcile with a single late cataclysm.

We argue that the survival of 4.6 - 3.9 AE old igneous plutonic rocks (23) and the lack of impact melt rocks older than 4.15 AE must not necessarily reflect an early epoch of extremely reduced impact rate. We present the following alternative views. All Apollo highland sites are heavily dominated by the Imbrium ejecta blanket. Only at Apollo 16 and 17, also Nectaris and Serenitatis ejecta are present. These deposits contain basin ejecta sensu stricto and local pre-Imbrian or pre-Nectarian surface rocks (24). The latter must contain a high concentration of impact melt rock clasts because impact melts are only formed at the surface. In contrast, basin ejecta are dominated by more deep seated rocks, e.g. plutonic igneous lithologies (besides some melt ejecta). The age ranges and the compositions of impact melt lithologies at Apollo 14 (3.75 - 3.95 AE (12)), Apollo 16 (3.74-4.14 AE (8, 11)) and Apollo 17 (3.83-3.96 AE (22)) reveal differences of the Imbrium and Nectaris ejecta deposits. The oldest age group (3.96-4.14 AE), only found in the Descartes region, is most probably related to pre-Nectarian impact melt formations at the Nectaris site. The lack of impact melts older than 4.15 AE can be explained by an intense early bombardment (non-cataclysmic model A of (3)) which prior to 4.2 AE "pulverized" and remelted older highland rocks to a depth of 1 - 5 km where all pre-Nectarian melt sheets were concentrated. Therefore, impact melt rocks survive only at later times whereas the > 4.2 AE old plutonic rocks are preserved because they were brought to the surface from greater depths by late basin impact events. The cut-off at 3.95 AE for the Apollo 14 and 17 impact melt ages may be explained by the special target situation at the Imbrium site where pre-Imbrian crust had been removed by earlier very large basin impacts (e.g. Procellarum and Insularum basins (22, 25)). This explains not only the observed impact melt ages but also the lack of Fe-anorthosite and of old pristine igneous rocks (23) at the Apollo 14 site (9).

The absolute ages of the basins mentioned above remain uncertain. We have argued in favor of a 3.77 - 3.75 AE age of Imbrium (8). The ages of Serenitatis and Nectaris must be in the 3.83 to 3.96 AE range if we accept the feldspathic fragment-laden impact melt breccias (3.96 - 4.14 AE) as pre-Nectarian rocks. However, Nectaris could still be as young as 3.85 AE if all melt rocks of North Ray, Apollo 16, were pre-Nectarian. Consequently, about 30 pre-Nectarian basins (22) were formed within 440 to 550 million years since 4.4 AE, and about 12 post-Nectaris basins fall into a time period of 110 to 210 million years.

REFERENCES: (1) Tera, F. & G.J. Wasserburg (1974) Proc. Lunar Sci. Conf. 5th, 1571-1599. (2) Hartmann, W.K. (1975) Icarus 24, 181-187. (3) Hartmann, W.K. (1980) Proc. Conf. Lunar Highlands Crust, 155-171. (4) Taylor, S.R. (1982) Planetary Science: A lunar perspective, Plenum Press, N.Y. (5) Wilhelms, D.E. (1984) Moon, in: The Geology of Terrestrial Planets, NASA SP-469, 107-206. (6) Ryder, G. (1988) Workshop on Moon and Transition: Apollo 14, KREEP, and Evolved Lunar Rocks, 71-74. (7) Ryder, G. (1989) Lunar Planet. Sci. Conf. XX, 934-935. (8) Deutsch, A. & D. Stöffler (1987) Geochim. Cosmochim. Acta 51, 1951-1964. (9) Stöffler, D. et al. (1988) Workshop on Moon in Transition: Apollo 14, KREEP, and Evolved Lunar Rocks, 101-104. (10) Maurer, P.P. et al. (1978) Geochim. Cosmochim. Acta 42, 1687-1720. (11) Stöffler, D. et al. (1985) Proc. Lunar Planet. Sci. Conf. 15th, C449-C506. (12) Stadermann, F.J. et al. (1988) Workshop on Moon in Transition: Apollo 14, KREEP, and Evolved Lunar Rocks, 105. (13) Wacker, K. (1984) Dipl. thesis, Universität Heidelberg. (14) Heusser, E. (1985) Dipl.thesis, Max-Planck-Institut für Kernphysik, Heidelberg. (15) Lingner, S. et al. (1988) Workshop on Moon in Transition: Apollo 14, KREEP, and Evolved Lunar Rocks, 23-26. (16) Schaeffer, G.A. & Q.A. Schaeffer (1977) Proc. Lunar Sci. Conf. 8th, 2253-2300. (17) Jessberger, E.K. et al. (1977) Lunar Planet. Sci. XIII, 511-513. (18) Jessberger, E.K. et al. (1978) Proc. Lunar Planet. Sci. Conf. 9th, 841-854. (19) James, O.B. (1981) Proc. Lunar Planet. Sci. Conf. 12th, 209-233. (20) Spudis, P.D. & G. Ryder (1981) Proc. Lunar Planet. Sci. Conf. 12th, 133-148. (21) Spudis, P.D. & G. Ryder (1985) Trans. Am. Geophys. Union 66, 724. (22) Wilhelms. D.E. (1987) The Geologic History of the Moon, U.S. Geol. Survey, Prof. Paper 1348, pp. 301. (23) Shih, C.-Y. et al. (1989) Lunar Planet. Sci. Conf. XX, 1004-1005. (24) Oberbeck, V.R. (1975) Rev. Geophys. Space Phys. 13, 337-362. (25) Spudis, P.D. et al. (1987) Proc. Lunar Planet. Sci. Conf. 18th, 155-168.

Sudbury, Canada: Remnant of the only multi-ring (?) impact basin on Earth. Stöffler, D.[1], Avermann, M.[1], Bischoff, L.[1], Brockmeyer, P.[1], Deutsch, A.[1], Dressler, B.O.[2], Lakomy, R.[1], Müller-Mohr, V..[1] (1) Institut für Planetologie and Geologisch-Paläontologisches Institut, Universität Münster, FRG. (2) Ontario Geol. Surv., Toronto, Ont., Canada.

The Sudbury Structure is located at the present boundary between the Archean Superior Province and the Proterozoic Southern Province of the Canadian Shield. Its origin by impact or endogenic explosion is a matter of debate (1, 2). In a recent list of terrestrial impact structures (3) Sudbury is entered as a 1.85 Ga old complex crater with a diameter of 140 km. Field analysis and mapping, petrographic, chemical and isotope analysis (2, 5 to 18) in combination with a reevaluation of published observations (2, 19, 20) and the application of impact mechanical models in a planetological context (4, 19) led us to the following interpretation of the lithologies and stratigraphy of the various rock units of the structure.

a) The footwall underlying the 1.85 Ga old (2) Sudbury Igneous Complex (SIC) consists of Precambrian rocks and represents the autochthonous to parautochthonous crater basement. Pseudotachylites (Sudbury Breccia) cross-cut these Precambrian rocks which immediately below the SIC are shock-metamorphosed up to ~ 20 GPa. The discontinuous heterolithic Footwall Breccia, exposed in the North Range, and the footwall rocks at the lower contact of the SIC represent the uplifted crater floor and have been subjected to contact metamorphism by the SIC (12). b) The four units of the SIC (Sublayer, Norite, Quarz Gabbro and Granophyre) and the fragment-rich Basal Member (including the Melt Bodies) of the overlying Onaping Formation are part of a silicate melt system which according to isotopic signatures has a common origin in the Precambrian crust (13, 17). We believe that this system in total or at least large parts of it was formed by impact-induced melting of target rocks. c) The allochthonous polymict breccias of the upper Onaping Formation consist of Gray Member and Black Member. The Gray Member is a melt-bearing polymict suevitic breccia. The uppermost Black Member in large parts consists of reworked material. Groundsurging, air-born ejection and fall back and subaquaeous redeposition readily account for the sedimentary features of this allochthonous crater filling.

We conclude from our observations and from the published literature (e.g. 2) that the exposed section of shocked rocks, breccias and impact melt rock represent the eroded central depression inside the "peak ring" of a multi-ring impact basin. The ring itself and possibly additional rings including the crater rim have been eroded. Based on the distribution and extend of breccias, impact melt, and shatter cones and based on the location of the ~ 7.5 GPa isobar (2, 19, 21) we arrive at a range of 100 - 120 km for the diameter of the transient crater of the Sudbury Structure. According to empirical relations (22) the following geometrical parameters characterize the Sudbury Structure: depth of transient crater = 25 - 38 km, depth of excavation = 12 - 19 km; volume of impact melt = 5000 - 12000 km^3 (23) to 11000 - 24000 km^3 (22), diameter of apparent crater: 155 - 240 km. The depth of the impact-induced melt zone must have been at least equal to the depth of excavation (19 km (22)). Consequently impact melting affected a major part of the Precambrian crust. This result is compatible with isotope characteristics of the above defined melt system (17, 18).

REFERENCES: (1) DIETZ, R.S. (1964) J. Geol., **72**, 412 p.. (2) PYE, E.G., NALDRETT, A.J. & GIBLIN, P.E. (1984) Ont. Geol. Survey Spec. Vol.1. (3) GRIEVE, R.A.F. (1987) Ann. Rev. Earth Planet. Sci., **15**: 245-270. (4) SCHULTZ, P.H. & MERRILL, R.B. (ed.) (1981) Proc. Lunar Planet. Sci., **12A**. (5) BROCKMEYER, P. (1986) Unpublished Diploma Thesis, 100p; Münster. (6) LAKOMY, R. (1986) Unpublished Diploma Thesis, 135p; Münster. (7) AVERMANN, M. (1988) Unpublished Diploma Thesis, 113p; Münster. (8) MÜLLER-MOHR, V. (1988) Unpublished Diploma Thesis, 106p; Münster. (9) DEUTSCH, A., BUHL, D. & LAKOMY, R. (1988) Lunar Planet. Sci. Conf. 19th, 275-276. (10) LAKOMY, R. (1988) Fortschr. Miner., **66**,Beih. 1: 94. (11) LAKOMY, R., DEUTSCH, A. & BUHL, D. (1988) Fortschr. Miner., **66**, Beih. 1: 95. (12) DEUTSCH, A., LAKOMY, R. & BUHL, D. (1989) Earth Planet. Sci. Lett., (in press). (13) BROCKMEYER, P. & DEUTSCH, A. (1989) Lunar Planet. Sci. Conf. 20th, Abstracts: 113-114. (14) LAKOMY, R. (1989) Unpublished Ph. D. Thesis, 156p; Münster. (15) BROCKMEYER, P. (1989) Ph. D. Thesis, in prep; Münster. (16) DRESSLER, B.O., MORRISON, G.G., PEREDERY, W.V. & RAO, B.V. (1987) In: POHL, J. (ed.): 39-68. (17) FAGGART, B.E., BASU, A.R. & TATSUMOTO, M. (1985) Science, **230**: 436-439. (18) NALDRETT, A.J., RAO, B.V. & EVENSEN, N.M. (1988) The Institution of Mining and Metallurgy, London: 75-91. (19) STÖFFLER, D., BISCHOFF, L., OSKIERSKI, W. & WIEST, B. (1988) In: BODEN, A. & ERIKSSON, K.G. (eds.): Vol. 1: 277-297. (20) GRIEVE, R.A.F., DENCE, M.R. & ROBERTSON, P.B. (1977) In: RODDY, D.J., PEPIN, R.O. & MERRILL, R.B. (ed.): 791-814. (21) WIEST, B. (1987) Unpublished Ph. D. Thesis, 167p; Münster. (22) MELOSH, H.J. (1989) Oxford University Press, 245pp. (23) LANGE, M.A. & AHRENS, T.J. (1979) Lunar Planet. Sci. Conf. 10th: 2707 pp.

FISSION TRACK EVIDENCE FOR MULTIPLE SOURCE COMPONENTS OF ZHAMANSHIN IMPACTITES, AND NEW FISSION TRACK AGES. Dieter Storzer[1] and Christian Koeberl[2]. [1]Laboratoire de Mineralogie, Museum, 61 Rue Buffon, F-75005 Paris, France. [2]Institute of Geochemistry, University of Vienna, A-1010 Vienna, Austria.

Impact glasses from the Zhamanshin impact crater have been the subject of several recent investigations (e.g., [1,2]). The Zhamanshin crater is situated in the semi-arid regions of Khazakhstan, and according to recent remote sensing studies [3], has a diameter of about 13 km. The geological setting is complex and involves Paleozoic metamorphic crystalline rocks, Upper Paleozoic volcanic-sedimentary series, and rare ultrabasic dikes. Numerous types of impact glasses are found at the crater. The Si-rich varieties include the so-called irghizites (which are small, and tektite-like), Si-rich zhamanshinites (which have a structure and chemistry similar to Muong Nong type tektites), and blue zhamanshinites. Si-poor varieties include basic irghizites, and Si-poor zhamanshinites. Previous attempts to date samples of Si-poor zhamanshinites have yielded results that were inconclusive and not in agreement with ages determined for Si-rich zhamanshinites [4]. We have recently shown [2] that careful fission track age determinations of Si-poor zhamanshinites give ages that are indistinguishable from Si-rich zhamanshinites. In the course of this work, we have determined fission track ages for additional samples (size-corrected; in Ma): a. blue zhamanshinites, BZ8601: 1.09 +/- 0.14; BZ8602: 1.08 +/- 0.14. b. Si-poor zhamanshinite Zh 57/4b: 0.96 +/- 0.26.

In addition, we studied the microdistribution of uranium in a number of Zhamanshin impactites. Fig. 1 gives an overview of some of our results. In most samples, U is homogeneously distributed on a large scale. On a small scale (10-100 μm), U enrichments occur in a net-like pattern with large local enrichments. In several samples we found local enrichments (diameter about 20 μm) of up to 190 ppm U, probably decomposition products of zircons. The blue layers in blue zhamanshinites have higher u concentrations than the brown layers. The different U contents and the inhomogeneous microdistribution of U in the glasses indicate the presence of at least three different precursor components.

References: [1] Koeberl, C. (1988) GCA **52**, 779-784. [2] Koeberl, C., and Storzer, D. (1987) 2nd Inter.Conf. Natural Glasses, Prague, 207-213. [3] Garvin, J.B., et al. (1989) Proc. Intern. Conf. Global Catastr., subm. [4] Kashkarov, L.L., et al. (1987) 2nd Inter.Conf. Natural Glasses, Prague, 199-202.

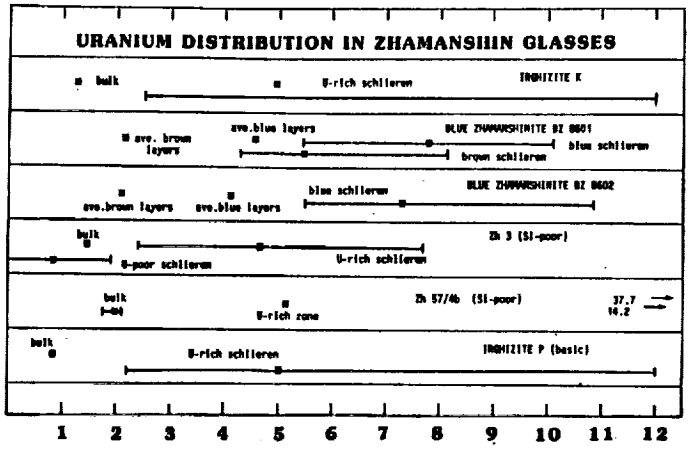

A PRELIMINARY REPORT ON NITROGEN ABUNDANCES AND ISOTOPES IN LL CHONDRITES; N.Sugiura and K.Hashizume, Geophysical Institute, University of Tokyo, Tokyo Japan.

A new system for measuring nitrogen abundances and isotopes was constructed. Nitrogen was extracted from meteorites by stepped combustion. The gas extraction system and handling are similar to those described by Frick and Pepin[1]. But in our system, a quadrupole mass spectrometer was used for detecting nitrogen molecules. The cold blank is about 0.5 ng of N, while the hot blank at 1200 C is about 3 ng of N. Nitrogen isotopic ratio can be determined with a precision of better than 3 permil according to repeated measurements of air nitrogen. Canyon Diablo (IA) was measured to confirm that we can reproduce the isotope anomaly reported by Prombo and Clayton[2]. Ar is also measured to provide evidence for the origin of nitrogen.

LL chondrites, Chainpur(LL3), Yamato74442(LL4) and St.Severin (LL6) have been measured so far. The nitrogen abundances range from 4.1 to 70.5 ppm, while the bulk isotopic ratios range from -13.8 to 8.2 permil. The respective values are shown in table 1. Duplicate measurements on Chainpur and St.Severin show that isotopic ratio vs. temperature diagram is fairly reproducible, while nitrogen release pattern could be variable at sample sizes of 50 mg. It was observed that at the highest temperatures (1100 - 1200 C) nitrogen isotope tends to be heavy, which may be due to cosmogenic nitrogen. At low temperatures, it is not easy to distinguish contamination (adsorbed air and organic nitrogen) from indigenous nitrogen. Similar release patterns of nitrogen and 36-argon in many samples suggest that contamination is not serious. On the other hand, a slight bump on isotope profile at 500 C suggests some contamination. If the data at 700 - 900 C are selected to avoid the effect of possible contamination and that of cosmogenic nitrogen, then a trend of increasing isotopic ratio with the increase in petrologic type is observed.

Table 1 Bulk results for nitrogen and 36-argon.

Sample	Nitrogen(ppm)	Delta-15N(permil)	36-Argon(ccSTP/g)
Chainpur	23.2	-13.8	4.2e-7
Chainpur	70.5	-9.1	6.3e-7
Y74442	7.0	-10.1	4.8e-8
St.Severin	4.1	+7.8	4.5e-8
St.Severin(S)	6.8	+8.2	2.4e-8
Canyon Diablo	21.7	-45.6	8.4e-8

(S) for St.Severin denotes silicate portion.

References: [1] U.Frick and R.O.Pepin (1981) Earth Planet.Sci.Lett. 56,64. [2] C.A.Prombo and R.N.Clayton (1983) Lunar Planet. Sci. XIV, 620.

SHOCK METAMORPHISM IN THE KOEFELS STRUCTURE (Tyrol,Austria)

Rouben SURENIAN
(Geologische Bundesanstalt,Vienna, Austria).

ABSTRACT:

Quartz and feldspars of gneiss and the famous pumice-like glass ("Bimsstein") from KOEFELS were analysed in detail with SEM to determine their structure and character. Features observed in quartz and some also in feldspars (like cone-shaped patterns, flow structures, partitioning, fine fracturing, cleavages and minute cavities) are compared to identical but more pronounced and more common features observed in samples of shocked gneiss from the RIES CRATER (Otting/Bavaria).

Some mineral phases within the etchted pumice (like lechatelierite and euhedral crystals of quartz and feldspars), the effects of rapid cooling of the molten material (partial fusion of quartz and feldspars), the shape of vents in the walls of the bubbles in the pumice as well as the crystallographically controlled planar features in quartz of gneiss are strong indicators for a meteorite impact, which triggered the largest post-glacial landslide in the crystalline Alps at KOEFELS.

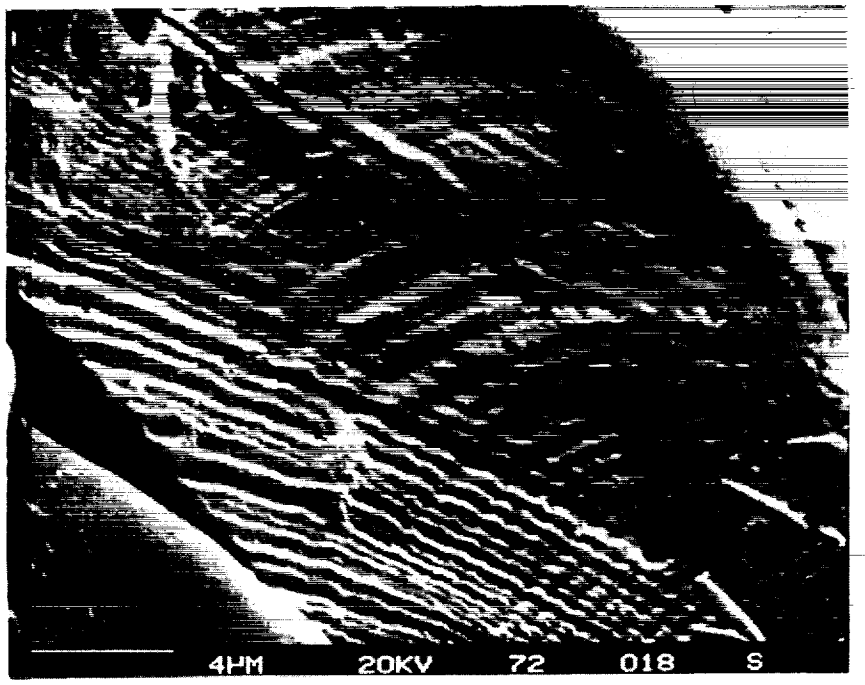

Fig.1: Quartz grain of an etched, autochthonous gneiss sample from Schartle/Koefels, showing well developed and cone-shaped lamellae ("shatter cones") under influence of shock waves.

DENSITY ESTIMATES FOR ELEVEN COSMIC DUST PARTICLES BASED ON SYNCHROTRON X-RAY FLUORESCENCE ANALYSES, S.R. Sutton[1] and G. J. Flynn[2], (1) Dept. of Geophysical Sciences, The Univ. of Chicago, and Brookhaven Nat. Lab, (2) Dept. of Physics, SUNY-Plattsburgh.

Cosmic dust particle density is an important parameter in calculating the orbital evolution time scale (and thus solar flare track density) and peak temperature reached on atmospheric entry. Both track density and peak temperature have been used to distinguish between cometary and asteroidal sources of the particles. We have previously reported densities of three chondritic cosmic dust particles from the Johnson Space Center (JSC) stratospheric collection [1]. Particle masses were inferred from direct measurements of Fe mass by synchrotron x-ray fluorescence and particle Fe/Si from the JSC catalog spectra. Volumes were determined from the two dimensional cross-section in the JSC catalog photo and an estimate of apparent thickness. We have improved the volume determinations by using an optical microscope to estimate particle dimensions and shapes. Control experiments using this procedure on two small fragments of standard glass (SRM 1876 K546) of known density (2.2 g/cc) gave density estimates of 2.0 and 3.8 g/cc. Thus we estimate the accuracy of this approach to be about $\pm$ 50%. Our density estimates for nine new chondritic particles and reevaluation of two of the previously reported particles are given in Table 1.

For the two particles previously reported, the density of one, W7029*A27, was unchanged from our earlier value of 1.6 g/cc. The optical observation that the second, U2015-G1, is sharply pointed in the depth dimension gives rise to density estimate of 1.6 g/cc compared to 1.2 g/cc using the previous technique. The new particles have densities in the range from 0.4 to 2.0 g/cc, consistent with the range from 0.7 to 2.2 g/cc reported by Fraundorf et al. [2] on seven smaller (all but one $\leq$ 11 μm) chondritic particles. Our largest particle, W7027-C5, exceeded the dimensions of the x-ray beam, thus the measured Fe mass is an underestimate of total Fe present and we can infer only a lower limit on its density. The mean particle density is 1.2 g/cc, suggesting a density of about 1 g/cc is appropriate for orbital evolution and entry heating models.

REFERENCES: [1] Flynn G. J. and Sutton S. R. (1988) Meteoritics, 23, 268-269. [2] Fraundorf P. et al. (1982) LPSC 13, 225-226.

Table 1: Particle Densities

Particle	Shape*	Dimensions (x,y,z in μm)	Density (g/cc)
W7029*A27	S	diameter = 10	1.6
U2015-G1	P	17,20,20	1.6
W7027-C5	P	22,30,35	> 0.5
U2022-G17	E	8,8,14	0.4
W7013-H17	P	12,12,15	0.8
W7013-A11	P	17,12,26	1.7
U2022-G2	R	15,7,15	2.0
U2022-B2	P	12,18,15	0.8
U2022-C18	R	11,9,14	0.9
U2001-B6	C	diam = 25, 15	0.6
W7066*A4	R	7,6,8	1.7

*SHAPE: R = rectangular box: C = cylinder: E = ellipsoid: S = sphere: P = intermediate to R and E [Vol(P) = 0.75 Vol(R)].

EXCESS FISSION XENON IN METEORITES; T. D. Swindle, Lunar and Planetary Laboratory, University of Arizona, Tucson, AZ 85721; C. M. Hohenberg, R. H. Nichols and C. T. Olinger, McDonnell Center for Space Science, Washington University, St. Louis, MO; and D. H. Garrison, NASA/JSC, Houston, TX.

All gas-rich lunar highland breccias, and some other lunar samples, contain excess fission xenon, xenon which was apparently produced by decay of ^{244}Pu and ^{129}I within the moon, and then somehow incorporated near the surfaces of grains within the regolith [1]. Finding the same effect in a gas-rich meteorite might be useful both to determine the timing of asteroidal regolith exposures and to constrain models of incorporation of excess fission xenon on the Moon.

Xenon matching many characteristics of lunar excess fission xenon has been identified in two howardites. In Kapoeta, grain-size separates reveal a surface-correlated fission-like component [2], although ordinate-intercept plots give a composition closer to H-Xe than to a true fission xenon component. In Bholghati, a lightly-bound (low-temperature) fission-like component has been found in stepwise heating [3], although the spectrum is again uncertain. These data, along with data from two other gas-rich meteorites, have been re-analyzed to try to pin down the fission composition.

For the Kapoeta data, three individual data sets (two grain-size separate experiments [2] and stepwise heating data [2,4]) define linear correlations on three-isotope plots of $^{x}Xe/^{130}Xe$ vs. $^{126}Xe/^{130}Xe$. Assuming that there are two components, and that one component is solar xenon plus a fission component, the composition of the assumed fission component can be calculated from the values of the correlation lines at $^{126}Xe/^{130}Xe=0.0263$ (the solar value). A weighted average of the three compositions is consistent with either H-Xe or ^{238}U fission. For Bholghati, a similar analysis gives a composition close to ^{238}U for $^{132}Xe/^{134}Xe/^{136}Xe$, but with anomalously high ^{131}Xe. Combined, these suggest the possibility of U fission, which would suggest that the component was acquired more recently than 4Ga ago. However, Kapoeta and Bholghati have "fission" components with $^{129}Xe/^{136}Xe$ of 0.73 ± 0.48 and 0.80 ± 0.26, respectively, which suggests an earlier acquisition (since the progenitor, ^{129}I, has such a short halflife).

In each stepwise heating experiment on Pesyanoe [5,6] and Fayetteville [7], a low-temperature step is enriched in heavy (fission-derived) xenon isotopes, although in some cases, the enrichment is apparently generated by terrestrial contamination. Since the data do not define linear correlations, the decomposition was done assuming a mixture of SUCOR, an appropriate fission-poor temperature step (which also contains some SUCOR) and the unknown component. Choosing the appropriate fission-poor component is somewhat arbitrary, but two Pesyanoe samples analyzed by [5] seem most consistent with ^{244}Pu fission, while the Fayetteville data could be consistent with either ^{244}Pu or terrestrial contamination.

In summary, there is clear evidence for excess fission xenon in meteorites. However, the present data are not sufficiently precise to determine the progenitor with accuracy for any class of meteorite, suggesting the need for more work.

References: [1] T. D. Swindle et al. (1986) Origin of the Moon, 331. [2] D. H. Garrison et al. (1987) Meteoritics 22, 382. [3] T. D. Swindle et al. (1989) LPS XX, 1095. [4] M. W. Rowe (1970) GCA 34, 1019. [5] K. Marti (1969) Science 166, 1263. [6] Yu. A. Shukolyukov et al. (1983) Geochem. Int. 20 (5), 96. [7] O. K. Manuel (1967) GCA 31, 2413.

Asteroidal Sources of Dust at the Earth's Orbit

Mark V. Sykes (Steward Observatory, Univ. of Arizona, Tucson, AZ 85721)

Collisional dust production in the asteroid belt is evidenced by the zodiacal dust bands discovered by the Infrared Astronomical Satellite (1). Small particles are removed from the asteroid belt by radiation forces, including Poynting-Robertson drag which secularly reduces their semi-major axes. The spatial distribution of particles deriving from the dust bands at a given time is defined by a torus having a squarish radial cross-section (see figure). Particle number densities increase toward the edges and are maximum at the "corners" (the locus of pericenters and apocenters of the particle orbits). As the particle orbits decay and their eccentricities decrease, the radial width of the torus decreases. Secular gravitational perturbations cause these tori to be inclined with respect to the ecliptic plane with an angle and ascending node which are a function of semi-major axis. Eventually these tori come within 1 AU of the sun and are intercepted by the earth. The result is an annual modulation in the flux of interplanetary dust as the earth samples different locations within a given torus. Only tori having low proper inclinations are likely to have their maximum densities sampled. The initial density and orbital elements of the dust in their source region will determine the amplitude of modulation at the earth's orbit and the ecliptic longitude of peak flux of dust deriving from that source. The principal asteroidal sources of modulations in the interplanetary dust flux at the earth's orbit is expected to derive from the low-inclination α and β bands, which have been associated with the Themis (C-type) and Koronis (S-type) asteroid families, respectively (2). By determining the components of interplanetary dust which are varying, and the longitudes of their maximum spatial density, it will be possible to identify material from these and possibly other source regions in the asteroid belt, thereby determining the minerologies associated with specific asteroid taxa.

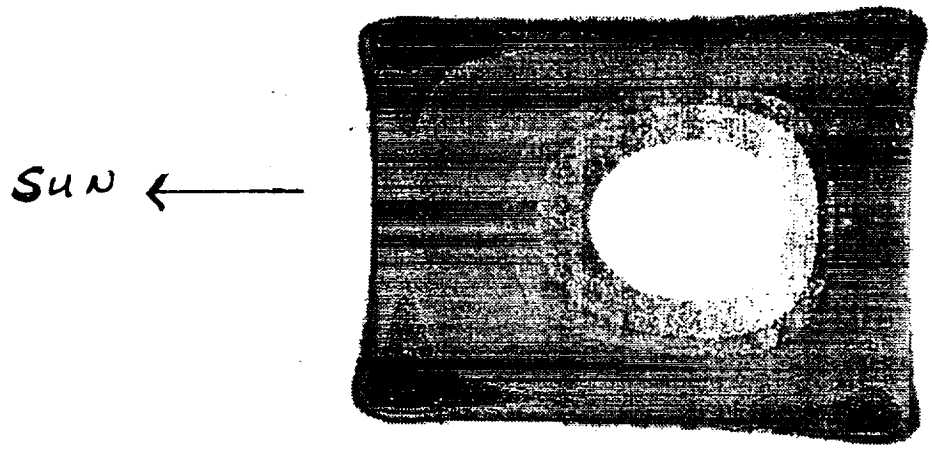

(1) Low, F.J., *et al.* (1984). *Astrophys. J. (Letters)* **278**, L19-L22.
(2) Sykes, M.V., *Icarus*, submitted.

CHEMICAL COMPOSITIONS OF FREMDLINGE FROM AN ALLENDE INCLUSION; P. Sylvester, B. Ward, and L. Grossman*, Department of the Geophysical Sciences, The University of Chicago, Chicago, IL 60637 USA *Also Enrico Fermi Institute.

Egg 6 is a type B1 calcium-, aluminum-rich inclusion (CAI) from the Allende meteorite. It contains numerous metal-magnetite-sulfide-phosphate nodules known as Fremdlinge. These include Zelda (504 μg) [1], Zorba (18 μg) and six smaller ones (~10 μg) whose bulk compositions were measured previously [2, 3]. In this study, we determined the bulk chemical compositions of an additional nine, tiny (0.2 - 10.5 μg) Fremdlinge from the same inclusion by INAA. These analyses were used to calculate mineral modes for all Fremdlinge, assuming that their mineral compositions are like those of Zelda [1]. The results suggest that the Fremdlinge are largely mixtures of FeNi metal, pyrrhotite and pentlandite (65.0 - 97.1%), with relatively minor magnetite (0 - 29.4%), molybdenite (.01 - 3.7%), whitlockite (0 - 9.4%) and refractory metal nuggets (.01 - 4.5 %). Metal/sulfide ratios range from 0.02 to 15.8. Chondrite-normalized refractory siderophile element abundances are shown in order of decreasing condensation temperature in the figure. Data are corrected for attached fassaite. For the three samples (F5, F6, F12) whose weights were too small to be measured accurately, the analyses were normalized to 100% after the masses of S, O and P were calculated from the inferred mineralogy. Interpretations below are based on all published trace element analyses of Fremdlinge from Egg 6.

For Re, Os, Ir and Rh, average inter-element ratios are within 14% of C1 ratios. On average, ratios of Re, Os and Ir to Ru and Pt are greater than C1 values by 48 - 81%, but Rh/Ru and Rh/Pt are within 15 - 20% of the C1 ratio. This suggests that, on average, the more volatile elements, Ru and Pt, were preferentially excluded from Fremdlinge relative to the more refractory elements, Re, Os and Ir, presumably due to the high nebular equilibration temperatures of the condensate alloys from which Fremdlinge were constructed. The 1 σ standard deviations of these ratios are very large, varying from 28 - 103%, with the notable exception of that for Re/Os, which is only 12%. The relative lack of fractionation of Re from Os is due to the fact that they have similarly high condensation temperatures and probably also reflects their condensation into a common alloy. The much larger fractionations seen among the rest of these elements in individual Fremdlinge are due to their differing volatilities from one another, their condensation into different host alloys from one another, or both.

Compared to the above elements, W and Mo show both enrichments and depletions relative to C1 chondrites. In cases where both are depleted, the W depletion is larger. This is opposite to what is expected from condensation from an oxidizing gas, a model used previously [4] to explain W and Mo depletions in Fremdlinge and bulk CAIs. It is likely that W was removed from Fremdlinge during secondary alteration [3], but it is clear that F5 originally had a W/Mo ratio that was greater than the cosmic ratio. An alternative explanation for fractionation of W and Mo from the other refractory siderophiles is based on crystal structures. At high temperatures, W and Mo form complete solid solutions in an alloy with a body-centered cubic structure, whereas the other refractory siderophiles form face-centered cubic and hexagonal close-packed crystal structures. Thus, W and Mo may have condensed into a different alloy from the other refractory siderophiles and different Fremdlinge may have accumulated from different proportions of these alloy phases.

References: [1] Armstrong J.T. et al. (1987) GCA 51, 3155-3173. [2] Grossman L. et al. (1986) LPSC XVII, 295-296. [3] Palme H. et al. (1989) LPSC XX, 814-815. [4] Fegley B. and Palme H. (1985) EPSL 72, p. 311-326.

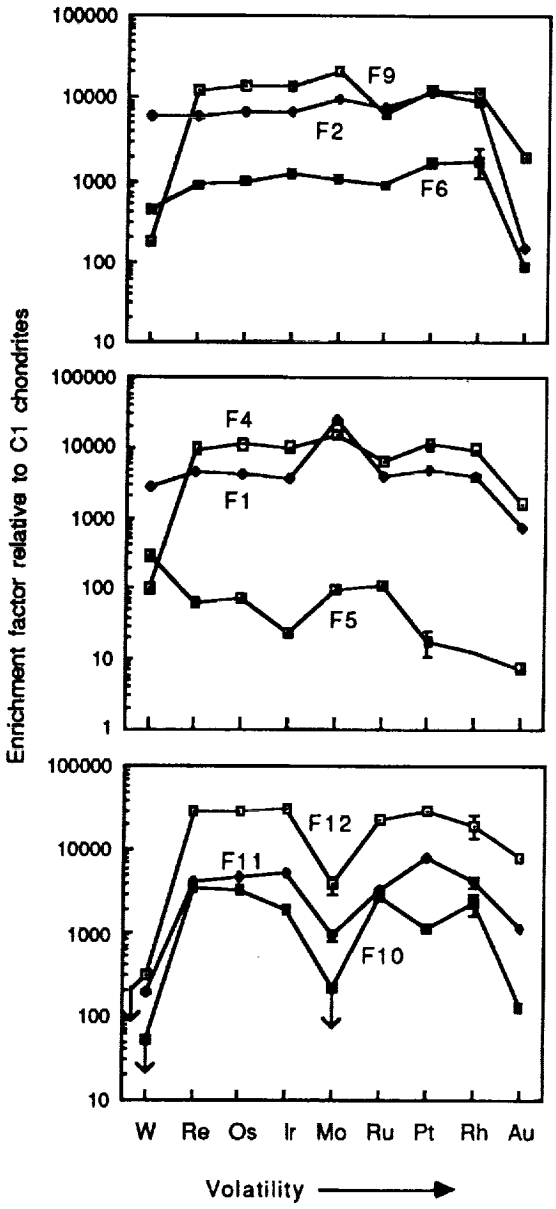

ASSOCIATION OF DIOGENITES AND CUMULATE EUCRITES IN YAMATO 791439 AND THEIR GENETIC LINK. Hiroshi Takeda and O. Hidaka, Mineralogical Inst., Faculty of Science, Univ. of Tokyo, Hongo, Tokyo 113, Japan.

Crystallization and impact histories of the HED (Howardites, Eucrites, Diogenites) achondrite parent body have been deciphered from the mineralogy and chemistry of a suite of the Yamato achondrites intermediate to diogenite and cumulate eucrite and represented by Y75032 (Takeda and Mori, 1985). A new specimen Y791439,51 has been investigated by electron microprobe and compared with the Y75032 group. The shock textures and mineral chemistry indicate that Y791439 is similar to the Y75032 group and contains clasts intermediate between diogenite and cumulate eucrite. One characteristics of Y791439 is that cumulate eucrites as Fe-rich as Serra de Magé and Moore Co. (MC) are abundant as clasts and pyroxene fragments. The amount of plagioclase in such clasts is larger than those in the Y75032 group. The exsolution textures of inverted pigeonites and chemistry of such clasts are similar to those of Serra de Magé. Six clasts of this kind up to 2.8X2.3 mm in size have been found in the thin section. Two pyroxene fragments contain thick (001) exsolution lamellae similar to MC. Y791200 and Y791201 contained rare cumulate eucrite clasts, but they are similar to Binda (BD) or Moama.

Pyroxene compositions in Y791439 fall in a limited range from mg number=MgX100/(Mg+Fe)=70 to 50 and are compatible with the continuum of rock types produced presumably by differentiation on the HED parent body. The chemical variation of pyroxene is wider than that of the monomict Y75032 group. The Mg-rich end is an Fe-rich diogenite-like pyroxene ($Ca_2Mg_{66}Fe_{31}$) common in Y75032, but the range extends more to Fe-rich side. Y791439 contains pyroxene clasts ($Ca_{11}Mg_{53}Fe_{36}$) texturally like that in MC. Y791439 also contains small fragments of ordinary eucrites such as Juvinas. Chemical compositions (An Mol %) of all plagioclase fragments in the section fall between 93 to 87 and the range is smaller than that of the diogenite-rich members of the Y75032 group. Chromite crystals are present in pyroxenes and show intermediate nature.

An versus mg number of the clasts distribute along cumulate eucrite (mg 63.5, An 91.5) to ordinary eucrite (mg 48.7, An 88.0) crystallization trend. This trend contrasts with that of diogenite-rich member such as Y791466, which shows an An-variation trend with nearly constant mg number. In summary, Y791439 sampled more cumulate eucrite components, especially of the MC-type than diogenitic ones, but the BD-type are also present. Y791439 shows a more polymict nature than the other Y75032 group, but the lithic variability is more limited and large lithic clasts are more abundant than normal howardites. The association of large amounts of smaller numbers of clast types suggests that it sampled by an impact three or four layers of the layered crust or pluton produced by the crystal fractionation, but did not sample deeper Mg-rich diogenites as in howardites and diogenites. Y791439 may best be classified as a polymict cumulate eucrite with small diogenitic and rare ordinary eucrite components. The presence of such a link material is a good indication of their genetic relationship.

We thank NIPR for the sample.

Reference: Takeda H. and Mori H. (1985) Proc. Lunar Planet. Sci. Conf. 15th. in J. Geophys. Res. 90, Suppl., C636-C648.

LUNAR REGOLITH: ITS CHARACTERIZATION AS A POTENTIAL RESOURCE FOR A LUNAR BASE. LAWRENCE A. TAYLOR. Department of Geological Sciences, University of Tennessee, Knoxville, TN 37996 USA.

The entire lunar surface is covered by a layer of fragmental and unconsolidated rock material - the **"regolith"**. In fact, all of the 382 kg of lunar samples returned by the 9 lunar missions were collected from this. The unconsolidated nature of the regolith makes it relatively easy to move, mine, and otherwise manipulate. Indeed, the rocks, minerals, and regolith on the moon will be the raw materials with which to construct a lunar base.

The **soil**, the finer fraction (< 1cm) of the unconsolidated regolith, was formed by three basic processes: 1) simple **comminution** - disaggregation of rocks and minerals into smaller particles by micrometeorites (which are also incorporated into the soil); 2) **agglutination** - the welding of lithic and mineral fragments together by the glass resulting from micrometeorite-produced impact melt; and 3) solar-wind **spallation and implantation**. The soil consists of rock, mineral, and glass fragments and agglutinates. The glasses are of two origins: 1) impact melt and 2) volcanic magma, explosively discharged and with coatings of volatile components. The presence of solar-wind H and C caused an "auto-reduction" of the soil during impact melting to produce single-domain (40-330 Å) Fe^{o} in the agglutinitic glass. Unfortunately this abundant native Fe metal in the soil is too fine-grained for easy concentration; beneficiation, involving grain-size coarsening, will be necessary to bring this native Fe up to "ore" grade. The single-domain signature, **"I_s/FeO"**, was recognized by McKay et al. (1974) as a measure of the quantity of agglutinitic glass and maturity (exposure age) of a soil. Morris (e.g., 1976) performed measurements of this parameter on numerous soils, thereby providing invaluable data for use in surveying soils for particular raw materials. In fact, this I_s/FeO is also indicative of the solar-wind content of the soil - higher maturity indicating greater amounts of H, He, C, etc.

Raw Materials - In order to consider habitation on the Moon, it is necessary to have abundant **WATER**. Ilmenite and possibly spinel are starting materials from which **oxygen** can be easily extracted by reduction processing (Gibson & Knudson, 1988). Solar-wind **hydrogen** is abundant (≅ 100 ppm) in lunar soil and is easily recovered by heating to 600°C (Carter, 1985). Another valuable solar-wind component of the soil is **helium** (≅ 40 ppm) which is the most prized of the reactants for nuclear fusion - in fact, it may be the only true economic "ore" on the Moon (Kulcinski, 1988). **Native Fe** is abundant in mare basalts and soils, particularly in the agglutinates. Volcanic glass beads possess abundant coatings of **volatile elements (e.g., Cl, Na, Zn, S)**. Concentrations of this material occurs in certain deposits, such as in the Apollo 17 "orange soil" (74220). **Sulfur** is also abundant in the soil in the mineral troilite (FeS). Several metals can be extracted from the soils and rocks, such as **Al, Si, Ti, Co, Ni**, etc. As a bulk material, lunar soil can be used as for housing insulation against cosmic rays, as well as within space vehicles. Perhaps agglutinitic glass can be concentrated by magnets (attraction of single-domain native Fe) and used for the fabrication and casting of certain structures. And of course, there is always the use of lunar soil as feed for making cement (àla T.D. Lin, 1988). The numerous potential uses for lunar regolith and soil only await fertile imaginations.

REFERENCES: Carter, 1985, Lunar Bases & Sp. Act. 21st Century, 571; Gibson M.A., and C.W. Knudsen, 1988, Proc. Space 88, ASCE, 400; Kulcinski, G.L., 1988, Univ. Wisc. Press, 20 pp; Lin, T.D., et al., 1988, Proc. Space 88, 146; McKay, D.S., et al., 1974, PLSC 5, 887; Morris, R.V., 1976, PLSC 7, 315.

Twenty years since Apollo 11
What have we learned about the Moon?

Stuart Ross Taylor
Lunar and Planetary Institute and Australian National University

Before the Apollo landing on July 20, 1969, firm facts about the moon were restricted to dynamical information about the lunar orbit, angular momentum and density. Speculations about its composition and origin were effectively unconstrained. Thus statements that running water carved the lunar rilles, that many of the large craters were volcanic calderas, that ice was present in a permafrost layer, that the maria were full of dust, that the maria were only a few million years old, that the lunar highlands were composed of granite or covered with volcanic ash-flows, that a 'lunar grid' reflected tectonic stress patterns, that tektites came not only from the Moon, but from the crater Tycho, and that the Moon was essentially a primitive undifferentiated object, were all published in the serious scientific literature.

The initial Apollo landing in Mare Tranquillitatis immediately swept away much of this speculation. The maria were shown to be composed of basaltic lava flows, with ages close to 4 billion years. By the time of the last landing of Apollo 17 in the Taurus-Littrow Valley on December 11, 1972, it was well established that the postulated calderas were all due to meteoritic impact, that the lunar highlands were mainly composed of anorthosite, that the highland plains were ejecta sheets from large basin impacts, that the 'lunar grid' was an artifact of the overlapping basin ejecta patterns, that tektites were terrestrial, and the basic lunar stratigaphy was well understood.

By 1974 the major conclusions about the evolution of the Moon had been established. At least 50% of the Moon was shown to have been melted, either during or shortly following accretion. The 100 km thick feldspathic highland crust had crystallised and floated on this 'magma ocean'. The interior had crystallised by about 4.4 billion years into a zoned sequence of cumulate minerals. The enigmatic 'KREEP' was shown to be derived from the final few percent of residual melt from this magma ocean, thus accounting for the extraordinary near surface concentrations of the incompatible elements. The mare basalts represented partial melts derived from this zoned interior, erupting up to a billion years later as radioactive heating induced mantle melting. Probably a small metallic core had formed. The Moon was bone-dry, depleted in volatile and siderophile elements and enriched in refractory elements relative either to the composition of the Earth or to that of the primordial solar nebula.

By the tenth anniversary of the initial landing, we understood the composition and evolution of the Moon rather better than that of the Earth. The question of lunar origin, frequently expected to be resolved by the initial lunar landing, remained stubbornly enigmatic. All the pre-Apollo theories collapsed following the overdose of lunar data. Capture and Double Planet hypotheses failed to account for the chemistry. Fission from the Earth, a truly testable hypothesis, failed to provide the predicted compositional match with the terrestrial mantle.

A successful theory to account for the new information required a synthesis of the dynamical and geochemical data with an understanding of the role of very large collisions, extrapolating by an order of magnitude beyond the impacts needed to produce the Imbrium and Orientale basins. The integration of all this disparate information probably explains why it was not until after the Kona Conference in 1984 that a consensus was reached that the Moon originated as the result of the glancing collision of an impactor larger than Mars, whose mantle, rather than that of the Earth, spun out to form the Moon.

It is ironic that the Moon, the most obvious astronomical object, accessible even to naked eye observation, as Harold Urey often reminded us, turned out to be unique in the Solar System. However it does provide some part of the often hoped for Rosetta Stone. "The lunar pre-Nectarian system provides our clearest look at the early Solar System" [Wilhems, D. E. 1987, *USGS Prof. Paper 1348*, p. 139] so providing a key to events before 3.8 billion years. It demonstrates clearly and dramatically the importance of stochastic events and stupendous collisions during the accretion of the planets. It enables us to contemplate with equanimity the collisional removal of the silicate mantle of Mercury, and the absence of a Moon and the slow backward rotation of Venus, due to a massive collision at a different angle. The dated lunar cratering record provides a benchmark with which to compare the cratering history of the planets and satellites. Although the hoped for geological correlation across the Solar System turns out to be unattainable, the detailed understanding of the variations observed in cratering throws much light on the differences of accretionary rates in the inner and outer parts of the Solar System.

Jaques Monod, in *Chance and Necessity,* remarked on the unlikely sequence of evolutionary events which led to *Homo sapiens.* It appears that an equally unlikely set of chance encounters resulted in the unique terrestrial satellite and that inspiration to poets, the Moon.

BULK CHEMISTRY AND MINERAL COMPOSITION OF A CHONDRITIC INTERPLANETARY DUST PARTICLE

K.L. Thomas[1], W. Klöck[2], M.E. Zolensky[3], D.S. McKay[2], [1]Lockheed, 2400 Nasa Rd.1, Houston, TX, 77058; [2]SN14, NASA/JSC, Houston, TX, 77058; [3]SN21, NASA/JSC, Houston, TX, 77058

INTRODUCTION AND METHODS Several refractory minerals similar in composition to those found in CAI's have been previously reported in a single interplanetary dust particle (IDP) [1]. Here we report on another IDP (W7027H14) which also contains refractory mineral grains. This particle is also unusual because it has a measured bulk carbon content of 23 wt.% [2]. We shall discuss the bulk chemistry and mineral chemistry of this particle in an attempt to determine where the carbon is located, and the possible effect of silicone oil contamination on both the meausred silicon and carbon compostion of this particle.

The bulk particle was analyzed using a JEOL 35 CF SEM at 15 kV equipped with a windowless Si(Li) detector which allows us to detect carbon x-rays. The particle was then embedded in epoxy and thin sectioned with an ultramicrotome and examined in a transmission electron microscope with a Be window X-ray spectrometer. Individual mineral phases and matrix areas within the sections were analyzed using the Cliff-Lorimer method [3].

RESULTS Particle W7027H14 is an anhydrous chondritic aggregate of 11x14 micrometers. The particle is very porous in thin sections. It consists mainly of enstatite, iron-sulfides as a mixture of pyrrhotite and pentlandite, and matrix. Rare olivine grains are also present. Pyroxenes range in composition from Fs 0.1 to 17.6 and olivines ranging from Fa 0.4 to 22.7 are present. The Ni content of the iron-sulfides varies from 1-13 wt%. Grains of an Fe-Ni phase with Ni contents of 20 wt% (assuming a metal) were also found. However, these grains could be oxides. The refractory mineral phases, identified by EDS analyses, are perovskite, fassaite, and forsterite. Perovskite grains measure 0.5 micrometers and a single rounded fassaite grain measures 0.3 micrometers in diameter.

All the individual mineral grains are embedded in an abundant silicon-rich matrix. Other elements detected in the matrix in varying amounts are sulfur and potassium. The amount of silicon, calculated as SiO_2, can be as high as 97 wt% neglecting the possible existence of carbon in the matrix. The matrix material is soft compared to the enclosed minerals as determined by behavior during sectioning. We suggest that the matrix consists of carbonaceous material which soaked up collector silicone oil which was not removed during hexane rinsing. Sulfur is highly variable and is sometimes the most abundant component in this matrix (neglecting carbon). It is also never associated with iron. This suggests that the matrix sulfur is most likely due to contamination from stratospheric sulfur aerosols [4].

In order to evaluate the degree of silicone oil contamination for this particle, we can assume that all of the Mg from the bulk analysis is present in enstatite, which is the dominant silicon-containing mineral phase present. With this assumption, the bulk silicon value should be 10.1 wt% instead of the measured 14.6 wt% silicon in the particle. As we found no significant silicon-rich phase other than the enstatite and matrix, we assume that the excess 4.5 wt% silicon is present as silicone oil absorbed in the matrix. This means that not only silicon is enriched but carbon, which is present in silicone oil, is then calculated to be too high by 12 wt% in the bulk analysis, assuming the Si/C ratio of silicone oil. In Figure 1, element abundances are compared to CI for the bulk particle with and without compensation for silicone oil contamination. Although correction for possible silicone oil contamination greatly reduces the carbon content, it is still considerably above CI levels.

CONCLUSION Particle W7027H14 is an unequilibrated anhydrous IDP, probably belonging to the pyroxene class, containing high temperature phases (perovskite, fassaite) and possibly low temperature phases (carbonaceous matrix). The inferred carbonaceous matrix apparantly has a strong affinity for silicone oil and sulfur aerosols.

REFERENCES: [1] Christoffersen R. and Buseck P.R.(1986) Science, 234, 590-592 [2] Thomas K.L., Klöck W., Blanford G.E., McKay D.S.(1988) Meteoritics, 23, 305 [3] Cliff G. and Lorimer G.W. (1975) J. Microscopy, 103, 203-207 [4] Mackinnon I.D.R. and Mogk D.W.(1985) Geophys Res Lett, 12, 93-96.

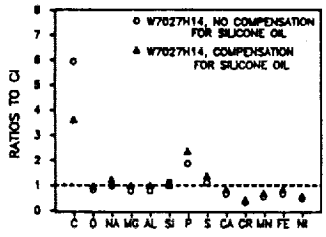

Figure 1: W7027H14 element abundances compared to CI

AR-AR AGES OF LL CHONDRITES; Mario Trieloff, Elmar K. Jessberger, and Josefa Oehm, Max-Planck-Institut für Kernphysik, P.O. Box 103980, 6900 Heidelberg, FRG

Scenarios concerning the formation and metamorphism of ordinary chondrite parent bodies (Grimm, 1985) range from the simple "onion-shell" model to fragmentation and reassembling models or the "metamorphosed-planetesimal" model (Scott and Rajan, 1981), where small planetesimals of one or two different petrologic types accreted to a larger body before the last stage of cooling.

Assuming internal heating, the "onion-shell" model predicts an inverse correlation of petrologic type with both, cooling rate and radiometric age. This is not expected for the other mentioned scenarios, because of the random layering depth after accretion or reassembling.

Cooling rates derived by ^{244}Pu fission track thermometry (Pellas and Storzer, 1981; Pellas and Fieni, 1988) seem to confirm an inverse correlation of FT-cooling rate and petrologic type among the H chondrites, which is in contrast to metallographic cooling rates (Taylor at al. 1987). If the "onion-shell" model is applicable, the different petrologic types of chondrites should find a reflection in ^{40}Ar-^{39}Ar age differences, but these could be small.

This is a report of ^{40}Ar-^{39}Ar age determinations of seven LL-chondrites in order to test the "onion-shell" hypothesis for the (possible) LL-parent body. The dated meteorites are Uden (LL7), St. Severin light and dark (LL6), the new fall Trebbin (LL5 or LL6), and the four antarctic meteorites ALHA 83070 (LL6), ALHA 84027 (LL7), ALHA 78109 (LL5), and EEtA 82608 (LL6). To keep the error of the relative ages small, all samples were irradiated together in the same capsule.

As a first result we did not obtain the 0.04 Ga age difference between St. Severin light and dark that had been found by Hohenberg et al. (1981), although the age patterns are quite similar. Our ^{40}Ar-^{39}Ar age of St. Severin (light and dark) is 4.34 ± 0.03 Ga. All results will be discussed at the meeting.

References: Grimm R.E. (1985) J. Geophys. Res. **90** B2, 2022-2028. Hohenberg C.M., Hudson P., Kennedy P.M. and Podosek F.A. (1981) Geochim. Cosmochim. Acta **45,** 535-546. Pellas P. and Storzer D. (1981) Proc. R. Soc. Lond. **A 374**, 253-270. Pellas P. and Fieni C. (1988) Lunar Planet. Sci. XIX. Scott E. R.D. and Rajan R.S. (1981) Geochim Cosmochim. Acta **45**, 53-67. Taylor G.J., Maggiore P., Scott E.R.D., Rubin A.E. and Keil K. (1987) Icarus **69,** 1-13.

CONDENSATION EXPERIMENTS AND THEIR APPLICATION TO THE CHEMICAL COMPOSITIONS OF CHONDRITES; A.Tsuchiyama, Department of Geology and Mineralogy, Kyoto University, Sakyo, Kyoto, 606, JAPAN.

In the last few years, condensation experiments have been carried out to reproduce condensates in the primordial solar nebula (e.g., Nagahara et al., 1988; Tsuchiyama et al., 1988). Tsuchiyama (1989) carried out condensation experiments in the system Mg-Si-O-H by using forsterite as a vaporization source, and obtained condensates of forsterite, enstatite, amorphous silicates and silicon, as a function of temperature and redox condition at low pressures. Phase diagrams of the system were also constructed independently by thermochemical calculations to compare with the experimental results. The calculations showed that the locations of some phase boundaries in the phase diagrams are fixed for $p<10^{-3}$bar and $(Mg+Si+O)/H<10^{-2}$. The condensation sequences were same as those predicted by the phase diagrams. From these studies (1) correspondence between the condensation experiments and the thermochemical calculations and (2) an experimental method for studying fractionation of isotopes and minor elements with condensation (e.g., Ueda et al. (1989) for the Mg isotopes) have been established.

The result of (1) means that applicability of solid-gas equilibria to condensation in the nebula at high temperatures is verified by experiments. It was also revealed that the phase diagrams of simplified systems are useful for the application to condensation (and also vaporization) in the nebula in stead of the classical method dealing directly with natural complex systems, such as of Grossman and Larimer (1974). In this point of view, several phase diagrams were constructed in simple systems including H and major elements for refractory minerals (Mg, Si, Fe and O). Effects of H and O contents were also examined from these diagrams. The chemical and mineral compositions of the chondrites was explained in the light of these phase diagrams.

References:

Grossman,L. and Larimer,J.W. (1974) Rev. Geophys. Space Phys., **12**, 71-101.

Nagahara,H., Kushiro,I., Mysen,B.O., and Mori,H. (1988) Nature, **331**, 516-518.

Tsuchiyama,A. (1989) Lunar Planet. Sci. **XX**.

Tsuchiyama,A., Kushiro,I., Mysen,B.O. and Morimoto,N. (1988) Proc. NIPR Antarctic Meteorite, **1**, 185-196.

Ueda,C., Okano,J. and Tsuchiyama,A. (1989) Abstract of this meeting.

IS THERE MARTIAN SURFACE WATER IN NAKHLA? G Turner, R Burgess and E Chatzitheodoridis, Department of Geology, University of Manchester, Manchester M13 9PL, UK.

In recent years we have demonstrated how it is possible to use the ^{40}Ar-^{39}Ar technique to disentangle mixtures of radiogenic, parentless (excess) and atmospheric argon in terrestrial fluid inclusions through interelement and isotopic correlations with K, Cl and ^{36}Ar [1]. The technique has been applied to a variety of minerals, most especially quartz and fluorite from areas of mineralisation. Recently Cl correlated excess 40Ar has even been observed in volatile rich fluids in diamond [2]. The presence of argon with near atmospheric $^{40}Ar/^{36}Ar$ ratios coupled with concentrations of ^{36}Ar around 10^{-6} ccSTP/g in the hydrothermal brines in vein quartz and fluorite is a clear indication of the presence of water which equilibrated with the terrestrial atmosphere. The presence in Nakhla of aqueous alteration products of possible martian origin and xenon with a high $^{129}Xe/^{132}Xe$ (coupled with a low Kr/Xe ratio relative to the martian atmosphere) suggests that it could be worthwhile searching for evidence of noble gases introduced by martian sub-surface water in Nakhla. Clearly the evidence will be less obvious than in terrestrial minerals because of the much lower atmospheric pressure on Mars and the absence of any evidence as yet for fluid inclusions in the submicroscopic 'martian' alteration products. Below are two instructive calculations.

Typical concentrations of ^{40}Ar, ^{84}Kr and ^{132}Xe in terrestrial surface waters are respectively, $3x10^{-4}$, $4x10^{-8}$ and $4x10^{-9}$ ccSTP/g. Hydrothermal minerals typically trap water at the per-cent level so that bulk concentrations are a factor of 100 lower. Concentrations in any present day martian sub-surface water will be roughly two orders of magnitude lower than in terrestrial water due to the lower atmospheric pressure, implying that bulk concentrations of the three isotopes in martian alteration products could be of the order of $3x10^{-8}$, $4x10^{-12}$ and $4x10^{-13}$ ccSTP/g. Presumably bulk concentrations in the meteorite itself are considerably smaller.

Terrestrial hydrothermal fluids in inclusions are usually brines with NaCl concentrations commonly in the range 3 - 30 wt% and molar ratios of Cl to atmospheric ^{40}Ar of $4x10^{4}$ to $4x10^{5}$. Given the low water content of Mars it seems likely that martian sub-surface water may be very saline and (assuming NaCl and ^{40}Ar saturated 0°C brine) have a molar Cl to ^{40}Ar ratio of the order of $2x10^{7}$. Published Cl concentrations for Nakhla are variable ranging from 80ppm to 1000ppm. If all this chlorine were introduced by sub-surface water the associated complement of atmospheric ^{40}Ar would be from $2.5x10^{-9}$ to $3.1x10^{-8}$ ccSTP/g. In comparison with the conclusions of the previous paragraph these values are uncomfortably high and suggest that only a small proportion of the chlorine can be associated with trapped martian water.

We searched for evidence of a correlation between Cl and ^{40}Ar in the published ^{40}Ar-^{39}Ar measurements on Nakhla [3] but without success. However the use of stepped heating and the high concentration of in-situ radiogenic argon ($7x10^{-6}$ ccSTP/g) would certainly obscure any effects at the levels estimated above. We are currently repeating these experiments with the use of in vacuo crushing prior to stepped heating in order to release any argon associated with micro-inclusions. Results will be presented at the meeting. Preliminary crushing experiments on a 50mg unirradiated sample released $\leqslant(4\pm2)x10^{-9}$ ccSTP/g of non terrestrial ^{40}Ar, the dissolved argon equivalent of 0.1% of martian water or 140 ppm Cl.

[1] Turner G, GCA, **52**, 1443-1448 (1988); [2] Turner G and Burgess R, Lunar and Planet Sci **XX**, 1140-1141, (1989); [3] Podosek FA, EPSL, **19**, 135-144, (1973).

C-3

CHEMISTRY AND ISOTOPIC COMPOSITION OF XENOLITHS IN CARBONACEOUS CHONDRITES

A.A.Ulyanov[1], N.N.Kononkova[1], M.A.Korovkin[2]
[1]V.I.Vernadsky Institute of Geochemistry and Analytical Chemistry, USSR Academy of Sciences, Moscow, USSR; [2]M.V.Lomonosov Moscow State University, Moscow, USSR

Xenoliths in carbonaceous chondrites are important to understand the early history and evolution of the Solar System. Recently Olsen et al. [1] reported the presence of C3 xenoliths in Murchison. Our studies of Allende and Efremovka samples have shown that there are many small dark xenoliths ranging from 3 to 20 mm within C3V-hosts. In the present study, we examined three of these xenoliths (ALD-08,E39, and E53) by petrographic and electron scaning microscopes (NU-2 and CAMSCAN, respectively) and electron microprobe analysis (CAMEBAX MICROBEAM). Major element analyses of different areas of xenoliths by SEM and EPMA reveal some variability, but are in a good agreement (Fig.1). In our preliminary isotope investigations [2,3] of the Efremovka meteorite we presented data for oxygen and hydrogen isotopic compositions of xenoliths E39 and E53. Recently we reported [4] the oxygen and hydrogen isotope data for Allende xenolith ALD-08. Oxygen isotope analyses of Efremovka xenoliths E39 and E53 fall between terrestrial and CM-matrix fractionation lines on the tree isotope diagram. Analysis of Allende xenolith ALD-08 plots close to crossing of the CO-CV mixing line and CM-matrix fractionation lines. Oxygen isotope analyses of Efremovka and Allende xenoliths discribed here fall on a single fractionation line (R=.999) with a slope .58, which is close to the slope of mass-fractionation line. Hydrogen isotope analyses of xenoliths ALD-08 and E39 fall within the fields of CM and CV chondrites, respectively. Hydrogen isotope data suggest that Allende and Efremovka xenoliths have undergone extraterrestrial hydrous alteration to varying degree. All xenoliths of Efremovka and Allende described here represent chondritic-like lithologies. Xenolith clasts in Allende and Efremovka show a relativly narrow range of bulk element chemistries. Their mineral chemistries are similar to those of known types of carbonaceous chondrites except for some enriched in Fe of chondrule minerals (olivines and pyroxenes). The major element ratios to Si of Efremovka xenoliths (E39 and E53) are different from average values of known types of carbonaceous chondrites (Table). These Efremovka xenoliths may represent of new types of meteorite matter and they were simultaneously accerted with other components (chondrules, CAIs, etc) of carbonaceous chondrites. As xenoliths are quite abundant in meteorites, the chemical data of them may be very important for future interpretations of Phobos-mission data.

Type	Mg/Si	Al/Si	Ca/Si	Fe/Si
CI	.90±.03	.080±.002	.089±.002	1.77±.06
CM	.91±.03	.086±.003	.096±.003	1.66±.06
CO	.92±.02	.088±.001	.097±.002	1.64±.02
CV	.93±.01	.112±.004	.118±.002	1.48±.03
ALD-08	.90±.04	.125±.011	.115±.025	1.50±.07
E39	.91±.02	.084±.009	.098±.007	1.58±.03
E53	.92±.03	.086±.012	.070±.018	1.57±.02

CI, CM, CO and CV - after [5]; ALD-08, E39, and E53 - our data

REFERENSES: [1] Olsen E.J., et al. (1988) - GCA, 52, 1615; [2] Devirts A.L., et al., (1984) - X Symp. Stable Isot.,145 (in Russian); [3] Ustinov V.I.,et al. (1987) - Dokl. Acad. Sci. USSR, 296, 2, p. 441 (in Russian); [4] Ulyanov A.A., et al. - Meteoritika (in press) (in Russian); [5] Yavnel' A.A.(1988) 27th Int. Geol. Congr., Sec. C.11, p.79.

MAGNESIUM ISOTOPE ABUNDANCES OF SILICATES PRODUCED IN GAS-CONDENSATION FURNACE; C.Uyeda and J.Okano, College of General Education, Osaka Univ. Toyonaka, Osaka 560 Japan. A.Tsuchiyama, Dept. Geology & Mineralogy, Kyoto Univ. Sakyo, Kyoto 606 Japan.

Isotopic abundances of magnesium have been measured for silicate samples produced in a gas condensation furnace(Tsuchiyama,1989) to investigate the mechanism of mass fractionation in the primitive solar nebula. In particular, the relation between condensation temperature Tc and the amount of Mg mass fractionation was studied for the silicate condensates.

The starting material (powders of Mg_2SiO_4 synthetic crystals) was evaporated around 1630 °C under constant H_2 gas pressure of 1.4×10^{-5} barr which is close to that of the solar nebula. Condensates of different Tc were produced within a single run. Forsterite, forsterite-enstatite mixtures and amorphous material condensed at 1400 °C-900 °C, 900 °C-600 °C and below 600 °C, respectively(Tsuchiyama,1989). Seven samples with different Tc were collected and the amount of mass fractionation, Δ26, were measured for each sample, where Δ26 is $\Delta 26 = \{(^{26}Mg/^{24}Mg)_{sample}/(^{26}Mg/^{24}Mg)_{strart} - 1\} \times 1000$ ‰. Mg isotope abundances were measured by SIMS(modified Hitachi IMA-2A) with 10.5keV, O_2^+ ions as primaries. The diameter and current of the primary ion beam on the sample surface were 200μm and 1.5-2.0μA, respectively(Okano et al.1985). The scattering of $^{26}Mg/^{24}Mg$ values due to instrumental effect was estimated to be less than ±4‰ in the present measurement.

The condensates of the room temperature were highly enriched in the light Mg isotope and Δ26 amounted to -52±4‰, however Δ26 tend to increase with Tc and became positive above Tc=1200 °C. At Tc=1400 °C, Δ26 amounted to +12±5‰. The residue was enriched in the heavy isotope and Δ26=+8±4‰. The results indicate that the Mg mass fractionation in silicates produced through evaporation-condensation process strongly depends on its condensation temperature , and that the condensates are not necessarily enriched in light isotopes. The results will be compared with those of other workers(Esat et al. 1986), and the mechanism of this large mass fractionation of condensates will be discussed based on the correlation of Δ26 and Tc.

References

1)Tsuchiyama,A.(1989): Abstracts of the 52th Annual Meteoritical Society Meeting, to be published; Tsuchiyama,A.(1989):Proc. Lunar and Planetary Science XX.

2) Okano,J., Uyeda,C. and Nishimura,H.(1985) : Mass Spectroscopy 33,245-253.

3) Esat,M.T.,Spear,R.H. and Taylor,R.S.(1986): Nature 319, 576-578

METEORITIC SOURCE OF LARGE-ION LITHOPHILE ELEMENTS IN TERRESTRIAL NESQUEHONITE FROM ANTARCTIC METEORITE LEW 85320 (H5).

M.A. Velbel[1], D.T. Long[1] and J.L. Gooding[2] [1]*Dept. of Geological Sciences, Michigan State University, East Lansing, MI 48824-1115* [2]*SN21/Planetary Science Branch, NASA/Johnson Space Center, Houston, TX 77058*

Recent studies of evaporite minerals and their distribution on Antarctic meteorites have suggested that at least some of the cationic constituents of the evaporites are derived from the meteorites themselves, rather than from the terrestrial environment [1,2]. The presence of surficial evaporite deposits is associated with below-average alkali- and alkaline-earth element (especially Rb) contents in meteorite interiors [1]. This suggests that evaporites and element depletion may be causally related [1]. In order to test the hypothesis that evaporite formation results from redistribution of meteoritic elements, rather than by terrestrial contamination, major and trace element analyses are being performed on evaporite deposits from the Lewis Cliffs, Antarctica, LEW 85320 (H5) ordinary chondrite.

Here we report analyses for Na, Mg, K, Ca, and Rb for two samples of evaporite material from LEW 85320. Sample ,81 is a split of material which was present when the meteorite was recovered. Sample ,81 consists entirely of soluble material. Sample ,82 is a split of an efflorescence which formed in the laboratory during storage of the parent meteorite under dry nitrogen [2]. Another split (,22) from the same parent possesses a salt-and-pepper texture, most likely due to contamination of the evaporite with fusion crust or other meteoritic material [2]. Sample ,82 consists of 5.7 wt % non-magnetic insoluble material, 5.3 wt % magnetic insoluble material, and 89.0 wt % soluble material. X-ray diffraction (XRD) of both samples indicated that the dominant crystalline phase is nesquehonite [2]. The non-magnetic insoluble fraction of sample ,82 contains lepidocrocite, which we interpret to be an alteration product of fusion crust.

Element-ratio diagrams (below) suggest that the observed contents of large-ion lithophile elements would require only modest fractionation of meteoritic elements (below left), whereas substantial fractionation would be required to derive the observed element ratios from terrestrial seawater (below right). Therefore, evaporite minerals on Antarctic meteorites are most likely not products of contamination by terrestrial (marine) salts. The low level of Rb in the evaporite contradicts the hypothesis that evaporite formation is responsible for the anomalously low Rb contents in the interiors of evaporite-bearing Antarctic ordinary chondrites [1]. The association between evaporites and low interior Rb contents may indicate that whatever (pre-terrestrial?) phenomenon that caused low Rb contents also made the meteorite more vulnerable to weathering and evaporite formation.

References: [1] Velbel M.A. (1988) *Meteoritics*, **23**, 151-159. [2] Jull A.J.T., Cheng S., Gooding J.L. and Velbel M.A. (1988) *Science*, **242**, 417-419.

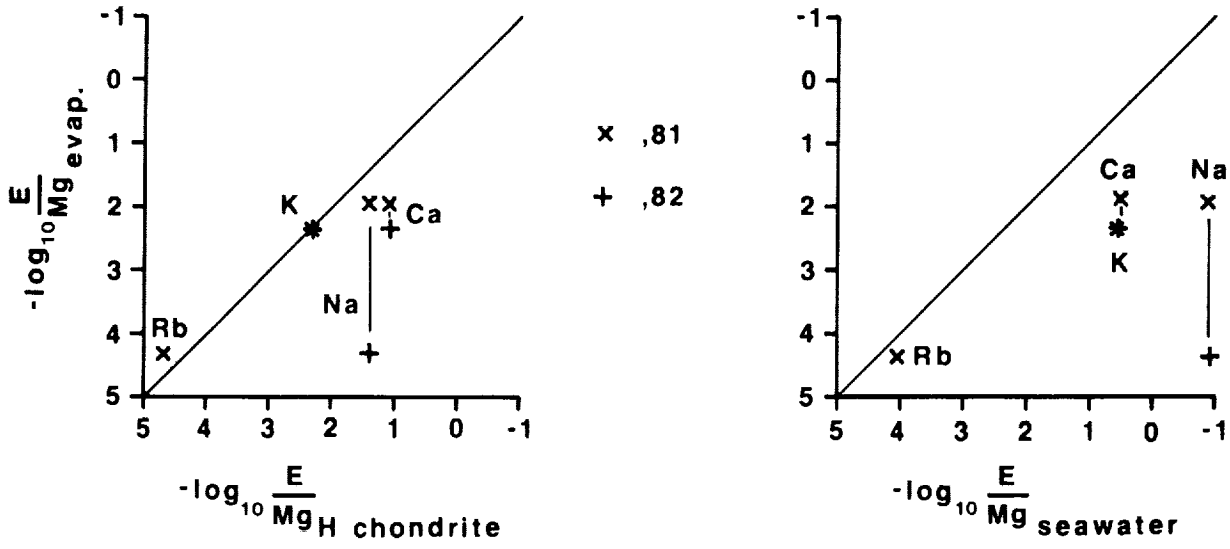

OXYGEN ISOTOPIC COMPOSITIONS OF SPINEL AND CORUNDUM GRAINS FROM THE MURCHISON CARBONACEOUS CHONDRITE; A. Virag+, E. Zinner+, R. S. Lewis* and S. Amari*, +McDonnell Center for the Space Sciences and Physics Department, Washington University, St. Louis, MO 63130, USA; *Enrico Fermi Institute and Department of Chemistry, University of Chicago, Chicago, IL 60637, USA.

Previous ion probe measurements by McKeegan (1987) and Zinner and Epstein (1987) indicated that individual spinel grains from Murchison residue CFOc show different ^{16}O enrichments. Grossman *et al.* (1988) found that large spinel grains (>100μm) from the Murchison matrix have isotopically normal oxygen. Here we report O isotopic compositions of more carefully selected and characterized spinels (5 to 30 μm in size) from Murchison CFOc as well as the first O isotopic measurements on individual corundum grains obtained from the coarse grained (>10μm) Murchison separate LU (Amari and Lewis, 1989).

Only $^{18}O/^{16}O$ ratios were determined in 161 pure spinel grains. Contrary to the previous results of McKeegan (1987) and Zinner and Epstein (1987), there is no evidence for substantial oxygen isotopic heterogeneity (Fig. 1). Only one grain lies outside the major range of CFOc grains whose width is not significantly different from that obtained on the Burma Spinel standard grains ($\chi^2 = 1.07 < \chi^2_{crit}(69, 161,5) = 1.30$). This observation is borne out by 9 randomly chosen spinel grains, in addition to the isotopically heavier grain, for which we measured all O isotopes (Fig. 2). While the spinel grains are isotopically homogeneous, the corundum grains show a large range in ^{16}O enrichments. Specifically, one of the corundum grains has substantially smaller $\delta^{17}O$ and $\delta^{18}O$ values than have previously been observed.

Clayton *et al.* (1977) and Clayton and Mayeda (1984) assumed the ^{16}O-rich endmember to be represented by spinel with an ^{16}O excess of 40‰. There is now mounting evidence (cf. Fahey *et al.*, 1987, Ireland and Zinner, 1989) that at least in Murchison this value is an average and that much higher ^{16}O enrichments exist. It is unlikely that the fairly uniform composition of the CFOc spinels resulted from partial equilibration of originally ^{16}O-richer spinel after their formation. More likely, these spinels formed from a reservoir that was itself a mixture of the original ^{16}O-rich endmember and normal O.

Acknowledgements: Murchison separate CFOc was kindly provided by Yang and Epstein. A. Virag wants to thank the "Fond zur Förderung der wissenschaftlichen Forschung," Austria, for financial support of this work.

References: Amari S. and Lewis R.S. (1989) this volume; Clayton R.N. *et al.* (1977) EPSL **34**, 209; Clayton R.N. and Mayeda T. (1984) EPSL **67**, 151; Fahey A.J. *et al.* (1987) Ap.J. **323**, L91; Grossman L. *et al.* (1988) Lunar Planet. Sci. XIX, 435; Ireland T.R. and Zinner E. (1989) this volume; McKeegan K. D. (1987) Science **237**, 1468; Zinner E. and Epstein S. (1987) EPSL **84**, 359.

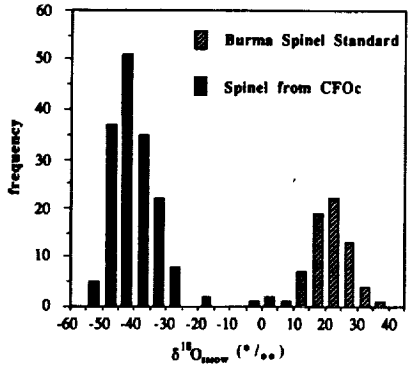

Fig. 1: Distribution of $\delta^{18}O$ values measured in single spinel grains from Murchison and the Burma spinel standard.

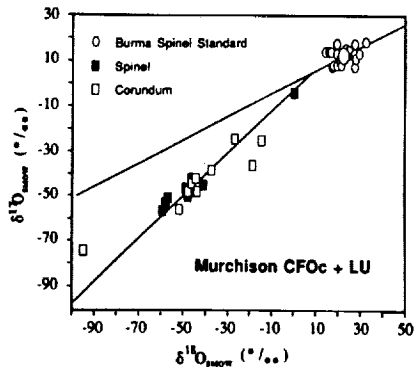

Fig. 2: Oxygen isotopic compositions of single spinel and corundum grains from the Murchison meteorite.

CORROSION OF THE SANTA CATHARINA METEORITE; L. Vistisen and N.O. Roy-Poulsen, *Niels Bohr Institute, Blegdamsvej 17, DK-2100 Copenhagen Ø, Denmark*

R.S. Clarke, Jr., *Division of Meteorites, National Museum of Natural History, Smithsonian Institution, Washington, D.C. 20560*

Mössbauer spectroscopy has shown that the Santa Catharina meteorite is composed of two Fe-Ni phases, low-Ni taenite (<25% Ni) and high-Ni taenite (~50% Ni). In a rather well preserved sample (USNM 6293) the high-Ni taenite is nearly pure tetrataenite. In a more corroded sample (USNM 3043) the Mössbauer spectrum shows that the high-Ni taenite is mostly tetrataenite but disordered taenite (~50% Ni) is also present. Furthermore, there is relatively more low-Ni taenite in the well preserved sample than in the corroded sample (Vistisen et al., 1987).

Santa Catharina is polycrystalline with crystals of 2-8 cm in size (Buchwald, 1975). We do not know the relationship between the two examined samples and they might originate in different crystals. The difference between the samples could thus be explained by different compositions of the crystals. As the two samples have different degrees of corrosion, another explanation for the observed differences might be that corrosion converts low-Ni taenite (<25% Ni) into high-Ni, disordered taenite (~50% Ni).

To investigate the last suggestion we have searched for a much more corroded sample. The piece of Santa Catharina from which the most corroded sample (USNM 3043) has been cut is surrounded by a rusty shell where metal is hardly seen. From this rusty part small, irregular metallic grains (~100-500 μm) have been separated. A Mössbauer absorber was made of the grains being polished to small plates with a thickness of 10-15 μm. For comparison a piece of the nearby metallic part (the already examined corroded sample (USNM 3043)) has been polished by the same procedure to the same thickness.

Transmission Mössbauer spectra of the grains and of the metallic sample have almost the same relative contribution from the low-Ni taenite (<25% Ni), suggesting that this Fe-Ni phase is not preferentially attacked by corrosion. The high-Ni taenite (~50% Ni), on the other hand, has by the corrosion been altered to have a higher content of disordered taenite (~50% Ni), showing that tetrataenite disorders by heavy corrosion. This difference is reflected in the Mössbauer parameters of the high-Ni taenite which are H = 290 kG, ϵ = 0.18 mm/s for the metallic sample and H = 292 kG, ϵ = 0.16 mm/s for the grains from the rusty part.

The Mössbauer results suggest that the differences between the two first examined samples are not due to corrosion effects, but might be explained by assuming that the samples were originally of different composition. This indicates that the crystals which make up the Santa Catharina meteorite do not have the same Ni-content.

Buchwald, V.F. (1975) *Handbook of Iron Meteorites,* University of California Press, Berkeley.

Vistisen, L., Hansen, H., Roy-Poulsen, N.O. and Clarke, R.S., Jr. (1987) *Meteoritics* **22**, 518.

Fe ISOTOPE ANOMALIES; J. Völkening and D. A. Papanastassiou, Lunatic Asylum, Div. Geol. & Planet. Sci., 170-25, Caltech, Pasadena, CA 91125.

We have developed techniques for the measurement of Fe isotopic abundances and applied them to Fe in whole samples and in FUN and non-FUN refractory inclusions of carbonaceous meteorites. Correlated isotope anomalies for Ca, Ti and Cr have proven critical for the identification of distinct nucleosynthetic components, especially based on compositions for the FUN inclusions, and later on large effects in hibonites using the ion microprobe. Measurements in Ni and Zn [1,2] provide faint hints of anomalies for elements just above Fe. Based on the Fe peak of solar abundances, the measurement of Fe appears important. We used samples with known Ca, Ti and Cr effects. Fe was separated (anion) in a HCl medium. Separation from Cr was important, given the much higher ionization efficiency (IF) of Cr vs. Fe. Fe was measured as Fe^+ using Si-gel and boric acid as an emitter. Typically, 5µg Fe yield $(1.5\text{-}2)\times10^{-11}$A $^{56}Fe^+$, for several hours, IF = $(3\text{-}6)\times10^{-5}$ for Fe, as compared to $\sim1\times10^{-3}$ for Cr. Mass interferences: at 54amu, $^{54}Cr^+/^{54}Fe^+ < 4$ ε-units (εu); at 58amu, no interference from Ni with an upper limit $^{58}Ni^+/^{58}Fe^+$ of 10 εu, since the ^{58}Fe abundance is only 0.3%. No other interferences were seen; a small hydrocarbon peak at 58.2amu was monitored but was well-resolved. The data are shown in the Table. For isotope fractionation (F_{Fe}) normalization we used $^{54}Fe/^{56}Fe$ and an exponential law. For reagent Fe we observe: a) a narrow range in F_{Fe} of 10±2°/₀₀/amu; b) uncertainties of ±2 to ±4 εu for $^{57}Fe/^{56}Fe$ and of ±10 to ±20 εu for $^{58}Fe/^{56}Fe$ (both $2\sigma_{mean}$), reflecting the low abundance of ^{58}Fe. Fe in whole samples (acid soluble) of Allende and Murchison show normal Fe with a hint of ^{58}Fe excess for Murchison. Some non-FUN inclusions show small effects in ^{57}Fe at the 4σ level and effects at ^{58}Fe which cannot be resolved from normal. FUN inclusion C-1, surprisingly, shows only hints of effects at ^{57}Fe and ^{58}Fe. By contrast, FUN inclusion EK-1-4-1 has normal ^{57}Fe and a very large excess in ^{58}Fe of 279±16εu. We conclude that, for Fe: a) only small endemic effects may be present in non-FUN inclusions; b) FUN inclusion EK-1-4-1 shows normal ^{57}Fe and an excess in ^{58}Fe which may be correlated with effects in Ca, Ti and Cr; c) no large Fe effects are present in C-1 which would correlate with the distinct components seen in C-1 for Ca, Ti and Cr; and d) there is no evidence (at the limit of ±2°/₀₀) for intrinsic Fe isotope fractionation, even for FUN inclusions. The correlation of ^{48}Ca, ^{50}Ti, ^{54}Cr and ^{58}Fe excesses appears well-defined for EK-1-4-1; it implies a neutron-rich equilibrium process, presumably with multiple zone mixing skewed towards zones with slightly lower neutron excess values, to enhance ^{58}Fe [3]. Production of excess ^{54}Fe and ^{58}Fe, e.g. in SN carbon deflagrations [4], would also be consistent with excesses in ^{58}Fe (after normalization for F_{Fe}); however the constancy in $^{54}Fe/^{56}Fe$ (i.e., F_{Fe}) and the absence of ^{57}Fe effects provide no direct support for this possibility. (#676).

Fe results		F(Fe)	$^{57}Fe/^{56}Fe$	$^{58}Fe/^{56}Fe$
FUN	EK-1-4-1	11.3 - 8.5	-0.4 ± 1.7	279 ± 16
	C-1(S1)a	10.3 - 9.0	-10.0 ± 4	27 ± 16
	b	9.4 - 7.7	-2.6 ± 4.7	8 ± 15
non-FUN	Egg 2	5.9 - 3.8	-3.4 ± 2.2	14 ± 11
	Egg 3 a	0 - (-6.9)	-0.4 ± 6.0	13 ± 22
	b	9.8 - 8.3	1.3 ± 2.1	-12 ± 11
	Egg 6A a	9.0 - 7.8	-3.4 ± 2.2	-6 ± 8
	b	10.0 - 2.2	-3.9 ± 2.6	-18 ± 6
Whole	Murchison	9.9 - 8.2	0.9 ± 2	29 ± 10
Met.	Allende	11.1 - 4.7	1.3 ± 1.3	-17 ± 6
Fe Standard		11.0 - 10.0	0.0 ± 4	19 ± 22
		10.0 - 9.8	-0.4 ± 3	10 ± 19
		9.1 - 2.1	0.9 ± 2	-11 ± 6
		10.8 - 9.9	-1.3 ± 2	-18 ± 5

F(Fe) = isotope fractionation factor in °/₀₀/amu calculated from measured $^{54}Fe/^{56}Fe$. Fractionated Egg-3a measurement at high T. $^{57,58}Fe/^{56}Fe$ deviations from normal, in parts in 10^4; $2\sigma_m$ uncertainties for data corrected for isotope fractionation using the exponential law. Normal Fe: $^{54}Fe/^{56}Fe \equiv 0.062669$; $^{57}Fe/^{56}Fe = 0.023261\pm0.000002$; $^{58}Fe/^{56}Fe = 0.0031170\pm0.0000054$.

Ref. 1. Birck & Lugmair (1988) EPSL 90, 131; 2. Loss & Lugmair (1989) LPS XX, 588; 3. Hartmann et al. (1985) Ap. J. 297, 837; 4. Woosley & Weaver (1986) in Lect. Notes Phys. 255, 91 (Springer-Verlag); & (1986) Ann. Rev. Astron. Astrophys. 24, 205.

PETROLOGY AND CHEMISTRY OF PROBABLE IMPACT MELT ROCKS AT THE SEVETIN CRATER;

S. Vrána, Ústřední ústav geologický, Malostranské nám. 19, 118 21 Praha 1, Czechoslovakia

There are two types of probable melt rocks interpreted as injections in the fundament of the deeply eroded Sevětín structure (1, 2): 1. Pyroxene-biotite quartz monzodiorite /MD/, 2. Microgranodiorite /MG/. These rocks, endemic to the Sevětín structure, were dated as Upper Permian (3). MD is exposed as a dyke and as loose blocks at other two localities. The rock is moderately clast-laden: quartz clasts show rims of clinopyroxene + Kfs-Qtz intergrowth; centimetric granite clasts are transformed to granophyre with lathy plagioclase; host rock mafic granulite clasts are rare; fibrolitic sillimanite microclasts, showing reaction to hercynitic spinel, corundum and diaspore, appear to be inherited from paragneiss of the basement. A vesicular facies is rare. MD has subophitic texture of plagioclase and augite, contains ~15 vol.% biotite /> 5 wt.% TiO_2/ and minor brown-green hornblende. Chlorite spheroids ϕ 0.5 - 1.5 mm make 8 vol.% of the rock. Rare lechatelierite relics occur exclusively in the spheroids. Sulphide grains and aggregates are enriched in the spheroids /pyrhotite, pentlandite, pyrite, sphalerite, chalcopyrite, galena and Ni-cobaltite with ~11 wt.% Ni/. Altogether 34 minerals identified in MD /26 analyzed with microprobe/ demonstrate the highly disequilibrium nature of this rock. Four pyroxenes are identified: major augite / Wo_{42} $En_{45}Fs_{13}$/, rare low-Ca augite /10 wt.% CaO/, pigeonite /5 wt.% CaO/ is the major pyroxene from one locality of MD, and very rare hypersthene mainly altered to "bastite". The early accessory minerals - zircon /<10 μm/, ilmenite /up to 0.4 wt.% Cr_2O_3/ and apatite are in skeletal crystals and indicate a high cooling rate during the early stages of crystallization. The chlorite spheroids are interpreted as drops of an immiscible liquid dispersed and solidified in the main mass of melt (cf. 4, 5). The rock composition is similar to that of mafic granulite, but Ni and Cr are enriched in MD by factors of 15 and 3 respectively, relative mafic granulite.

Microgranodiorite /MG/ is close in its composition to quartz monzonite and quartz monzodiorite, i.e. very similar to the biotite /sillimanite/ paragneiss of the Moldanubian crystalline complex (6). MG is enriched in Ni and Cr but HREE are lower compared to paragneiss. The rock is fine-grained, contains <5 vol.% of clasts, mainly minor plagioclase and quartz xenocrysts which give the rock a pseudoporphyritic texture. Biotite gneiss and fibrolitic sillimanite clasts were also observed. The rock was first introduced (1) under the name granodiorite microporphyry. The texture is dominated by lathy plagioclase, interstitial K-feldspar, chlorite and quartz. Primary pyroxene is chloritized, relics of hypersthene are very rare. Apatite, ilmenite, pyrite and pyrhotite are accessory. Mineralogy of this fine-grained rock is not completely studied.

Pre-impact platform cover sediments - Stephanian C - Lower Permian preserved in two downthrown segments indicate a two layer target with sedimentary cover> 1 000 m, overlying basement. This provides for two kinds of melt. Estimates of the target composition at the present erosion level give 65% paragneiss and migmatitic gneiss, 25% biotite granite, 8% felsic granulite and acid orthogneiss, 2% mafic granulite for the central uplift area. At the pre-impact setting, paragneiss and migmatitic gneiss possibly constituted about 80% of the target below the Stephanian-Permian cover. Petrochemical data for the cover sediments are lacking for mixing calculations.

REFERENCES (1) Vrána S. /1967/ Geol. Rundschau 76, 505-528; (2) Vrána S. /1988/ Lunar and Planetary Sci. XIX, 1222-1223; (3) Jessberger E.K., Buzek F. /unpublished/ K-Ar dating of dyke rocks from the Sevětín impact structure; (4) Dence M.R., von Engelhardt W., Plant A.C., Walter L.S. /1974/ Contrib. Mineral. Petrol 46, 81-97; (5) Grieve R.A.F. /1975/ Geol. Soc. Amer. Bull. 86, 1617-1629; (6) Bouška V., Jelínek E., Pačesová M. /1985/ Geochemistry of the Moldanubian paragneisses.- Charles University, Prague.

Fe ISOTOPE ANOMALIES; J. Völkening and D. A. Papanastassiou, Lunatic Asylum, Div. Geol. & Planet. Sci., 170-25, Caltech, Pasadena, CA 91125.

We have developed techniques for the measurement of Fe isotopic abundances and applied them to Fe in whole samples and in FUN and non-FUN refractory inclusions of carbonaceous meteorites. Correlated isotope anomalies for Ca, Ti and Cr have proven critical for the identification of distinct nucleosynthetic components, especially based on compositions for the FUN inclusions, and later on large effects in hibonites using the ion microprobe. Measurements in Ni and Zn [1,2] provide faint hints of anomalies for elements just above Fe. Based on the Fe peak of solar abundances, the measurement of Fe appears important. We used samples with known Ca, Ti and Cr effects. Fe was separated (anion) in a HCl medium. Separation from Cr was important, given the much higher ionization efficiency (IF) of Cr vs. Fe. Fe was measured as Fe^+ using Si-gel and boric acid as an emitter. Typically, 5µg Fe yield $(1.5\text{-}2)\times10^{-11}$A $^{56}Fe^+$, for several hours, IF = $(3\text{-}6)\times10^{-5}$ for Fe, as compared to $\sim1\times10^{-3}$ for Cr. Mass interferences: at 54amu, $^{54}Cr^+/^{54}Fe^+ < 4$ ε-units (εu); at 58amu, no interference from Ni with an upper limit $^{58}Ni^+/^{58}Fe^+$ of 10 εu, since the ^{58}Fe abundance is only 0.3%. No other interferences were seen; a small hydrocarbon peak at 58.2amu was monitored but was well-resolved. The data are shown in the Table. For isotope fractionation (F_{Fe}) normalization we used $^{54}Fe/^{56}Fe$ and an exponential law. For reagent Fe we observe: a) a narrow range in F_{Fe} of 10±2°/₀₀/amu; b) uncertainties of ±2 to ±4 εu for $^{57}Fe/^{56}Fe$ and of ±10 to ±20 εu for $^{58}Fe/^{56}Fe$ (both $2\sigma_{mean}$), reflecting the low abundance of ^{58}Fe. Fe in whole samples (acid soluble) of Allende and Murchison show normal Fe with a hint of ^{58}Fe excess for Murchison. Some non-FUN inclusions show small effects in ^{57}Fe at the 4σ level and effects at ^{58}Fe which cannot be resolved from normal. FUN inclusion C-1, surprisingly, shows only hints of effects at ^{57}Fe and ^{58}Fe. By contrast, FUN inclusion EK-1-4-1 has normal ^{57}Fe and a very large excess in ^{58}Fe of 279±16εu. We conclude that, for Fe: a) only small endemic effects may be present in non-FUN inclusions; b) FUN inclusion EK-1-4-1 shows normal ^{57}Fe and an excess in ^{58}Fe which may be correlated with effects in Ca, Ti and Cr; c) no large Fe effects are present in C-1 which would correlate with the distinct components seen in C-1 for Ca, Ti and Cr; and d) there is no evidence (at the limit of ±2°/₀₀) for intrinsic Fe isotope fractionation, even for FUN inclusions. The correlation of ^{48}Ca, ^{50}Ti, ^{54}Cr and ^{58}Fe excesses appears well-defined for EK-1-4-1; it implies a neutron-rich equilibrium process, presumably with multiple zone mixing skewed towards zones with slightly lower neutron excess values, to enhance ^{58}Fe [3]. Production of excess ^{54}Fe and ^{58}Fe, e.g. in SN carbon deflagrations [4], would also be consistent with excesses in ^{58}Fe (after normalization for F_{Fe}); however the constancy in $^{54}Fe/^{56}Fe$ (i.e., F_{Fe}) and the absence of ^{57}Fe effects provide no direct support for this possibility. (#676).

Fe results		F(Fe)	$^{57}Fe/^{56}Fe$	$^{58}Fe/^{56}Fe$
FUN	EK-1-4-1	11.3 - 8.5	-0.4 ± 1.7	279 ± 16
	C-1(Sl)a	10.3 - 9.0	-10.0 ± 4	27 ± 16
	b	9.4 - 7.7	-2.6 ± 4.7	8 ± 15
non-FUN	Egg 2	5.9 - 3.8	-3.4 ± 2.2	14 ± 11
	Egg 3 a	0 - (-6.9)	-0.4 ± 6.0	13 ± 22
	b	9.8 - 8.3	1.3 ± 2.1	-12 ± 11
	Egg 6A a	9.0 - 7.8	-3.4 ± 2.2	-6 ± 8
	b	10.0 - 2.2	-3.9 ± 2.6	-18 ± 6
Whole Met.	Murchison	9.9 - 8.2	0.9 ± 2	29 ± 10
	Allende	11.1 - 4.7	1.3 ± 1.3	-17 ± 6
Fe Standard		11.0 - 10.0	0.0 ± 4	19 ± 22
		10.0 - 9.8	-0.4 ± 3	10 ± 19
		9.1 - 2.1	0.9 ± 2	-11 ± 6
		10.8 - 9.9	-1.3 ± 2	-18 ± 5

F(Fe) = isotope fractionation factor in °/₀₀/amu calculated from measured $^{54}Fe/^{56}Fe$. Fractionated Egg-3a measurement at high T. $^{57,58}Fe/^{56}Fe$ deviations from normal, in parts in 10^4; $2\sigma_m$ uncertainties for data corrected for isotope fractionation using the exponential law. Normal Fe: $^{54}Fe/^{56}Fe \equiv 0.062669$; $^{57}Fe/^{56}Fe = 0.023261\pm0.000002$; $^{58}Fe/^{56}Fe = 0.0031170\pm0.0000054$.

Ref. 1. Birck & Lugmair (1988) EPSL 90, 131; 2. Loss & Lugmair (1989) LPS XX, 588; 3. Hartmann et al. (1985) Ap. J. 297, 837; 4. Woosley & Weaver (1986) in Lect. Notes Phys. 255, 91 (Springer-Verlag); & (1986) Ann. Rev. Astron. Astrophys. 24, 205.

PETROLOGY AND CHEMISTRY OF PROBABLE IMPACT MELT ROCKS AT THE SEVETIN CRATER;

S. Vrána, Ústřední ústav geologický, Malostranské nám. 19, 118 21 Praha 1, Czechoslovakia

There are two types of probable melt rocks interpreted as injections in the fundament of the deeply eroded Sevětín structure (1, 2): 1. Pyroxene-biotite quartz monzodiorite /MD/, 2. Microgranodiorite /MG/. These rocks, endemic to the Sevětín structure, were dated as Upper Permian (3). MD is exposed as a dyke and as loose blocks at other two localities. The rock is moderately clast-laden: quartz clasts show rims of clinopyroxene + Kfs-Qtz intergrowth; centimetric granite clasts are transformed to granophyre with lathy plagioclase; host rock mafic granulite clasts are rare; fibrolitic sillimanite microclasts, showing reaction to hercynitic spinel, corundum and diaspore, appear to be inherited from paragneiss of the basement. A vesicular facies is rare. MD has subophitic texture of plagioclase and augite, containing ~15 vol.% biotite /> 5 wt.% TiO_2/ and minor brown-green hornblende. Chlorite spheroids ϕ 0.5 - 1.5 mm make 8 vol.% of the rock. Rare lechatelierite relics occur exclusively in the spheroids. Sulphide grains and aggregates are enriched in the spheroids /pyrhotite, pentlandite, pyrite, sphalerite, chalcopyrite, galena and Ni-cobaltite with ~11 wt.% Ni/. Altogether 34 minerals identified in MD /26 analyzed with microprobe/ demonstrate the highly disequilibrium nature of this rock. Four pyroxenes are identified: major augite / Wo_{42} $En_{45}Fs_{13}$/, rare low-Ca augite /10 wt.% CaO/, pigeonite /5 wt.% CaO/ is the major pyroxene from one locality of MD, and very rare hypersthene mainly altered to "bastite". The early accessory minerals - zircon /<10 μm/, ilmenite /up to 0.4 wt.% Cr_2O_3/ and apatite are in skeletal crystals and indicate a high cooling rate during the early stages of crystallization. The chlorite spheroids are interpreted as drops of an immiscible liquid dispersed and solidified in the main mass of melt (cf. 4, 5). The rock composition is similar to that of mafic granulite, but Ni and Cr are enriched in MD by factors of 15 and 3 respectively, relative mafic granulite.

Microgranodiorite /MG/ is close in its composition to quartz monzonite and quartz monzodiorite, i.e. very similar to the biotite /sillimanite/ paragneiss of the Moldanubian crystalline complex (6). MG is enriched in Ni and Cr but HREE are lower compared to paragneiss. The rock is fine-grained, contains <5 vol.% of clasts, mainly minor plagioclase and quartz xenocrysts which give the rock a pseudoporphyritic texture. Biotite gneiss and fibrolitic sillimanite clasts were also observed. The rock was first introduced (1) under the name granodiorite microporphyry. The texture is dominated by lathy plagioclase, interstitial K-feldspar, chlorite and quartz. Primary pyroxene is chloritized, relics of hypersthene are very rare. Apatite, ilmenite, pyrite and pyrhotite are accessory. Mineralogy of this fine-grained rock is not completely studied.

Pre-impact platform cover sediments - Stephanian C - Lower Permian preserved in two downthrown segments indicate a two layer target with sedimentary cover> 1 000 m, overlying basement. This provides for two kinds of melt. Estimates of the target composition at the present erosion level give 65% paragneiss and migmatitic gneiss, 25% biotite granite, 8% felsic granulite and acid orthogneiss, 2% mafic granulite for the central uplift area. At the pre-impact setting, paragneiss and migmatitic gneiss possibly constituted about 80% of the target below the Stephanian-Permian cover. Petrochemical data for the cover sediments are lacking for mixing calculations.

REFERENCES (1) Vrána S. /1967/ Geol. Rundschau 76, 505-528; (2) Vrána S. /1988/ Lunar and Planetary Sci. XIX, 1222-1223; (3) Jessberger E.K., Buzek F. /unpublished/ K-Ar dating of dyke rocks from the Sevětín impact structure; (4) Dence M.R., von Engelhardt W., Plant A.C., Walter L.S. /1974/ Contrib. Mineral. Petrol 46, 81-97; (5) Grieve R.A.F. /1975/ Geol. Soc. Amer. Bull. 86, 1617-1629; (6) Bouška V., Jelínek E., Pačesová M. /1985/ Geochemistry of the Moldanubian paragneisses.- Charles University, Prague.

A SURVEY OF 26-ALUMINUM IN ANTARCTIC METEORITES; J. F. Wacker, Battelle, Pacific Northwest Laboratories, P. O. Box 999, Richland, WA 99352

Since 1979, Battelle, Pacific Northwest Laboratories has continued to assay Antarctic meteorites for ^{26}Al ($t_{1/2}$=7.05 x 10^5 yr). Over 490 meteorites have been analyzed for ^{26}Al, which is measured rapidly and nondestructively by multiparameter gamma-ray spectroscopy. The ^{26}Al data are used to estimate the terrestrial residence time of meteorites that have accumulated on the Antarctic ice. While the ^{26}Al method alone cannot provide completely reliable ages for individual samples, ^{26}Al data are useful for evaluating trends for large groups of samples and providing guidance for selecting samples for more detailed study by other methods, such as analysis of noble gases or other radionuclides (*e.g.*, ^{10}Be, ^{14}C, ^{36}Cl, and ^{53}Mn).

The main emphasis to date have been the analysis of ordinary chondrites. The ^{26}Al activities in our data set range from 11 dpm/kg (ALH76008) to 117 dpm/kg (ALH79036), with most activities falling between 30 and 50 dpm/kg. The peak in the activity distribution of the Antarctic meteorites is lower than the equilibrium saturation activities of 59 and 55 dpm/kg for L and H chondrites [1], but is consistent with an average terrestrial age of ~200,000 years [2]. Some of the samples have ^{26}Al activities that fall outside the normal range, indicating unusual histories, such as long terrestrial residence times or exposure to solar cosmic rays. Samples with unusually low or high activities are listed in the Table, along with new data for 5 ureilites.

The lowest activities cluster around 20 dpm/kg, suggesting that ~1 million years is the approximate age cutoff for Allan Hills region. Low activities are indicative of short exposure ages or shielding effects. In particular, ALH76008 has an ^{26}Al activity of 11 dpm/kg, corresponding to a terrestrial age of ~1.6 Myr, but analyses of other radionuclides indicate a complex exposure history and a relatively short terrestrial age [1,3]. Samples with high activities are generally small, consistent with the requirement that these samples experienced low ablation to preserve solar cosmic ray effects. ALH79036 has an ^{26}Al activity of 117±7 dpm/kg -- the highest activity ever measured in an ordinary chondrite -- and should be analyzed for other radionuclides and noble gases to confirm exposure to solar cosmic rays.

The ureilite data show two groups, one with low activities (~30-40 dpm/kg), the other with high activities (~50-80 dpm/kg). The origin of low ureilite ^{26}Al activities was discussed by [4], who suggested that the undersaturation was due to peculiar orbital geometry. More recently, [5] concluded that most ureilites are near-surface samples and suggested that the LEW 85440 (67.8 dpm/kg) experienced significant solar cosmic ray irradiation. Our data indicate that ALH84136, and possibly ALH82106/ALH82130, were irradiated by solar cosmic rays. This question will be addressed as more ureilite data become availible.

[1] Evans J.C. and J.H. Reeves (1987) Earth Planet. Sci. Lett., **82**, 223. [2] Nishiizumi K. (1984) Smithsonian Contri. Earth Sci., **26**, 105. [3] Fireman E.L. (1983) Lunar Planet. Sci. XIV, 195-196. [4] Wilkening L.L., Herman G.F. and Anders E. (1973) Geochim. Cosmochim. Acta. **37**, 1803-1810. [5] Aylmer D., Herzog G.F., Vogt S., Middleton R., Fink D., and Klein J. (1989) Lunar Planet. Sci. XX, 54-55.

specimen	class	mass*	^{26}Al†	specimen	class	mass*	^{26}Al†	specimen	class	mass*	^{26}Al†
ALH76008	H6	281.3	11±1	ALH77131	H6	25.9	86±11	ALH81101	URE	119.2	35±2
ALH77026	L6	20.3	17±9	ALH78027	H5	29.2	78±8	ALH82106	URE	35.1	63±4
ALH77111	H6	52.3	20±7	ALH78080	H5	24.8	74±7	ALH82130	URE	44.6	62±5
ALH77174	H5	32.4	25±12	ALH78141	H5	24.1	75±8	ALH84136	URE	83.5	77±7
ALH77175	L3	23.3	24±14	ALH79036	H5	20.2	117±7	EET83225	URE	44.0	54±4
ALH77258	H6	597.3	29±2	ALH80126	H6	34.5	76±8				
ALH77278	LL3	312.9	28±3	ALH81099	L6	151.6	80±4				
ALH78153	LL6	151.7	22±1	MET78019	H6	91.1	108±6				
ALH83002	L5	367.1	28±1	OTT80301	H3	35.5	82±3				
ALH84080	L6	286.8	26±1								

* recovered mass in g †dpm/kg

ON THE ORIGIN OF TRAPPED NOBLE GASES IN METEORITES; J. F. Wacker, Battelle-Pacific Northwest Laboratories, P.O. Box 999, Richland, WA 99352

Chondritic meteorites contain a variety of trapped noble gas components that are carried mainly by elemental carbon [1]. Most of the gas is isotopically normal but elementally fractionated, with lighter gases progressively depleted by up to 10^{-6} relative to solar abundances. This component, often called "planetary" due to its similarity to noble gases found in planetary atmospheres, itself is complex, having at least five subcomponents [1]. Trapped noble gas components can provide important information about the conditions during the formation of the solar system, but knowledge about trapping mechanisms is needed to properly interpret the data.

Results of experimental studies of the sorption of Ne, Ar, Kr, and Xe by elemental carbon have been recently reported [2]. Elemental carbon (*e.g.*, carbon black) traps substantial amounts of tightly sorbed gas (defined as gas remaining after pumping for 24 hrs) upon exposure to noble gases. The temperature dependence of tightly sorbed gas on carbon black yields apparent heats of adsorption (ΔH) in the range for physical adsorption (-2 to -8 kcal/mole). Both the ΔH's and elemental fractionation patterns match those obtained from equilibrium-type experiments, where the sorbed phase is measured during solid/gas equilibrium. Nevertheless, the sorption behavior depends strongly upon the type of carbon and its heat treatment. Surprisingly, most samples trapped large amounts of Ne, implying significant solubility of Ne at 23°C.

The new results corroborate the "labyrinth" model of [3] and [4], which describes trapping of gases by physical adsorption on interior surfaces within amorphous carbons to account for the paradoxical properties of planetary noble gases (*e.g.*, phase **Q**): surface-siting and high retentivity. The interior surfaces are formed by a network of pores with atomic dimension (the pore labyrinth). The new data for Ar, Kr, and Xe show that 1) the adsorption/desorption times are controlled by choke points that restrict the movement of noble gas atoms within the pore labyrinth, and 2) the temperature behavior and elemental fractionation patterns are controlled by physical adsorption. Ne, and by analogy He, are trapped by solubility.

These results strongly support the hypothesis that surface-sited planetary components (*e.g.*, phase **Q** and polymer) are trapped by physical adsorption on interior surfaces of carbon grains. The elemental fractionations produced between 300 and 400 K in the laboratory match those observed for phase **Q**, implying a solar nebular origin for **Q**. The planetary component found in ureilites is volume-sited, but the elemental patterns and Xe/C ratio are indicative of initial trapping by adsorption, as suggested by [5], followed by processing to convert a surface-sited component into a volume-sited one. Such a conversion process also has implications for Xe-HL and its associated He-Kr, a volume-sited component carried by diamonds [6]. Xe-HL could have been trapped by adsorption since its elemental pattern is enriched in heavy gases [7], and no comparable amounts of the neighboring barium isotopes accompany the xenon [8], as would be expected if trapping occurred by ion implantation [9]. Although complications arise in explaining the low $^{129}Xe/^{132}Xe$ ratio of Xe-HL [9], the adsorption model is attractive as it avoids some of the pitfalls of ion implantation.

Adsorption apparently played an important role in the trapping of noble gases in the early solar system and in pre-solar environments. The labyrinth model accounts for many of the elemental and retentivity features of noble gases in meteorites. Furthermore, the model provides a framework for designing laboratory experiments to address questions posed by isotopic structures and concentrations of meteoritic noble gases.

[1] Tang M. and Anders E. (1988) *Geochim. Cosmochim. Acta* **52**, 1245-1254. [2] J.F. Wacker (1989) *Geochim. Cosmochim Acta*, in press. [3] Wacker J.F., Zadnik M.G. and Anders E. (1985) *Geochim. Cosmochim. Acta* **49**, 1035-1048. [4] Zadnik M.G., Wacker J.F. and Lewis R.S. (1985) *Geochim. Cosmochim. Acta* **49**, 1049-1059. [5] Ott U., Löhr H.P. and Begemann F. (1985) *Lunar Planet. Sci. XVI*, 639-640. [6] Lewis R.S., Tang M., Wacker J.F., Anders E. and Steel E. (1987) *Nature* **326**, 160-162. [7] Lewis R.S., Srinivasan B. and Anders E. (1975) *Science* **190**, 1251-1261. [8] Lewis R.S., Anders E., Shimamura T. and Lugmair G.W. (1983) *Science* **222**, 1013-1015. [9] Lewis R.S. and Anders E. (1981) *Astrophys. J.* **247**, 1122-1124.

VOLATILE/MOBILE TRACE ELEMENTS IN ANGRITES, M.-S. Wang and M. E. Lipschutz, Dept. of Chemistry, Purdue Univ., W. Lafayette, IN 47907.

Until the discovery of LEW 86010, Angra dos Reis (ADOR) was the only known angrite: these 2 have now been joined by LEW 87051. Only ADOR has been studied previously: it is an early basaltic achondrite with one of the least radiogenic initial $^{87}Sr/^{86}Sr$ ratios [1]. Howardite, eucrite and diogenite (HED) achondrites may be about as ancient as ADOR but exhibit much more complicated chronologies (e.g. [2-6]).

As part of the Angrite Consortium led by G. McKay to study ADOR and LEW 86010, we are carrying out RNAA determinations of Ag, Au, Bi, Cd, Co, Cs, Ga, In, Rb, Sb, Se, Te, Tl, U and Zn. Our results, while incomplete at the time of abstract submission, indicate that the thermal history of the angrites is rather different from that of HED meteorites or lunar samples. Both angrites have rather similar lithophile element contents, lower than in HED meteorites and lunar samples. For the remaining elements analyzed to date, contents in LEW 86010 are significantly lower than those in ADOR and generally lower than those in other extraterrestrial basalts. Tentatively, it appears that during formation of angrite parent material, separation of volatiles was more complete than during formation of other extraterrestrial basalts and/or post-formation volatile addition was minimal.

Reference

[1] G. J. Wasserburg, F. Tera, D. Papanostassiou and J. C. Huneke (1977) Isotopic and chemical investigations on Angra dos Reis. Earth Planet. Sci. Lett. 35, 294-316.

[2] R. L. Paul, R. O. Sack, H. Kruse and M. E. Lipschutz (1988) Simple and non-so-simple mixing in the howardite-eucrite-diogenite (HED) parent body (abstr.). Meteoritics 23, 296

[3] M.-S. Wang, R. L. Paul and M. E. Lipschutz (1989) Volatile/mobile trace elements in Bholghati howardite. Geochim. Cosmochim. Acta, in preparation.

[4] T. D. Swindle, C. M. Hohenberg, R. Nichols and C. T. Olinger (1989) Parentless fission xenon in the meteorite Bholghati? (abstr.). Lunar Planet. Sci. XX, 1095-1096.

[5] L. Nyquist, H. Wiesmann, B. Bansal and C.-Y. Shieh (1989) Rb-Sr age of an eucrite clast in the Bholghati howardite and initial Sr composition of the Lewis Cliff 86010 angrite (abstr.). Lunar Planet. Sci. XX, 798-799.

[6] D. D. Bogard and D. H. Garrison (1989) ^{39}Ar-^{40}Ar ages of eucrites: Did the HED parent body experience a long period of thermal events due to major impacts? (abstr.). Lunar Planet. Sci. XX, 90-91.

GEOCHEMISTRY OF SEVEN UREILITES: THE CASE OF THE MISSING ALUMINUM

Paul H. Warren and Gregory W. Kallemeyn
Institute of Geophysics and Planetary Physics, University of California, Los Angeles, CA 90024, USA

We have analyzed seven Antarctic ureilites (ALHA77257, ALHA78262, ALHA81101, ALH84136, MET78008, PCA82506, and RKPA80239) by INAA. Most had never been analyzed before. Our high-precision results for Al are consistently low, compared to an average of literature data for all ureilites. The mean of our 7 results is 1.30±46 mg/g; they range from 0.84 mg/g (ALHA77257) to 2.33 mg/g (MET78008). For comparison, the mean of all previous analyses for "monomict" ureilites (pre-averaged for each of 13 samples) is 2.56 mg/g. With our new results added to the data base, this mean shifts to 2.19 mg/g (for 19 samples). Weathering is probably not a problem with our data, because many of the highest literature values are for Antarctic ureilites. We also note that all unusually high Al results in ureilites are based on wet-chemical analysis. If wet-chemistry data are excluded from the present data base, the mean for 15 "monomict" ureilites shifts to 1.44 mg/g — and our new data appear quite normal. The oxygen-isotopic results of Clayton and Mayeda [1988; *Geochimica*] prove that ureilites did not form by igneous fractionation from a common batch of matter. However, the uniformly low Al contents of "monomict" ureilites are difficult to explain by models invoking derivation from one (or worse, more than one) small, little-differentiated asteroid. Ureilite genesis involved some process that resulted in a remarkably clean separation of basaltic matter from ultramafic matter, such that even the polymict ureilites contain only 2.3-3.7 mg/g of Al. We [Warren and Kallemeyn, 1988; *LPS XIX*] suggest that this process was a giant impact, which simultaneously enriched the ultramafic (ureilitic) portion of the parent asteroid in carbon, ^{16}O, and noble gases.

None of our analyses shows the light REE enrichment found among several of the first REE analyses of ureilites. MET78008 has the highest contents of heavy REE (Yb = 84±12 ng/g, Lu = 32±6 ng/g) of any known ureilite. Presumably these unusual HREE concentrations are linked to the exceptionally high-Ca nature of the MET78008 pyroxenes [Takeda et al., 1988; *Proc. Symp. Antarctic Meteorites*]. With our results added to the literature data base, the mean chondrite-normalized bulk-rock Lu/Sm ratio for "monomict" ureilites is 5.3, whereas La/Sm is only 2.0. We find that ALH84136 has an unprecedentedly low Fe/Mn ratio (17.5), which is consistent with a correlation previously noted [Takeda, 1988; *EPSL*] between Mn/Fe and the *mg* ratio of ureilite mafic silicates.

Clayton and Mayeda [1988] showed a plot of wt% carbon (literature data) vs. $\Delta^{17}O$, manifesting little correlation; and concluded that the carbon must be "indigenous to the rocks, not injected later." However, we still think it possible that most of the carbon was added by a giant impact. Data for carbon in ureilites show tremendous scatter, even for single ureilites; presumably due to real heterogeneities. Based on a more extensive compilation of literature carbon data, we find a fairly strong anticorrelation between C and $\Delta^{17}O$. The only samples that fall well away from the regression line are North Haig, which is polymict, and Dyalpur. However, if in place of C we plot concentration of noble gases in pure-carbon residue samples [data mainly from Göbel et al., 1978; *JGR*], a similar anticorrelation is found, except with Dyalpur on the opposite side of the regression line. Clearly, more data for $\Delta^{17}O$, carbon, and noble gases are needed.

CHONDRULE MAGNETIC PROPERTIES.

P. J. Wasilewski, Code 691 - NASA/Goddard Space Flight Center

Thermomagnetic curves (left figure), saturation remanence (SIRM) alternating field demagnetization curves (top right) and SIRM backfield demagnetization curves (bottom right) are used to evaluate the magnetic character of chondrules from the indicated meteorites. Thermomagnetic curves suggest that chondrules from a given meteorite are similar indicating similar magnetic phase relations. Chondrules from different meteorites have dissimilar thermomagnetic curves suggesting distinctive magnetic phase relations for each meteorite. Demagnetization curves indicate a broad range of magnetic hardness. The dominant magnetically hard component in the chondrules is tetrataenite. Magnetic techniques appear to be useful for characterization and classification of the chondrules.

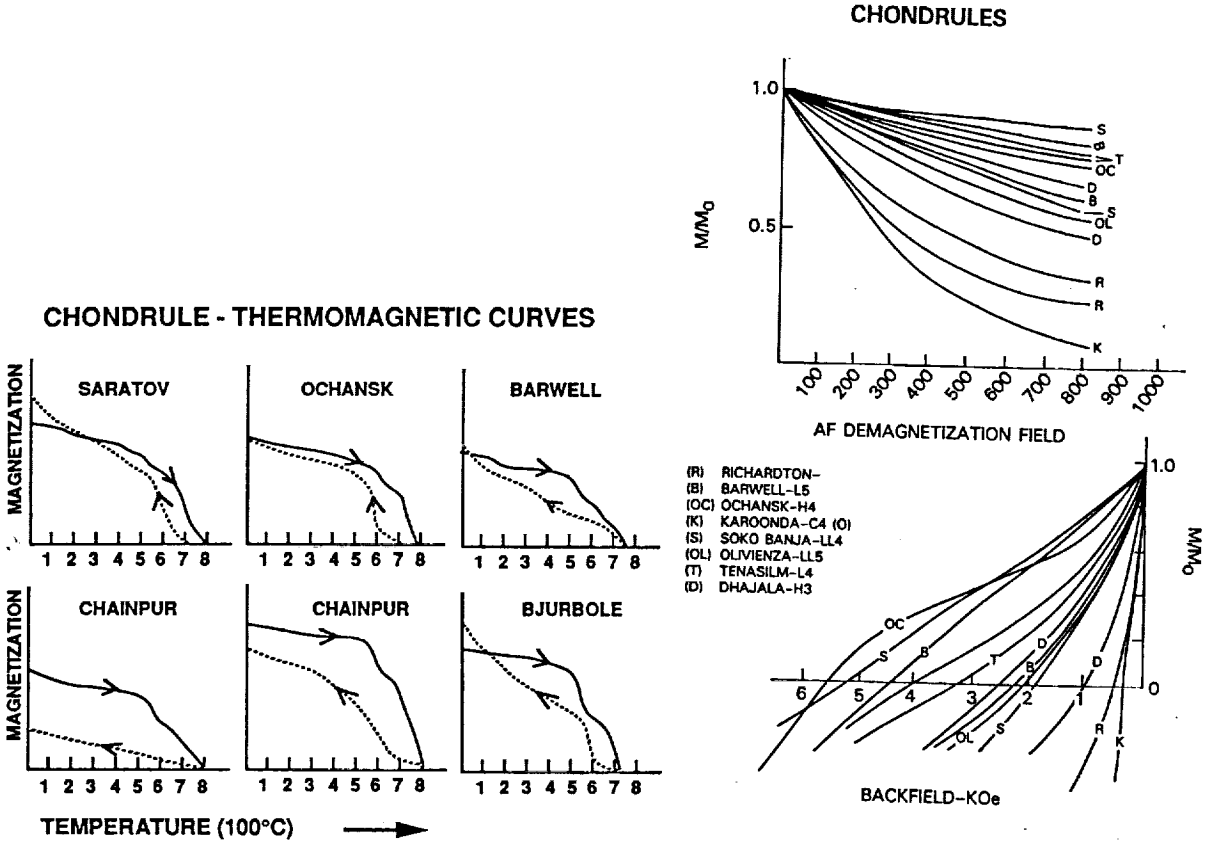

THERMOMAGNETIC CHARACTERIZATION OF METEORITES.

P. J. Wasilewski, Code 691 – NASA/Goddard Space Flight Center

Measurement of saturation magnetization (M_S) as a function of temperature gives us a Curie point curve or what is referred to as a thermomagnetic curve. Normally this experiment is done using an applied magnetic field of the order of 0.2 Telsa or greater, the field magnitude is not critical. The purpose of the experiment is to identify the magnetic phases; irreversibility between the heating and cooling curves being associated with redox effects or thermal decomposition eg. of $\gamma Fe_2O_3 \rightarrow \alpha Fe_2O_3$. In FeNi alloys most notably in meteorites we must contend with Martensite (M_S)–Austenite (A_S) irreversibility in kamacite; with order–disorder in tetrataenite/taenite; and with chemical gradients and thermal metastability in the cloudy zone. Additionally the applied magnetic field is critical because of the magnetization–field dependence contrasts between tetrataenite and taenite. In many cases it is necessary to cycle the specimen to cryogenic temperatures to achieve an adequate understanding of the magnetic phase relations.

Thermomagnetic characterization is effective with individual metal grains, chondrules, or other specific components in chondrite meteorites. During the thermomagnetic analysis, the heating or cooling might be interupted for a few minutes at any temperature and a magnetic hysteresis loop produced. This will allow composition and structure sensitive parameterization of the magnetic phase relations and thereby suggest the nature of thermally induced changes when heating and cooling data are compared. Stepwise experiments are conducted in order to resolve the contribution of the tetrataenite→taenite order/disorder to the total thermomagnetic behavior, and to resolve thermally induced magnetic phase modifications in the cloudy zone.

Though considerable work remains to be done, we have at present an outline for thermomagnetic procedures.

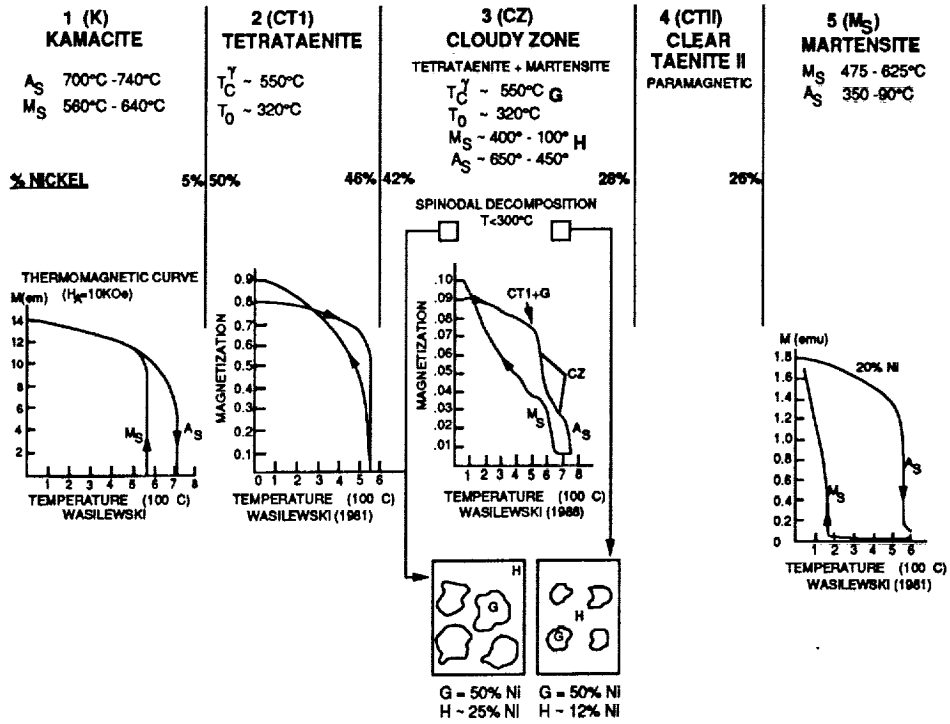

CLIMATE AND TEKTITE ORIGIN; John T. Wasson, Institute of Geophysics and Planetary Physics, University of California, Los Angeles, CA 90024, USA

Only four tektite fields are recognized to have been formed during the past 40 Ma of earth history, a surprisingly small number. A possible explanation is that large craters are required, but the cratering rate estimated by Wetherill and Shoemaker (1982) shows that 120 craters with diameters ≥10 km should have formed on the continents during this period. Perhaps 100 of these were in regions with sedimentary deposits ≥10 m thick. There appears to be nothing in the mechanics of crater formation that implies that tektitic melt should not be formed in craters as small as 1 km, but the distribution of tektites over distances larger than a few crater radii requires the local deposition of enough energy to push the ejecta cloud through the Earth's atmosphere.

Why did 100 large (and many more smaller) craters produce only four tektite fields? Why do the Arizona crater and other well preserved craters in suitable sedimentary materials not have associated tektites? Even allowing for incomplete preservation, the conclusion seems inevitable that tektite formation requires very special conditions, either special kinds of projectiles or special properties in the target. The latter seems more likely to be the deciding factor.

What sorts of target materials are most suitable for generating large amounts of melt more-or-less free of unmelted crystals? During impact the fraction of melt is maximum in targets that are porous, fine-grained and dry. Ideal targets are thick (≥5 m) deposits of aeolian dust such as loess. Such deposits are widespread on the continents during periods when the climate is cold and dry, and strong winds are associated with the large equator-pole temperature gradients. Loess was deposited in SE Asia during the most recent ice age.

Several authors have mentioned loess as a possible target material melted to produce the Australasian tektites. Glass showed that relict grains have sizes and shapes characteristic of loess, and Taylor noted the close compositional relationship to Nanjing loess. In a recent paper Barnes summarized the evidence and strongly endorsed loess as a precursor material for these tektites.

I propose to carry this conclusion a step farther and propose that it is not just the Australasian tektites that were formed in loess, but that similarly dry and porous targets are required to produce the large ratio of melt to unmelted materials observed in tektites. According to this picture tektites can only be formed when climatic conditions are suitable for producing such layers of aeolian dust. Because dry, porous deposits are generally within a few tens of m of the surface, weak objects that break up and rain down over an extensive area may be more efficient at producing tektites than are strong, compact objects that make a single crater.

EXPOSURE AGES OF H4-CHONDRITE FALLS; H. W. Weber, L. Schultz and F. Begemann, Max-Planck-Institut für Chemie, D-6500 Mainz FRG.

About 45% of all H-group chondrites have cosmic ray exposure ages which cluster around 7 My. This is generally interpreted to reflect a major collisional event which, at that time, broke up a considerable part of the H-group chondrite parent body. The fact that this exposure age peak contains all petrological-chemical groups it is taken as an argument for a parent body of H-chondrites which was fragmented and reassembled into a megabreccia (see e.g. [1]). The strength of this argument rests on the assumption that the peak records one event only. This is hard to verify from the existing exposure age data because many of them are based on noble gases measured more than 20 years ago. At that time instrumental fractionation as well as background corrections for atmospheric Ne were based on $^{20}Ne/^{22}Ne = 10.3$ rather than the present 9.8 [2] which leads to considerable uncertainties, in particular of the cosmogenic $^{22}Ne/^{21}Ne$. This ratio is then used for shielding corrections of the ^{21}Ne production rate and hence affects the calculated cosmic ray exposure age.

To extend and improve the existing data base we have measured the noble gases in more than half of the 44 reported H4-chondrite falls. Exposure ages are calculated from cosmogenic ^{3}He, ^{21}Ne and ^{38}Ar using $^{22}Ne/^{21}Ne$ as a parameter for shielding corrections. The exposure age distribution of H4-falls will be presented and compared with that of H-falls to see whether there is any evidence in the exposure age distributions or in correlations between trapped and radiogenic gases that different parent bodies exist for the individual petrological-chemical groups.

References: [1] J.Crabb and L.Schultz, Geochim.Cosmochim.Acta 45, 2151, 1981. [2] P. Eberhardt et al., Z. Naturf. 20a, 623, 1966.

Chemical Fractionation of Primitive Meteorites

Gerd Weckwerth, Max-Planck-Institut f. Chemie, Saarstr. 23, D-6500 Mainz, Germany

The variation of the chemical composition of Chondrites is mainly defined by condensation- and volatilization processes in the early solar nebula. Therefore the fractionation of the elements depend strongly on their volatility, which can be approximately described by the condensation temperature. To find specific fractionation parameters of the different chondrite groups, C1-normalized concentrations have been studied as function of the respective condensation temperatures.
With the exception of enstatite chondrites (E3,E4) the most refractory elements are unfractionated and show the highest abundances relative to C1-Chondrites. Their concentrations can be approximated with a horizontal line. The depletion of more volatile elements increases almost exponentially with the condensation temperature. The logarithmic concentration values have been approximated by a slope-line. The starting point of the slope, its steepness and the average concentration of the refractory elements have been the approximation parameters of the used regression.
The results show, that the starting point is fixed for carbonaceous chondrites at a condensation temperature between 1400 and 1500 K and for the ordinary chondrites at around 1200 K. A characteristic of ordinary chondrites are also the anomalous concentrations of Si, Mg and the alkaline elements, what seems to be rather a consequence of a mineralogical fractionation, independent from the volatility.
The slope is almost constant over all types of ordinary chondrites with the exception of highly volatile elements with a condensation temperature below 600 K. These elements show an additional depletion in the higher types of ordinary chondrites. For carbonaceous chondrites the regression yield high correlation coefficients, showing that their abundances fulfil the used model very well. Only a few exceptions of deviating concentrations of elements have been found, which should be not due to the measurements (Na, K, Br in C2). A more global deviation is the changing of the slope starting at 1100 K from a slope more similar to C2 to a slopes similar to the only real C4 meteorite, Coolidge. Other carbonaceous chondrites classified petrologically as C4, C5 or C6 are chemically only subtypes of C3, with an additional depletion of the highly volatile elements. The increase of the average content of refractory elements from C2 to C4 is correlated with the increase of the steepness found for the volatile elements. Higher content of refractory elements should be only a consequence of the relative deficit of main elements (Mg, Si, Fe, S, C, H_2O) giving a possibility of recalculating the original water content.
A comparison with primitive mantle material of planetary bodies (only lithophile elements) shows that earth and moon belongs to the material with high starting point of the slope and EPB, SPB and the Earth/Moon-ratio belong to a fractionation starting with a condensation temperature of around 1200 K. The condensation temperatures of the main elements Mg, Si and Fe lie in the middle of the starting points of these two groups. This implies that the fractionation with higher starting point derived from condensation processes and those with the lower starting point from volatilization processes during heating up to that temperature.

OXYGEN-ISOTOPIC COMPOSITIONS OF ALLENDE OLIVINES. S. Weinbruch[1+2], E.K. Zinner[1], I.M. Steele[3], A. El Goresy[2], and H. Palme[4]. [1] McDonnell Center for the Space Sciences and Physics Department, Washington University, St.Louis, MO 63130, USA, [2] Max-Planck-Institut für Kernphysik, P.O. Box 103980, D-6900 Heidelberg, FRG, [3] Department of Geophysical Sciences, University of Chicago, 5734 S. Ellis Ave., Chicago, IL 60637, USA, [4] Max-Planck-Institut für Chemie, Saarstr. 23, D-6500 Mainz, FRG.

Ion microprobe determinations of the oxygen-isotopic composition have been made on individual Allende olivines including 1) forsteritic core and fayalitic rim of two isolated grains; 2) core and rim samples from a compact granular olivine chondrule; 3) surrounding matrix grains; 4) three blue-luminescing grains of uncertain textural association. The analytical technique is described by McKeegan (1987). Terrestrial mantle olivine and Burma Spinel were used as isotopic standards.
These data show (see also Figure):
1) Mg-rich cores (1.5-20 wt.% FeO) of the two zoned single grains are enriched in ^{16}O with respect to Fe-rich rims (26-36 wt.% FeO). These data lie within error on the slope unity Allende mixing line.
2) A similar pattern is seen for the chondrule samples. Again, the Mg-rich interiors of individual grains (3-13 wt.% FeO) are more enriched in ^{16}O than their fayalitic rims (26-33 wt.% FeO), but the mean value of the forsterites lies above the mixing line. The Fe-rich rims show a large scatter, probably resulting from the sampling of rim material from the outer and inner part of the chondrule.
3) While most matrix olivines have oxygen compositions similar to the Fe-rich rims, about 10 % show much larger ^{16}O-enrichments, exceeding even that of the forsteritic cores. The most ^{16}O-rich grains are shown in Fig. 1.
4) The three blue-luminescing grains (FeO < 0.5 wt.%) show O-isotopic compositions similar to the Mg-rich core olivine of the single grains.
The O-isotopic pattern of forsteritic cores and fayalitic rims can be interpreted as the result of partial equilibration of originally ^{16}O-rich olivine with an isotopically normal reservoir. Unfortunately, the mechanism and timing of this process is not obvious. The partial equilibration of originally ^{16}O-rich forsterite with the same reservoir also occured for olivines from the fractionated Allende inclusion TE (Zinner et al., 1989). The essentially identical O-isotopic composition of relict forsterite grains and more iron-rich forsterites may indicate that these two different types of forsterites formed in the same isotopic environment. On the other hand, because forsterite from TE must have formed in a more ^{16}O-rich environment (Zinner et al., 1989), it cannot be excluded that the forsterites described above were more enriched in ^{16}O and have equilibrated to their present O-isotopic composition. The ^{16}O-rich matrix olivines indicate that at least some of the matrix formed in the same isotopic environment as the Mg-rich grains in spite of their distinct minor and major element chemistry (see also Weinbruch et al., 1989).
Ref.: McKeegan K.D. (1987) Science 237, 1468. Weinbruch S. et al. (1989) LPS XX, 1187. Zinner E.K. et al. (this volume).
Fig. 1: Oxygen-isotopic composition of Allende olivines (mean values except for matrix olivines).

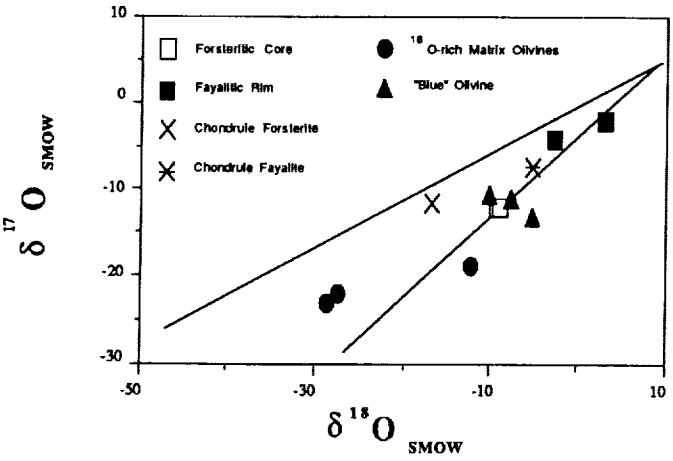

THE RENAZZO-TYPE CR CHONDRITES. M.K. Weisberg[1,2], M. Prinz[1], R.N. Clayton[3] and T.K. Mayeda[3]. (1) Amer. Mus. Nat. Hist., NY, NY 10024 (2) Brooklyn College, CUNY, B'klyn, NY 11210 (3) Enrico Fermi Institute, University of Chicago, Chicago, IL 60637.

The Renazzo-type CR chondrites are important for several reasons. Their FeNi metal records a primitive nebular condensation event [1]. Renazzo has a ^{15}N-rich component which may also be the result of early nebular processes [2, 3, 4]. CR chondrite matrix has some petrologic and oxygen isotopic similarities to CI chondrites [5, 6, 7], also indicative of primitive processes. CR chondrites exhibit multi-layer rimming which has important implications for chondrule forming processes [8]. The CR chondrites appear to be closely related to other important primitive meteorites (which are anhydrous); i.e., ALH85085 and Bencubbin/Weatherford [1]. In this study we present petrologic and oxygen isotopic data on four Renazzo-type chondrites (Renazzo, Al Rais, Y790112, Y793495) in order to better characterize the CR group and its implications in understanding nebular processes. These are the first results of a comprehensive study of this unusual group. Components of the CR chondrites include: (1) chondrules, (2) CAI's, (3) AOA's (amoeboid olivine aggregates), (4) DI's (dark inclusions), and (5) matrix. **CHONDRULES** make up 40-60 vol.%, are up to 2 mm across, with most from 0.5 - 1.5 mm, and exhibit subtle elongation and lineation. Many are FeNi metal-rich (3-6 vol.%, some up to 20%) and most are rimmed by layers and multi-layers of ol, pyx, hydrous silicates and FeNi metal. Most chondrules (>90%) are type I, the rest are type II. Chondrule rims are generally finer grained than cores and systematic compositional changes are observed from core to rim. Core ol has slightly higher MgO and CaO (up to 0.6%); FeO, MnO and Cr_2O_3 (up to 0.8%) are higher in rim ol. Both cores and rims contain hydrous silicates, but rims have higher abundances. Hydrous silicates also occur as brown glassy spheres on chondrule rims and as isolated spheres in the matrix. FeNi metal in cores is generally more Ni-rich (~7-12%) than FeNi in rims (~5-6%). Therefore, if FeNi metal is a condensation product [1], rim metal condensed later, and at a lower temperature than core metal. Preliminary results on the oxygen isotopic compositions of chondrules show that they are similar to whole rock, and overlap with those from CV3 chondrites. However, further work is being carried out on a larger population of chondrules in order to better define their oxygen isotopic characteristics. **CAI's** are relatively rare in CR chondrites. They are irregularly shaped and most are up to 1 mm in maximum dimension. Preliminary results indicate two types. One consists of Mg-Al spinel with perovskite inclusions, with the spinel rimmed by a fine band of diopside with an interlayer of Fe-rich phyllosilicates. Similar inclusions have been described in CM chondrites [9]. The other type consists almost entirely of melilite with trace amounts of Mg-Al spinel. Melilite is close to the gehlenite endmember having 40% CaO and 4% MgO. **AOA's** are also found, and these contain calcite intermixed with the ol ($Fo_{\sim 98}$). **FeNi METAL** is compositionally similar in all four meteorites, and the FeNi metal has a positive Ni vs. Co trend which overlaps with calculated nebular condensation paths. FeNi metal in ALH85085 and Bencubbin/Weatherford is similar [1]. **MATRIX** contains anhydrous and hydrous silicates, angular fragments of calcite, blades of sulfide and magnetite framboids and platelets similar to those in CI chondrites. In some cases magnetite framboids occur in clusters containing spheres of variable size. The bulk composition of the CR matrix has higher volatiles (Na, K, and S) and higher Fe/Mg than that of the whole rock. Matrix oxygen isotopic compositions lie on the terrestrial mass fraction line relatively close to the CI chondrites. **DI's** are similar to those described in CV3 chondrites [10]. These clasts contain chondrule-like objects and CAIs, but on a much finer scale (50 - 100μm) than those in the host chondrites. The DI matrix is opaque and contains features similar to those of the host CR matrix, including magnetite framboids and hydrous silicates. The bulk compositions of the DI's are similar to those of the host CR matrix; in many cases the boundary between DI and host matrix is unclear. **CONCLUSIONS:** (1) CR chondrites have similar petrologic and oxygen isotopic characteristics which are unique to this group, and should be distinguished from all other carbonaceous chondrite groups. (2) CR chondrites contain a variety of highly primitive components in terms of nebular history. These include FeNi metal, ^{15}N, CAI's, AOA's, DI's, and C1-like matrix. (3) Dark inclusions in CR chondrites are analogous to those in CV3 chondrites, and record a preaccretionary chondritic component which has experienced a replacement process, probably with a oxidizing nebular gas..

REFERENCES: [1] Weisberg et al. (1988) EPSL 91, 19-32. [2] Kung, C. and Clayton, R.N. (1978) EPSL 38. [3] Robert, F. and Epstein, S. (1982) GCA 46, 81-95. [4] Prombo, C.A. and Clayton, R.N. (1985) Science 323, 935-937. [5] Fredriksson et al. (1981) Meteoritics 16, 316. [6] Clayton, R.N. and Mayeda, T.K. (1977) LPSC VIII, 193-195. [7] Kallemeyn, G.W. and Wasson, J.T. (1982) GCA 46, 2217-2228. [8] Prinz et al. (1985) LPSC 16, 677-678. [9] MacPherson et al. (1988) In: Meteorites and the Early Solar System, 746-807. [10] Johnson, C.A. et al. (1989) LPSC XX, 468-469.

A NON-EQUILIBRIUM ISOTOPIC FRACTIONATION: THERMAL DECOMPOSITION OF OZONE; Jun-Shan Wen and Mark H. Thiemens, Chemistry Dept., B-017, University of California, San Diego, La Jolla, California 92093-0317

It is well known both theoretically and experimentally that chemical equilibrium or diffusional processes normally result in mass dependent isotopic fractionations, which define a line with a slope of ~0.5 for $\delta^{17}O/\delta^{18}O$. However, recent measurements, most of them gas phase or non-equilibrium processes, have demonstrated a wide variety of fractionations which did not obey the mass dependent pattern. Since gas phase reactions play an essential role in the early chemical history of the solar system, it is important to study the general isotopic fractionations in non-equilibrium gas phase reactions.

A series of thermal decomposition experiments of O_3 of known amount and isotopic composition were performed. Oxygen produced from 90°C ozone decomposition at ~ 60 torr pressure was collected and analyzed, as previously described (1).

The residual ozone was collected, separated and measured for yield, $\delta^{17}O$ and $\delta^{18}O$. At room temperature, O_3 decomposition produces isotopically light O_2 (~ 20‰ lighter in essentially a mass dependent fashion in $\delta^{18}O$ than the precursor O_3), as expected on the basis of differential isotopic vibrational frequencies (1). The present experiments, at 90°C, produce isotopically heavy oxygen, ~40‰ with respect to the O_3 initial, which is mass independently fractionated with $\delta^{17}O \cong \delta^{18}O$. A kinetic evaluation demonstrates that the gas phase rate constant for 90°C ozone decomposition is $\sim 2.6 \times 10^{-23}$ cm^3s^{-1}, essentially identical to literature values (2). Recycling to O_3, via $O + O_2$, is insignificant due to the slow kinetics for the experimental conditions. The product oxygen is derived from (a) $O_3 + \Delta \rightarrow O_2 + O$ and (b) $O + O_3 \rightarrow 2O_2$, and both must be considered in accounting for the observed fractionation. If the source of the anomalous fractionation were step (a), no existing theory successfully accounts for the observation, if (b), it may be that the transition state, [O··O··O··O] is subject to symmetry constraints, in which case, this is the first demonstration of a mass independent fractionation involving a 4-atom molecule transition state, though there is an insufficient theoretical framework for this type of process. Future experiments will be dedicated towards resolution of the source of the anomalous fractionation and reported.

These experiments, as well as those for $O + O_2$, $O + CO$ and $SF_5 + SF_5$, demonstrate that gas-phase mass independent fractionation may, in fact, be rather general and widespread. A well developed theoretical and experimental basis for non-equilibrium mass independent fractionations is needed. This is particularly true for meteoritics where meteoritic material may bear the isotopic signature for a wide variety of early gas phase processes.

References:

(1) Bhattacharya S. K. and Thiemens M. H. (1988) Geophys. Res. Lett., 15, 9-12.

(2) Benson S. W. and Axworthy A. E. Jr. (1957) J. Chem. Phys. 26, 1718-1726.

GLASSES IN LUNAR METEORITE Y82193: COMPARISONS TO APOLLO 16 FELDSPATHIC FRAGMENTAL AND REGOLITH BRECCIAS; S. J. Wentworth[1], D. S. McKay[2], and H. Takeda[3]; [1]Lockheed, 2400 NASA Rd. 1, Houston, TX 77058; [2]SN14, NASA Johnson Space Center, Houston, TX 77058; [3]Mineralogical Institute, Faculty of Science, University of Tokyo, Hongo, Tokyo 113, Japan.

Background All known lunar meteorites have been identified as regolith breccias. Meteorites Y82192 and Y82193 (a probable pair) contain little evidence of a regolith component [1,2,3] and may be more similar to Apollo 16 feldspathic fragmental breccias than to regolith breccias [4]. Apollo 16 feldspathic fragmental breccias are very similar to Apollo 16 regolith breccias, especially to the ancient (~4 Gy) regolith breccia suite [5,6], except that the feldspathic fragmental breccias do not contain an identifiable regolith component. Relationships among Apollo 16 feldspathic fragmental breccias, regolith breccias, and present-day soils are poorly understood. Perhaps feldspathic fragmental breccia material was a precursor to the ancient Apollo 16 regolith breccias [6]. Therefore, it is important to understand the relationship of lunar meteorites to feldspathic fragmental breccias and regolith breccias. For this study, we determined populations and compositions of glass clasts in polished thin section Y82193,91-1 by SEM and electron microprobe for comparison with glass data for Apollo 16 feldspathic fragmental breccia 67016, regolith breccias, and soils [6,7].

Results and Discussion Thin section Y82193,91-1 contains no homogeneous glass clasts; all glass clasts are at least partly recrystallized, and some are clast-bearing. Using our standard compositional classification [7], 80.6% of the 31 analyzed glasses are of highland basalt composition (i.e., feldspathic with Al_2O_3 > 23 wt%), 16.1% are LKFM (low-K Fra Mauro), and 3.2% are KREEPy. Similarities between glass populations of Y82193,91-1 and those of feldspathic fragmental breccia 67016 include the lack of homogeneous glasses, lack of mare glasses, and the predominance of glasses of highland basalt composition (78.3% of 67016 glasses). Differences include more glass clasts in Y82193 (only 23 were found in 8 thin sections of 67016), a trace of regolith-derived spherules in Y82193 not found in 67016, and a greater range of compositions for Y82193 glasses. In contrast to Y82193 and 67106, Apollo 16 regolith breccias and soils contain greater abundances of glass clasts, including significant amounts of KREEP glass. The glass data indicate that Y82193 is more similar to Apollo 16 feldspathic fragmental breccias than it is to even the most immature Apollo 16 regolith breccias. Differences between Y82193 and 67016 glass populations are consistent with other evidence that Y82193 did not come from an area near Apollo 16 and may have a farside origin [8]. Because Y82192 and Y82193 contain a small regolith component, these meteorites may be transitional between feldspathic fragmental breccias and true regolith breccias. Therefore, the meteorites may fill a sampling gap and be of key importance in understanding the history of the lunar highlands and its regolith.

References [1] Takeda et al. (1988) *Proc. LPSC 18th*, 33-43; [2] Bischoff et al. (1987) *Mem. Natl. Inst. Polar Res., Spec. Issue, 46*, 21-42; [3] Eugster and Niederman (1988) *EPSL 89*, 15-27; [4] Takeda et al. (1989) *LPS XX*, 1103-1104; [5] McKay et al. (1986) *Proc. LPSC 16th*, D207-D303; [6] Wentworth and McKay (1988) *LPS XIX*, 1263-1264; [7] Wentworth and McKay (1988) *Proc. LPSC 18th*, 67-77; [8] Warren and Kallemeyn (1988) *13th Symp. Antarctic Meteorites*, 12-14.

COMETARY CRATERING RATES ON THE TERRESTRIAL PLANETS;
G. W. Wetherill, DTM, Carnegie Institution of Washington, Washington, D.C. 20015

The larger terrestrial planet and lunar impact craters are produced by astronomically observable planet-crossing bodies. These bodies are derived from collisions in the main asteroid belt as well as from the sources of comets in the outermost solar system (35 – 10^5 A.U.). It has been shown that the asteroidal region probably supplies about 1/3 of the cratering flux, the remainder being cometary (Wetherill, 1989). Although the contribution from active comets is significant (Weissman et al. 1989) most of the impacting cometary population probably consists of extinct or at least dormant comets of asteroidal appearance, primarily in orbits only barely distinguishable statistically from those of Apollo-Amor objects of asteroidal origin.

These conclusions have been augmented by new Öpik-Arnold Monte Carlo calculations of the probability of gravitationally decoupling short-period comets from Jupiter's influence by close encounters with Earth and Venus. The probability of decoupling is found to be $\sim 3 \times 10^{-3}$. When combined with observational data on the observed number of active short period comets and the observed number of Apollo-Amors, a model of planetary cratering is obtained that is also consistent with the mass flux and orbital distribution of the survivable small-size end member Earth-crossing population, the meteorites.

Duncan et al. (1988) have shown by numerical integration that the orbital distribution of Jupiter family comets corresponds to that expected from an otherwise unobserved "Kuiper belt" of comets just beyond Neptune, and is inconsistent with the earlier hypothesis of capture of long-period Oort cloud comets by Jupiter. By use of more approximate Monte Carlo methods, this work has been extended to include the entire cometary source region. It is found that any highly flattened inclination distribution, such as may be expected to be found for cometary aphelia as large as $\sim$ 2000 A.U., is acceptable, but no isotropic distribution corresponding to derivation of short period comets by capture of an isotropic distribution from either the inner or outer Oort cloud at greater aphelia agrees with the observed orbital distribution of short period comets. This new work also suggests the speculation that the approximate factor of two discrepancy between the observed lunar and terrestrial cratering rates could be a stochastic effect of the most deeply penetrating passing star having perturbed the most distant portion of the inner non-isotropic region (aphelion $\sim$ 2000 A.U.) about 500 m.y. ago, supplying a moderate pulse of Neptune-crossing comets with dynamic lifetimes 10^8 – 10^9 years, that then slowly evolved into Jupiter family comets and Apollo objects.

REFERENCES:

Wetherill G. W. (1989) Cratering of the terrestrial planets by Apollo objects. In press, *Meteoritics.*

Weissman P. R., A'Hearn M. F., McFadden L. A., and Rickman H. (1989) Evolution of comets into asteroids. In press, *Asteroids II*, Univ. of Arizona Press.

Duncan M., Quinn T., and Tremaine S. D. (1988) Origin of short period comets. *Astrophys. J.* **328**, L69 - L73.

COARSE-GRAINED OLDHAMITE IN AN IGNEOUS CLAST IN THE NORTON COUNTY AUBRITE. M.M. Wheelock, K. Keil and G.J. Taylor, Dept. of Geology and Institute of Meteoritics, University of New Mexico, Albuquerque, NM 87131

A series of igneous clast lithologies in the Norton County aubrite have been interpreted as a fractional crystallization sequence [3,5]. A coarse-grained, igneous-textured sulfide+forsterite clast is described here, representing a new igneous lithology for the Norton County suite. The sulfide portion consists of a single euhedral crystal of oldhamite (2 cm diameter) containing 13 vol% of other sulfides and traces of metal (Table 1). Modal mineral composition is given in Table 1. The identification of oldhamite was confirmed by XRD analysis. Measured d-spacings (in order of decreasing intensity: 2.842, 2.011, 1.643, 1.279, 1.422A) agree well with published values for synthetic CaS [2]. Electron microprobe analyses were performed on all phases. The bulk composition of the clast (Table 2) was computed from the mode and measured compositions.

The textures of multi-phase inclusions in oldhamite suggest that this clast formed from an immiscible sulfide melt. Although it contains minute oriented alabandite inclusions, most larger inclusions are round, or have sweeping, curved boundaries; they contain up to five phases and are up to several mm in size. These inclusions apparently did not form by exsolution from oldhamite, but probably formed from trapped melt inclusions. The absence of silicate inclusions indicates that the sulfide melt separated from the silicate melt before crystallizing, supporting the immiscibility hypothesis. This texture also indicates that the oldhamite is of igneous origin and cannot be a refractory residue; if the oldhamite were a product of nebular condensation, it would not have grown around multi-phase blobs that contain low temperature sulfides (such as caswellsilverite, $NaCrS_2$). The following sequence of events is proposed for the origin of this clast: (1) Immiscible sulfide melt formed in the silicate magma. (2) Oldhamite began to crystallize, taking up all the Ca and some Mg and Mn. Since oldhamite can accommodate very little Fe [4], Fe and other elements were concentrated in the residual melt. (3) The remaining (Fe,Mg,Mn,Na,Cr,Ti,Ni)S melt was trapped in melt pockets inside the growing oldhamite crystal. (4) Melt inclusions crystallized to form: FeNi metal, Ti-bearing troilite, alabandite, daubreelite, and caswellsilverite. (5) As oldhamite cooled, it could no longer accommodate MgS+MnS in solid solution [4] and numerous tiny, euhedral alabandite crystals exsolved.

Recent analyses found REE enrichment (at about 100xCI) in oldhamite in the Bishopville aubrite [1]. In the aubrite parent magma, the following elements were concentrated in sulfide and metal phases: Fe,Ti,Na,Mg,Mn,Ni,Cr, REE and some Ca,Mg. Throughout most of Norton County's crystallization history, none of these elements behaved incompatibly. This complicates interpretation of the detailed crystallization history of the Norton County suite (chiefly pyroxenites), since traditional "incompatible"-element enrichment trends do not develop. One potentially useful minor element is Al, since it is incompatible in all minerals present (until plagioclase forms in the final stages). Progressive crystallization would cause progressive Al-enrichment in pyroxenes, providing evidence of the crystallization sequence of the pyroxenite lithologies. Hints of such Al enrichment were reported in [3].

TABLE 1.
MODAL COMPOSITION (vol%)

Oldhamite (CaS)	86.6
Alabandite (Mg,Mn,Fe)S	9.6
Troilite (Fe,Ti)S	2.2
Daubreelite ($FeCrS_2$)	.85
Caswellsilverite ($NaCrS_2$)	.65
Metal (FeNi)	tr

TABLE 2.
BULK COMPOSITION (wt%)

Na	0.16	Cr	0.7
Mg	2.1	Mn	4.1
S	43.9	Fe	4.6
Ca	44.5	Ni	0.02
Ti	0.04	TOTAL	100.1

REFERENCES: 1)Heavilon et al.(1989), Meteoritics 24. 2)Min. Powd. Diff. File, ICDD (1986). 3) Okada et al.(1988), Meteoritics 23:1, 59-74. 4)Skinner and Luce (1971), Am. Min. 56, 1269ff. 5) Taylor et al.(1988), LPSC 19, 1185ff.

PLANETARY NOBLE GASES IN NITRIC ACID-SOLUBLE FRACTIONS OF CARBONACEOUS CHONDRITES; **R. Wieler, H. Baur, P. Signer,** *ETH-Zürich, NO C61, 8092 Zürich, Switzerland*; **R. S. Lewis,** *Enrico Fermi Institute, University of Chicago, Chicago, IL 60637-1433 USA.*

In carbonaceous chondrites, most of the planetary Ar-Kr-Xe and also a minor fraction of the planetary He-Ne (the isotopically "normal" portion) are sited in phase "Q", defined as that part of an HF-HCl residue that loses its noble gases upon oxidation, e.g. treatment with HNO_3. Due to the elusive character of their carrier, Q-gases had to be inferred either by difference between untreated and oxidized residue or at best were partially isolated by stepwise heating. We now are able to study Q-gases by closed system stepwise etching of HF-HCl residues with HNO_3 [1].

Allende: A residue of this meteorite released upon HNO_3 oxidation more than 90% of its Ar-Kr-Xe as well as some 10% of the He-Ne [1], confirming earlier statements [2] that Q indeed contains a minor part of the light planetary noble gases. The isotopic composition of these trapped gases was virtually constant in all steps, proving that the HNO_3 treatment essentially tapped a single, distinct noble gas component. Q-Ne in Allende has $^{20}Ne/^{22}Ne = 10.65 \pm .15$ and $^{21}Ne/^{22}Ne \leq 0.0316$. This component and Ne-A2 in oxidized Allende residues [3] are not related by a simple mass fractionation process.

Murchison: As in Allende, closed system oxidation of a Murchison HF-HCl residue released besides the major fraction of the heavy planetary gases ($^{36}Ar/^{38}Ar = 5.33$, Kr-Xe approximately AVCC) also some of the planetary He-Ne. In the first step, a ratio $^{20}Ne/^{22}Ne = 10.3 \pm .2$ is observed, a value only slightly lower than that of Q-Ne in Allende. This confirms suggestions [4] that Q in Murchison contains a Ne component very similar to that in Allende, despite the fact that the $^{20}Ne/^{22}Ne$ ratio of the HNO_3-soluble part was inferred by difference to be 6.8 only [5]. In contrast to Allende, however, further etching resulted in the release of progressively lighter Ne, with $^{20}Ne/^{22}Ne$ ratios in the final steps slightly below the atmospheric value of 9.8. Probably this is due to a second major Ne component of lower 20/22 ratio (Ne-A of Pepin, or "polymer Ne" of [5]), but contributions of minor amounts of Ne-E cannot be ruled out.

Despite this ambiguity, the Murchison data confirm that Q-Ne is present not only in CV3 chondrites but in at least one other class of carbonaceous chondrites (CM2). Q-Ne is isotopically similar to planetary Ne in ureilites, suggesting that this component may be rather common in primitive meteorites [6].

Acknowledgements: Work supported by the Swiss National Science Foundation and NASA Grant NAG 9-52.

References: [1] Wieler R. *et al.*, (1989) *Lun. Planet. Sci.* **20**, 1201. [2] Lewis R. S. *et al.*, (1975) *Science* **190**, 1251. [3] Ott U. *et al.*, (1981) *Geochim. Cosmochim. Acta* **45**, 1751. [4] Alaerts L. *et al.* (1980) *Geochim. Cosmochim. Acta* **44**, 189. [5] Srinivasan B. *et al.*, (1977) *J. Geophys. Res.* **82**, 762. [6] Ott U. *et al.*, (1985) *Proc. Conf. Isotopic Ratios in the Solar System* (Paris), 129.

TWO NEW CM CHONDRITES FROM ANTARCTICA: DIFFERENT MINERALOGY, BUT SAME CHEMISTRY.

F. WLOTZKA, B. SPETTEL, H. PALME AND L. SCHULTZ,
Max-Planck-Institut fuer Chemie, Mainz.

Among the 199 meteorites found in 1988 in the Allan Hills by a German-American team were two small black stones,which looked different from the rest and turned out to be CM chondrites: ALH88045 (18g) and ALH88052 (7g).

Table 1:

	MUR aver.	ALHA 88045	ALHA 88052		MUR aver.	ALHA 88045	ALHA 88052
Fe %	21.22	20.10	19.98	Sc ppm	8.36	7.75	7.14
Ca %	1.31	0.80	0.83	La ppm	0.32	0.31	0.31
Cr ppm	3040	2940	2780	Sm ppm	0.21	0.22	0.20
Na ppm	1400-4230	4140	2900	Eu ppm	0.080	0.085	0.065
				Yb ppm	0.24	0.22	0.22
K ppm	250-350	455	300				
	moderately volatile			siderophile elements			
Au ppb	166	177	160	Ni %	1.40	1.25	1.29
Mn ppm	1580	1650	1560	Co ppm	571	553	541
As ppm	1.76	1.73	1.77	Os ppb	858	690	680
Ga ppm	7.61	8.43	7.86	Ir ppb	638	563	600
Se ppm	13.3	13.3	13.3	Re ppb	54	85	80
Zn ppm	176	194	176				

MUR-average: 3 Murchison samples

In Table 1 are listed preliminary INAA-results of the two new CM meteorites. An average of three Murchison samples analyses in this lab is given for comparison. Contents of moderately volatile elements are diagnostic for the various carbonaceous chondrites. The new CMs closely match the average Murchison in their contents of moderately volatile elements. The alkali elements are notoriously variable in carbonaceous chondrites. The new members are no exception. The only difference in chemistry to other CM-chondrites are the comparatively high Re contents of the new meteorites. The reason is unknown.

Despite their close match in chemistry the new CMs are quite different in their mineralogy. 88052 contains olivine and pyroxene in chondrules and fragments in the usual phyllosilicate matrix. Metal and coarser sulfides are rare. In 88045, on the other hand, no olivines or pyroxenes were found, it consists mainly of phyllosilicates, carbonates and rather coarse-grained sulfides. The rare sulfides in 88052 are pyrrhotite and pentlandite, 88045 contains in addition a K- and Cr-containing ironsulfide (2-3% K, 0.1-4% Cr, 18% Ni). Calcium carbonate was found in 88052 only in the center of an CAI, where it is surrounded by a layer of small perovskites and a mantle of spinel. In 88045 carbonates are more abundant; they occur in inclusions and aggregates, not in veins. Most of it is rather pure calcium carbonate, one inclusion contains $Na_2Ca(CO_3)_2$, nyerereite (note that 88045 has also a rather high bulk Na content).

It appears that 88045 is a highly altered CM, where most primary minerals were transformed into phyllosilicates, only Cr-spinel grains survived this alteration. 88045 also does not contain the Fe-S-O-Ni bearing PCP phases, which are found in 88052. Probably the massive Fe-sulfides in 88045 were formed from PCP by this alteration. This process was isochemical, as the similar bulk compositions of 88052 and 88045 show. The altered 88045 has a distinct texture with preferred orientation of altered inclusions and phyllosilicate aggregates, which indicates that the alteration took place under stress on a parent body.

CALCULATION OF MINERAL EQUILIBRIA IN THE NEBULA BY ENERGY-MINIMIZATION TECHNIQUES: J. A. Wood and A. Hashimoto, Harvard-Smithsonian Center for Astrophysics, Cambridge MA USA

Several energy-minimization techniques for determining equilibrium mineral assemblages are reviewed by [1]. We have tested two methods, those of White *et al.* [2] and Van Zeggeren and Storey (summarized in the Appendix of [3]). Both have problems, which will be discussed briefly.

An obstacle of long standing in exercises of this sort is the treatment of oxide components in the melt phase, under those conditions where a melt would be stable. We approximate the chemical potentials of these components by a method Hashimoto has developed, wherein the melt is considered to be an ideal mixture of magnesian, ferrous, and calcic liquids. The magnesian liquid is an ideal mixture of two binary liquids, MgO-SiO_2 and MgO-$AlO_{1.5}$; the ferrous liquid is an analogous system. The calcic liquid is a non-ideal mixture of the binary liquids CaO-SiO_2 and CaO-$AlO_{1.5}$. The literature provides information about the non-ideal behavior of the six binary systems.

Use of this approach in energy-minimization calculations predicts the occurrence of melts under plausible conditions, and the ranges of melt composition are also largely plausible. For example, when the condensation sequence is calculated for a system of cosmic composition except for H, which is 0.001x cosmic (corresponding to circumstances where nebular dust, ices, and organics settled to the midplane and concentrated to that degree before high-energy transient events created chondrules), melt phase is found to be stable between ~2200 and 1300K. Between 2200 and ~1900K, the melt consists mostly of Al_2O_3 and CaO, other oxides being mostly uncondensed. (Between ~2000 and 1820K, the melt coexists with melilite and spinel.) Below ~1900K, the melt composition evolves to an essentially normal gabbroic character. Below ~1500K the melt becomes increasingly ferrous, trending to an unrealistic ~85 wt. pct. FeO at 1300K.

References

1. Van Zeggeren, F., and Storey, S. H. (1970) *The Computation of Chemical Equilibria.* Cambridge Univ. Press.
2. White, W. B., Johnson, S. M., and Dantzig, G. B. (1958) Chemical equilibrium in complex mixtures. *J. Chem. Phys.* **28**, 751-755.
3. Wood, B. J. and Holloway, J. R. (1984) A thermodynamic model for subsolidus equilibria in the system CaO-MgO-Al_2O_3-SiO_2. *Geochim. Cosmochim. Acta* **48**, 159-176.

ISOTOPIC AND OPTICAL PROPERTIES OF LARGE INDIVIDUAL SiC CRYSTALS FROM THE MURCHISON CHONDRITE; B. Wopenka[1], A. Virag[1], E. Zinner[1], S. Amari[2], R. S. Lewis[2], and E. Anders[2]; [1]McDonnell Center for the Space Sciences and Physics Department, Washington University, St. Louis, MO 63130, USA; [2]Enrico Fermi Institute and Department of Chemistry, University of Chicago, Chicago, IL 60637, USA.

Single SiC crystals, being pure rather than mixtures, give direct clues to the isotopic composition of their parent stars (Tang *et al.*, 1989). A new separation of a large (88.2g) Murchison sample (Amari and Lewis, 1989) provided the opportunity to extend isotopic measurements to a larger statistical sample. 18 grains from 1×1.5 μm to 14×20 μm in size were extracted from separates LS and LU and analyzed in the ion microprobe for their C, N and Si isotopic compositions. Laser Raman microprobe spectra on 16 of these grains and 4 additional single grains from Murchison HO (Tang *et al.*, 1989) were also obtained to provide information on their crystal structures.

The C data confirm the previous observation that large crystals on the average have smaller ^{13}C excesses than fine-grained SiC from Murchison whose average is $\delta^{13}C \approx +1250$ ‰ (Tang *et al.*, 1988). The $\delta^{13}C$ in the LS + LU grains shows a curious distribution: 8 grains have $\delta^{13}C = 800$ to 900 ‰, 7 grains $\delta^{13}C = -50$ to 0 ‰ and only 3 lie outside these bands. While 2 of the latter have intermediate $\delta^{13}C$, the third has $\delta^{13}C = +28625 \pm 67$ (1σ) ‰, exceeding the highest previous value by 3×, corresponding to $^{12}C/^{13}C = 3.0$. This is close to the equilibrium ratio for the CNO cycle (Iben, 1975), but the $\delta^{15}N = +1690 \pm 106$ ‰ in this crystal is much too high and indicates a nova origin. With one exception, the two carbon groups separate rather well on a Si isotope plot (Fig. 1), heavy C correlating with heavy Si and "normal" C with "normal" Si. Besides the crystal with $\delta^{13}C = +28625$ ‰, only a second one shows heavy N ($\delta^{15}N = +96 \pm 34$ ‰), 3 are normal, and the others measured (11) are depleted in ^{15}N. It is interesting that normal C and Si compositions occur with substantial frequency. Since the grains studied are single crystals that could not have been formed in a solar gas, these compositions must reflect those of their stellar sources, not a fortuitous mixture from an interstellar cloud.

Including the HO samples, only 5 crystals have a triplet TO Raman line, indicative of a non-cubic (hexagonal, rhombic) crystal structure. It is remarkable that these 5 grains have isotopically normal C and Si. While a terrestrial contamination origin cannot be excluded for two grains with normal N, 3 of them show distinctly anomalous N isotopes. However, not all grains with this isotopic signature are non-cubic: the grain with $\delta^{15}N = +96$ ‰ has terrestrial C and Si but a single TO line, characteristic of cubic SiC. The SiC grains show a variety of morphologies, including surfaces with conchoidal fractures, smooth surfaces with cleavage features, euhedral forms, and fluffy appearance. All grains with conchoidal fracture surfaces are non-cubic but no other correlations can be established at this time.

References: Amari S. and Lewis R. S. (1989) This volume; Iben I., Jr. (1975) Ap. J. **196**, 525; Tang M. *et al.* (1988) LPS XIX, 1177; Tang M. *et al.* (1989) Nature, in press.

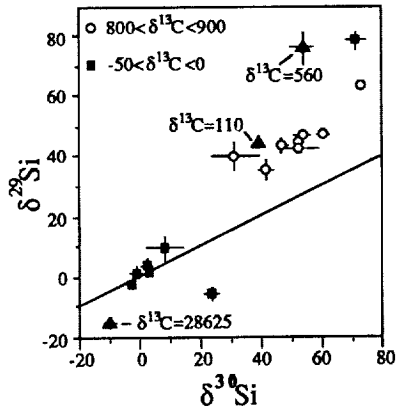

Fig. 1: Si isotopic compositions of 18 individual SiC grains from Murchison LS + LU.

C and N in LEW 86010; I.P.Wright, M.M.Grady and C.T.Pillinger, Planetary Sciences Unit, Department of Earth Sciences, The Open University, Milton Keynes, MK7 6AA, England.

Prinz *et al.* (1) have alluded to the possibility that, although exhibiting an igneous texture, the LEW 86010 meteorite may not be an achondrite. Indeed, this and other angrite materials (*i.e.* Angra dos Reis, and clasts in Nilpena and North Haig) appear to have affinities with type B CAI and the opaque matrices of unequilibrated ordinary chondrites. The melting which produced the igneous textures of angrites may have taken place in a nebular environment. In addition to the unusual nature of the mineralogy (*e.g.* fassaite, kirschteinite, celsian, plagioclase up to An_{100} *etc.*, ref. 2) some interesting geochemical properties have also been reported; for instance, an apparent disequilibrium in oxygen isotopic composition between coexisting olivine and pyroxene (3) and a Rb-Sr age of 1.3×10^9 y (4, although see, for example, 5 which does not confirm this result).

As part of a consortium effort to study LEW 86010 (led by G.McKay) ~50mg of an homogenised powder (taken from 800 mg of starting material) was made available for carbon and nitrogen studies. As the sample was not crushed in our laboratory it is unknown what precautions were taken to avoid contamination and, indeed, the carbon analysis yielded a total of 350 ppm C with nearly 80% of this probably due to terrestrial organic contamination. Regardless, incremental heating allowed partial resolution of the contamination and it appears that LEW 86010 contains a single major indigenous carbon component, equivalent to 80 ppm C, with $\delta^{13}C$ of -14 ± 4‰. The combustion (decomposition?) temperature of 450-700°C would be commensurate with identification as either a carbonate or amorphous carbon. A relatively straightforward acid treatment of the bulk sample should constrain this further. Note that carbonates are not confined to regolith breccias such as C1/C2 meteorites; a CAI from Murchison has been determined to contain 45% by volume of calcite (6) and carbonates are present in SNC meteorites (7,8).

The nitrogen distribution in LEW 86010 appears to be more complicated than that of the carbon. At temperatures above 1000°C, ^{15}N-enriched nitrogen is liberated. Assuming reasonable production rates and using an exposure age of 18×10^6 y (9) this effect can be explained by spallogenic reactions. However, this is at odds with the fact that no accompanying ^{13}C-enrichment was evident at high temperatures (the calculated effect in $\delta^{13}C$ is modest but should have been easily observed). Nitrogen released at lower temperatures (20 ppm in total) shows one major release (200-600°C) but $\delta^{15}N$ values appear to exhibit variations commensurate with a number of components. There is an overall enrichment in ^{15}N (excluding any nitrogen which could be spallogenically produced) resulting in a whole-rock $\delta^{15}N$ value of +12‰. It is interesting that the nature of the release profile is similar to that obtained from certain whole-rock unequilibrated ordinary chondrites (PSU unpublished data); the ^{15}N-enrichment on the other hand could be ascribed to either a carbonaceous (*e.g.* 10) or ordinary (*e.g.* 11) chondrite source.

Refs: (1) Prinz *et al.*, (1988), *LPSC*, **XIX**, 949, (2) Prinz *et al.*, (1977), *EPSL*, **35**, 317, (3) Clayton *et al.*, (1976), *EPSL*, **30**, 10, (4) Birck *et al.*, (1975), *Meteoritics*, **10**, 364, (5) Lugmair and Marti, (1977), *EPSL*, **35**, 273, (6) Armstrong *et al.*, (1982), *GCA*, **46**, 575, (7) Carr *et al.*, (1985), *Nature*, **314**, 248, (8) Wright *et al.*, (1988), *GCA*, **52**, 917, (9) Eugster *et al.*,(1989), *LPSC*, **XX**,272,(10) Kerridge (1985),*GCA*,**49**,1707,(11) Alexander *et al.*,(1989),*LPSC*,**XX**, 7.

IMPACT-PRODUCED FLUIDIZATION OF DUOLUN CRATER, CHINA

Wu Siben, Institute of Mineral Deposits, Chinese Academy of Geological Sciences, Baiwanzhuang Road, Beijing 100037, China

The conspicuous 70 km-diameter Duolun ring structure, located in 200 km north of Beijing (42 ° 3′N, 116 ° 15′E), is a complex impact crater with ring structures. It has a 70 km-diameter inner ring which is a peripheral trough now occupied by the Lower Cretaceous coal-bearing formation etc. and has a 170 km-diameter outmost ring marked monomict megablock breccia. (1, 2, 3) Duolun crater is similar in size and feature to the famous Manicouagan crater in Canada. In constrast to Manicouagan croded more deeply, Duolun crater has some better-preserved uppermost impact-produced materials of fluidization, such as suevite, ejecta blanket, impact melt sheets with concentric hummocky ridges, and ground surge mear the impact point. Research on some rare phenomena of Duolun will be able to provide an opportunity to get some reasonable answers of unsolved problems: the origin of basin rings, the identity of the boundary of excavation, etc.

Concentric hummocky ridges and impact melt sheets At the north-western part of Duolun, at impact melt sheets outside the inner ring, there are the concentric hummocky ridges, in general, which has been regarded as preserved crests of standing shock waves moving outward through the surrounding rock which was momemtarily fluidized by impact.

Impact melt sheets occur at the central and western part of Duolun, and extend to the distances 120 km (3.4 inner ring radii) from the cratering centre. Near Taipusiqi city, the impact melt sheet has a thickness more than 200 m, and has some cooling fracture of more than 35m high and 1m in size.

Ground surge near cratering centre. Near the centre of Duolun, there are some lobes of ground surges which appear to be a lot of festoons consisting of a series of arclike ridges with steep outer slopes and gentle inner slopes. The highness of ridges has a centripetal gradual decrease up to apparent disappearance. The phenomenon indicates that the flow of ground surge had a subhorizontal outward novement. The outer edge of the ground surge forms an incomplete ring peaks of 18-22 km in diameter. It seems probably to be interpreted a product of oscillatory uplift near cratering centre and to suggest the previous fluidization or Tsunami hypothesis on origin of basin rings in the Moon. (4, 5)

Ejecta blanket and suevite. The ejecta blanket at southwestern part of Duolun is located outside 82 km-diameter inner rim which consists of Archean quartzite and schist, and the Lower Permian limestone, and impact melt. The lack of ejecta blanket inside inner rim suggests that the inner rim may be the boundary of excavation. The ejecta blanket contains radial lineations of various impact glass body, maybe up to 100 m × 600 m in size. The matrix of impact glass body appears obvious floded and contorted schlieren with vortex behind tail of shock-produced molten glassy rock fragment, this phenomenon indicates that there is extremely large velocity difference between the glass ejecta blanket and the overtaken rock fragment.

The suevite at western and south-western parts of Duolun extends to the distances 75 km − 100 km from the cratering centre. It forms individual complexes up to 100 km × 500 km in size and more than 20 m in thickness, and contains black-color, vitreous impact glass bombs aerodynamically-sharped in the micron to decimeter.

This research is supported by NSF of China, and by the Chinese Foundation for Development of Geological Sciences and Techniques.

REFERENCES: (1) Wu Siben (1987) Lunar and Planet. Sci., XVIII, 920-921. (2) Wu Siben et al. (1987) Meteoritics, 22 (4), 502-503. (3) Wu Siben (1989) Lunar and Planet. Sci., XX, In press. (4) Murray J. B. (1980) Moon and Planets, 22, 269. (5) Baldwin R. B. (1981) Proc. Lunar Planet. Sci., 12A, 275-288.

OVER 2,000 NEW ANTARCTIC METEORITES, RECOVERED NEAR THE SOR RONDANE MOUNTAINS, EAST ANTARCTICA: Keizo Yanai, Department of meteorites, National Institute of Polar Research, 9-10, Kaga 1-chome, Itabashi-ku, Tokyo, Japan

Over 2,000 new Antarctic meteorites named Asuka-87 and Asuka-88 meteorites were recovered on the bare ice fields around the Sør Rondane Mountains, near the Japanese Base Asuka, East Antarctica by the Japanese Antarctic Research Expedition 1987-1989. Of preliminary processed specimens of over new 2,000 meteorites, there were several irons, numerous achondrites contain anorthositic breccia and chondrites with many carbonaceous chondrites. It may be to found possible new specimen(s) in the collection. Total weight of the collection is about 500kg with the largest specimen of 46kg chondrite.

WEATHERING IN ORDINARY CHONDRITES AS EVIDENCED BY CHEMICAL ANALYSES (OLD AND NEW); A. M. Yates, Department of Chemistry, Arizona State University, Tempe, AZ 85287

In order to draw conclusions about the pre-terrestrial intra-group homogeneity (or heterogeneity) of ordinary chondrites, it is essential that only "good" (i.e. unweathered) samples be compared. "Good" samples and "falls" have often been assumed to be synonymous. To verify or refute this assumption, over 150 recent (after 1950) chemical analyses of ordinary chondrites (falls and finds) were compiled from the literature. Most of these analyses were done by Wiik, Jarosewich or D'yakonova and Kharitonova utilizing wet chemical methods (literature references available from author).

Comparison of the data sets reveals that several chondrites classified as falls have undergone weathering. This is usually evidenced by low values for metallic iron and/or inclusion of values for ferric oxide in the analytical results. Although the oxidation of metallic iron is usually the first indication of weathering, (Buddhue, 1957), other phases may also be affected. For example, the alkali oxides exhibit a variability which can be ascribed to weathering.

In the second phase of this work, 30 equilibrated L and H chondrites were analyzed by x-ray fluorescence. The results obtained further support the fact that falls cannot be assumed to be unweathered and that feldspars also participate in the weathering process - at least in some cases.

Buddhue, J.D. (1957) The Oxidation and Weathering of Meteorites, University of New Mexico Press.

ISOTOPICALLY HEAVY CARBON IN DEEP-SEA SPHERULES: P.D. Yates, I.P. Wright, C.T. Pillinger, Planetary Sciences Unit, Department of Earth Sciences, The Open University, Milton Keynes, MK7 6AA. R. Hutchison, British Museum (Natural History), Cromwell Road, London, SW7 5BD, England.

Wright *et al.* (1988) revealed the presence of four distinct carbonaceous components in deep-sea spherules (DSS). Of these only one could be believed to be indigenous to the samples. This component had a $\delta^{13}C$ of –20 to –16‰ and burned between 600 and 1200°C. In an attempt to study this component further, six DSS (kindly supplied by D.E. Brownlee) have been anlaysed using the new 'low blank' preparation technique of Yates *et al.* (1989). Even so, it has been necessary to apply a blank correction - to remove the effects of contamination from the sample vessel.

Diagram 1 shows the results of Wright *et al.* plotted together with those of this work. Note that only the type S DSS are considered, this being the group that contains the component. of interest. Neither set of data have been blank corrected. The most striking difference on a plot of amount of carbon liberated between 600 and 1200°C vs. the corresponding $\delta^{13}C$ measurement calculated as the average of the extraction steps that constitute the release, is in the carbon content; Wright *et al.* showing concentrations in the range of 200 to 2500 ppm, this study 40 to 370 ppm. It is not apparent at this stage whether this difference can be attributed solely to the differing preparation techniques used, or whether an actual difference exists. The results for the spherules analysed in this work redefine the $\delta^{13}C$ of the component in a range of –19 to –8‰ - a considerable increase in the degree of ^{13}C enrichment previously observed.

From comparisons between sample analyses and blank experiments performed on the days before and after measurement of the samples, it could be seen that a major proportion of the high temperature carbon release was still due to contamination. In order to elucidate the true $\delta^{13}C$ value of the sample carbon,a blank correction can be estimated. Diagram 2 shows the results of such blank corrections on sample KKF. The 'starting position' is the average value for the carbon obtained over 600°C, assuming that there is no blank contribution to this. The curve shows how this value changes when corrections are applied assuming that a proportion of the total is supplied from the blank (the average $\delta^{13}C$ measured for the blank experiments was –30‰). Experience from a large number of blank experiments suggests that the blank supplies between 75 and 90% of the total, giving $\delta^{13}C$ values of between +57 to +171‰ for the sample component. Notwithstanding the problems and associated errors of the technique, it is now possible to accept some heavy carbon exists in the DSS and as such they probably contain a pre-solar component.

From the Type S DSS so far analysed by us and Wright *et al.*, it would seem that such anomalously heavy carbon is a minor but common constitutent. This is in direct contrast to the chondritic meteorites, where only type 3 or lower petrographic types show evidence of heavy carbon in bulk samples. The presence of such material obviously has important implications for the petrogenesis of the DSS, and their relationships to other extraterrestrial reservoirs, and further work will hopefully help us to elucidate these questions.

Diagram 1

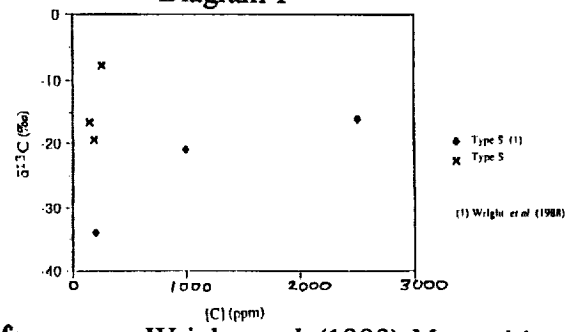

Diagram 2

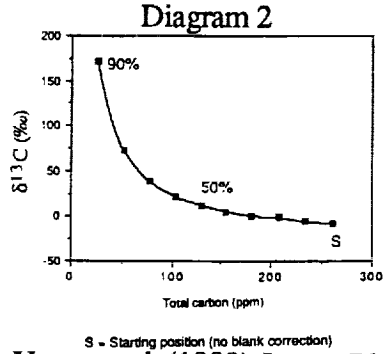

References: Wright *et al.* (1988) *Meteoritics* **23**,339.. Yates *et al.* (1989) *Lunar Planet. Sci.*, **XX**, 1227.

INFLUX OF COSMIC SPHERULES TO THE EARTH DURING THE LAST ~ 10^5 YEARS AS DEDUCED FROM CONCENTRATIONS IN ANTARCTIC ICE CORES

F. Yiou and G.M. Raisbeck

IN2P3 - Centre de Spectrométrie Nucléaire et de Spectrométrie de Masse

Bât. 108 - 91405 Campus ORSAY - FRANCE

At this meeting two years ago, we reported the discovery of 5 "cosmic spherules" from an ice core drilled at Dome C in Antarctica (Yiou and Raisbeck, 1987). Although the concentration of these particles is very low, we pointed out two rather important advantages of this type of reservoir for studying such particles: (i) the parameters necessary to calculate an absolute flux from such observations can be quite reliably estimated (ii) one can look for possible time variations in this flux.

During the past year we have pursued these studies in several other Antarctic ice cores, in particular one drilled at Vostok by a Soviet team, which is believed to cover a time period of ~ 150,000 years. From samples spaced roughly uniformly over this latter core we have isolated more than 50 spherules of >50μ in diameter. From previous experience we know that a significant fraction of these spherules could be terrestrial contamination (natural or anthropogenic) introduced during the recovery and handling of the ice. This contamination can usually be quite easily recognized by electron microprobe analysis. While we have not yet had the opportunity of carrying out such analyses, we hope to do so before the meeting. This would enable us to give at least a rough estimate of the global flux of extraterrestrial matter in this form during the past ~10^5 years. We also hope eventually to be able to measure iridium in the filters from which these spherules were extracted, and from this to also estimate the flux of unmelted extraterrestrial particles.

Yiou F. and Raisbeck G.M. (1987), Meteoritics 22, 539

Organic Analysis of Individual Meteorite Inclusions by Two-Step Laser Desorption/Laser Multiphoton Ionization Mass Spectrometry

Renato Zenobi, Jean-Michel Philippoz, Peter R. Buseck*, and Richard N. Zare

Department of Chemistry, Stanford University, Stanford, CA 94305
*Departments of Geology and Chemistry, Arizona State University, Tempe, AZ 85281

A complex array of organic molecules has been identified in carbonaceous chondrites. In typical analytical schemes, gram amounts of material are pulverized, the compounds of interest are extracted, purified, separated by chromatography, and finally identified by mass spectrometry. These procedures are not only very time-consuming, but artifacts may also arise because of contamination or from chemical reactions occurring during sample processing. In addition, with these traditional methods it is impossible to obtain information on the spatial distribution of organic matter within heterogeneous samples. Since meteorite samples are known to be heterogeneous, even on a millimeter scale or below, the possibility of organic analysis with such a spatial resolution is desirable.

We report here the direct analysis of organic compounds in mm-sized regions and inclusions of meteorites, using a highly selective and sensitive two-step laser desorption/multiphoton ionization mass spectrometric method. First, the pulsed output of an infrared laser is focused onto the surface of a freshly fractured or ablated sample. Intact neutral molecules are released from its surface in a rapid laser-induced thermal desorption process. After approximately 40 μs, an ultraviolet laser pulse induces 1 + 1 resonance-enhanced multiphoton ionization (REMPI) of the desorbed molecules 2 mm above the surface. Finally, the ions are detected in a reflectron time-of-flight mass spectrometer.

Combining the desorption of intact neutrals with the soft ionization characteristics of REMPI results in parent molecular ion signals dominating the mass spectra. These features of our method easily allow us to interpret spectra of complex mixtures and therefore to circumvent complicated sample preparation procedures. Small pieces of meteorites are mounted onto a sample holder with a thermoplastic polymer and introduced into the source region of the laser mass spectrometer with no further treatment. The infrared laser pulse desorbs material from about 1 mm^2 of the sample surface, and by overlapping consecutive laser shots complete spectral information can be obtained from as little as 1 μg of the sample. At an ionization wavelength of 266 nm, aromatic compounds are easily ionized whereas substances fail to resonantly absorb this wavelength are suppressed. Detection sensitivities lie in the femtomole range or below.

We investigated small splits as well as individual chondrules from the Allende meteorite and compared their spectra with matrix material. Polycyclic aromatic hydrocarbons (PAHs) are readily detected, and their distribution within the meteorite could be probed. Dominating the spectra are naphthalene (128 amu) and its alkyl-substituted homologs (128 + n•14 amu), as well as phenanthrene/anthracene (178 amu) and their alkyl substituted homologs (178 + n•14 amu), with up to eight additional carbon atoms attached to the aromatic skeleton. Spectra taken from interior surfaces obtained by fracturing the meteorite generally showed a significant enhancement of the aromatic signal compared to the average distribution of organics obtained from powder samples. This suggests that PAHs are primarily associated with the fine-grained matrix that is adjacent to inner surfaces and cracks in the meteorite. An experiment was conducted on unexposed interior of individual chondrules which were carefully machined using a diamond tool. Blanks were treated in the same fashion. Within our detection limits, no aromatic compounds have been detected inside the chondrules whereas on the outside, signals resembling those from matrix material were found.

Our results will provide information about the formation and history of meteorites, and about the possible role PAHs played in the early solar system.

WHERE IS THE TETRATAENITE PHASE IN THE IRON METEORITE SANTA CATHARINA? J.Zhang, D.B.Williams and J.I.Goldstein Department of Materials Science and Engineering, Lehigh University, Bethlehem PA 18015 USA

The iron meteorite Santa Catharina is a severely weathered meteorite and has a bulk Ni composition of about 35wt%.[1] It is one of the few high Ni anomalous irons.[1] Oxygen containing regions and the Tetrataenite phase have been found in the metallic portion of the meteorite.[2,3] Although Santa Catharina has been studied by many authors, there is little agreement on the relationship of the Tetrataenite phase to the microstructure of the meteorite. There are also discrepencies about the existence of an oxide phase. In this study we have investigated the Santa Catharina meteorite (USNM#3043 specimen) using analytical electron microscope (AEM) and electron probe microanalyser(EPMA).

Figure 1 is a backscattered electron(BSE) image of a non-etched sample of Santa Catharina. The dark and the light regions, 1 to 100μm in size, are the typical microstructural features observed by most other research groups.[4-6] Quantitative X-ray chemical analysis using the EPMA shows that the light region has 34.9±0.35wt% Ni with Fe as remainder and the dark region has 45.3±0.43wt% to 50.0±0.48wt% Ni and 6.98±0.07wt% to 11.6±0.11wt% O with Fe as remainder. No oxygen was detected in the light region. The existence of a large amount of oxygen in the high Ni dark regions lowers the average atomic number at the regions and is the reason why these regions are darker in the BSE image. Figure 2 is a TEM bright field image of Santa Catharina showing the interface between the two different regions labelled 'FeNi+Oxide' and 'FeNi+γ' respectively. Chemical analysis using the AEM has shown that the right hand side of figure 2 which has a distinct two phase structure is the 'dark region' in BSE image and the region on the left hand side of figure 2 is the 'light region' in BSE image. A two phase structure very similar in morphology to that of 'dark region' also exists in the 'light region' but is much less distinctive. The electron diffraction and dark field images show that the Tetrataenite exists in the island phase of both regions and that the domains are about 10nm in size. The honeycomb phase of the 'dark region' is an oxide phase. The honeycomb phase of the 'light region' is a disordered fcc taenite phase. We argue that the Santa Catharina meteorite originally had a uniform microstructure, that is a 20nm scale cloudy zone type structure. During terrestrial corrosion the low Ni honeycomb phase in part of the meteorite was oxidized forming the dark regions. The Tetrataenite remains unaffected by the corrosion process.

REFERENCES 1. Buchwald,V.F.(1975)Handbook of Iron Meteorites, Univ. of California Press v.3 p.1068 2. Lovering,J.F. and C.A.Andersen(1965)Science 147,734 3. Danon,J. et al.(1977)Nature 277,283 4. Bowles,J.S. et al.(1978)Nature 276,168 5. Jago,R.A. et al.(1982)Physica Status Solidi (a)74,247 6. Saito,J. and H.Takeda(1988) Abs. 51st Annu. Meteo. Soc. Meet. P1, Fayetteville, AK, USA

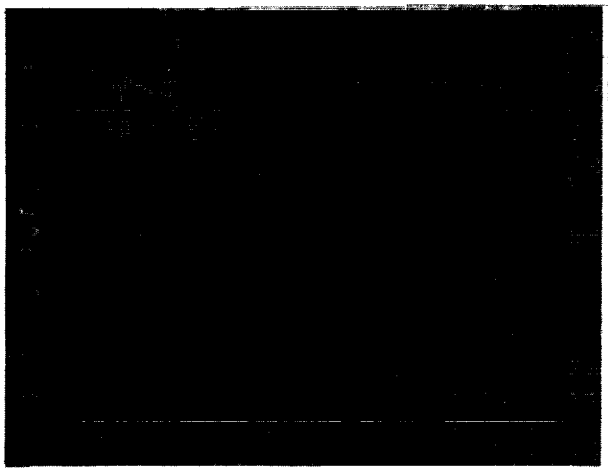

Fig.1 SEM BSE image of Santa Catharina

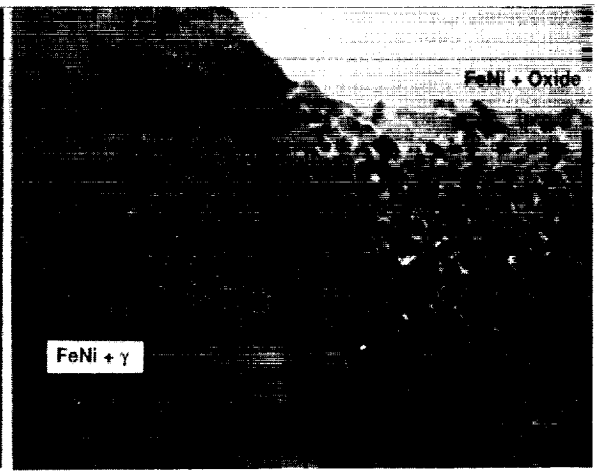

Fig.2 TEM BF image of Santa Catharina

A MIXED MODEL ON THE PERMIAN-TRIASSIC BOUNDARY EVENT Zhou Yaoqi Chai Chifang Mao Xueying Ma Shulan Ma Jianguo (Institute of High Energy Physics, Academia Sinica, P.O.Box 2732, Beijing, China)

A large mass extinction occured at the end of the Permian. What caused the extinction? Extraterrestrial impact or terrestrial volcanicty?Some researchers think the mass extinction may be caused by a large-scale impact event (e.g. Sun,et al.,1984; Xu,et al.,1985; He,1985; Zhou,et al.,1987).This hypothesis is based on Pt-group element anomaly and presence of microspherules and clastics of metamophic rocks in boundary clays, which were thought to be related to impact event. However, Kastner,et al.(1980), Asaro,et al.(1982), He,(1981) and Yin, (1987) considered the Permian/Triassic event as a volcanic one. Their reasons are as follows: (1)The volcanic rhyotaxitic structure was found at the boundary clays; (2)Many high-temperature β-quartzs formed by volcanic activity were discovered from the boundary clay; and (3) there are 3 to 7 clay layers near the P/T boundary, which are similar to the boundary clay on the elemental composition. The two points of view seem all right, but what is the better explanation? In order to answer the question, we checked eleven sections of Permian/Triassic boundary in China and the Nammal section in Pakistan by NAA.
A slight Ir anomaly has been detected at the black shale on the P/T boundary (366ppt in Nammal section, Pakistan; 52ppt and 42ppt in Duansan and Changxing sections, China). And a very clear siderophile anomalies (82.5ppm Co,347ppm Ni and 232ppm Cr) were found in Fusui section of China. Those anomalies may be caused by the enrichment process of the black shale, but Ir and Ni abundances, 5 times higher than the background of the shale, may be difficuty to explain by the normal enrichment of black shale. There may be another siderophile source in addition to the background of sea water. The Fe, As, Sb, and Se anomalies at the bottom of boundary clay layer are related to the reduction environment at that time.
The REE abundances in clays at and near the P/T boundary in different section of South China were detected by INAA. And the REE patterns of boundary clays differ from those of non-boundary clays indicadted their different sources. As a comparison, we also determined the REE of the acidic-intermediate volcano rocks of Triassic, and the Pre€/€,D/C and C/T boundary clays. From those REE patterns and some other evidences, we put forward a proposal that the P/T boundary clay may be a mixed product consisting of the acidic-intermediate ash and the upper crust substance representing sputtering component (here use the data of C/T boundary clay). and the calculated mixing fraction of the former and latter is 7:3.
The mixed model of forming boundary clay can better explain the experimental facts from two aspects:i.e. the volcanic activity and impact event. A possible scenario is that at the end of the Permian, an large-scale impact triggered severe activity of volcanos. Or these two interactions simultaneously occured at that time.
REFERENCES Asaro,F.,Alvarez,W.,Alvarez,L.W.Michel,H.V.,Geol.Soc.Amer.Spec.Pap. 190(1982) 517. Chai,C.F.,Ma,S.L.Mao,X.Y.Zhou,Y.Q.,Sun,Y.Y.,Xu,D.Y.,Zhang,Q.W., and Yang,Z.Z.Journal of Radioanalytical and Nuclear Chemistry,Articles,Vol.114 No.2(1987) 293-301. He,J.W.,Chai,C.F.,Ma,S.L., Science Bulletin, Vol.32, No.14 (1988),1088-1091. Xu,D.Y.,Chai,C.F.,Ma,S.L.,Mao,X.Y.,Sun,Y.Y.,Zhang,Q.W.,Yang, Z.Z., ature Vol.314,(1985),154-156. Zhou,Y.Q.,Chai,C.F.,Ma,S.L.,Mao,X.Y.,He,J. W.,Sun,Y.Y.,Science Bulletin,Vol.31,No.23(1986),1838-1839.Zhou,Y.Q.,Chai,C.F., Ma,J,G.,Kong,P.,Hu,G.M.,Science Bulletin, Vol.33,No.5(1988),397-398.

ALLENDE TE REVISITED II: MAGNESIUM AND OXYGEN ISOTOPIC STRATIGRAPHY.

E. ZINNER[1], A. VIRAG[1], S. WEINBRUCH[1,2], AND A. EL GORESY[2]; [1]MCDONNELL CENTER FOR THE SPACE SCIENCES AND THE PHYSICS DEPARTMENT, WASHINGTON UNIVERSITY, ST. LOUIS, MO 63130, USA; [2]MAX-PLANCK-INSTITUT FÜR KERNPHYSIK, POB 103980, D-6900 HEIDELBERG, FRG.

Allende TE, a forsterite-bearing F inclusion, has non-linear isotopic effects in Ti and Ca that are in the range seen in "normal" Allende CAIs (Jungck et al. ,1984; Niederer et al., 1985). Here we report first results from a detailed ion microprobe investigation made in conjunction with petrologic studies (El Goresy et al., 1989).

Magnesium measured *in situ* in olivine and fassaite of lithology A and in spinel and fassaite of lithology B (see El Goresy et al., 1989, for a description) is isotopically heavy with F_{Mg} = +14‰/amu, confirming the results of Clayton et al. (1984). No significant differences in F_{Mg} between different phases were found nor between spinels in the interior and the rim of lithology A. Hibonite from the rim of lithology A shows ^{26}Mg excess, together with neighboring spinel it defines a line with $(^{26}Al/^{27}Al)_0=5.1x10^{-5}$.

Oxygen isotopes were measured in individual mineral grains from different preselected areas of the TE PTS (El Goresy et al., 1989): 1) the interior of lithology A (forsterite and fassaite), 2) oxidized olivines from lithology A, 3) the interior of a xenolith from lithology B (spinel, fassaite) and 4) rim layers of another xenolith of B (spinel, hibonite). Measured compositions (Fig. 1) in areas 1 and 2 lie on the fractionated mixing line (≡"TE mixing line") established by Clayton et al. (1984). Forsterite and fassaite in area 1 are indistinguishable from the most ^{16}O-rich fraction of Clayton et al. (1984), but olivines in area 2 are shifted toward normal O, with Fa-rich grains lying closest to normal. Oxygen measured in the interior and rim layers of the xenoliths shows isotopic heterogeneity in its fractionation, in addition to mixing with normal O. Spinels in region 3 spread along the "^{16}O-rich fractionation line" from the Allende mixing line to the TE mixing line, by far exceeding the experminental uncertainty. On the other hand, spinels in the rim of lithology B (area 4) are even more fractionated than the TE mixing line, while a few hibonites in the outermost layer of this rim lie close to the Allende mixing line. This indicates that, at least in lithology B, different grains experienced different degrees of fractionation. Apparently, while Mg and O in olivine and fassaite of lithology A equilibrated during the fractionation event, this was not the case for O in spinel and hibonite in the xenoliths.

References: Clayton et al. (1984) *GCA* **48**, *535*; El Goresy et al. (1989) *this volume*; Jungck et al. (1984) *GCA* **48**, *2651*; Niederer et al. (1985) *GCA* **49**, *835*.

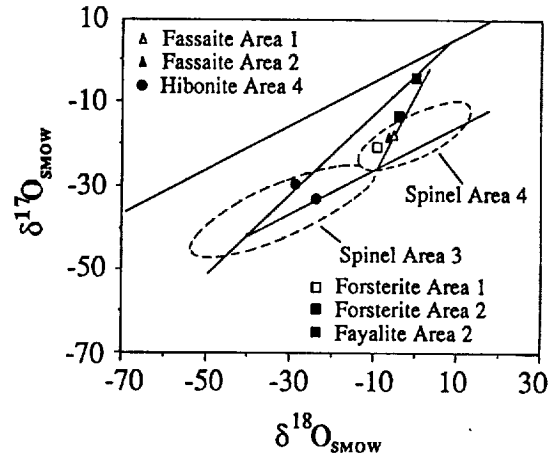

Figure 1

THE COMPOSITION OF EET 83334: A PROGRESS REPORT

M.E. Zolensky[1], D.W. Mittlefehldt[2], M.E. Lipschutz[3], X. Xiao[3], R.N. Clayton[4], T.K. Mayeda[4] and R.A. Barrett[2], [1]NASA/JSC, Houston, TX, [2]Lockheed Science and Engineering Co., 2400 NASA Rd.1, Houston, TX, [3]Dept. of Chemistry, Purdue University, West Lafayette, IN, [4]Enrico Fermi Institute, University of Chicago, Chicago, IL.

INTRODUCTION We report here preliminary results from a consortium study of the bulk mineralogical, trace element, and oxygen isotopic composition of EET 83334. We then use the data to place this meteorite within proper petrological context.

MINERALOGY AND PETROLOGY As previously revealed [1], EET 83334 contains abundant rounded to irregularly shaped rimmed aggregates (<1 mm) of coarse- to fine-grained Fe-Mg phyllosilicates and, sometimes, Ca-carbonates, dispersed within a matrix of Fe-Mg phyllosilicates, magnetite, Ca-carbonates, pyrrhotite, and pentlandite. Rare grains of magnetite-rimmed kamacite, chromite, and Ca-phosphate are also present.

BULK COMPOSITION The bulk Fe-Si-Mg-S composition of the matrix and aggregate rim material of EET 83334 is similar only to that for previously analyzed CM matrices [1]. The oxygen isotopic composition of a whole rock sample of EET 83334 is $\delta^{18}O$=+5.90‰ and $\delta^{17}O$=+0.79‰, relative to SMOW, and falls along the CM matrix line [2]. The results of analyses for major and minor elements by INAA and RNAA are presented in a CI-normalized plot in Fig.2 (average CI composition from [3]). The composition of EET 83334 is very similar to Murchison (CM2) [4-5].

CLASSIFICATION EET 83334 contains phyllosilicate-rich aggregates set within a matrix whose bulk composition is most similar to CM2 chondrite matrices. Similarly, the whole rock composition of this meteorite is most similar to CM2s. However, no true chondrules are present; phyllosilicate aggregates are present as in Y-86720 and B-7904 [6], which are CIs, and Y-82042, tentatively classified as a CM1 [4]. EET 83334 is of lower petrologic type than CM2, and is best described as a CM1.

REFERENCES [1] Zolensky and Barrett (1988) Meteoritics 23, 314; [2] Clayton et al. (1976) EPSL 30, 10; [3] Anders and Grevesse (1989) GCA 53, 197; [4] Grady et al. (1997) Proc. 11th Symp. Antarc. Meteor., 162; [5] Lipschutz and Paul (in press) Zeit. Naturfor.; [6] Zolensky et al. (1989) 14th Symp. Antarc. Meteor.

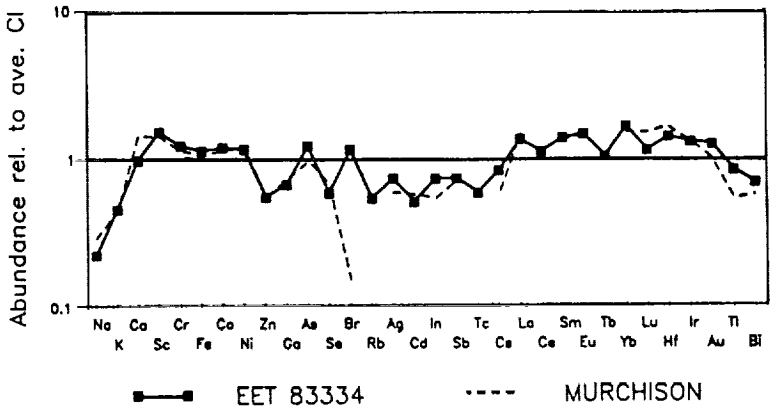

*U.S.GOVERNMENT PRINTING OFFICE:1989-661-008/00250

Author Index